

http://researchcommons.waikato.ac.nz/

Research Commons at the University of Waikato

Copyright Statement:

The digital copy of this thesis is protected by the Copyright Act 1994 (New Zealand).

The thesis may be consulted by you, provided you comply with the provisions of the Act and the following conditions of use:

- Any use you make of these documents or images must be for research or private study purposes only, and you may not make them available to any other person.
- Authors control the copyright of their thesis. You will recognise the author's right to be identified as the author of the thesis, and due acknowledgement will be made to the author where appropriate.
- You will obtain the author's permission before publishing any material from the thesis.

Uplift History and Geomorphic Development of the Southern Alps, New Zealand, Assessed by Fission Track Analysis

A thesis

submitted in fulfilment

of the requirements for the Degree

of

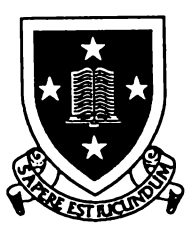
Doctor of Philosophy in Earth Sciences

at the

University of Waikato

by

John Mark Tippett



University of Waikato

1992

ABSTRACT

The uplift history and geomorphic development of the Southern Alps has been studied, using fission track analysis of basement samples in combination with measurement of the present geomorphology of the Southern Alps.

During the late Cenozoic the Pacific plate has been converging obliquely with the Australia plate in South Island, New Zealand. A result of this convergence has been the growth of a major mountain range - the Southern Alps - at the leading edge of the Pacific plate. The results of fission track analysis of 140 samples from 13 transects across the 300 km-long central sector of the Southern Alps reported here, establish the late Cenozoic vertical kinematics (amount, age, and rate of rock uplift) of the Pacific crust underlying the Southern Alps. The pattern of late Cenozoic rock uplift is asymmetrical with respect to the Alpine Fault, being a maximum (19 km) immediately east of the central part of the Fault, with lesser values at the eastern (3 km), northern (10 km) and southern (8 km) extremities of the Southern Alps. The age of the start of rock uplift varies spatially across the Southern Alps, the earliest indications from fission track analysis being at 8 Ma ago at the southern end of the Southern Alps, decreasing to 5 Ma ago at the northern end and 3 Ma ago along the southeastern margin. This age variation reflects the longer time over which the southern parts of the Southern Alps have been in collision. The rate of propagation of rock uplift southeastwards into the Pacific plate has been 30 mm/a, nearly 4 times the late Cenozoic average rate of convergence normal to the plate boundary. Late Cenozoic mean rock uplift rates range from a maximum of ~2.8 mm/a at the Alpine Fault to a minimum of ~1.0 mm/a in the east. Uplift has accelerated over time, but only significantly since 1.3 ± 0.3 Ma ago.

The fission track data in combination with topographic data have been analysed to quantify the response of the surface of the Pacific plate to the late Cenozoic continent-continent collision. The rates of mean surface uplift, the rates of work done against gravity during the mountain building, and the erosional, isostatic and tectonic components (amounts and rates) of rock uplift, have been derived and mapped over the central 300 km length of the Southern Alps. The data do not support the notion of erosional-mechanical coupling of the two wedges in the two-sided orogen model of *Koons* [1990], but are consistent with overriding of the Australia plate by the Pacific plate. The late Cenozoic rate of mean surface uplift in the Southern Alps ranges from

<0.1 mm/a adjacent to the Alpine Fault to >0.3 mm/a over most of the area east of the Main Divide. The highest rates of mean surface uplift do not coincide spatially with the regions of highest mean elevation. The rate of work done in elevating the mean surface ranges from ~2.5 mWm^{-2} to ~10 mWm^{-2}, although most areas have experienced similar rates of energy input of ~7.5 mWm^{-2}. The amount of denudation ranges from ~18 km adjacent to the Alpine Fault to ~2 km along the southeast margin of the Southern Alps; the late Cenozoic mean rate of denudation ranges from ~2.5 mm/a at the Fault to ~0.5 mm/a in the southeast parts of the Southern Alps. The amount of tectonic uplift decreases from ~4 km at the Alpine Fault to ~1 km along the eastern margin of the Southern Alps.

The fission track data have been used to assess the role of faulting in the late Cenozoic uplift of the Pacific plate crust. For the Moonlight, Ostler, Harper, Torlesse, Porter's Pass and Hope faults, the vertical offset in all cases lies within the uncertainty of the data, typically ± 2 km, and is less than 30% of the surrounding uplift. Over a scale of kilometres the uplift is continuous and regular, and deformation in the plate boundary zone can therefore be treated as if it were ductile.

The regression of the mean surface, summit, and valley elevations on the amount, age, and rate of uplift for each of 82 sample sites is used to establish the nature of the relationship between uplift and geomorphology. The preferred regression models have uniform slope but varying elevation response between transects. Uplift explains 80-90 % of the variation in elevation. Substitution of space for time has allowed the evolution of landforms to be studied. To the east of the Main Divide, elevation and relief are proportional to and closely related to the age of initiation of rock uplift and the amount of rock uplift (r^2>0.8). Mean surface uplift was delayed for ~2 Ma after the start of rock uplift, a result of the stripping of a soft cover rock succession that prior to rock uplift overlaid the harder greywacke basement. Under a rock uplift rate of 0.8 km/Ma, uplift of the mean surface proceeded at 0.4 km/Ma, while the summits increased in elevation at a rate of 0.6 km/Ma and valleys increased in elevation at 0.2 km/Ma. The mountains east of the Main Divide have continued to increase in elevation and relief and evolve in form over time since the start of uplift. Mountain elevation has little relationship with late Cenozoic mean rock uplift rates of 0.8-1.0 km/Ma or inferred contemporary rock uplift rates (r^2~0.3). In contrast, to the west of the Main Divide, elevation is shown to be closely related to rock uplift rate (r^2>0.8). Transects with higher rock uplift rates support higher topography.

Landforms are therefore in a stable equilibrium with rock uplift rate, and the landscape contains no residual evidence of the total amount of rock uplift, or the age of uplift. Lithological variation appears to have no relationship with elevation.

The new uplift and geomorphic data allow the construction of a new model of the geomorphic evolution of the Southern Alps. The model quantifies the development over time and space of rock uplift, mean surface elevation, exhumation of crustal section, and relief. The earliest indications of mean surface uplift are between 4 and 5 Ma ago at the Alpine Fault. Mean surface uplift propagated southeastward from the Alpine Fault at a rate of 30 km/Ma. At 3 Ma ago greenschist was exposed in the southern parts of the Southern Alps near Lake Wanaka, and since then has become exhumed along a narrow strip east of the Alpine Fault. Amphibolite grade schist has been exhumed adjacent to the Alpine Fault only in the last 0.3 Ma. At the southeast margin of the Southern Alps a 1.0-1.5 km step in the basement topography separates the Southern Alps from the non-uplifted plains to the east. The existing models of the geomorphic development of the Southern Alps - the dynamic cuesta model of *J. Adams* [1980 and 1985] and the numerical model of *Koons* [1989] - are compared with the new data. Particular constraints unrealised by these two earlier models include: the earlier age of rock uplift (8 Ma ago) and its spatial variation (8 Ma ago to 3 Ma ago) across the Southern Alps; the lower long-term rock uplift rate (0.8-1.0 mm/a) of the Southern Alps for most of the late Cenozoic; the lag between the start of rock uplift and the start of mean surface uplift; and the patterns of rock uplift and erosion across the Southern Alps. The age of the start of rock uplift, and the amount and rate of rock uplift, all of which vary spatially, are considered to be the dominant influences on the development of the landscape in the Southern Alps.

ACKNOWLEDGEMENTS

I thank the following people who have helped me produce this D. Phil. thesis:

My chief supervisor Dr Peter Kamp for suggesting a Southern Alps fission track project, and for the benefit of his expertise, enthusiasm, and guidance throughout the duration of the study.

Professor Michael Selby, as supervisor, for his assistance with the geomorphic parts of the thesis.

Dr Paul Green for providing Otway Basin fission track data for use in paleotemperature calibration.

Chairperson Professor Cam Nelson, whose consideration in the arrangement of my teaching duties enabled me to make headway with research.

Dr Richard Stevenson for undertaking microprobe analyses, and for his friendship and interest in the thesis.

The landowners who allowed me to obtain samples from their properties, and who provided hospitality.

Mum, Dad, and Gran for their close concern and support, and financial assistance when the dollars disappeared.

Other fission trackers for their company, including Thomas, Kerry, Edy, Chris and Gerry; in particular I thank Ian and Ivan for friendship and humour in the lab, and for useful discussion.

Earth Sciences Department staff and graduate students who have helped make a happy and productive environment in which to work.

My extended family who have always been interested in my progress and have given me encouragement.

My friends who have given me support, particularly Chris and Anne Mills and Michael and Carole Hughes for their special friendship.

My beloved wife, Sharleen ('Sharky'), for her love, understanding, and patience while I finished the thesis.

TABLE OF CONTENTS

ABSTRACT ii

ACKNOWLEDGEMENTS v

TABLE OF CONTENTS vi

CHAPTER 1: Introduction 1
OBJECTIVE 2
TECTONIC, GEOLOGICAL, AND GEOMORPHIC SETTING OF THE SOUTHERN ALPS 2
Tectonic Setting 2
Geological Setting 2
Geomorphic Setting 4
PREVIOUS STUDIES OF THE UPLIFT OF THE SOUTHERN ALPS 6
PREVIOUS STUDIES OF THE GEOMORPHIC DEVELOPMENT OF THE SOUTHERN ALPS 7
PROBLEMS TO BE ADDRESSED 8
FISSION TRACK ANALYSIS INTRODUCED 9
THESIS FORMAT 10
Content 10
Format 11
Data Appendix 12
REFERENCES 12

CHAPTER 2: Fission track analysis 16
INTRODUCTION 16
LATENT AND ETCHED TRACKS 18
Source of latent tracks 18
Formation of a latent fission track 18
Latent track etching 20
Anisotropic etching 20
FISSION TRACK DATING 22
Identification of tracks 22
Fission track age equation 22
Age determination methods 23
Thermal neutron fluence (ϕ) and λ_f 25
The zeta calibration approach 27
Standardisation of fission track dating calibration 28
Fission track age error analysis 29
ETCHED FISSION TRACK LENGTH PARAMETER 31
ANNEALING 35
Definition 35
Mechanism of latent fission track annealing 35
Annealing studies 38
(1) Laboratory annealing studies 38
(2) Natural studies 40
(3) Physically-based mathematical models 41
Factors controlling annealing 42
(1) Mineral type 42

(2) Temperature and time 42
(3) Mineral composition (apatite) 44
(4) Orientation of tracks 44
THERMAL AND TECTONIC HISTORIES FROM FTA 45
(1) Closure temperature studies - cooling and uplift rates (apatite and zircon) 45
(2) Typical track length distribututions (apatite) 47
(3) Empirical comparison with Otway Basin (apatite) 49
(4) Forward models (apatite) 51
(5) Inverse models (apatite) 54
REFERENCES 56

CHAPTER 3: Fission track analysis of the late Cenozoic vertical kinematics of continental Pacific crust, South Island, New Zealand 62
ABSTRACT 64
INTRODUCTION 64
GEOLOGICAL SETTING 66
TECHNIQUES 67
Fission Track Analysis 67
Sampling Design 68
Experimental Procedures 70
Calibration of Fission Track Analysis 71
RESULTS AND INTERPRETATIONS 76
Apatite Data 76
Zircon Data 84
Paleotemperature Estimation 84
Qualitative Comparison of Otway Basin and S. Alps Apatite Data Sets 92
Correction of Age and Length Data for late Cenozoic Uplift 94
Pre-uplift Sample Paleotemperatures 94
AMOUNT OF ROCK UPLIFT 96
Spatial Pattern of Amount of Rock Uplift 98
TIMING OF LATE CENOZOIC UPLIFT 100
Discussion of Uplift Age 103
RATES OF ROCK UPLIFT AND IMPLICATIONS 105
Late Cenozoic Mean Uplift Rates 107
Uplift Rates Derived From Reset Zircon Ages 109
SUMMARY 113
ACKNOWLEDGEMENTS 114
REFERENCES 115

CHAPTER 4: Dynamics of Pacific plate continental crust in the South Island collision zone (New Zealand) 120
ABSTRACT 122
INTRODUCTION 122
UPLIFT TERMS 124
TECTONIC SETTING 124
MEAN SURFACE UPLIFT 125
Initial Mean Surface Elevation (Eim) 125
Present Mean Surface Elevation (Em) 128
AGE OF UPLIFT 128
RATES OF MEAN SURFACE UPLIFT 134

WORK DONE BY MEAN SURFACE UPLIFT 135
ROCK UPLIFT 137
DENUDATION 138
ISOSTATIC AND TECTONIC COMPONENTS OF UPLIFT 140
TWO-SIDED OROGEN EVALUATED 146
Outline of Two-Sided Orogen 146
Discussion 147
CONCLUDING REMARKS 150
REFERENCES 151

CHAPTER 5: On the role of faulting in rock uplift in the Southern Alps 154
INTRODUCTION 156
PRINCIPLES AND METHOD OF INVESTIGATION 158
MOONLIGHT FAULT 160
OSTLER FAULT 164
PORTER'S PASS, TORLESSE AND HARPER FAULTS 164
HOPE FAULT 166
DISCUSSION 166
CONCLUDING REMARKS 169
REFERENCES 169

CHAPTER 6: Fission track analysis enables determination of quantitative relationships between uplift and geomorphology of the Southern Alps, New Zealand 171
ABSTRACT 172
INTRODUCTION 173
TECTONIC DEVELOPMENT AND GEOMORPHOLOGY OF THE SOUTHERN ALPS 175
APPROACH TO STUDY 175
METHODS 177
Fission track analysis 177
How estimates of amount, age, and rate of rock uplift were derived for the Southern Alps 179
Geomorphic analysis 180
APPROACH TO DATA ANALYSIS 180
Regression models 184
Example: regression of mean surface elevation on rock uplift 184
RESULTS: REGRESSION OF GEOMORPHIC VARIABLES ON ROCK UPLIFT AND UPLIFT AGE (EAST OF MAIN DIVIDE) 188
Regressions on rock uplift 188
Regressions on uplift age 188
DISCUSSION: AREA TO THE EAST OF THE MAIN DIVIDE 190
Description of regressions 190
Substitution of space for time 194
Landscape evolution east of the Main Divide 195
REGRESSION OF GEOMORPHIC VARIABLES ON TECTONIC UPLIFT (EAST OF THE MAIN DIVIDE) 198
REGRESSION OF GEOMORPHIC VARIABLES ON ROCK UPLIFT RATE (WEST OF THE MAIN DIVIDE) 200
SUMMARY AND CONCLUSIONS 203
APPENDIX 1: Regression Equations 205
REFERENCES 208

CHAPTER 7: Geomorphic evolution of the Southern Alps, New Zealand 210
ABSTRACT 211
INTRODUCTION 213
EXISTING MODELS FOR THE EVOLUTION OF THE SOUTHERN ALPS 213
Dynamic cuesta model (Adams 1980, 1985) 213
Numerical model (Koons, 1989) 215
CONSTRAINTS ON A NEW MODEL 217
Initial conditions 217
Rock uplift amount 219
Rock uplift age 219
Rock uplift rate 219
Final conditions 221
A MODEL FOR THE GEOMORPHIC EVOLUTION OF THE SOUTHERN ALPS 221
Uplift domains and regimes 221
Increase in elevation of the mean surface 222
Progressive exposure of lithology 225
Landform and relief development 231
DISCUSSION 231
SUMMARY 234
REFERENCES 235

CHAPTER 8: SUMMARY 237

DATA APPENDIX 245

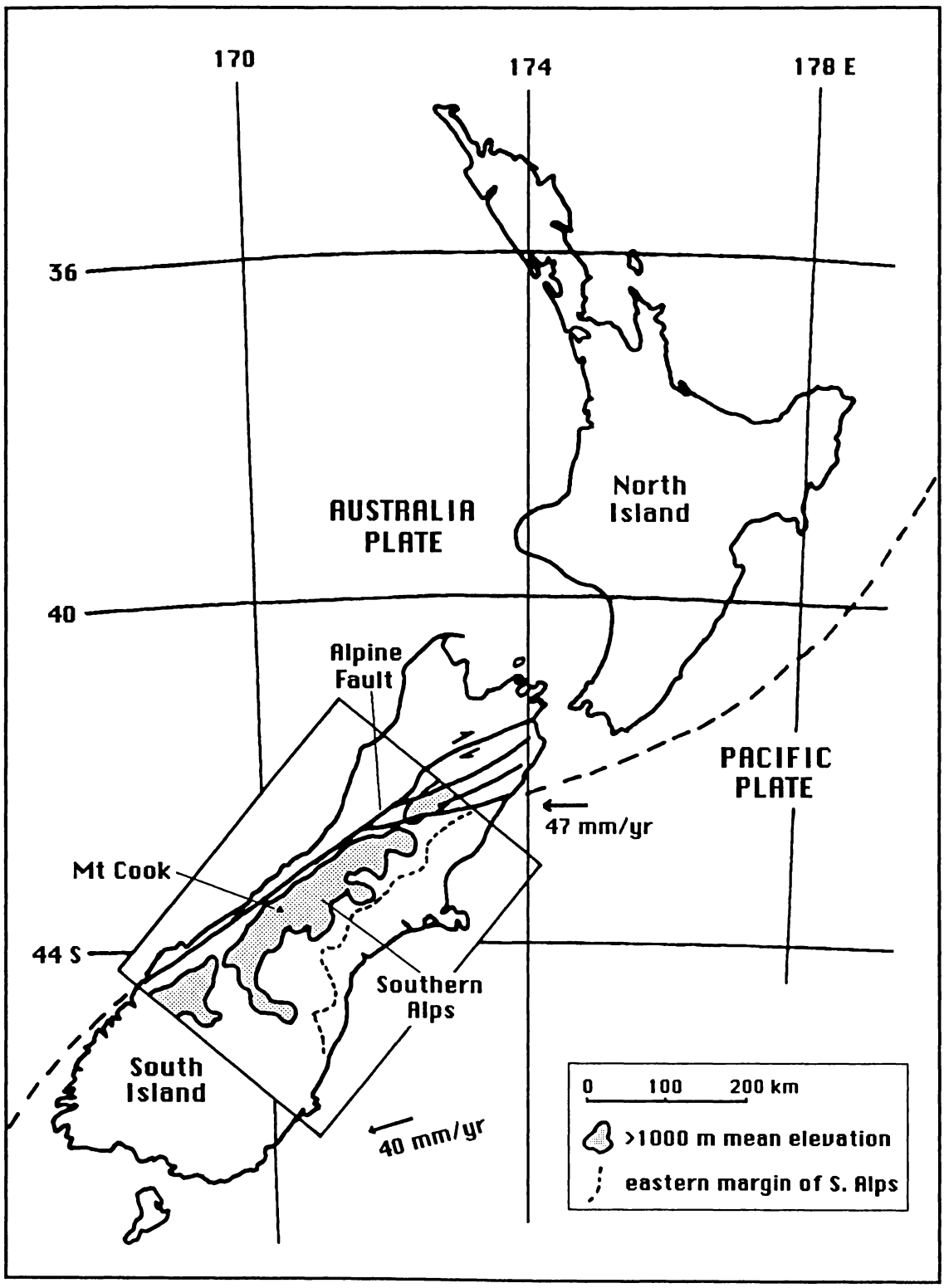


Fig. 1. Tectonic setting of the Southern Alps, New Zealand. Arrows indicate directions and rates of convergence [from *Walcott*, 1984]. The box contains the area investigated.

CHAPTER 1: Introduction

OBJECTIVE

The objective of this study was to work towards a new model of the late Cenozoic uplift history and geomorphic development of the Southern Alps, New Zealand, using fission track analysis.

TECTONIC, GEOLOGICAL, AND GEOMORPHIC SETTING OF THE SOUTHERN ALPS

Tectonic Setting

The Southern Alps (S. Alps) have been formed by uplift of Pacific plate continental crust as a result of late Cenozoic collision of the Pacific and Australia plates (Fig. 1). The Alpine Fault, the boundary in South Island between the two plates, has accommodated 480 km of dextral displacement since about 25 Ma ago [e.g. *Kamp*, 1986; *Cooper et al.*, 1987]. Convergence across the plate boundary is predicted from plate rotation parameters to have started at about anomaly 5 (9.8 Ma ago) [*Stock and Molnar*, 1982], as a result of a change in the direction of migration of the Australia-Pacific pole of rotation. At present, the displacement vector trends at about 30° to the strike of the Alpine Fault (Fig. 1); therefore the current relative plate motion in the vicinity of the S. Alps of 46 mm/a is resolved into 40 mm/a parallel to and 22 mm/a perpendicular to the fault [*Walcott*, 1979]. Since transpression started, there has been 70-80 km of shortening normal to the plate boundary in central South Island [*Walcott*, 1979; *Allis*, 1986]. However, only about 50 km of this has been accommodated in the Pacific plate part of the plate boundary zone [*Allis*, 1986].

Geological Setting

The basement exposed in the Southern Alps comprises mostly Triassic Torlesse Terrane greywacke and its metamorphosed equivalent, the Haast Schist (Fig. 2). The Haast Schist is divided geographically into Otago Schist and Alpine Schist. The Otago Schist belt forms a northwest-striking anticlinorium of greenschist facies rocks (chlorite and biotite zones) decreasing in metamorphic grade to prehnite-pumpellyite grade Torlesse greywackes. Metamorphism is considered to have occurred in the earliest Jurassic [*Adams et al.*, 1985]. Post-metamorphic deformation of the schists

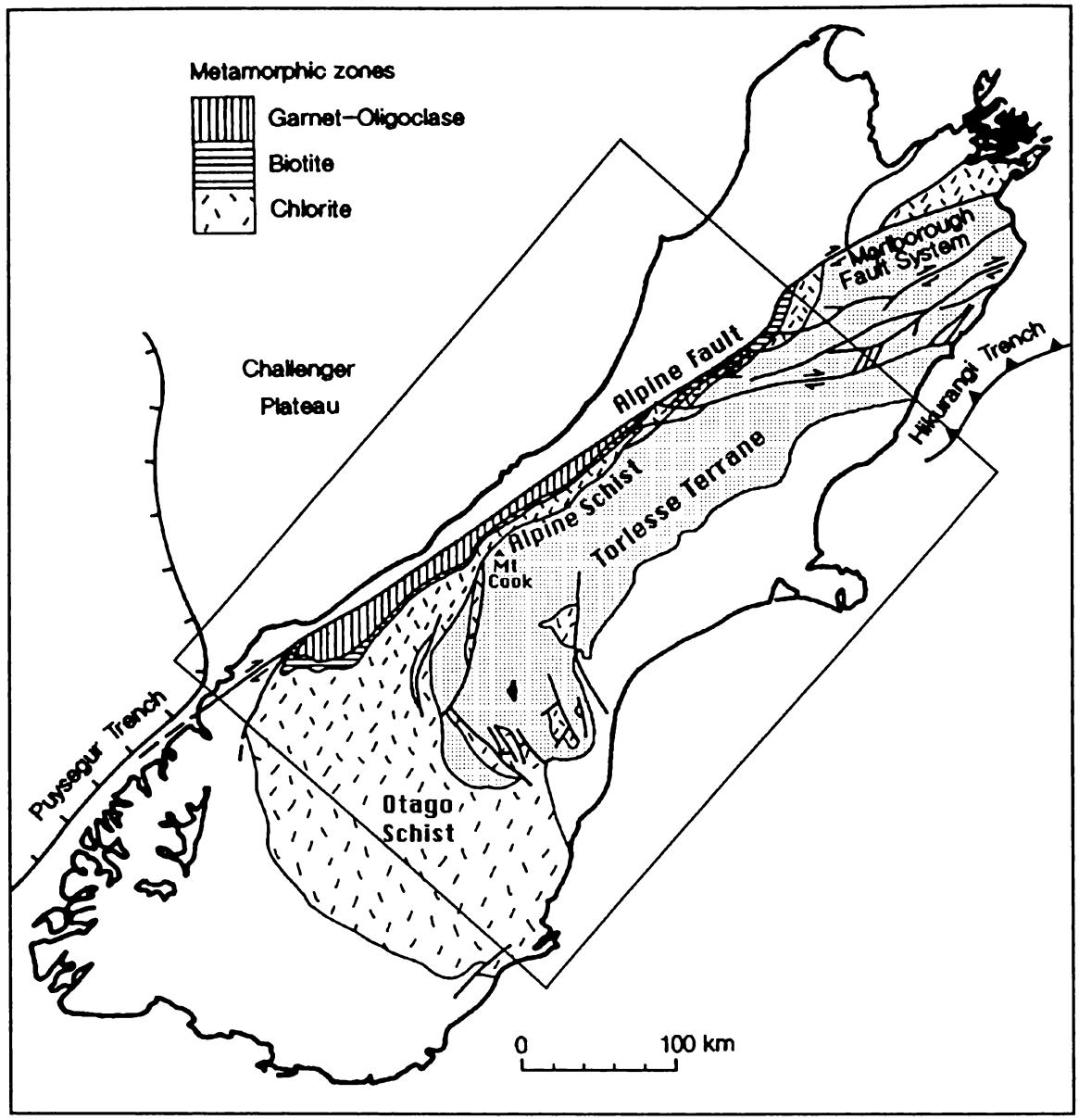


Fig. 2. Geological map of South Island [adapted from *New Zealand Geological Survey*, 1972].

includes crenulations and kinkfolds [*Turnbull*, 1981], and high-angle northeast-trending reverse faults [*Beanland and Barrow-Hurlbert*, 1988].

The Alpine Schist crops out in a narrow belt immediately to the east of the Alpine Fault (Fig. 2). Mid-amphibolite grade rocks (oligoclase zone) pass southeastward into the garnet, biotite, and chlorite zones of greenschist facies [*Mason*, 1962]. Estimates of the peak temperature of the oligoclase zone in the central Alpine Fault area range from between 490° and 570°C [*Grapes and Otsuki*, 1983; *Johnstone and White*, 1983; *Findlay*, 1985]. The Alpine Schist passes eastward into Torlesse greywacke of pumpellyite-actinolite and then prehnite-pumpellyite metamorphic grade. The depositional ages of the Torlesse range from Permian to Triassic in the S. Alps, and as young as Cretaceous in Marlborough to the north. Alpine Schist and Torlesse greywacke have suffered several phases of deformation prior to the late Cenozoic. *Findlay* [1979 and 1987] showed that the schists display zones of folding and ductile shear. The greywacke strata are steeply dipping, with crush zones, jointing, and folding being widely present [*Bradshaw*, 1972; *Spörli*, 1979; *Findlay and Spörli*, 1984].

Late Cenozoic deformation in the S. Alps is a consequence of the distributed strain of collision and dextral transform movement across the plate boundary [*Walcott*, 1978]. Many of the features of the late Cenozoic fault pattern in the greywacke are inherited from Cretaceous fractures [*Spörli*, 1979], with northeast and northwest trending faults accommodating varying amounts of strike-slip and reverse movement [*Berryman*, 1979]. In addition to the seismic deformation resulting in fault movements, an aseismic ductile flow of crustal rocks has been identified by *Walcott* [1978]. The late Cenozoic deformation is responsible for a component of the dextral arcuate structure of the basement terranes in southern South Island [*Walcott*, 1978; *Norris*, 1979; *Kamp*, 1987] (Fig. 2).

Geomorphic Setting

Fig. 3 shows the variation in mean surface elevation across the Southern Alps. Topographically, the S. Alps form an elongated asymmetric dome located immediately to the southeast of, and sub-parallel to, the Alpine Fault (Fig. 3). In the 300 km-long central sector of the S. Alps, the range has a width of 90-150 km. In the west, the mountains rise steeply from a coastal plain to the Main Divide 15-30 km southeast of the fault. In the vicinity of the Main Divide, mean surface elevations reach almost 2000 m,

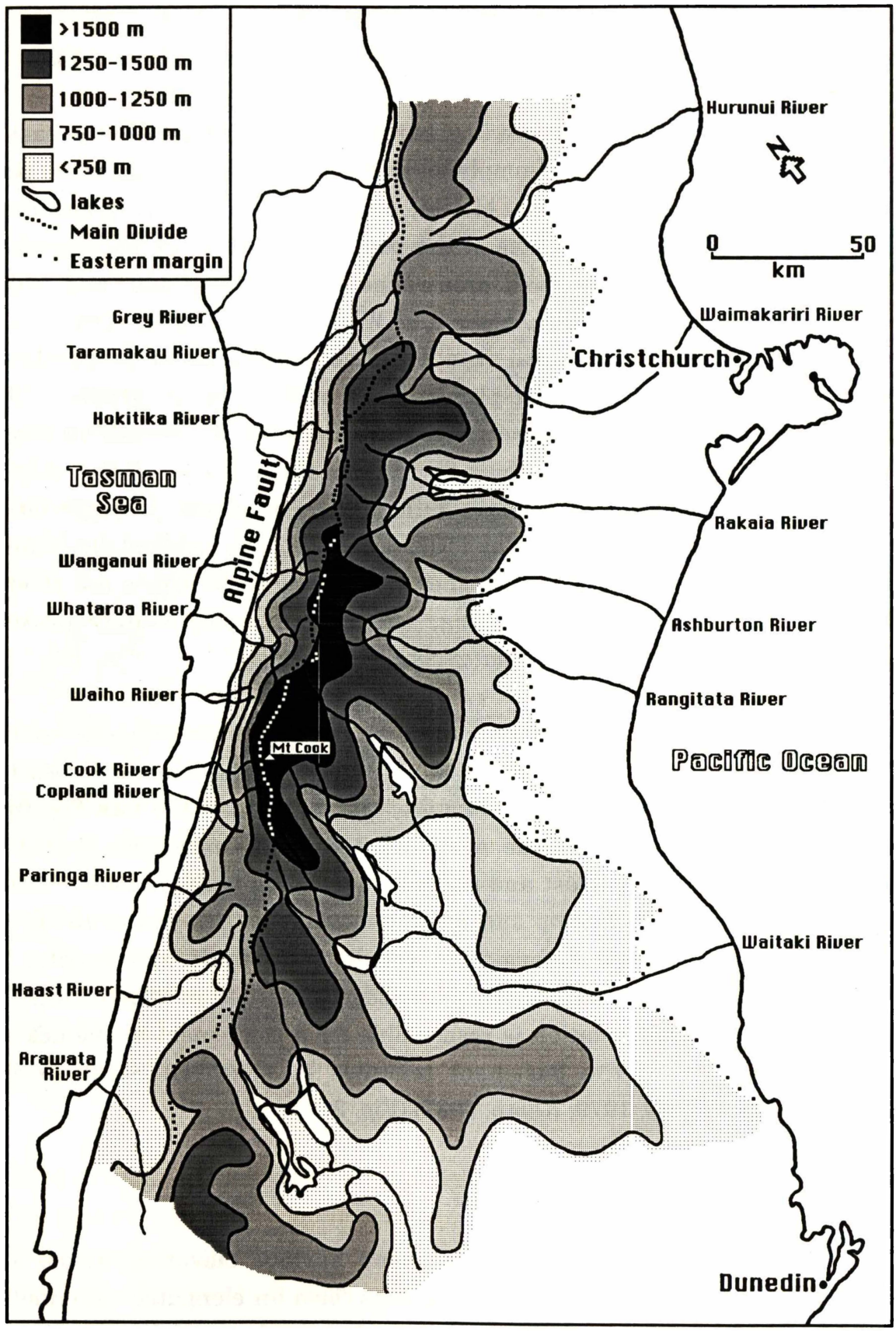


Fig. 3. Geomorphology of the Southern Alps, showing mean surface elevation, location of the Main Divide [from *Whitehouse*, 1987], drainage pattern, and the eastern margin of basement outcrop.

individual summits attain elevations of 3000 m, and glacial landforms predominate. To the east of the Main Divide, mountain mean elevations decrease to 750 m over a distance of 80-140 km. In this region, scree-sided ranges are separated by braided-river valleys. To the east of the S. Alps, coalesced fans comprising gravels derived from the S. Alps form an extensive alluvial plain 20-70 km wide.

PREVIOUS STUDIES OF THE UPLIFT OF THE SOUTHERN ALPS

The Southern Alps have been the focus of a number of studies that have sought to understand the nature of their uplift. K-Ar ages reported by *Mason* [1961], *Sheppard et al.* [1975], *Adams* [1979 and 1981], and *Adams and Gabites* [1985] have been interpreted in terms of the amount and age of late Cenozoic uplift for rocks lying <10 km from the Alpine Fault. The ages have been interpreted as implying some 18-20 km of Mesozoic uplift of the Alpine Schists, thereby restricting vertical movement in the late Cenozoic to 5-10 km [*Adams*, 1979 and 1981]. Schist was inferred to have been exposed at the Alpine Fault prior to late Cenozoic uplift. In this model, the rocks, prior to late Cenozoic uplift, were viewed as having resided at crustal levels with temperatures below that of the K-Ar closure temperature (~300° C). A zone of young (<10 Ma) K-Ar ages within 10 km of the Alpine Fault was therefore attributed to a thermal event, associated with the start of late Cenozoic uplift, that caused complete argon loss from the K-rich minerals of these rocks. The timing of this event (estimated from K-Ar 'isochron ages') has been put at 4 ± 2 Ma ago [*Sheppard et al.*, 1975], 5 ± 2 Ma ago [*Adams*, 1981], and 12 ± 5 Ma ago [*Adams and Gabites*, 1985]. Although these estimates pertain to successively more southern parts of the S. Alps, the implication by each author was that each estimate of the timing of the start of late Cenozoic uplift applied to the whole of the S. Alps, that is, uplift started everywhere at the same time.

In an alternative model, the amount of late Cenozoic uplift of the Alpine Schists near the Alpine Fault has greatly exceeded 10 km [*Wellman*, 1979; *Adams*, 1980; *Allis*, 1981 and 1986; *Kamp et al.*, 1989]. *Wellman* [1979] established post-glacial ('contemporary') uplift rates that showed a pattern of 10 mm/a at the Alpine Fault declining approximately exponentially to the southeast. *Wellman* [1979] and *Adams* [1980] assumed that the contemporary uplift rate pattern had exposed schists adjacent to the Alpine Fault in the last 2.5 Ma. *Allis* [1986] estimated the amount of late Cenozoic uplift and erosion for 3 profiles across the S. Alps, by determining the

amount of crustal shortening predicted by plate rotation data, and subtracting the amount of crustal thickening as inferred from the gravity pattern. This yielded estimates of a maximum of ~17 km of late Cenozoic uplift in the southern part of the S. Alps (Haast), and up to 30 km in the central parts (Mt Cook - Franz Josef area) adjacent to the Alpine Fault. Importantly, *Allis* [1986] estimated uplift and erosion not only at the Alpine Fault as in previous studies, but also was able to estimate the pattern of the amount of uplift and erosion to 80 km southeast of the fault. The pattern showed that the amount of uplift was greatest at the Alpine Fault and declined non-linearly to the southeast.

The work of *Kamp et al.* [1989] gave important insights into the nature of the late Cenozoic uplift of the S. Alps. *Kamp et al.* [1989] re-interpreted the young K-Ar ages in the zone <10 km from the Alpine Fault as cooling ages, implying that these rocks prior to late Cenozoic uplift lay stratigraphically below the K-Ar closure temperature. This implied that the amount of late Cenozoic uplift exceeded 5-10 km, contrary to previous interpretations of the K-Ar data. *Kamp et al.* [1989], using fission track analysis of S. Alps basement samples, studied 3 transects across the S. Alps (Haast, Mt Cook, and Arthur's Pass), and showed that profiles of the amount of late Cenozoic uplift increased exponentially toward the Alpine Fault. The profiles showed that adjacent to the Alpine Fault there had been 18 ± 4 km of late Cenozoic uplift at Haast in the south, 18 ± 4 km near Mt Cook in the central S. Alps, and 14 ± 2 km at Arthur's Pass to the north. The asymmetric nature of the late Cenozoic uplift pattern was therefore shown to be responsible for the exhumation of the Alpine schists near the Alpine Fault. The study also showed that there was a regional difference in the timing of the start of uplift between Haast (~6.6 Ma ago) to the south and Arthur's Pass (~4.3 Ma ago) to the north, and that there had been an acceleration in the rate of uplift through the late Cenozoic for rock samples near the Alpine Fault.

PREVIOUS STUDIES OF THE GEOMORPHIC DEVELOPMENT OF THE SOUTHERN ALPS

Both *J. Adams* [1980 and 1985] and *Koons* [1989] have proposed models that attempt to explain simultaneously the tectonic and geomorphic development of the S. Alps. These studies aimed to establish the relationship between uplift and the landscape evolution of the S. Alps.

Adams [1980 and 1985] proposed that the contemporary rate of erosion of the Southern Alps is equal to the rate of uplift. Under *Adams'* [1980] uplift pattern, the modern-day uplift rates increased from 15 mm/a at the Alpine Fault to 22 mm/a some 7 km southeast of the fault, then declined exponentially to reach zero about 70 km southeast of the fault. *Adams* [1980] found that both the rate of sediment deposition offshore, and river sediment loads, appeared to equal the average uplift rate of the S. Alps. *Adams* [1980] also modelled the geomorphic evolution of the S. Alps over a 2.5 Ma period, by establishing empirical relationships between present mountain height, present runoff, and present uplift rate. In his model, erosion started to lower the crests when the non-steady state 'flat-topped' mountains attained a height of 2 km, at which point they became 'spiky' ('steady state') mountains. At that point the erosion rate was calculated from the relationship between uplift rate, mountain height, and runoff, assuming that the erosion rate equals the uplift rate (i.e. 'steady state' equilibrium). The spiky mountains appeared to reach their present state after about 1.5 Ma of uplift. Mountains in the far east of the S. Alps were viewed by *Adams* [1980 and 1985] as flat-topped 'time-dependent' landforms that represent an uplifted peneplain. They were noted to change further inland to spiky 'time-independent' landforms at about the 0.5 mm/a post-glacial uplift rate contour of *Wellman* [1979].

Koons [1989] numerically modelled the simultaneous uplift and erosion of the Southern Alps using the diffusion equation for a moving medium. In doing so he examined the relative importance to morphology of uplift rates, stream density, and variations in diffusivity (material transport parameter). Models were run with an uplift rate pattern compatible with the modern uplift pattern in the S. Alps as proposed by *Wellman* [1979], and the development of topography at intervals up to 5 Ma after the start of uplift was simulated. The numerical models predicted that near-'steady state' elevations would be reached in the region to the west of the Main Divide within 0.25 to 0.5 Ma of the start of uplift. *Koons* [1989] inferred that the mountain elevations in the region to the east of the Main Divide are unlikely to have reached 'steady state equilibrium', with pre-uplift surfaces likely to be preserved.

PROBLEMS TO BE ADDRESSED

From the preceding discussion, uncertainty remains over the following fundamental questions that this study attempts to answer:

(1) What is the pattern of the amount of late Cenozoic uplift across the S. Alps?
(2) When did late Cenozoic uplift start, and does the timing of uplift vary across the S. Alps?
(3) What is the pattern of the rate of late Cenozoic uplift across the S. Alps?
(4) What is the nature of the relationship between uplift and the geomorphic development of the S. Alps?

In this study, data on the amount of rock uplift, the age of initiation of rock uplift, and the rate of rock uplift (questions 1, 2, and 3) have been established by fission track analysis. The geomorphic development of the S. Alps (question 4) has been studied by establishing and measuring parameters of landscape morphology, and relating the measured values to the fission track estimates of the amount, age, and rate of uplift.

FISSION TRACK ANALYSIS INTRODUCED

The primary technique used in this study is fission track analysis of apatite and zircon. Fission tracks in uranium bearing minerals are created by the spontaneous fission of ^{238}U, and can be made visible by etching polished sections of uranium-bearing minerals such as apatite and zircon. The density of fission tracks that intersect a crystal surface, and the lengths of subsurface horizontal tracks, are the two variables routinely measured in fission track analysis that provide information about the thermal history of the host rocks. Fission tracks begin to be recorded in a crystal as it cools below a critical temperature, which for apatite is ~110°-125° C [*Gleadow and Duddy*, 1981; *Green et al.*, 1989] and for zircon is in the range 240° ± 25° C [*Hurford*, 1986]. The tracks in apatite are unstable at ambient temperatures of ~20° to 125° C and for zircon are unstable in the temperature range ~200° to 265° C. The instability is manifested in track length reduction ('annealing'), which leads to track density reduction in a randomly cut crystal section, and hence age reduction. The distribution of single-grain ages, and track length distributions, will therefore reflect the thermal history of a sample. When the geothermal gradient and initial elevation of

the land surface are known independently or can be reasonably assumed, a thermal (cooling) history can be interpreted in terms of an uplift history, to yield information about the amount, age, and rate of rock uplift.

Fission track analysis has previously been applied in thermo-tectonic studies of collisional, extensional, and intraplate tectonic settings. *Hurford* [1986] used apatite and zircon ages to constrain cooling and inferred uplift patterns in the European Alps, while *Zeitler* [1985] reported fission track ages from the Himalaya of northern Pakistan, and interpreted the data in terms of the amount, timing, and rate (0.1-4 mm/yr) of uplift. The Transantarctic Mountains were studied by *Gleadow and Fitzgerald* [1987] who were able to estimate the timing (~50 Ma) of the start of uplift, as well as uplift amounts and rates, from apatite fission track data. *Moore et al.* [1986] examined the thermal evolution of the rifted continental margin in southeastern Australia, and interpreted apatite fission track ages in terms of a rift-related thermal event at ~80-100 Ma. *Green* [1986], in a study of the thermal and tectonic evolution of Northern England, showed that several kilometres of uplift and erosion at ~60 Ma were required to explain the observed pattern of fission track parameters.

THESIS FORMAT

Content

The body of the thesis includes 5 discrete manuscripts that are either in press or submitted at the time of thesis submission. A brief outline of these manuscripts in the context of the thesis is as follows:

Chapter 1 Introduction

Chapter 2 Fission track analysis: The theory of fission track analysis and its application to establishing thermal histories of host rocks is outlined.

Chapter 3 Fission track analysis of the late Cenozoic vertical kinematics of continental Pacific crust, South Island, New Zealand (paper by *Tippett and Kamp*, Journal of Geophysical Research, in press): Fission track dating calibration data and S. Alps fission track data are reported. Pre-uplift sample paleotemperatures are estimated, and the amount, age, and rate of late Cenozoic rock uplift of the Pacific crust underlying the S. Alps are derived.

Chapter 4 Dynamics of Pacific plate continental crust in the South Island collision zone (New Zealand) (manuscript by *Kamp and Tippett*, submitted to Journal of Geophysical Research): The amount and rate of mean surface uplift are established. The erosional, isostatic, and tectonic components of rock uplift are derived. The two-sided orogen model of *Koons* [1990] is tested against the new data.

Chapter 5 On the role of faulting in rock uplift in the Southern Alps (manuscript by *Tippett and Kamp*, submitted to New Zealand Journal of Geology and Geophysics): The nature of vertical deformation in the S. Alps is assessed to determine whether or not deformation in the plate boundary zone can be viewed as being ductile.

Chapter 6 Fission track analysis enables determination of quantitative relationships between uplift and geomorphology of the Southern Alps, New Zealand (manuscript by *Tippett and Kamp*, submitted to Earth Surface Processes and Landforms): Geomorphic parameters are established and measured, and related to the fission track data on the amount, age, and rate of rock uplift. The nature of the relationship between uplift and geomorphology in the S. Alps is determined, and aspects of the landscape development of the S. Alps are analysed quantitatively.

Chapter 7 Geomorphic evolution of the Southern Alps, New Zealand (manuscript by *Tippett and Kamp*, submitted to Earth Surface Processes and Landforms): New fission track data on the age, amount and rate of rock uplift in the S. Alps allow the construction of a new model of the geomorphic evolution of the S. Alps. The model emphasises the development of rock uplift, mean surface elevation, exhumation of crustal section, and relief. The models of *J. Adams* [1980 and 1985] and *Koons* [1989] are compared with the new data.

Chapter 8 Summary

Format

Because the major chapters of the thesis comprise discrete manuscripts intended for publication in different journals, there are differences between the chapters in format and measurement units used. The different measurement units are defined and used as follows:

Parameter	Chapters 2,3,4, and 5.	Abstract, Introduction, Chapters 6 and 7, and Summary.
rate	mm/yr or km/m.y.	mm/a or km/Ma
age interval	m.y.	Ma
datum	Ma	Ma ago

Data Appendix

A data appendix is included in this volume. The appendix contains for Southern Alps samples data on single grain fission track ages for apatite and zircon, and horizontally confined fission track lengths for apatite.

REFERENCES

Adams, C.J., Age and origin of the Southern Alps, *Bull. R. Soc. N. Z., 18*, 73-78, 1979.

Adams, C.J., Uplift rates and thermal structure in the Alpine fault zone and Alpine Schists, Southern Alps, New Zealand, *Spec. Publ. Geol. Soc. London, 9*, 211-222, 1981.

Adams, C.J., and J. E. Gabites, Age of metamorphism and uplift in the Haast Schist Group at Haast Pass, Lake Wanaka and Lake Hawea, South Island, New Zealand, *N. Z. J. Geol. Geophys., 28*, 85-96, 1985.

Adams, C.J., D.G. Bishop, and J.E. Gabites, Potassium-argon age studies of a low-grade, progressively metamorphosed greywacke sequence, Dansey Pass, South Island, New Zealand, *J. Geol. Soc. London, 142*, 339-349, 1985.

Adams, J., Contemporary uplift and erosion of the Southern Alps, New Zealand, *Geol. Soc. Am. Bull., 91*, 1-114, 1980.

Adams, J., Large-scale tectonic geomorphology of the Southern Alps, New Zealand, in *Tectonic Geomorphology*, editors M. Morisawa and J. T. Hack, Proc. 15th Ann. Binghamton Geomorphology Symposium, Allen and Unwin, 105-128, 1985.

Allis, R.G., Continental underthrusting beneath the Southern Alps of New Zealand, *Geology, 9*, 303-307, 1981.

Allis, R.G., Mode of crustal shortening adjacent to the Alpine fault, New Zealand, *Tectonics, 5*, 15-32, 1986.

Beanland, S., and S. A. Barrow-Hurlbert, The Nevis-Cardrona fault system, Central Otago, New Zealand: late Quaternary tectonics and structural development, *N. Z. J. Geol. Geophys., 31*, 337-352, 1988.

Berryman, K., Active faulting and derived PHS directions in the South Island, New Zealand, *Bull. R. Soc. N. Z., 18*, 29-34, 1979.

Bradshaw, J.D., Stratigraphy and structure of the Torlesse Supergroup (Triassic-Jurassic) in the foothills of the Southern Alps near Hawarden (S60-61), Canterbury, *N. Z. J. Geol. Geophys., 15*, 71-87, 1972.

Cooper, A.F., B.A. Barreiro, D.L. Kimbrough, and J.M. Mattinson, Lamprophyre dike intrusion and the age of the Alpine fault, New Zealand, *Geology, 15*, 941-944, 1987.

Findlay, R.H., Summary of structural geology of Haast Schist terrane, central Southern Alps, New Zealand, *Bull. R. Soc. N. Z., 18*, 113-120, 1979.

Findlay, R.H., Metamorphic low to high 2Vx K-feldspar in kyanite zone rocks within the Alpine schists of Copland Valley, South Westland, New Zealand, *N. Z. J. Geol. Geophys., 28*, 77-83, 1985.

Findlay, R.H., Structure and interpretation of the Alpine schists in Copland and Cook River valleys, South Island, New Zealand, *N. Z. J. Geol. Geophys., 30*, 117-138, 1987.

Findlay, R.H., and K.B. Spörli, Structural geology of the Mount Cook Range and Main Divide, Hooker Valley region, New Zealand, *N. Z. J. Geol. Geophys., 27*, 257-276, 1984.

Gleadow, A.J.W., and I.R. Duddy, A natural long-term track annealing experiment for apatite, *Nucl. Tracks, 5*, 169-174, 1981.

Gleadow, A.J.W., and P.G. Fitzgerald, Uplift history and structure of the Transantarctic Mountains: new evidence from fission track dating of basement apatites in the Dry Valleys area, southern Victoria Land, *Earth Planet. Sci. Lett., 82*, 1-14, 1987.

Grapes, R., and Otsuki, H., Peristerite compositions in quartzofeldspathic schists, Franz Josef - Fox Glacier area, New Zealand, *J. Metamorph. Geol., 1*, 47-61, 1983.

Green, P.F., On the thermo-tectonic evolution of Northern England: evidence from fission track analysis, *Geol. Mag., 123*, 493-506, 1986.

Green, P.F., I.R. Duddy, G.M. Laslett, K.A. Hegarty, A.J.W. Gleadow, and J.F. Lovering, Thermal annealing of fission tracks in apatite 4, *Chem. Geol, 79*, 155-182, 1989.

Hurford, A.J., Cooling and uplift patterns in the Lepontine Alps, South Central Switzerland, and an age of vertical movement of the Insubric fault line, *Contrib. Mineral. Petrol., 92,* 413-427, 1986.

Johnstone, D.C., and S.H. White, Shear heating associated with movement along the Alpine fault, New Zealand, *Tectonophysics, 92*, 241-252, 1983.

Kamp, P.J.J., Late Cretaceous-Cenozoic tectonic development of the southwest Pacific region, *Tectonophysics, 121*, 225-251, 1986.

Kamp, P.J.J., Age and origin of the New Zealand Orocline in relation to Alpine fault movement, *J. Geol. Soc. London., 144*, 641-652, 1987.

Kamp, P.J.J., P.F. Green, and S.H. White, Fission track analysis reveals character of collisional tectonics in New Zealand,*Tectonics, 8*, 169-195, 1989.

Kamp, P.J.J., P.F. Green, and J.M. Tippett, Tectonic architecture of the mountain front-foreland basin transition, South Island, New Zealand, assessed by fission track analysis, *Tectonics, 11*, 98-113, 1992.

Koons, P.O., The topographic evolution of collisional mountain belts: a numerical look at the Southern Alps, New Zealand, *Am. J. Sci., 289*, 1041-1069, 1989.

Koons, P.O., Two-sided orogen: Collision and erosion from the sandbox to the Southern Alps, New Zealand, *Geology, 18*, 679-682, 1990.

Mason, B., Potassium-argon ages of metamorphic rocks and granites from Westland, New Zealand, *N.Z. J. Geol. Geophys., 4*, 352-356, 1961.

Mason, B., Metamorphism in the Southern Alps of New Zealand, *Bull. Am. Mus. Nat. Hist., 123*, 217-248, 1962.

Moore, M.E., A.J.W. Gleadow, and J.F. Lovering, Thermal evolution of rifted continental margins: new evidence from fission tracks in basement apatites from southeastern Australia, *Earth Planet. Sci. Lett.*, 78, 255-270, 1986.

New Zealand Geological Survey, *South Island (1st Ed.) Geological Map of New Zealand 1:1,000,000*, Department of Scientific and Industrial Research, Wellington, New Zealand, 1972.

Norris, R.J., A geometrical study of finite strain and bending in the South Island, *Bull. R. Soc. N. Z., 18*, 21-28, 1979.

Sheppard, D.S., C.J. Adams, and G.W. Bird, Age of metamorphism and uplift in the Alpine Schist belt, New Zealand, *Geol. Soc. Am. Bull., 86*, 1147-1153, 1975.

Spörli, K.B., Structure of the South Island Torlesse in relation to the origin of the Southern Alps, *Bull. R. Soc. N. Z., 18*, 99-104, 1979.

Stock J., and P. Molnar, Uncertainties in the relative positions of the Australia, Antarctica, Lord Howe, and Pacific plates since the Late Cretaceous, *J. Geophys. Res., 87B*, 4697-4714, 1982.

Turnbull, I.M., Contortions in the schists of the Cromwell district, Central Otago, New Zealand, *N. Z. J. Geol. Geophys., 24*, 65-86, 1981.

Walcott, R.I., Present tectonics and late Cenozoic evolution of New Zealand, *Geophys. J.R. Astr. Soc., 52*, 137-164, 1978.

Walcott, R.I., Plate motion and shear strain rates in the vicinity of the Southern Alps, in Origin of the Southern Alps, *Bull. R. Soc. N. Z., 18*, 5-12, 1979.

Walcott, R.I., The kinematics of the plate boundary zone through New Zealand: a comparison of short- and long-term deformations, *Geophys. J. R. Astr. Soc., 79*, 613-633, 1984.

Wellman, H.W., An uplift map for the South Island of New Zealand, and a model for the uplift of the Southern Alps, *Bull. R. Soc. N. Z., 18*, 13-20, 1979.

Whitehouse, I.E., Geomorphology of a compressional plate boundary, Southern Alps, New Zealand, in *International Geomorphology*, chief editor V. Gardiner, John Wiley and Sons Ltd, Part 1, 897-924, 1987.

Zeitler, P.K., Cooling history of the NW Himalaya, Pakistan, *Tectonics, 4*, 127-151, 1985.

CHAPTER 2: Fission track analysis

INTRODUCTION

Fission track analysis is a new technique, based upon the measurement and geological interpretation of the density and lengths of fission tracks that occur in uranium-bearing crystals, that is able to provide information about the thermal histories of host rocks.

Fission track dating is based on the slow but constant decay of radioactive nucleides. The absolute rate at which spontaneous fission tracks accumulate within a crystal is proportional to the rate of decay and the concentration of ^{238}U; therefore it is necessary to measure both the spontaneous track density and the uranium content in order to determine a fission track age. A measurable fraction of ^{235}U can be induced by exposing the crystal to a specific dose of thermal neutrons in a nuclear reactor. A count of the tracks produced from the ^{235}U fission across a crystal surface can be related to the ^{238}U concentration of the crystal via the known $^{235}U/^{238}U$ isotopic ratio. Therefore, determination of the ratio of the densities of spontaneous tracks to induced tracks in a mineral, together with a measure of the neutron dose, allows a fission track age to be calculated [*Price and Walker*, 1963].

The density of tracks that intersect a randomly cut crystal surface is dependent on the lengths of the tracks. Because fission tracks shorten (anneal) over time in response to elevated temperatures, the distribution of track lengths in a crystal will reflect the thermal history of the sample. Particular length distributions for the mineral apatite are known to be characteristic of particular styles of thermal history [e.g. *Gleadow et al.*, 1986a], and therefore the parameters of the measured sample track length distribution can be interpreted in terms of temperature. Fission track analysis (FTA) combines the information about density (time) and length (temperature), and the data can therefore be interpreted in terms of the thermal history of a sample. A thermal history of cooling can be interpreted in terms of a denudation history when the geothermal gradient is known or assumed. When the initial elevation of the land surface is also known, an uplift history can be determined.

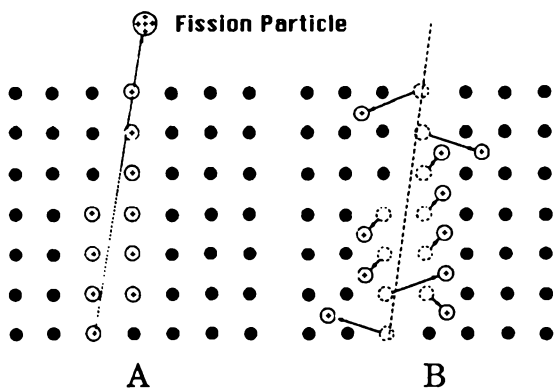


Fig. 1. Ion explosion spike mechanism: track formation in a crystalline solid. In A the atoms are ionized by passage of a charged fission particle. In B, instability causes ions to eject into the lattice forming the fission track damage zone by mutual repulsion. From *Naeser* [1979], after *Fleischer et al.* [1965].

LATENT AND ETCHED TRACKS

Source of latent tracks

The number of possible particle track origins in natural materials is limited by the low sensitivities of crystals and glasses [*Fleischer et al.*, 1975]. This means that for practical purposes, tracks in terrestrial samples are due either to fission [e.g. *Price and Walker*, 1963] or to recoil nuclei that are heavier than α-particles [*Huang and Walker*, 1967]. Etched tracks of recoil nuclei are three orders of magnitude shorter than etched fission tracks, and are dominated by ^{238}U fission tracks. The half-lives of fissionable isotopes other than ^{238}U (e.g. ^{235}U, Pb) are too long to produce measurable track densities. Therefore, for terrestrial materials, it can be safely assumed that particle tracks originate from the spontaneous fission of ^{238}U.

Formation of a latent fission track

Fragments produced by fission of a uranium nucleus create trails of damage on an atomic scale. A latent fission track is a path of ionization-produced defects dominated by vacancies and displaced atoms that occupy interstitial sites [*Fleischer et al.*, 1965] (Fig. 1). Latent tracks need to be etched by chemical means before being optically observed [*Price and Walker*, 1962a].

Early transmission electron microscope (TEM) studies of latent fission tracks suggested that the zones of disruption are approximately cylindrical, and measure only a few nanometres [e.g. *Price and Walker*, 1962a]. A very recent TEM study [*Paul and Fitzgerald*, 1992] has reported that latent fission tracks in fluorapatite display widths of ~5-10 nm, and that near the atomic scale the tracks are not cylindrical, nor perfectly linear, nor continuous along their length. The TEM observations also suggested that the width of latent fission tracks may be crystallographically controlled, with tracks oriented parallel to the c-axis having the greatest average width (9 nm average) and tracks perpendicular to the c-axis having average widths of 5 nm. This difference may reflect the different amounts of energy required to disrupt the bond forces in different orientations within a crystal during the formation of a latent fission track.

Fleischer et al. [1965] described the formation of a track in terms of the 'ion explosion spike.' An ionization burst along the path of the fission

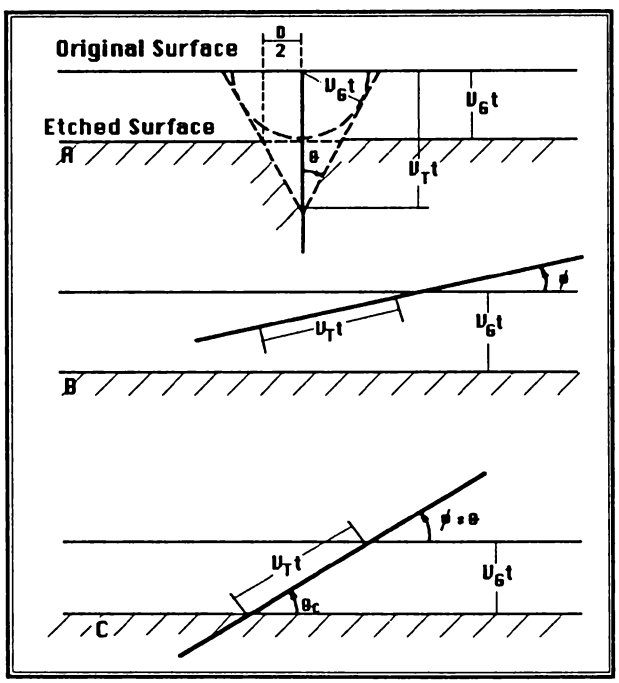


Fig. 2. Track registration geometry: (A) track geometry is determined by the comparative rates of general attack V_G, and preferential attack, V_T along the track; (B) no track is registered if the angle of incidence is less than arcsin (V_G/V_T), i.e. the general rate of etching is greater than the track etching rate; (C) arcsin (V_G/V_T) = θ and therefore the track just fails to be registered. Above this critical angle θ_c, tracks are able to be registered [from *Fleischer et al.*, 1975]. Note that t = etching time.

fragment creates an electrostatically unstable array of adjacent ions which displace one another from normal positions into interstitial sites, as the electrostatic stresses exceed atomic bonding strengths. Subsequently, elastic relaxation reduces the local stresses by dissipating the strain.

A fission track results from the interaction of a charged particle (produced from fission) with electrons attached to atoms [*Price and Walker*, 1962b and c]. The recoil energy and linear momentum of the two fragments is dissipated before coming to rest in the solid primarily through electronic losses (Coulomb attraction of electrons to the positive atomic ore). The fission fragment energises (attracts) electrons as it passes, forming δ-particles. The δ-particles, once removed from the parent atoms, undergo collisions before being brought to rest. The ions then move by electrostatic displacement creating vacancies and filling interstices. It is the energy lost by the fission fragments to the δ-particles that is stored as radiation damage (a latent track) in the solid. The nature of the solid state characteristics of the detector (e.g. crystal structure) - before, during, and after a fission spike - determines the anatomy of the final latent track [*Chadderton*, 1988].

Latent track etching

The locations of latent tracks can be optically displayed by etching - the preferential attack by a suitable chemical reagent [*Price and Walker*, 1962a]. Etching enlarges tracks to reveal cylinders or cones with dimensions in the order of micrometres.

The efficiency and geometry of track etching is controlled by the relative rates of chemical dissolution along the track (V_T), and the general attack on the solid surface and interior of the etched track (V_G) (Fig. 2). The etching efficiency (the fraction of latent tracks crossing a particular surface that are revealed by etching) is close to 100% when $V_T >> V_G$, and is low when the excess of V_T over V_G is small. When $V_T \leq V_G$, tracks are not revealed; also, tracks at shallow angles to the surface are not revealed when the vertical component of $V_T \leq V_G$ [*Fleischer and Price*, 1963].

Anisotropic etching

V_G is anisotropic for most crystals [*Fleischer et al.*, 1975], that is, V_G varies as a function of crystal surface orientation. When V_G is anisotropic, etching efficiency is still high when $V_T >> V_{G\,(normal)}$ (the value of V_G

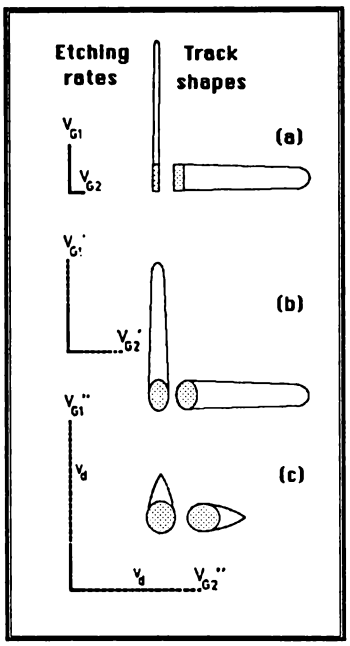


Fig. 3. Alpha-recoil damage effects on etching: Etching characteristics of an anisotropic mineral (A) with no alpha damage; (B) with some alpha damage, where the initial anisotropic etching properties are modified to be more isotropic; and (C) with immense radiation damage, where the mineral has a very high bulk etching rate in all directions. From *Gleadow* [1981].

normal to the etched surface) [Fleischer et al., 1975]. In this case, the cross-section shape of the etched track will be determined by the relative rates of the $V_{G\ (parallel)}$ etching directions.

Gleadow [1978] showed that, for sphene, the anisotropy of V_G decreases with increasing amounts of radiation damage from α-decay of U and Th. This is because the etching rate of the damaged material is added equally to all etching directions, and therefore the etching of tracks in different orientations becomes more uniform with increasing α-damage [*Gleadow*, 1981] (Fig. 3). Low etching efficiencies are found in low-damage crystals, with efficiencies approaching 100% being found in crystals of higher radiation damage. The alpha damage was found by Gleadow [1981] to be removed with heating to a temperature lower than that required for track annealing.

Gleadow [1981] suggested that the effect of α-damage on etching anisotropy for apatite can be safely neglected, as the α-damage is not stable over geological time even at ambient surface temperatures. However for sphene and zircon, the damage does have an effect on etching properties as high temperatures are required to remove the damage.

V_T is also likely to be anisotropic in crystals, as the variable atomic spacing along different orientations controls the density of radiation damage along a latent track and hence controls V_T [*Gleadow*, 1981].

FISSION TRACK DATING

Identification of tracks

Fleischer and Price [1964] and *Fleischer et al.* [1975] outlined the characteristics of etched fission tracks that distinguish them from other etch features. Fission tracks are straight line defects, of limited length, and randomly oriented.

Fission track age equation

Price and Walker [1963] proposed a technique of dating mica samples based on the fact that the number of tracks derived from the spontaneous fission of ^{238}U is a function of the age of the specimen. They suggested that the best method of determining an age was to compare the counts of

spontaneous tracks arising from ^{238}U, and tracks induced by thermal neutron irradiation of ^{235}U. This was because the rate at which spontaneous fission tracks accumulate in crystals is proportional to the uranium concentration. Determination of the ratio of the densities of spontaneous tracks to induced tracks, together with a measure of the neutron dose, allows an age to be calculated. One version of the age equation [from *Hurford and Green*, 1983] is:

$$T = \frac{1}{\lambda_D} ln \left[1 + \frac{\lambda_D \Phi \sigma I g \rho_s}{\lambda_f \rho_i}\right] \qquad \textit{equation 1}$$

λ_D = total decay constant for ^{238}U; 1.55125×10^{-10} yr^{-1} [*Jaffrey et al.*, 1971].

λ_f = spontaneous fission decay constant of ^{238}U; two values: 7.03×10^{-17} or 8.42×10^{-17} [*Spadavecchia and Hahn*, 1967; *Roberts et al.*, 1968].

I = isotopic ratio $^{235}U/^{238}U$; 7.2527×10^{-3} [*Conran and Adler*, 1976].

σ = thermal neutron cross-section for ^{235}U; $580.2\ 10^{-24}$ cm^2 /atom [*Hannah et al.*, 1969]

Φ = thermal neutron fluence (neutrons cm^{-2}).

g = geometry factor (= 1 for population dating method; 0.5 for external detector method).

ρ_s = spontaneous track density (tracks cm^{-2}).

ρ_i = neutron-induced track density (tracks cm^{-2}).

T = age in years.

Age determination methods

Gleadow [1981] proposed that an ideal fission track (FT) dating method is one where both spontaneous and induced tracks are measured under identical conditions of track registration, etching, and counting. The various FT dating strategies differ in the registration geometries and etching efficiencies of the surfaces used to record spontaneous and induced tracks. Other differences are whether tracks are measured on single grains or averaged over a number of grains, and whether or not spontaneous tracks are annealed before neutron irradiation. All methods use internal surfaces for measuring spontaneous track density. Alternative FT dating strategies include the population method, external detector method, subtraction method, re-etch method, and re-polish method. *Hurford and Green* [1982] showed that problems of registration geometry, inhomogeneous uranium

distribution, accumulated radiation damage and anisotropic etching, rule out all but the population and external detector methods.

The features of the population method (PM) have been summarised by *Hurford and Green* [1982]. The spontaneous and induced track counts are made on separate fractions of the sample. Induced tracks are measured on crystals that before irradiation have been annealed, removing all (latent) spontaneous tracks. This method allows spontaneous and induced tracks to be revealed under equivalent etching conditions and track registration geometries and efficiencies. However, the assumption that the two fractions have equal uranium concentrations will not hold if there is significant inter-crystal variation in uranium content.

The external detector method (EDM) [e.g. *Gleadow*, 1981; *Hurford and Green*, 1982] allows ages to be determined for individual crystals. This has proved vital in examining the effect of crystal composition on fission track annealing, in identifying different populations of crystals [e.g. *Hurford et al.*, 1984], and elucidating the thermal histories of samples. All fission track ages reported in this thesis have been determined using the EDM. In this method, the spontaneous tracks are counted on an internal surface of the (etched) crystal; the induced tracks are counted in the corresponding area of a low uranium mica detector held against the crystal surface during irradiation and later etched. Intra- and inter-crystal variation in uranium distribution are therefore accounted for.

In the EDM, spontaneous tracks across the internal surface result from fissions centred both above and below the surface, thereby producing a 4π registration geometry. On the other hand, induced tracks result from the passage of fission fragments travelling from the crystal into the external mica detector, producing a 2π geometry. This difference in geometry should in theory be corrected by the introduction of a geometry factor (=0.5) (equation 1), when it is assumed that the etching efficiencies of the crystal and mica are equal (~100%). The results of *Gleadow and Lovering* [1977] and *Green and Durrani* [1978] demonstrated that the 0.5 geometry factor is ideal when using the EDM for crystal surfaces with low V_G. Practically, surfaces with low V_G can be identified as having narrow (<1.5 μm) polishing scratches after etching [*Gleadow,* 1978 and 1981].

The effect of α-damage on the anisotropy of V_G has implications for the PM of dating for some minerals. Laboratory annealing used in the PM

anneals both spontaneous fission tracks and the α-damage, thereby restoring the initial anisotropic pattern of V_G to minerals such as zircon and sphene [*Gleadow,* 1978 and 1981]. Etching of induced tracks will be anisotropic, with weakly etched tracks being missed during counting [*Gleadow*, 1981]; therefore the usual geometry factor of one for the PM is not valid as spontaneous and induced densities have been determined under different etching conditions. Therefore sphene and zircon can be dated only using the EDM.

Thermal neutron fluence (ϕ) and λ_f

Since the values of the constants I, λ_D, and σ are well established, only ρ_s and ρ_i, λ_f and ϕ need to be measured to obtain the age. ρ_s and ρ_i can be ascertained by counting, which leaves ϕ and λ_f to be determined. The neutron fluence can be determined by: (1) Measuring neutron-induced gamma or beta activity in a metal activation foil of Au, Cu, or Co (*Hurford and Green*, 1982); or (2) Neutron-irradiating a standard track detector (glass dosimeter) of fixed uranium content, and then using [after *Fleischer and Hart*, 1972]:

$$\phi = B\rho_d \qquad \textit{equation 2}$$

where ρ_d is the track density of the dosimeter, and B is a constant determined empirically. Glass has a low track etching efficiency, and therefore an external mica detector adjacent to the glass dosimeter is used to register induced tracks.

The detection efficiency of method (2) above is poorly known and therefore the systems must be calibrated prior to their use for neutron fluence determinations of subsequent irradiations [*Hurford and Green*, 1982]. One way of calibrating a neutron dosimeter is with reference to metal activation foils. *Hurford and Green* [1982] calibrated SRM glasses against Au and Cu activation monitors. Using glass SRM 962 they calculated values of B for Au and Cu monitors that differed by 11%. They also showed that the value of B (calculated by measuring ϕ with a Co activation monitor, and ρ_d with a mica detector on glass SRM 612) varied significantly with time over irradiations done over six years. *Hurford and Green* [1982] concluded that 'an absolute unique neutron fluence value is exceedingly difficult to define.'

Hurford and Green [1983] calibrated the standard dosimeter glasses SRM 612, CN1, and CN2, against Co monitors in 79 irradiations to determine values of B for each glass, and compared the relative variation of one dosimeter against another to show which of the four dosimeters was most consistent and hence suitable for neutron fluence measurement in FT dating. They showed that CN1 and CN2 (natural U glasses) gave a more consistent measure of neutron fluence than SRM 612, which in turn was considerably better than the Co wire which gave unacceptably inconsistent results. *De Corte et al.* [1990], however, measured thermal neutron fluence with Au, Co, and Cu wire monitors, and found apparently consistent fluences (within 1.5% of each other) between them.

There exists a range of estimates of the value of λ_f. The values have tended to cluster around 7×10^{-17} y^{-1} and around 8.5×10^{-17} y^{-1} [*Bigazzi*, 1981], a difference of about 20%. The problems of measurement of λ_f and ϕ have traditionally been circumvented by selecting values of λ_f and ϕ to yield a calibration ratio (ϕ/λ_f) that gives a 'correct' answer when a sample of independently known age is dated [*Hurford and Gleadow*, 1977; *Hurford and Green*, 1982 and 1983]. The calibration ratio can be found either by measuring B (and hence ϕ) by calibrating a glass dosimeter against another dosimetry system (as outlined above) and then selecting the appropriate value of λ_f to give the 'right' age of a sample of known age; or, if a particular value of λ_f is used, an appropriate value of B (and hence ϕ) can be selected. The effect is to split the calibration ratio into two parts: a notional λ_f and a notional ϕ, obviating the need for an absolute value of λ_f. A value of the calibration ratio is valid only for that particular dosimetry scheme, and must be shown to give consistent and accurate results for multiple age determinations on standards [*Hurford and Green*, 1982 and 1983]. The use of this system also shows that as λ_f is a physical constant with an absolute unique value, and as different workers have reported FT results apparently consistent with measurements of standard sample ages, differences must exist in the dosimetry systems used [*Hurford and Green*, 1983].

Until reliable and independent values for λ_f and ϕ are known, FT dating will need to be empirically calibrated against standards of independently known age. The complexities of wire activation techniques and their apparently inconsistent measurements of neutron fluence determination, prompted *Hurford and Green* [1982, 1983] to propose the zeta (ζ) calibration approach to FT dating.

The zeta calibration approach

Fleischer and Hart [1972] initially suggested that a constant, ζ, could be used in conjunction with measured ρ_s, ρ_i, and ρ_d, to replace the constants in the age equation and yield a FT age:

$$T = \zeta \frac{\rho_s}{\rho_i} \rho_d \qquad \textit{equation 3}$$

Fleischer and Hart [1972] argued that, in principle, ρ_s, ρ_i, and ρ_d, can be measured for a sample whose age T_{STD} is independently known. ζ is then given by $(T_{STD} \frac{\rho_i}{\rho_s} \rho_d)$, yielding a number that can be used to determine unknown ages (T_{UNK}) of other samples when ρs, ρ_i, and ρ_d are measured for those samples. *Fleischer and Hart* [1972] calibrated for over 30 samples the FT age against known ages over a wide age span, and hence measured ζ. They also appreciated the problem of the plethora of values of λ_f if wanting to calculate an age using a preferred value of λ_f. *Fleischer and Hart* [1972] concluded 'measuring ζ directly is the simple, more precise, and more reliable procedure that is recommended.'

After a decade of confusion concerning FT dating system calibration, *Hurford and Green* [1982 and 1983] re-proposed the ζ calibration approach, and refined and extended it. They argued that a uranium glass dosimeter can be calibrated against age standards. For this calibration system, the neutron fluence ϕ is represented by ρ_d, and the age equation is rewritten as [*Hurford and Green*, 1983]:

$$T_{UNK} = \frac{1}{\lambda_D} ln \left[1 + \lambda_D \zeta \frac{\rho_s}{\rho_i} g \rho_d\right] \qquad \textit{equation 4}$$

where the value of ζ for a particular glass dosimeter is determined from age standards by [*Hurford and Green*, 1983]:

$$\zeta = \frac{e^{\lambda_D T_{STD}} - 1}{\lambda_D [\rho_s / \rho_i]_{STD} g \rho_d} \qquad \textit{equation 5}$$

where T_{STD} is an age standard of independently known age.

Hence ζ is also given by [*Hurford and Green*, 1983]:

$$\zeta = \frac{\sigma I B}{\lambda_f} \qquad \textit{equation 6}$$

When ζ has been evaluated, unknown ages of samples can be determined using equation 4, having measured ρ_s, ρ_i, and ρ_d. Because a single ζ determination may be subject to large errors, a large number of determinations of ζ should be made, calibrated against appropriate age standards. *Hurford and Green* [1983] made repeated determinations of ζ for the three dosimeter glasses SRM 612, CN1, and CN2 against zircon age standards, and recommended suitable age standards having demonstrated the reproducibility of ζ determinations between different age standards and between dosimeters. They recommended that other FT workers make multiple measurements of ζ on age standards, appreciating that the ζ is personal and related to particular conditions of track etching, and track identification and counting. *Green* [1985] extended the earlier work on zircons by applying the ζ approach to apatite and sphene.

Standardisation of fission track dating calibration

The problems in calibration of FT dating led to the recommendation by the International Union of Geological Sciences Subcommission of Geochronology, for a uniform approach to system calibration [*Hurford*, 1990]. The recommendations were that: (1) Age standards must form the basis for all FT dating system calibrations (age standards that fulfill the appropriate criteria were identified). (2) Unknown samples should be irradiated as far as possible under the same conditions as used for the calibration irradiations. (3) Two approaches were recommended for FT age determination: (i) For the population method: either an "absolute' calibration approach with selection of a value for λ_f and direct measurement of ϕ using both Co and Au activation monitors which should agree within experimental error (<5%); or the zeta calibration approach. (ii) For single-grain methods (including EDM), the zeta (ζ) approach alone is recommended. The ζ value is specific to the dosimeter glass, mineral phase, operator, and experimental conditions including reactor and microscope.

The minimum requirements for establishing a system calibration for either the zeta or absolute approaches are five analyses per mineral phase, each being a separate mount. For apatite and zircon, the minimum five analyses should include more than a single age standard and represent at least three different irradiations. FT-daters should check their calibrations periodically. The ζ calibration approach to fission track dating has been used exclusively in this thesis.

Fission track age error analysis

Statistical models for the calculation of the error in a fission track age that has been determined by the EDM have been discussed by *Johnson et al.* [1979], *McGee and Johnson* [1979], *Green* [1981a], *Galbraith* [1981], *Bardsley* [1983], *Galbraith* [1984], and *Galbraith and Laslett* [1985].

Green [1981a] formalised the error analysis used by FT daters at about that time, terming it the 'conventional analysis.' Errors in ρ_s, ρ_i, and ϕ were combined to give a relative uncertainty in the age T:

$$\frac{\sigma(T)}{T} = \left\{ \left(\frac{\sigma(\rho_s)}{\rho_s} \right)^2 + \left(\frac{\sigma(\rho_i)}{\rho_i} \right)^2 + \left(\frac{\sigma(\phi)}{\phi} \right)^2 \right\}^{1/2} \qquad \textit{equation 7}$$

where $\sigma(\rho_s) = \frac{\sqrt{N_s}}{A_s}$ and $\sigma(\rho_i) = \frac{\sqrt{N_i}}{A_i}$

and where N_s and N_i are the respective total numbers of spontaneous and induced tracks counted, and A_s and A_i are the respective areas over which spontaneous and induced tracks are counted.

Using track numbers instead of densities, and for fission track ages determined using the ζ approach, equation 7 can be rewritten as:

$$\frac{\sigma(T)}{T} = \left\{ \left(\frac{1}{Ns} \right) + \left(\frac{1}{Ni} \right) + \left(\frac{1}{Nd} \right) + \left(\frac{\sigma(\zeta)}{\zeta} \right)^2 \right\}^{1/2} \qquad \textit{equation 8}$$

where N_s, N_i, and N_d are the total number of tracks counted for spontaneous, induced, and standard glass respectively.

The error determined by equations 7 and 8 is an estimate of the distribution of possible ages that could be obtained from the amount of uranium in the area analysed. The age calculated is termed the 'pooled' age, as it is calculated (from equation 4) using the total track counts for the sample mean densities (ρ_s/ρ_i).

The assumption underlying this error analysis is that the random fluctuation in the rate of uranium fission is the only source of uncertainty in the measurements [*Green*, 1981a]. The Poisson law can be derived from mathematical conditions that closely approximate the underlying physical process, and therefore the 'Poisson assumption' is appropriate [*Galbraith and Laslett*, 1985]. This assumption states that the numbers of spontaneous and induced tracks that have formed from given amounts of uranium have independent Poisson distributions with means proportional to the amounts of uranium. For the EDM, as N_s and N_i are counted for each grain, only within-grain variation contributes to the error [*Galbraith and Laslett*, 1985]. *Galbraith* [1981] developed a χ^2 test that can be used to examine departures from the Poisson model. If the χ^2 statistic is too large (that is, $P\chi^2<5\%$) then extra-Poissonian error is present. This additional source of variation may be due to inept counting or experimental procedures [*Green*, 1981a], or significant compositional variation between single grains [e.g. *Green*, 1989b] the effect of which is manifest in particular thermal histories. Alternatively, if the χ^2 statistic is consistently smaller that the predictions of the Poisson model, then this may be due to sampling or counting biases.

Galbraith [1981] showed that if observed track counts are acceptable under the χ^2 criterion, then the conventional analysis gives the best estimate of the error in ρ_s, ρ_i, ρ_d, and the error in ρ_s/ρ_i and the age 'T' calculated is termed the 'pooled age'. In the case of extra-poissonian variation being detected by the χ^2 test, then the conventional analysis provides only a minimum estimate of the error. *Green* [1981a] recommended that in this case, a better estimate of the error on the ratio ρ_s/ρ_i is one which is calculated from the standard deviation on the weighted mean value of ρ_s/ρ_i from the individual crystal ratios:

$$\sigma(N_s/N_i) = \frac{\sqrt{\sum_{J=1}^{n} \left(\overline{\rho_s/\rho_i}\right)_J^2 - \left[\sum_{J=1}^{n} (\rho_s/\rho_i)_j\right]^2}}{n(n-1)} \qquad \textit{equation 9}$$

In this case the age calculated is termed the 'mean' age as it is calculated using the mean of the individual crystal ratios $\overline{\rho s/\rho i}$ (or $\overline{Ns/Ni}$):

$$\left(\frac{\rho_s}{\rho_i}\right)_{mean} = \sum_{j=1}^{n} \frac{(\rho_s/\rho_i)_j}{n} \qquad \textit{equation 10}$$

In this case the error on the FT age is:

$$\frac{\sigma(T)}{T} = T\left\{\left(\frac{\sigma(\rho_s/\rho_i)}{\overline{\rho_s/\rho_i}}\right)^2 + \left(\frac{\sigma(\rho_d)}{\rho_d}\right)^2 + \left(\frac{\sigma(\zeta)}{\zeta}\right)^2\right\}^{1/2} \qquad \textit{equation 11}$$

or using track numbers instead of densities:

$$\frac{\sigma(T)}{T} = T\left\{\left(\frac{\sigma(N_s/N_i)}{\overline{N_s/N_i}}\right)^2 + \left(\frac{1}{N_d}\right) + \left(\frac{\sigma(\zeta)}{\zeta}\right)^2\right\}^{1/2} \qquad \textit{equation 12}$$

The error when the population method 'fails' the χ^2 test is problematic.

ETCHED FISSION TRACK LENGTH PARAMETER

Although FT density is the parameter used when calculating a FT age, the length of an etched FT is a more fundamental measure, as the density of tracks that intersect a crystal surface is a function of the distribution of track lengths. The FT length is also important as the parameter allows assessment of the degree of annealing a sample has experienced and therefore aspects of its thermal history can be evaluated. Fission tracks in a crystal have a certain distribution of lengths due to differences in the range of fission fragments, crystallographic anisotropy, anisotropic V_G, and shortening of tracks due to annealing [*Laslett et al.*, 1982].

There are two approaches to measuring the lengths of fission tracks:

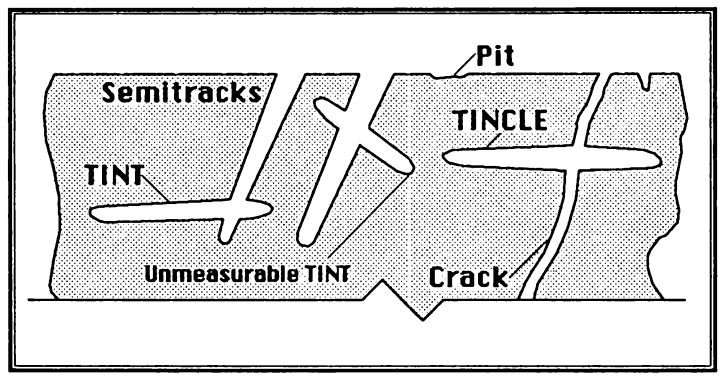


Fig. 4. Fission track lengths: Schematic representation of a cross-section through the crystallographic c-axis showing measurable and unmeasurable confined tracks, and semi-tracks [modified from *Lal et al.*, 1969].

(i) Measurement of tracks intersecting the exposed internal surface of a crystal: (a) measurement of lengths of tracks intersected by and projected on an exposed (and polished) internal surface ('projected semi-track length') [e.g. *Wagner and Storzer*, 1972; *Wagner*, 1988; *Wagner et al.*, 1989; *Dakowski*, 1978]; (b) measurement of the true length of the tracks intersecting a surface by correcting for the dip of the track into the surface ('semi-track length') [*Bhandri et al.*, 1971; *Dakowski*, 1978] (Fig. 4).

(ii) Measurement of tracks confined within the crystal that have been etched without themselves intersecting the surface, via another track (= 'TINT' or 'Track IN Track') or via a fracture or cleavage (= 'TINCLE' or 'Track IN CLEavage') connected to the surface: (a) measurement of both dipping and horizontal tracks ('confined track length') [e.g. *Lal et al.*, 1969; *Bhandri et al.*, 1971]; (b) measurement of only confined tracks that are horizontal ('horizontally confined track length') [e.g. *Gleadow et al.*, 1983; *Gleadow et al.*, 1986a and b; *Donelick*, 1991; *Green et al.*, 1986, 1989] (Fig. 4).

The measurement of a number of tracks for a sample results in a FT length distribution. In practice, projected (semi-track) track lengths and horizontally confined track lengths are most commonly measured. The relative merit of the two approaches is contentious. *Dakowski* [1978], *Green* [1981b], *Laslett et al.* [1982], and *Gleadow et al.* [1986a], amongst others, have supported the measurement of horizontally confined tracks. *Laslett et al.* [1982] showed that measurements of all FT length distributions are biased with respect to the true length distribution, and recommended that FT length distributions should be constructed from horizontally confined tracks, as the observed distribution of these tracks is closely related to the true distribution, and the bias is more easily corrected than for projected track lengths. Also, observed projected semi-track lengths appear to obscure detail in the distribution of lengths, and therefore differences between samples are subtle. [*Laslett et al.*, 1982; *Gleadow et al.*, 1986a]. *Gleadow et al.* [1986a] concluded that projected length distributions are sensitive only to major differences in thermal history, and recommended the measurement of horizontally confined track lengths in order to maximise information about thermal history. All fission track lengths measured and reported in this thesis are horizontally confined track lengths.

Wagner [1988] and *Wagner et al.* [1989] equated the fraction of projected track lengths >10 μm to a 60° C cooling age, and with *Wagner and Heijl* [1991] suggested that other useful temperature-time information could

be extracted from the distribution of projected track lengths. *Galbraith et al.* [1990] suggested that although horizontally confined tracks are preferable to measure, projected semi-tracks may provide useful information when the numbers of confined tracks are low.

Bias of the measured horizontally confined track length distribution includes [*Laslett et al.*, 1982; *Galbraith et al.*, 1990]:

(i) Length bias, where longer tracks have a grater probability of intersecting cleavages or tracks connected to the surface, e.g. a 10 μm track has twice the chance of being etched and measured as does a 5 μm track.
(ii) Multiple cleavage bias, where a track intersects more than one cleavage or semi-track, e.g. a track that intersects two cleavages should be counted twice.
(iii) Edge bias, where if only tracks lying totally inside a crystal are sampled, shorter tracks are more likely to be included.
(iv) Cleavage angle bias, where a track of a given length is more likely to intersect a cleavage if its angle to the cleavage is higher (closer to 90° than 0°).
(v) Orientation bias, where due to anisotropic etching tracks present a wider face in the direction perpendicular to the c-axis, producing a blade shaped track and favouring the sampling of TINTS at high angles to the c-axis.
(vi) Cleavage thickness bias, where long tracks that intersect a cleavage have a higher chance of having both ends shown than shorter tracks.
(vii) Measurement bias, where for instance both ends of short tracks may be hidden by shadows of cleavages.

The most important of these is length bias, which also affects other biases (e.g. measurement and cleavage angle biases).

Horizontally confined tracks should be measured on only those polished surfaces that are parallel to the crystallographic c-axis, as the etchable length of a track in apatite varies with crystallographic orientation due to anisotropic annealing. Tracks oriented parallel to the c-axis are longer than those lying perpendicular [*Green and Durrani*, 1978; *Green*, 1981b; *Green et al.*, 1986; *Donelick*, 1991]. In a section parallel to the c-axis, horizontally confined tracks will be present in all orientations from 0°-90° C to the c-axis, whereas in a basal section all tracks seen and measured are perpendicular to the c-axis and will be shorter than tracks in other

orientations, introducing considerable bias to the observed length distribution.

ANNEALING

Definition

Annealing is the repair of latent fission track damage over time. The phenomenon of 'track fading' was observed by *Price and Walker* [1963] who noted that the number and average length of fission tracks in mica as revealed by etching was reduced by heating. *Price and Walker* [1963] realised that the effect of track fading over geological time would be to lower observed FT ages below the 'true' age.

Mechanism of latent fission track annealing

Repair of FT damage involves translations of atoms over distances of 0.5-1.0 nm from their displaced positions into proper crystallographic sites [*Carlson*, 1990]. The atomic repositioning is driven by the strain energy stored in the disrupted zone area of the crystal.

The ability to detect a damage zone (a latent track) by etching will depend on the threshold value of defect density for a particular etching procedure. The damage zone is termed 'annealed' when the defect density is too low to allow preferential etching of the zone; a density exceeding the threshold allows this region of the crystal to be etched and the region is termed 'unannealed' [*Green et al.*, 1988; *Carlson*, 1990].

Most studies of FT annealing in crystals have been on the mineral apatite, and have involved measurements of etched tracks to infer characteristics of latent track annealing. *Green et al.* [1986] studied the degree of annealing of induced fission tracks in samples of Durango apatite that were heated for between 20 mins and 500 days at temperatures of between 95° and 400° C. Two distinct stages of annealing were identified: (1) A systematic reduction in mean etchable (horizontally confined) track length and slight broadening in the length distribution to a length reduction of ~0.65 of the initial length (i.e. from ~16 to ~11 μm); (2) Below ~11 μm, a greatly accelerated reduction in mean etchable track length and a larger spread of track lengths about the mean. The first stage of annealing was interpreted as representing a progressive shrinking of tracks from their ends towards

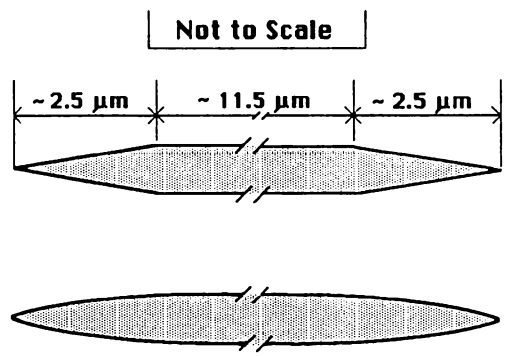


Fig. 5. Schematic representations of a latent track (modified from *Carlson* [1990]): (Top) Cylindrical zone of disruption terminated by two conical tips; (Bottom) Alternative representation in which the radius decreases monotonically and non-linearly from the axial centre to its tips. *Carlson* [1990] favoured the first representation as it yielded less cumbersome kinetic equations when describing fission track annealing.

their centres. The second stage was interpreted in terms of the development of unetchable gaps in tracks, and the anisotropy of annealing of tracks according to their orientation within the crystals.

Carlson [1990] studied the annealing of tracks in apatite by constructing a physical model of the atomic scale processes involved in annealing. The observations of *Green et al.* [1986] were used to constrain parts of the model. *Carlson* [1990] proposed that a latent FT in apatite consists of an ~11 μm cylindrical disrupted zone terminated by two conical tips each ~2.5 μm in length (Fig. 5). In Carlson's [1990] model, annealing produces both a systematic decrease in the radius of the damage zone and a decrease in the length, with the anisotropy of annealing being the only contributer to the spread of track lengths about the mean. The rate of shortening to ~11 μm is controlled by the rate of radial shrinkage, which in turn is controlled by the taper angle of the conical tips. As the length of the damage zone approaches ~11 μm the track radius necessarily approaches zero. Slight variations of defect density along this length were considered to cause the track to segment at random positions along its length, a process that continues until annealing is complete. This stage is defined by a rapid decrease in mean length and an increase in spread in lengths. These two stages equated to the two stages of *Green et al.* [1986] and explain reasonably the experiments of that study. The two stages were termed by *Carlson* [1990] as 'axial shortening' and 'segmentation.' *Carlson* [1990] also argued that the rate of elimination of defects in the annealing process is constant and uniform throughout a crystal at a constant temperature and that the rate increases exponentially with temperature. The initial distribution of radial defects is one where defect density is greatest at the radial centre of the track and declines under a power function to a minimum at the perimeter of the damage zone. This accounts for the fact that, given a constant rate of defect elimination during annealing, rates of axial shortening decrease over time at constant temperature, as shown by the experiments of *Green et al.* [1986]. For example, at 210° C, the first hour of annealing produces a 1 μm reduction in etched track length while the next 1 μm takes 100 hrs. The process of tracks segmentation is more difficult to examine than axial shortening, as the process is probably random. For this reason *Carlson* [1990] analysed segmentation by relating the amount of segmentation to the mean track length.

Paul and Fitzgerald [1992], using TEM studies of latent fission tracks in fluorapatite, have suggested that track annealing anisotropy may be

controlled by the anisotropy of track width; the greater resistance to annealing of tracks parallel to the c-axis is viewed as resulting from the greater time needed to anneal an initial wider track.

Annealing studies

Three approaches to the study of annealing of etched fission tracks in apatite are apparent in the literature: (1) Laboratory studies, (2) Natural studies, and (3) Physically-based mathematical studies. These studies provide information that assists in interpretation of sample FT data in terms of thermal histories over geological timescales.

(1) Laboratory annealing studies

These studies involve measuring track length distributions and track densities in crystals subjected to controlled thermal histories where temperature ranges from ~100°-500° C for times ranging from a few minutes to ~1 year (e.g. *Fleischer and Price*, 1964; *Green et al.*, 1986; *Crowley et al.*, 1991). The results have traditionally been presented in the form of an arrhenius plot where each straight line represents a certain degree of annealing. This allows the relationship between track density or track length reduction and temperature to be extrapolated to geological timescales. The degree of annealing is portrayed usually on a diagram of logarithm of annealing time versus inverse absolute temperature [e.g. *Storzer and Wagner*, 1969; *Green et al*, 1985; *Laslett et al.*, 1987]. The arrhenius equation is:

$$\ln(t) = A + BT^{-1}$$

where t = annealing time; T = annealing temperature in Kelvins; A = a constant; and B is normally interpreted in terms of E/k, where k = Boltzmann's constant and E is an activation energy.

Early studies showed that annealing in apatite occurred after heating at 250°-300° C for one hour. Arrhenius plots typically showed a fanning pattern whereby a given proportion of track loss had a characteristic slope or activation energy, with the activation energy increasing with the degree of annealing. The predictions of the arrhenius plots were able to be tested subsequent to studies of the variation in FT parameters with depth (temperature) in deep boreholes [*Naeser and Forbes*, 1976; *Gleadow and*

Duddy, 1981; *Naeser*, 1981]. These studies showed that annealing occurred over a narrower temperature interval over geological times than that predicted by laboratory annealing data, although the results of *Gleadow et al.* [1983] when extrapolated showed better comparison with borehole data.

The studies by *Green et al.* [1985] and *Laslett et al.* [1987] showed that the widely fanning plots of earlier studies may have been due to the presence of apatites of different compositions that had different annealing properties (different activation energies). The slightly fanning relationships of *Green et al.* [1985] and *Laslett et al.* [1987] were in much closer agreement with natural annealing observed in borehole samples. *Laslett et al.* [1987] also suggested that different crystallographic orientations may be characterised by different activation energies.

However, *Crowley et al.* [1991] preferred a widely-fanning model for both their own data and that of *Green et al.* [1986]. Activation energies increased from about 20 kcal/mol at the start of annealing to about 66 kcal/mol at the final stages of annealing, which implied that the rate of annealing is a function not only of temperature and time, but also of track length. This was interpreted as showing that tracks become more resistant to shortening as annealing progresses. *Crowley et al.* [1991] interpreted the point of intersection of the lines as representing the limit of stability of tracks in apatite (the point of instantaneous track annealing).

Green [1980 and 1988] showed that annealing occurs even at low (20° C) ambient temperatures over geologic timescales. *Donelick et al.* [1990] demonstrated that mean etchable FT lengths decrease by ~0.5 μm at temperatures of ~23° C during the first three weeks after being induced by irradiation. This phenomenon of low ambient temperature annealing almost certainly occurs for spontaneous tracks in apatite. The slightly fanning model of *Laslett et al.* [1987] predicted that a track would be shortened by 1 μm to ~15 μm at a temperature of 20° C sustained over 10 m.y. The fanning models of *Crowley et al.* [1991] predicted ~10% shortening after 1 m.y. heating duration at 25° C.

Green [1988] examined the relationship between track shortening and FT age reduction for both induced and spontaneous tracks in laboratory annealing experiments. The relationship was ~1:1 for lower amounts of length reduction, but as annealing proceeded, age was more rapidly reduced than length. This was understood principally in terms of the bias against

the revelation of short tracks. Data for samples that have undergone 'natural' annealing in geological conditions showed similar trends, suggesting that a laboratory-based description of annealing can be applied to geological conditions of temperature and time.

Tagami et al. [1990] studied the annealing characteristics of spontaneous fission tracks in zircon in a series of one hour annealing experiments. They measured on zircon crystals, track density, horizontally confined track length and track orientation, for temperatures between 400° and 700° C. Significant reductions in length and density appeared to begin at ~450° C and reached zero at ~750° C. Anisotropy of track etching increased dramatically at temperatures of >500° C due to the repair of α-damage. The density-length relationship for zircon appeared to be linear and showed that density reduction occurs more rapidly than length reduction, although the departure is not as great as that for apatite.

(2) Natural studies

Naeser and Forbes [1976] found in a 3 km deep borehole in Alaska that apatite age decreased with depth from ~100 Ma near the surface to ~14 Ma at the bottom where the temperature was 96° C. The apatite ages extrapolated to zero at 105° C. The samples had been heated for ~100 m.y. In another hole (in New Mexico) *Naeser* [1979] found that apatite age decreased to zero at a temperature of 135° C, due to the shorter heating time (~1 m.y.) in this hole.

However, the Otway Basin boreholes provide probably the best constraints on the annealing behaviour of apatite fission tracks in geological situations and over geological timescales [*Green et al.*, 1989a]. Importantly, these boreholes have geologically well-constrained thermal histories, and show both the beginning and ending of FT annealing [*Gleadow and Duddy*, 1981; *Gleadow et al.*, 1983; *Green et al.*, 1989a and b]. Sedimentary sequences in these wells have experienced thermal histories that have involved a steady increase in temperature to present values over an effective heating time of 10-40 m.y. [*Green et al.*, 1989a].

Apatite FT ages decrease from 120 Ma near the surface of the wells to zero at ~125° C, while mean horizontally confined track lengths decrease from ~15 μm to zero over the same temperature interval. Significant track annealing occurs between ~70° C and 125° C, with both mean length and age decreasing rapidly [*Gleadow et al.*, 1983; *Gleadow and Duddy*, 1981; *Green et*

al., 1989]. This temperature range is termed the 'annealing zone,' and shows the range of temperatures through which significant annealing occurs over geological time. *Gleadow and Duddy* [1981] also noted that there was considerable variation in the single grain ages of Otway Basin annealing zone samples, implying that apatites of different composition anneal by different amounts at the same temperature.

(3) Physically-based mathematical models

Carlson [1990] developed a physical model of the atomic-scale processes that occur in FT annealing in apatite. From this model he developed a kinetic equation to describe the relationship between the length of a FT and its thermal history during axial shortening. The equation described the length of an annealed FT in terms of initial track length, time, and temperature, and three empirically determined quantities. In the absence of an atomic-scale theory for segmentation (a complex and random process), segmentation was analysed by adding to the initial equation a parameter that quantified the fraction of segmented tracks as a function of mean track length.

Carlson [1990] suggested that the different annealing rates for apatite of different composition as observed by e.g. *Green et al.* [1985] may vary as functions of the total ionic porosity of the apatite crystals. The lowest estimated ionic porosity is seen in Cl-apatites, which are less easily annealed than F- and OH-apatites. *Carlson* [1990] also explained the effect on annealing rate of track orientation within a crystal. He concluded that anisotropy of annealing rates must be due to anisotropy of variations in the widths and taper angles of the disrupted zones, as neither the activation energy nor the radial defect distribution showed orientational anisotropy.

Carlson [1990] argued that as the kinetic model is based on a physical model of the annealing mechanism, extrapolation of annealing rates to the lower temperatures and longer timescales of natural annealing were more soundly based than empirical relationships fitted to laboratory annealing data. *Carlson* [1990] suggested that previous fanning arrhenius plots that showed variable activation energies as annealing progresses, may be reflecting a problem of using the same equation to describe the two (kinetically different) stages of annealing.

Factors controlling annealing

Neglecting the effect of mineral type, the factors of temperature and time are dominant in annealing, and crystal composition and track orientation are secondary [e.g. *Green et al.*, 1986 and 1989a].

(1) Mineral type

In practice, the three minerals used in FT dating are apatite, zircon, and sphene, in order of decreasing frequency of use. Fission tracks are more stable at a given temperature in sphene than zircon than apatite, reflected in the closure temperatures of ~300° C (sphene), ~240° C (zircon), and ~110° C (apatite).

(2) Temperature and time

Awareness of the sensitivity of fission tracks to elevated temperatures, as shown by the reduction of FT length and age, was apparent at an early stage of FT dating [e.g. *Fleischer et al.*, 1965b; *Storzer and Wagner*, 1969; *Wagner and Storzer*, 1970; *Fleischer and Hart*, 1972].

Although annealing in apatite has been shown to occur even at ambient temperatures of ~20° C [e.g. *Green* 1980; *Donelick et al.*, 1990], it is most significant between ~70° and 125° C [e.g. *Gleadow and Duddy*, 1981; *Green et al.*, 1989]. Tracks are not retained over geological (>10 m.y.) timescales at temperatures of >~125° C. At shorter annealing times, the temperature of non-retention of tracks increases.

Gleadow et al. [1983] were able to estimate the relative effects of temperature and time on FT annealing by comparing Otway basin borehole data and experimental annealing results using the arrhenius relationship. The annealing zone for 100 m.y. heating duration was inferred to be ~25° C lower than the annealing zone for 1 m.y. heating. *Duddy et al.* [1988] showed that FT mean length is far more sensitive to temperature than to time. In a situation of a linear increase in temperature to a maximum, a ~10° C change in maximum temperature was shown to be equivalent to a change in timescale of an order of magnitude. For example, a similar amount of annealing is experienced by tracks in apatites that reside for 10 m.y. at 100° C as tracks that reside for 100 m.y. at 90° C. Once the maximum

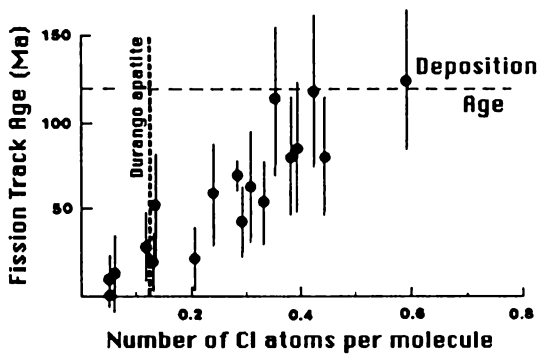


Fig. 6. Compositional control on apatite annealing: Variation in single grain ages in an apatite sample, derived from the Flaxmans-1 borehole at a present day temperature of 92° C [from *Green et al.*, 1985].

temperature is reached, ~10 m.y. is required for FT lengths to attain a distribution characteristic of that temperature.

(3) Mineral composition (apatite)

Annealing has been shown to be influenced by composition. *Green et al.* [1985] showed empirically the compositional control on annealing: apatites richest in chlorine are more resistant to annealing, while F-apatites are more easily annealed (Fig. 6). Pure fluorapatites were inferred by *Green et al.* [1989] to totally anneal at ~90° C in the Otway Basin boreholes, whereas the chlorapatites totally anneal at ~ 125° C.

Crowley et al. [1990] examined the effects of apatite composition on the annealing of tracks in Cl-, F-, OH-, and Sr-F-apatite in 300 isochronal annealing experiments (at 10, 100, 1000 hours) at temperatures ranging from 40° - 400° C. Their data showed that the pattern of annealing resistance in apatite is Cl-apatite > Sr-F-apatite = F-apatite ~ OH-apatite. The difference in annealing resistance of Cl-apatites with the others is large (to 30° C in the experiments). *Hughes et al.* [1990] investigated differences in crystal structure among the different apatites and related these variations to observed differences in annealing resistance. The structure of Cl-apatites was found to differ from OH- and F-apatites in terms of polyhedron volume and bond length. The differences in structure between the end-member apatites correlated in magnitude and direction with observed differences in annealing resistance.

(4) Orientation of tracks

Green and Durrani [1977], *Green* [1981b], *Green et al.* [1986], *Donelick et al.* [1990], *Donelick* [1988 and 1991], and *Crowley et al.* [1991] have all demonstrated that the length of annealed fission tracks in apatites varies according to crystallographic orientation (that is, annealing is anisotropic). Specifically, tracks at high angles to the c-axis are shorter than tracks at lower angles.

Tracks perpendicular to the c-axis enter the second stage of annealing sooner than tracks parallel to the c-axis [*Donelick*, 1988]. *Carlson* [1990] inferred from the data of *Donelick* [1988] that the ratio between length reduction of tracks parallel to the c-axis and those perpendicular to the c-axis appeared to be constant for mean lengths ≥ 11 μm. This implied that the

anisotropy of track annealing is not a result of the variation in activation energy with respect to orientation. *Donelick* [1991] developed an empirical model in which the mean etchable FT length at an angle to the c-axis is defined by the radius of an ellipse that has semi-axes equal to the mean lengths parallel and perpendicular to the c-axis.

THERMAL AND TECTONIC HISTORIES FROM FTA

Knowledge of the systematics of fission track annealing (the stability of fission tracks over time with respect to temperature) is the key to interpreting FT data in terms of thermal (and inferred tectonic) histories. There are several approaches:

(1) Closure temperature studies - cooling and uplift rates (apatite and zircon)

The principle of a simple closure temperature for FT retention in apatite (110° ± 10° C) and zircon (240° ± 50° C) has been applied in many studies to constrain cooling and uplift/erosion rates since the time that the closure temperature was attained. Examples include studies of the European Alps [e.g. *Hurford*, 1986], the Himalaya [e.g. *Zeitler et al.*, 1982; *Zeitler*, 1985], the Andes [*Benjamin et al.*, 1987], the New Zealand Southern Alps [*Kamp et al.*, 1989], and the Transantarctic Mountains [e.g. *Fitzgerald, 1987*; *Gleadow and Fitzgerald*, 1987]. Three methods are commonly used:

(a) The cooling rate is simply the closure temperature divided by the FT age.
(b) The gradient of FT age versus sample elevation is interpreted as the apparent uplift rate over the period of the apatite ages.
(c) Apatite and zircon FT age pairs can be used to calculate a cooling rate during the intervening interval.

The methods make several assumptions, including that of a constant geothermal gradient over time (that is, the cooling rate equals the erosion rate). This assumption is unlikely to hold if the rate of uplift exceeds ~2 mm/yr [*Koons*, 1987].

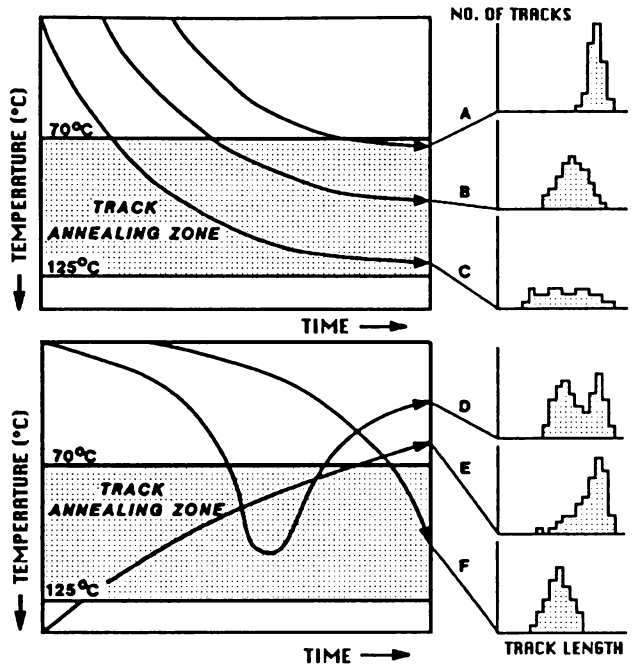
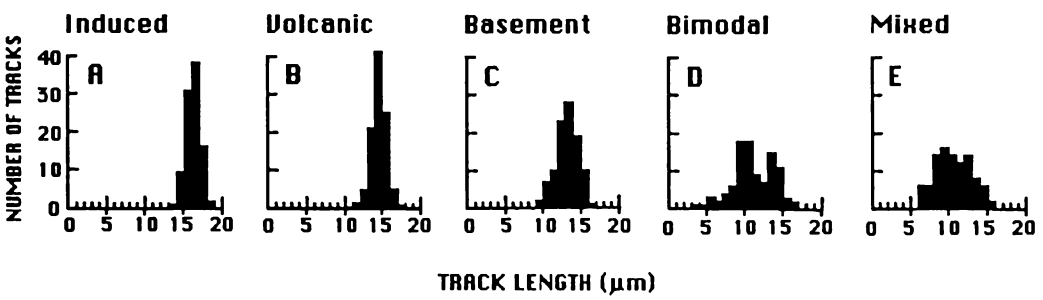


Fig. 7. Temperature-time paths and the resulting apatite horizontally confined fission track length distributions for rocks of varying thermal history [from *Gleadow et al.*, 1983].



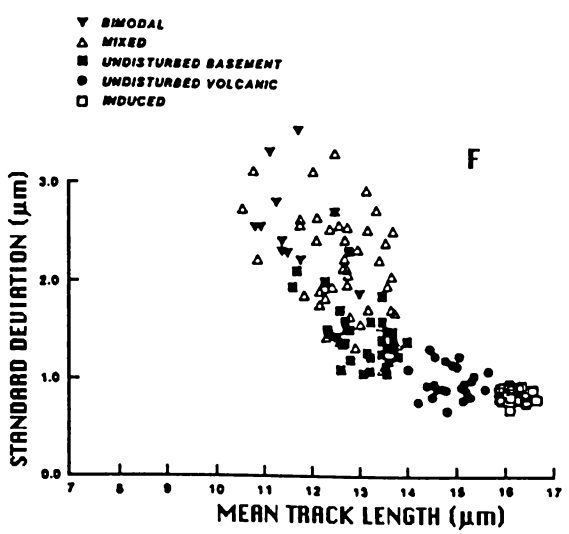


Fig. 8. Fission track (horizontally confined) length data for characteristic geological environments [from *Gleadow et al.*, 1986a].

(2) Typical track length distribututions (apatite)

The distribution of horizontally confined track lengths in apatite is diagnostic of the style of thermal history [e.g. *Gleadow et al.*, 1986a]. In theory, because fission tracks accumulate over time and have a constant birth length of ~16 μm, the whole of the thermal history since the sample cooled through the closure temperature will be reflected in the statistics of the length distribution. One way of extracting thermal history information from 'unknown' samples is to compare FT length distribution statistics with the 'typical' shapes of e.g. *Gleadow et al.* [1983] and Gleadow et al. [1986a].

Gleadow et al. [1983] presented temperature-time paths and typical (hypothetical) tracks length distributions for rocks possessing different thermal histories (Fig. 7). Fig. 7A, B, and C show a simple and progressive burial history (such as experienced in the Otway Basin) with length distributions essentially in equilibrium with the modern annealing zone range of temperatures. D shows the bimodal distribution expected from a sample now at low temperature which has experienced heating. E shows a skewed distribution typical of slow cooling through an annealing zone. F shows a shortened distribution resulting from a recent heating event.

Gleadow et al. [1986a] divided confined track length distributions into a number of characteristic shapes that corresponded to distinct geological environments (Fig. 8). Fig. 8A shows the distribution of lengths of induced tracks, characterised by a mean length of ~16.3 μm, and a standard deviation of ~0.9 μm. B shows the distribution corresponding to volcanic rocks that have cooled rapidly and not been reheated, with a mean length of 14.5-15 μm, and a standard deviation of ~1.0 μm. C shows the distribution that reflects slow cooling from 120° C to ambient surface temperatures, typical of granitic basement terranes. The distribution has a mean length of ~12-13 μm and a standard deviation of between 1.2 and 2 μm. D shows the bimodal distribution resulting from the mixture of shorter tracks from a past thermal event, and long tracks formed after the samples cooled to lower temperatures. Standard deviations exceed 2 μm. E shows a mixed distribution (of which the bimodal distribution of D is a special type) resulting from heating but where the two track components of D are not so well resolved. Mean lengths vary typically from 10.5-13.5 μm, and standard deviations are >1.3 μm. F shows the relationship between mean track length and standard deviation for the five length distribution types.

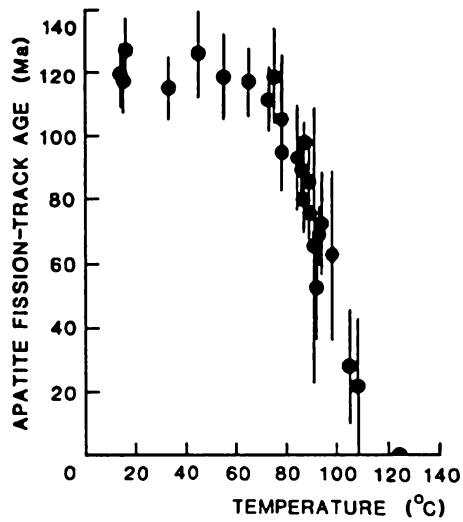


Fig. 9. Otway Basin data: Variation of fission track age (± 2σ) with present day down-hole temperature [modified from *Gleadow and Duddy*, 1981 in *Green et al.*, 1989].

(3) Empirical comparison with Otway Basin (apatite)

The Otway Basin, in Southern Victoria, Australia, was formed during the early stages of rifting between Australia and Antarctica [*Gleadow and Duddy*, 1981]. A 3.5 km thick sequence of terrigenous volcanogenic sediment was deposited during the early Cretaceous; concordant apatite, zircon and sphene FT ages of outcrop samples (~120 Ma) indicate that source volcanism was contemporaneous with deposition [*Gleadow and Duddy*, 1981]. Stratigraphic evidence suggests that the sediments reached their maximum burial depth at about 30 Ma, and have remained at about the same depth since then. Four wells penetrating the Otway Group have been sampled for the purposes of FTA [e.g. *Gleadow and Duddy*, 1981; *Gleadow et al.*, 1983]. The rocks in these wells have progressively increased temperature to present values and have stayed within a few degrees of their present values for the last 10-40 m.y. [*Green et al.*, 1989a]. As annealing is dominated by the highest temperatures experienced [*Duddy et al.*, 1988], FT parameters from the well samples will be determined by annealing in the last 10-40 m.y. and therefore will be essentially in equilibrium with current formation temperatures. The simple and well-constrained thermal history of the basin means that the Otway wells provide an ideal reference with which to compare annealing characteristics of 'unknown' samples. Valid comparison is only assured if the thermal history of the unknown samples is similar (i.e. a virtual equilibrium situation) and the compositional spread is similar (in particular, the unknown samples need to have a proportion of Cl-apatites).

The four wells show a variation of annealing of fission tracks in apatite with depth (temperature) [e.g. *Gleadow and Duddy*, 1981; *Gleadow et al.*, 1983; *Green et al.*, 1989b]. *Green et al.* [1989b] examined the variation with depth (temperature) of five FT parameters: FT age, distribution of single grain ages, χ^2 values, mean confined track length, and the distribution of confined FT lengths.

Fig. 9 shows the variation of FT age with present downhole temperature for the four Otway Basin wells. Samples residing at ~70° C yield formation ages, indicating little thermal disturbance. Samples between 70° and 125° C (apatite annealing zone) show progressive annealing as shown by steadily decreasing ages, until zero age is reached at ~125° C.

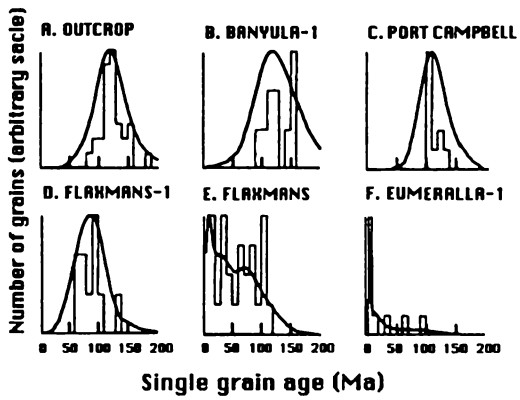


Fig. 10. Otway Basin data: Variation in the single grain age distribution with temperature [from*Green et al.*, 1989]. A, ~20° C (outcrop); B, 45° C; C, 73° C; D, 86° C; E, 92° C; F, 109° C.

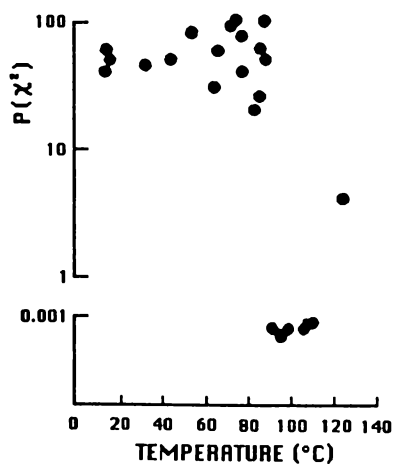


Fig. 11. Otway Basin data: Variation in $P(\chi^2)$ with downhole temperature in the 4 Otway Basin wells [from *Green et al.*, 1989b].

Fig. 10 shows the variation in distribution of single grain ages with temperature for six Otway samples. Distributions for samples <90° C retain a tight symmetric shape. Above ~90° C the distributions show a wide spread of single grain ages resulting from the spread of apatite compositions present in the samples: Cl-apatites have older single grain ages than the F-apatites. The Cl-apatites are totally annealed at ~125° C, while the F-apatites are fully annealed at ~90° C (the first appearance of zero age grains) [*Green et al.*, 1989a]. The effect of the compositional spread is also reflected in the variation in the value of the χ^2 statistic [*Galbraith*, 1981] with temperature. Fig. 11 shows values of $P(\chi^2)$ of samples taken from the Otway wells. All samples at temperatures <90° C have values of $P(\chi^2)$ >5%, showing that the variation in single grain ages is small and consistent with a single age. Samples between 90° - 125° C show very low $P(\chi^2)$ values due to the spread in single grain ages resulting from the range of apatite compositions.

Fig. 12 shows the variation in mean confined track length of Otway apatites with present formation temperature. The progressive reduction in mean length accelerates with increasing temperature so that the decrement from 8 μm to total erasure of tracks occurs between ~115° C and 125° C.

Fig. 13A shows the variation in the distribution of confined FT lengths with temperature. The distribution is a narrow symmetric form at low temperatures, but changes to increasingly flattened distributions at progressively higher temperatures. The increase in standard deviation of the length distributions with temperature reflects the combined effects of annealing anisotropy and apatite composition. Fig. 13B shows the relationship between standard deviation and mean track length.

Several studies have used the Otway Basin as a reference in order to infer thermal histories of unknown samples. Both *Dumitru* [1988] (Great Valley forearc basin in California) and *Kamp et al.* [1989] (New Zealand southern Alps) assigned paleotemperatures to samples by comparing track length distributions and single grain age distributions with Otway Basin fission track data.

(4) Forward models (apatite)

The term 'forward' refers to the model prediction of FT age and length distributions (with which are compared observed distributions from geological samples) that result from given thermal histories. *Green et al.*

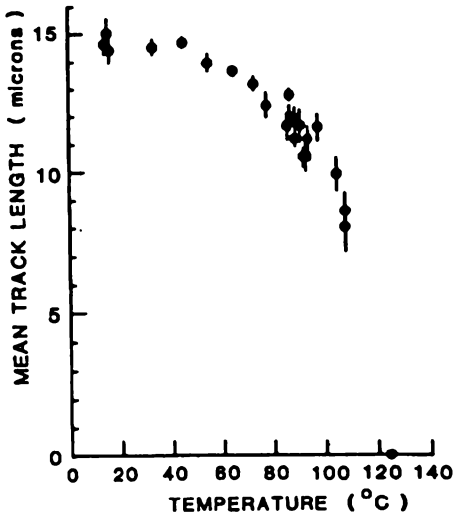


Fig. 12. Otway Basin data: Variation in mean confined track length with temperature [*Green et al.*, 1989b]. Note the rapid decrease in length from 8 μm to zero in the final 15° C from 110° to 125° C.

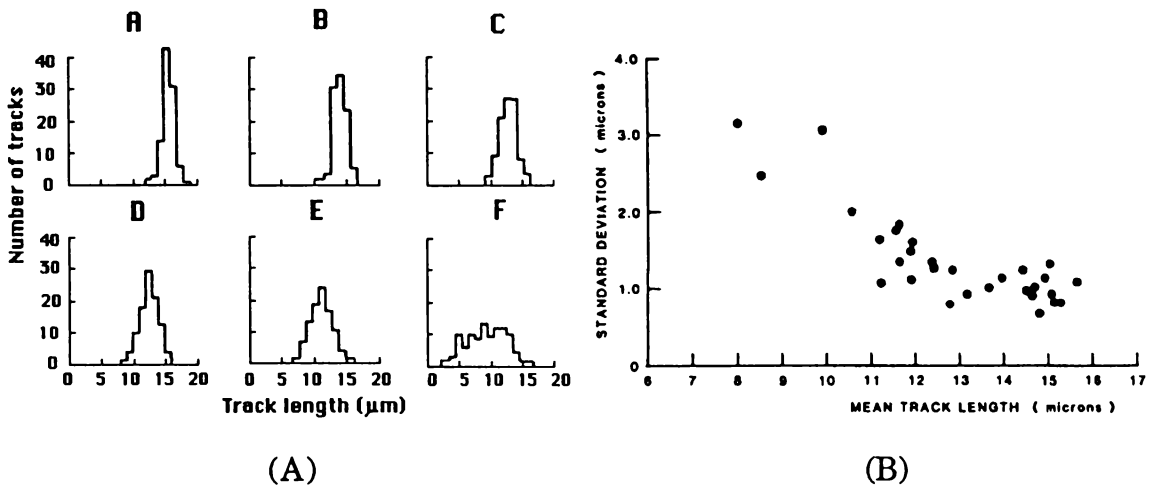


Fig. 13. Otway Basin data: (A) Composite mixed distributions of confined track lengths derived from samples in the 4 wells. A, ~20° C (outcrop); B, 40° to 50° C; C, 60° C; D, 80° to 90° C; E, 90° to 101° C; F, 102° to 110° C. All distributions are 'normalised' to 100 tracks. (B) Relationship between standard deviation and mean confined track length. From *Green et al.* [1989b].

[1985] and *Laslett et al.* [1987] derived parallel or only slightly fanning arrhenius plots [using the laboratory annealing data of*Green et al.*, 1986] that were in close agreement with the natural annealing observed in borehole samples. The isothermal annealing model based on these laboratory FT length annealing data [*Laslett et al.*, 1987], together with the observed relationship between track length and track density reduction [*Green et al.*, 1986; *Green*, 1988], and the variable temperature annealing model of *Duddy et al.* [1988], can be used as the basis for a model that predicts the FT length and age parameters resulting from a given thermal history.

Green et al. [1989a] constructed such a model, based on the annealing characteristics of the compositionally uniform Durango apatite. *Green et al.* [1989a] tested the extrapolation of the laboratory model to geological timescales by applying the model to geological situations for which apatite data were available and where the thermal history was well-constrained [e.g. the Otway Basin, and the 'volcanic' and 'basement' distributions of *Gleadow et al.*, 1986a]. The FT parameters predicted by the model agreed well with observations, implying that the extrapolation and model were valid, and suggesting that the kinetics of annealing are the same at both laboratory and geological timescales. The model predicted the distributions of mean length and age at various stages for heating, cooling, short timescale heating, and uplift and erosion. The model therefore afforded the basis of a method of paleotemperature estimation, particularly in sedimentary basins.

The model is however limited by its reliance on a single apatite composition. Although Durango apatite composition approximates the modal composition for a variety of rocks [*Sieber*, 1986, in *Green et al.*, 1989a], the model will be unsuitable for samples that exhibit a wide spread of compositions including Cl-apatites that will anneal at higher temperatures than Durango apatite. Also, the forward modeling predicts FT data from a given thermal history, when the aim is usually to predict the thermal history from observed data. Thus, identifying the range of thermal histories compatible with the observed FT data (or identifying the uncertainties associated with one possible thermal history) proceeds by trial and error; a goodness of fit test with which to compare predicted and observed data is needed.

Crowley et al. [1991] have also constructed an equation, based on laboratory annealing data, that describes the decrease in mean track length

with increasing temperature or time. However, *Crowley et al.* [1991] emphasised that the model needs to be tested [as in *Green et al.*, 1989a] before its extrapolation to geological timescales is possible.

Jones and Dokka [1990] however have argued that the equations for parallel and fanning models cannot be used directly to describe annealing over geological timescales as the effect of continuous track production throughout the history is not accounted for.

The forward model of *Carlson* [1990] has been adequately described above.

(5) Inverse models (apatite)

Inverse methods of modeling thermal histories from apatite FT data involve systematically modifying an initial thermal history until the predicted and observed FT age and length distribution agree statistically [*Lutz and Omar*, 1991; *Corrigan*, 1991]. This approach is the inverse of the forward model approach, as it determines the range of thermal histories compatible with the data, as opposed to predicting data from thermal histories.

Lutz and Omar [1991] made use of the fanning arrhenius isothermal annealing model of *Laslett et al.* [1987] and the variable temperature extension of *Duddy et al.* [1988] as the forward model, although their method can be used for any model of annealing. The approach of *Lutz and Omar* [1991] made use of the fact that forward models predict FT age and length of a specified thermal history. The inverse method uses the differences between the predicted and observed age and length to progressively modify an initial simple thermal history of linear cooling until the predicted and observed data are not significantly different. A thermal history that provides such an agreement between the predicted and observed data then guides the generation of a spectrum of additional Monte Carlo models of thermal histories. Not all of the histories may be geologically reasonable in non-synthetic data situations, and geological information is useful in constraining a smaller range of possible histories by providing time or temperature information.

Lutz and Omar [1991] used the predictions of the forward model (that is, synthetic data) as observed data in order to examine the accuracy and

precision of the results of the inverse method by comparing the spectrum (or envelope) of possible thermal histories produced from the method with the perfectly known (defined) thermal history used to generate the synthetic data. Typical uncertainties on observed age and length determinations were incorporated into the model (e.g. 10 % for 1σ on mean age). Thermal histories were defined by temperature-time segments, with the simplest history having one segment, and progressively more complex histories invented by doubling the number of segments until a satisfactory agreement is reached between the predicted (model) data and observed data. The results showed that the age at which a sample cooled through the closure temperature and the most general characteristics of the thermal history can be revealed. However, samples that have spent protracted or episodic periods in the annealing zone have a wide range of possible thermal histories permitted by the data (in these cases, geological information is helpful in eliminating implausible histories).

Corrigan [1991] also proposed an inverse method. *Corrigan* [1991] used the annealing model for track axial shortening of *Carlson* [1990], with empirical parameters taken from the experimental data for Durango of *Green et al.* [1986]. *Corrigan* [1991] analysed the thermal history spectra in terms of probability-contour plots of the density of time-temperature space compatible with the data. For perfect (synthetic) data subject to typical uncertainties, the resolution for the best-constrained parts of the thermal history was ± 10° C.

Corrigan [1991] noted the shortcomings of the forward modeling approach, which were that the spectrum of possible thermal histories compatible with a particular set of data cannot be identified except by trial and error, and that the effect of data uncertainty on the resolution of thermal history cannot be addressed directly. *Corrigan* [1991] concluded that 'the fundamental limitation on application of this inversion method to real data is the current imprecise state of knowledge of FT annealing in apatite of various anion compositions at time and temperature conditions of geological interest.'

REFERENCES

Bardsley, W.E., Confidence limits for fission-track dating, *Mathematical Geology, 15/6*, 649-658, 1983.

Benjamin, M.T., N.M. Johnson, and C.W. Naeser, Recent rapid uplift in the Bolivian Andes: evidence from fission track dating, *Geology, 15*, 680-683, 1987.

Bhandari, N., S.G. Bhat, D. Lal, G. Rajagopalana, A.S. Tamhare, and V.S. Venkatavardam, Fission track lengths in apatite: recordable track lengths, *Earth and Planetary Science Letters, 13*, 191-199, 1971.

Bigazzi, G., The problem of the decay constant λ_f of ^{238}U, *Nucl. Tracks, 5*, 35-44, 1981.

Carlson, W.D., Mechanisms and kinetics of apatite fission-track annealing, *American Mineralogist, 75*, 1120-1139, 1990.

Chadderton, L.T., On the anatomy of a fission fragment track, *Nuclear Tracks, 15*, 11-29, 1988.

Conran, G.A., and H.H. Adler, The variability of the natural abundance of ^{235}U, *Geochimica et Cosmochimica Acta, 40*, 1487-1490, 1976.

Corrigan, J., Inversion of apatite fission track data for thermal history information, *J. Geophys. Res., 96/B6*, 10347-10360, 1991.

Crowley, K.D., M. Cameron, and B.J. McPherson, Annealing of etchable fission-track damage in F-, OH-, Cl-, and Sr-apatite: 1. Systematics and preliminary interpretations, *Nuclear Tracks, 17*, 409-410, 1990.

Crowley, K.D., M. Cameron, and R.L. Schaeffer, Experimental studies of annealing of etched fission tracks in fluorapatite, *Geochimica et Cosmochimica Acta, 55*, 1449-1465, 1991.

Dakowski, M., Length distributions in thick crystals, *Nuclear Tracks, 2*, 181-189, 1978.

De Corte, F., P. Van den haute, A. De Wispelaere, and R. Jonckheere, Calibration of the fission-track dating method: is Cu useful as an absolute thermal neutron fluence monitor?, *Chemical Geology (Isotope Geoscience Section), 86*, 187-194, 1991.

Donelick, R.A., Etchable fission track length reduction in apatite: experimental observations, theory and geological apalications, Unpubl. Ph.D. thesis, Rensselaer Polytechnic Institute, New York, 414 pp, 1988.

Donelick, R.A., Crystallographic orientation dependence of mean etchable fission track length in apatite: an empirical model and experimental observations, *American Mineralogist, 76*, 83-91, 1991.

Donelick, R.A., M.K. Rowden, J.D. Mooers, B.S. Carpenter, and D.S. Miller, Etchable length reduction of induced fission tracks in apatite at room temperature (~23° C): crystallographic orientation effects and "initial" mean lengths, *Nuclear Tracks, 17/3*, 261-265, 1990.

Duddy, I.R., P.F. Green, and G.M. Laslett, Thermal annealing of fission tracks in apatite 3. Variable temperature behaviour, *Chemical Geology (Isotope Geoscience Section), 73*, 25-38, 1988.

Dumitru, T.A., Subnormal geothermal gradients in the great valley forearc basin, California, during Franciscan subduction: a fission track study, *Tectonics, 7/6*, 1201-1221, 1988.

Fitzgerald, P.G., Uplift history of the Transantarctic Mountains in the Ross Sea Sector, (Unpublished) Ph.D., University of Melbourne, 1987.

Fleischer, R.L., and Price, P.B., Charged particle tracks in glass, *J. Appl. Phys., 34*, 2903-2904, 1963.

Fleischer R.L., and P.B. Price, Fission track evidence for the simultaneous origin of tektites and other natural glasses, *Geochimica et Cosmochimica Acta, 28*, 755-760, 1964.

Fleischer, R.L., and H.R. Hart, Fission track dating: Techniques and problems. In W.W. Bishop, D.A. Miller, and S. Cole (Editors), *Calibration of hominoid evolution*, Scottish Academic Press, Edinburgh, pp. 135-170, 1972.

Fleischer, R.L., P.B. Price, and R.M. Walker, The ion explosion spike mechanism for formation of charged particle tracks in solids, *J. Appl. Phys., 36*, 3645-3652, 1965a.

Fleischer, R.L., P.B. Price, and R.M. Walker, Effects of temperature, pressure, and ionization on the formation and stability of fission tracks in minerals and glasses, *J. Geophys. Res., 70*, 1497-1502, 1965b.

Fleischer, R.L., P.B. Price, and R.M. Walker, *Nuclear tracks in solids*, University of California Press, 605 pp., 1975.

Galbraith, R.F., On statistical models for fission track counts, Mathematical *Geology, 13*, 471-478, 1981.

Galbraith, R.F., On statistical estimation in fission track dating, Mathematical *Geology, 16/7*, 653-669, 1984.

Galbraith, R.F., and G.M. Laslett, Some remarks on statistical estimation in fission track dating, *Nuclear Tracks, 10*, 361-363, 1985.

Galbraith, R.F., G.M. Laslett, P.F. Green, and I.R. Duddy, Apatite fission track analysis: geological thermal history analysis based on three-dimensional random process of linear radiation damage, *Phil. Trans. R. Soc. Lond., 332*, 419-438, 1990.

Gleadow, A.J.W., Anisotropic and variable track etching characteristics in natural sphenes, *Nuclear Tracks, 2*, 105-117, 1978.

Gleadow, A.J.W., Fission track dating methods: what are the real alternatives?, *Nuclear Tracks, 5*, 3-14, 1981.

Gleadow, A.J.W., and K.A. Lovering, Geometry factor for external detectors in fission track dating, *Nuclear Tracks*, 1, 99-106, 1977.

Gleadow, A.J.W., and I.R. Duddy, A natural long-term track annealing experiment for apatite, *Nuclear Tracks, 5*, 169-174, 1981.

Gleadow, A.J.W., and P.G. Fitzgerald, Uplift history and structure of the Transantarctic Mountains: new evidence from fission track dating of basement apatites in the Dry Valleys area, southern Victoria Land, *Earth and Planetary Science Letters, 82*, 1-14, 1987.

Gleadow, A.J.W., Duddy, I.R., and Lovering, K.A., Fission track analysis: a new tool for the evaluation of thermal histories and hydrocarbon potential, *Petrol. Explor. Assoc. Aust. J., 23*, 9-102, 1983.

Gleadow, A.J.W., I.R. Duddy, P.F. Green, and J.F. Lovering, Confined fission track lengths in apatite: a diagnostic tool for thermal history analysis, *Contrib. Mineral. Petrol., 94*, 405-415, 1986a.

Gleadow, A.J.W., I.R. Duddy, P.F. Green, and K.A. Hegarty, Fission track lengths in the apatite annealing zone and the interpretation of mixed ages, *Earth and Planetary Science Letters, 78*, 245-254, 1986b.

Green, P.F., On the cause of shortening of spontaeous fission tracks in certain minerals, *Nuclear Tracks, 4*, 91-100, 1980.

Green, P.F., A new look at statistics in fission track dating, *Nuclear Tracks, 5*, 77-86, 1981a.

Green, P.F., Track-in-track length measurements in annealed apatites, *Nuclear Tracks, 5*, 121-128, 1981b.

Green, P.F., Comparison of zeta calibration baselines for fission track dating of apatite, zircon and sphene, *Chemical Geology, 58*, 1-22, 1985.

Green, P.F., The relationship between track shortening and fission track age reduction in apatite: influences of inherent instability, annealing anisotropy, length bias and system calibration, *Earth and Planetary Science Letters, 89*, 335-352, 1988.

Green, P,F., and Durrani, S.A., A quantitative assessment of geometry factors for use in fission track studies, *Nuclear Tracks, 2*, 207-213, 1978.

Green, P.F., and Hurford, A.J., Neutron dosimetry for fission track dating, *Nuclear Tracks, 9*, 231-241, 1984.

Green, P.F., I.R. Duddy, A.J.W. Gleadow, and P.R. Tingate, Fission-track annealing in apatites: track length measurements and the form of the arrhenius plot, *Nuclear Tracks, 10*, 323-328, 1985.

Green, P.F., I.R. Duddy, A.J.W. Gleadow, I.R. Tingate, and G.M. Laslett, Thermal annealing of fission tracks in apatite 1, *Chem. Geol., 59*, 237-253, 1986.

Green, P.F., I.R. Duddy, and G.M. Laslett, Can fission track annealing in apatite be described by first-order kinetics?, *Earth and Planetary Science Letters, 87*, 216-228, 1988.

Green, P.F., I.R. Duddy, G.M. Laslett, K.A. Hegarty, A.J.W. Gleadow, and J.F. Lovering, Thermal annealing of fission tracks in apatite 4, *Chem. Geol., 79*, 155-182, 1989a.

Green, P.F., I.R. Duddy, A.J.W. Gleadow, and J.F. Lovering, Apatite fission track analysis as a paleotemperature indicator for hydrocarbon exploration, in *Thermal history of sedimentary basins*, editors N.D. Naeser, and T.H. McCulloch, Springer-Verlag, New York, 1989b.

Hannah, G.C., C.H. Wescott, H.D. Lemmel, B.R. Leonard, J.S. Story, and P.M. Attree, Revision of values for the 2200 m/s neutron constants for four fissile nuclides, *Gen. Elec. Co. Atomic Energy Rev.*, 7, 3-92, 1969.

Huang, W.H., and R.M. Walker, Fossil α particle recoil tracks: a new method of age determination, *Science, 155*, 1103-1106, 1967.

Hughes, J.M., M. Cameron, and K.D. Crowley, Annealing of etchable fission-track damage in F-, OH-, Cl- and Sr-apatite: 2. Correlations with crystal structure, , *Nuclear Tracks, 17*, 417-418, 1990.

Hurford, A.J., Cooling and uplift patterns in the Lepontine Alps, South Central Switzerland, and an age of vertical movement of the Insubric fault line, *Contrib. Mineral. Petrol., 92*, 413-427, 1986.

Hurford, A.J., International union of geological sciences, subcommission and geochronology: recommendation for the standardization of the fission track dating calibration and data reporting, *Nuclear Tracks, 17*, 233-236, 1990.

Hurford, A.J., and A.J.W. Gleadow, Calibration of fission track dating parameters, *Nuclear Tracks, 1*, 41-48, 1977.

Hurford, A.J., and P.F. Green, A users guide to fission track dating calibration, *Earth and Planetary Science Letters, 59*, 343-354, 1982.

Hurford A.J., and P.F. Green, The zeta age calibration of fission-track dating, *Isotope Geosci., 1*, 285-317, 1983.

Hurford, A. J., F. J. Fitch, and A. Clarke, Revelation of the age structure of the detrital zircon population of two lower Cretaceous sandstones from the Weald of England by fission track dating, *Geol. Mag., 121*, 269-277, 1984.

Jaffrey, A.H., K.F. Flynn, L.E. Glendenin, W.C. Bentley, and A.M. Essling, Precision measurements of the half-lives and specific activities of ^{235}U and ^{238}U, *Phys. Rev., 4*, 1889-1906, 1971.

Johnson, N.M., V.E. McGee, and C.W. Naeser, A practical method of estimating standard error of age in the fission track dating method, *Nuclear Tracks, 3*, 93-99, 1979.

Jones, S.M., and R.K. Dokka, Modelling fission track annealing: an assessment of uncertainties, *Nuclear Tracks, 17*, 255-260, 1990.

Kamp, P.J.J., P.F. Green, and S.H. White, Fission track analysis reveals character of collisional tectonics in New Zealand,*Tectonics, 8*, 169-195, 1989.

Koons, P.O., Some thermal and mechanical consequences of rapid uplift: an example from the Southern Alps, New Zealand, *Earth and Planetary Science Letters, 86*, 307-319, 1987.

Lal, D., R.S. Rajan, and A.S. Tamhane, Chemical composition of nuclei of Z > 22 in cosmic rays using meteoritic minerals and detectors, *Nature, 221*, 33-37, 1969.

Laslett, G.M., W.S. Kendal, A.J.W. Gleadow, and I.R. Duddy, Bias in measurement in fission track length distributions, *Nuclear Tracks, 6*, 79-85, 1982.

Laslett, G.M., P.F. Green, I.R. Duddy, and A.J.W. Gleadow, Thermal modelling of fission tracks in apatite: 2. A quantitative analysis, *Chemical Geology, 65*, 1-13, 1987.

Lutz, T.M., and G. Omar, An inverse method of modeling thermal history from apatite fission track data, *Earth and Planetary Science Letters, 104*, 181-195, 1991.

McGee, V.E., and N.M. Johnson, Statistical treatment on experimental errors in the fission track dating method, *Mathematical Geology, 11*, 255-268, 1979.

Naeser, C.W., Fission track dating and geological annealing of fission tracks, in E. Jager and J.C. Hunziker (Editors), *Lectures in isotope geology*, Springer Verlag, New York, pp. 154-169, 1979.

Naeser, C.W., The fading of fission tracks in the geologic environment - data from deep drill holes (abstract), *Nuclear Tracks, 5*, 248-250, 1981.

Naeser, C.W., and R.B. Forbes, Variation of fission track ages with depth in two deep drill holes (Abstract), *Trans. Amer. Geophys. Union, 57*, 353, 1976.

Paul, T.A., and P.G. Fitzgerald, Transmission electron microscope investigation of fission tracks in fluorapatite, *Amer. Mineral., 77*, 336-344, 1992.

Price, P.B., and R.M. Walker, Chemical etching of charged particle tracks in solids, *J. Appl. Phys., 33*, 3407, 1962a.

Price, P.B., and R.M. Walker, Observation of charged particle tracks in solids, *J. Appl. Phys., 33,* 3400, 1962b.

Price, P.B., and R.M. Walker, Observation of fossil particle tracks in natural micas, *Nature, 196*, 732-734, 1962c.

Price, P.B., and R.M. Walker, Fossil tracks of charged particles in mica and the age of minerals, *J. Geophys. Res.*, 68, 4847-4862, 1963.

Roberts, J.H., R. Gold, and R.J. Armani, Spontaneous fission decay constant of ^{238}U, *Phys. Rev., 174*, 1482-1484, 1968.

Sieber, K.G., Compositional variation in apatites, Unpublished B.Sc. (Hons) Report, University of Melbourne, 1986.

Spadavecchia, A., and B. Hahn, *Die Rotationskammer und einige Anwendungen, Helv. Phys. Acta., 40*, 1063-1079, 1967.

Storzer, D., and G.A. Wagner, Correction of thermally lowered fission track ages of tektites, *Earth and Planetary Science Letters, 5*, 463-468, 1969.

Tagami, T., H. Ito, and S. Nishimura, Thermal annealing characteristics of spontaneous fission tracks in zircon, *Chemical Geology (Isotope Geoscience Section), 80*, 159-169, 1990.

Wagner, G.A., Apatite fission-track geochrono-thermometer to 60° C: projected length studies, *Chemical Geology (Isotope Geoscience Section), 72*, 145-153, 1988.

Wagner, G.A., and G.W. Reimer, Fission track tectonics: the tectonic interpretation of fission track apatite ages, *Earth and Planetary Science Letters, 14*, 263-268, 1972.

Wagner, G.A., and D. Storzer, Fission track length reductions in minerals and the thermal histories of rocks, *Trans. Am. Nucl. Soc., 15*, 127-128, 1972.

Wagner, G.A., and E. Hejl, Apatite fission-track age-spectrum based on projected track-length analysis, *Chemical Geology (Isotope Geoscience Section), 87*, 1-9, 1991.

Wagner, G.A., A.J.W. Gleadow, and P.G. Fitzgerald, The significance of the partial annealing zone in apatite fission track analysis: projected track length measurements and uplift chronology of the Transantarctic Mountains, *Chemical Geology (Isotope Geoscience Section), 79*, 295-305, 1989.

Zeitler, P.K., Cooling history of the NW Himalaya, Pakistan, *Tectonics, 4*, 127-151, 1985.

Zeitler, P.K., N.M. Johnson, C.W. Naeser, and R.A.K. Tahirkeli, Fission track evidence for Quaternary uplift of the Nanga Parbat region, Pakistan, *Nature, 298*, 255-257, 1982.

CHAPTER 3

Fission track analysis of the late Cenozoic vertical kinematics of continental Pacific crust, South Island, New Zealand

(Paper in press, *Journal of Geophysical Research*)

J. Mark Tippett
Peter J.J. Kamp

Geochronology Research Unit,
Department of Earth Sciences,
University of Waikato,
Private Bag 3105,
Hamilton 2001, New Zealand.

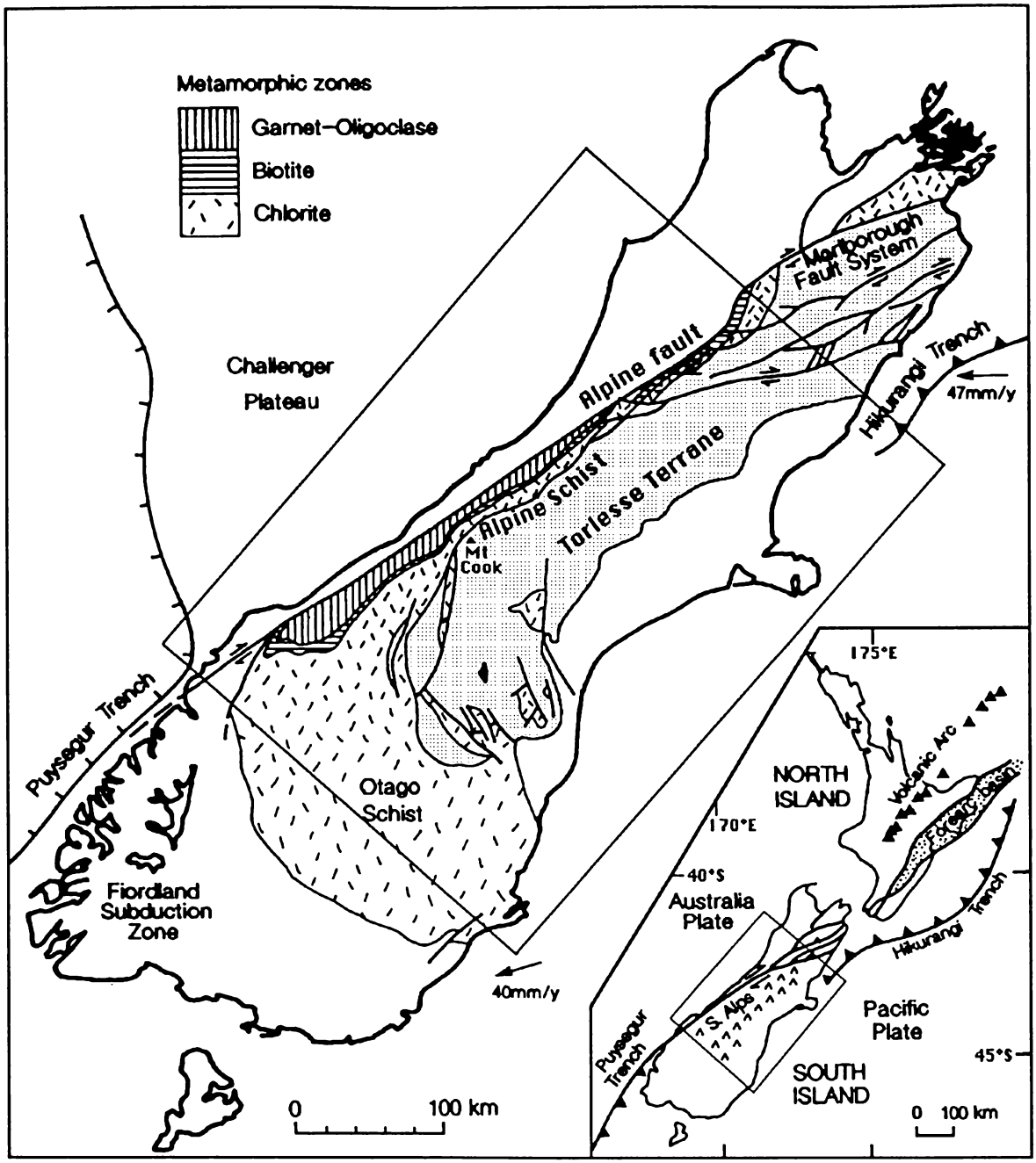


Fig. 1. Tectonic and geological map of South Island, New Zealand. Arrows indicate directions and rates of convergence. Box indicates area investigated, as outlined in Fig. 2.

ABSTRACT

During the late Cenozoic the Pacific plate has been converging obliquely with the Australia plate in South Island, New Zealand. A result of this convergence has been the growth of a major mountain range - the Southern Alps - at the leading edge of the Pacific plate. The results of fission track analysis of 140 samples from 13 transects across the alps reported here establish the late Cenozoic vertical kinematics (amount, age, and rate of rock uplift) of the Pacific crust underlying the alps. The late Cenozoic rock uplift of the Pacific crust is asymmetrical with respect to the Alpine fault, being a maximum (19 km) immediately east of the central part of the fault, with lesser values at the eastern (3 km), northern (10 km) and southern (8 km) extremities of the alps. The age of the start of rock uplift varies spatially across the Southern Alps, the earliest indications from fission track analysis being at 8 Ma at the southern end of the alps, decreasing to 5 Ma at the northern end and 3 Ma along the southeastern margin. This age variation reflects the longer time over which the southern parts of the alps have been in collision. The rate of propagation of rock uplift southeastwards into the Pacific plate has been 30 mm/yr, nearly 4 times the late Cenozoic average rate of convergence normal to the plate boundary. Late Cenozoic mean rock uplift rates range from a maximum of ~2.8 mm/yr at the Alpine fault to a minimum of ~1.0 mm/yr in the east, and have been sustained for periods of 3 - 8 m.y. Accompanying denudation has exhumed amphibolite grade rocks immediately east of the Alpine fault. Comparison of the late Cenozoic mean uplift rates with uplift rates derived from reset zircon data (2 - 10 mm/yr) near the Alpine fault shows that uplift has accelerated over time, but only significantly since 1.3 ± 0.3 Ma. There has not been any vertical drag on the Alpine fault. The amount of Mesozoic uplift ranged from minimal amounts north of Arthur's Pass, to ~3 km near Mount Cook, to 10 km in the south at Lake Wanaka.

INTRODUCTION

South Island of New Zealand contains an active zone of oblique continent-continent collision, involving the Australia and Pacific plates (Fig. 1). The Alpine fault is the locus of much of the oblique plate motion, and in its central segment, facilitates ramping of continental Pacific plate over continental Australia plate [*Allis*, 1981; *Kamp et al.*, 1992]. A major mountain range, the Southern Alps (S. Alps), is the surface manifestation of uplift of the leading edge of the Pacific plate, uplift which was initiated soon

after anomaly 5 (9.8 Ma) as a result of a change in the direction of migration of the Australia-Pacific pole of rotation [*Stock and Molnar*, 1982].

To date several attempts have been made to characterise the vertical kinematics of the Pacific plate part of the collision zone. Post-glacial rates of uplift have been estimated by *Wellman* [1979]. In the central segment of the collision zone modern rates of uplift vary considerably across the strike of the S. Alps, decreasing from ~10 mm/yr at the Alpine fault to 1 mm/yr near the eastern coastline of South Island. Various estimates of the "age" of the S. Alps have been proposed based on sedimentolgical [e.g. *Nathan et al.*, 1986] and geochronological evidence [e.g. *Adams*, 1981; *Adams and Gabites*, 1985; *Kamp et al.*, 1989]. These ages have ranged from 2 Ma to 12 Ma, and there has been a tendency by most authors to infer that the uplift ages estimated for particular sites apply to the whole of the S. Alps; that is, uplift started everywhere at the same time. The fission track study of three transects across the S. Alps by *Kamp et al.* [1989] indicated that there was a regional difference in the timing of uplift along the S. Alps: they showed that uplift was underway by ~6.6 Ma in the south at Haast Pass and by ~4.3 Ma in the north at Arthur's Pass. Their study also showed that profiles of the total amount of late Cenozoic uplift increased exponentially toward the Alpine fault, and that there had been an acceleration in the rate of uplift through the late Cenozoic.

This study extends the approach taken by *Kamp et al.* [1989] to the whole of the 300 km-long central sector of the S. Alps to obtain a more detailed understanding of regional variations in the vertical kinematics of the leading edge of the Pacific plate. We present 140 new apatite fission track sample ages and associated track length statistics, and 140 new zircon fission track sample ages, and interpret them in terms of pre-uplift paleotemperatures, amounts of rock uplift, rates of rock uplift, and timing of rock uplift. These data establish very clearly the structure of uplift of Pacific crust along 300 km of the oblique continent-continent collision zone.

Fission track analysis has previously been applied in thermo-tectonic studies of collisional, extensional, and intraplate tectonic settings. *Hurford* [1986] used apatite and zircon ages to constrain cooling and uplift patterns in the European Alps, while *Zeitler* [1985] reported reset fission track ages from the Himalaya of northern Pakistan, and interpreted the data in terms of the amount, timing, and rate (0.1-4 mm/yr) of uplift. The Transantarctic Mountains were studied by *Gleadow and Fitzgerald* [1987] who were able to

estimate the timing (~50 Ma) of the start of uplift, as well as uplift amounts and rates, by distinguishing between reset and annealed apatite fission track ages. *Moore et al.* [1986] examined the thermal evolution of the rifted continental margin in southeastern Australia. Apatite fission track ages that younged towards the margin represented a rift-related thermal event at ~80-100 Ma. *Green* [1986], in a study of the thermal and tectonic evolution of Northern England, showed that several kilometres of uplift and erosion at ~60 Ma were required to explain the observed pattern of fission track parameters.

GEOLOGICAL SETTING

The basement exposed in the S. Alps comprises mostly Triassic Torlesse Terrane greywacke and its metamorphosed equivalent, the Haast Schist (Fig. 1). The Haast Schist is divided geographically into Otago Schist and Alpine Schist (Fig. 1).

The Otago Schist belt forms a northwest-striking anticlinorium. Approaching the belt from the northeast, prehnite-pumpellyite grade Torlesse greywackes pass through pumpellyite-actinolite facies to greenschist facies rocks (chlorite and biotite zones). The chlorite zone has been divided into textural zones (1-4) on the basis of the development of schistosity [*Hutton and Turner*, 1936; *Mason*, 1962; *Bishop*, 1972; *Cooper*, 1972]. The maximum temperature and pressure conditions attained by the Otago Schist in the biotite zone are estimated at about 400°C and 4.5 kbar [*Yardley*, 1982; *Jamieson and Craw*, 1987]. Metamorphism is considered to have occurred in the earliest Jurassic [*Adams et al.*, 1985]. Post-metamorphic deformation of the schists includes crenulations and kinkfolds [*Turnbull*, 1981], and high-angle northeast-trending reverse faults, which are responsible for the basin and range topography of the Otago region [*Yeats*, 1987; *Beanland and Barrow-Hurlbert*, 1988].

The Alpine Schist crops out in a narrow belt immediately to the east of the Alpine fault (Fig. 1). Mid-amphibolite grade rocks (oligoclase zone) pass southeastward into the garnet, biotite, and chlorite zones of greenschist facies [*Mason*, 1962]. The chlorite zone has been divided into four textural zones as in the Otago Schist. The Alpine Schist attains higher grade than the Otago Schist: estimates of the peak temperature of the oligoclase zone in the central Alpine fault area range from 490-570°C [*Grapes and Otsuki*, 1983; *Johnstone and White*, 1983; *Findlay*, 1985]. The Alpine Schist passes

eastward into Torlesse greywacke of pumpellyite-actinolite and then prehnite-pumpellyite metamorphic grade. The Torlesse greywacke appears to have been accreted in belts which young to the northeast (with respect to present-day geography) [*Spörli*, 1978]. The depositional ages range from Permian to Triassic in the S. Alps, and as young as Early Cretaceous in Marlborough.

Both the Alpine Schist and Torlesse greywacke have suffered multiple phases of deformation prior to the late Cenozoic. *Findlay* [1979,1987] showed that the schists display Cenozoic regional folds (amplitude >3 km) in which steeply dipping zones of ductile shear separate km-scale pod-shaped domains of low dipping limbs within which Mesozoic deformational structures are preserved. The greywacke strata are steeply dipping, with crush zones, intense jointing, disruption of bedding, and folding being widely present [*Bradshaw*, 1972; *Mackinnon*, 1980; *Spörli*, 1979]. *Findlay and Spörli* [1984] recognised several episodes of folding related to the Mesozoic Rangitata Orogeny.

Late Cenozoic deformation in the S. Alps is a consequence of the distributed strain of collision and dextral transform movement across the plate boundary [*Walcott*, 1978]. Many of the features of the late Cenozoic fault pattern in the greywacke are inherited from Cretaceous fractures [*Spörli*, 1979], with northeast and northwest trending faults accommodating varying amounts of strike-slip and reverse movement [*Berryman*, 1979]. In addition to the seismic deformation resulting in fault movements, an aseismic ductile flow of crustal rocks has been identified by *Walcott* [1978]. The late Cenozoic deformation is responsible for a component of the dextral arcuate structure of the basement terranes in southern South Island [*Walcott*, 1978; *Norris*, 1979; *Kamp*, 1987] (Fig. 1).

TECHNIQUES

Fission Track Analysis

Fission track analysis is a method of analysing low temperature (zircon <265° C; apatite <125° C) thermal histories, involving measurement under an optical microscope of the density and lengths of fission tracks in apatite and zircon crystals separated from host rocks. A latent fission track is a linear path of atomic-scale disruption caused by spontaneous fission of ^{238}U within a crystal [*Fleischer et al.*, 1965]. Latent tracks need to be

chemically etched to become observable. The areal density of (etched) fission tracks across a cut and polished crystal surface is proportional to both time and ^{238}U concentration. By comparing the counts of spontaneous tracks arising from ^{238}U, and tracks induced from fission of ^{235}U by thermal neutron irradiation, inter-crystal differences in uranium concentration can be normalised and fission track ages calculated. Track length data are derived from 'horizontally confined' tracks that lie within the crystal and parallel to the etched surface.

Fission track damage in apatite is unstable over geological (10^7 m.y.) time at temperatures in the range ~20°-125° C [*Green*, 1980; *Gleadow and Duddy*, 1981], and tracks shorten (anneal) depending on the maximum temperature experienced [*Duddy et al.*, 1988]. Annealing involves repair of latent fission track damage whereby atoms are driven by strain energy from their displaced positions into proper crystallographic sites [*Carlson*, 1990]. The final length of an etched fission track is determined primarily by the maximum temperature to which it is exposed [*Duddy et al.*, 1988]; however, because fission tracks accumulate continuously over time and have a constant 'birth' length of about 16 ± 1 μm, the whole of the thermal history since the last resetting event will be reflected in the statistics of the track length distribution. The distribution of horizontally confined track lengths in apatite is therefore diagnostic of the style of thermal history experienced by a sample [*Gleadow et al.*, 1986a]. An apatite fission track age must similarly be interpreted in terms of both the time over which tracks have been accumulating and the degree of annealing that has taken place; that is, the thermal history of a sample.

Sampling Design

Because it had been established earlier that the axis of uplift trends northeast [*Wellman*, 1979; *Kamp et al.*, 1989], we sampled a number of transects starting at the Alpine fault and extending to the southeast across the S. Alps. The variation in fission track (FT) data across the S. Alps transects studied by *Kamp et al.* [1989] also formed a guide for sample location and density within each transect. In particular, from the locations of the bases of the exhumed apatite and zircon annealing zones identified by *Kamp et al.* [1989], it is possible to predict the likely locations of the same features in other transects, allowing a higher sample density to be obtained where required. Identification of the bases of the annealing zones is

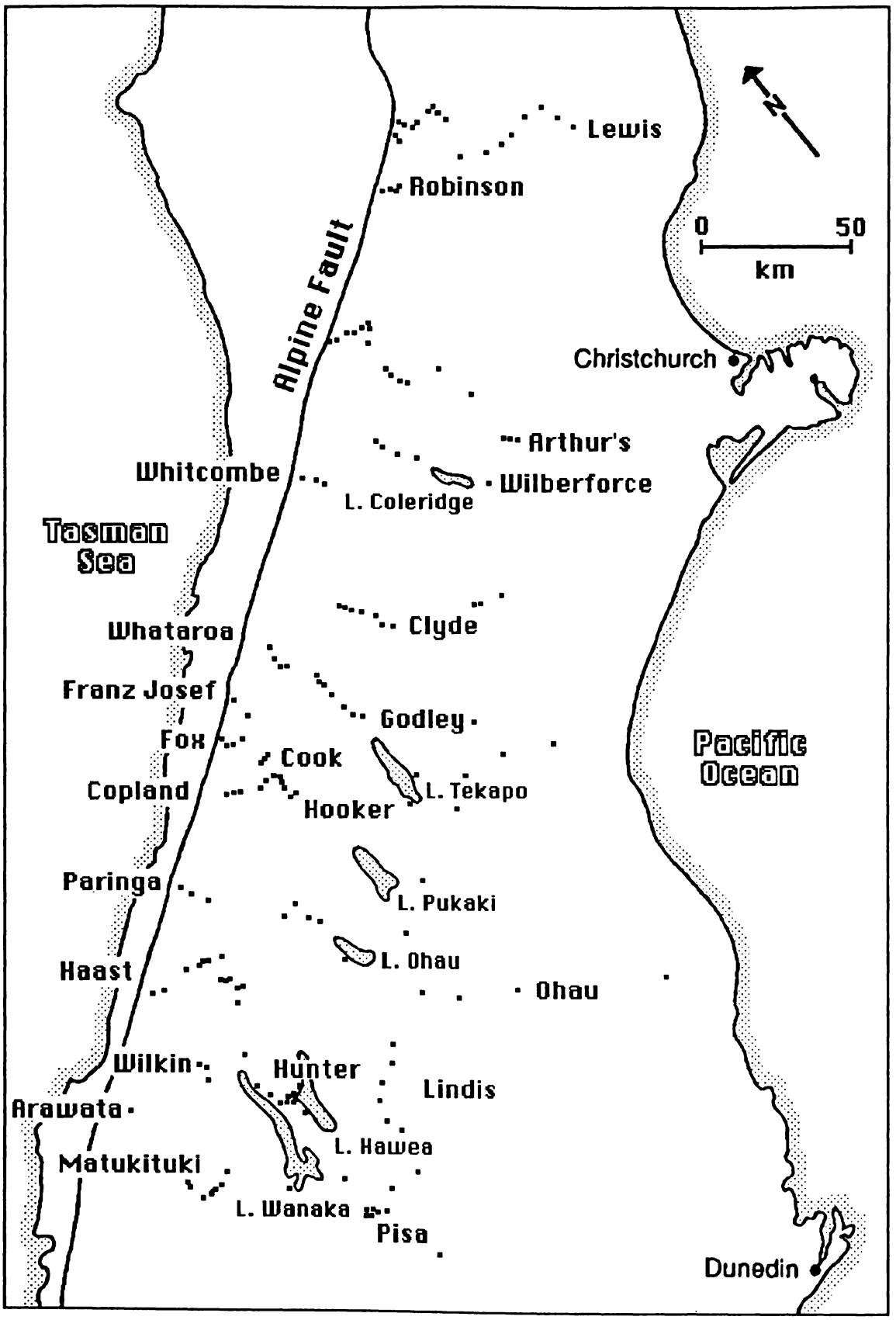


Fig. 2. Locations of samples [including those of *Kamp et al.*, 1989] used in this study, and locations and names of transects referred to in the text. Location data for each sample are reported in Table 3.

important in terms of establishing the age of initiation of late Cenozoic uplift. Sample locations are shown in Fig. 2.

Experimental Procedures

The experimental procedures used in this study followed those reported by *Green* [1986]. Apatite and zircon concentrates were separated from 4 kg whole rock samples using standard magnetic and heavy liquid techniques. Apatite separates were mounted in Petropoxy™ resin at 140°C on glass slides, then ground with silicon carbide paper to reveal internal surfaces of crystals. After polishing with a slurry of alumina powder, the crystals were etched in 5M HNO_3 for 20 seconds at 24°C. Zircon separates were embedded in FEP Teflon™ at ~300°C, ground to reveal internal surfaces, and polished using alumina slurry followed by 1μm diamond powder. Etching of zircons took place in molten KOH-NaOH eutectic at ~205°C for times ranging from 8 to 56 hours. After etching, zircon mounts were cleaned by immersion in dilute HF for one hour.

After etching, all mounts were cut down to 1 x 1.5 cm and cleaned with detergent and alcohol. Low-uranium mica external detectors were then sealed in intimate contact with the mounts using envelopes of heat-shrink plastic. Pinpricks were made at the corners of each mount-mica sandwich for purposes of alignment during subsequent track counting. Each batch of mounts for irradiation was then stacked vertically, between two pieces of uranium dosimeter glass (SRM 612 for apatites, CN1 for zircons) each of which had also been sealed in intimate contact with a mica detector. Each stack was packed into a cannister and irradiated in the X-7 facility of the HIFAR reactor, New South Wales, Australia. Nominal fluences of 1×10^{16} n cm $^{-2}$ to 5×10^{16} n cm $^{-2}$ for apatites and 3×10^{15} n cm $^{-2}$ for zircons were used.

After irradiation, the mica detectors were etched in 40% HF for 24 minutes at 24°C. Each mount-mica pair was mounted in a mirror-image relationship on a glass slide ready to be counted. Fission track density determinations were undertaken using a Zeiss Axioplan™ optical microscope, using 100x dry objectives with 10x eyepieces and 1.25x tube factor. Tracks were counted in a 10 x 10 unit eyepiece grid, the dimensions of which were calibrated against a diffraction grating. Because of anisotropic annealing in both apatite and zircon, only apatites with sharp polishing scratches indicating a section parallel to the c-axis, and zircons

with well-etched tracks in all orientations, were counted. In order to measure the thermal dose received by the samples, track densities of the mica detectors contacting the standard glasses at the top and bottom of each cannister were counted.

Lengths of horizontally confined fission tracks in apatites were measured using a Nikon™ Optiphot optical microscope at 1250x with a digitizing tablet interfaced with a Macintosh™ computer. The length of each suitable track was measured by digitizing the track ends using an image of the digitizing tablet superimposed onto the field of view via a drawing tube. Tracks were measured on grains (as for density determinations) with sharp polishing scratches. Only horizontal tracks were measured. As many suitable tracks as possible up to 100 were measured on each mount.

Calibration of Fission Track Analysis

Fission track ages reported here have been determined by using the zeta calibration approach, which eliminates the need for explicit thermal neutron dosimetry and selection of a value for the spontaneous fission decay constant of ^{238}U. Details of this approach are reported in *Hurford and Green* [1983] and *Green* [1985]. Personal calibration of fission track density measurements for both apatite and zircon was carried out on recommended age standards [*Hurford and Green*, 1983; *Green*, 1985; *Hurford and Watkins*, 1987], the results of which are presented in Table 1. Mean weighted zetas for JMT of 354.9 ± 4.3 (SRM 612) for apatite and 133.9 ± 1.4 (CN1) for zircon were determined.

Calibration of length measurements of horizontally confined tracks in apatite was performed by using the age standards on which density calibrations were made. The resulting mean track lengths and track length distributions for JMT are similar to those reported by *Gleadow et al.* [1986a]. Table 2 shows results of track length measurement calibration.

Table 1. Results of calibration of fission track age determinations by the zeta approach.

Age Standard and Irradiation No.	Mineral and No. crystals	Spontaneous ρ_s	Spontaneous N_s	Induced ρ_i	Induced N_i	$P(\chi^2)$ (%)	$\overline{\rho_s/\rho_i} \pm 1\sigma$	Glass	Dosimeter ρ_d	Dosimeter N_d	$\zeta \pm 1\sigma$
Durango pt836	apatite (21)	0.157	873	1.111	6179	35		SRM 612	1.2200	15415	365.2 ± 13.8
Durango pt836	apatite (21)	0.153	182	1.121	1332	96		SRM 612	1.2200	15415	377.7 ± 30.1
Durango wk043	apatite (20)	0.157	339	0.814	1763	100		SRM 612	0.8876	5267	368.9 ± 22.6
Durango wk044	apatite (19)	0.155	302	0.768	1492	59		SRM 612	0.8950	4426	347.5 ± 22.7
Fish Canyon pt836	apatite (25)	0.167	209	1.258	1572	63		SRM 612	1.2200	15415	344.8 ± 25.9
Fish Canyon pt836	apatite (25)	0.197	508	1.424	3673	49		SRM 612	1.2200	15415	331.4 ± 16.4
Fish Canyon wk043	apatite (25)	0.173	233	0.959	1292	78		SRM 612	0.8876	5267	349.3 ± 25.7
Fish Canyon wk044	apatite (25)	0.176	298	1.031	1749	78		SRM 612	0.8950	4426	366.7 ± 24.1
Mt Dromedary pt836	apatite (25)	0.624	3023	1.356	6571	8		SRM 612	1.2200	15415	354.4 ± 8.5
Mt Dromedary pt836	apatite (25)	0.688	3329	1.491	7219	42		SRM 612	1.2200	15415	353.6 ± 8.2
Mt Dromedary wk043	apatite (20)	0.656	702	1.098	1175	43		SRM 612	0.8876	5267	375.1 ± 18.7
Mt Dromedary wk044	apatite (18)	0.845	872	1.313	1356	86		SRM 612	0.8950	4426	345.6 ± 16.0
									Apatite	Mean ζ	354.9 ± 4.3
Buluk wk029	zircon (21)	0.640	403	2.029	1278	10		CN1	0.7927	3920	129.8 ± 7.7
Buluk pt845	zircon (15)	0.742	306	1.161	479	37		U3	0.5556	2698	91.4 ± 6.9
Tardree wk029	zircon (30)	4.568	2643	4.286	2480	6		CN1	0.8006	3959	138.2 ± 4.6
Tardree wk029	zircon (28)	5.344	4445	4.745	3947	74		CN1	0.8083	3997	129.6 ± 3.7
Tardree pt845	zircon (15)	5.460	2176	2.537	1011	9		U3	0.5556	2698	98.6 ± 4.3
Mt Dromedary wk029	zircon (18)	9.739	2013	5.656	1169	67		CN1	0.8162	4036	141.5 ± 5.7
Mt Dromedary wk029	zircon (24)	10.571	5008	5.961	2824	27		CN1	0.8239	4074	136.1 ± 4.0
Mt Dromedary pt845	zircon (6)	8.355	471	2.306	130	68		U3	0.5556	2698	98.8 ± 10.0
Mt Dromedary pt845	zircon (4)	12.504	371	3.269	97	75		U3	0.5556	2698	93.6 ± 10.8
Mt Dromedary pt845	zircon (6)	9.459	1001	2.551	270	92		U3	0.5556	2698	96.6 ± 6.9
Fish Canyon wk029	zircon (29)	3.982	3525	7.864	6961	<0.1	0.512 ± 0.017	CN1	0.8396	4152	130.1 ± 5.1
Fish Canyon pt845	zircon (19)	4.364	2857	3.747	2453	32		U3	0.5556	2698	86.4 ± 3.1
Fish Canyon pt845	zircon (8)	4.553	815	4.246	760	83		U3	0.5556	2698	93.9 ± 5.2
Fish Canyon pt845	zircon (29)	4.578	3690	4.438	3577	88		U3	0.5556	2698	97.6 ± 3.2
Lake Mountain wk029	zircon (3)	15.001	816	2.335	127	24		CN1	0.8473	4190	139.0 ± 13.4
Lake Mountain pt846	zircon (7)	12.210	797	3.891	254	17		U3	2.5420	6033	94.9 ± 7.0
Lake Mountain pt846	zircon (10)	15.046	1741	5.090	589	57		U3	2.5420	6033	100.7 ± 5.0
Mt Warning wk029	zircon (12)	2.700	916	6.527	2214	49		CN1	0.8708	4306	126.8 ± 5.5
Mt Warning pt845	zircon (6)	3.589	614	3.945	675	12		U3	0.5556	2698	90.4 ± 5.4

Age Standard and Irradiation No.	Mineral and No. crystals	Spontaneous ρ_s	Spontaneous N_s	Induced ρ_i	Induced N_i	$P(\chi^2)$ (%)	$\overline{\rho_s/\rho_i} \pm 1\sigma$	Glass	Dosimeter ρ_d	Dosimeter N_d	$\zeta \pm 1\sigma$
Mt Warning pt845	zircon (13)	3.470	2694	3.954	3070	<0.1	0.918 ± 0.058	U3	0.5556	2698	89.5 ± 6.0
										Zircon Mean ζ	133.9 ± 1.4

(i) Analyses of apatite and zircon age standards by external detector method; track densities (ρ) are ($x10^6$ cm^{-2}); N = number of tracks counted. (ii) $P(\chi^2)$ is the probability of obtaining χ^2 value for v degrees of freedom where v = (No. of crystals - 1) [*Galbraith*, 1981]; pooled p_s/p_i ratio used to calculate ζ and uncertainty where $P(\chi^2)$ >5%; mean p_s/p_i ratio used to calculate ζ and uncertainty where $P(\chi^2)$ <5% [Green, 1981]. (iii) Standard ages used are: Fish Canyon Tuff 27.8 ± 0.7 Ma, Tardree Rhyolite 58.7 ± 1.1 Ma [*Hurford and Green*, 1983]; Durango Apatite 31.4 ± 0.5, Mount Dromedary Igneous Complex 98.7 ± 0.6 Ma, Lake Mountain Rhyodacite 367.6 ± 1.5 Ma, Mount Warning Complex 22.8 ± 0.5 [*Green*, 1985]; Buluk Member tuff 16.2 ± 0.2 Ma [*Hurford and Watkins, 1987*]. (iv) An uncertainty component from independent age is included in the error on each ζ value; apatite/zircon mean ζ and its error weighted according to uncertainties on individual ζ values. (v) Apatite and zircon ζ determinations fulfill the requirements proposed by *Hurford* [1990]. (vi) Zircon mean ζ calculated for CN1, with U3 sample determinations being converted to CN1 terms by using the factor of *Green* [1985].

Table 2. Results of calibration of horizontally confined track length determinations on apatite.

Standard	Sample number	Number of tracks	Mean length (μm) ± 1σ	Standard deviation (μm)
Durango	8794-1,2,3	40	14.71 ± 0.18	1.14
Durango	Sample mean		14.71 ± 0.18	
Fish Canyon	8794-4	63	15.15 ± 0.15	1.17
Fish Canyon	8794-5	51	15.35 ± 0.13	0.90
Fish Canyon	8794-23	79	15.14 ± 0.10	0.87
Fish Canyon	Sample mean		15.20 ± 0.07	
Mt Dromedary	8794-6/1	49	14.84 ± 0.15	1.07
Mt Dromedary	8794-6/2	67	14.83 ± 0.14	1.14
Mt Dromedary	8794-7	70	14.66 ± 0.14	1.19
Mt Dromedary	Sample mean		14.77 ± 0.08	

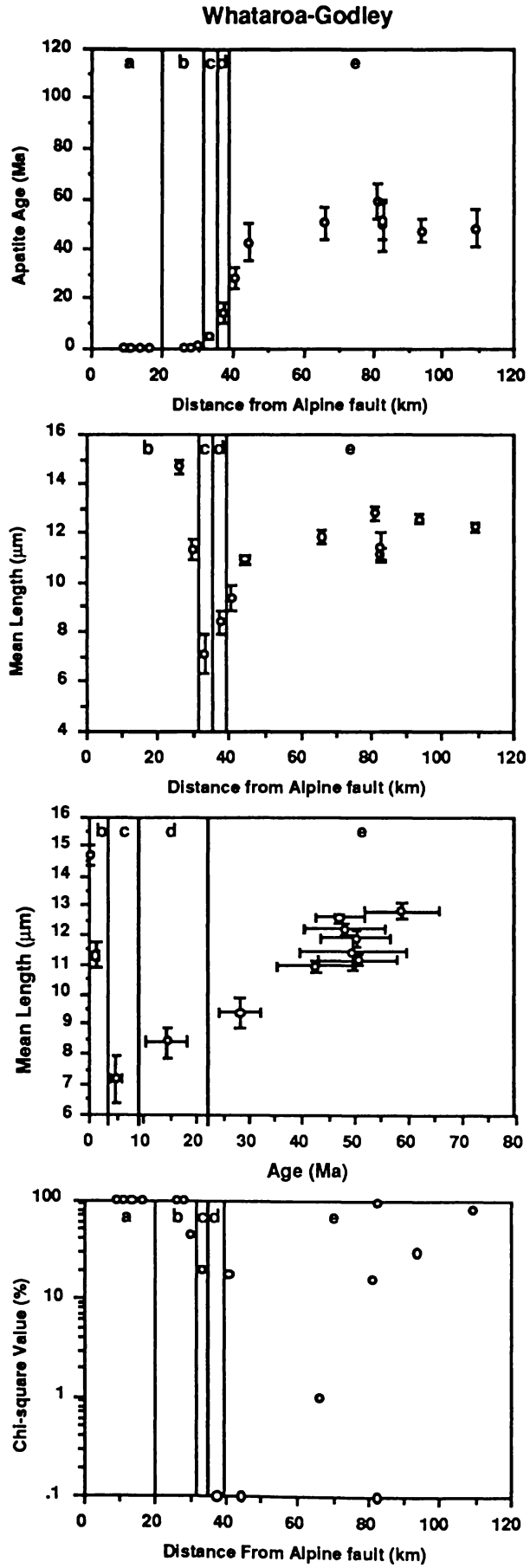


Fig. 3. Apatite FT data for the Whataroa-Godley transect. Lettering a-e refers to sample zones described in text. Errors are 1σ.

RESULTS AND INTERPRETATIONS

Apatite Data

One hundred and forty new apatite FT ages are reported as part of this study. In addition statistics about horizontally confined track lengths for 56 samples are reported. All the data are presented in Table 3.

The apatite data show a simple pattern: in each transect, apatite age increases monotonically to the southeast normal to the Alpine fault, while mean length decreases initially and then increases with distance from the fault. This pattern is inferred to have resulted from rapid uplift of a crustal section such that apatites with reset ages occur in a zone adjacent to the Alpine fault, and an exhumed apatite annealing zone occurs in a parallel zone farther to the southeast. The zone of reset apatite data corresponds to crustal section uplifted from depths greater than those of the exhumed annealing zone. The data from which this interpretation is drawn are illustrated in a series of graphs for a selected transect (Fig. 3).

In zone a (Fig. 3) apatite ages are close to zero and chi-squared values [*Galbraith*, 1981] are very high (close to 100%) representing a tight peaked distribution. In zone b ages increase slightly and confined track lengths are typically 12-16 μm. Samples from zones a and b are inferred to be reset, meaning that before uplift started their apatites contained no latent fission tracks. Farther from the Alpine fault, each transect typically has a sample (zone c) with a high $P(\chi^2)$ value, a short mean length (~8 μm) and a wide distribution of track lengths including some very short (1-2 μm) tracks. This zone would have resided at or near the base of the annealing zone prior to the start of uplift. The next zone (d) southeast of the Alpine fault contains samples with greater age than zones to the northwest, and in particular samples have a broad range of single grain ages ($P(\chi^2)$ <5%) and a low mean length value (~9 μm). These parameters indicate that zone d contains annealed samples. In zone e the mean sample ages increase farther as does the mean length, suggesting lesser amounts of annealing and lower ambient temperatures prior to uplift.

Fig. 4 illustrates all of the apatite data from the S. Alps for which there are length measurements. Samples with reset signatures are clearly distinguished by their longer mean lengths and younger ages from those that belong to the exhumed annealing zone. The data from the former

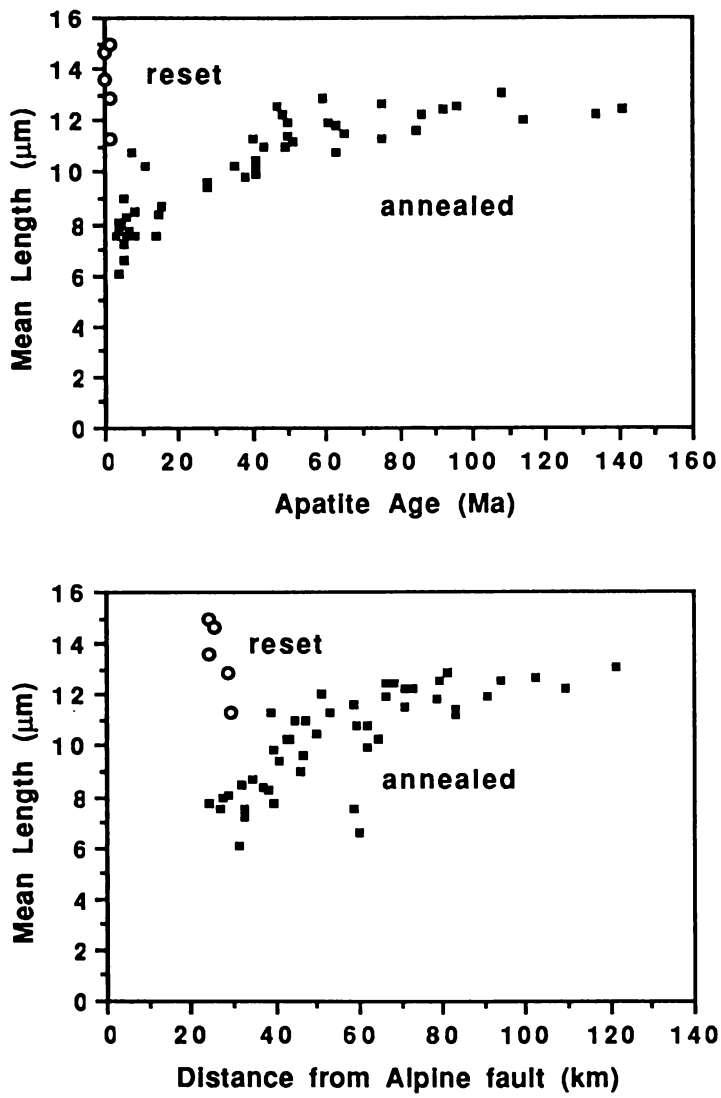


Fig. 4. Variation of mean length with apatite age, and mean length with distance from the Alpine fault, for all S. Alps samples on which lengths were measured except Lindis, Pisa, and Matukituki transects. Note the distinction between annealed and reset samples.

Table 3. Fission track data for Southern Alps samples.

Sample Number	Transect	Coordinate x	Coordinate y	Elevation (m)	Distance from Alpine fault (km)	Mineral	No. crystals	Spontaneous ρ_s	Spontaneous N_s	Induced ρ_i	Induced N_i	$P(\chi^2)$ (%)	$\overline{\rho_s/\rho_i}$ ± 1σ	ρ_d	N_d	Age (Ma) ±1σ	Mean Track Length ± 1σ (μm)	Standard Deviation (μm)	No. Lengths
20	Matukituki	2537	4424	535	33.1	Apatite	15	0.000	0	0.025	0			4.580	3623	0 ± ∞			
						Zircon	2	4.449	44	10.313	102	65		0.997	4929	29 ± 5			
21	Matukituki	2532	4411	520	34.3	Apatite	15	0.000	0	0.122	87			4.539	3591	0 ± ∞			
						Zircon	2	3.623	43	7.920	94	5.2		0.989	4891	30 ± 6			
22	Matukituki	2544	4348	490	39.3	Apatite	15	0.000	0	0.037	9			4.497	3558	0 ± ∞			
23	Matukituki	2579	4341	395	42.8	Apatite	15	0.000	0	0.094	52			4.456	3526	0 ± ∞			
						Zircon	3	3.559	88	4.975	123	12		0.981	4863	47 ± 7			
24	Matukituki	2590	4344	455	43.3	Apatite	15	0.000	0	0.034	13			4.415	3493	0 ± ∞			
25	Matukituki	2629	4342	365	45.0	Apatite	15	0.000	0	0.679	219			4.374	3460	0 ± ∞			
						Zircon	11	7.930	698	8.793	774	5.4		0.974	4815	59 ± 3			
26	Matukituki	2675	4363	365	45.8	Apatite	15	0.000	0	0.071	87			4.333	3428	0 ± ∞			
27	Matukituki	2813	4171	335	66.4	Apatite	20	0.193	93	2.522	1217	81		4.261	3371	58 ± 6	12.64 ± 0.62	1.64	7
						Zircon	11	5.300	456	4.405	379	22		1.065	5265	85 ± 6			
28	Pisa	2994	4072	120	83.5	Apatite	20	0.123	88	1.764	1263	85		4.291	3395	53 ± 6	12.91 ± 0.31	0.98	10
						Zircon	9	13.512	588	9.123	397	3.0	1.541 ± 0.159	1.065	5265	109± 11			
29	Pisa	3110	3934	290	100.9	Apatite	40	0.202	202	3.155	3155	34		4.250	3363	48 ± 4	12.66 ± 0.56	2.11	14
						Zircon	13	6.977	1318	4.997	944	17		0.950	4700	88 ± 4			
30	Pisa	3043	3885	610	100.4	Apatite	15	0.000	0	0.028	17			4.209	3330	0 ± 0			
						Zircon	4	9.635	162	7.256	122	95		1.065	5265	94 ± 11			
31	Pisa	3026	3895	870	98.7	Apatite	20	0.014	8	0.388	220	100		4.168	3297	27 ± 10			
						Zircon	10	6.329	795	4.363	548	76		0.935	4624	90 ± 3			
32	Pisa	3017	3905	1400	97.5	Apatite	15	0.000	0	0.041	25			4.127	3265	0 ± ∞			
33	Pisa	3011	3909	1630	96.8	Apatite	15	0.000	0	0.068	70			4.085	3232	0 ± ∞			
						Zircon	4	8.658	137	6.320	100	79		0.927	4586	86 ± 11			
34	Pisa	3004	3910	1965	96.3	Apatite	15	0.000	0	0.007	6			4.044	3200	0 ± ∞			
						Zircon	3	6.450	185	4.916	141	86		1.065	5265	93 ± 11			
35	Pisa	3092	3638	185	120.8	Apatite	30	0.049	75	1.060	1618	96		4.003	3167	33 ± 4	13.06 ± 0.58	1.43	6
						Zircon	13	8.542	735	6.694	576	65		1.065	5265	90 ± 5			
36	Arawata	2543	4763	90	8.2	Apatite	15	0.000	0	0.054	29			4.674	3698	0 ± ∞			
						Zircon	14	0.906	147	11.597	1881	22		1.065	5265	5.6 ± 0.5			
37	Wilkin	2855	4745	610	25.3	Apatite	15	0.000	0	0.015	6			4.640	3671	0 ± ∞			
						Zircon	10	3.033	237	11.813	923	33		0.897	4433	15 ± 1			
38	Wilkin	2857	4740	610	25.7	Apatite	15	0.000	0	0.118	71			4.607	3645	0 ± ∞			
						Zircon	4	1.171	22	8.887	167	24		0.889	4395	7.8 ± 1.8			
39	Wilkin	2869	4718	610	27.9	Apatite	15	0.000	0	0.210	42			4.573	3618	0 ± ∞			
						Zircon	7	3.033	219	8.061	582	98		0.881	4357	22 ± 2			
40	Wilkin	2844	4675	335	30.3	Apatite	15	0.000	0	0.150	92			4.540	3592	0 ± ∞			
						Zircon	6	4.118	167	8.706	353	52		0.873	4319	28 ± 3			
41	Wilkin	3010	4665	305	39.8	Apatite	15	0.000	0	3.789	667			4.506	3565	0 ± ∞			
						Zircon	4	3.184	233	3.443	252	88		1.065	5265	66 ± 6			
42	Wilkin	2986	4487	305	50.8	Apatite	20	0.002	1	1.893	790	100		4.473	3539	1.0 ± 1.0			
						Zircon	13	6.720	844	8.360	1050	89		1.025	5064	55 ± 3			
43	Hunter	2991	4438	395	55.5	Apatite	15	0.000	0	0.386	132			4.439	3512	0 ± ∞			
						Zircon	5	6.587	228	6.673	231	97		1.065	5265	70 ± 7			
44	Hunter	3006	4436	365	56.5	Apatite	15	0.005	1	0.292	62			4.406	3486	0 ± ∞			
						Zircon	9	9.010	802	7.437	662	94		1.007	4979	81 ± 5			
45	Hunter	3015	4436	395	57.0	Apatite	15	0.000	0	0.379	69			4.339	3433	0 ± ∞			
						Zircon	7	6.258	359	4.690	289	85		1.065	5265	95 ± 8			

Table 3 ctd

Sample Number	Transect	Coordinate x	Coordinate y	Elevation (m)	Distance from Alpine fault (km)	Mineral	No. crystals	Spontaneous ρ_s	Spontaneous N_s	Induced ρ_i	Induced N_i	$P(\chi^2)$ (%)	$\overline{\rho_s/\rho_i}$ ± 1σ	ρ_d	N_d	Age (Ma) ±1σ	Mean Track Length ± 1σ (μm)	Standard Deviation (μm)	No. Lengths
46	Hunter	3032	4435	425	58.0	Apatite	15	0.000	0	0.133	49			4.305	3406	0 ± ∞			
						Zircon	6	10.245	699	6.721	452	67		0.990	4894	100 ± 6			
47	Hunter	3042	4435	380	58.5	Apatite	10	0.000	0	1.334	91			1.080	2136	0 ± ∞			
						Zircon	7	10.681	581	7.207	392	7		0.962	4852	97 ± 7			
48	Hunter	3057	4439	410	59.0	Apatite	25	0.079	20	2.994	761	<0.1	0.072 ± 0.026	1.072	2120	14 ± 5	7.50 ± 1.57	2.98	6
						Zircon	12	8.930	892	4.986	498	23		0.973	4809	116 ± 7			
49	Hunter	3084	4443	380	60.2	Apatite	20	0.056	15	1.768	472	98		0.888	5267	5.0 ± 1.3	6.55 ± 1.70	3.69	7
						Zircon	6	5.812	684	3.237	381	2.0	1.881 ± 0.163	1.065	5265	133 ± 12			
50	Hunter	3090	4452	395	59.7	Apatite	20	0.080	32	2.858	1142	3.0	0.039 ± 0.011	1.055	2088	7.3± 2.0	10.74 ± 0.65	1.05	5
						Zircon	7	10.720	827	6.183	477	58		1.065	5265	122 ± 7			
51	Haast	3098	5028	75	17.4	Apatite	15	0.000	0	0.085	37			4.238	3353	0 ± ∞			
						Zircon	5	0.556	22	9.707	384	61		0.947	4682	3.6± 0.8			
52	Haast	3117	5031	90	18.1	Apatite	15	0.000	0	0.133	47			4.533	3586	0 ± ∞			
						Zircon	6	0.945	86	10.628	967	27		0.939	4640	5.6± 0.6			
53	Haast	3130	5023	90	19.4	Apatite	15	0.000	0	0.057	25			4.497	3558	0 ± ∞			
54	Haast	3128	4935	135	25.3	Apatite	15	0.011	7	4.046	2809	100		4.288	3393	2.0± 0.8			
						Zircon	9	0.757	125	6.291	1039	83		0.921	4555	7.4± 0.7			
55	Haast	3135	4928	170	26.4	Apatite	15	0.000	0	1.874	621			4.460	3529	0 ± ∞			
56	Haast	3146	4919	290	27.8	Apatite	15	0.000	0	0.004	3			1.207	2984	0 ± ∞			
						Zircon	7	4.780	156	13.757	449	25		1.065	5265	25 ± 2			
57	Haast	3148	4878	455	30.6	Apatite	25	0.022	3	2.996	406	98		4.388	3471	5.8 ± 3.3			
						Zircon	8	6.930	562	4.131	335	<0.1	1.891 ± 0.241	0.896	4428	112± 15			
58	Haast	3167	4868	1310	32.4	Apatite	22	0.069	20	2.855	833	<0.1	0.050 ± 0.024	0.888	5267	7.8 ± 3.8	7.50 ± 1.36	2.94	7
						Zircon	7	9.210	1758	5.506	1051	42		0.887	4385	99 ± 4			
59	Lindis	3226	3926	305	107.3	Apatite	15	0.071	21	1.559	458	100		4.351	3443	35 ± 8			
						Zircon	10	11.020	1188	8.534	920	38		0.878	4343	76 ± 4			
60	Lindis	3276	4078	395	97.0	Apatite	29	0.321	162	3.572	1805	100		4.315	3414	68 ± 6	11.56 ± 0.62	2.46	16
61	Lindis	3256	4140	470	91.3	Apatite	30	0.709	239	1.951	658	100		0.888	5267	57 ± 4	11.78 ± 0.39	2.18	31
						Zircon	8	7.821	526	6.275	422	100		0.907	4485	75 ± 5			
62	Lindis	3287	4218	520	86.3	Apatite	30	0.286	165	3.909	2254	97		4.279	3385	55 ± 5	12.38 ± 0.38	1.91	25
						Zircon	7	5.548	406	4.564	334	89		0.898	4441	73 ± 6			
63	Lindis	3335	4265	715	85.8	Apatite	23	0.717	319	1.654	736	77		0.888	5267	68 ± 5	10.83 ± 0.39	2.67	46
						Zircon	9	10.204	1211	4.676	555	58		0.890	4398	129± 7			
64	Lindis	3412	4298	775	87.5	Apatite	24	1.001	190	2.854	542	38		1.111	2746	69 ± 6	11.17 ± 0.27	2.66	97
						Zircon	3	7.583	105	5.633	78	78		0.881	4355	79 ± 12			
65	Lindis	3459	4351	640	85.3	Apatite	20	0.916	116	3.128	396	14		1.099	2716	57 ± 6	12.60 ± 0.56	2.52	20
						Zircon	1	15.456	107	7.800	54	100		0.872	4312	115± 19			
66	Paringa	3230	5301	30	1.5	Apatite	15	0.000	0	0.998	819			1.086	2686	0 ± ∞			
						Zircon	8	0.446	15	16.446	553	55		1.065	5265	1.9 ± 0.5			
67	Paringa	3248	5258	60	6.6	Apatite	15	0.000	0	0.043	65			4.243	3357	0 ± ∞			
68	Paringa	3279	5196	170	12.8	Apatite	15	0.000	0	0.025	7			1.062	2627	0 ± ∞			
						Zircon	8	0.445	48	10.204	1100	70		1.065	5265	3.1± 0.5			
69	Ohau	3456	4974	760	38.3	Apatite	20	0.012	5	2.169	884	15		1.050	2597	1.1 ± 0.5			
						Zircon	11	10.457	1665	5.495	875	15		0.846	4182	107± 5			
70	Ohau	3516	4983	640	40.5	Apatite	19	0.000	0	1.802	360			1.038	2567	0 ± ∞			
						Zircon	6	8.531	540	4.187	265	4.7	2.024 ± 0.231	0.837	4139	112 ± 13			
71	Ohau	3521	4914	640	46.0	Apatite	26	0.059	37	2.693	1691	97		1.253	3100	4.9 ± 0.8	8.99 ± 1.18	3.28	10
						Zircon	10	11.964	1834	5.121	785	38		0.828	4095	128 ± 6			
72	Ohau	3544	4877	550	49.8	Apatite	21	0.525	225	2.767	1185	3.0	0.187 ± 0.022	1.244	3076	41 ± 5	10.47 ± 0.48	2.74	32
						Zircon	8	11.372	1822	2.796	448	10		0.819	4052	219 ± 12			
73	Ohau	3528	4711	565	62.3	Apatite	23	0.666	201	1.528	461	39		0.814	2014	63 ± 6	10.76 ± 0.36	2.49	48
						Zircon	17	10.957	2254	3.505	721	0.3		0.811	4009	182± 13			

Table 3 ctd

Sample Number	Transect	Coordinate x	Coordinate y	Elevation (m)	Distance from Alpine fault (km)	Mineral	No. crystals	Spontaneous ρ_s	Spontaneous N_s	Induced ρ_i	Induced N_i	$P(\chi^2)$ (%)	$\overline{\rho_s/\rho_i}$ ± 1σ	ρ_d	N_d	Age (Ma) ±1σ	Mean Track Length ± 1σ (μm)	Standard Deviation (μm)	No. Lengths
74	Ohau	3673	4431	425	90.8	Apatite	20	0.653	142	2.307	502	19		1.224	3027	61 ± 6	11.87 ± 0.35	2.27	41
						Zircon	9	11.398	2480	2.758	600	0.8	4.298 ± 0.335	0.802	3965	227± 18			
75	Ohau	3766	4333	410	102.5	Apatite	20	1.011	424	2.420	1015	3.0	0.348 ± 0.038	1.214	3002	75 ± 8	12.64 ± 0.20	1.84	89
						Zircon	3	9.116	577	3.239	577	26		1.065	5265	198 ± 16			
76	Ohau	3951	4217	320	121.3	Apatite	20	1.276	410	1.851	595	33		0.888	5267	108 ± 7	13.03 ± 0.18	1.84	100
						Zircon	6	10.230	516	3.232	163	55		1.065	5265	222 ± 20			
77	Ohau	4403	3911	120	166.3	Apatite	14	0.151	25	0.285	47	58		1.194	2963	112 ± 28			
						Zircon	4	11.684	208	4.775	85	73		1.067	6342	173 ± 22			
78	Copland	3586	5461	260	7.7	Apatite	15	0.000	0	0.529	533			4.206	3328	0 ± ∞			
						Zircon	5	0.015	1	11.998	795	4.7	0.003 ± 0.003	1.067	6342	0.2 ± 0.2			
79	Copland	3612	5451	410	9.7	Apatite	15	0.000	0	0.655	232			4.170	3299	0 ± ∞			
						Zircon	8	0.057	6	5.207	551	45		0.758	3749	0.6± 0.2			
80	Copland	3629	5439	595	11.5	Apatite	15	0.000	0	0.264	179			4.134	3270	0 ± ∞			
						Zircon	11	0.159	51	9.716	3123	75		0.930	4596	1.0± 0.1			
81	Copland	3695	5403	775	17.3	Apatite	15	0.000	0	5.784	1905			4.097	3242	0 ± ∞			
						Zircon	11	0.441	72	7.366	1202	7		0.922	4558	3.7± 0.5			
82	Copland	3734	5411	1080	18.3	Apatite	15	0.000	0	2.890	483			1.145	2830	0 ± ∞			
						Zircon	2	0.722	10	14.372	199	72		0.914	4520	3.1± 1.0			
83	Hooker	3766	5406	1830	20.3	Apatite	10	0.000	0	2.196	215			1.243	3074	0 ± ∞			
						Zircon	13	14.185	1908	10.111	1360	7		0.907	4483	85 ± 4			
84	Hooker	3769	5405	1575	20.5	Apatite	15	0.000	0	1.186	435			1.125	2781	0 ± ∞			
						Zircon	13	9.361	2333	4.004	998	18		0.899	4445	139 ± 6			
85	Hooker	3773	5404	1320	20.7	Apatite	15	0.006	2	1.292	442	82		1.115	2756	0.9± 0.6			
						Zircon	15	14.755	3619	5.785	1419	9		0.891	4407	150 ± 6			
86	Hooker	3775	5399	1140	21.3	Apatite	15	0.004	1	1.577	421	92		1.105	2732	0.5 ± 0.5			
						Zircon	10	10.573	1809	3.331	570	15		0.884	4369	185 ± 10			
87	Hooker	3766	5347	825	24.8	Apatite	15	0.014	2	2.552	376	99		1.095	2707	1.0± 0.7			
						Zircon	10	12.071	1158	4.347	417	39		0.876	4331	161± 10			
88	Hooker	3786	5307	715	28.9	Apatite	22	0.018	9	2.799	1420	23		1.235	3055	1.4 ± 0.5	12.84		1
						Zircon	7	12.386	735	5.410	321	53		0.868	4393	132 ± 9			
89	Hooker	3937	4753	550	78.8	Apatite	20	0.793	215	2.742	743	9		1.223	3025	63 ± 5	11.86 ± 0.33	2.47	57
						Zircon	14	7.997	1645	2.693	554	25		0.861	4256	169± 9			
90	Hooker	3763	4642	425	79.3	Apatite	20	1.184	746	2.630	1657	<0.1	0.452 ± 0.037	1.211	2994	98 ± 8	12.60 ± 0.20	2.09	106
						Zircon	18	7.982	1871	2.713	636	0.3	2.974 ± 0.197	0.850	4218	167± 12			
91	Fox	3703	5807	230	2.3	Apatite	10	0.000	0	0.404	124			4.061	3213	0 ± ∞			
92	Fox	3725	5595	380	4.5	Apatite	8	0.000	0	0.283	47			4.643	3673	0 ± ∞			
93	Whataroa	4058	5791	150	8.5	Apatite	15	0.000	0	1.267	450			4.616	3652	0 ± ∞			
						Zircon	11	0.190	33	11.128	1937	96		0.830	4104	0.9± 0.2			
94	Whataroa	4044	5745	200	11.1	Apatite	12	0.000	0	3.126	470			4.589	3630	0 ± ∞			
						Zircon	29	0.263	167	7.594	4814	<0.1	0.041 ± 0.006	0.822	4066	2.2± 0.3			
95	Whataroa	4039	5709	350	13.4	Apatite	15	0.000	0	1.563	1062			1.150	2843	0 ± ∞			
						Zircon	12	0.220	107	5.280	2569	62		0.815	4029	2.3± 0.2			
96	Whataroa	4061	5695	655	15.7	Apatite	10	0.000	0	7.253	1162			4.561	3609	0 ± 0			
						Zircon	17	0.728	136	13.219	2471	53		1.067	6342	3.9 ± 0.4			
97	Godley	4120	5599	1065	25.8	Apatite	15	0.000	0	1.020	327			1.125	2783	0 ± ∞	14.69 ± 0.31	0.44	2
						Zircon	20	12.835	3732	3.790	1102	1.0	3.409 ± 0.218	0.799	3953	180± 12			
98	Godley	4117	5573	1005	27.8	Apatite	15	0.000	0	0.991	147			1.113	2752	0 ± ∞			
						Zircon	22	11.528	2816	3.832	936	10		0.993	4912	197± 8			
99	Godley	4118	5554	960	29.5	Apatite	20	0.013	6	2.312	1052	44		1.101	2722	1.1± 0.5	11.32 ± 0.42	0.94	5
						Zircon	7	13.819	984	3.764	268	16		0.984	4868	238 ± 17			
100	Godley	4118	5506	915	32.8	Apatite	25	0.073	24	2.425	794	20		0.888	5267	4.8± 1.0	7.17 ± 0.82	3.72	22
						Zircon	11	12.007	2755	3.521	808	1.0	3.214 ± 0.221	0.975	4824	207± 15			

Table 3 ctd

Sample Number	Transect	Coordinate x	Coordinate y	Elevation (m)	Distance from Alpine fault (km)	Mineral	No. crystals	Spontaneous ρ_s	Spontaneous N_s	Induced ρ_i	Induced N_i	P(χ^2) (%)	$\overline{\rho_s/\rho_i}$ ± 1σ	ρ_d	N_d	Age (Ma) ±1σ	Mean Track Length ± 1σ (μm)	Standard Deviation (μm)	No. Lengths
101	Godley	4122	5443	825	37.0	Apatite	20	0.117	73	2.043	1275	<0.1	0.076 ± 0.021	1.077	2862	14 ± 4	8.40 ± 0.49	2.90	35
						Zircon	14	11.743	2555	4.077	887	<0.1	2.907 ± 0.190	0.966	4779	185± 13			
102	Godley	4133	5401	790	40.6	Apatite	20	0.286	58	1.904	386	18		1.064	2631	28 ± 4	9.37 ± 0.52	2.74	29
						Zircon	5	8.742	415	2.970	141	30		0.958	4735	186± 18			
103	Godley	4155	5371	760	44.6	Apatite	20	0.382	195	1.603	818	<0.1	0.229 ± 0.039	1.052	2601	43 ± 7	10.97 ± 0.2	1.70	70
						Zircon	10	11.722	1994	3.645	620	10		0.949	4691	201± 10			
105	Godley	4085	5008	810	66.5	Apatite	20	0.650	169	2.814	732	1.0	0.239 ± 0.030	1.187	2936	50 ± 6	11.88 ± 0.27	2.31	75
						Zircon	18	10.295	3360	3.864	1261	1.0	2.772 ± 0.155	0.931	4803	171± 10			
106	Godley	4208	4884	715	83.0	Apatite	20	0.620	168	2.591	702	<0.1	0.243 ± 0.036	1.178	2912	51 ± 8	11.16 ± 0.22	2.26	103
						Zircon	16	10.805	1432	4.361	578	<0.1	2.639 ± 0.231	0.922	4559	161± 14			
107	Godley	4312	4968	440	83.0	Apatite	15	0.224	31	0.932	129	96		1.168	2888	50 ± 10	11.44 ± 0.58	3.13	29
						Zircon	7	4.364	82	2.767	52	71		0.913	4515	96 ± 17			
108	Godley	4461	5093	490	81.3	Apatite	7	0.917	98	3.193	341	16		1.158	2864	59 ± 7	12.83 ± 0.30	0.85	8
						Zircon	7	9.614	599	2.359	147	87		0.904	4471	242± 23			
109	Godley	4472	4932	395	93.8	Apatite	20	0.638	142	2.750	612	30		1.148	2839	47 ± 5	12.57 ± 0.19	1.38	51
						Zircon	11	11.735	1091	3.690	343	<0.1	3.258 ± 0.380	0.895	4427	192± 23			
110	Godley	4636	4846	200	109.0	Apatite	8	0.653	51	2.739	214	80		1.139	2815	48 ± 8	12.21 ± 0.21	1.50	52
						Zircon	12	10.384	1027	4.075	403	7		0.886	4383	150± 9			
111	Clyde	4354	5753	915	27.0	Apatite	15	0.003	1	2.332	821			1.129	2791	0 ± ∞			
						Zircon	27	10.929	6204	3.981	2260	<0.1	2.850 ± 0.130	0.877	4338	165 ± 8			
112	Clyde	4366	5735	855	29.1	Apatite	9	0.000	0	1.046	119			1.119	2767	0 ± ∞			
						Zircon	17	9.617	1750	3.676	669	<0.1	2.614 ± 0.240	0.868	4294	150± 14			
113	Clyde	4378	5711	810	31.4	Apatite	26	0.042	28	2.119	1400	73		1.109	2743	3.9 ± 0.8	6.11 ± 0.97	2.33	8
						Zircon	7	8.701	654	3.805	286	68		0.860	4250	130± 10			
114	Clyde	4402	5683	715	34.8	Apatite	25	0.108	74	1.410	962	<0.1	0.078 ± 0.022	1.100	2719	15 ± 4	8.73 ± 0.55	3.18	33
						Zircon	9	6.434	1298	2.295	463	<0.1	2.797 ± 0.257	0.851	4206	157± 15			
115	Clyde	4433	5637	655	39.9	Apatite	21	0.249	90	1.283	463	97		1.090	2695	38 ± 4	9.82 ± 0.53	3.11	35
						Zircon	10	6.777	811	2.390	286	87		0.842	4162	158± 11			
116	Clyde	4428	5595	610	43.5	Apatite	21	0.348	170	1.521	743	1.0	0.214 ± 0.030	1.080	2671	41 ± 6	10.27 ± 0.29	2.68	83
						Zircon	7	7.979	947	3.160	375	1.0	2.603 ± 0.241	0.961	4750	165 ± 16			
117	Clyde	4459	5566	595	47.3	Apatite	20	0.463	168	2.245	815	0.1	0.258 ± 0.033	1.070	2649	49 ± 6	11.03 ± 0.20	2.01	106
						Zircon	14	9.353	2331	4.482	1117	<0.1	2.285 ± 0.134	0.954	4716	144± 9			
118	Clyde	4741	5436	550	70.8	Apatite	20	0.857	273	2.581	822	2.0	0.346 ± 0.037	1.061	2622	65 ± 7	11.51 ± 0.20	2.05	106
						Zircon	12	12.635	1512	5.925	709	16		0.947	4681	134± 7			
119	Clyde	4762	5424	520	72.9	Apatite	20	2.151	834	4.684	1816	<0.1	0.463 ± 0.045	1.051	2598	86 ± 9	12.27 ± 0.14	1.34	98
						Zircon	6	8.804	505	4.567	262	5.8		0.940	4646	120± 9			
120	Clyde	4844	5396	440	80.0	Zircon	15	11.529	2269	7.743	1524	<0.1	1.545 ± 0.088	0.933	4611	98 ± 6			
121	Whitcombe	4557	6208	105	2.0	Apatite	10	0.000	0	0.804	109			1.171	2895	0 ± ∞			
						Zircon	10	0.279	32	13.415	1539	95		0.926	4577	1.3± 0.2			
122	Whitcombe	4591	6173	185	6.3	Apatite	15	0.000	0	1.978	497			1.164	2876	0 ± ∞			
						Zircon	10	0.241	20	12.158	1010	47		0.919	4542	1.2± 0.3			
123	Whitcombe	4606	6142	410	9.3	Apatite	15	0.000	0	0.195	72			4.507	3565	0 ± ∞			
						Zircon	6	0.662	19	14.051	403	99		1.067	6342	3.4 ± 0.8			
124	Wilberforce	4855	6143	760	24.3	Apatite	14	0.000	0	1.906	409			1.150	2843	0 ± ∞	13.63 ± 0.65	1.46	5
						Zircon	16	14.907	2123	6.727	958	3.0	2.251 ± 0.107	0.904	4472	135 ± 7			
125	Wilberforce	4857	6110	670	27.8	Apatite	27	0.058	22	2.868	1095	48		1.143	2825	4.1 ± 0.9	7.90 ± 0.93	3.63	17
						Zircon	15	13.873	686	6.936	343	14		0.898	4438	119± 8			
126	Wilberforce	4886	6057	700	32.0	Apatite	30	0.167	55	3.895	1306	1.0	0.042 ± 0.011	1.136	2808	8.4 ± 2.2	8.49 ± 0.74	2.77	16
						Zircon	5	12.711	176	5.200	72	42		0.890	4403	144± 20			
127	Wilberforce	4933	6003	670	38.7	Apatite	25	0.640	355	3.143	1744	<0.1	0.202 ± 0.022	1.129	2790	40 ± 5	11.27 ± 0.25	2.20	75
						Zircon	13	13.500	2163	6.217	996	66		0.883	4368	127± 5			
128	Wilberforce	5080	5758	520	62.3	Apatite	20	0.440	101	2.275	522	<0.1	0.207 ± 0.049	1.122	2772	41 ± 10	9.98 ± 0.32	2.84	79
						Zircon	9	10.491	1629	4.083	634	8		0.876	4334	149± 8			

Table 3 ctd

Sample Number	Transect	Coordinate x	Coordinate y	Elevation (m)	Distance from Alpine fault (km)	Mineral	No. crystals	Spontaneous ρ_s	Spontaneous N_s	Induced ρ_i	Induced N_i	$P(\chi^2)$ (%)	$\overline{\rho_s/\rho_i}$ ± 1σ	ρ_d	N_d	Age (Ma) ±1σ	Mean Track Length ± 1σ (μm)	Standard Deviation (μm)	No. Lengths
129	Arthur's	4980	6524	170	2.3	Apatite	15	0.000	0	2.311	304			1.115	2755	0 ± ∞			
						Zircon	4	0.253	12	8.721	414	69		0.869	4299	1.7± 0.5			
130	Arthur's	5045	6506	245	6.7	Apatite	15	0.007	2	2.408	705	90		1.108	2737	0.6± 0.4			
						Zircon	19	0.700	321	8.710	3997	98		0.862	4264	4.6± 0.3			
131	Arthur's	5082	6500	245	9.3	Apatite	15	0.000	0	6.737	2685			4.479	3544	0 ± ∞			
						Zircon	15	2.127	469	9.009	1987	7		0.855	4229	14 ± 1			
132	Arthur's	5104	6498	290	10.5	Apatite	15	0.000	0	3.040	451			1.093	2702	0 ± ∞			
						Zircon	6	2.654	42	6.825	108	8		0.848	4195	22 ± 4			
133	Arthur's	5063	6297	810	24.0	Apatite	16	0.042	9	9.138	1952	34		4.452	3522	3.6 ± 1.2	7.69 ± 2.40	3.86	5
						Zircon	10	10.270	1097	3.539	378	8		0.841	4160	161± 10			
134	Arthur's	5064	6264	760	26.8	Apatite	21	0.053	22	2.856	1178	3.0	0.029 ± 0.009	1.079	2667	5.5± 1.8	7.56 ± 2.65	4.26	5
						Zircon	15	10.947	2252	3.797	781	5.6		0.968	4786	184± 8			
135	Robinson	5464	6844	335	1.0	Apatite	15	0.000	0	4.767	594			4.425	3501	0 ± ∞			
						Zircon	3	0.449	4	12.583	112	78		1.067	6342	2.6 ± 1.3			
136	Robinson	5492	6831	380	3.5	Apatite	15	0.022	2	6.480	596	98		4.398	3479	2.6 ± 1.9			
137	Robinson	5500	6815	425	5.1	Apatite	15	0.006	1	3.525	638	93		1.718	3396	0.5 ± 0.5			
						Zircon	2	0.822	26	10.238	324	28		1.067	6342	5.7 ± 1.2			
138	Robinson	5505	6814	425	5.6	Apatite	15	0.000	0	4.437	746			1.706	3374	0 ± ∞			
						Zircon	9	1.553	169	12.565	1367	1.0	0.120 ± 0.015	0.947	4682	7.6 ± 1.0			
139	Robinson	5519	6816	455	6.1	Apatite	20	0.012	3	3.523	885	66		1.695	3351	1.0± 0.6			
						Zircon	9	10.992	761	7.468	517	39		0.940	4648	92 ± 6			
140	Lewis	5628	6974	1115	0.8	Apatite	15	0.000	0	0.288	121			1.683	3328	0 ± ∞			
						Zircon	9	0.396	29	11.628	851	86		0.933	4613	2.1 ± 0.4			
141	Lewis	5630	6972	1050	1.0	Apatite	15	0.000	0	0.672	363			4.370	3457	0 ± ∞			
						Zircon	12	0.596	221	12.317	4568	60		0.926	4579	3.0 ± 0.2			
142	Lewis	5670	7004	610	0.9	Apatite	15	0.000	0	0.256	144			4.343	3436	0 ± ∞			
						Zircon	5	0.626	26	11.965	497	90		1.067	6342	3.7 ± 0.8			
143	Lewis	5672	7004	655	1.0	Apatite	15	0.000	0	0.109	22			4.316	3414	0 ± ∞			
						Zircon	7	0.337	17	9.437	476	62		0.912	4510	2.2 ± 0.5			
144	Lewis	5670	6993	490	1.6	Apatite	15	0.000	0	2.434	508			1.637	3238	0 ± ∞			
						Zircon	17	0.531	246	9.340	4323	11		0.905	4476	3.4 ± 0.2			
145	Lewis	5678	6986	550	2.6	Apatite	15	0.019	4	3.853	804	99		1.626	3215	1.4± 0.7			
						Zircon	16	0.793	211	9.029	2402	24		0.898	4441	5.3± 0.4			
146	Lewis	5699	6958	610	5.8	Apatite	11	0.000	0	3.751	601			1.614	3192	0 ± ∞			
						Zircon	17	8.902	1708	6.447	1237	3.0	1.420 ± 0.076	0.891	4407	84 ± 5			
147	Lewis	5723	6959	595	7.0	Apatite	15	0.005	1	3.120	688	100		1.603	3169	0.4 ± 0.4			
						Zircon	15	12.797	1987	7.168	1113	<0.1	1.864 ± 0.125	0.884	4372	109± 8			
148	Lewis	5784	6969	775	9.7	Apatite	15	0.000	0	3.286	741			1.591	3147	0 ± ∞			
						Zircon	13	13.326	1766	5.999	795	2.0	2.331 ± 0.156	0.877	4338	136± 9			
149	Lewis	5807	6969	915	11.0	Apatite	20	0.006	1	2.467	427	96		1.580	3124	0.7 ± 0.7			
						Zircon	9	14.065	779	6.067	336	98		1.067	6342	164 ± 11			
150	Lewis	5809	6939	825	14.0	Apatite	20	0.011	3	2.517	692	98		1.568	3101	1.2± 0.7			
						Zircon	11	11.877	1621	3.407	465	34		0.863	4267	198 ± 11			
151	Lewis	5812	6901	730	16.2	Apatite	20	0.012	2	4.262	725	99		1.557	3079	0.8± 0.5			
						Zircon	15	15.523	3439	4.622	1024	1.0	3.380 ± 0.191	0.856	4234	191± 11			
152	Lewis	5764	6760	595	24.0	Apatite	20	0.019	3	3.142	491	100		1.545	3056	1.7 ± 1.0	14.96 ± 0.91	1.81	4
						Zircon	15	14.908	1725	4.606	533	47		0.849	4200	181± 10			
153	Lewis	5853	6708	455	32.3	Apatite	20	0.031	9	2.474	707	80		1.331	3291	3.0 ± 1.0	7.57 ± 2.18	4.70	7
						Zircon	11	10.688	1131	4.186	443	2.0	2.977 ± 0.292	1.067	6342	209± 21			
154	Lewis	5917	6697	425	36.8	Zircon	5	14.521	517	4.578	163	28		0.918	4538	192± 18			
155	Lewis	5968	6703	410	39.5	Apatite	28	0.028	13	1.376	630	3.0	0.027 ± 0.012	1.322	3270	6.4 ± 2.8	7.70 ± 1.39	4.14	11
						Zircon	6	8.932	477	2.958	158	3.0	3.099 ± 0.356	0.909	4499	186± 22			

Table 3 ctd

Sample Number	Transect	Coordinate x	Coordinate y	Elevation (m)	Distance from Alpine fault (km)	Mineral	No. crystals	Spontaneous ρ_s	Spontaneous N_s	Induced ρ_i	Induced N_i	$P(\chi^2)$ (%)	$\overline{\rho_s/\rho_i}$ ± 1σ	ρ_d	N_d	Age (Ma) ±1σ	Mean Track Length ± 1σ (μm)	Standard Deviation (μm)	No. Lengths
156	Lewis	6047	6724	380	43.0	Apatite	16	0.077	21	1.603	436	14		1.313	3248	11 ± 3	10.23 ± 1.34	4.42	13
						Zircon	12	12.322	1438	5.613	655	<.01	2.542 ± 0.292	0.902	4460	152± 18			
157	Lewis	6116	6716	335	46.8	Apatite	19	0.342	106	2.513	778	0.1	0.121 ± 0.030	1.305	3226	28 ± 7	9.66 ± 0.55	2.79	26
						Zircon	15	12.749	2257	5.044	893	2.0	2.824 ± 0.161	1.067	6342	199± 12			
158	Lewis	6139	6643	290	53.3	Apatite	20	0.418	155	1.273	472	35		1.296	3204	75 ± 7	11.28 ± 0.24	2.23	87
						Zircon	12	10.292	2168	5.288	1114	<.1	2.140 ± 0.255	0.886	4383	126± 15			
159	Lewis	6159	6584	245	58.8	Apatite	21	1.290	213	3.433	567	95		1.287	3183	85 ± 7	11.58 ± 0.20	1.87	89
						Zircon	14	9.767	1758	3.428	617	1.0	3.170 ± 0.207	0.879	4345	184± 13			
90017	Cook	3784	5478	2530	15.2	Zircon	6	8.089	408	4.223	213	17		1.067	6342	135± 12			
90016	Cook	3797	5474	3230	16.3	Apatite	10	0.006	1	1.267	223	6		0.831	2055	0.7 ± 0.7			
						Zircon	9	9.967	552	4.911	272	11		1.067	6342	143± 11			
90015	Cook	3802	5476	3660	16.3	Apatite	11	0.000	0	1.961	318			0.820	2027	0 ± ∞			
						Zircon	6	10.203	444	5.400	235	49		1.067	6342	134± 11			

(i) X and y coordinates refer to New Zealand Map Series 1. (ii) Track densities (ρ) are x 10^6 tr cm^{-2}. (iii) All analyses by external detector method using 0.5 for the $4\pi/2\pi$ geometry correction factor. (iv) Apatite ages calculated using dosimeter glass SRM 612 and zeta-612 = 354.9 ± 4.3 (1σ); zircon ages calculated using dosimeter glass CN1 and zeta-CN1 = 133.9 ± 1.4 (1σ). (v) $P(\chi^2)$ is the probability of obtaining χ^2 value for v degrees of freedom (where v = No. crystals - 1) [*Galbraith*, 1981]; pooled ρ_s/ρ_i ratio is used to calculate age and uncertainty where $P(\chi^2)$ >5%; mean ρ_s/ρ_i ratio is used to calculate age and uncertainty where $P(\chi^2)$ <5% [*Green*, 1981].

annealing zone form a remarkably coherent data set considering that the samples originate from 13 transects across the S. Alps with a total separation of 300 km.

Zircon Data

The zircon data are reported in Table 3. The pattern of zircon FT age variation across the S. Alps is similar to that for the apatite ages, with age increasing monotonically away from the Alpine fault. Fig. 5 shows the results for a typical transect. Very close to the Alpine fault there are always very young ages up to ~5-7 Ma which increase linearly away from the Alpine fault. These ages are considered to be reset ages. The oldest of these young ages, which is usually the sample farthest east, records the age when uplift started (e.g. 5.3 Ma in Lewis transect). Farther southeast from this point on the transects zircon ages increase rapidly. These ages belong to an exhumed zircon annealing zone, which in turn merges with 150-200 Ma ages that were reset by Mesozoic burial and uplift.

Paleotemperature Estimation

Several different approaches to paleotemperature estimation from FT data have been proposed in the literature. One is based on a quantitative treatment of annealing achieved by forward modeling of track shortening and age evolution through likely thermal histories for an average (Durango) apatite composition [*Green et al.*, 1989a]. This approach was not adopted here because there are few stratigraphic constraints on the vertical movement of the S. Alps basement prior to the start of uplift, and the apatites have a wider compositional spread than the composition of Durango apatite. Another suggested modeling approach is based on kinetic equations derived from physical models of the processes involved in fission track annealing [*Carlson*, 1990]. This approach is in its infancy and needs further development before it becomes practical. A third possible approach involves modeling thermal histories directly from FT data, whereby a given thermal history is systematically modified until statistical agreement is reached between the predicted and observed data [*Lutz and Omar*, 1991]. This approach cannot at present give unique solutions in all cases.

The approach adopted in this study was (i) to pick the location of the base of the exhumed zircon annealing zone for each transect and assign an appropriate paleotemperature value, and (ii) for samples from within the

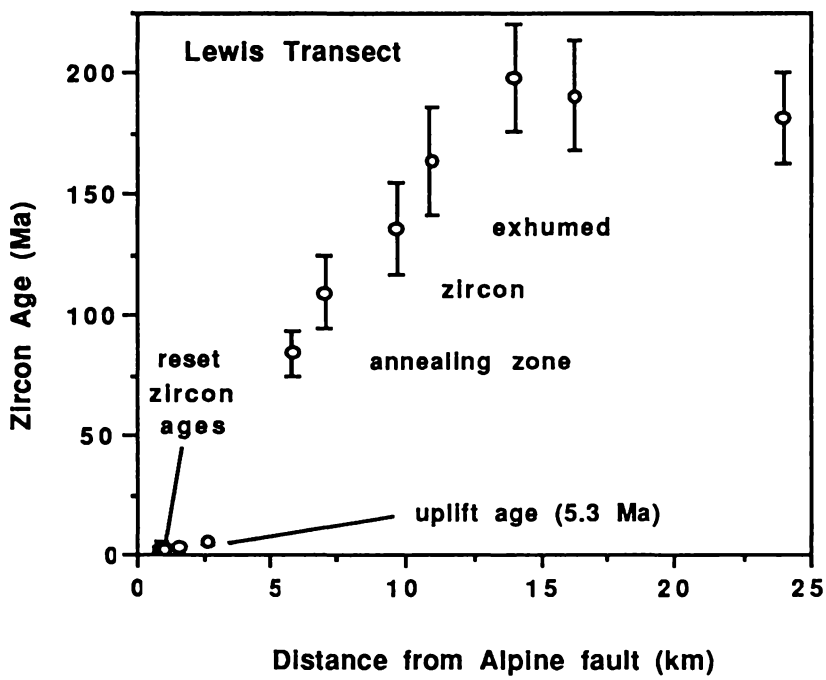


Fig. 5. Variation of sample zircon ages with distance from the Alpine fault for Lewis transect. Errors are 2σ.

exhumed apatite annealing zone, apply the empirically derived relationships between formation temperatures, mean FT age and length statistics established for Otway Basin reference wells [e.g. *Gleadow et al.*, 1986b; *Green et al.*, 1989b] (Fig. 6). This approach is possible for the S. Alps because the rocks analysed have recently and rapidly been uplifted from depths where the FT parameters had been in equilibrium with the ambient temperatures. In this situation the age and length data will not have been modified greatly by the addition of a component of tracks that have accumulated since uplift started. This assumes that for samples within the exhumed apatite annealing zone the component of track length and density attributable to the cooling/uplift phase can be separated from that of the pre-uplift (now exhumed) annealing zone. We describe below a procedure for separating the track components which allows paleotemperature estimation with reference to the Otway Basin data. We first discuss possible limitations on this approach to paleotemperature estimation.

Green et al. [1989a] have demonstrated that apatite FT parameters for samples from different levels in the Otway Basin reference wells (Flaxman's-1, Eumeralla-1, Port Campbell-4 and Banyula-1) have equilibrated to within a few degrees of their current formation temperatures. This has occurred over a period of 10-40 m.y. The Southern Alps samples would also have to have been equilibrated with the ambient pre-uplift temperatures if Otway data are to be used to estimate paleotemperatures for the S. Alps samples. This would have been the case, as following late Jurassic-early Cretaceous uplift, the Triassic basement in the S. Alps was eroded to a low relief landscape which foundered below sea level throughout the Paleogene [*Suggate et al.*, 1978]. The marine transgression across New Zealand reached its peak during the late Oligocene (~25 Ma), having accommodated several hundred metres of marine sediments in Canterbury [*Wilson*, 1956], within and east of the future S. Alps. The sea regressed over parts of Canterbury in the early Miocene and consequently coal measures accumulated. Widespread regressive facies are not recorded until the latest Miocene to Pliocene. This stratigraphic history implies that prior to uplift, the FT parameters in apatites of the S. Alps samples would have had more than 10 m.y. to equilibrate with ambient temperatures, and therefore the timescale of heating is not a limitation in applying to the S. Alps data, FT-temperature relationships established for the Otway Basin.

The method of paleotemperature estimation adopted here assumes that the apatites in the S. Alps samples have similar compositions to apatites

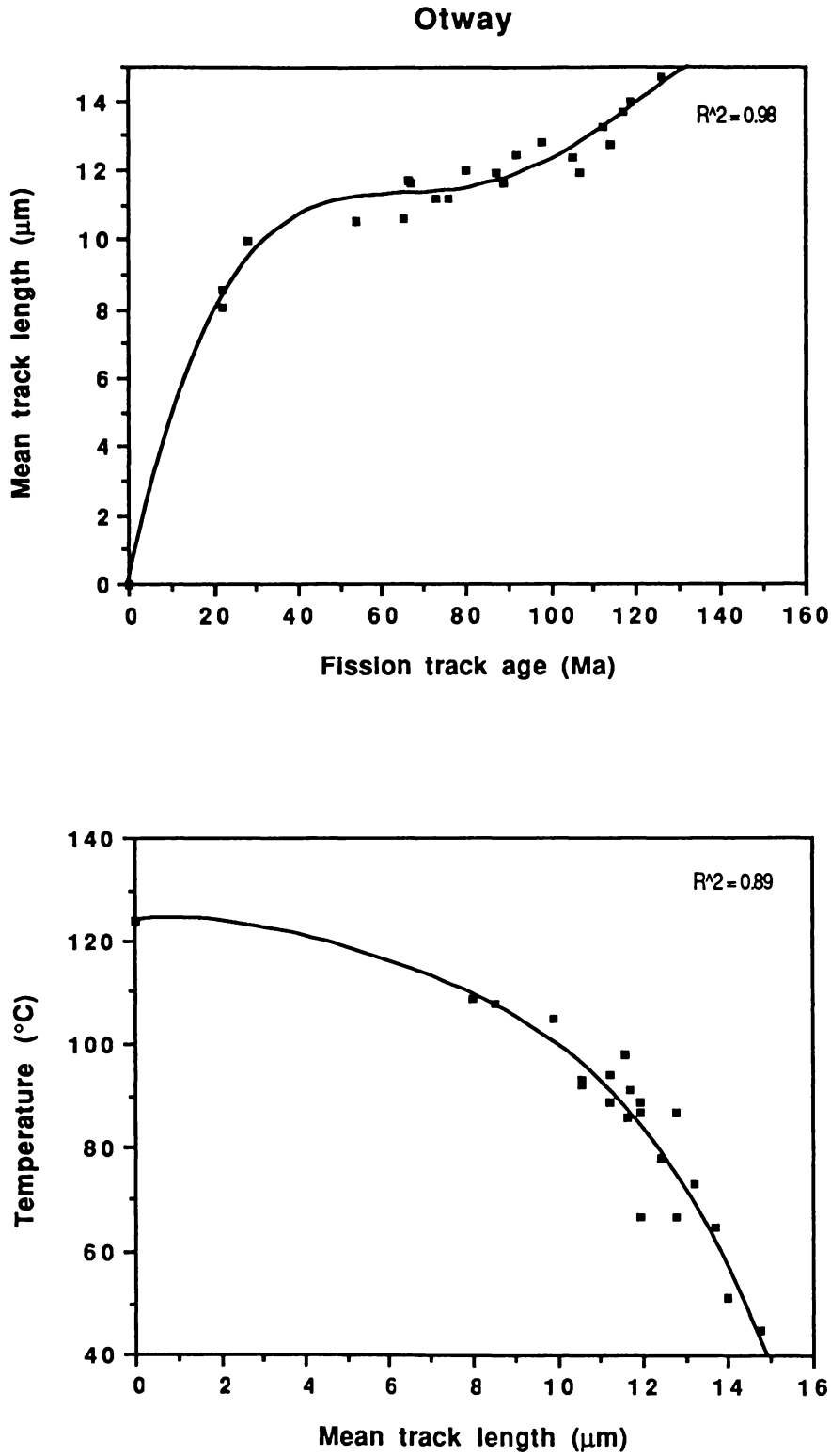


Fig. 6. Calibration curves (4th order polynomials), using data from the Otway Basin, to predict (top) the mean fission track length expected for a given apatite FT age, and (bottom) the paleotemperature expected for a given mean track length.

in the Otway Basin succession, which are known to have a wide compositional spread [*Green et al.*, 1985; *Green et al.*, 1989a]. Chlorapatites are less susceptible to annealing than fluorapatites [*Green et al.*, 1985; *Crowley et al.*, 1990], and it has been shown that the Cl/(Cl+F) ratio describes the compositional control on annealing [*Green et al.*, 1989a]. Durango apatite has a ratio value of 0.10. To test the assumption of the similarity of apatite compositions between the S. Alps basement and Otway Basin succession, apatites from 5 samples from the exhumed annealing zone in the Godley transect were probed (Fig. 7). As our paleotemperature estimates are based primarily on confined track length information, we analysed the composition of crystals containing horizontally confined tracks. The results are illustrated in Fig. 7, which gives the frequency of grains in particular classes of Cl/(Cl+F) ratio for each sample. Overall, 28 out of 83 (34 %) of the crystals probed have a Cl content greater that Durango apatite, and range up to 0.35 Cl/(Cl+F). Sample 100, taken from near the base of the exhumed annealing zone, has a ratio of 0.15, and 60 % of the grains have a Cl/(Cl+F) ratio of >0.10. These figures are lower for the other annealing zone samples; samples 101 and 105 average about 0.10 Cl/(Cl+F) and contain a fairly high proportion (~40 %) of chlorapatites. Samples 102 and 103 retain 15-25 % chlorapatite.

These data show that the S. Alps apatites have a wide compositional spread and importantly contain a significant number of chlorapatites; application of Otway Basin FT-temperature relationships to estimate pre-uplift paleotemperatures for S. Alps host rocks is therefore largely valid. The temperature of total annealing in S. Alps apatites will be higher than that for Durango apatite (~110° C), particularly for samples 100 and 101, which contain a high percentage of chlorapatites and formerly resided near the base of the late Cenozoic annealing zone. Because Otway Basin samples probed generally have a higher proportion of chlorapatites [*Green et al.*, 1985], the temperature of total overprinting in S. Alps samples may not be as high as 125°, but is probably within 5° C of this figure. A difference of 5° C is well within the error on the derived paleotemperature estimates (Table 4), but the sample mean paleotemperature estimates within the exhumed annealing zone may be a little high by a few degrees. This translates into a possible overestimate of rock uplift amounts of 100 to 200 m within the parts of the S. Alps containing the exhumed apatite annealing zone (east of the Main Divide); this amount lies within the uncertainties of uplift amount estimated from other sources of error (Table 4).

Table 4. Paleotemperature and rock uplift amount estimates for Southern Alps samples.

Transect	Mineral	Sample Number	Age (Ma) ± 2σ	Uplift Age (Ma) ± 2σ	Corrected Age (Ma) ± 2σ	Sample Mean Length (μm) ± 2σ	Corrected Mean Length (μm) ± 2σ	Pre-uplift Paleotemp. (°C) ± 2σ	Elevation (km)	Amount of Rock Uplift (km) ± 2σ
Hunter	Apatite	48	13.7 ± 9.8	5.7 ± 2.2	8.0 ± 10.0	7.5 ± 3.1	5.4 ± 6.1	118 ± 15	0.41	4.3 ± 0.6
Hunter	Apatite	49	5.0 ± 2.6	5.7 ± 2.2	0 ± 3.4	6.6 ± 3.4	3.6 ± 4.1	122 ± 7	0.38	4.5 ± 0.5
Hunter	Apatite	50	7.3 ± 4.0	5.7 ± 2.2	1.6 ± 4.6	10.7 ± 1.3	8.0 ± 3.3	111 ± 13	0.40	4.1 ± 0.6
Hunter	Apatite	8326-3	35 ± 20	5.7 ± 2.2	29 ± 20	10.2 ± 0.9	9.6 ± 3.6	102 ± 18	0.46	3.8 ± 0.7
Haast	Apatite	58	7.8 ± 7.6	6.7 ± 5.0	1.1 ± 9.1	7.5 ± 2.7	4.3 ± 6.5	121 ± 14	1.31	5.3 ± 0.6
Ohau	Apatite	71	4.9 ± 1.6	5.8 ± 10.4	0 ± 10.5	9.0 ± 2.4	5.9 ± 6.7	117 ± 19	0.64	4.5 ± 0.7
Ohau	Apatite	72	41 ± 10	5.8 ± 10.4	35 ± 14	10.5 ± 1.0	10.0 ± 1.8	100 ± 10	0.55	3.8 ± 0.5
Ohau	Apatite	73	63 ± 12	5.8 ± 10.4	57 ± 16	10.8 ± 0.7	10.7 ± 0.7	96 ± 6	0.57	3.7 ± 0.4
Ohau	Apatite	74	61 ± 12	5.8 ± 10.4	55 ± 16	11.9 ± 0.7	11.8 ± 0.7	87 ± 8	0.43	3.2 ± 0.4
Ohau	Apatite	75	75 ± 16	5.8 ± 10.4	69 ± 19	12.6 ± 0.4	12.6 ± 0.5	78 ± 7	0.41	2.9 ± 0.4
Ohau	Apatite	76	108 ± 14	5.8 ± 10.4	102 ± 17	13.0 ± 0.4	12.6 ± 1.6	75 ± 20	0.32	2.7 ± 0.5
Ohau	Apatite	77	112 ± 56	5.8 ± 10.4	106 ± 57			74 ± 16	0.12	2.5 ± 0.6
Hooker	Apatite	89	63 ± 10	5.6 ± 5.0	57 ± 11	11.9 ± 0.7	11.8 ± 0.7	87 ± 7	0.55	3.3 ± 0.4
Hooker	Apatite	90	96 ± 16	5.6 ± 5.0	90 ± 17	12.6 ± 0.4	12.3 ± 1.2	79 ± 13	0.43	3.0 ± 0.4
Godley	Apatite	100	4.8 ± 2.0	5.4 ± 4.6	0 ± 5.0	7.2 ± 1.6	4.3 ± 3.5	121 ± 16	0.92	5.0 ± 0.5
Godley	Apatite	101	14.4 ± 8.0	5.4 ± 4.6	9.0 ± 9.0	8.4 ± 1.0	6.5 ± 4.6	115 ± 13	0.83	4.6 ± 0.6
Godley	Apatite	102	28 ± 8	5.4 ± 4.6	23 ± 9	9.4 ± 1.0	8.4 ± 2.5	108 ± 10	0.79	4.3 ± 0.5
Godley	Apatite	103	43 ± 14	5.4 ± 4.6	38 ± 15	11.0 ± 0.4	10.6 ± 1.4	96 ± 10	0.76	3.8 ± 0.5
Godley	Apatite	105	50 ± 12	5.4 ± 4.6	45 ± 13	11.9 ± 0.5	11.7 ± 0.8	88 ± 9	0.81	3.6 ± 0.4
Godley	Apatite	106	51 ± 16	5.4 ± 4.6	46 ± 17	11.2 ± 0.4	11.0 ± 0.9	94 ± 8	0.72	3.8 ± 0.4
Godley	Apatite	107	50 ± 20	5.4 ± 4.6	45 ± 21	11.4 ± 1.2	11.3 ± 1.6	91 ± 14	0.44	3.4 ± 0.6
Godley	Apatite	108	59 ± 14	5.4 ± 4.6	54 ± 15	12.8 ± 0.7	12.8 ± 0.8	76 ± 11	0.49	2.9 ± 0.4
Godley	Apatite	109	47 ± 10	5.4 ± 4.6	42 ± 11	12.6 ± 0.4	12.3 ± 0.8	81 ± 10	0.40	2.9 ± 0.4
Godley	Apatite	110	48 ± 16	5.4 ± 4.6	43 ± 17	12.2 ± 0.4	12.0 ± 1.1	85 ± 12	0.20	2.9 ± 0.5
Clyde	Apatite	113	3.9 ± 1.6	4.3 ± 4.2	0 ± 4.5	6.1 ± 1.9	3.8 ± 3.3	122 ± 7	0.81	4.9 ± 0.5
Clyde	Apatite	114	15.3 ± 8.4	4.3 ± 4.2	11.0 ± 9.4	8.7 ± 1.1	7.3 ± 4.4	112 ± 15	0.72	4.4 ± 0.6
Clyde	Apatite	115	38 ± 8	4.3 ± 4.2	34 ± 9	9.8 ± 1.1	9.4 ± 1.6	103 ± 8	0.66	4.1 ± 0.4
Clyde	Apatite	116	41 ± 12	4.3 ± 4.2	37 ± 13	10.3 ± 0.6	10.0 ± 1.4	100 ± 8	0.61	3.9 ± 0.4
Clyde	Apatite	117	49 ± 12	4.3 ± 4.2	45 ± 13	11.0 ± 0.4	10.9 ± 0.8	94 ± 7	0.60	3.7 ± 0.4
Clyde	Apatite	118	65 ± 14	4.3 ± 4.2	61± 15	11.5 ± 0.4	11.5 ± 0.4	90 ± 5	0.55	3.5 ± 0.4
Clyde	Apatite	119	86 ± 18	4.3 ± 4.2	82 ± 18	12.3 ± 0.3	12.2 ± 0.8	82 ± 7	0.52	3.2 ± 0.4
Wilberforce	Apatite	125	4.1 ± 1.8	4.7 ± 3.0	0 ± 3.5	7.9 ± 1.9	5.4 ± 2.9	118 ± 7	0.67	4.6 ± 0.5
Wilberforce	Apatite	126	8.4 ± 4.4	4.7 ± 3.0	3.7 ± 5.3	8.5 ± 1.5	6.4 ± 3.5	116 ± 10	0.70	4.5 ± 0.5
Wilberforce	Apatite	127	40 ± 10	4.7 ± 3.0	35 ± 10	11.3 ± 0.5	10.9 ± 1.3	94 ± 9	0.67	3.7 ± 0.4
Wilberforce	Apatite	128	41 ± 20	4.7 ± 3.0	36 ± 20	10.0 ± 0.6	9.6 ± 2.3	102 ± 12	0.52	3.9 ± 0.5
Arthur's	Apatite	133	3.6 ± 2.4	4.2 ± 1.8	0 ± 3.0	7.7 ± 4.8	5.4 ± 5.2	118 ± 13	0.81	4.8 ± 0.6
Arthur's	Apatite	134	5.5 ± 3.6	4.2 ± 1.8	1.3 ± 4.0	7.6 ± 5.3	5.5 ± 6.0	118 ± 15	0.76	4.7 ± 0.6
Arthur's	Apatite	rp1	134 ± 14	4.2 ± 1.8	130 ± 14	12.2 ± 0.3		70 ± 16	0.57	2.8 ± 0.5
Arthur's	Apatite	rp2	141 ± 16	4.2 ± 1.8	137 ± 16	12.4 ± 0.3		69 ± 16	0.61	2.8 ± 0.5
Arthur's	Apatite	rp3	92 ± 22	4.2 ± 1.8	88 ± 22	12.4 ± 0.4	12.2 ± 1.3	81 ± 14	0.73	3.3 ± 0.4
Arthur's	Apatite	rp4	114 ± 22	4.2 ± 1.8	110 ± 22	12.0 ± 0.4		73 ± 16	0.65	2.9 ± 0.6
Arthur's	Apatite	rp5	6.0 ± 3.6	4.2 ± 1.8	1.8 ± 4.0	8.3 ± 2.1	6.2 ± 3.4	116 ± 10	0.61	4.5 ± 0.5
Arthur's	Apatite	rp6	3.9 ± 1.4	4.2 ± 1.8	0 ± 2.3	8.0 ± 2.4	5.8 ± 2.8	117 ± 7	0.67	4.6 ± 0.5

Transect	Mineral	Sample Number	Age (Ma) ± 2σ	Uplift Age (Ma) ± 2σ	Corrected Age (Ma) ± 2σ	Sample Mean Length (μm) ± 2σ	Corrected Mean Length (μm) ± 2σ	Pre-uplift Paleotemp. (°C) ± 2σ	Elevation (km)	Amount of Rock Uplift (km) ± 2σ
Lewis	Apatite	153	3.0 ± 2.0	3.4 ± 2.2	0 ± 3.0	7.6 ± 4.4	5.7 ± 4.8	117 ± 12	0.46	4.4 ± 0.6
Lewis	Apatite	155	6.4 ± 5.6	3.4 ± 2.2	3.0 ± 6.0	7.7 ± 2.8	6.1 ± 4.8	116 ± 14	0.41	4.3 ± 0.6
Lewis	Apatite	156	11.2 ± 5.0	3.4 ± 2.2	7.8 ± 5.5	10.2 ± 2.7	8.9 ± 4.0	106 ± 19	0.38	3.9 ± 0.7
Lewis	Apatite	157	28 ± 14	3.4 ± 2.2	25 ± 14	9.7 ± 1.0	9.1 ± 3.6	105 ± 16	0.34	3.8 ± 0.6
Lewis	Apatite	158	75 ± 14	3.4 ± 2.2	72 ± 14	11.3 ± 0.5	11.2 ± 0.5	91 ± 5	0.29	3.3 ± 0.4
Lewis	Apatite	159	85 ± 14	3.4 ± 2.2	82 ± 14	11.6 ± 0.4	11.5 ± 0.7	89 ± 5	0.25	3.1 ± 0.4
Wilkin	Zircon	38						265 ± 50	0.61	9.9 ± 2.0
Arawata	Zircon	36						265 ± 50	0.09	9.4 ± 2.0
Haast	Zircon	54						265 ± 50	0.14	9.4 ± 2.0
Copland	Zircon	82						265 ± 50	1.08	10.4 ± 2.0
Whataroa	Zircon	96						265 ± 50	0.66	9.9 ± 2.0
Arthur's	Zircon	130						265 ± 50	0.25	9.5 ± 2.0
Robinson	Zircon	137						265 ± 50	0.43	9.7 ± 2.0
Lewis	Zircon	145						265 ± 50	0.55	9.8 ± 2.0
Whitcombe	Zircon	123						265 ± 50	0.41	9.7 ± 2.0
Haast	Zircon	8326-82						265 ± 50	0.09	9.4 ± 2.0

(i) All paleotemperatures assigned to apatite samples (except 77, RP1, RP2, RP4) have been determined by using the curves of Fig. 6 and the calculation procedure described in the text. (ii) All paleotemperature and rock uplift estimates are mean values. Errors on paleotemperature estimates from apatite data have been calculated by propagating errors through the curves whereby the error in $y = \frac{dy}{dx}\delta x$ where δx is the error in x, and by combining errors in subtractions using standard methods. Errors on paleotemperature estimates from zircon data are as suggested by *Hurford* [1986]. Rock uplift estimates combine errors from paleotemperature, geothermal gradient, initial mean surface elevation, and sea level change. (iii) "Corrected" refers to data having been corrected for uplift age. (iv) Paleotemperatures for samples 77 (no lengths), and RP1, RP2, and RP4 (inherited length and density) have been estimated with reference to paleotemperature determinations of neighbouring samples. (v) FT data for samples RP1-RP6 and 8326-82 taken from *Kamp et al.* [1989].

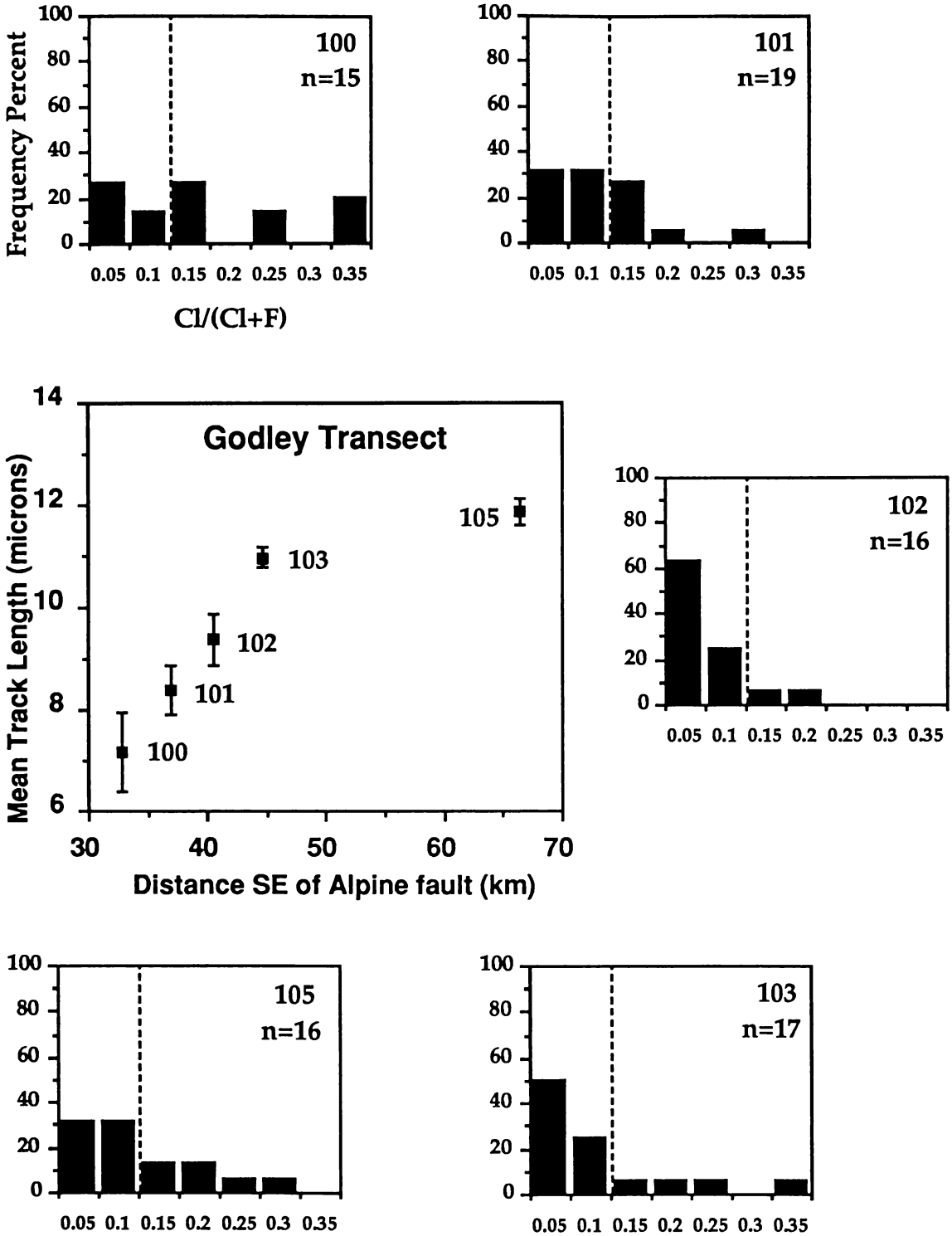


Fig. 7. Composition (Cl/(Cl+F)) of apatites from exhumed annealing zone samples of the Godley transect. Classes of Cl/(Cl+F) start at 0-0.05and increase at 0.05 intervals. Vertical broken line indicates Durango composition.

Another aspect of the empirical comparison of Otway Basin FT-temperature relationships with S. Alps FT data to derive paleotemperatures, is the fact that the S. Alps host rocks have cooled recently via uplift from the temperatures at which the FT parameters had equilibrated. This requires a correction to be made to the S. Alps FT data set to account for the accumulation of spontaneous tracks and the consequent modification of the track length distributions since cooling via uplift started. The details of this correction are outlined in the next section.

Qualitative Comparison of Otway Basin and S. Alps Apatite Data Sets

Fig. 8 shows graphs of mean age versus mean length (top) and mean length versus standard deviation (bottom) for Otway Basin and S. Alps data. The two data sets clearly show the same broad pattern. However for ages less than 110 Ma, the S. Alps samples have less age than would be expected from their lengths by comparison with the Otway data. This difference could be due to the slight compositional differences between the Otway Basin and S. Alps apatite, as on average the S. Alps samples contain slightly higher proportions of fluorapatites. Such a compositional difference would have the effect of reducing the age more than the length, as the reduction in age is affected by all the grains, whereas the mean length is biased by the longer tracks measured from the more Cl-rich grains. Fig. 8 (bottom) shows that S. Alps samples have slightly higher standard deviations than Otway samples of equivalent length, indicating that the length distributions are broader. This reflects the addition of long tracks to the exhumed apatite annealing zone since late Cenozoic uplift started, in addition to slight compositional differences.

For ages greater than ~110 - 115 Ma, the S. Alps samples have greater ages than would be expected from lengths in comparison with the Otway Basin data. This involves data for samples RP1, 2, and 4 from *Kamp et al.* [1989]. These three samples are regarded as having a population of fission tracks inherited from earlier thermo-tectonic events; inherited tracks would increase the age of a sample while the effect on track length would probably be to reduce the mean length. The paleotemperatures for these samples have therefore not been estimated using the calibration curves in Fig. 6. The rest of the samples are regarded as having been in equilibrium with ambient temperatures prior to uplift, with no inherited track component present.

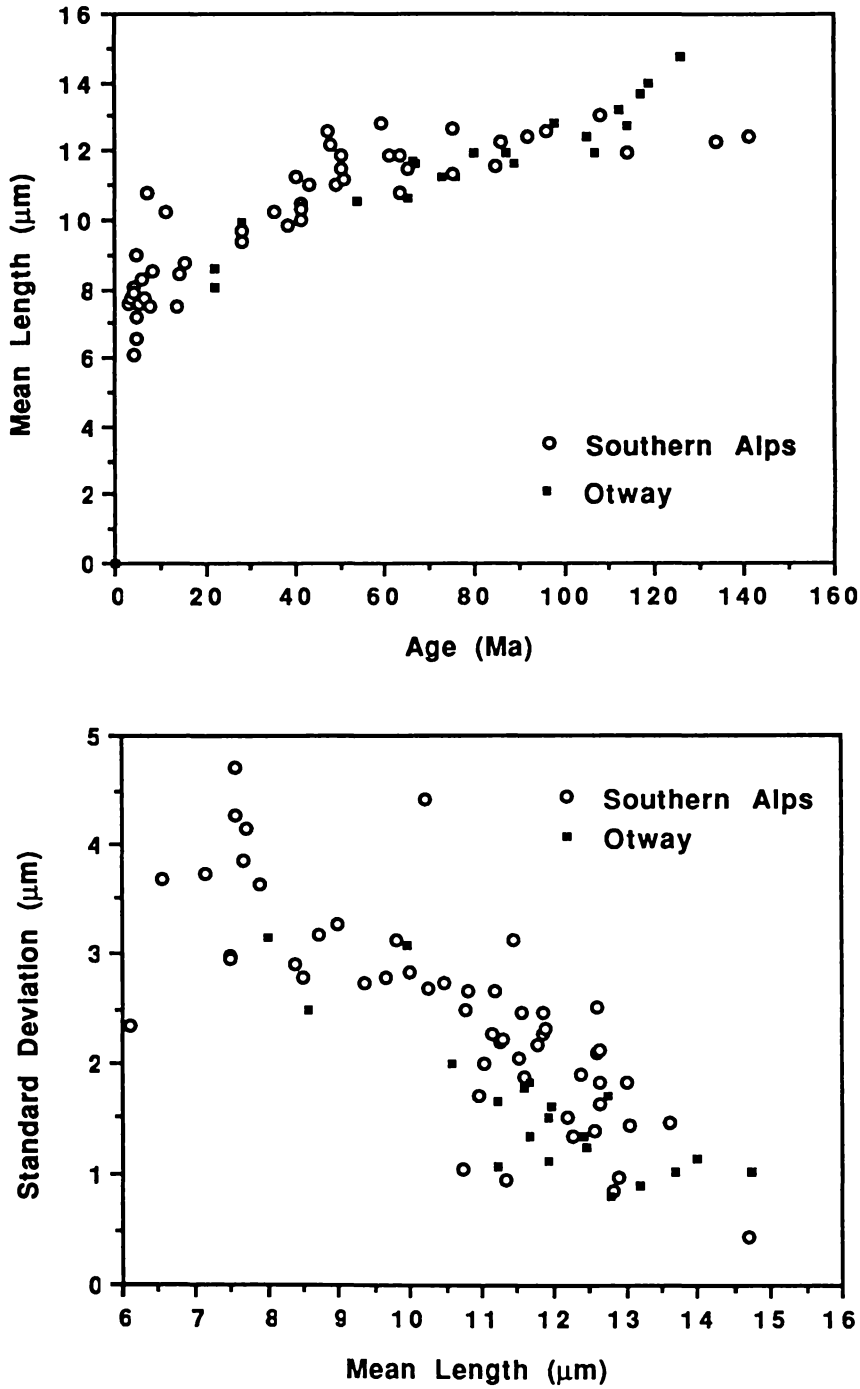


Fig. 8. (Top) Relationship between mean track length and apatite age for S. Alps and Otway Basin samples. Note the close similarity between the two data sets. (Bottom) Relationship between standard deviation and mean length for S. Alps and Otway Basin sample data.

Correction of Age and Length Data for late Cenozoic Uplift

The S. Alps samples were collected from surface outcrops and therefore the apatites have experienced a cooling phase that is primarily responsible for the systematic shift in the value of the S. Alps FT parameters from the comparable Otway Basin FT values (Fig. 8). The effect of the cooling on the S. Alps FT data is to increase the age of each sample in the exhumed annealing zone by the uplift age, and to increase the mean length of each sample by the addition of a component of 'long' tracks that originated during rapid cooling via uplift. This means that paleotemperature estimates of samples using raw lengths will be too low and a correction needs to be applied.

Calibration curves were constructed from the Otway data to estimate paleotemperatures of S. Alps samples (Fig. 6). For each S. Alps exhumed annealing zone sample, the Otway mean track length versus fission track age calibration curve (Fig. 6, top) was used to estimate a mean length corresponding to the fission track sample age. A 'corrected age' (that is, one corrected for the influence of the uplift phase) was derived by subtracting the uplift age from the sample age (we give details of the approach to, and results of, estimation of uplift age below). The mean length corresponding to the 'corrected age' was then estimated using the length versus age curve (Fig. 6, top). The difference between the two estimates of mean track length was then subtracted from the sample mean length to give a 'corrected mean length' (that is, one corrected for the influence of the uplift phase) (Table 4). This length is an estimate of the equilibrium mean length of the sample prior to uplift. The pre-uplift paleotemperature corresponding to this length was then determined using the Otway temperature versus length curve (Fig. 6, bottom).

Pre-uplift Sample Paleotemperatures

The pre-uplift mean paleotemperature estimates and errors for all samples from the exhumed apatite annealing zone are given in Table 4. In each transect an additional paleotemperature estimate could be made from the zircon data corresponding to the base of the zircon annealing zone. In each transect the base of the zircon annealing zone corresponds to a major inflexion in the age versus distance from the Alpine fault plot (e.g. Fig. 5). The paleotemperature assigned to this point in each transect is 265 ± 50°C (±

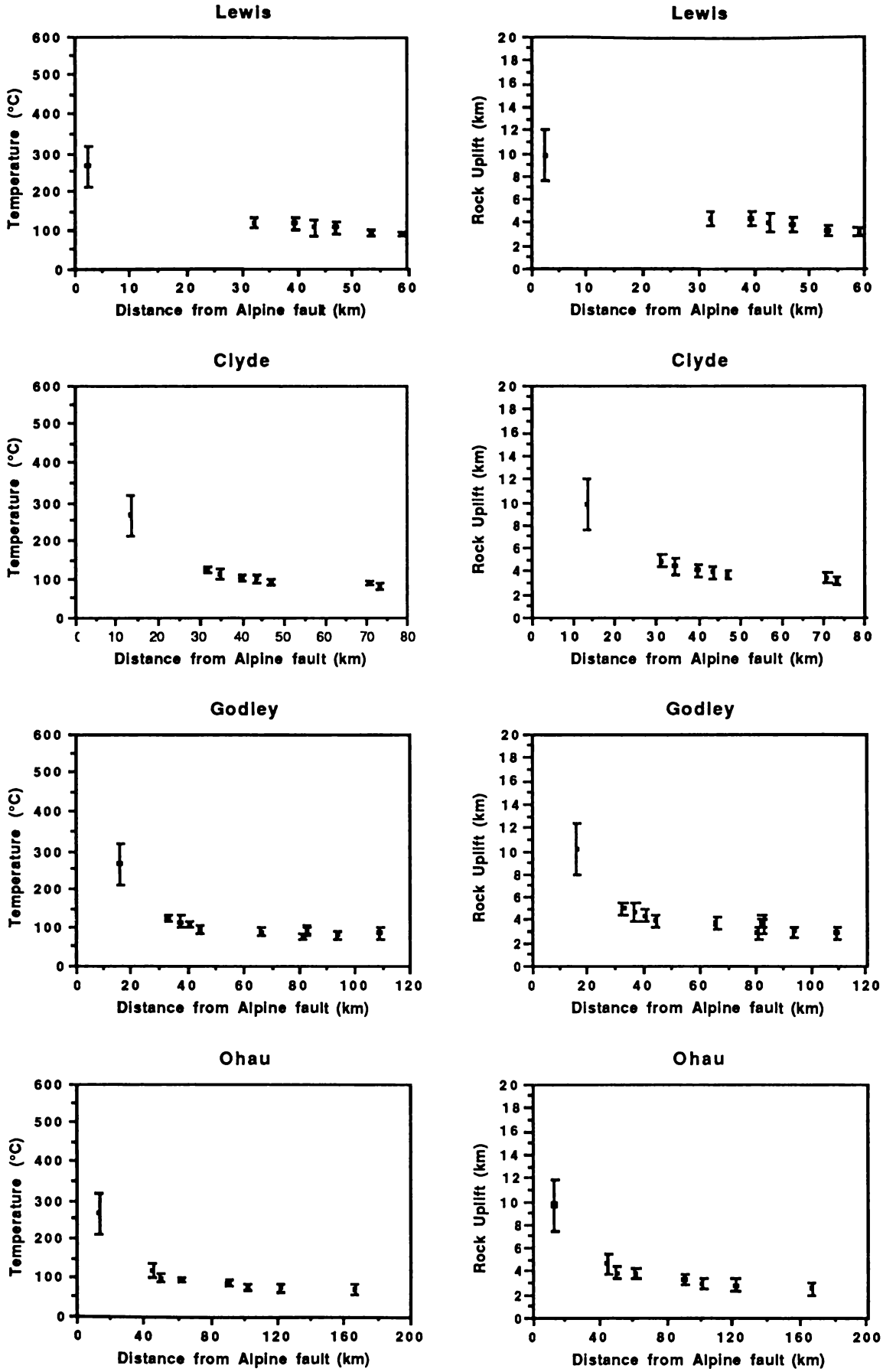


Fig. 9. (Left) Variation of pre-uplift paleotemperature with distance from the Alpine fault for samples from selected S. Alps transects. Errors on point mean values are 2σ. (Right) Variation of uplift amount with distance from the Alpine fault for samples from selected S. Alps transects. Errors on point mean values are 2σ.

2σ), following *Kamp et al.* [1989]. The samples to which this paleotemperature were assigned are included in Table 4.

Fig. 9 (left) illustrates for four transects data about paleotemperature versus sample distance from the Alpine fault. In all transects, sample paleotemperatures increase consistently with increasing proximity to the Alpine fault.

AMOUNT OF ROCK UPLIFT

An estimate of the total amount of rock uplift for each sample was made using the following relationship [modified from *Brown*, 1990]:

$$U_r = \frac{T_p - T_s}{G} + E_s - E_{im} + \Delta E_{msl} \quad (1)$$

where
U_r = amount of rock uplift (km)
T_p = pre-uplift paleotemperature (°C)
T_s = pre-uplift surface temperature (assume = 10°C)
G = pre-uplift geothermal gradient (assume = 27.5 ± 2.5°C (2σ))
E_s = present sample elevation above mean sea level (km)
E_{im} = initial mean elevation of land surface (assume 0 km)
ΔE_{msl} = difference between pre-uplift mean sea level and present day mean sea level (assume = 0 km)

The mean sea level from 25 Ma - 10 Ma was similar to that of the present day [*Haq et al.*, 1987], and therefore ΔE_{msl} is assumed to be zero. There may have been a difference of ~100 m at most, but this is not significant in light of the total amount of rock uplift as discussed below. The existence of a low relief terrestrial environment from about 25 Ma - 10 Ma means E_{im} for all samples is taken as zero [*Kamp and Tippett*, submitted]. The pre-uplift geothermal gradient is assumed to have been that of a 'normal' continental lithosphere, and the figure of 27.5°C used is the mid-point of the oft-quoted range of 25 - 30°C.

Estimates of the total amount of uplift for each sample are given in Table 4. We emphasise that the uplift estimates pertain to the amount of

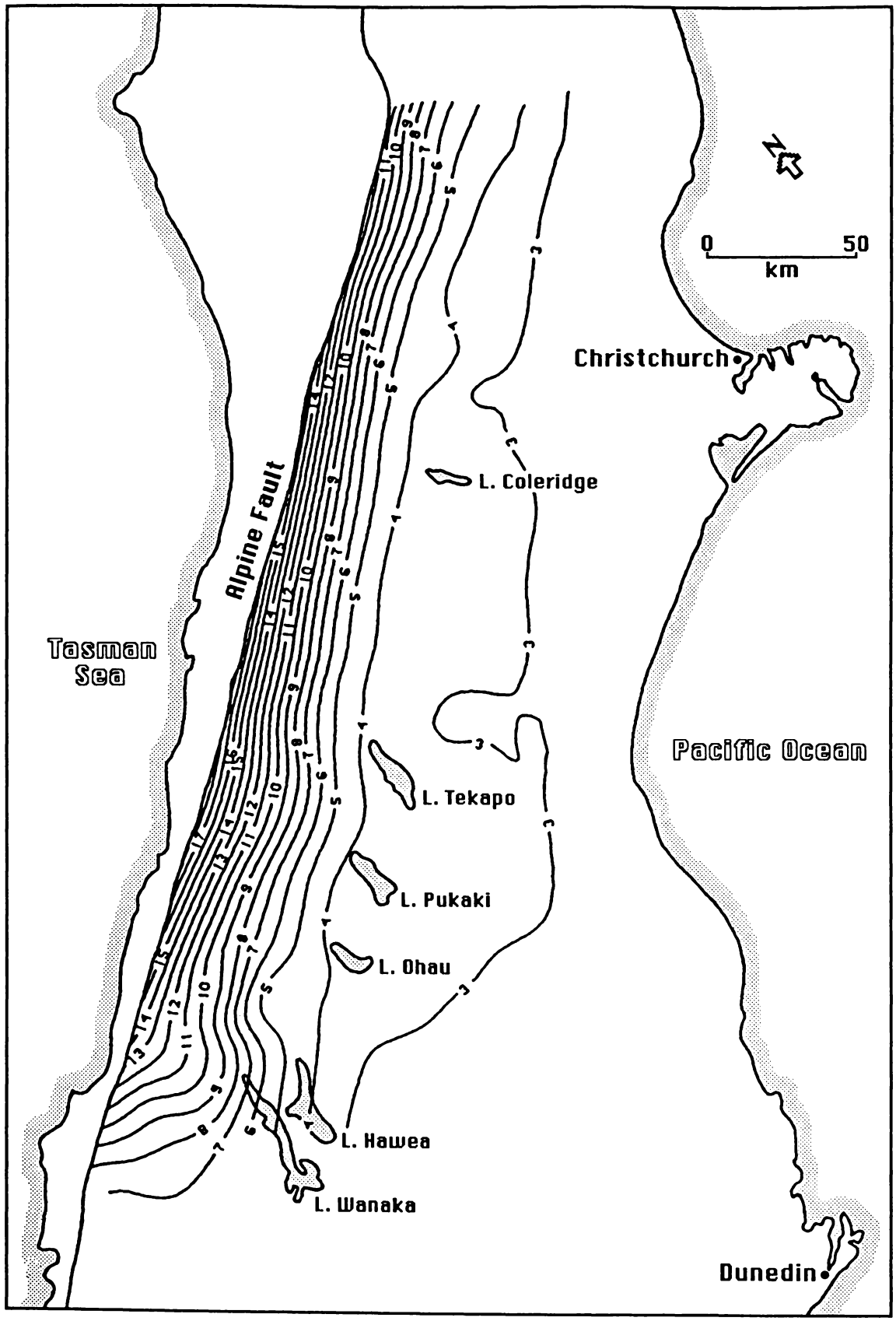


Fig. 10. Map of amount of late Cenozoic rock uplift (in km) of the S. Alps, constructed with the uplift data contained in Table 4 based on a trend surface model described in the text.

rock uplift [*England and Molnar*, 1990], and not to mean surface uplift or any other definition of uplift.

Spatial Pattern of Amount of Rock Uplift

Fig. 9 (right) shows for selected transects that the amount of uplift increases smoothly with increasing proximity to the Alpine fault. The spatial variation in the amount of late Cenozoic uplift over the S. Alps derived from all the data is illustrated in Fig. 10. The variation was initially approximated using a fourth order polynomial trend surface function. Inspection of residual plots showed that residuals are homoscedastic and not spatially correlated, suggesting that the trend surface model is appropriate. The surface was significant at better than the 99% level of confidence, and therefore it is most unlikely that the spatial pattern is a random effect. In order to produce a slightly more realistic geological surface, the residuals from the trend surface model were added into the trend surface (Fig. 10).

From the base of the exhumed zircon annealing zone, corresponding to approximately 10 km of uplift, the amount of uplift is extrapolated to the Alpine fault reaching a maximum of ~19 km at the fault between Copland River and Fox Glacier. The easternmost bedrock cropping out in South Island has been uplifted 3 km. To the north at Lewis Pass, uplift amounted to about 10 km, and it is 8 km near Arawata in the south. Considering the distance over which the data extend (~300 km), the pattern of uplift is remarkably simple. Previous estimates of late Cenozoic uplift at the Alpine fault fall into two groups: (1) Mesozoic uplift has accounted for 18-20 km of uplift, restricting late Cenozoic uplift to 5-10 km [e.g. *Sheppard et al.*, 1975; *Adams* 1979, 1981; *Adams and Gabites*, 1985], (2) late Cenozoic uplift has accounted for much greater than 10 km of uplift [e.g. *J. Adams*, 1980; *Cooper*, 1980; *Kamp et al.*, 1989]. This study supports the latter model.

The contours of equal uplift amount cross-cut the geological boundaries presently cropping out in the S. Alps, most noticeably to the south of Mount Cook. This originates from the effect of Mesozoic uplift. The amount of Mesozoic (or pre-late Cenozoic) uplift can be estimated by subtracting the amount of late Cenozoic uplift from the total uplift calculated from peak metamorphic temperatures. The boundary between chlorite subzones 2 and 3 approximates the transition from pumpellyite-actinolite metamorphic facies to greenschist facies rocks [e.g. *Bishop*, 1972]. The peak

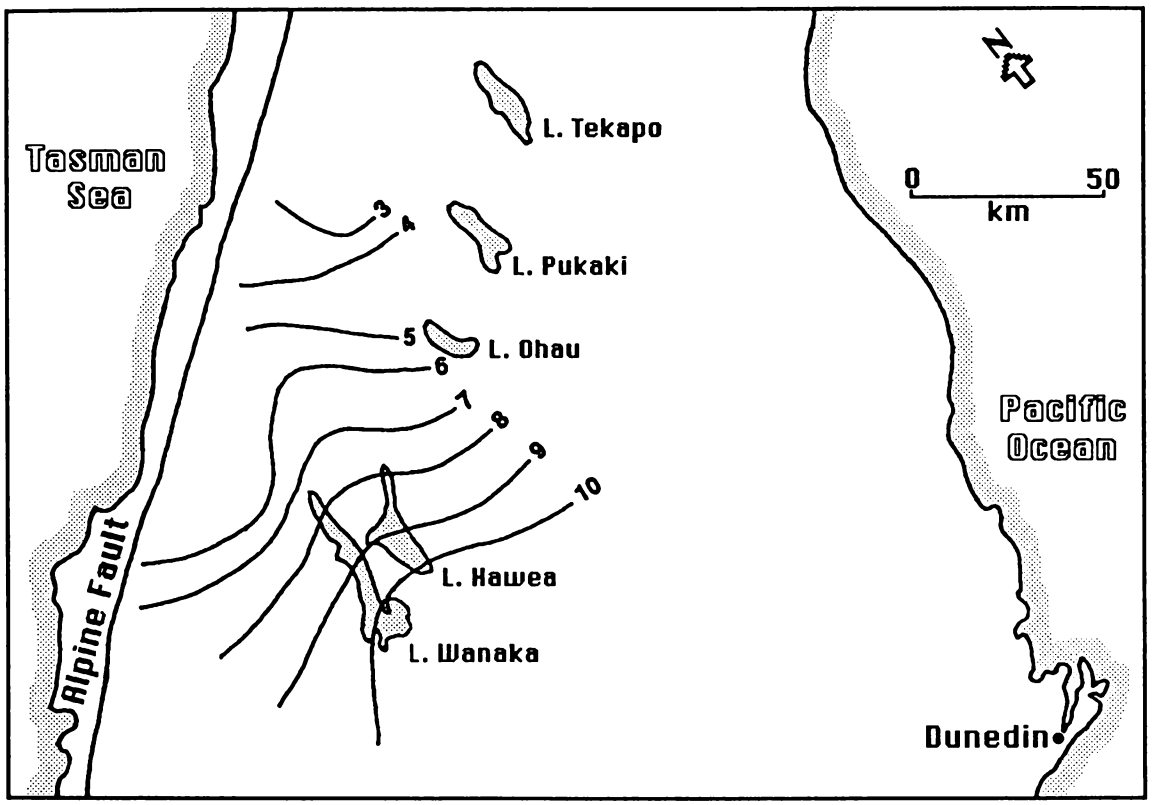


Fig. 11. Map of amount of rock uplift (in km) prior to the late Cenozoic, constructed by subtraction of the late Cenozoic uplift amount from the total amount of uplift as indicated by the metamorphic grade of the basement rocks.

metamorphic temperature of this boundary is ~300°C [*Essene*, 1989] and that of the biotite isograd is about 400°C at 4.5 kilobar [*Mason*, 1962; *Jamieson and Craw*, 1987]. Assuming a 25-30°C geothermal gradient, these temperatures represent approximately 11.5 km and 15 km of total rock uplift respectively, incorporating a correction for elevation.

Fig. 11 shows the amount, pattern and extent of the pre-late Cenozoic uplift in the southern part of the S. Alps produced by subtraction of the late Cenozoic uplift at the points where the uplift contours and geological boundaries cross. The amount of pre-late Cenozoic uplift increases from north to south, and in the south, from northwest to southeast away from the Alpine fault to reach a maximum of 10 km at the southern ends of Lakes Wanaka and Hawea. Pre-late Cenozoic uplift near Mount Cook amounted to ~3 km, and north of Arthur's Pass there is no evidence for uplift prior to the late Cenozoic. Distributed late Cenozoic strain within the schists east of the Alpine fault has probably caused the orientation of the contour pattern of pre-late Cenozoic uplift to be bent dextrally. Further investigation into uplift episodes prior to the late Cenozoic, integrating this information with other fission track data, is proceeding [*Kamp and Tippett*, in preparation].

TIMING OF LATE CENOZOIC UPLIFT

Within each transect apatite FT age decreases towards the Alpine fault (Fig. 3). In terms of estimating the age of initiation of uplift, the annealing zone age ($P(\chi^2)<5\%$) of zone d in Fig. 3 will slightly over-estimate the age of uplift, because it already had a finite age prior to uplift. By comparison, the reset age ($P(\chi^2)>5\%$) immediately to the west (zone c in Fig. 3) will slightly under-estimate the age of uplift because uplift was already underway before tracks could accumulate. The estimate we have used of the age of the start of uplift is the weighted mean of the reset and annealing zone age pair in each transect, and relates to the geographic mid-point of the sample pair. These estimates for each transect are given in Table 5. These ages will be minimum ages (probably by a maximum of a few hundred thousand years) as the short mean length of the annealing zone age and very low frequency of horizontally confined tracks preclude application of a length correction to the mean age.

The age of initiation of uplift in different parts of each transect can also be established from the zircon data. We have identified the transition from reset to exhumed zircon annealing zone ages in each transect by the

Table 5. Uplift age estimates for Southern Alps samples.

Transect	Mineral	Sample Number	Ages used in calculation (Ma) ± 1σ	P(χ^2) (%)	Uplift Age (Ma) ± 1σ	Location
Hunter	apatite	49	5.0 ± 1.3	98		
		50	7.3 ± 2.0	3.0		
					5.7 ± 1.1	s107/087448
Haast	apatite	57	5.8 ± 3.3	96		
		58	7.8 ± 3.8	<0.1		
					6.7 ± 2.5	s98/158873
Haast	zircon	54			7.4 ± 0.7	s98/126935
Haast	zircon	8326-82			6.6 ± 0.8	s87/118031
Ohau	apatite	71	4.9 ± 0.8	97		
		72	41.2 ± 5.0	2.8		
					5.8 ± 5.7	s99/532896
Godley	apatite	100	4.8 ± 1.0	20		
		101	14.4 ± 4.0	<0.1		
					5.4 ± 2.3	s80/120475
Clyde	apatite	113	3.9 ± 0.8	58		
		114	15.3 ± 4.2	<0.1		
					4.3 ± 2.1	s72/390697
Wilberforce	apatite	125	4.1 ± 0.9	48		
		126	8.4 ± 2.2	1.2		
					4.7 ± 1.5	s65/872084
Arthur's	apatite	133	3.6 ± 1.2	34		
		134	5.5 ± 1.8	3.0		
					4.2 ± 0.9	s59/059281
Arthur's	zircon	RP14			4.3 ± 0.9	s51/953537
Arthur's	zircon	130			4.6 ± 0.3	s52/045506
Robinson	zircon	137	5.7 ± 1.2	28		
		138	7.6 ± 1.0	1.0		
					6.8 ± 0.9	s46/503815
Lewis	apatite	153	3.0 ± 1.0	80		
		155	6.4 ± 2.8	2.5		
					3.4 ± 1.1	s54/911706
Lewis	zircon	145			5.3 ± 0.4	s46/678986

(i) Location grid coordinates refer to New Zealand Map Series 1. (ii) FT data for samples 8326-82 and RP14 taken from *Kamp et al.* [1989].

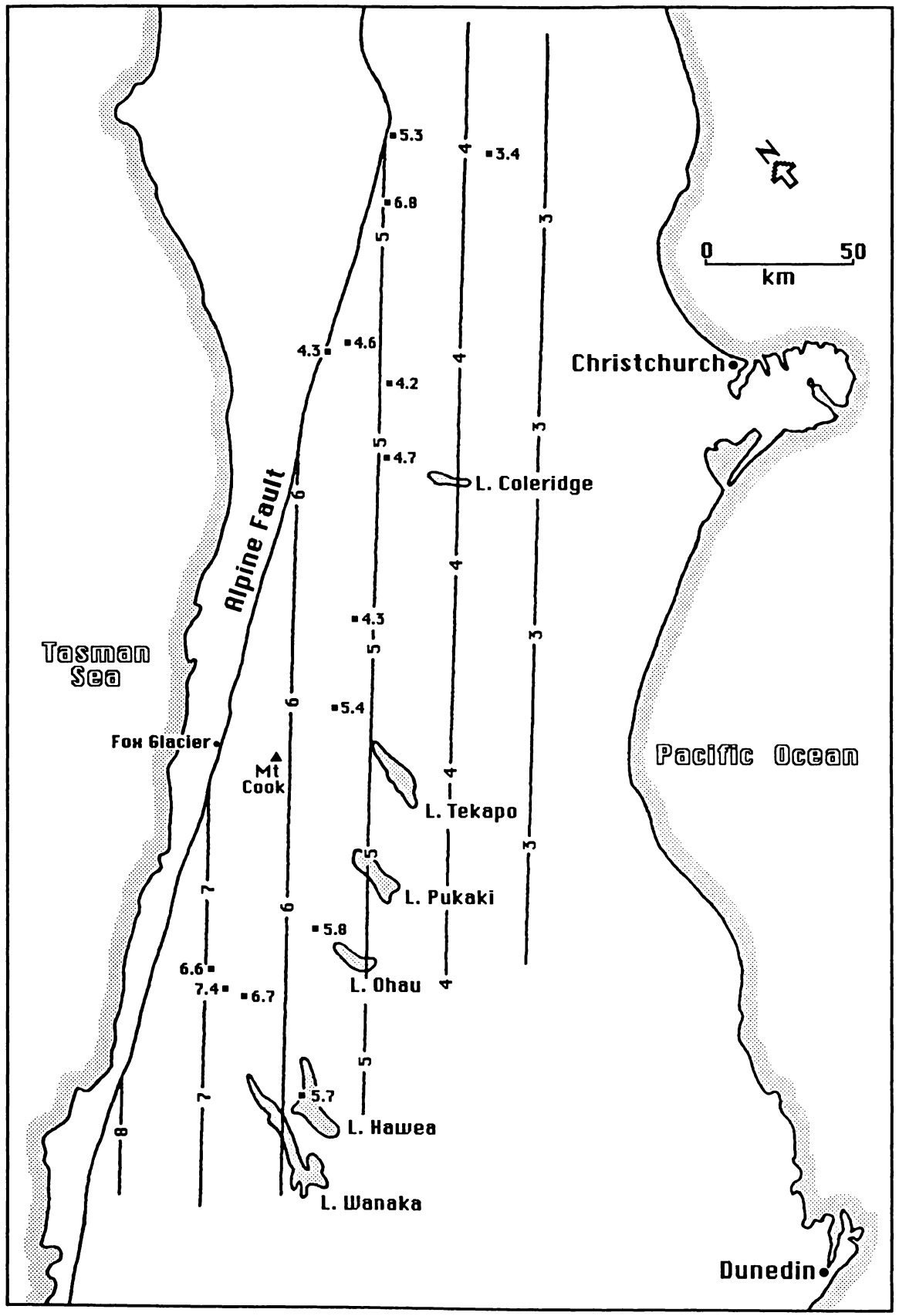


Fig. 12. Map of the spatial variation in uplift age (in Ma) across the S. Alps (first order trend surface). Details of map construction are described in the text. Filled squares show the locations and point mean values of the uplift age estimates (Table 5) used to construct the surface.

sudden increase in age southeast of the Alpine fault (Fig. 5). This point of inflexion is best shown in the Lewis, Arthur's, Haast and Robinson transects. The sample marking the base of the exhumed annealing zone records the uplift age for each transect. Uplift ages derived in this way are also incorporated in Table 5.

Discussion of Uplift Age

The uplift age data of Table 5 were modelled using a first order polynomial trend surface function. Fig. 12 is the resulting map and shows the regional variation in the age of uplift initiation across the S. Alps together with the point mean values of uplift age. Inspection of residual plots shows that the residuals are homoscedastic and not spatially correlated, suggesting that the trend surface model is appropriate. The surface is significant at the 99% level of confidence, and therefore the spatial pattern is not a random effect.

The pattern of the iso-age lines in Fig. 12 shows that there is clearly significant spatial variation in the age of uplift initiation within the S. Alps; rocks now at the surface in different places started to be uplifted at different times. The two major features about the pattern of the iso-age lines are that the 8 - 5 Ma iso-age lines project to intersect the Alpine fault, and that there is a southeastward younging in the age of uplift initiation.

The intersection of the iso-age lines with the Alpine fault indicates that uplift of the leading edge of the Pacific plate at the present position of the Alpine fault began about 3 m.y. earlier in the southern part of the S. Alps (at about 8 Ma) compared with the northern part of the S. Alps (at about 5 Ma). This difference in timing confirms that inferred by *Kamp et al.* [1989] from a much more limited amount of FT data. The age of uplift initiation given in Fig. 12 for different positions along the Alpine fault should be regarded as minimum estimates of the age of uplift initiation at the paleo-Alpine fault. The first rocks in the central sector of the S. Alps to be uplifted were those in the south at ~8 Ma, 2 m.y. after the Alpine fault is predicted from plate rotation parameters to have became obliquely convergent [9.8 Ma; *Stock and Molnar*, 1982].

There is a strong south-eastward younging across the strike of the S. Alps in the age of uplift initiation (Fig. 12). The uplift was clearly controlled by the Alpine fault and propagated southeastwards. The rate of

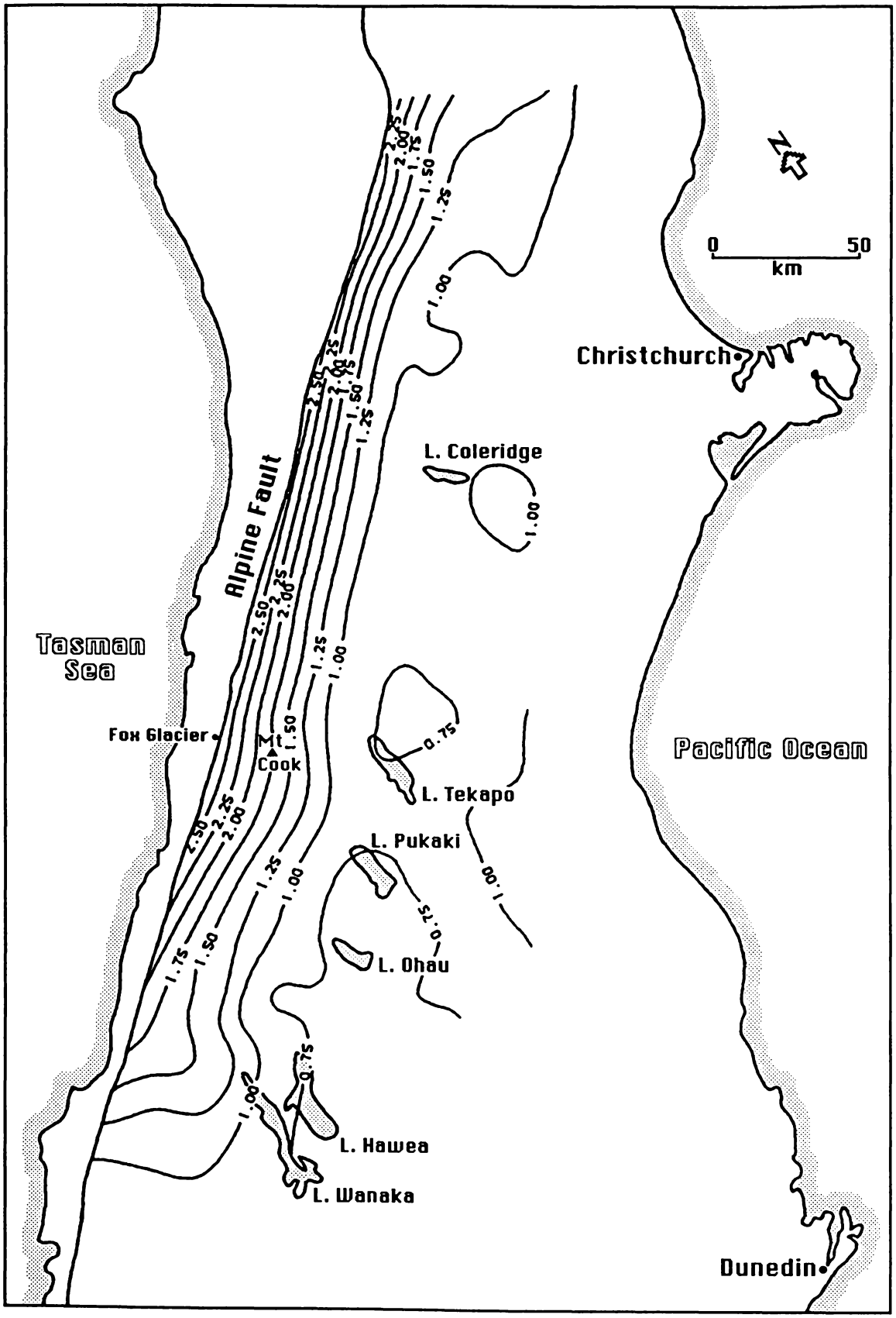


Fig. 13. Map of the spatial variation in late Cenozoic mean uplift rate (in mm/yr), derived by dividing uplift amount (Fig. 10) by uplift age (Fig. 12).

southeastward propagation of uplift initiation was 30 mm/yr; this exceeds the average rate of convergence perpendicular to the Alpine fault since 9.8 Ma of ~8 mm/yr (*Allis* [1986] has inferred ~80 km of shortening across the Australia-Pacific plate boundary in the vicinity of the S. Alps since ~10 Ma).

The intersection of the iso-age lines with the Alpine fault is considered to result from the longer time over which the southern part of the S. Alps has been under collision (~8 Ma) compared with the northern part (~5 Ma). At the time the southern part of the S. Alps started to be uplifted, the northern parts may still have been in a purely strike-slip portion of the plate boundary zone (see reconstructions of *Walcott* [1984] and *Kamp* [1987]). As dextral transcurrent movement (330 ± 110 km since 9.8 Ma [*Stock and Molnar*, 1982]) brought the northern parts of the S. Alps into the collision zone, so uplift started there later. This implies that mountain-building started in the southwest and propagated to the northeast and southeast; that is, uplift propagated both along the length and across the width of the present S. Alps.

The strike of the iso-age lines in Fig. 12 obliquely intersects the strike of the contours of rock uplift (Fig. 10), which are more parallel to the strike of the Alpine fault. This indicates that late Cenozoic mean uplift rates have varied regionally across the S. Alps.

RATES OF ROCK UPLIFT AND IMPLICATIONS

Two approaches to the derivation of uplift rates have been taken in this study. Firstly, late Cenozoic mean uplift rates have been calculated by dividing the total amount of uplift by the age of uplift initiation (Fig. 13). Secondly, uplift rates have been estimated from the reset zircon ages near the Alpine fault. A potential problem in calculating the amount and rate of uplift from FT data is the possibility of perturbation of the geotherms during uplift, resulting in higher geothermal gradients near the surface. This may have the effect of leading to an overestimation of the amount and rate of uplift. However, all data from the exhumed apatite and zircon annealing zones cannot be affected by the effect of uplift subsequently dragging up the geotherms, as the rise of the geotherms must postdate the 'setting' of ages at the base of the annealing zones; that is, regionally, the geotherms cannot rise before uplift is initiated. Therefore, the calculated uplift amounts, ages, and rates (Tables 4, 5, and 6; Figs 9b, 10, 12, and 13) based on a pre-uplift

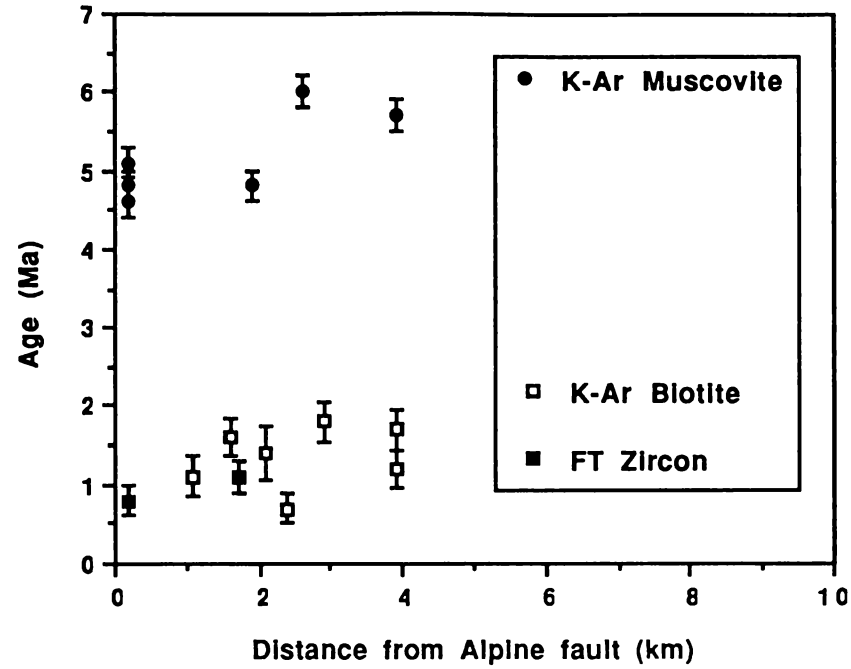


Fig. 14. Relationship between age and distance from the Alpine fault for the Mt Cook region for samples <5 km from the fault (Havelock Creek, Cook River, Fox Glacier, Franz Josef Glacier and Dry Creek). K-Ar data are from *Adams* [1981]; FT data are from *Kamp et al.* [1989] and this study. Errors are 1σ.

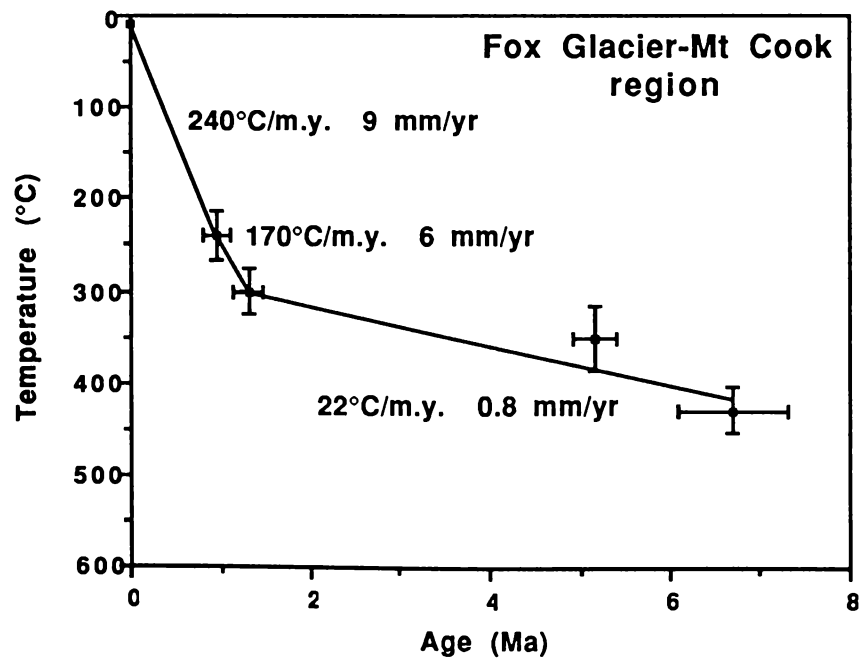


Fig. 15. Cooling history of rocks from <5 km from the Alpine fault (from Fig. 14) in the Mt Cook region. The sample ages have been averaged for each dating system (K-Ar biotite, K-Ar muscovite, FT zircon). The age of initiation of uplift at 6.7 ± 0.6 Ma is from Fig. 12, and Fig. 3 of *Kamp and Tippett* [submitted]. Errors are 1σ.

geothermal gradient of 27.5°C/km are considered to be reliable. We also show below that the passage of most of the reset zircon samples through the zircon FT closure temperature of 240° ± 50° C (± 2σ) [*Hurford*, 1986] occurred before the geotherms could have been perturbed significantly.

Late Cenozoic Mean Uplift Rates

The late Cenozoic mean uplift rates for the S. Alps range from a minimum of ~0.7 mm/yr along the eastern margin of the alps to a maximum of ~2.8 mm/yr adjacent to the central part of the Alpine fault (Fig. 13). Fig. 13 indicates the magnitude of longer-term rates that over 5 to 8 m.y. can expose amphibolite grade schists. The rates are considerably lower than the contemporary uplift rates of *Wellman* [1979], and the estimates of uplift rates derived below from reset zircon samples.

The thermal development of the continental lithosphere during uplift depends upon the rate of erosion (which cools the rocks) and the rate at which the geotherms rise in response to the uplift. The thermal evolution of the lithosphere adjacent to the Alpine fault during the uplift of the S. Alps has been modelled by *Allis et al.* [1979] and *Koons* [1987]. The thermal model of *Koons* [1987] relies upon uplift rate data from other published sources to provide constraints and boundary conditions; uplift rates of 10 mm/yr have been extrapolated back in time to 4 Ma. *Koons* [1987] predicts temperatures after 2.25 m.y. of uplift at 10 mm/yr of more than 400°C at 5 km depth, with geothermal gradients of up to 100°C/km in the upper 3 km. Over periods longer than 2.5 m.y., the vertical temperature distribution is shown to change little, given the boundary conditions adopted by Koons [1987].

The results of this study indicate that the boundary conditions of uplift age and rate previously used in thermal models can now be more tightly constrained. The age when rock uplift started in the Mt Cook region (~6.7 Ma) is actually earlier, and the average uplift rate in that region is lower (~2.8 mm/yr) than the values assumed by *Koons* [1987] in his thermal model.

Fig. 14 shows the variation in age of K-Ar and zircon FT data with distance from the Alpine fault in the Mount Cook region (Copland - Fox Glacier - Franz Josef Glacier - Whataroa). The data in Fig. 14 have been used to construct a cooling curve for the region adjacent to the Alpine fault near Mt Cook (Fig. 15). For these localities the K-Ar biotite and muscovite ages are younger than the uplift age inferred from fission track data (Fig.

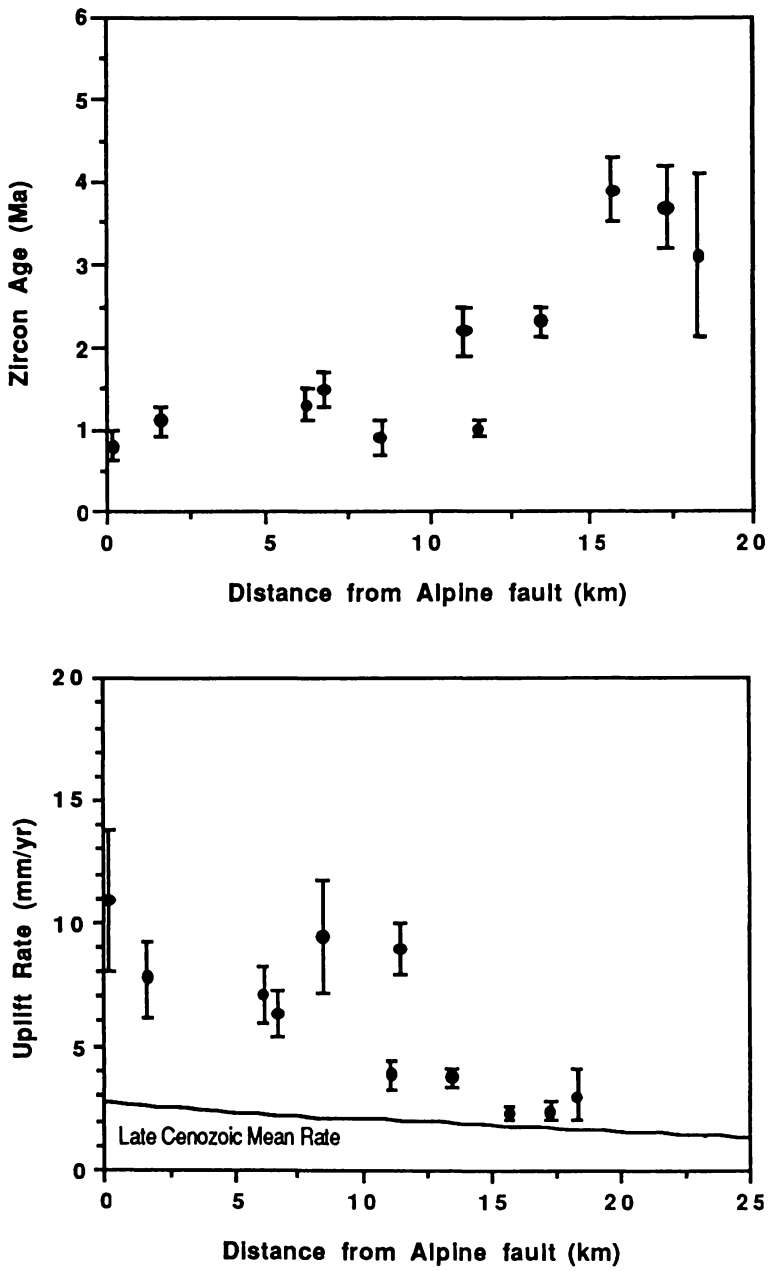


Fig. 16. (Top) Variation in zircon age with distance from the Alpine fault in the Mt Cook region. Data from *Kamp et al.* [1989] and this study, taken from Copland River, Fox Glacier, Franz Josef Glacier and Whataroa River. Errors are 1σ. (Bottom) Variation in uplift rate (derived from reset zircon sample ages) with distance from the Alpine fault in the Mt Cook region. Errors are 1σ.

12), and the K-Ar ages decrease towards the Alpine fault (Fig. 14). Therefore the problem of excess argon within the schists encountered to the south at Haast Pass [*Adams and Gabites*, 1985] is unlikely to be a major problem with the K-Ar ages from the Alpine Schist in the Mt Cook region. The estimate of the pre-late Cenozoic uplift temperature of the schist rocks of 430°C in Fig. 15 is an extrapolation from the exhumed apatite and zircon annealing zone data. Four hundred and thirty degrees celsius seems a reasonable value given that the likely maximum temperature attained by the schists 2-3 km from the fault in the Franz Josef area was ~520°C [530°C, *Grapes and Otsuki*, 1983; 540°C, *Findlay*, 1985; 490°C, *Johnstone and White*, 1983], and that there is evidence of ~90°C of Mesozoic cooling of the rocks in this area (Fig. 11). The rock uplift rates from ~6.7 to 1.3 Ma would have been in the order of 0.8 mm/yr for a gradient of 27.5°C/km (Fig. 15), which is probably too low to have substantially perturbed the geotherms prior to about 1.3 Ma; uplift rates of up to 2 mm/yr evidently have little impact on the thermal structure of the crust [*Koons*, 1987]. Uplift has accelerated to 6-9 mm/yr only since 1.3 ± 0.3 Ma (2σ) (Fig. 15), and therefore the geotherms will have been perturbed significantly only since then. This means that meaningful uplift rates can be calculated from the reset zircon ages that are greater than 1.3 ± 0.3 Ma using a geothermal gradient of 27.5°C/km. Samples with zircon ages younger than 1.3 ± 0.3 Ma will have been affected significantly by the effect of rising geotherms, and therefore uplift rates based on a constant gradient of 27.5°C/km overestimate the rate of uplift. This affects samples 79, 80, 93, 122, cw21 and cg13.

Uplift Rates Derived From Reset Zircon Ages

Table 6 contains data pertaining to the samples with reset zircon ages including calculated uplift rates. The calculation of uplift rates near the Alpine fault using these reset ages assumes that the land surface prior to the uplift period was at sealevel. Fig. 16 (top) shows a trend of increasing age with increasing distance from the Alpine fault for the Mt Cook region. Other transects show a similar trend. Fig. 16 (bottom) shows the derived uplift rates for the same samples based on a gradient of 27.5°C/km in relation to the late Cenozoic mean uplift rate for the region. Uplift rates increase from ~3 mm/yr 15 km from the fault to ~11 mm/yr right at the fault. Other transects (Fig. 17) show similar patterns of higher uplift rates closer to the fault.

Table 6. Rock uplift rates calculated from reset zircon sample ages.

Sample Number	Zircon age (Ma) ± 1σ	Distance from Alpine fault (km)	Elevation (km)	Uplift amount (km)	Uplift rate (mm/yr) ± 1σ
36	5.6 ± 0.5	8.2	0.09	8.5	1.5 ± 0.2
38	7.8 ± 1.8	25.7	0.61	9.0	1.2 ± 0.3
51	3.6 ± 0.8	17.4	0.08	8.4	2.4 ± 0.6
52	5.6 ± 0.6	18.1	0.09	8.5	1.5 ± 0.2
8326-2	4.2 ± 0.8	4.6	0.05	8.4	2.0 ± 0.4
8326-6	4.8 ± 0.4	6.6	0.06	8.4	1.8 ± 0.2
8326-9	3.8 ± 0.3	11.4	0.09	8.5	2.2 ± 0.2
66	1.9 ± 0.5	1.5	0.03	8.4	4.4 ± 1.2
68	3.1 ± 0.5	12.8	0.17	8.5	2.8 ± 0.5
79	0.6 ± 0.2	9.7	0.41	8.8	14.6 ± 5.0
80	1.0 ± 0.1	11.5	0.60	9.0	9.0 ± 1.1
81	3.7 ± 0.5	17.3	0.78	9.1	2.5 ± 0.4
82	3.1 ± 1.0	18.3	1.08	9.4	3.1 ± 1.0
cw21	0.8 ± 0.2	0.2	0.34	8.7	10.9 ± 2.8
fox4	1.5 ± 0.2	6.7	1.22	9.6	6.4 ± 1.0
cg3	1.1 ± 0.2	1.7	0.19	8.6	7.8 ± 1.5
cg13	1.3 ± 0.2	6.2	0.91	9.3	7.1 ± 1.2
93	0.9 ± 0.2	8.5	0.15	8.5	9.5 ± 2.2
94	2.2 ± 0.3	11.1	0.20	8.6	3.9 ± 0.6
95	2.3 ± 0.2	13.4	0.35	8.7	3.8 ± 0.4
96	3.9 ± 0.4	15.7	0.66	9.0	2.3 ± 0.3
121	1.3 ± 0.2	2.0	0.11	8.5	6.5 ± 1.1
122	1.2 ± 0.3	6.3	0.19	8.6	7.1 ± 1.9
123	3.4 ± 0.8	9.3	0.41	8.8	2.6 ± 0.6
129	1.7 ± 0.5	2.3	0.17	8.5	5.0 ± 1.5
RP11	2.7 ± 0.3	3.3	0.22	8.6	3.2 ± 0.4
RP14	4.3 ± 0.9	0.6	0.15	8.5	2.0 ± 0.4
135	2.6 ± 1.3	1.0	0.34	8.7	3.4 ± 1.7
137	5.7 ± 1.2	5.1	0.43	8.8	1.5 ± 0.3
140	2.1 ± 0.4	0.8	1.12	9.5	4.5 ± 0.9
141	3.0 ± 0.2	1.0	1.05	9.4	3.1 ± 0.3
142	3.7 ± 0.8	0.9	0.61	9.0	2.4 ± 0.6
143	2.2 ± 0.5	1.0	0.66	9.0	4.1 ± 1.0
144	3.4 ± 0.2	1.6	0.49	8.9	2.6 ± 0.2

(i) Uplift rate is determined by calculating uplift amount since passing through the 240°C closure temperature (equation 1) and dividing by the sample age. (ii) Error on uplift rate incorporates errors on zircon age, zircon closure temperature, and geothermal gradient. (iii) FT data for samples 8326-2, 6, 9, 82; cw21, fox 4, cg3, cg13; RP11, 14 taken from *Kamp et al.* [1989].

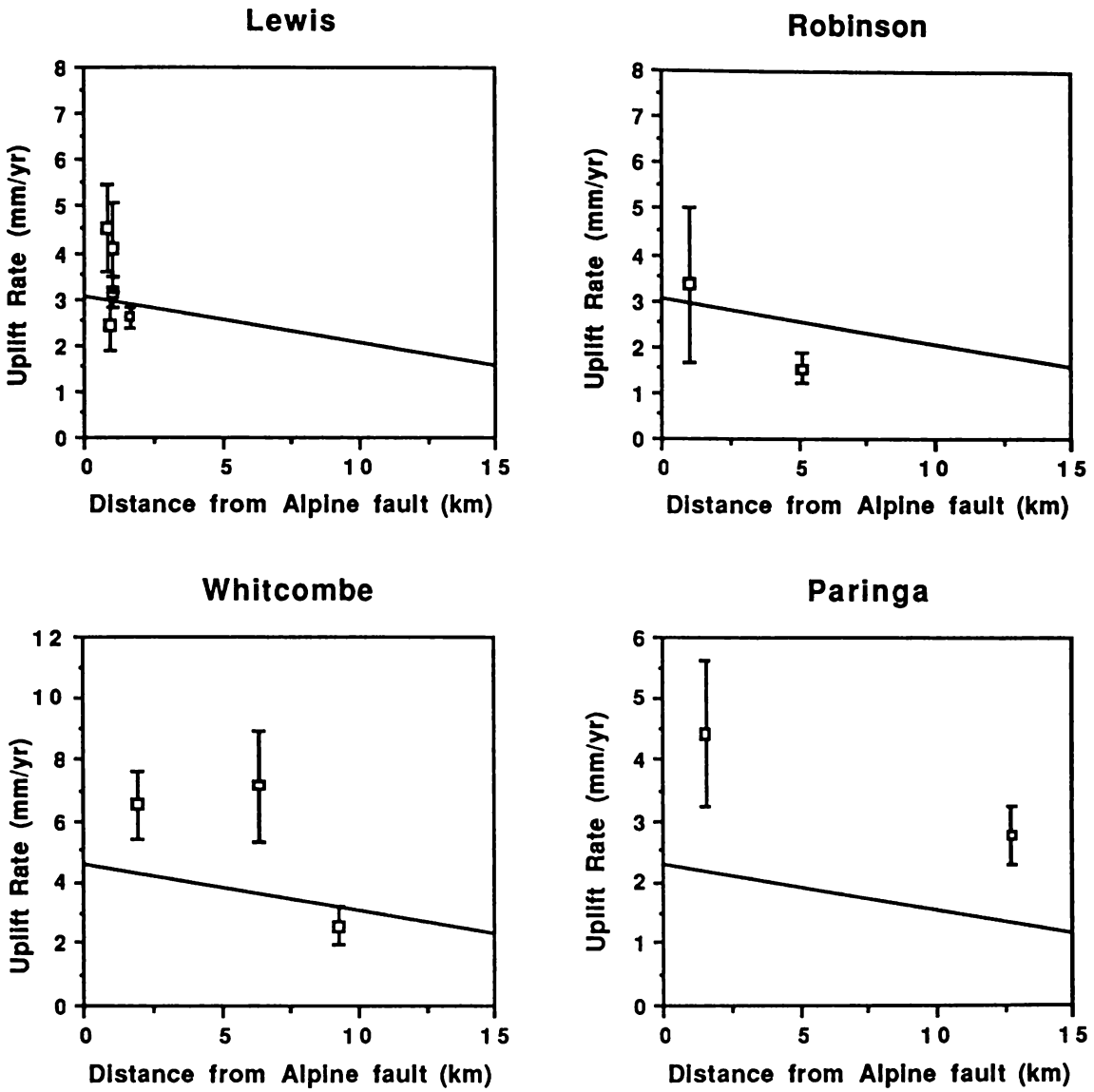


Fig. 17. Variation in uplift rate (in mm/yr) derived from reset zircon sample ages with distance from the Alpine fault for selected transects. Dotted line represents the late Cenozoic mean uplift rate from Fig. 13. Errors are 1σ.

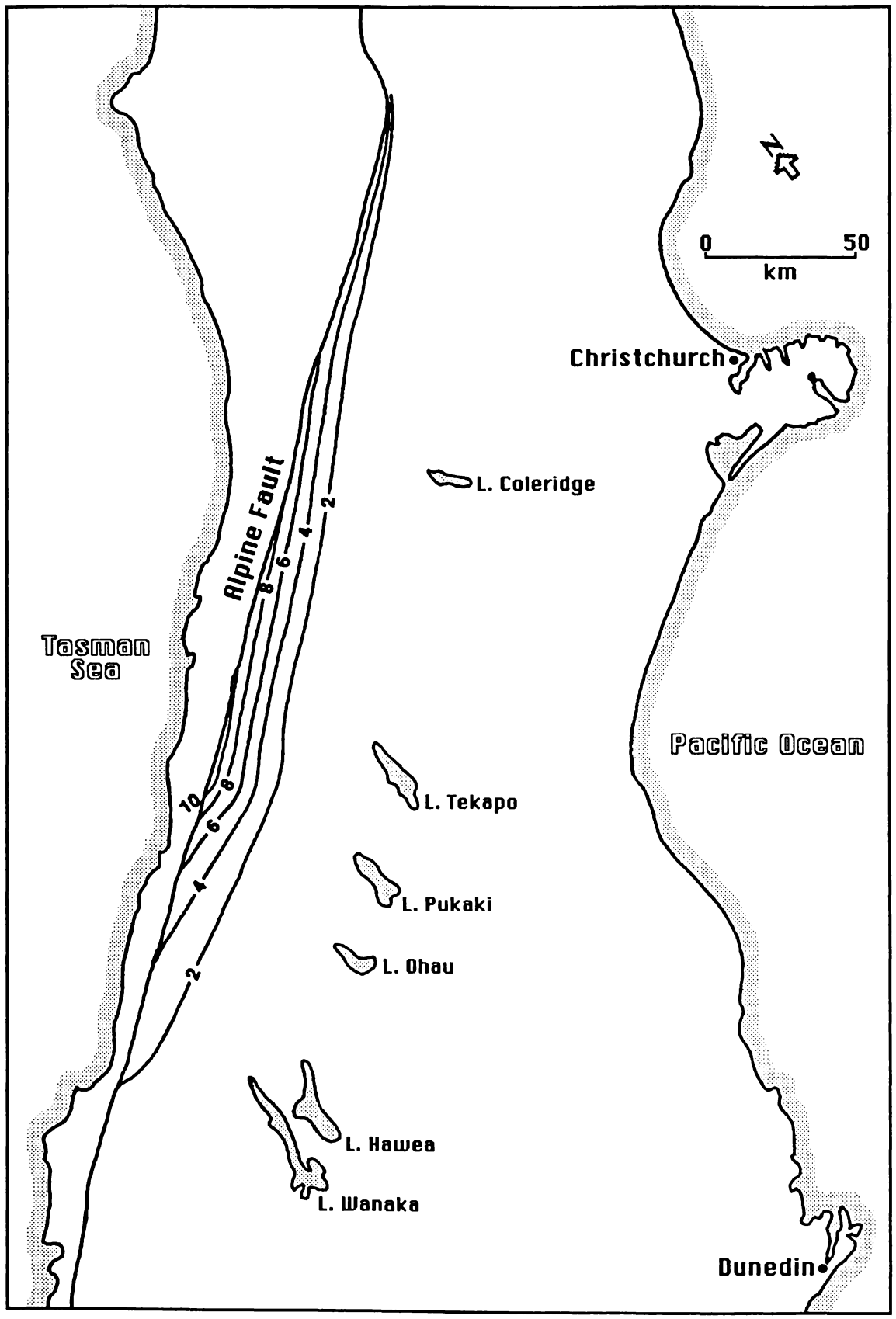


Fig. 18. Map of uplift rates (in mm/yr) derived from reset zircon sample ages.

Fig. 18 shows all the transect data in the form of a map. The uplift rates derived from reset zircon sample ages consistently exceed the estimated late Cenozoic mean uplift rates (Fig. 17). Near the Alpine fault the rates are high and of the same order as estimates of contemporary (post-glacial) uplift rates [*Wellman*, 1979], although the region of maximum uplift rate is further south than for the contemporary rates shown by *Wellman* [1979]. Farther to the southeast where the zircons have been recording uplift over longer periods of time, the uplift rates decrease quickly to almost equal the late Cenozoic mean uplift rate (Fig. 17).

J. Adams [1979] postulated that vertical drag has occurred on the Alpine fault, with the result that the highest uplift rates are found not right at the fault but at some distance (5 to 8 km) to the southeast. Figs 16 (bottom) and 17 show from a comprehensive data set that this has not happened, a conclusion arrived at earlier by *Kamp et al.* [1989].

SUMMARY

We have used fission track analysis of apatite and zircon to investigate the late Cenozoic vertical kinematics of the Pacific continental crust in South Island, New Zealand. We have presented new data which constrain the spatial variations in the amount, age and rate of late Cenozoic rock uplift across the leading edge of the Pacific plate presently in collision with the Australia plate.

The pattern of late Cenozoic uplift is strongly asymmetrical with respect to the Alpine fault, and varies from a maximum of ~19 km at the Alpine fault near Fox Glacier, to ~3 km at the east. To the north at Lewis Pass, the maximum uplift is 10 km, and it reaches 8 km at Arawata in the south.

There are major differences along the S. Alps in the age of the start of late Cenozoic rock uplift. Uplift started earlier in the southern part of the central S. Alps (at about 8 Ma) than the northern part (5 Ma). The uplift age also youngs to the southeast, and the rate of uplift propagation is 30 mm/yr in that direction, which exceeds the late Cenozoic average rate of convergence normal to the Alpine fault of ~8 mm/yr. The 8 Ma estimate of uplift initiation lags the predicted age of the start of compression across the Alpine fault by about 2 m.y.

Late Cenozoic uplift rates have averaged no more than 2.8 mm/yr right at the Alpine fault near Fox Glacier, but have been sufficient in 5 - 8 m.y. to expose amphibolite grade schist near the fault. The lowest mean rates of 1 mm/yr occur in the southern and eastern parts of the Alps. The mean rates have been sustained for periods of 3 - 8 m.y. Uplift has accelerated over time to reach ~7-10 mm/yr at Fox Glacier, with lower rates to the north, south and east. Significant acceleration of cooling and uplift has occurred only since 1.3 ± 0.3 Ma in the Fox Glacier region, which has the highest uplift rates.

From 6.7 to 1.3 Ma, cooling rates were in the order of 22°C/m.y., and inferred uplift rates of 0.8 mm/yr are too low to have significantly perturbed the geotherms. Geotherms have however been perturbed in areas adjacent to the Alpine fault in the period of accelerated uplift since 1.3 ± 0.3 Ma, as evidenced by the contemporary geothermal gradient of 60 ± 10°C/km [*Allis*, 1981]. The fission track data derived from within the zircon and apatite exhumed annealing zones are unaffected by geotherm perturbation as the uplift of geotherms must have postdated the setting of ages in the respective exhumed annealing zones. Also, the timing of significant perturbation (1.3 Ma) even post-dates the uplift of most of the rocks now exposed at the surface that contain reset zircons.

The pattern of increasing uplift rate with increasing proximity to the Alpine fault suggests that uplift has not been constrained by vertical drag on the Alpine fault during the late Cenozoic.

Differences between the peak metamorphic temperatures of the host rocks, and the ambient temperatures just prior to late Cenozoic uplift, allow estimates to be made of the amount of Mesozoic uplift across the S. Alps. These estimates range from negligible uplift north of Arthur's Pass, increasing to ~3 km at Mt Cook, to a maximum of 10 km at Lakes Wanaka and Hawea.

ACKNOWLEDGEMENTS

We acknowledge the University of Waikato Research Committee and the New Zealand University Grants Committee for funding support to P.J.J.K. We thank Dr Paul Green for providing Otway Basin data and Dr Richard Stevenson for kindly undertaking microprobe analyses at the Analytical Facility, Victoria University of Wellington. We thank Associate Editor Andrew Griscom and two anonymous referees for constructive and helpful comments on the original manuscript.

P.J.J. Kamp and J.M. Tippett, Geochronology Research Unit, Department of Earth Sciences, University of Waikato, Private Bag 3105, Hamilton 2001, New Zealand.

REFERENCES

Adams, C.J., Age and origin of the Southern Alps, *Bull. R. Soc. N. Z., 18*, 73-78, 1979.

Adams, C.J., Uplift rates and thermal structure in the Alpine fault zone and Alpine Schists, Southern Alps, New Zealand, *Spec. Publ. Geol. Soc. London, 9*, 211-222, 1981.

Adams, C.J., and J. E. Gabites, Age of metamorphism and uplift in the Haast Schist Group at Haast Pass, Lake Wanaka and Lake Hawea, South Island, New Zealand, *N. Z. J. Geol. Geophys., 28*, 85-96, 1985.

Adams, C.J., D.G. Bishop, and J.E. Gabites, Potassium-argon age studies of a low-grade, progressively metamorphosed greywacke sequence, Dansey Pass, South Island, New Zealand, *J. Geol. Soc. London, 142*, 339-349, 1985.

Adams. J., Vertical drag on the Alpine fault, New Zealand, *Bull. R. Soc. N. Z., 18*, 47-54, 1979.

Adams, J., Contemporary uplift and erosion of the Southern Alps, New Zealand, *Geol. Soc. Am. Bull., 91*, 1-114, 1980.

Allis, R.G., Continental underthrusting beneath the Southern Alps of New Zealand, *Geology, 9*, 303-307, 1981.

Allis, R.G., Mode of crustal shortening adjacent to the Alpine fault, New Zealand, *Tectonics, 5*, 15-32, 1986.

Allis, R.G., R.W. Henley, and A.F. Carman, The thermal regime beneath the Southern Alps, *Bull. R. Soc. N. Z., 18*, 79-85, 1979.

Beanland, S., and S. A. Barrow-Hurlbert, The Nevis-Cardrona fault system, Central Otago, New Zealand: late Quaternary tectonics and structural development, *N. Z. J. Geol. Geophys., 31*, 337-352, 1988.

Berryman, K., Active faulting and derived PHS directions in the South Island, New Zealand, *Bull. R. Soc. N. Z., 18*, 29-34, 1979.

Bishop, D.G., Progressive metamorphism from prehnite-pumpellyite to greenschist facies in the Dansey Pass area, Otago, New Zealand, *Geol. Soc. Am. Bull., 83*, 3177-3197, 1972.

Bradshaw, J.D., Stratigraphy and structure of the Torlesse Supergroup (Triassic-Jurassic) in the foothills of the Southern Alps near Hawarden (S60-61), Canterbury, *N. Z. J. Geol. Geophys., 15*, 71-87, 1972.

Brown, R.W., Backstacking apatite fission-track "stratigraphy": a method for resolving the erosional and isostatic rebound components of tectonic uplift histories, *Geology, 19*, 74-77, 1990.

Carlson, W.D., Mechanisms and kinetics of apatite fission-track annealing, *Am. Mineral., 75*, 1120-1139, 1990.

Cooper, A.F., Progressive metamorphism of metabasic rocks from the Haast Schist Group, *J. Petrol., 13*, 457-492, 1972.

Cooper, A.F., Retrograde alteration of chromian kyanite in metachert and amphibolite whiteschist from the Southern Alps, New Zealand, with implications for uplift on the Alpine fault, *Contrib. Mineral. Petrol., 75*, 153-164, 1980.

Crowley, K.D., M. Cameron, and B.J. McPherson, Annealing of etchable fission-track damage in F-, OH-, Cl-, and Sr-apatite: 1. Systematics and preliminary interpretations, *Nucl. Tracks radiat. Meas., 17*, 409-439, 1990.

Duddy, I.R., P.F. Green, and G.M. Laslett, Thermal annealing of fission tracks in apatite 3. Variable temperature behaviour, *Chem. Geol. (Isot. Geosci. Sect.), 73*, 25-38, 1988.

England, P., and P. Molnar, Surface uplift, uplift of rocks, and exhumation of rocks, *Geology, 18*, 1173-1177, 1990.

Essene, E.J., The current status of thermobarometry in metamorphic rocks, in Evolution of metamorphic belts, editors J.S. Daly, R.A. Cliff, and B.W.D. Yardley, *Geol. Soc. Spec. Publ., 43*, 1-44, 1989.

Findlay, R.H., Summary of structural geology of Haast Schist terrane, central Southern Alps, New Zealand, *Bull. R. Soc. N. Z., 18*, 113-120, 1979.

Findlay, R.H., Metamorphic low to high 2Vx K-feldspar in kyanite zone rocks within the Alpine schists of Copland Valley, South Westland, New Zealand, *N. Z. J. Geol. Geophys., 28*, 77-83, 1985.

Findlay, R.H., Structure and interpretation of the Alpine schists in Copland and Cook River valleys, South Island, New Zealand, *N. Z. J. Geol. Geophys., 30*, 117-138, 1987.

Findlay, R.H., and K.B. Spörli, Structural geology of the Mount Cook Range and Main Divide, Hooker Valley region, New Zealand, *N. Z. J. Geol. Geophys., 27*, 257-276, 1984.

Fleischer, R.L., P.B. Price, and R.M. Walker, The ion explosion spike mechanism for formation of charged particle tracks in solids, *J. Appl. Phys., 36*, 3645-3652, 1965.

Galbraith, R.F., On statistical models for fission track counts, *Math. Geol., 13*, 471-478, 1981.

Gleadow, A.J.W., and I.R. Duddy, A natural long-term track annealing experiment for apatite, *Nucl. Tracks, 5*, 169-174, 1981.

Gleadow, A.J.W., I.R. Duddy, P.F. Green, and J.F. Lovering, Confined fission track lengths in apatite: a diagnostic tool for thermal history analysis, *Contrib. Mineral. Petrol., 94*, 405-415, 1986*a*.

Gleadow, A.J.W., I.R. Duddy, P.F. Green, and K.A. Hegarty, Fission track lengths in the apatite annealing zone and the interpretation of mixed ages, *Earth Planet. Sci. Lett., 78*, 245-254, 1986*b*.

Gleadow, A.J.W., and P.G. Fitzgerald, Uplift history and structure of the Transantarctic Mountains: new evidence from fission track dating of basement apatites in the Dry Valleys area, southern Victoria Land, *Earth Planet. Sci. Lett., 82*, 1-14, 1987.

Grapes, R., and Otsuki, H., Peristerite compositions in quartzofeldspathic schists, Franz Josef - Fox Glacier area, New Zealand, *J. Metamorph. Geol., 1*, 47-61, 1983.

Green, P.F., On the cause of shortening of spontaeous fission tracks in certain minerals, *Nucl. Tracks, 4*, 91-100, 1980.

Green, P.F., Comparison of zeta calibration baselines for fission track dating of apatite, zircon and sphene, *Chem. Geol, 58*, 1-22, 1985.

Green, P.F., On the thermo-tectonic evolution of Northern England: evidence from fission track analysis, *Geol. Mag., 123*, 493-506, 1986.

Green, P.F., I.R. Duddy, A.J.W. Gleadow, and P.R. Tingate, Fission-track annealing in apatites: track length measurements and the form of the arrhenius plot, *Nucl. Tracks, 10*, 323-328, 1985.

Green, P.F., I.R. Duddy, A.J.W. Gleadow, I.R. Tingate, and G.M. Laslett, Thermal annealing of fission tracks in apatite 1, *Chem. Geol, 59*, 237-253, 1986.

Green, P.F., I.R. Duddy, G.M. Laslett, K.A. Hegarty, A.J.W. Gleadow, and J.F. Lovering, Thermal annealing of fission tracks in apatite 4, *Chem. Geol, 79*, 155-182, 1989*a*.

Green, P.F., I.R. Duddy, A.J.W. Gleadow, and J.F. Lovering, Apatite fission track analysis as a paleotemperature indicator for hydrocarbon exploration, in *Thermal History of Sedimentary Basins*, editors N.D. Naeser, and T.H. McCulloch, Springer-Verlag, New York, 1989*b*.

Haq, B.U., J. Hardenbol, and P.R. Vail, Chronology of fluctuating sea levels since the Triassic, *Science, 235*, 1156-1167, 1987.

Hurford, A.J., Cooling and uplift patterns in the Lepontine Alps, South Central Switzerland, and an age of vertical movement of the Insubric fault line, *Contrib. Mineral. Petrol., 92,* 413-427, 1986.

Hurford A.J., and P.F. Green, The zeta age calibration of fission-track dating, *Isotope Geosci., 1*, 285-317, 1983.

Hurford A.J., and Watkins R.T., Fission track age of the tuffs of the Buluk Member, Bakate Formation, northern Kenya: a suitable fission track age standard, *Chem. Geol., 66*, 209-216, 1987.

Hutton, C.O., and F.J. Turner, Metamorphic zones in north-west Otago, *Trans. R. Soc. N.Z., 65*, 405-406, 1936.

Jamieson, R.A., and D. Craw, Sphalerite geobarometry in metamorphic terranes: an appraisal with implications for metamorphic pressure in the Otago Schist, *J. Metamorph. Geol., 5*, 87-99, 1987.

Johnstone, D.C., and S.H. White, Shear heating associated with movement along the Alpine fault, New Zealand, *Tectonophysics, 92*, 241-252, 1983.

Kamp, P.J.J., Age and origin of the New Zealand Orocline in relation to Alpine fault movement, *J. Geol. Soc. London., 144*, 641-652, 1987.

Kamp, P.J.J., P.F. Green, and S.H. White, Fission track analysis reveals character of collisional tectonics in New Zealand,*Tectonics, 8*, 169-195, 1989.

Kamp, P.J.J., P.F. Green, and J.M. Tippett, Tectonic architecture of the mountain front-foreland basin transition, South Island, New Zealand, assessed by fission track analysis, *Tectonics, 11*, 98-113, 1992.

Kamp, P.J.J. and J.M. Tippett, Dynamics of Pacific plate continental crust in the south Island collision zone (New Zealand), *J. Geophys. Res., B series*, (submitted).

Koons, P.O., Some thermal and mechanical consequences of rapid uplift: an example from the Southern Alps, New Zealand, *Earth Planet. Sci. Lett., 86*, 307-319, 1987.

Lutz, T.M., and G. Omar, An inverse method of modeling thermal history from apatite fission track data, *Earth Planet. Sci. Lett., 104*, 181-195, 1991.

Mackinnon, T.C., Geology of Monotis-bearing Torlesse rocks in Temple Basin near Arthur's Pass, South Island, New Zealand, *N. Z. J. Geol. Geophys., 23*, 63-81, 1980.

Moore, M.E., A.J.W. Gleadow, and J.F. Lovering, Thermal evolution of rifted continental margins: new evidence from fission tracks in basement apatites from southeastern Australia, *Earth Planet. Sci. Lett.*, 78, 255-270, 1986.

Mason, B., Metamorphism in the Southern Alps of New Zealand, *Bull. Am. Mus. Nat. Hist., 123*, 217-248, 1962.

Nathan, S., H.J. Anderson, R.A. Cook, R.H. Herzer, R.H. Hoskins, J.I. Raine, and D. Smale, Cretaceous and Cenozoic sedimentary basins of the West coast Region, South Island, *New Zealand, N. Z. Geol. Surv. Basin Studies 1*, D.S.I.R. (Wellington), 90pp, 1986.

Norris, R.J., A geometrical study of finite strain and bending in the South Island, *Bull. R. Soc. N. Z., 18*, 21-28, 1979.

Sheppard, D.S., C.J. Adams, and G.W. Bird, Age of metamorphism and uplift in the Alpine Schist belt, New Zealand, *Geol. Soc. Am. Bull., 86*, 1147-1153, 1975.

Spörli, K.B., Mesozoic tectonics, North Island, New Zealand, *Geol. Soc. Am. Bull., 89*, 415-425, 1978.

Spörli, K.B., Structure of the South Island Torlesse in relation to the origin of the Southern Alps, *Bull. R. Soc. N. Z., 18*, 99-104, 1979.

Stock J., and P. Molnar, Uncertainties in the relative positions of the Australia, Antarctica, Lord Howe, and Pacific plates since the Late Cretaceous, *J. Geophys. Res., 87B*, 4697-4714, 1982.

Suggate, R.P., G.R. Stevens, and M.T. Te Punga (editors), *The geology of New Zealand*, Government Printer, Wellington, 820 pp, 1978.

Turnbull, I.M., Contortions in the schists of the Cromwell district, Central Otago, New Zealand, *N. Z. J. Geol. Geophys., 24*, 65-86, 1981.

Walcott, R.I., Present tectonics and late Cenozoic evolution of New Zealand, *Geophys. J.R. Astr. Soc., 52*, 137-164, 1978.

Walcott, R.I., The kinematics of the plate boundary zone through New Zealand: a comparison of short- and long-term deformations, *Geophys. J. R. Astr. Soc., 79*, 613-633, 1984.

Wellman, H.W., An uplift map for the South Island of New Zealand, and a model for the uplift of the Southern Alps, *Bull. R. Soc. N. Z., 18*, 13-20, 1979.

Wilson, D.D., The Late Cretaceous and early Tertiary transgression in South Island, New Zealand, *N. Z. J. Sci. Tech., B37*, 610-622, 1956.

Yardley, B.W.D., The early metamorphic history of the Haast Schists and related rocks of New Zealand, *Contrib. Mineral. Petrol., 81*, 317-327, 1982.

Yeats, R.S., Tectonic map of central Otago based on landsat imagery, *N. Z. J. Geol. Geophys., 30*, 261-271, 1987.

Zeitler, P.K., Cooling history of the NW Himalaya, Pakistan, *Tectonics, 4*, 127-151, 1985.

CHAPTER 4

Dynamics of Pacific plate continental crust in the South Island collision zone (New Zealand)

(Manuscript submitted to *Journal of Geophysical Research*)

Peter J.J. Kamp
J. Mark Tippett

Geochronology Research Unit,
Department of Earth Sciences,
University of Waikato,
Private Bag 3105,
Hamilton 2001, New Zealand.

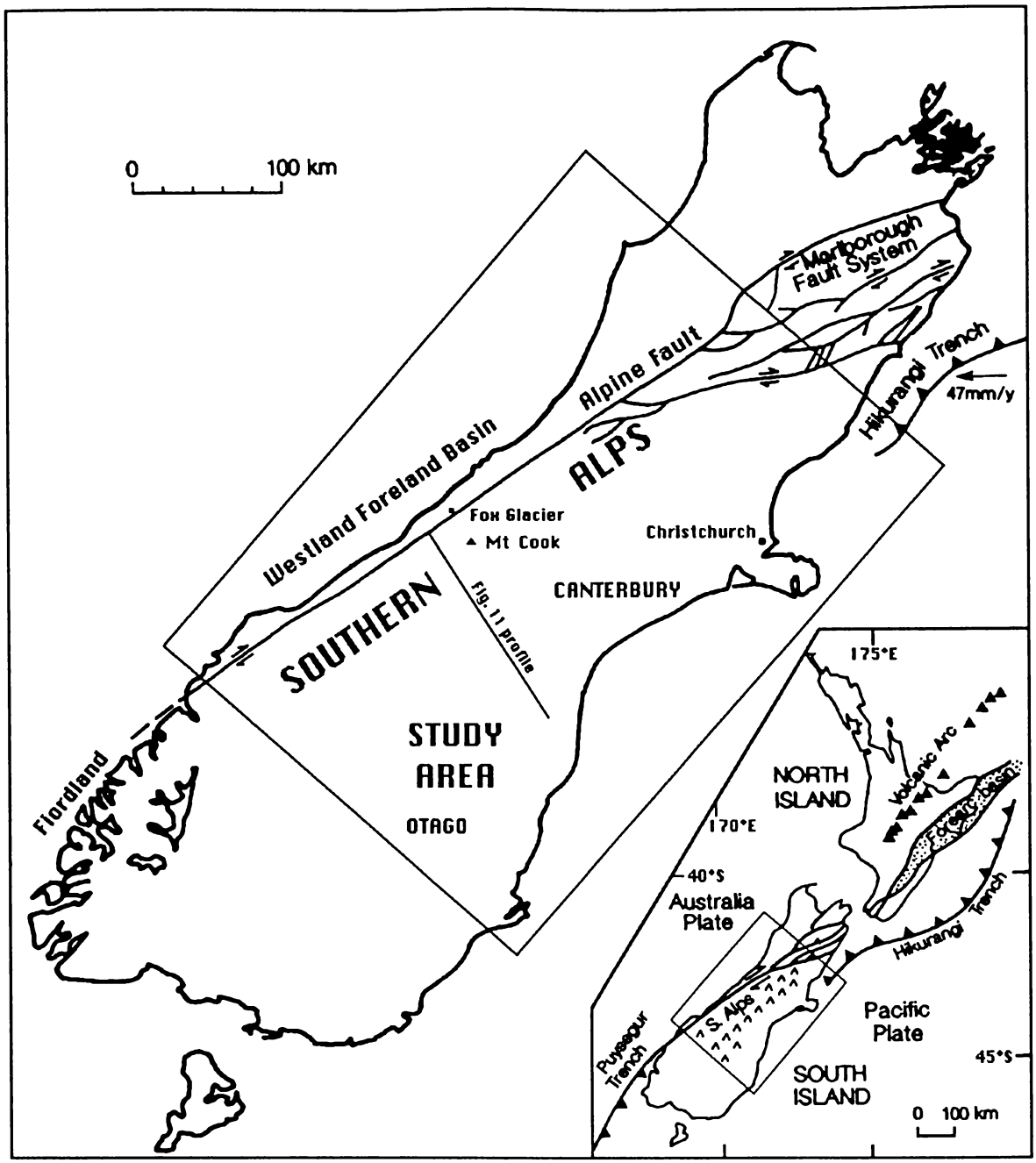


Fig. 1. Map of South Island, New Zealand showing extent of the study area, which includes the central 300 km length of the Southern Alps, in relation to the main tectonic features. Inset is a plate tectonic map of New Zealand.

ABSTRACT

Here we analyse topographic and fission track data to quantify the response of the surface of the Pacific plate to the late Cenozoic continent-continent collision in South Island, New Zealand. We derive and map over the central 300 km length of the Southern Alps mountain chain the rates of mean surface uplift, the rates of work done against gravity during the late Cenozoic mountain building, the isostatic and tectonic components (amounts and rates) of the uplift, and the amounts and rates of denudation. We fully assess the uncertainties associated with these quantities. These data bear on the mode of crustal deformation in the collision zone. The data do not support the notion of erosional-mechanical coupling of the two wedges in the description of the collision zone as a two-sided orogen [*Koons*, 1990], but are consistent with overriding of the Australia plate by the Pacific plate.

The rate of mean surface uplift ranges from <0.1 mm/yr adjacent to the Alpine fault to >0.3 mm/yr over most of the area east of the Main Divide. The highest rates of mean surface uplift do not coincide spatially with the regions of highest mean elevation, or highest topography, or greatest relief, but lie further to the southeast. The rate of work done in elevating the mean surface ranges from ~2.5 mWm^{-2} in the SW to ~10 mWm^{-2} in the central-eastern part of the Southern Alps. Areas of lower mean elevation uplifted more recently have experienced similar rates of energy input as the areas of higher mean elevation, where uplift started earlier. The amount of denudation ranges from ~18 km adjacent to the Alpine fault to ~2 km along the SE margin of the Southern Alps, and is large compared with the mean surface uplift. The late Cenozoic mean rates of denudation range from ~2.5 mm/yr to ~0.5 mm/yr with increasing distance from the Alpine fault across the Southern Alps to the SE. The amount of isostatic uplift ranges from a maximum of 14 km adjacent to the Alpine fault to ~2 km along the SE margin of Southern Alps. A tectonic uplift component is resolvable, ranging from ~4 km along the Alpine fault to ~1 km along the eastern margin of the Southern Alps.

INTRODUCTION

Zones of continent-continent convergence, such as the South Island collision zone in New Zealand (Fig. 1), typically exhibit very high rates of denudation, resulting in the exhumation of mid-crustal level metamorphic rocks. Despite the degree of exhumation, overall the crust thickens during

periods of continent-continent convergence, as evidenced, for example, by the occurrence of mountain chains and their coincidence with major negative gravity anomalies.

To quantitatively describe the mechanics controlling crustal thickening in collisional setting, basic data are required about crustal thickness changes through time across the orogenic belt; this is, the rates of surface uplift, and the rates of deepening of the crust-mantle boundary. Data are also required about the rates of denudation that act to thin the crust across the orogen.

In a recent contribution, *England and Molnar* [1990] commented "We are aware of no reliable, quantitative estimates of rates of surface uplift in mountain ranges that place useful constraints on tectonic processes" [*England and Molnar*, 1990, p.1176]. Despite comments to the contrary [*Hatfield*, 1991; *Pinter and Keller*, 1991], *England and Molnar* have recently reiterated their view [*England and Molnar*, 1991a, 1991b]. As we are aware of no reliable quantitative estimates of rates of deepening of the crust-mantle boundary in mountain ranges, we are forced to acknowledge that as geoscientists we do not have the basic data to quantitatively describe the dynamics of continental collision zones and of mountain building.

In an attempt to go some way to understanding the dynamics of the South Island collision zone, we quantify in this paper the response of the surface of the Pacific plate to the continental collision in South Island by analysing farther the fission track data reported by *Tippett and Kamp* [submitted]. In particular, we derive the late Cenozoic rates of mean surface uplift of the Southern Alps (New Zealand) mountain chain, and the rates of work done (against gravity) by the late Cenozoic mountain building. We evaluate fully all the sources of uncertainty associated with the derivation of these quantities. We also derive the isostatic and tectonic components (amounts and rates) of the uplift, and the amounts and rates of denudation, and their respective uncertainties. These quantities are mapped over the central 300 km length of the collision zone/mountain chain SE of the Alpine fault. These data allow us to test the idea [*Koons*, 1990] of erosional-mechanical coupling of the inboard and outward wedges in the description of the South Island collision zone as a two-sided orogen.

UPLIFT TERMS

England and Molnar [1990] have recently emphasised the differences between surface uplift (displacement of Earth's surface with respect to the geoid), rock uplift (displacement of rocks with respect to the geoid) and denudation or exhumation (displacement of rocks with respect to the surface). The three displacements are related such that surface uplift = rock uplift - exhumation. In this paper we apply these definitions and understandings of the types of uplift to the South Island collision zone.

TECTONIC SETTING

Central South Island of New Zealand contains an active zone of oblique continent-continent collision, involving the Australia and Pacific plates (Fig. 1). The Alpine fault is the suture between the plates, and at present the displacement vector trends at about 30° to this structure. The total dextral horizontal displacement on the Alpine fault amounts to 480 km and it started at about 25 Ma [*Kamp*, 1986a, 1991; *Cooper et al.*, 1987]. By comparison, convergence across the plate boundary started much later, at about anomaly 5 (9.8 Ma) [*Stock and Molnar*, 1982; *Kamp et al.*, 1989]. Thus the Alpine fault had an initial 15 m.y. history as a transcurrent fault, and subsequently a ~10 transpressional history. Since transpression started, shortening normal to the collision zone has been estimated at about 70 km in the central part of South Island [*Allis*, 1986], compared with about 330 km of horizontal displacement.

The oblique continental collision has resulted in the formation of a mountain chain, wholly contained within the Pacific plate. The Southern Alps (S. Alps) trend NE-SW and occur immediately SE of the Alpine fault throughout its length, and have a width of 90-150 km. The mountains have an asymmetric topographic profile. In the west they rise steeply over a distance of 15 km from a narrow coastal plain, to the Main Divide with summits at 2500-3000 m above sea level. East of the Main Divide the mountain heights decrease less rapidly over a distance of 80-140 km. The southeastern margin of the S. Alps, in East Otago, are characterised by Laramide-style range and basin structure; this does not characterise more northern parts of the eastern margin in Canterbury, where there is a broad alluvial piedmont.

The gravity field over the South Island has a pronounced NE-SE trending lineation that (sub)parallels the plate boundary [*Reilly and Whiteford*, 1979]. A negative Bouguer anomaly lies beneath the S. Alps, and has been interpreted as originating from crustal thickening [*Woodward*, 1970; *Allis*, 1986]. *Allis* [1986] noted that the most negative part (< -50 mgal) of the Bouguer anomaly was restricted to the southern part of the S. Alps, and trends at about 15° to the Alpine Fault; this suggests that the maximum crustal thickness lies at an increasing distance from the Alpine fault, southward along the fault.

MEAN SURFACE UPLIFT

England and Molnar [1990] defined surface uplift as:

$$\underset{(Us)}{\text{Surface uplift}} = \underset{(Ur)}{\text{rock uplift}} - \underset{(\Delta E)}{\text{exhumation}} \qquad (1)$$

In the simplified case where the initial mean surface elevation (Eim) was at or close to sea level, the amount of mean surface uplift (Us) would be equivalent to the present mean elevation (Em). This is the case for the S. Alps, therefore we define mean surface uplift as:

$$Us = Em - Eim \qquad (2)$$

The rate of mean surface uplift (Usr) of the orogen can then be calculated by dividing the mean surface uplift by the uplift age (ΔT):

$$Usr = \frac{Em - Eim}{\Delta T} \qquad (3)$$

Initial Mean Surface Elevation (Eim)

The central South Island collision zone presents a rather ideal situation in that prior to the start of surface uplift associated with the collision, the mean surface elevation was at or close to sea level. This is evident from the distribution and lithofacies of late Cretaceous-Cenozoic cover sequences preserved beneath the piedmont and around the margins of the S. Alps. Details of the Cenozoic stratigraphic and paleogeographic development of the region have been synthesised in *Wilson* [1963], *Suggate et al.* [1978], *Kamp* [1986b] and *Field and Browne et al.* [1989]. In Canterbury

and North Otago a cover sequence up to 1000 m thick accumulated prior to uplift of the S. Alps. The cover rocks accumulated during a late Cretaceous to late Oligocene New Zealand-wide marine transgression, and a subsequent more local and irregular marine regression. Within the main part of the S. Alps the cover rocks are not preserved, but outliers such as the Castle Hill Basin and Harper River Basin occur within 28 km of the Main Divide.

At the late Oligocene peak of the transgression, carbonate facies characterised by disconformities associated with bored greensand horizons and phosphatic nodules dominated the sedimentation patterns. It is inferred that at this time the New Zealand landmass was almost completely inundated by the sea, which resulted from thermal relaxation following the late Cretaceous separation of the subcontinent from Australia and Antarctica. The absence of any major terrigenous sediment sources suggest that the region now occupied by the S. Alps was below sea level in the late Oligocene. *Field and Browne et al.* [1989] map a ~16 Ma shoreline in Canterbury subparallel to the Alpine fault and 50 km to the SE of it, with probable terrestrial sedimentation to the NW of the shoreline and over the current central part of the S. Alps. Terrestrial coal measure facies accumulated widely across North Otago and South Canterbury during the Middle Miocene, whereas shelf environments persisted over large parts of northern Canterbury. During the late Miocene a widespread erosion surface developed across the cover rock sequence, which was completely removed over what became the main part of the S. Alps. This was followed by the deposition of an apron of Pliocene-Pleistocene basement derived conglomerates, particularly along the eastern margin of the S. Alps. This apron has prograded to the east during the late Pleistocene, forming the present piedmont and coastline.

The cover rock stratigraphy indicates that uplift over the bulk of the S. Alps started from at or near sea level in the late Miocene. This timing is consistent with the fission track data. That uplift started from near sea level is related to the origin of uplift: the pre-existing transform fault (Alpine fault) suddenly became transpressive due to a change in migration direction of the pole of rotation to which the Alpine fault was initially a small circle. In this respect the S. Alps are unlike most continent-continent collision zones in that there was not an early "soft" collision as the two facing passive margin sedimentary wedges impacted.

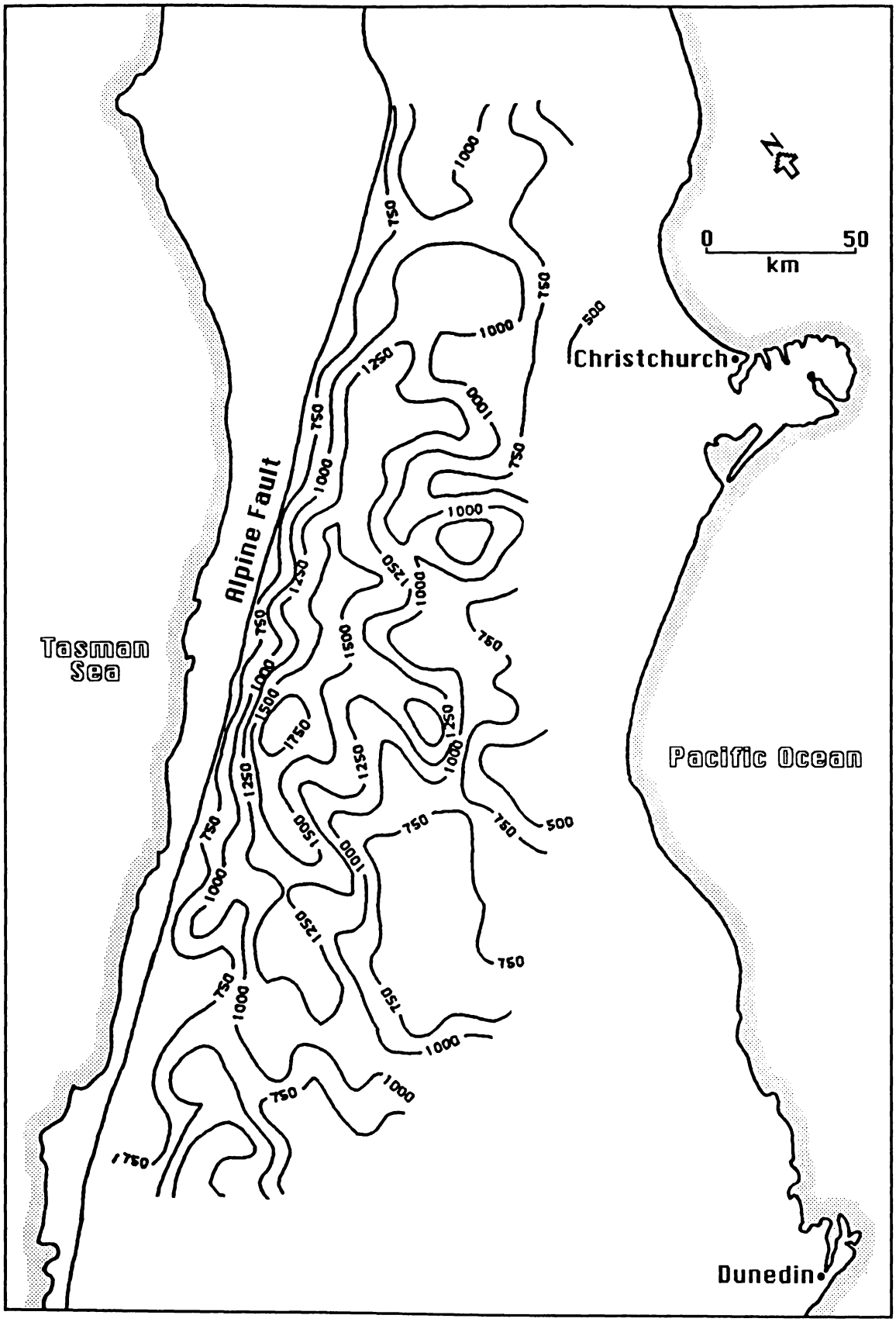


Fig. 2. Map of the present mean surface elevation of the Southern Alps, New Zealand. Elevation in metres above sea level. This is also a map of the amount of mean surface uplift associated with the late Cenozoic continental collision.

Present Mean Surface Elevation (Em)

The variation in mean elevation over the 300 km-long central section of the S. Alps was established by constructing an elevation matrix from the 1:63,360 NZMS 260 topographic map series. The elevation matrix was established by recording the elevation of the centre of 20 km^2 grid squares over the mountain range. The error on each of these estimates is ± half the contour interval of 100 ft. The contour values reflect the average value of the nearest nine grid square elevations.

Fig. 2 is a map of the present mean surface elevation of the central parts of the S. Alps expressed in metres above sea level; it is also a map of the amount of mean surface uplift. It shows that mean surface uplift has been greatest along a zone fairly consistently located about 20 km to the SE of the Alpine fault (Fig. 1). Along this line (corresponding to the Main Divide) mean surface elevation rises from 1000 m above sea level in the NE to 1750 m near Mt Cook and then falls to 500 m above sea level farther to the SW. From the Main Divide surface uplift declines rapidly northwestward to the Alpine fault, which lies at 500 m above sea level or lower, and less rapidly southeastward to the piedmont. The mean surface uplift pattern of the central section of the S. Alps conforms to an asymmetric dome elongated parallel to the Alpine fault.

AGE OF UPLIFT

A major contribution of Fission Track Analysis (FTA) to tectonic studies is its capacity to reveal the age when rock uplift started in active orogens, particularly those where sedimentary rocks still occur at the surface. Moreover, FTA can be applied to at least two minerals, apatite and zircon, that have different temperatures at which the respective systems are reset. The determination of rock uplift ages rely on identification of the base of the exhumed annealing zones for the apatite and zircon systems. The only major limitations on obtaining a detailed understanding of possible variations in rock uplift age across an orogen include the number of transects sampled, and the pattern of rock uplift. The latter is a limitation in that information can only be obtained for sites corresponding to the base of the exhumed apatite and zircon annealing zones. The locations of these sites are dependent on the pattern of uplift. These are, however, minor limitations compared with the difficulty of establishing the age(s) of uplift in

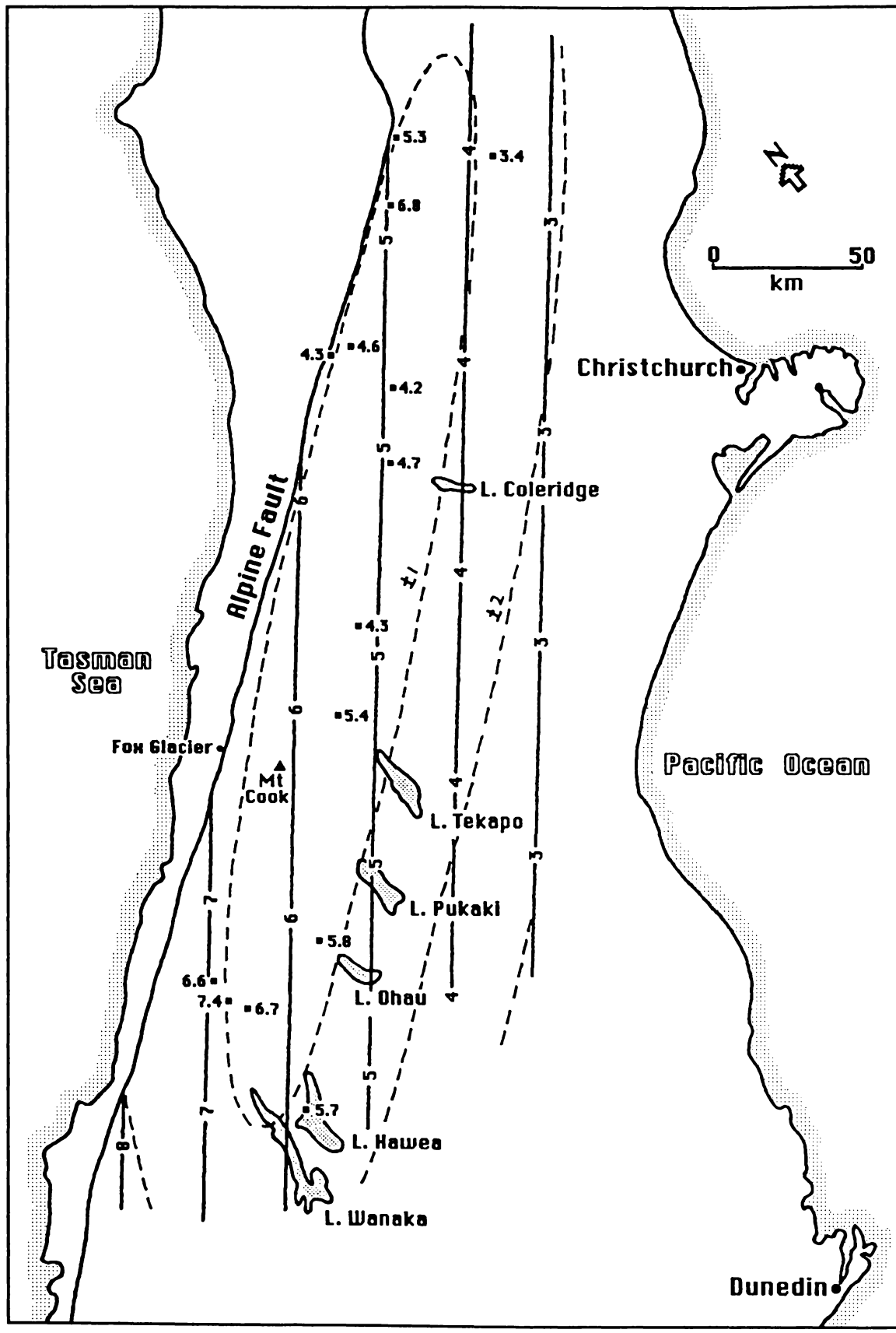


Fig. 3. Map of Southern Alps showing (i) sites and corresponding age in Ma of the start of rock uplift, (ii) a first order polynomial trend surface with one m.y. spacing, and (iii) and error surface (broken lines of ±1, ±2, ±3 m.y.) on the uplift age trend surface.

major orogenic belts from stratigraphic evidence, mainly because stratigraphic evidence is rarely preserved in orogenic belts.

In our study of the S. Alps we have identified 14 sites for which we are confident that the age of the start of rock uplift has been reliably estimated; eight are based on apatite fission track measurements of samples from the base of the exhumed apatite annealing zone, and six are based on zircon measurements of samples from the base of the zircon annealing zone [*Kamp et al.* 1989; *Tippett and Kamp*, submitted]. These values have been modelled using a first order polynomial trend, which is significant at the 99% level of confidence, indicating that there is real spatial variation in the age of rock uplift initiation across the S. Alps [*Tippett and Kamp*, submitted] (Fig. 3). Fig. 3 also shows an error surface on the uplift age trend surface. The error lines correspond to ±1, ±2 and ±3 m.y. and range from 20% to 66% of the mean uplift age estimates. As part of the latter part of this paper we have estimated (by interpolation using the trend surface) the rock uplift age and error for 59 sample locations for which we have estimated the amount of rock uplift (Table 1). These samples originate mainly from the exhumed apatite annealing zone and hence came from sites east of the Main Divide.

From this information the rocks now at the surface and adjacent to the Alpine fault in the southern part of the S. Alps started to be uplifted at 8 ± 2 Ma (2 σ error), before the rocks adjacent to the Alpine fault in the north started to be uplifted (5 ± 1 Ma). The age of uplift initiation also younged to the SE across the trend of the S. Alps, not starting at the eastern extremities of the S. Alps until 3 ± 2 m.y. ago.

It is worth noting that the differences in age of uplift initiation across the S. Alps collision zone amount to about 50% of the time since rock uplift first started. This is significant and resolvable because the uplift is so young, but the regional differences in uplift age only encompass four million years. If the South Island collision zone was of Cretaceous or older age, it is doubtful that regional differences in uplift age of this magnitude could be resolved by fission track analysis.

Fission track analysis, as with any other geothermochronometer, can only establish the age when rock uplift started, because the clock is set at depth in the crust beneath the initial topographic surface. The technique (FTA) cannot date directly when the mean surface elevation started to rise. We assume in the following section that this happened when rock uplift

Table 1: Uplift data for the Southern Alps, New Zealand

Transect	Sample No.	Mineral	Sample Elevation (km)	Rock Uplift (km)	Mean Elevation (km)	d (km)	Denudation (km)	Isostatic Uplift (km)	Tectonic Uplift (km)	Surface Uplift (km)	Uplift Age (Ma)	Rock Uplift Rate (mm/yr)	Denudation Rate (mm/yr)	Tectonic Uplift Rate (mm/yr)	Isostatic Uplift Rate (mm/yr)	Surface Uplift Rate (mm/yr)
Hunter	48	Ap	0.4	4.3±0.7	0.7±0.3	-0.3±0.3	3.6±0.7	2.9±0.6	1.4±0.9	0.7±0.3	5.7±1.1	0.8±0.2	0.6±0.2	0.2±0.2	0.5±0.3	0.1±0.1
Hunter	49	Ap	0.4	4.5±0.5	0.7±0.3	-0.3±0.3	3.7±0.5	3.1±0.4	1.4±0.7	0.7±0.3	5.7±1.2	0.8±0.2	0.7±0.2	0.2±0.1	0.5±0.3	0.1±0.1
Hunter	50	Ap	0.4	4.1±0.6	0.9±0.3	-0.5±0.3	3.2±0.6	2.6±0.5	1.5±0.8	0.9±0.3	5.7±1.2	0.7±0.2	0.6±0.2	0.3±0.1	0.5±0.3	0.2±0.1
Hunter	8326-3	Ap	0.5	3.8±0.7	0.6±0.2	-0.1±0.2	3.3±0.7	2.7±0.6	1.2±0.9	0.6±0.2	5.6±1.3	0.7±0.2	0.6±0.2	0.2±0.2	0.5±0.3	0.1±0.0
Haast	58	Ap	1.3	5.3±0.6	1.0±0.3	0.3±0.3	4.3±0.7	3.5±0.5	1.8±0.8	1.0±0.3	6.4±0.8	0.8±0.1	0.7±0.1	0.3±0.1	0.6±0.3	0.2±0.0
Ohau	71	Ap	0.6	4.5±0.8	1.1±0.3	-0.4±0.3	3.5±0.8	2.8±0.7	1.7±1.0	1.1±0.3	5.6±0.8	0.8±0.2	0.6±0.2	0.3±0.2	0.5±0.3	0.2±0.1
Ohau	72	Ap	0.6	3.8±0.5	1.1±0.3	-0.5±0.3	2.8±0.5	2.2±0.4	1.6±0.7	1.1±0.3	5.5±0.9	0.7±0.1	0.5±0.1	0.3±0.1	0.4±0.2	0.2±0.1
Ohau	73	Ap	0.6	3.7±0.4	0.8±0.3	-0.3±0.3	2.9±0.5	2.3±0.4	1.4±0.5	0.8±0.3	5.2±1.2	0.7±0.2	0.6±0.2	0.3±0.1	0.5±0.3	0.2±0.1
Ohau	74	Ap	0.4	3.2±0.4	0.5±0.1	-0.1±0.1	2.7±0.4	2.2±0.3	1.0±0.5	0.5±0.1	4.2±2.2	0.8±0.4	0.6±0.3	0.2±0.2	0.5±0.4	0.1±0.1
Ohau	75	Ap	0.4	2.9±0.4	0.6±0.2	-0.2±0.2	2.3±0.4	1.9±0.3	1.0±0.5	0.6±0.2	3.7±2.6	0.8±0.6	0.6±0.5	0.3±0.2	0.5±0.5	0.2±0.1
Ohau	76	Ap	0.3	2.7±0.5	0.5±0.2	-0.2±0.2	2.2±0.5	1.8±0.4	0.9±0.6	0.5±0.2	3.0±3.3	0.9±1.0	0.7±0.8	0.3±0.4	0.6±0.7	0.2±0.2
Ohau	77	Ap	0.1	2.5±0.6	0.2±0.0	0.0±0.0	2.3±0.3	1.9±0.3	0.6±0.7	0.2±0.1	1.2±5.1	2.0±8.6	1.9±8.1	0.5±2.1	1.6±3.3	0.1±0.6
Hooker	89	Ap	0.6	3.3±0.4	0.6±0.1	0.0±0.1	2.8±0.4	2.3±0.3	1.1±0.5	0.6±0.1	4.2±1.9	0.8±0.4	0.7±0.3	0.3±0.2	0.5±0.4	0.1±0.1
Hooker	90	Ap	0.4	3.0±0.4	0.5±0.1	-0.1±0.1	2.4±0.4	2.0±0.3	1.0±0.5	0.5±0.1	4.4±1.8	0.7±0.3	0.5±0.2	0.2±0.1	0.5±0.3	0.1±0.1
Godley	100	Ap	0.9	5.0±0.5	1.4±0.2	-0.5±0.2	3.5±0.5	2.9±0.4	2.1±0.7	1.4±0.3	5.4±0.6	0.9±0.1	0.7±0.1	0.4±0.1	0.5±0.3	0.3±0.1
Godley	101	Ap	0.8	4.6±0.6	1.2±0.2	-0.4±0.2	3.4±0.6	2.8±0.5	1.8±0.8	1.2±0.2	5.3±0.6	0.9±0.2	0.6±0.1	0.3±0.2	0.5±0.3	0.2±0.1
Godley	102	Ap	0.8	4.3±0.5	1.2±0.2	-0.4±0.2	3.1±0.5	2.6±0.4	1.8±0.7	1.2±0.2	5.1±0.7	0.9±0.2	0.6±0.1	0.3±0.1	0.5±0.3	0.2±0.1
Godley	103	Ap	0.8	3.9±0.5	1.0±0.1	-0.2±0.1	2.9±0.5	2.4±0.4	1.5±0.6	1.0±0.1	5.0±0.8	0.8±0.2	0.6±0.1	0.3±0.1	0.5±0.3	0.2±0.0
Godley	105	Ap	0.8	3.6±0.4	0.8±0.0	0.0±0.0	2.9±0.4	2.3±0.3	1.3±0.5	0.8±0.1	4.4±1.5	0.8±0.3	0.6±0.2	0.3±0.2	0.5±0.4	0.2±0.1
Godley	106	Ap	0.7	3.8±0.4	0.7±0.1	0.0±0.1	3.0±0.4	2.5±0.3	1.3±0.5	0.7±0.1	3.8±2.1	1.0±0.6	0.8±0.5	0.3±0.2	0.7±0.5	0.2±0.1
Godley	107	Ap	0.4	3.4±0.6	0.6±0.1	-0.1±0.1	2.8±0.6	2.3±0.5	1.1±0.7	0.6±0.2	3.7±2.1	0.9±0.5	0.8±0.5	0.3±0.3	0.6±0.5	0.2±0.1
Godley	108	Ap	0.5	2.9±0.4	0.6±0.1	-0.1±0.1	2.3±0.4	1.9±0.4	1.0±0.6	0.6±0.1	3.6±2.1	0.8±0.5	0.6±0.4	0.3±0.2	0.5±0.5	0.2±0.1
Godley	109	Ap	0.4	3.0±0.4	0.4±0.1	0.0±0.1	2.6±0.4	2.1±0.3	0.9±0.5	0.4±0.1	3.3±2.5	0.9±0.7	0.8±0.6	0.3±0.3	0.6±0.6	0.1±0.1
Godley	110	Ap	0.2	2.9±0.5	0.2±0.1	0.0±0.1	2.7±0.5	2.2±0.4	0.7±0.6	0.2±0.1	2.7±3.1	1.1±1.2	1.0±1.2	0.3±0.4	0.8±0.9	0.1±0.1
Clyde	113	Ap	0.8	4.9±0.5	1.5±0.2	-0.7±0.2	3.4±0.5	2.8±0.4	2.1±0.6	1.5±0.2	5.2±0.5	0.9±0.1	0.7±0.1	0.4±0.1	0.5±0.3	0.3±0.1
Clyde	114	Ap	0.7	4.4±0.6	1.3±0.3	-0.6±0.3	3.1±0.7	2.5±0.6	1.9±0.8	1.3±0.3	5.1±0.6	0.9±0.2	0.6±0.2	0.4±0.2	0.5±0.3	0.3±0.1
Clyde	115	Ap	0.7	4.1±0.5	1.2±0.3	-0.5±0.3	2.9±0.5	2.3±0.4	1.7±0.6	1.2±0.4	4.9±0.7	0.8±0.2	0.6±0.1	0.3±0.1	0.5±0.3	0.2±0.1
Clyde	116	Ap	0.6	3.9±0.4	1.0±0.4	-0.4±0.4	2.9±0.6	2.4±0.5	1.5±0.6	1.0±0.4	4.8±0.8	0.8±0.2	0.6±0.2	0.3±0.1	0.5±0.3	0.2±0.1
Clyde	117	Ap	0.6	3.7±0.4	0.9±0.3	-0.3±0.3	2.8±0.5	2.3±0.4	1.4±0.6	0.9±0.3	4.7±0.9	0.8±0.2	0.6±0.2	0.3±0.1	0.5±0.3	0.2±0.1
Clyde	118	Ap	0.6	3.5±0.4	0.8±0.2	-0.2±0.2	2.7±0.4	2.2±0.3	1.2±0.5	0.8±0.2	3.7±1.8	0.9±0.5	0.7±0.4	0.3±0.2	0.6±0.5	0.2±0.1
Clyde	119	Ap	0.5	3.2±0.4	0.7±0.2	-0.2±0.2	2.4±0.4	2.0±0.3	1.2±0.5	0.7±0.2	3.6±2.0	0.9±0.5	0.7±0.4	0.3±0.2	0.6±0.5	0.2±0.1
W'force	125	Ap	0.7	4.6±0.5	1.4±0.2	-0.8±0.2	3.2±0.5	2.6±0.4	2.0±0.6	1.4±0.2	4.9±1.8	0.9±0.4	0.6±0.3	0.4±0.2	0.5±0.4	0.3±0.1
W'force	126	Ap	0.7	4.5±0.5	1.2±0.3	-0.5±0.3	3.3±0.6	2.7±0.5	1.8±0.7	1.2±0.3	4.7±1.9	1.0±0.4	0.7±0.3	0.4±0.2	0.6±0.4	0.3±0.1
W'force	127	Ap	0.7	3.7±0.5	1.0±0.3	-0.4±0.3	2.7±0.5	2.2±0.4	1.5±0.6	1.0±0.3	4.5±1.3	0.8±0.3	0.6±0.2	0.3±0.2	0.5±0.3	0.2±0.1
W'force	128	Ap	0.5	3.9±0.5	0.6±0.1	-0.1±0.1	3.2±0.5	2.6±0.4	1.2±0.7	0.6±0.2	3.6±0.6	1.1±0.2	0.9±0.2	0.3±0.2	0.7±0.4	0.2±0.1
Arthur's	133	Ap	0.8	4.8±0.6	1.3±0.2	-0.5±0.2	3.4±0.6	2.8±0.5	2.0±0.8	1.3±0.2	4.8±0.7	1.0±0.2	0.7±0.2	0.4±0.2	0.6±0.3	0.3±0.1

Transect	Sample No.	Mineral	Sample Elevation (km)	Rock Uplift (km)	Mean Elevation (km)	d (km)	Denudation (km)	Isostatic Uplift (km)	Tectonic Uplift (km)	Surface Uplift (km)	Uplift Age (Ma)	Rock Uplift Rate (mm/yr)	Denudation Rate (mm/yr)	Tectonic Uplift Rate (mm/yr)	Isostatic Uplift Rate (mm/yr)	Surface Uplift Rate (mm/yr)
Arthur's	134	Ap	0.8	4.7±0.6	1.3±0.2	-0.6±0.2	3.3±0.7	2.7±0.5	2.0±0.8	1.3±0.2	4.7±0.9	1.0±0.2	0.7±0.2	0.4±0.2	0.6±0.4	0.3±0.1
Arthur's	rp1	Ap	0.6	2.8±0.6	0.8±0.2	-0.2±0.2	1.9±0.4	1.6±0.3	1.2±0.7	0.8±0.2	3.2±1.7	0.9±0.5	0.6±0.4	0.4±0.3	0.5±0.4	0.3±0.1
Arthur's	rp2	Ap	0.6	2.8±0.6	1.0±0.2	-0.4±0.2	1.8±0.4	1.5±0.3	1.3±0.7	1.0±0.2	3.3±0.6	0.8±0.2	0.5±0.2	0.4±0.2	0.4±0.3	0.3±0.1
Arthur's	rp3	Ap	0.7	3.3±0.4	1.0±0.2	-0.2±0.2	2.3±0.5	1.9±0.4	1.4±0.6	1.0±0.2	3.4±0.7	1.0±0.2	0.7±0.2	0.4±0.2	0.6±0.4	0.3±0.1
Arthur's	rp4	Ap	0.7	2.9±0.6	1.1±0.2	-0.5±0.2	1.8±0.4	1.5±0.3	1.5±0.7	1.1±0.2	3.8±1.8	0.8±0.4	0.5±0.3	0.4±0.3	0.4±0.3	0.3±0.2
Arthur's	rp5	Ap	0.6	4.5±0.5	0.8±0.2	-0.2±0.2	3.7±0.5	3.0±0.4	1.5±0.7	0.8±0.2	4.2±0.9	1.1±0.3	0.9±0.2	0.3±0.2	0.7±0.4	0.2±0.1
Arthur's	rp6	Ap	0.7	4.6±0.5	1.1±0.2	-0.5±0.2	3.4±0.5	2.8±0.4	1.8±0.6	1.1±0.2	4.6±0.7	1.0±0.2	0.7±0.2	0.4±0.1	0.6±0.3	0.2±0.1
Lewis	153	Ap	0.5	4.4±0.6	1.0±0.2	-0.5±0.2	3.4±0.6	2.8±0.5	1.6±0.8	1.0±0.2	3.7±1.2	1.2±0.4	0.9±0.3	0.4±0.2	0.8±0.5	0.3±0.1
Lewis	155	Ap	0.4	4.3±0.6	0.8±0.2	-0.4±0.2	3.5±0.6	2.8±0.5	1.4±0.8	0.8±0.2	3.4±1.4	1.3±0.5	1.0±0.5	0.4±0.3	0.8±0.6	0.2±0.1
Lewis	156	Ap	0.4	3.9±0.7	0.7±0.2	-0.3±0.2	3.2±0.7	2.6±0.6	1.3±0.9	0.7±0.2	3.2±1.5	1.2±0.6	1.0±0.5	0.4±0.3	0.8±0.7	0.2±0.1
Lewis	157	Ap	0.3	3.8±0.6	0.4±0.1	-0.1±0.1	3.4±0.6	2.8±0.5	1.0±0.8	0.4±0.1	3.0±1.6	1.3±0.7	1.1±0.6	0.3±0.3	0.9±0.8	0.1±0.1
Lewis	158	Ap	0.3	3.3±0.4	0.5±0.1	-0.2±0.1	2.8±0.3	2.3±0.3	1.0±0.5	0.5±0.1	2.8±1.8	1.2±0.8	1.0±0.7	0.3±0.3	0.8±0.7	0.2±0.1
Lewis	159	Ap	0.2	3.1±0.4	0.3±0.1	0.0±0.1	2.8±0.3	2.3±0.3	0.8±0.5	0.3±0.1	2.7±2.0	1.2±0.9	1.0±0.8	0.3±0.3	0.9±0.8	0.1±0.1
Wilkin	38	Zi	0.6	9.9±2.0	1.0±0.2	-0.4±0.2	8.8±2.0	7.2±1.6	2.6±2.6	1.0±0.2	6.9±1.0	1.4±0.4	1.3±0.3	0.4±0.4	1.0±0.6	0.2±0.0
Arawata	36	Zi	0.1	9.4±2.0	0.6±0.3	-0.5±0.3	8.8±2.0	7.2±1.6	2.2±2.6	0.6±0.3	7.8±1.6	1.2±0.4	1.1±0.3	0.3±0.3	0.9±0.6	0.1±0.0
Haast	54	Zi	0.1	9.4±2.0	0.7±0.2	-0.6±0.2	8.7±2.0	7.1±1.6	2.3±2.6	0.7±0.2	6.7±0.9	1.4±0.4	1.3±0.3	0.3±0.4	1.1±0.6	0.1±0.0
Haast	8326-82	Zi	0.1	9.4±2.0	0.5±0.2	-0.4±0.2	8.8±2.0	7.2±1.6	2.1±2.6	0.5±0.2	6.9±1.1	1.4±0.4	1.3±0.4	0.3±0.4	1.0±0.7	0.1±0.0
Copland	82	Zi	1.1	10.4±2.0	1.7±0.4	-0.6±0.4	8.7±2.0	7.1±1.7	3.2±2.6	1.7±0.4	6.2±0.7	1.7±0.4	1.4±0.4	0.5±0.4	1.1±0.7	0.3±0.1
Whataroa	96	Zi	0.7	9.9±2.0	1.5±0.2	-0.9±0.2	8.4±2.0	6.9±1.6	3.0±2.6	1.5±0.2	6.0±0.7	1.7±0.4	1.4±0.4	0.5±0.4	1.1±0.7	0.3±0.0
Whitcombe	123	Zi	0.4	9.7±2.0	1.1±0.3	-0.6±0.3	8.6±2.0	7.1±1.6	2.6±2.6	1.1±0.3	5.6±0.7	1.7±0.4	1.5±0.4	0.5±0.5	1.3±0.8	0.2±0.1
Arthur's	130	Zi	0.2	9.5±2.0	0.6±0.2	-0.3±0.2	8.9±2.0	7.3±1.6	2.2±2.6	0.6±0.3	5.3±0.8	1.8±0.5	1.7±0.4	0.4±0.5	1.4±0.8	0.1±0.1
Robinson	137	Zi	0.4	9.7±2.0	1.0±0.1	-0.5±0.1	8.7±2.0	7.1±1.6	2.6±2.6	1.0±0.2	4.8±0.8	2.0±0.5	1.8±0.5	0.5±0.5	1.5±0.9	0.2±0.1
Lewis	145	Zi	0.6	9.8±2.0	0.8±0.2	-0.2±0.2	9.0±2.0	7.4±1.6	2.4±2.6	0.8±0.2	4.7±0.9	2.1±0.6	1.9±0.6	0.5±0.6	1.6±1.0	0.2±0.1

Note: (i) Transects and sample numbers are as reported in Table 3 of Tippett and Kamp [submitted]. (ii) Rock uplift estimates are as reported in Table 4 of Tippett and Kamp [submitted]. (iii) 'Ap' = Apatite; 'Zi' = Zircon; 'd' is as defined in the text. (iv) All errors are 2σ.

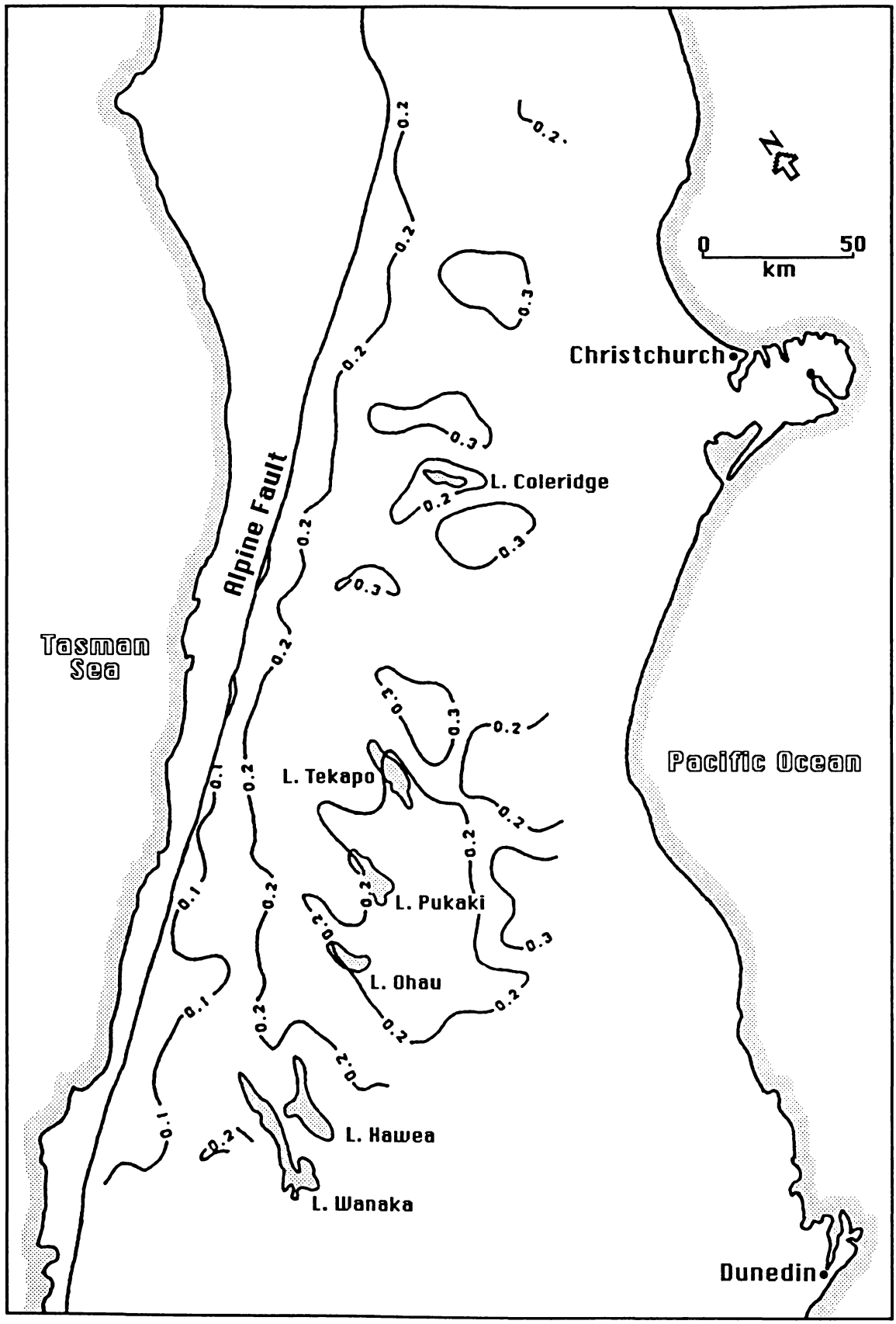


Fig. 4. Map of the rate of late Cenozoic mean surface uplift (in mm/yr) in the Southern Alps.

started. At present there is no alternative to this assumption as we are not aware of any stratigraphic record within the S. Alps that contains evidence of the timing of the growth of topography, let alone multiple stratigraphic records that would give a spatial dimension to the timing of the growth of topography.

RATES OF MEAN SURFACE UPLIFT

We derive the rate of mean surface uplift by equation (3) and express the results as a map giving contours in mm/yr (Fig. 4). This map was produced by dividing the mean surface elevation by the trend surface describing the mean uplift ages. The contours in Fig. 4 give the mean rate of mean surface uplift. Errors will be associated with these values, and will originate from several variables, including present mean surface elevation (Em), initial mean surface elevation (Eim), the difference between pre-uplift mean sea level and present mean sea level (Δ Emsl), and the errors on the uplift age trend surface. We have combined the uncertainties associated with these components to estimate the error on the rate of surface uplift for the 59 locations within the S. Alps for which we have estimated the amount of rock uplift. The surface uplift rate and rate error values (2 σ) are listed in Table 1. For three samples (5% of 59 sites) the 2σ error values exceed the mean value, in a further seven samples (12%) the magnitude of the error values lie between 50% and 75% of the mean values, and for all other samples (83%) the 2σ error values are 17 to 50% of the magnitude of the mean uplift rate values. Accordingly, we take the three-fold variation across the S. Alps in the rate of surface uplift to be very significant.

The rate of mean surface uplift ranges from <0.1 mm/yr adjacent to the Alpine fault in the SW to >0.3 mm/yr for most of the area east of the Main Divide and north of Lake Tekapo (Fig. 4). Hence the rate of surface uplift increases toward the NE, in a more easterly direction than the strike of the Alpine fault. This results, predictably, from the combined variations in the mean elevation and the uplift age; the lower mean elevations and earlier uplift in the SW give very low values (<0.1 mm/yr) adjacent to the Alpine fault, whereas higher elevations and younger uplift age combine to give much higher rates farther to the east and northeast. The comparatively little variation in rates in any NW-SE transect east of the Main Divide emphasizes particularly the control of the eastward propagation of uplift (Fig. 3) on the surface uplift rates.

An important conclusion to be drawn from this section is that the highest rates of surface uplift do not coincide spatially with the regions of highest mean elevation, or the highest topography, or the greatest relief. Southward along the S. Alps the highest rates of surface uplift becomes progressively more displaced to the east of the Main Divide (Fig. 4).

The rates of surface uplift are by definition averaged over the interval of uplift, but these rates may have varied through the duration of uplift. We have shown elsewhere [*Kamp et al.*, 1989; *Tippett and Kamp*, submitted] that the rate of cooling and rock uplift increased by an order of magnitude at 1.3 ± 0.3 Ma. This increase would have been reflected in changes in the rate of denudation, but was probably not simply related to changes in mean elevation and hence rates of mean surface uplift. Rather than build in suspect assumptions, we prefer, at this stage, to present and work with average rates of mean surface uplift.

WORK DONE BY MEAN SURFACE UPLIFT

The formation of mountains and their crustal roots requires work to be done against gravity, and consequently there is an increase in gravitational potential energy during orogenesis. *Molnar and Lyon-Caen* [1988] have defined the potential energy created by mountain building and crustal thickening (i.e. the difference between the potential energy per unit area of mountainous and lowland regions, using the depth of the Moho as the common reference). Their analysis ignores elastic plates and viscous stresses, and therefore the calculated difference in potential energy is a minimum:

$$\text{Difference} = \rho_c\, gh(h/2 + Ho + \Delta H/2) \qquad (4)$$

where ρ_c is density of continental crust (2700 kg m^{-3}); g is gravitational acceleration (9.8 m s^{-2}); h is mean elevation; Ho is thickness of original (unthickened) crust (30,000 m); ΔH is increase in thickness of crustal root.

The equation assumes Airy isostatic equilibrium, so that the excess load is compensated beneath the position of the load whereby $\rho_c h = \Delta\rho\Delta H$ (where $\Delta\rho$ is density difference between mantle and crust = 600 kg m^{-3}). This style of compensation may not necessarily be the case in the S. Alps were rocks have travelled (and are travelling) both vertically and laterally through

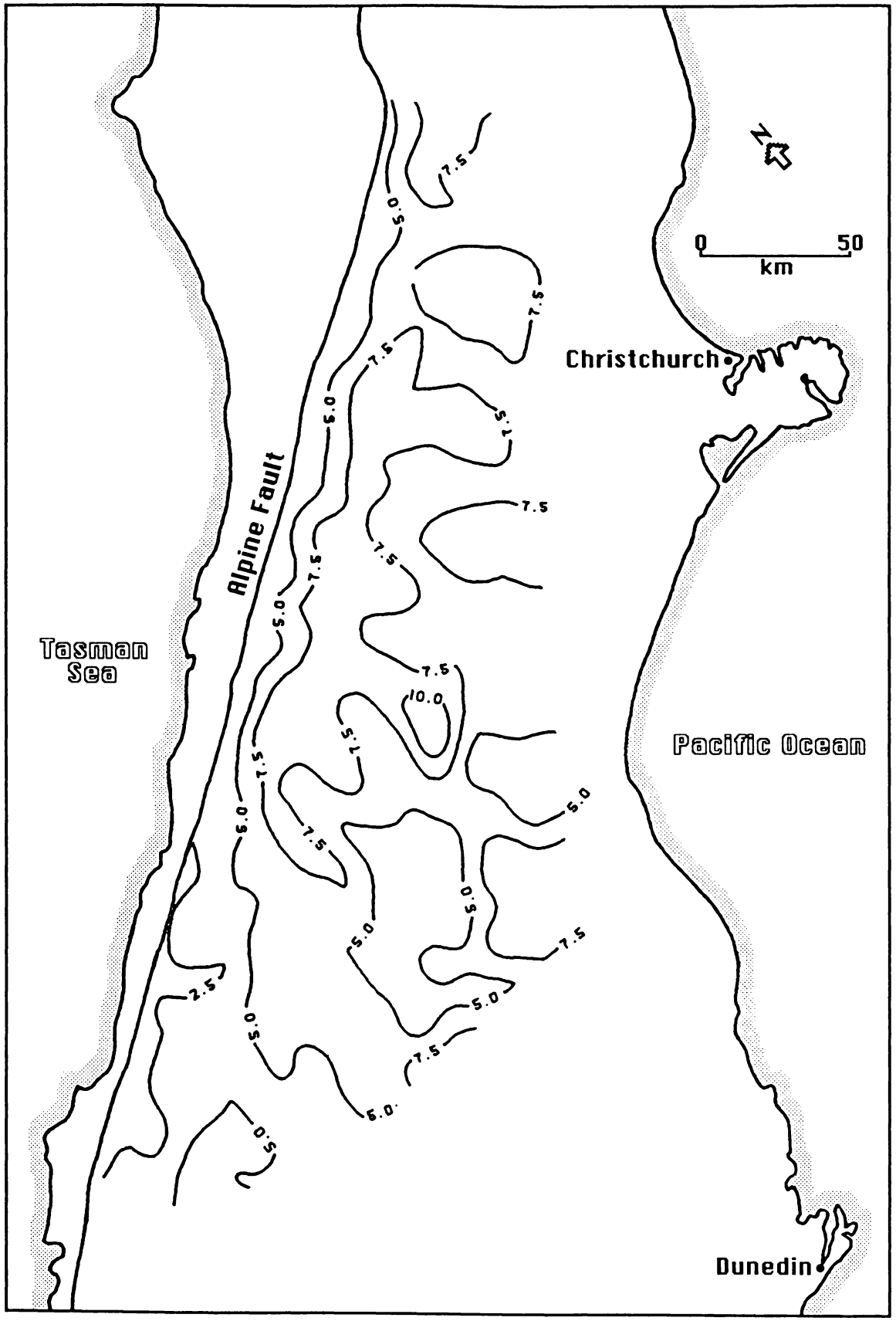


Fig. 5. Map of the rate of work done (in mWm^{-2}) in late Cenozoic uplift of the Southern Alps.

the system. *Reilly* [1970] inferred that the S. Alps are close to being in isostatic equilibrium, as corrections applied to the Bouguer anomaly map to obtain the isostatic anomaly map were similar to the Bouguer anomaly map itself. We have calculated the potential energy generated by the growth of the S. Alps with the simplifying assumption that the range is isostatically compensated.

The potential energy created (work done) by the uplift of the surface of the S. Alps was calculated from equation (4) and using the data of the mean elevation matrix. The rate of work done by the mountain building was calculated by dividing the work done by the uplift age.

Fig. 5 shows the spatial variation in the rate of work done by uplift of the mean surface of the S. Alps. The values range from 2.5 mWm^{-2} in the SW to 10 mWm^{-2} in the central-eastern part of the S. Alps. The striking feature of the map is that most of the S. Alps have values of ~5.0 to 7.5 mWm^{-2}; that is, the variation in power across the S. Alps is small. Therefore, although the Main Divide in the central part of the S. Alps occurs within the region of high values of potential energy due to its higher mean elevation, areas of lower topography uplifted more recently have experienced similar rates of energy input.

England Molnar [1990] suggested that surface uplift at a rate of about 1 mm/yr may represent a significant fraction of the work done in creating a mountain range. From equation (4) it is evident that the rate of work associated with a surface uplift of 1 mm/yr and an initial crustal thickness of 30 km is about 30 mWm^{-2}. The S. Alps have a maximum mean surface uplift rate of 0.3 mm/yr, and therefore the maximum rate of work done is ~10 mWm^{-2}. Average rates of mean surface uplift of 1 mm/yr and associated rates of working of ~30 mWm^{-2} may not be sustainable in an oblique continental collision zone such as the one in South Island.

ROCK UPLIFT

The uplift of rock above the mean elevation of the initial surface is one means of accommodating crustal shortening in a collisional orogen. Rock uplift accompanied by denudation is a process of thinning the crust. In the S. Alps this has resulted in the exhumation of mid-crustal level rocks. *Tippett and Kamp* [submitted] have reported and discussed the late Cenozoic amounts, rates and pattern of rock uplift in the leading edge of the Pacific

plate (see their Figs 9 and 12). The amount of rock uplift changes markedly across the collision zone, ranging from a maximum of ~18 km adjacent to the Alpine fault, to ~3 km along the eastern margin of the S. Alps. The contours of equal rock uplift subparallel the plate boundary such that the amount adjacent to the Alpine fault decreases to ~11 km at the northern end, and ~8 km at the southern end of the section of the collision zone investigated.

The errors associated with the amount and rate of rock uplift are given in Table 1 for the 59 samples for which rock uplift amounts could be estimated. These errors result from errors on measurement of the following variables: pre-uplift paleotemperature (Tp), pre-uplift geothermal gradient (G), sample elevation above sea level (Es), initial mean elevation of land surface (Eim), and the difference between pre-uplift mean sea level and present mean sea level (ΔEmsl).

Error estimates on pre-uplift sample paleotemperature have been reported by *Tippett and Kamp* [submitted, Table 4). A pre-uplift geothermal gradient of 27.5 ± 2.5°C was used in converting paleotemperature estimates into depths. We take the measurement of the sample elevation (Es) to be errorless (the topographic maps on which samples were located had 100 ft contours). The error on Eim is taken as ±100 m, and the error on ΔEmsl is taken as ±100 m. Errors (2σ) on the estimates of mean rock uplift were calculated by combining the errors on each of these variables, and are reported under rock uplift error in Table 1. The rock uplift 2σ errors all range between 10 and 21% of the mean values. Mean rock uplift rates and their errors have also been calculated and are included in Table 1. The rock uplift rate errors (2σ) represent combination of the errors associated with the rock uplift and uplift age.

DENUDATION

Denudation (ΔE) is defined as displacement of rocks with respect to the surface, such that [*Brown*, 1990]

$$\Delta E = (Tp - Ts)/G + d \qquad (5)$$

where

Tp = pre-uplift paleotemperature (°C)

Ts = pre-uplift surface temperature (assume 10°C)

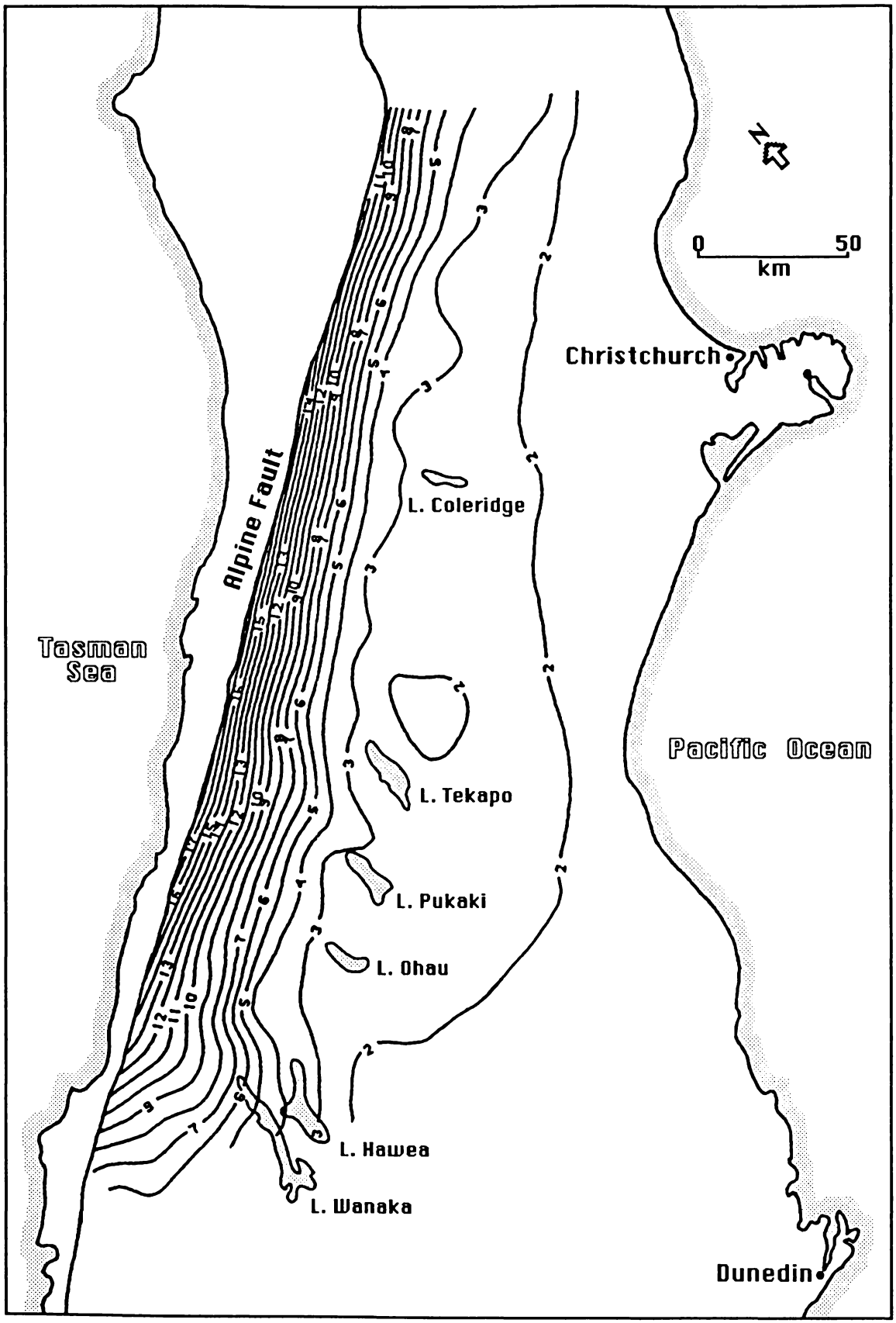


Fig. 6. Map of the amount of late Cenozoic denudation (in km) in the Southern Alps.

G = pre-uplift geothermal gradient (27.5 ± 2.5°C)
d = elevation difference between sample elevation and the present mean surface elevation (d is negative when mean surface elevation > sample elevation)

The amount of denudation and the associated 2σ errors estimated for each of 59 sample locations within the S. Alps for which there are paleotemperature (Tp) estimates, are reported in Table 1. The error values were calculated by combining the errors (listed in Table 1) on each of the variables included in Equation (5). The magnitude of these errors are virtually the same as the errors on mean rock uplift. Denudation rates and their errors are also included in Table 1, the errors having been derived by combination of the errors associated with the denudation amount and uplift age.

Fig. 6 is a contour map of the amount of late Cenozoic denudation of the Pacific plate east of the Alpine fault in South Island. The pattern of denudation is highly asymmetric, the amount ranging from 2 km along the eastern margin of the S. Alps to a maximum of ~18 km adjacent to the Alpine fault near Fox Glacier. At the northern end of the S. Alps the maximum denudation is ~10 km, and at the southern end of the study area it is ~7 km adjacent to the Alpine fault. The amount of denudation is large compared with the surface uplift, and therefore the amount and pattern of denudation is similar to the amount and pattern of rock uplift. The average rates of denudation and their errors are also comparable to the rates of uplift and their errors (compare Fig. 7 with Fig. 12 of *Tippett and Kamp*, submitted). The highest rates (~2.5 mm/yr) occur in the central section adjacent to the Alpine fault, but the contours of equal rate of uplift and denudation parallel the Alpine fault rather than slowly converge with it toward the north; this follows from the interaction of the amount of rock uplift, the amount of mean surface uplift and the age of uplift.

ISOSTATIC AND TECTONIC COMPONENTS OF UPLIFT

Molnar and England [1990] emphasised that surface uplift must be caused entirely by tectonic uplift; if the rock uplift is an isostatic response to the removal of material by erosion, then there is a decrease in the elevation of the mean surface. In any attempt to describe the dynamics of a collision zone, it is important, therefore, to calculate the amount of isostatic rebound of the mean surface resulting from the erosional unloading of the

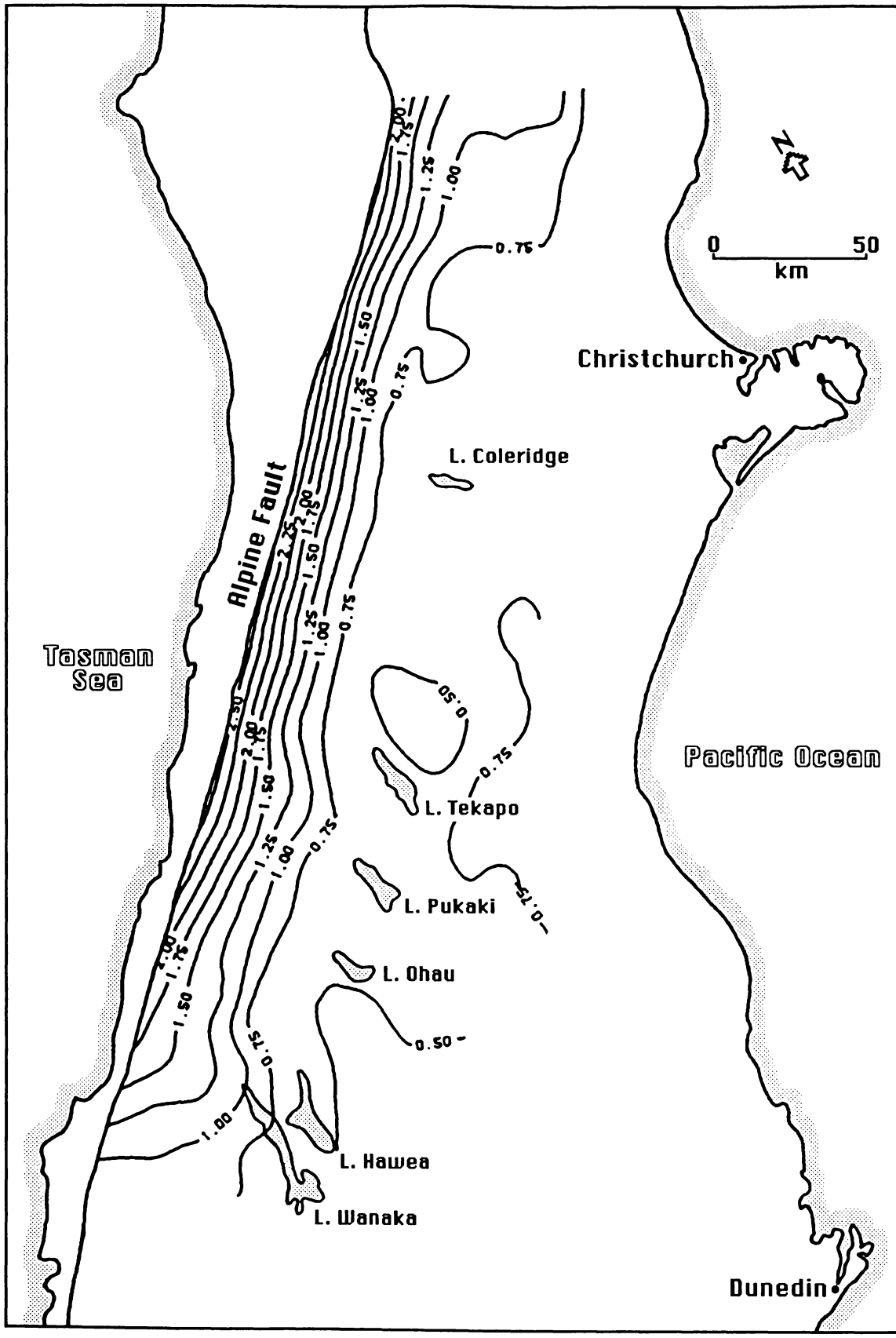


Fig. 7. Map of the rate of late Cenozoic denudation (in mm/yr) in the Southern Alps.

crust (measured relative to sea level), and thus establish whether or not there is a resolvable tectonic component to the surface uplift. Tectonic uplift (Ut) is the residual uplift component of the mean surface after subtracting the isostatic rebound due to denudation [*Brown*, 1991].

Having calculated the amount of erosion (ΔE) from equation (5), the amount of isostatic uplift is given by:

$$Ui = \frac{\rho c}{\rho m} \Delta E \qquad (6)$$

where ρ_c is the average density of continental crust (2700 kg m^{-3}), and ρ_m is the density of mantle (3000 kg m^{-3}). Assuming that Airy isostatic equilibrium applies to the S. Alps, Table 1 gives the amount of isostatic uplift and the isostatic uplift error for the 59 sample sites for which paleotemperatures were estimated. Fig. 8 is a contour map of the amount of isostatic uplift, which ranges from a maximum of 14 km at the Alpine fault near Fox Glacier to 2 km along the eastern margin of the S. Alps. Because the isostatic uplift is a constant proportion of the amount of denudation, the pattern of uplift is virtually identical and the relative errors are the same.

To isolate the tectonic uplift component (Ut) it is necessary to know independently the initial elevation of the mean surface [*Brown*, 1991]. In the case of the S. Alps the initial surface was at or close to sea level, and therefore:

$$Ut = Ur - Ui \qquad (7)$$

The tectonic uplift amount and error for each of the 59 sample sites are listed in Table 1, and Fig. 9 is a contour map of the amount of tectonic uplift. The 2σ errors range from 30 to 118% of the mean values, with 50% of the sites having errors less than the mean value. In all but six sites the 2σ errors are less than the mean values, indicating a resolvable tectonic uplift component, which is not surprising given that the study area is one of oblique continental collision. What consideration of the errors does indicate, however, is that given the inherent error associated with paleotemperature estimations from Fission Track Analysis, one needs to be studying a region with very high rock uplift rates to be able to resolve a tectonic component to the uplift where there is accompanying erosion. This conclusion becomes even more acute for tectonic uplift rates. The tectonic uplift rates and their

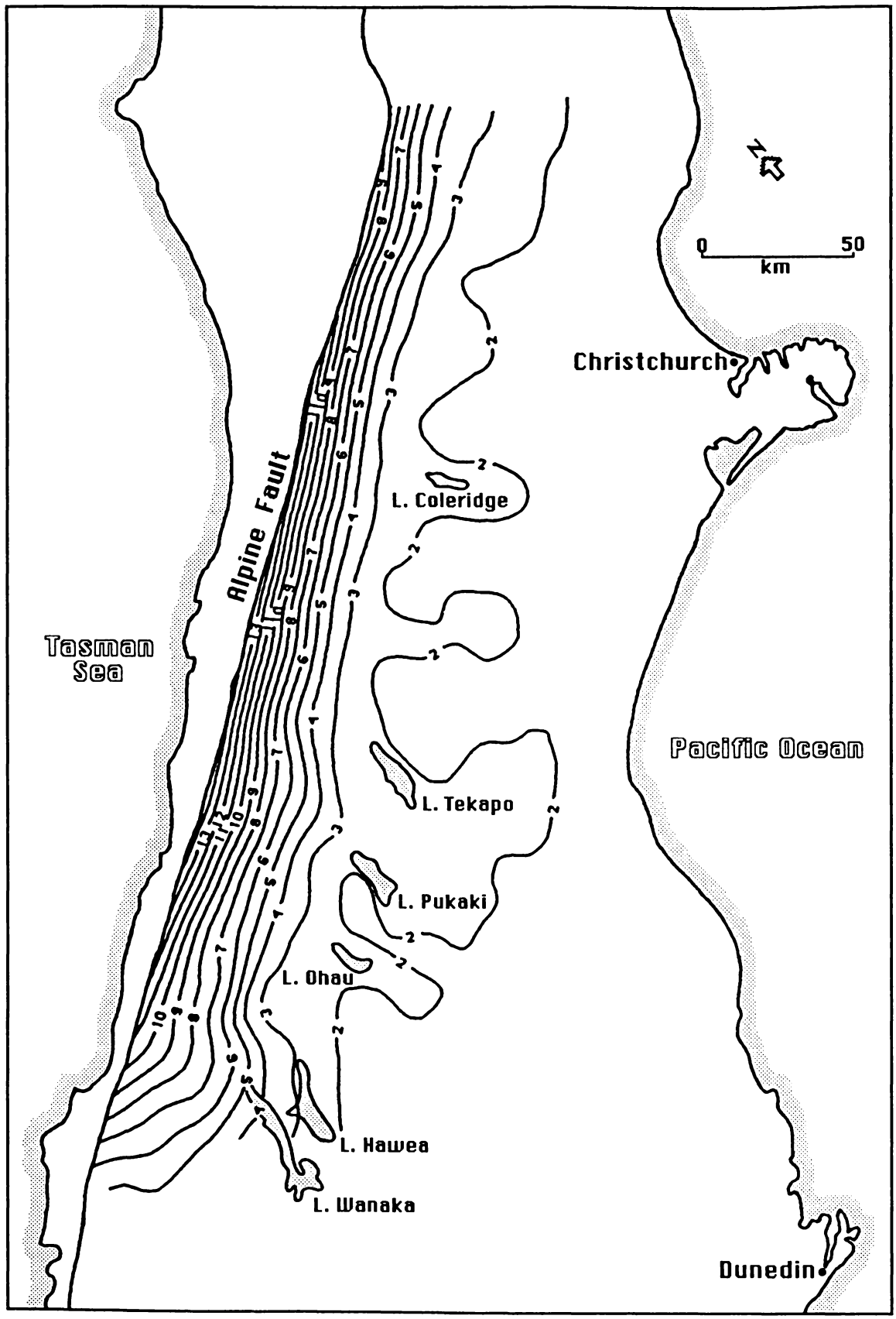


Fig. 8. Map of the amount of late Cenozoic isostatic uplift (in km) in the Southern Alps.

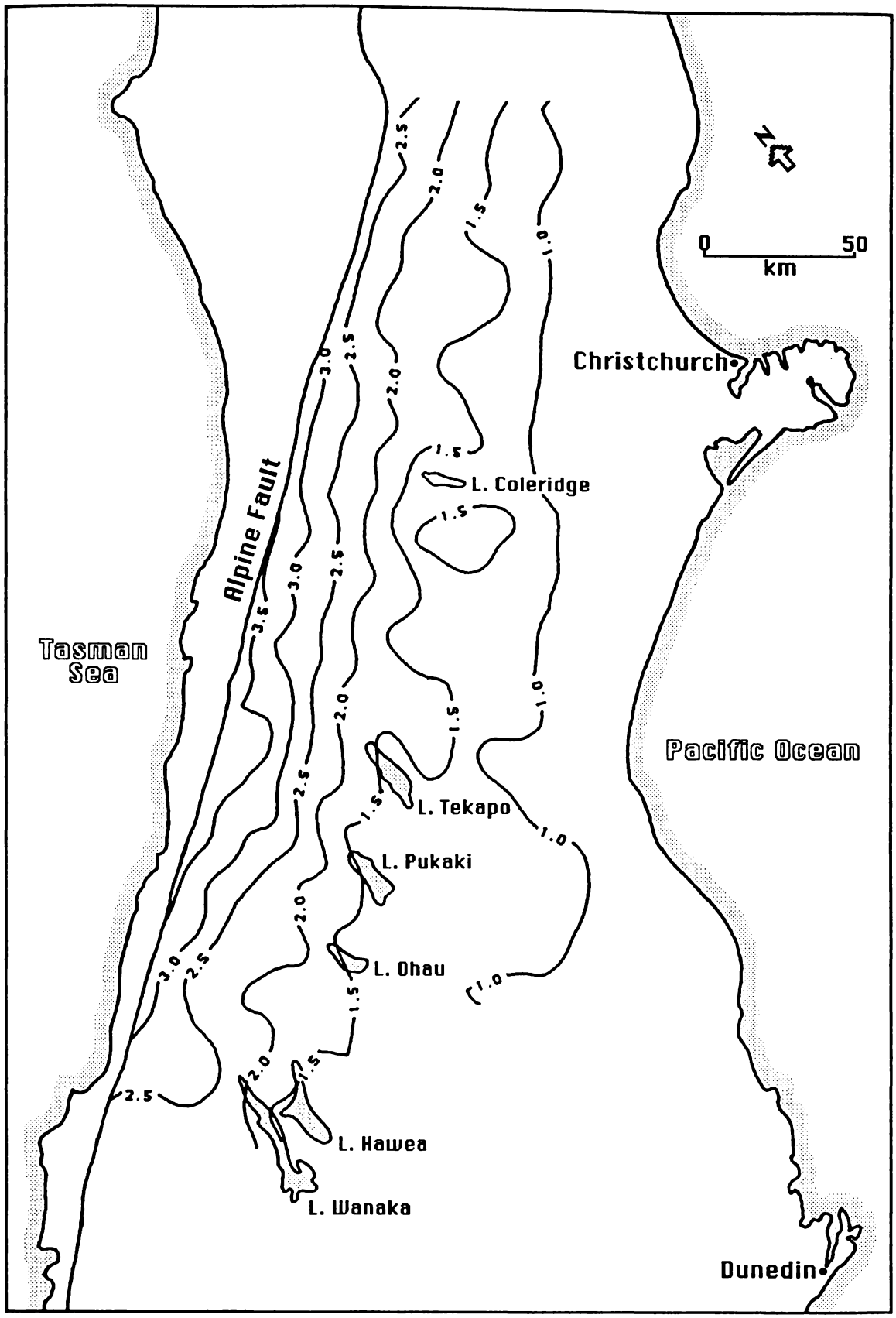


Fig. 9. Map of the amount of late Cenozoic tectonic uplift (in km) in the Southern Alps.

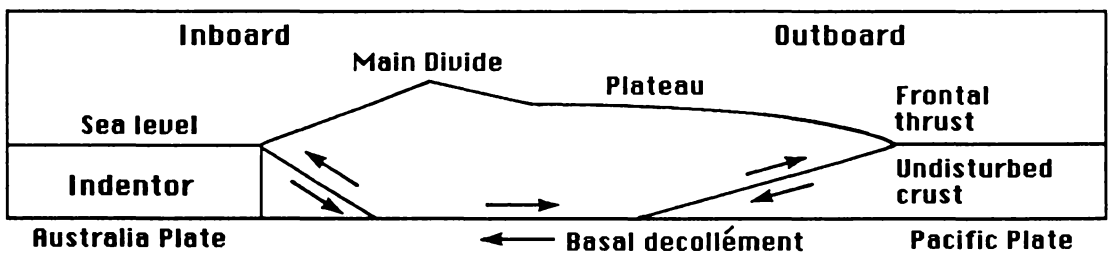


Fig. 10. Schematic representation of two-sided deforming orogen (modified from Fig. 4 of *Norris et al.* [1990]).

errors are also listed in Table 1. The 2σ errors range from 32 to 146% of the mean values, only 32% of the sites having errors less than 50% of their respective mean values, and 19% having errors larger than their mean value.

Keeping in mind the errors (Table 1), the amount of tectonic uplift (Fig. 9) ranges from almost 4 km at the Alpine fault near Fox Glacier to 1 km along the eastern margin of the S. Alps. The mean surface elevation is everywhere lower than the amount of tectonic uplift. This difference is a maximum NW of the Main Divide, but reduces from about 1.0 km at the Main Divide to 0.25 km at the eastern margin of the S. Alps. The average rate of tectonic uplift ranges from almost 0.6 mm/yr adjacent to the Alpine fault to about 0.3 mm/yr in the east.

TWO-SIDED OROGEN EVALUATED

The data on surface uplift, rock uplift and denudation presented above, bear on the mode and controls of crustal shortening in the South Island collision zone. *Koons* [1990] and *Norris et al.* [1990] have recently outlined the model of a two-sided orogen and proposed it as an analogy for the collisional tectonics in the S. Alps. *Koons* [1990] suggested that it has wider applicability to the Himalayas and the western European Alps. In this section we use our data to evaluate this model, and in particular the idea that there is an erosional-mechanical coupling of the inboard and outboard wedges.

Outline of Two-Sided Orogen

A two-sided orogen (Fig. 10) originates by convergence of continents with similar thicknesses, in which one, known as the indentor, remains roughly at sea level. The other develops two, opposite facing, asymmetrical wedges that are mechanically coupled. A steep inboard wedge faces the indentor, and is separated by the Main Divide from a broad outboard wedge that has a distinct break in slope. Crustal thickening is accommodated by the formation of a midcrustal décollement, with ponding of lower crustal material to form a root, and movement of middle and upper crustal material through the orogen and out through the inboard wedge. The structural development of the collision zone is considered to be a consequence of the interaction of high rainfall and consequent erosion rates in the inboard

wedge, which result in near steady state elevations and the exposure of deep crustal assemblages. In turn, this requires the orogen to keep feeding material into the inboard wedge in an attempt to restore the topography. The orogen grows to the east by thrusting of the outboard wedge over the undeformed material and by forward propagation of the fold-thrust belt. The outboard wedge undergoes minor erosion and maintains an upper crustal profile.

Discussion

The two-sided sandbox orogen (Fig. 10) essentially describes a developing, forward propagating thrust and ramp structure, as shown, for example, by the fact that the steep slope east of the "Main Divide" equates to the dip of the basal thrust. This model, which we refer to as the ramp model, is said to fail [*Koons*, 1990] as a complete analogy for the collisional tectonics of the S. Alps because it does not simulate the degree of differential erosion between the Main Divide and Alpine fault indicated by numerical modelling of the S. Alps [*Koons*, 1989]; the sandbox model does not imply erosional-mechanical coupling of the wedges. In his application to South Island of the two-sided orogen, *Koons* [1990] therefore outlines a modification of the sandbox model. We refer to this modification as the erosional-mechanical model. This model differs from the ramp model in that it must have a more dramatic vertical velocity gradient, increasing downwards from the surface to the décollement, than will be the case in the ramp model. In the erosional-mechanical model the additional velocity at increasing depths in the crust down to the décollement is inferred to be caused by strongly differential erosion across the inboard wedge, most erosion being concentrated at its toe adjacent to the indentor. This leads to a corresponding mechanical response, considered [*Koons*, 1990] to cause deep crustal material to be differentially exhumed along a narrow zone, most exhumation occurring adjacent to the indentor. The two models are clearly end-members of a spectrum of possible situations.

The two models will differ in the distribution of denudation across the orogen in a way that reflects the vertical velocity gradient. Because we have derived the distribution of denudation across the S. Alps, we can test the models. Unfortunately, *Koons* [1990] gives only an uplift (presumably rock uplift) profile, so in Fig. 11 we compare rock uplift profiles. We note several differences between the uplift profiles:

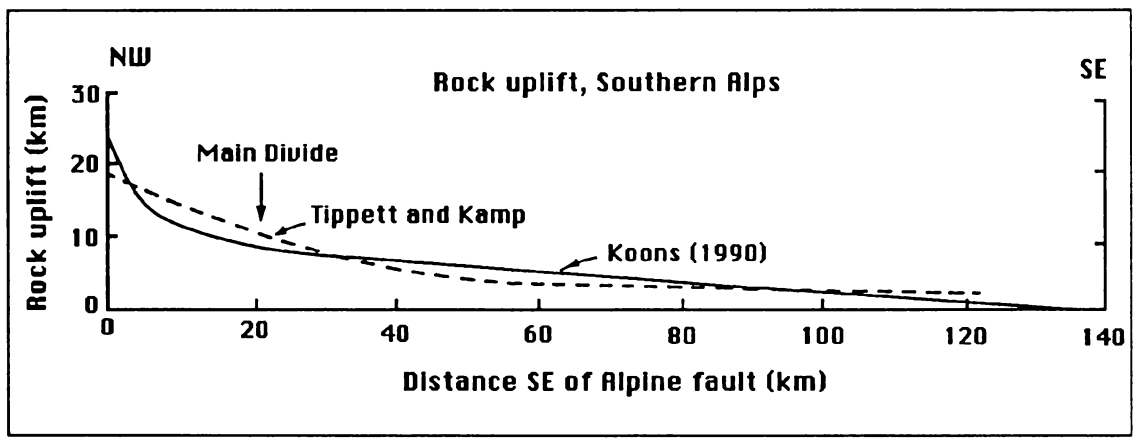


Fig. 11. Comparison of Southern Alps rock uplift profile from *Tippett and Kamp* [submitted] (line of section on Fig. 1) with uplift profile given in Fig. 2 of *Koons* [1990]. See text for discussion.

(i) The maximum uplift (23 to 24 km) in *Koons'* profile is much greater than the ~18 km maximum late Cenozoic uplift near Fox Glacier evident from our data. Consequently there has been less late Cenozoic exhumation at the toe of the inboard wedge than incorporated in the numerical model of *Koons* [1989]. Any mechanical response to erosion at the toe of the inboard wedge will therefore be less dramatic than envisaged by *Koons* [1990].

(ii) Over the majority of the inboard wedge, *Koons'* profile underestimates by about 3 km the amount of rock uplift. From 10 km east of the Main Divide out to 80 km east of the Main Divide, that is, over most of the outboard wedge, *Koons'* profile overestimates the amount of uplift, and along the eastern margin he underestimates the amount of rock uplift.

These differences between the profiles have lead us to wonder upon what sort of data *Koons'* [1990] uplift profile is based. We cannot find where this is documented, yet it is critical to the argument of an erosional-mechanical coupling of the two wedges. A fully documented denudation profile (or series of profiles) would seem to be a prerequisite to the construction of any model that attempted to show an erosional-mechanical coupling of the two wedges.

Our profile generally shows more uplift (and therefore more denudation) in the inboard wedge than *Koons'* [1990] profile, and vice versa in the outboard wedge. Does our profile then support the idea of erosional-mechanical coupling of two wedges as opposed to simple ramping of the Pacific plate over the Australia plate with consequent erosion? To assess this question we have estimated the volume of basement rock eroded during the late Cenozoic from the areas east and west of the Main Divide along the 300 km central section of the S. Alps considered in this paper. About 50% (~78 Tm^3) has been derived from the inboard wedge (NW of Main Divide), and about 50% (~80 Tm^3) has been derived from the outboard wedge (SE of Main Divide). Therefore there is not the strongly differential erosion between the inboard and outboard wedges envisaged by *Koons* [1990], and we are forced to doubt seriously the idea of erosional-mechanical coupling of the wedges. We emphasise that nothing dramatic occurs at the Main Divide in any of the parameters we have mapped; rock uplift and denudation that are important to this discussion vary smoothly between the so-called inboard and outboard wedges. We think that our data are better explained by the model of ramping of the Pacific plate over the Australia plate, with consequent erosion.

Another problem in application of the two-sided orogen to the South Island collision zone pertains to maintenance of the elevation of the indentor roughly at sea level throughout evolution of the orogen. In an associated study [*Kamp et al.*, 1992], we have identified the occurrence of a late Cenozoic foreland basin beneath the continental shelf and slope NW of the S. Alps. By integration of fission track data with the regional structure and stratigraphy, we have demonstrated that in the late Miocene - early Pliocene the foreland basin extended across Westland, and deepened toward the Alpine fault. This indicates that during the late Cenozoic the leading edge of the Pacific plate overrode and loaded the edge of the Australia plate. Oblique ramping was possible because the top of the Australia plate stood below sea level prior to the start of the continental collision. As a result of continuing convergence and thickening of the footwall by reverse faulting, the inner margin of the foreland basin has been inverted. The amount of inversion increases from south (~5 km) to north (~12 km) along the plate boundary. The surface elevation of the Australia plate, therefore, has clearly changed throughout the evolution of the South Island collision zone, and importantly, has not always been an effective indentor, and early in the evolution of the collision zone would have allowed the Pacific plate to ramp over the Australia plate. The patterns of mean surface uplift, rock uplift and denudation in the S. Alps are consistent with ramping of the Pacific plate over the Australia plate.

CONCLUDING REMARKS

This paper has addressed two current issues: the claim by *England and Molnar* [1990] that no one to date has produced reliable quantitative estimates of rates of surface uplift in mountain ranges that place useful constraints on tectonic processes, and the assertion by *Koons* [1990] that the South Island collision zone is an example of a two-sided orogen with erosional-mechanical coupling of the two wedges.

In their paper *England and Molnar* [1990] underestimated the potential of fission track thermochronology to quantitatively estimate rates of surface uplift in mountain ranges. We have successfully derived this information, including a rigorous estimation of the associated uncertainties, for the Southern Alps from a combination of topographic data and an extensive fission track data base. From the fission track data we have also derived information on the amounts and rates of denudation, and the isostatic and tectonic components of uplift that are important in better

understanding the dynamics of the crust in the continental collision zone. The essential contribution of fission track analysis to estimation of the rates of mean surface uplift lies in estimation of the ages of the start of uplift. The geological setting was favourable to the extent that the initial mean surface elevation was at or near sea level. Resolution of the amounts and rates of denudation and isostatic uplift, and of the amount of tectonic uplift is due largely to the very strong rock uplift signal, and the fact that the uplift has been so recent. Despite the constraints on the amount and timing of uplift, precise estimates of the rates of tectonic uplift could not be made.

For there to be substantial erosional-mechanical coupling between the two wedges in a two-sided orogen, most of the denudation must occur in the inboard wedge, and be strongly concentrated at its toe [*Koons*, 1990]. This condition is not satisfied in the Southern Alps as half of the total denudation over the 300 km long central section of the Southern Alps has occurred in the outboard wedge. In addition, we have shown elsewhere [*Kamp et al.*, 1992] that there has been substantial subsidence and rock uplift of the indentor (Australia plate) during the period of uplift of the Pacific plate; the collision zone throughout its history has not been characterised by a stationary indentor near sealevel.

REFERENCES

Allis, R.G., Mode of crustal shortening adjacent to the Alpine fault, New Zealand, *Tectonics, 5*, 15-32, 1986.

Brown, R.W., Backstacking apatite fission-track "stratigraphy": a method for resolving the erosional and isostatic rebound components of tectonic uplift histories, *Geology, 19*, 74-77, 1990.

Cooper, A.F., B.A.Barreiro, D.L. Kimbrough, and J.M. Mattinson, Lamprophyre dike intrusion and age of the Alpine fault, New Zealand, *Geology, 15*, 941-944.

England, P., and P. Molnar, Surface uplift, uplift of rocks, and exhumation of rocks, *Geology, 18,* 1173-1177, 1990.

England, P., and P. Molnar, Reply on "Surface uplift, uplift of rocks, and exhumation of rocks", *Geology, 19*, 1051-1052, 1991a.

England, P., and P. Molnar, Reply on "Surface uplift, uplift of rocks, and exhumation of rocks", *Geology, 19*, 1053-1054, 1991b.

Field, B.D., G.H. Browne and others, Cretaceous and Cenozoic sedimentary basins and geological evolution of the Canterbury region, South Island, New Zealand, *N.Z. Geol. Surv. Basin Studies 2*, 94pp, 1989.

Hatfield, C.B., Comment on "Surface uplift, uplift of rocks, and exhumation of rocks", *Geology, 19*, p.1051, 1991.

Kamp, P.J.J., Late Cretaceous-Cenozoic tectonic development of the southwest Pacific region, *Tectonophysics, 121*, 225-251, 1986a.

Kamp, P.J.J., Mid-Cenozoic Challenger Rift System of western New Zealand and its implications for the age of Alpine fault inception, *Bull. Geol. Soc. Am, 97*, 255-281, 1986b.

Kamp, P.J.J., Late Oligocene Pacific-wide tectonic event, *Terra Nova, 3*, 65-69, 1991.

Kamp, P.J.J., P.F. Green, and S.H. White, Fission track analysis reveals character of collisional tectonics in New Zealand, *Tectonics, 8* , 169-195, 1989.

Kamp, P.J.J., P.F. Green and J.M. Tippett, Tectonic architecture of the mountain front-foreland basin transition, South Island, New Zealand, assessed by fission track analysis, *Tectonics, 11*, 98-113, 1992.

Koons, P.O., The topographic evolution of collisional mountain belts: A numerical look at the Southern Alps, New Zealand, *American Journal of Science, 289*, 1041-1069, 1989.

Koons, P.O., Two-sided orogen: Collision and erosion from the sandbox to the Southern Alps, New Zealand, *Geology, 18*, 679-682, 1990.

Molnar, P., and H. Lyon-Caen, Some simple physical aspects of the support structure, and evolution of mountain belts. *Geol. Soc. Am. Special Paper, 218,* 179-207, 1988.

Norris, R.J., P.O. Koons, and A.F. Cooper, The obliquely-convergent plate boundary in the South Island of New Zealand: implications for ancient collision zones, *Journal of Structural Geology , 12*, 715-725, 1990.

Pinter, N., and E.A. Keller, Comment on "Surface uplift, uplift of rocks, and exhumation of rocks", *Geology, 19*, p.1053, 1991.

Reilly, W.I., New Zealand gravity map series, *New Zealand Journal of Geology and Geophysics, 15*, 3-15, 1972.

Reilly, W.I., and C.M. Whiteford, South Island Gravity Map of New Zealand, (1st Ed.), 1:1,000,000, Bougner Anomalies, New Zealand Department of Scientific and Industrial Research, Wellington, 1979.

Stock, J., and P. Molnar, Uncertainties in the relative positions of the Australian, Antarctica, Lord Howe, and Pacific plates since the late Cretaceous, *J. Geophys. Res., 87*, 4697-4714, 1982.

Suggate, R.P., G.R. Stevens, and M.T. Te Punga (editors), *The geology of New Zealand*, Government Printer, Wellington, 820pp., 1978.

Tippett, J.M. and P.J.J. Kamp, Fission track analysis of late Cenozoic vertical kinematics of the Pacific plate, South Island, New Zealand. *Journal of Geophysical Research* , (submitted).

Wilson, D.D., Geology of Waipara Subdivision, *Bull. N.Z. Geol. Surv., 64*, 122pp., 1963.

Woodward, D.J., The crustal structure of the Southern Alps, New Zealand, as determined by gravity, *Bull, R. Soc. N.Z., 18*, 95-98, 1979.

CHAPTER 5

On the role of faulting in rock uplift in the Southern Alps

(Manuscript submitted to *New Zealand Journal of Geology and Geophysics*)

J. Mark Tippett
Peter J.J. Kamp

Geochronology Research Unit,
Department of Earth Sciences,
University of Waikato,
Private Bag 3105,
Hamilton 2001, New Zealand.

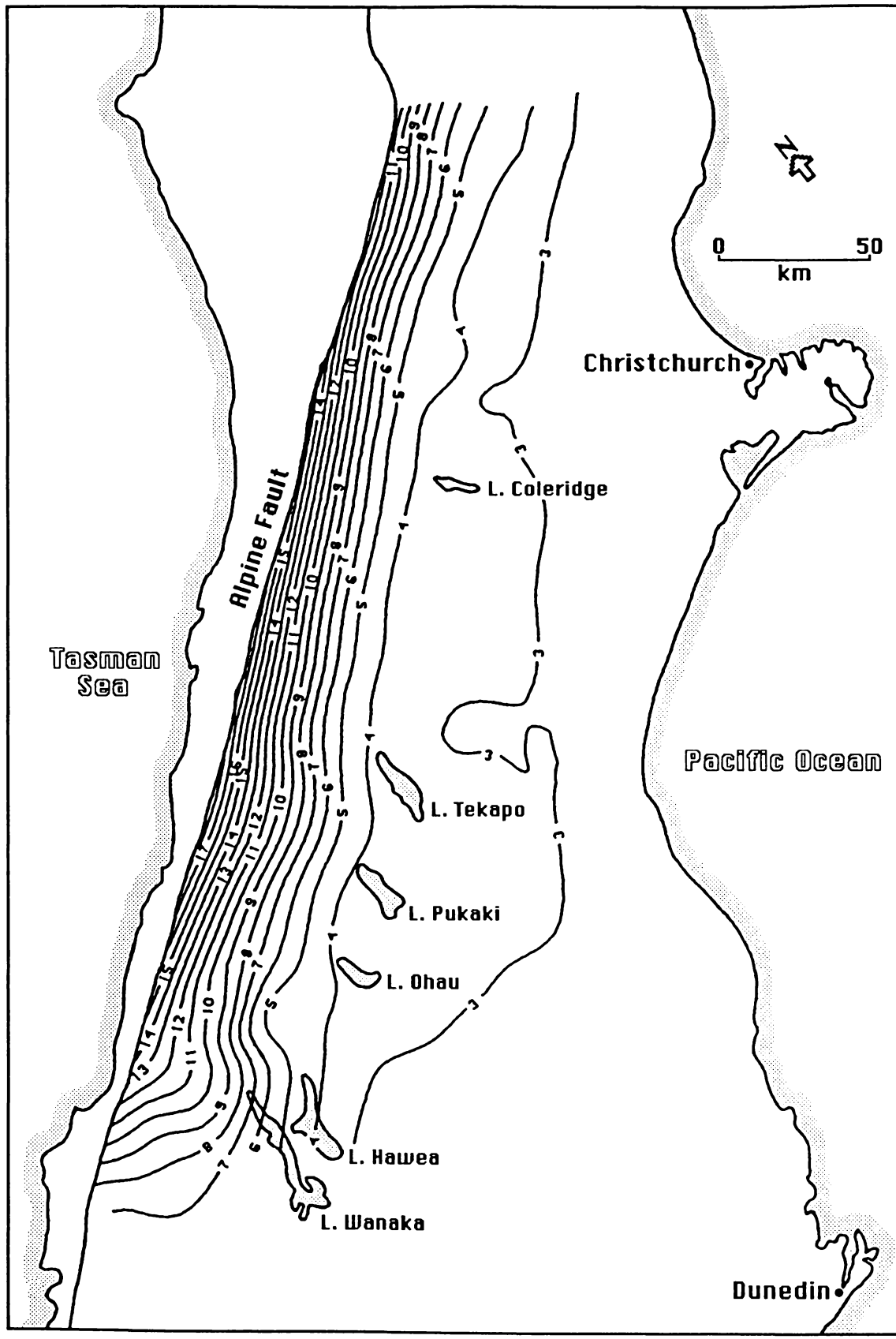


Fig. 1. Map of amount of late Cenozoic rock uplift (in km) in the Southern Alps (from Tippett and Kamp submitted).

ABSTRACT

We have used fission track data for a suite of basement rock samples from the central Southern Alps to assess the role of faulting in the late Cenozoic uplift of the Pacific plate. The fission track data for samples from sites on both sides of the Moonlight, Ostler, Harper, Torlesse, Porter's Pass and Hope faults show that in all cases the vertical offset lies within the uncertainty of the data, typically ± 2 km, and is less than 30% of the surrounding uplift. Major faults are conspicuously absent in the zone of greatest uplift. Over a scale of kilometres the uplift (dilatational strain) is continuous and regular. The results of this study support the conclusion reached by R.I. Walcott from geodetic data that deformation in the plate boundary zone can be treated as if it were a continuum with a ductile deformation.

INTRODUCTION

Throughout the late Cenozoic the Pacific plate has been converging obliquely with the Australian plate in central South Island. A consequence of this oblique continental collision has been substantial rock uplift at the leading edge of the Pacific plate such that an oblique section through the middle to upper part of the crust is now exposed over a zone ~120 km wide immediately southeast of the Alpine fault (e.g. Kamp et al. 1989). We have applied the technique of fission track analysis to 140 basement rock samples from the central part of the Southern Alps (Lewis Pass to Lake Wanaka) to establish details of the timing, amount and pattern of late Cenozoic uplift (Tippett and Kamp, submitted). Fig. 1 shows the distribution of the total amount of late Cenozoic rock uplift based on analysis of these data.

A question arising from the information contained in Fig. 1 is the mechanism of uplift, and in particular whether or not faulting within the Pacific plate has played a significant role in the uplift. A comparison of the region in the Southern Alps encompassing most of the uplift (Alpine fault SE to the 4 km uplift contour, Fig. 1) with the same region in Fig. 2 suggests that faulting may not be a significant uplift mechanism, because not many faults have been mapped within the region of greatest uplift. Alternatively, the absence of major faults generally in the central Southern Alps may merely reflect the difficulty of mapping faults within basement rocks. Many of the faults mapped in Fig. 2 are evident in the field because they involve displacement of the late Cretaceous-Cenozoic succession, or because (in SE

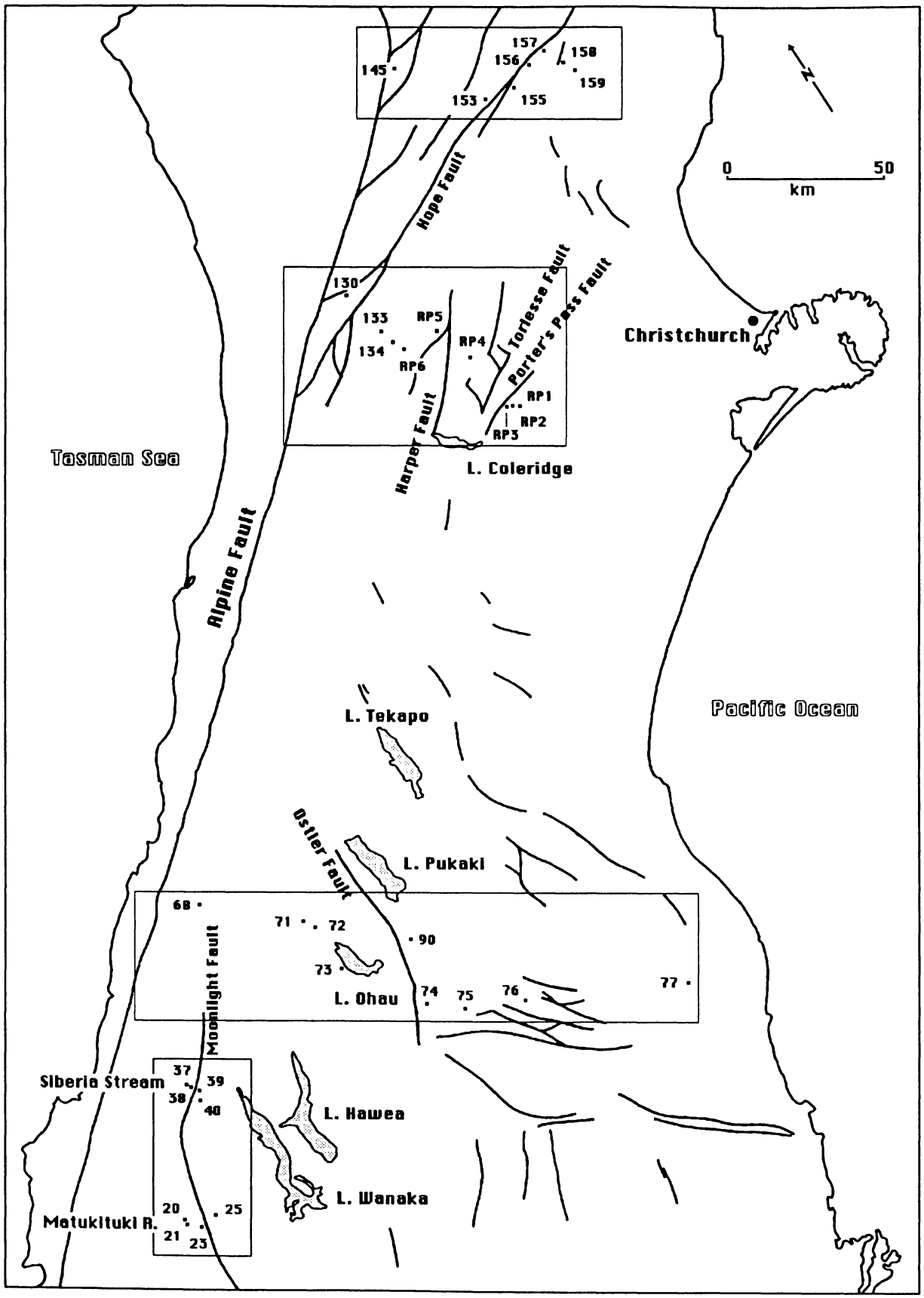


Fig. 2. Locations of fission track samples with respect to mapped faults in the Southern Alps (fault pattern from Spörli 1979; Craw 1985). Sample numbers correspond to Table 1.

Otago) of the offset of the Cretaceous peneplain cut across basement; these markers do not occur in the main part of the Southern Alps.

There are however several apparently major and more continuous faults occurring within or marginal to the zone of major uplift, including the Moonlight, Ostler, Torlesse, Porter's Pass, Harper and Hope faults (Fig. 2). Analysis of our fission track data indicates that the fault displacements are small compared with the total amount of uplift, suggesting that faulting within the Pacific plate part of central South Island is not a significant mechanism contributing to the uplift. Over the scale of the Southern Alps therefore, the effect of faulting can be ignored and the uplift treated as ductile deformation.

PRINCIPLES AND METHOD OF INVESTIGATION

As part of a wider fission track study of the Southern Alps, samples of basement rock were collected and analysed from sites on both sides of the more major faults mapped within the central Southern Alps (Fig. 2). The technique of analysis (fission track analysis) applied to apatite and zircon crystals is a well established method of determining the low temperature history of host rocks (e.g. Hurford 1986; Green et al. 1989; Kamp and Green 1990). Its application as a thermochronometer arises from the fact that over timescales of a few million years the fission track damage within the crystals is repaired (annealed) to different degrees within the range 20° to ~125°C.

The degree of annealing is reflected in the lengths of horizontally confined tracks, samples residing at deeper levels (higher temperatures) in the annealing zone having shorter mean lengths. At temperatures exceeding ~125°C fission track damage is not retained at all by apatite crystals, and when the host rocks are uplifted and cool through ~125°C, tracks start to be retained, and hence record the uplift age. Invariably, these ages will be minimum ages, as tracks produced during uplift will have been shortened to some extent, and therefore the density (age) of tracks intersecting a randomly cut surface will be less than if the rocks had cooled instantaneously. It follows that fission tracks in apatites that have been heated via burial and then resided for a few million years in the lower levels of an apatite annealing zone (70°-125°C) will have undergone significant annealing, and the measured ages will have no meaning in terms of geological events. This arises because the track density has been reduced,

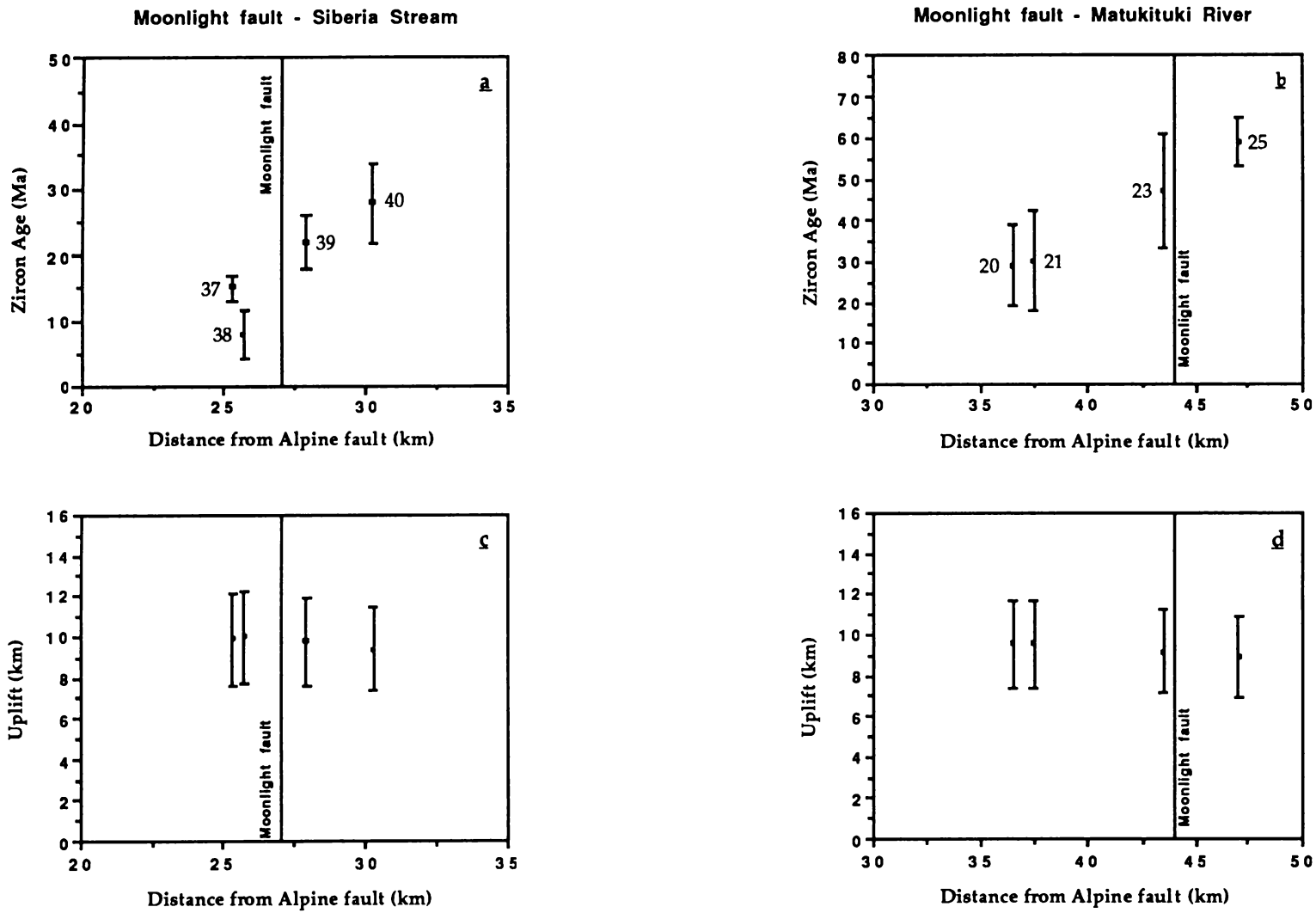


Fig. 3. Moonlight fault: Zircon fission track age (a) and uplift amount (c) versus distance from the Alpine fault for the Moonlight fault at the Siberia Stream transect. Zircon fission track age (b) and uplift amount (d) versus distance from the Alpine fault for the Moonlight fault at the Matukituki River transect. Errors are 2σ.

and hence age has been lost, due to the effects of annealing at elevated temperatures.

Because the length of a fission track is controlled primarily by the maximum temperature it has experienced (Duddy et al. 1988), outcrop samples from different localities that have recently been uplifted from similar depths within an annealing zone will have similar mean ages and mean track lengths. Disparate fission track ages and lengths for samples either side of faults will therefore indicate fault displacements. From the age and in particular the length data, estimates of the ambient temperatures prior to uplift are made via empirical relationships established for the Otway basin between modern formation temperatures and the fission track parameters of age and length. Details of paleotemperature estimations made for the Southern Alps samples are outlined fully in Tippett and Kamp (submitted). With the paleotemperature estimates for each sample and assuming a geothermal gradient (27.5° ± 2.5°C), the amount of uplift can be calculated by simple division. By this method, the amount of uplift can usually be constrained to better than ± 2 km (2σ).

The kinetics of annealing of fission tracks in zircon crystals are not as well understood as they are for apatite. Nevertheless, paleotemperature estimates and hence the amount of uplift can still be established by interpolation for samples, which prior to uplift, resided at temperatures between the base of the apatite annealing zone (~125°C) and the base of the zircon annealing zone (~265°C). We have done this in the case of the Moonlight fault because the apatites from the host rocks of Siberia Stream and Matukituki River have been uplifted from below the base of the apatite annealing zone.

Full details of fission track experimental procedures and calibration used in this study can be found in Tippett and Kamp (submitted). The fission track data and uplift data for this study are reported in Table 1.

MOONLIGHT FAULT

Fig. 3 a and b shows the spatial variation in zircon FT age, and amount of rock uplift, of rocks from the Siberia and Matukituki transects across the Moonlight fault. Zircon FT ages vary between 7.8 ± 1.8 Ma and 28 ± 3 Ma in the Siberia Stream transect, and between 30 ± 5 Ma and 59 ± 3 Ma in the Matukituki River transect. The ages differ because prior to uplift the

Table 1: Fission track data, derived pre-uplift paleotemperatures, and rock uplift amounts.

Sample Number	Area	Coordinate x	Coordinate y	Elevation (m)	Distance from Alpine Fault (km)	Mineral	Fission Track Age (Ma) ±2σ	Mean Track Length (μm) ±2σ	Pre-uplift Paleotemp. (°C) ±2σ	Amount of Uplift (km) ±2σ
20	Moonlight (Matukituki)	2537	4424	535	33	Apatite	0	-	-	-
						Zircon	29 ± 10	-	260 ± 50	9.6 ± 2.1
21	Moonlight (Matukituki)	2532	4411	520	34	Apatite	0	-	-	-
						Zircon	30 ± 12	-	260 ± 50	9.5 ± 2.1
22	Moonlight (Matukituki)	2544	4348	490	39	Apatite	0	-	-	-
23	Moonlight (Matukituki)	2579	4341	395	43	Apatite	0	-	-	-
						Zircon	47 ± 14	-	250 ± 50	9.1 ± 2.1
24	Moonlight (Matukituki)	2590	4344	455	43	Apatite	0	-	-	-
25	Moonlight (Matukituki)	2629	4342	365	45	Apatite	0	-	-	-
						Zircon	59 ± 6	-	245 ± 50	8.9 ± 2.0
37	Moonlight (Siberia)	2855	4745	610	25	Apatite	0	-	-	-
						Zircon	15 ± 2	-	265 ± 50	9.9 ± 2.2
38	Moonlight (Siberia)	2857	4740	610	26	Apatite	0	-	-	-
						Zircon	7.8 ± 3.6	-	265 ± 50	10.0 ± 2.2
39	Moonlight (Siberia)	2869	4718	610	28	Apatite	0	-	-	-
						Zircon	22 ± 4	-	260 ± 50	9.8 ± 2.2
40	Moonlight (Siberia)	2844	4675	335	30	Apatite	0	-	-	-
						Zircon	28 ± 6	-	260 ± 50	9.4 ± 2.1
68	Ostler	3279	5196	170	13	Zircon	3.1 ± 1.0	-	265 ± 50	9.4 ± 2.1
71	Ostler	3521	4914	640	46	Apatite	4.9 ± 1.6	8.99 ± 2.36	117 ± 19	4.5 ± 0.7
72	Ostler	3544	4877	550	50	Apatite	41 ± 10	10.47 ± 0.96	100 ± 10	3.8 ± 0.5
73	Ostler	3526	4711	565	62	Apatite	63 ± 12	10.76 ± 0.72	96 ± 6	3.7 ± 0.4
74	Ostler	3673	4431	425	91	Apatite	61 ± 12	11.87 ± 0.70	87 ± 8	3.2 ± 0.4
75	Ostler	3766	4333	410	103	Apatite	75 ± 16	12.64 ± 0.40	78 ± 7	2.9 ± 0.4
76	Ostler	3951	4217	320	121	Apatite	108 ± 14	13.03 ± 0.36	75 ± 20	2.7 ± 0.5
77	Ostler	4403	3911	120	166	Apatite	112 ± 56	-	74 ± 16	2.5 ± 0.6
90	Ostler	3763	4642	425	79	Apatite	96 ± 16	12.60 ± 0.40	79 ± 13	3.0 ± 0.4
130	Porter's/Harper	5045	6506	245	7	Zircon	4.6 ± 0.6	-	265 ± 50	9.5 ± 2.1
133	Porter's/Harper	5053	6297	810	24	Apatite	3.6 ± 2.4	7.69 ± 4.80	118 ± 13	4.8 ± 0.6
134	Porter's/Harper	5064	6264	760	27	Apatite	5.5 ± 3.6	7.56 ± 5.30	118 ± 15	4.7 ± 0.6

Sample Number	Area	Coordinate x	Coordinate y	Elevation (m)	Distance from Alpine Fault (km)	Mineral	Fission Track Age (Ma) ± 2σ	Mean Track Length (μm) ± 2σ	Pre-uplift Paleotemp. (°C) ± 2σ	Amount of Uplift (km) ± 2σ
RP1	Porter's/Harper	5262	5813	570	71	Apatite	134 ± 14	12.24 ± 0.26	70 ± 16	2.8 ± 0.5
RP2	Porter's/Harper	5239	5835	610	69	Apatite	141 ± 16	12.44 ± 0.30	69 ± 16	2.8 ± 0.5
RP3	Porter's/Harper	5233	5844	730	67	Apatite	92 ± 22	12.40 ± 0.38	81 ± 14	3.3 ± 0.4
RP4	Porter's/Harper	5237	6054	650	51	Apatite	114 ± 22	11.98 ± 0.42	73 ± 16	2.9 ± 0..6
RP5	Porter's/Harper	5205	6202	610	38	Apatite	6.0 ± 7.2	8.27 ± 2.10	116 ± 10	4.5 ± 0.5
RP6	Porter's/Harper	5082	6238	670	29	Apatite	3.9 ± 2.8	8.01 ± 2.40	117 ± 7	4.6 ± 0.5
145	Hope	5678	6986	550	2.6	Zircon	5.3 ± 0.8	-	265 ± 50	9.8 ± 2.2
153	Hope	5853	6708	455	32	Apatite	3.0 ± 2.0	7.57 ± 4.36	117 ± 12	4.4 ± 0.6
155	Hope	5968	6703	410	40	Apatite	6.4 ± 5.6	7.70 ± 2.78	116 ± 14	4.3 ± 0.6
156	Hope	6047	6724	380	43	Apatite	11 ± 6	10.23 ± 2.68	106 ± 19	3.9 ± 0.7
157	Hope	6116	6716	335	47	Apatite	28 ± 14	9.66 ± 1.10	105 ± 16	3.8 ± 0.6
158	Hope	6139	6643	290	53	Apatite	75 ± 14	11.28 ± 0.48	91 ± 5	3.3 ± 0.4
159	Hope	6159	6584	245	59	Apatite	85 ± 14	11.58 ± 0.40	89 ± 5	3.1 ± 0.4

Note: (i) Location coordinates refer to NZMS 1 topographic maps. (ii) Fission track data, derived paleotemperatures, and uplift amounts are taken from Kamp et al. (1989) and Tippett and Kamp (submitted). (iii) 'Uplift' refers to rock uplift (displacement of rocks with respect to the geoid).

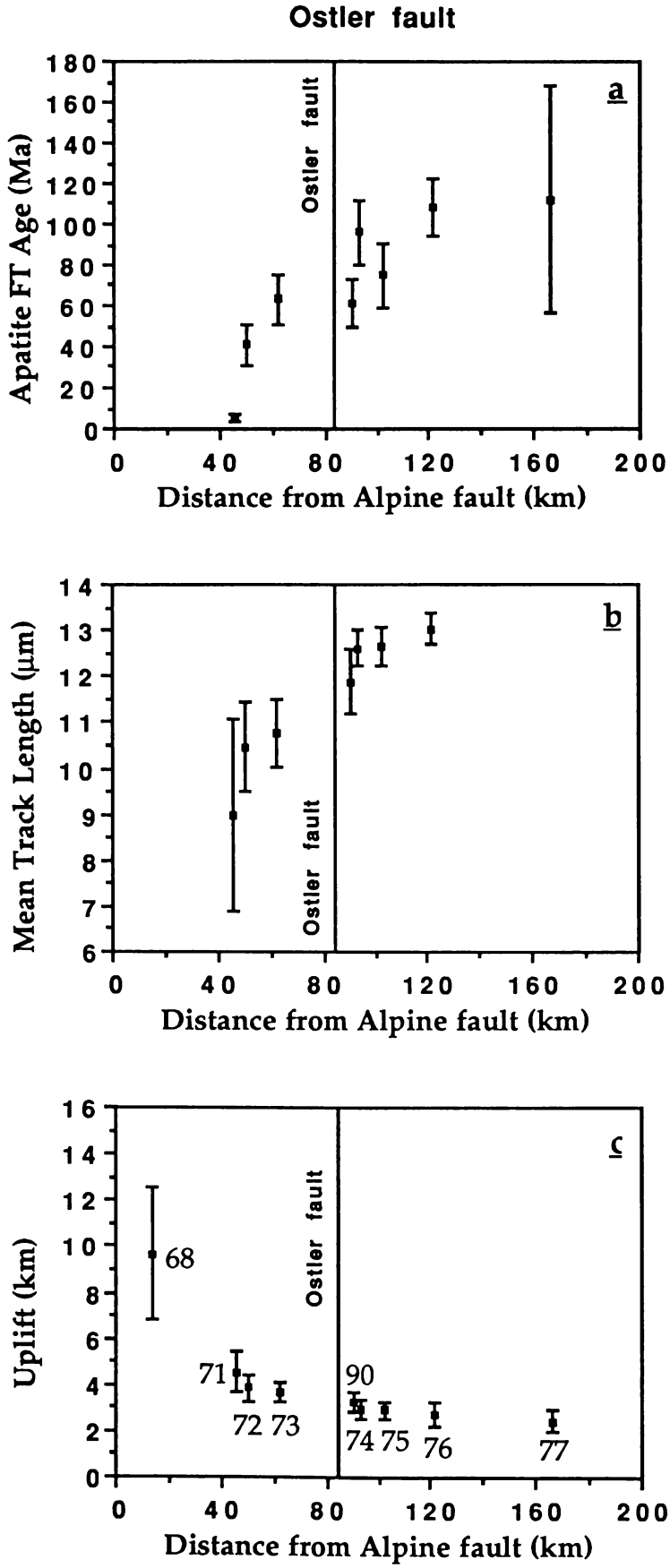


Fig. 4. Apatite fission track age (a) and mean track length (b), and uplift amount (c), versus distance from the Alpine fault for a transect across the Ostler fault. Errors are 2σ.

host rocks resided within the lower part of a zircon annealing zone where small changes in temperature have a large effect on annealing rate and hence age. We are confident that these ages originate from within the former annealing zone because all the ages exceed the uplift age for this part of the Southern Alps (~7 Ma, Kamp et al. 1989; Tippett and Kamp submitted) and the ages are much less than the ages of ~200 Ma preserved in the schists further east and outside the zone of major late Cenozoic uplift.

The paleotemperatures of the host rocks in Siberia Stream and Matukituki River have been estimated by interpolation (Table 1) and are displayed in Fig. 3 c and d. This method of paleotemperature estimation inherently has more uncertainty than where paleotemperatures are estimated for samples that were uplifted from within an apatite annealing zone, and so there is an uncertainty of about ± 2 km for data points in Fig. c and d. However, it is clear that in both transects the displacement across the Moonlight fault is no more than the 'most probable error' of 3 km (2σ) for differences between samples on opposite sides of the fault.

OSTLER FAULT

Fig. 4 a and b shows the variation of apatite FT age and mean track length for samples from either side of the Ostler fault. There are systematic changes in the apatite mean ages and mean lengths consistent with origination of the samples from an exhumed apatite annealing zone. The pattern of decreasing age and mean length westward is not disrupted by the Ostler fault.

Fig. 4 c shows the pattern of total late Cenozoic uplift across the Ostler fault near Lake Ohau. Sample 69 comes from the base of the exhumed zircon annealing zone, which prior to uplift had a temperature of 265 ± 50° C. Note that the amount of uplift increases smoothly with increasing proximity to the Alpine fault, and that any displacement on the Ostler fault probably lies within the uncertainty of the data (best shown by the difference 0.5 ± 0.6 km between samples 73 and 74).

PORTER'S PASS, TORLESSE AND HARPER FAULTS

Fig. 5 a and b shows the variation in apatite FT age and mean length of outcrop samples collected from a transect across the strike of the Porter's Pass, Torlesse and Harper faults. All of the samples in a and b resided in

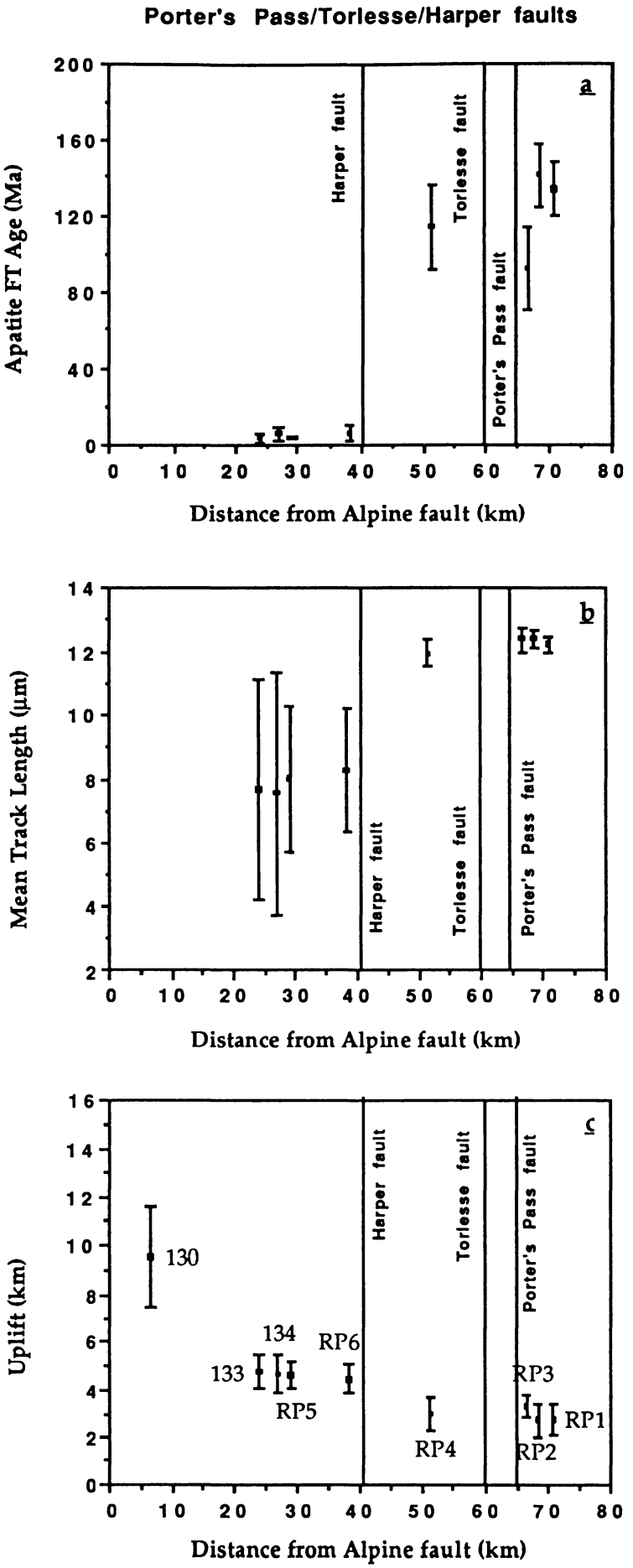


Fig. 5. Apatite fission track age (a) and mean track length (b), and uplift amount (c), versus distance from the Alpine fault for a transect across the Porter's Pass/Torlesse/Harper faults. Errors are 2σ.

the annealing zone prior to uplift, those at the eastern end of the transect lying at upper levels (low temperatures) and those at the western end lying at deeper levels near the base of the annealing zone. Sample 130, taken from a location 6.7 km southeast of the Alpine fault, has a zircon age of 4.6 ± 0.6 Ma, and prior to uplift lay at the base of a zircon annealing zone (~265° C).

Fig. 5 c shows the amount of uplift of each sample in the transect estimated from the age and length data. The primary signal is one where the amount of uplift increases systematically towards the Alpine fault. Between the western side of the Torlesse fault and the eastern side of the Porter's Pass fault the displacement lies within the uncertainty limits of the data. There may be more significant displacement on the Harper fault, measured by the difference between samples RP4 and RP6 of 1.7 ± 0.8 km.

HOPE FAULT

Fig. 6 a and b shows the variation in apatite FT age and mean track length of host rocks from positions either side of part of the Hope fault and a subparallel un-named fault. This suite of samples exhibits a very clear example of an exhumed apatite annealing zone. The samples for the western end of the transect prior to uplift resided in the reset zone below the annealing zone, and because of their low track densities, few confined track length measurements could be made. They would be expected to have long lengths however. Fig. 6 c shows the amount of rock uplift of the host rocks with respect to the faults in the transect. Note that samples 155, 156, and 157, which are equidistant from the Hope fault, show a pattern of decreasing uplift eastwards. Again, displacement across the faults is limited to ~1 km, within the uncertainties associated with the data.

DISCUSSION

The amount of displacement on the faults constrained by the fission track data applies strictly only to the vertical component of displacement. For example, the Hope fault in the region of Lewis Pass probably has a significant horizontal offset, but this type of displacement cannot be constrained by fission track data. In addition, it is probable that some of the faults considered here are long-lived structures that have reversed their sense of movement between the Mesozoic and late Cenozoic such that the net effect is minimal total offset. This type of fault behaviour would however be detected by fission track analysis, as there would have been sufficient time

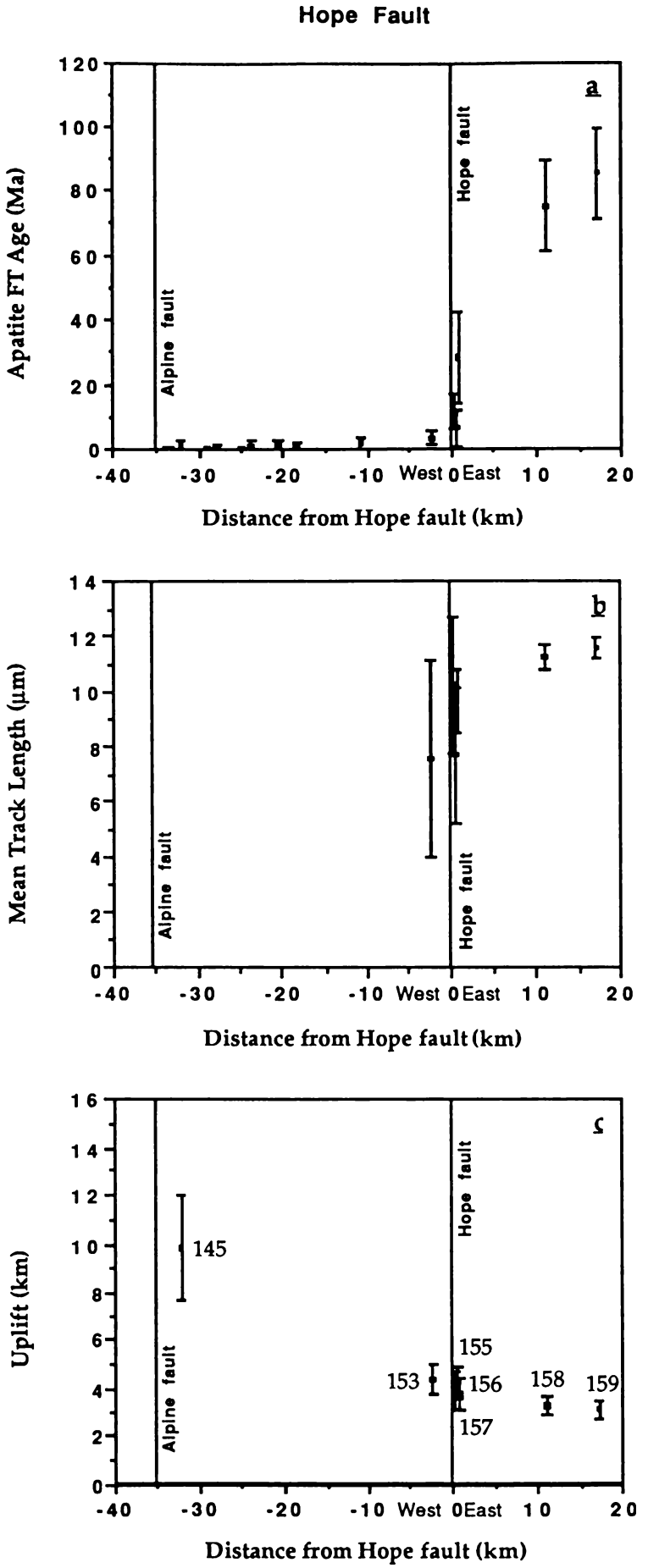


Fig. 6. Apatite fission track age (a) and mean track length (b), and uplift amount (c), versus distance from the Alpine fault for a transect across the Hope fault. Errors are 2σ.

between the change in sense of displacement on the fault(s) for the apatites to have equilibrated with the ambient crustal temperatures following the first (Mesozoic) phase of movement. A corollary of this is that the fission track data only constrain late Cenozoic displacement on the faults.

The principal conclusion from this study is that on all the faults considered, the maximum amount of late Cenozoic displacement that can have occurred is the uncertainty associated with the data. This corresponds to ± 3 km for the Moonlight fault in the study area, ± 1.5-2 km for the Harper fault, and ± 1 km for the Ostler, Porter's Pass, Torlesse and Hope faults. We do not imply that there has not been vertical displacement on these faults, but that the amount of displacement is only a proportion of the total amount of late Cenozoic uplift in each area. In all cases both sides of the faults have been uplifted, which in itself indicates that differential fault movement within the Pacific plate is not controlling its regional uplift.

We have noted earlier that there are few mapped faults in those parts of the Southern Alps where there is major rock uplift. No doubt some faults do occur there, but they are unlikely to have associated vertical displacements greater than those discussed above for the faults that lie mostly marginal to the region of major uplift. Even if faults as major as those discussed above do occur in the region of greater uplift, the proportional importance of their displacement becomes less and less significant towards the Alpine fault as the total amount of uplift increases. We suggest that over the greater part of the Southern Alps, vertical displacement on faults can be ignored as having any control on the uplift pattern. The profile of uplift is essentially a type of asymmetrical flexural upwarp centred on the Alpine fault and the rocks are mostly behaving in a ductile manner.

The fact that schistose rocks comprise the upper crust between the Alpine fault and the Main Divide in the Southern Alps probably has a major bearing on the mechanism of uplift, and the relative unimportance of faulting. The accumulation of strain in these rocks is probably prevented by slip on schistosity planes at microscopic and mesoscopic scales. Alpine schist encompasses the zone of major uplift from the Alpine fault southeastward to the 12 km uplift contour, and therefore most of the uplift has taken place in rocks that behave demonstrably in a ductile manner.

CONCLUDING REMARKS

In a comparison of short- and long-term kinematics of the plate boundary zone through New Zealand, Walcott (1984) concluded that while at a scale of a few hundred metres faulting is important and the deformation is continuous, at scale lengths of a few tens of kilometres the deformation is continuous and regular, and the effects of faulting can be ignored. Moreover, the plate boundary could be treated as if it were a continuum, with a ductile deformation. The results of our work support and extend this conclusion. Our work has been concerned with establishing the long-term uplift (dilatational strain) in central South Island. The principal conclusions of this study are (i) that the amount of vertical offset on the more major faults within the Pacific plate is a minor proportion of the total amount of surrounding uplift, and (ii) that no major fault displacements occur within the ~50 km wide zone of the central Southern Alps where most of the uplift takes place. The amount of uplift within central South Island increases nearly exponentially with increasing proximity to the Alpine fault, in a very clear continuum. This pattern is maintained with little variation over 300 km of the Southern Alps parallel to the Alpine fault. This pattern in itself is indicative of the important role of ductile deformation within the Pacific plate and the role of the Alpine fault as a major discontinuity.

REFERENCES

Craw, D. 1985: Structure of schist in the Mt Aspiring region, northwestern Otago, New Zealand. *New Zealand Journal of Geology and Geophysics 28*, 55-75.

Duddy, I.R.; Green, P.F.; Laslett, G.M. 1988: Thermal annealing of fission tracks in apatite 3. Variable temperature behaviour. *Chemical Geology (Isotope Geoscience section) 73*, 25-38.

Green, P.F.; Duddy, I.R.; Gleadow, A.J.W.; Lovering, J.F. 1989: Apatite fission track analysis as a paleotemperature indicator for hydrocarbon exploration. *In: Thermal History of Sedimentary Basins*. Editors N.D. Naeser; McCulloh, T.H., Springer-Verlag, New York.

Hurford, A.J. 1986: Cooling and uplift patterns in the Lepontine Alps, South Central Switzerland, and an age of vertical movement of the Insubric fault line. *Contributions to Mineralogy and Petrology 92,* 413-427.

Kamp, P.J.J.; Green, P.F.; White, S.H. 1989: Fission track analysis reveals character of collisional tectonics in New Zealand. *Tectonics 8*, 169-195.

Kamp, P.J.J. and Green, P.F. 1990: Thermal and tectonic history of selected Taranaki Basin (New Zealand) wells assessed by Apatite Fission Track Analysis. *The American Association of Petroleum Geologists Bulletin 74, (9)*, 1401-1419.

Spörli, K.B. 1979: Structure of the South Island Torlesse in relation to the origin of the Southern Alps. *Bulletin of the Royal Society of New Zealand 18,* 99-104.

Tippett, J.M. and Kamp, P.J.J. (submitted): Fission track analysis of the late Cenozoic vertical kinematics of continental Pacific crust, South Island, New Zealand. *Journal of Geophysical Research.*

Walcott, R.I. 1984: The kinematics of the plate boundary zone through New Zealand: a comparison of short- and long-term deformations. *Geophysical Journal of the Royal Astronomical Society 79*, 613-633.

CHAPTER 6

Fission track analysis enables determination of quantitative relationships between uplift and geomorphology of the Southern Alps, New Zealand

(Manuscript submitted to *Earth Surface Processes and Landforms*)

J. Mark Tippett
Peter J.J. Kamp

Geochronology Research Unit,
Department of Earth Sciences,
University of Waikato,
Private Bag 3105,
Hamilton 2001, New Zealand.

ABSTRACT

The Southern Alps mountain chain, New Zealand, has formed as a consequence of late Cenozoic collision of the continental parts of the Pacific and Australia plates. Fission track analysis has yielded estimates of the amount, age of initiation, and rate of late Cenozoic rock uplift for 82 surface samples taken from transects across the Southern Alps. The mean surface, summit, and valley elevations in the vicinity of each of the rock sample sites have also been measured. Regression of the geomorphic variables on the uplift variables has been used to establish quantitative relationships between uplift and geomorphology. There are strong and consistent linear associations between uplift and the elevations of the mean surface, summits, and valleys. The preferred regression models have uniform slope but varying elevation response between transects. Substitution of space for time has allowed the evolution of landforms to be studied.

To the east of the Main Divide, elevation and relief are proportional to and closely related to the age of initiation of rock uplift ('uplift age') and the amount of rock uplift (r^2>0.8). Mean surface uplift was delayed for ~2 Ma after the start of rock uplift, a result of the stripping of a soft cover rock succession that prior to rock uplift overlaid the harder greywacke basement. Inter-transect variations in regression response and x-intercept are inferred therefore to reflect the variable pre-uplift thickness of cover rocks. However, the regular regression slope for the transects reflects the consistent nature of the interaction between uplift and the erodibility of greywacke basement. Uplift of the mean surface proceeded at 0.4 km/km and 0.4 km/Ma of rock uplift, while the rock uplift rate was 0.8 km/Ma. Summit elevations have increased at a rate of 0.6 km/Ma and valley elevations have increased at 0.2 km/Ma. Both tectonic and isostatic uplift are required to explain the height of the summits. Regression lines relating mean surface, summit, and valley elevations to rock uplift and uplift age diverge from common intercepts; it is concluded therefore, that the mountains east of the Main Divide have continued to increase in elevation and relief and change in form over time since the start of uplift. Mountain elevation has little relationship with late Cenozoic mean rock uplift rates of 0.8-1.0 km/Ma or inferred contemporary rock uplift rates (r^2~0.3).

In contrast, to the west of the Main Divide, elevation is shown to be closely related to rock uplift rate (r^2>0.8). Transects with higher rock uplift rates support higher topography. Landforms are therefore in a stable

equilibrium with rock uplift rate, and the landscape contains no residual evidence of the total amount of rock uplift, or the age of uplift. Lithological variation appears to have no relationship with elevation.

INTRODUCTION

That geomorphology should be related functionally to uplift has become a paradigm in the geomorphic literature. Uplift (amount, age, and rate) exerts a primary control on the nature and evolution of landforms in both the 'classic' models of landscape evolution (Davis, 1899; Penck, 1953; King, 1953), and in the more recent models of Hack (1960) (dynamic equilibrium), and Brunsden and Thornes (1979) and Brunsden (1980) (landscape sensitivity). Indeed, any model of landscape evolution must take account of uplift as the basic constructional input leading to increase in relief and (often) mean surface elevation.

Therefore, although theoretical concepts concerning the relationship between uplift and landscape evolution have been considered extensively in the literature, there are few documented cases (e.g. Adams, 1980; Yoshikawa, 1985) where the relationship has been examined empirically. This is due to the difficulty of estimating accurately and precisely the amount, age, and rate of uplift. In mountainous regions, stratigraphic records that might be expected to retain evidence of the timing of uplift are generally not preserved. There is also the problem of extrapolating measures of 'contemporary' uplift rates back in time to draw inferences concerning the amount of uplift over longer timescales. Fission track analysis is a new technique for establishing the amount, age, and rate of rock uplift in basement terranes. It has previously been applied to obtain this type of information in parts of the Transantarctic mountains (Gleadow and Fitzgerald, 1987) and western European Alps (Hurford, 1986). In this study we use uplift data for South Island, New Zealand, derived by fission track analysis, to infer the landscape evolution of the Southern Alps.

The Southern Alps (S. Alps) provide an ideal situation for examining the relationships between uplift and landscape evolution on account of the simplicity of the uplift pattern. In a related paper (Tippett and Kamp, in press) we have used fission track analysis to derive the amount, age, and rate of rock uplift in the S. Alps. This was based on the analysis of 140 samples obtained from 13 transects across the S. Alps spaced along the 300 km-long central sector of the S. Alps. In another paper (Kamp and Tippett,

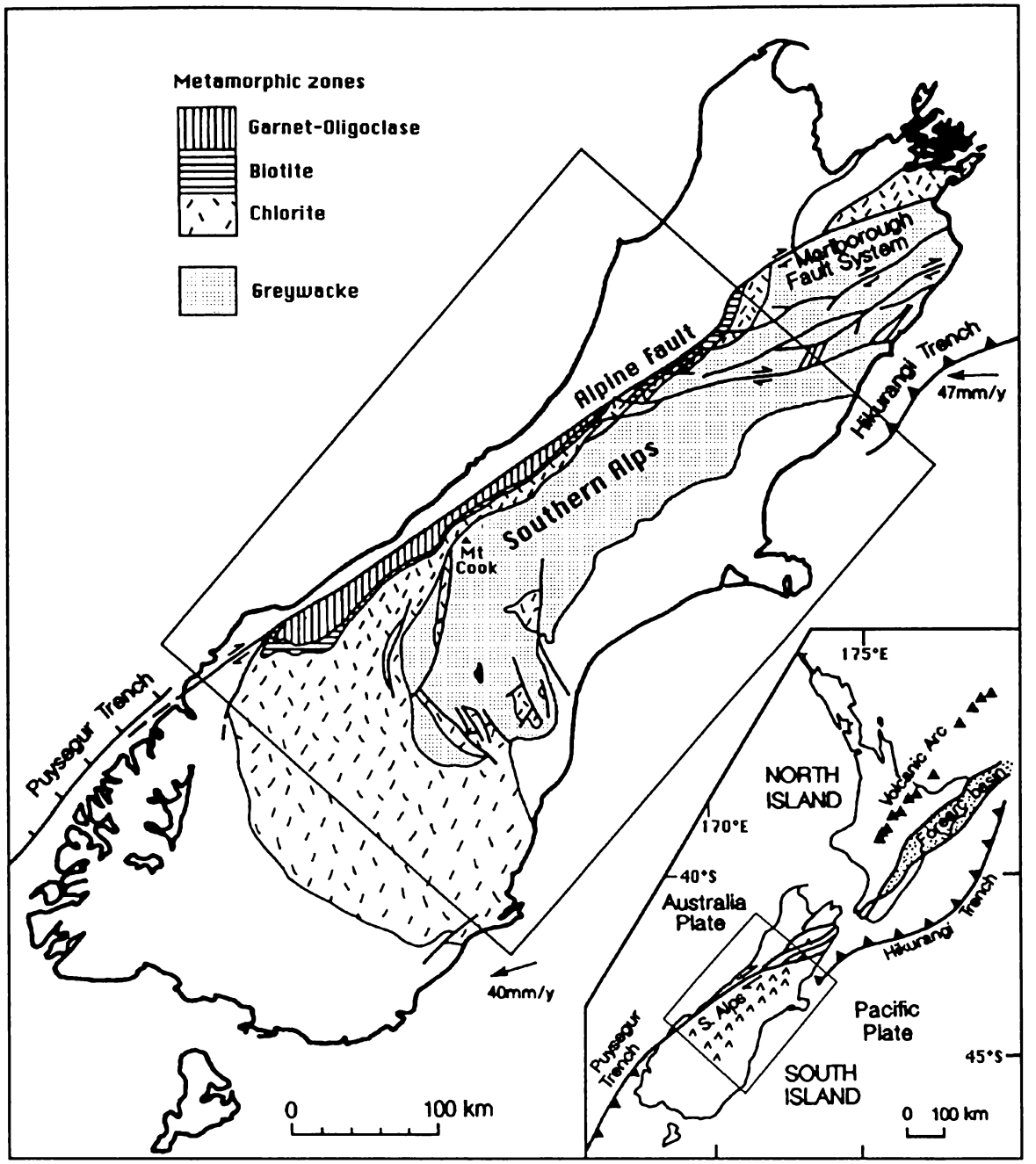


Fig. 1. Tectonic and geological setting of the Southern Alps (adapted from Kamp et al., 1989). Inset border indicates area covered by Figs 2 and 3.

submitted), we have calculated the tectonic component of the rock uplift; that is, the amount of the uplift due to plate driving forces, as opposed to the isostatic component of uplift that is due to denudation-induced rebound. In this study, we relate the uplift estimates of those studies to the present geomorphology of the S. Alps, and in doing so highlight the contribution of fission track analysis to quantifying aspects of the landscape evolution of the S. Alps.

TECTONIC DEVELOPMENT AND GEOMORPHOLOGY OF THE SOUTHERN ALPS

Throughout the late Cenozoic the Pacific plate has been converging obliquely with the Australia plate in central South Island as a result of a change in the direction of migration of the Australia-Pacific pole of rotation (Stock and Molnar, 1982). A consequence of this continental collision has been substantial rock uplift at the leading edge of the Pacific plate. The S. Alps mountain chain is the surface manifestation in the Pacific crust of the uplift, which was initiated at about 8 Ma ago (Kamp et al., 1989; Tippett and Kamp, in press). Fig. 1 shows the tectonic and geological setting of the S. Alps.

The S. Alps trend northeast-southwest and form an elongated asymmetric dome as shown by the variation in mean surface elevation (Fig. 2). From west to east, mountains rise steeply from a coastal plain to reach mean surface elevations at the Main Divide of almost 2 km, with a number of peaks exceeding 3 km in elevation. The Main Divide (Fig. 2) is the major drainage divide in the S. Alps and separates eastward-draining rivers from westward-draining ones. East of the Main Divide, mountain elevations decrease to 750 m over a distance of about 100 km. To the east of the S. Alps, mean surface elevation declines to sea level across gravel outwash plains.

APPROACH TO STUDY

In this paper we quantify the relationship between the uplift and geomorphology of the S. Alps, by using regression analysis of empirical data sets. We study the 'point to point' bivariate association (Hubert et al., 1985) between uplift and geomorphology, which refers to the correspondence between uplift and geomorphology over identical spatial locations.

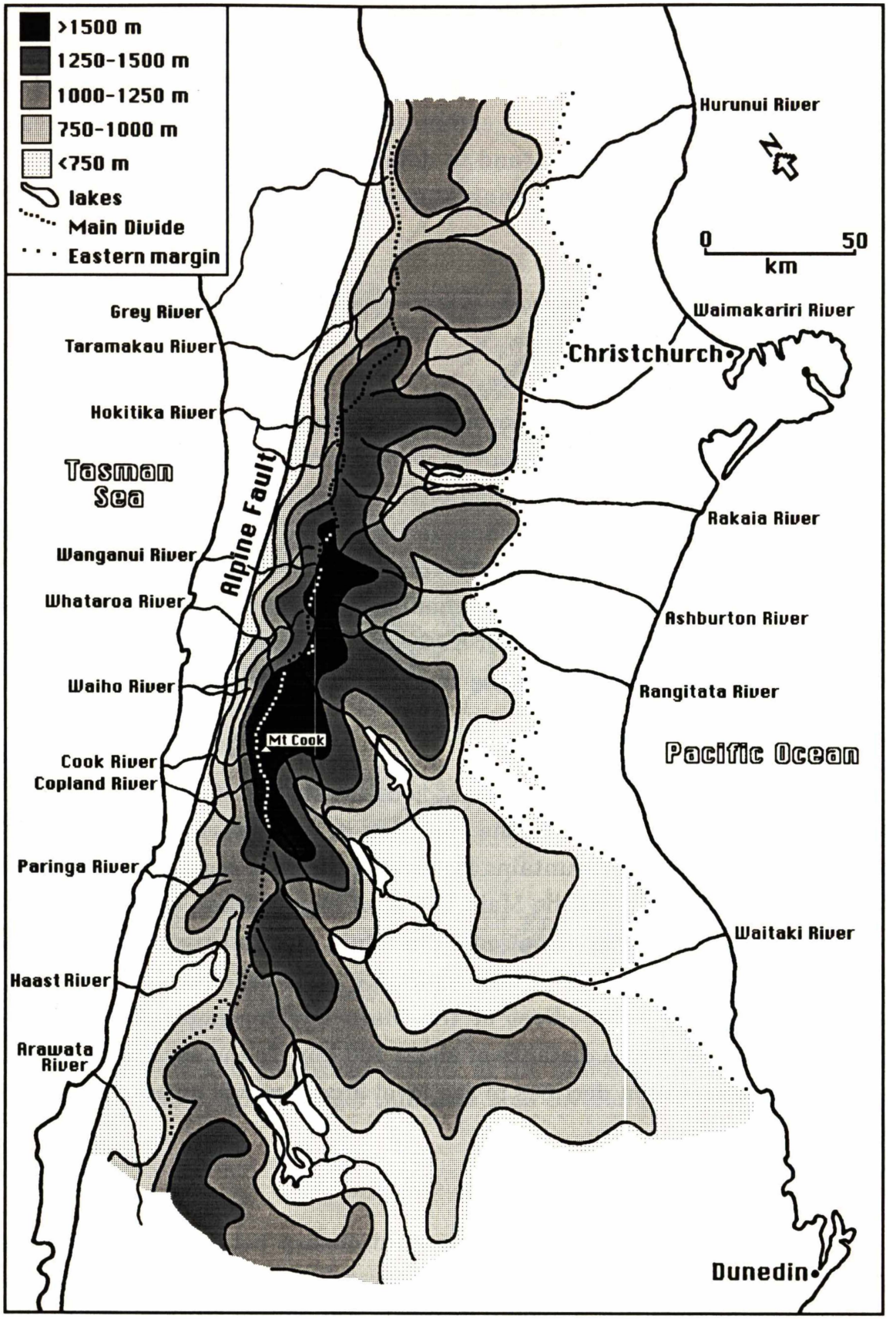


Fig. 2. Geomorphology of the Southern Alps, showing mean surface elevation, drainage pattern, location of the Main Divide (from Whitehouse, 1986), and the eastern margin of basement outcrop.

The uplift variables that we use are rock uplift (amount), uplift age (that is, the age of initiation of rock uplift), tectonic uplift (amount), and rock uplift rate. 'Rock uplift' is the displacement of rock with respect to the geoid, approximated as sea level. 'Tectonic uplift' is the component of rock uplift that is not attributable to isostatic uplift of the mean surface in response to erosion. 'Uplift' is used as a general term. The geomorphic variables that we use are mean surface elevation, summit (i.e. maximum) elevation, and valley (i.e. minimum) elevation.

We aim specifically to establish the character of the relationships between geomorphology and uplift, and to examine whether the relationships vary across the landscape. This will provide insights into landscape evolution in a continental collision zone.

METHODS

Fission track analysis

Fission tracks in uranium bearing minerals are created by the spontaneous fission of ^{238}U, and can be made visible by etching polished sections of uranium-bearing minerals such as apatite and zircon. The density of fission tracks that intersect a crystal surface, and the lengths of subsurface horizontal tracks, are the two variables routinely measured in fission track analysis that provide information about the thermal history of the host rocks. Fission tracks begin to be recorded in a crystal as it cools below a critical temperature, which for apatite is ~110°-125° C (Gleadow and Duddy, 1981; Green et al., 1989) and for zircon is in the range ~240°-265° C (Hurford, 1986; Kamp et al., 1989). The tracks in apatite are unstable at ambient temperatures of ~20° to 125° C and for zircon are unstable in the temperature range ~200° to 265° C. The instability is manifested in track length reduction, which leads to track density reduction in a randomly cut crystal section, and hence age reduction. The distribution of single grain ages, and track length distributions, will therefore reflect the thermal history of a sample. When the geothermal gradient and initial elevation of the land surface are known independently or can be reasonably assumed, a thermal (cooling) history can be interpreted in terms of an uplift history, to yield information about the amount, age, and rate of rock uplift.

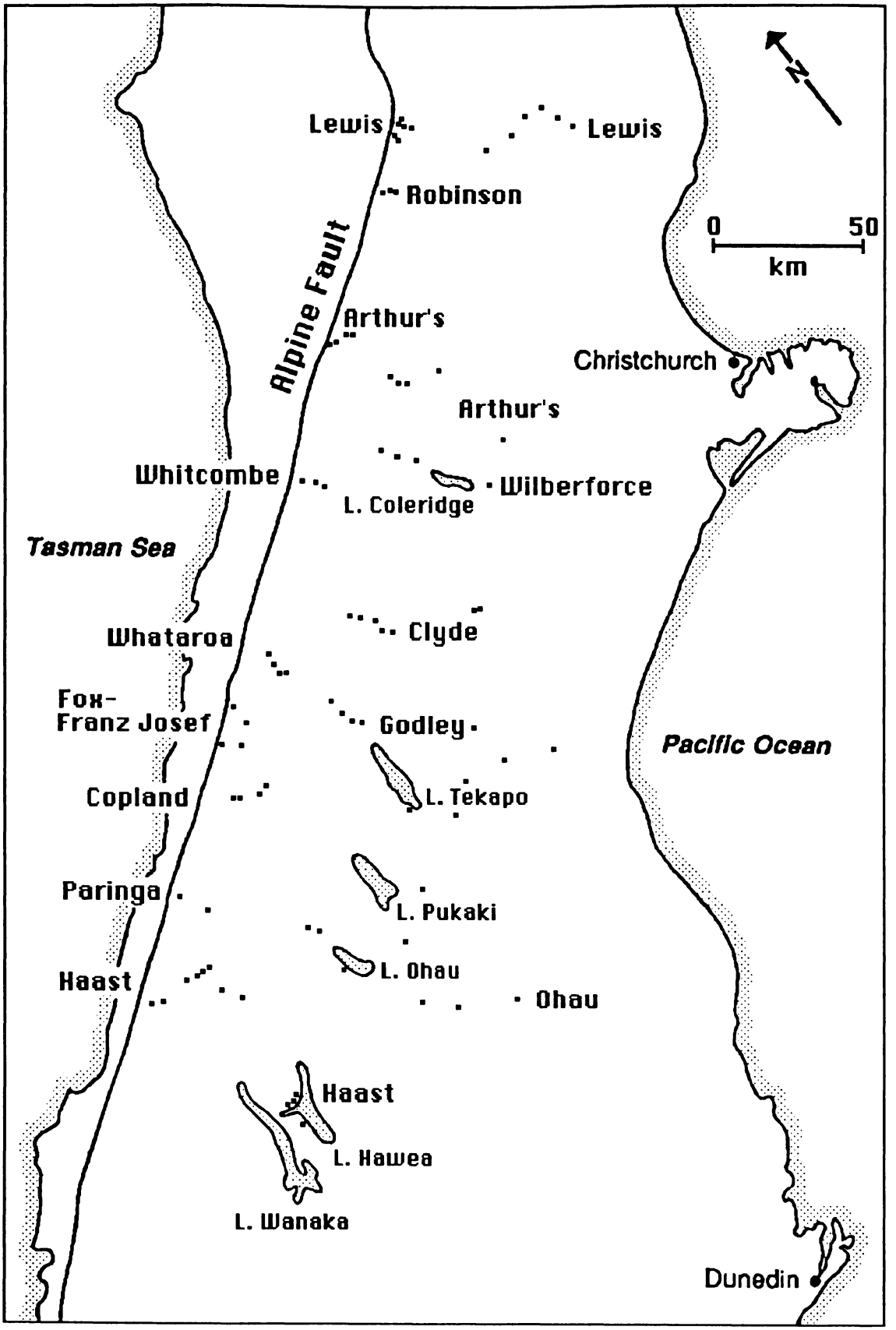


Fig. 3. Locations of transects and sample sites in the Southern Alps for which uplift data and geomorphic data were derived.

How estimates of amount, age, and rate of rock uplift were derived for the Southern Alps

Tippett and Kamp (in press) used fission track analysis of apatite and zircon crystals to establish the patterns of amount, age, and rate, of late Cenozoic rock uplift for the 300 km-long central section of the S. Alps. In that study, a number of transects starting at the Alpine Fault trace and extending to the southeast were sampled, as it had been established earlier (Wellman, 1979; Kamp et al., 1989) that the axis of uplift is oriented northeast-southwest. Fig. 3 shows the sample positions and transect locations. Tippett and Kamp (in press) estimated the pre-uplift paleotemperatures of apatites from each of the samples by comparing measured values of fission track age and mean length with published data relating these variables to temperature in deep hydrocarbon well sections in the Otway Basin, Australia. By assuming a normal pre-uplift geothermal gradient of 27.5 ± 2.5° C in the region that was to become the S. Alps, and showing that the initial mean elevation of the region was close to sea level, the amount of rock uplift was estimated for each of 45 apatite samples taken from the transects to the east of the Main Divide. The fission track data for these samples showed that they had resided in an annealing zone prior to late Cenozoic exhumation. Kamp and Tippett (submitted) calculated the amount of tectonic uplift of the samples by estimating the amount of isostatic rebound caused by denudation and subtracting this amount from the amount of rock uplift.

The rock uplift ages of 14 sites across the S. Alps were also established from fission track analysis (Tippett and Kamp, in press). A linear trend surface was fitted to these data to describe the spatial variation in uplift age across the S. Alps. Kamp and Tippett (submitted) used this trend surface to assign, by interpolation, uplift age estimates to the 45 samples for which estimates of the amount of rock uplift had been made. In addition, rates of rock uplift were estimated for each of 37 zircon samples taken from the transects to the west of the Main Divide by dividing the zircon closure temperature by the product of the sample age and geothermal gradient (Tippett and Kamp, in press); these estimates of rock uplift rate are averages over the last few million years, and have been shown to underestimate contemporary rock uplift rates.

Geomorphic analysis

Mean surface, summit, and valley (i.e. valley floor) elevations were chosen as the geomorphic variables to be measured in this study because these variables can be related to rock uplift. The values of these three variables for each sample point are necessarily averages of each surrounding area, as no one point has a mean surface, summit, or valley elevation, only a sample spot elevation.

Inspection of the maps used for data acquisition (New Zealand Map Series 1 1:63360 topographic maps) suggested that the average spacing between major river valleys is about 4-5 km. Therefore, a grid square of 20 km^2 placed systematically over the landscape should yield reasonable estimates of summit, valley, and mean surface elevations, as the size of each sampled area virtually assures inclusion of both valleys and summits. The maximum, minimum, and mean elevations within 20 km^2 grid squares were recorded for the 9 squares nearest each fission track sample location (mean elevation is the elevation of the grid square centre). The summit, valley, and mean surface elevations for each fission track sample location were estimated by the unweighted average of these 9 nearest-neighbour elevation measurements. Averaging overcomes the problem of using a single measurement from one grid square which may yield an unrepresentative value due to an 'accident' of precise grid location. The nine points sampled are regarded as a systematic sample of points in the related ~180 km^2 area.

APPROACH TO DATA ANALYSIS

Table 1 contains data of rock uplift, uplift age, tectonic uplift, and mean surface/summit/valley elevation, for the 45 sample sites located in the S. Alps to the east of the Main Divide. Also included in Table 1 are data on rock uplift rate and elevation for the 37 sample sites to the west of the Main Divide. The data have been divided geographically in this manner as it is evident from topographic maps, and the conclusions of previous work (e.g. Adams, 1985; Whitehouse, 1987; Koons, 1989), that two very different geomorphic domains exist to the east and west of the Main Divide.

Table 1: Uplift and geomorphic data for the Southern Alps, New Zealand.

Sample No.	Transect	Rock Uplift (km) ± 2σ	Uplift Age (Ma ago) ± 2σ	Tectonic Uplift (km) ± 2σ	Rock Uplift Rate (km/Ma) ± 2σ	Mean Surface Elevation (km) ± 2σ	Summit Elevation (km) ± 2σ	Valley Elevation (km) ± 2σ
8902-48	Haast (E)	4.3 ± 0.7	5.7 ± 1.1	1.4 ± 0.9	0.8 ± 0.2	0.73 ± 0.26	1.37 ± 0.23	0.38 ± 0.06
8902-49	Haast (E)	4.5 ± 1.0	5.7 ± 1.2	1.4 ± 0.7	0.8 ± 0.2	0.73 ± 0.26	1.37 ± 0.23	0.38 ± 0.06
8902-50	Haast (E)	4.1 ± 0.6	5.7 ± 1.2	1.5 ± 0.8	0.7 ± 0.2	0.89 ± 0.30	1.61 ± 0.22	0.49 ± 0.12
8326-3	Haast (E)	3.8 ± 0.7	5.6 ± 1.3	1.2 ± 0.9	0.7 ± 0.2	0.56 ± 0.20	1.16 ± 0.19	0.33 ± 0.02
8902-58	Haast (E)	5.3 ± 0.6	6.4 ± 0.8	1.8 ± 0.8	0.8 ± 0.1	1.04 ± 0.25	2.00 ± 0.20	0.68 ± 0.14
8902-71	Ohau (E)	4.5 ± 0.8	5.6 ± 0.8	1.7 ± 1.0	0.8 ± 0.2	1.06 ± 0.28	1.87 ± 0.33	0.66 ± 0.09
8902-72	Ohau (E)	3.8 ± 0.5	5.5 ± 0.9	1.6 ± 0.7	0.7 ± 0.1	1.06 ± 0.27	1.69 ± 0.36	0.63 ± 0.10
8902-73	Ohau (E)	3.7 ± 0.4	5.2 ± 1.2	1.4 ± 0.6	0.7 ± 0.2	0.84 ± 0.27	1.57 ± 0.26	0.62 ± 0.11
8902-74	Ohau (E)	3.2 ± 0.4	4.2 ± 2.2	1.0 ± 0.5	0.8 ± 0.4	0.52 ± 0.09	0.89 ± 0.17	0.41 ± 0.02
8902-75	Ohau (E)	2.9 ± 0.4	3.7 ± 2.6	1.0 ± 0.5	0.8 ± 0.6	0.59 ± 0.15	1.14 ± 0.23	0.37 ± 0.04
8902-76	Ohau (E)	2.7 ± 0.5	3.0 ± 3.3	0.9 ± 0.6	0.9 ± 1.0	0.50 ± 0.17	0.95 ± 0.20	0.30 ± 0.04
8902-89	Ohau (E)	3.3 ± 0.4	4.2 ± 1.9	0.6 ± 0.7	0.8 ± 0.4	0.58 ± 0.08	0.73 ± 0.09	0.51 ± 0.03
8902-90	Ohau (E)	3.0 ± 0.4	4.4 ± 1.8	1.1 ± 0.5	0.7 ± 0.3	0.53 ± 0.09	0.82 ± 0.23	0.44 ± 0.02
8902-100	Godley (E)	5.0 ± 0.5	5.4 ± 0.6	1.0 ± 0.5	0.9 ± 0.1	1.43 ± 0.24	2.39 ± 0.14	0.98 ± 0.09
8902-101	Godley (E)	4.6 ± 0.6	5.3 ± 0.6	2.1 ± 0.7	0.9 ± 0.2	1.21 ± 0.23	2.16 ± 0.18	0.89 ± 0.10
8902-102	Godley (E)	4.3 ± 0.5	5.1 ± 0.7	1.8 ± 0.8	0.9 ± 0.2	1.21 ± 0.23	2.16 ± 0.18	0.89 ± 0.10
8902-103	Godley (E)	3.9 ± 0.5	5.0 ± 0.8	1.8 ± 0.7	0.8 ± 0.2	0.99 ± 0.10	1.75 ± 0.27	0.81 ± 0.06
8902-105	Godley (E)	3.6 ± 0.4	4.4 ± 1.5	1.5 ± 0.6	0.8 ± 0.3	0.77 ± 0.04	0.93 ± 0.07	0.74 ± 0.03
8902-106	Godley (E)	3.8 ± 0.4	3.8 ± 2.1	1.3 ± 0.5	1.0 ± 0.6	0.73 ± 0.10	1.16 ± 0.11	0.59 ± 0.05
8902-107	Godley (E)	3.4 ± 0.6	3.7 ± 2.1	1.3 ± 0.6	0.9 ± 0.5	0.59 ± 0.14	1.00 ± 0.28	0.44 ± 0.04
8902-108	Godley (E)	2.9 ± 0.5	3.6 ± 2.1	1.1 ± 0.7	0.8 ± 0.5	0.57 ± 0.08	0.89 ± 0.14	0.48 ± 0.05
8902-109	Godley (E)	3.0 ± 0.4	3.3 ± 2.5	1.0 ± 0.6	0.9 ± 0.7	0.39 ± 0.08	0.59 ± 0.15	0.31 ± 0.04
8902-110	Godley (E)	2.9 ± 0.5	2.7 ± 3.1	0.9 ± 0.5	1.1 ± 1.2	0.23 ± 0.06	0.53 ± 0.13	0.15 ± 0.03
8902-113	Clyde (E)	4.9 ± 0.5	5.2 ± 0.5	0.7 ± 0.6	0.9 ± 0.1	1.47 ± 0.19	2.26 ± 0.12	0.87 ± 0.12
8902-114	Clyde (E)	4.4 ± 0.6	5.1 ± 0.6	2.1 ± 0.6	0.9 ± 0.2	1.33 ± 0.30	2.05 ± 0.19	0.73 ± 0.05
8902-115	Clyde (E)	4.1 ± 0.5	4.9 ± 0.7	1.9 ± 0.8	0.8 ± 0.2	1.18 ± 0.34	1.91 ± 0.26	0.67 ± 0.07
8902-116	Clyde (E)	3.9 ± 0.5	4.8 ± 0.8	1.7 ± 0.6	0.8 ± 0.2	1.01 ± 0.36	1.70 ± 0.30	0.65 ± 0.10
8902-117	Clyde (E)	3.7 ± 0.4	4.7 ± 0.9	1.5 ± 0.6	0.8 ± 0.2	0.91 ± 0.31	1.61 ± 0.32	0.65 ± 0.11
8902-118	Clyde (E)	3.5 ± 0.4	3.7 ± 1.8	1.4 ± 0.6	0.9 ± 0.5	0.76 ± 0.15	1.17 ± 0.12	0.58 ± 0.04
8902-119	Clyde (E)	3.2 ± 0.4	3.6 ± 2.0	1.3 ± 0.5	0.9 ± 0.5	0.73 ± 0.16	1.16 ± 0.11	0.52 ± 0.03
8902-125	Wilberforce (E)	4.6 ± 0.5	4.9 ± 1.8	1.2 ± 0.5	0.9 ± 0.4	1.45 ± 0.21	2.02 ± 0.09	0.75 ± 0.09
8902-126	Wilberforce (E)	4.5 ± 0.5	4.7 ± 1.9	2.0 ± 0.6	1.0 ± 0.4	1.21 ± 0.29	1.93 ± 0.08	0.68 ± 0.09
8902-127	Wilberforce (E)	3.7 ± 0.5	4.5 ± 1.3	1.8 ± 0.7	0.8 ± 0.3	1.02 ± 0.30	1.76 ± 0.24	0.62 ± 0.09
8902-128	Wilberforce (E)	3.9 ± 0.5	3.6 ± 0.6	1.5 ± 0.6	1.1 ± 0.2	0.65 ± 0.13	1.16 ± 0.27	0.45 ± 0.06
8902-133	Arthur's (E)	4.8 ± 0.6	4.8 ± 0.7	1.2 ± 0.7	1.0 ± 0.2	1.34 ± 0.22	1.92 ± 0.10	0.74 ± 0.06
8902-134	Arthur's (E)	4.7 ± 0.7	4.7 ± 0.9	2.0 ± 0.8	1.0 ± 0.2	1.34 ± 0.22	1.92 ± 0.10	0.74 ± 0.06
RP3	Arthur's (E)	3.3 ± 0.4	3.4 ± 0.7	1.4 ± 0.6	1.0 ± 0.2	0.96 ± 0.21	1.58 ± 0.19	0.44 ± 0.08
RP5	Arthur's (E)	4.7 ± 0.5	4.2 ± 0.9	1.5 ± 0.7	1.1 ± 0.3	0.79 ± 0.15	1.58 ± 0.18	0.60 ± 0.07
RP6	Arthur's (E)	4.6 ± 0.5	4.6 ± 0.7	1.8 ± 0.6	1.0 ± 0.2	1.13 ± 0.20	1.76 ± 0.09	0.68 ± 0.04
8902-153	Lewis (E)	4.4 ± 0.6	3.7 ± 1.2	1.6 ± 0.8	1.2 ± 0.4	0.96 ± 0.22	1.45 ± 0.18	0.48 ± 0.06
8902-155	Lewis (E)	4.3 ± 0.6	3.4 ± 1.4	1.4 ± 0.8	1.3 ± 0.5	0.79 ± 0.18	1.40 ± 0.12	0.43 ± 0.05
8902-156	Lewis (E)	3.9 ± 0.7	3.2 ± 1.5	1.3 ± 0.9	1.2 ± 0.6	0.69 ± 0.18	1.33 ± 0.11	0.43 ± 0.06
8902-157	Lewis (E)	3.8 ± 0.6	3.0 ± 1.6	1.0 ± 0.8	1.3 ± 0.7	0.42 ± 0.07	0.93 ± 0.13	0.33 ± 0.04
8902-158	Lewis (E)	3.3 ± 0.4	2.8 ± 1.8	1.0 ± 0.5	1.2 ± 0.8	0.45 ± 0.08	0.86 ± 0.15	0.31 ± 0.06
8902-159	Lewis (E)	3.1 ± 0.4	2.7 ± 2.0	0.8 ± 0.5	1.2 ± 0.9	0.29 ± 0.05	0.56 ± 0.12	0.23 ± 0.02
8902-51	Haast (W)				2.4 ± 1.1	0.61 ± 0.24	1.64 ± 0.14	0.20 ± 0.13
8902-52	Haast (W)				1.5 ± 0.4	0.52 ± 0.22	1.61 ± 0.13	0.18 ± 0.10
8902-54	Haast (W)				1.2 ± 0.3	0.72 ± 0.21	1.80 ± 0.19	0.31 ± 0.13
8326-2	Haast (W)				2.0 ± 0.8	0.65 ± 0.38	1.29 ± 0.14	0.05 ± 0.05
8326-6	Haast (W)				1.8 ± 0.4	0.70 ± 0.38	1.52 ± 0.14	0.10 ± 0.08
8326-9	Haast (W)				2.2 ± 0.5	0.61 ± 0.24	1.64 ± 0.14	0.20 ± 0.13
8326-82	Haast (W)				1.3 ± 0.4	0.52 ± 0.22	1.61 ± 0.13	0.18 ± 0.10
8902-66	Paringa (W)				4.4 ± 2.4	0.61 ± 0.34	1.31 ± 0.11	0.04 ± 0.01
8902-68	Paringa (W)				2.8 ± 1.0	1.13 ± 0.25	1.83 ± 0.17	0.27 ± 0.14
8902-79	Copland (W)				14.6 ± 10.0	1.10 ± 0.31	1.94 ± 0.14	0.31 ± 0.17
8902-80	Copland (W)				9.0 ± 4.4	1.28 ± 0.38	2.09 ± 0.19	0.51 ± 0.23
8902-81	Copland (W)				2.5 ± 0.8	1.59 ± 0.42	2.38 ± 0.22	0.72 ± 0.18
8902-82	Copland (W)				3.1 ± 2.0	1.67 ± 0.39	2.57 ± 0.26	0.90 ± 0.14
CW21	Fox-Franz Josef (W)				10.9 ± 5.7	1.04 ± 0.14	1.85 ± 0.17	0.39 ± 0.18
FOX4	Fox-Franz Josef (W)				6.4 ± 1.9	1.56 ± 0.44	2.35 ± 0.39	0.81 ± 0.32
CG3	Fox-Franz Josef (W)				7.8 ± 3.0	0.49 ± 0.23	1.55 ± 0.34	0.22 ± 0.08
CG13	Fox-Franz Josef (W)				7.1 ± 2.4	1.47 ± 0.52	2.26 ± 0.26	0.78 ± 0.30
8902-93	Whataroa (W)				9.5 ± 2.4	0.91 ± 0.30	1.69 ± 0.23	0.25 ± 0.13
8902-94	Whataroa (W)				3.9 ± 1.2	1.31 ± 0.35	1.95 ± 0.27	0.44 ± 0.16
8902-95	Whataroa (W)				3.8 ± 0.8	1.31 ± 0.35	1.95 ± 0.27	0.44 ± 0.16
8902-96	Whataroa (W)				2.3 ± 0.6	1.52 ± 0.22	2.30 ± 0.21	0.71 ± 0.21
8902-121	Whitcombe (W)				6.5 ± 2.2	0.86 ± 0.22	1.53 ± 0.23	0.20 ± 0.11
8902-122	Whitcombe (W)				7.1 ± 3.7	0.87 ± 0.22	1.62 ± 0.21	0.29 ± 0.13
8902-123	Whitcombe (W)				2.6 ± 1.3	1.06 ± 0.30	1.78 ± 0.19	0.47 ± 0.21
8902-129	Arthur's (W)				5.0 ± 3.0	0.46 ± 0.20	1.40 ± 0.02	0.20 ± 0.06
8902-130	Arthur's (W)				1.9 ± 0.4	0.62 ± 0.25	1.55 ± 0.18	0.23 ± 0.06
RP11	Arthur's (W)				3.2 ± 0.8	0.62 ± 0.25	1.55 ± 0.18	0.23 ± 0.06
RP14	Arthur's (W)				2.0 ± 0.9	0.46 ± 0.20	1.40 ± 0.02	0.20 ± 0.06
8902-135	Robinson (W)				3.4 ± 3.4	0.83 ± 0.10	1.49 ± 0.04	0.34 ± 0.04
8902-137	Robinson (W)				1.5 ± 0.7	1.01 ± 0.14	1.55 ± 0.07	0.43 ± 0.08

Table 1 ctd

Sample No.	Transect	Rock Uplift (km) ± 2σ	Uplift Age (Ma ago) ± 2σ	Tectonic Uplift (km) ± 2σ	Rock Uplift Rate (km/Ma) ± 2σ	Mean Surface Elevation (km) ± 2σ	Summit Elevation (km) ± 2σ	Valley Elevation (km) ± 2σ
8902-138	Robinson (W)				1.2 ± 0.3	1.01 ± 0.14	1.55 ± 0.07	0.43 ± 0.08
8902-140	Lewis (W)				4.5 ± 1.8	0.73 ± 0.17	1.42 ± 0.10	0.49 ± 0.06
8902-141	Lewis (W)				3.1 ± 0.6	0.73 ± 0.17	1.42 ± 0.10	0.49 ± 0.06
8902-142	Lewis (W)				2.4 ± 1.1	0.85 ± 0.22	1.40 ± 0.12	0.50 ± 0.03
8902-143	Lewis (W)				4.1 ± 2.0	0.85 ± 0.22	1.40 ± 0.12	0.50 ± 0.03
8902-144	Lewis (W)				2.6 ± 0.5	0.81 ± 0.16	1.46 ± 0.12	0.52 ± 0.05
8902-145	Lewis (W)				1.7 ± 0.4	0.81 ± 0.16	1.46 ± 0.12	0.52 ± 0.05

(i) All uplift estimates are taken from Tippett and Kamp (in press) and Kamp and Tippett (submitted). (ii) Fission track data used in uplift calculations for samples 8326-2, -3, -6, -9, -82; CW21; FOX4; CG3, 13; RP3, 5, 6, 11, 14 are taken from Kamp et al. (1989). (iii) Grid references for sample locations are reported in Kamp et al. (1989) and Tippett and Kamp (in press). (iv) (E) refers to a sample taken from a transect to the east of the Main Divide, (W) refers to a sample taken from a transect to the west of the Main Divide. (v) The rock uplift rates for samples from the east of the Main Divide are late Cenozoic mean rock uplift rates (that is, rock uplift amount divided by uplift age). (vi) The rock uplift rates for samples from the west of the Main Divide are derived from reset zircon ages. Most rock uplift rates quoted for these samples will be underestimates of contemporary rates as they necessarily average the periods of a few million years since the zircon samples were uplifted through the closure temperature (see Tippett and Kamp, in press). The amount of rock uplift is unable to be calculated for these samples.

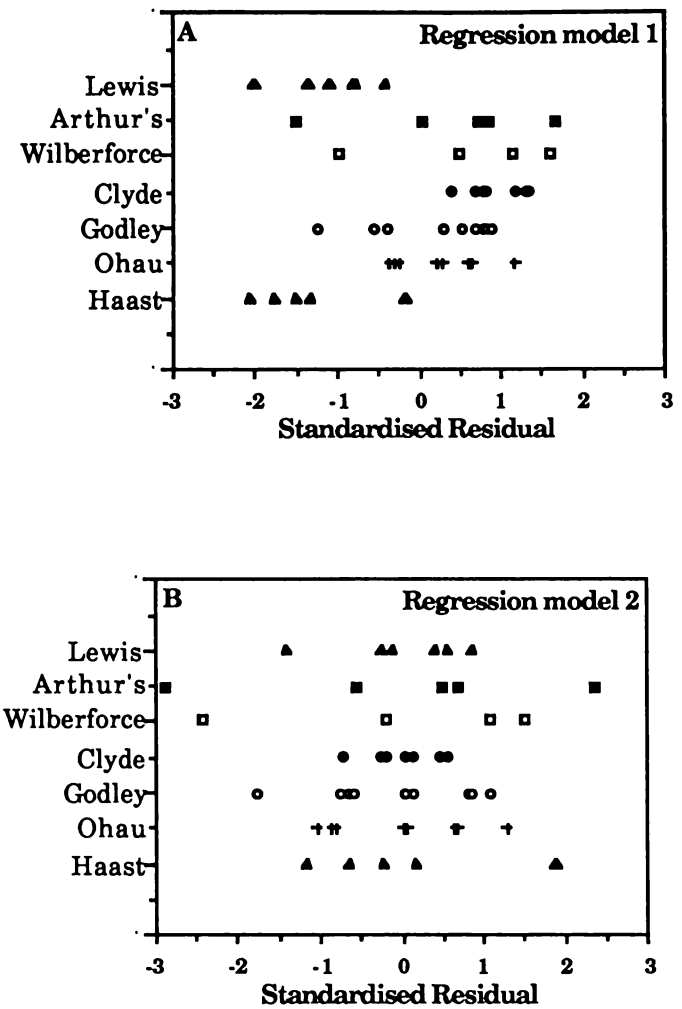


Fig. 4. Residual plots for the regression of mean surface elevation on rock uplift for transects located to the east of the Main Divide: (A) Residuals for regression on pooled data; (B) Residuals for regression using dummy variables.

Regression models

Linear regression has been used to analyse the relations between the variables identified earlier. Rock uplift, uplift age, tectonic uplift, and rock uplift rate, are regarded as the independent (x) variables, the variation within which causes variation in the dependent (y) geomorphic variables of mean surface/summit/valley elevations. We start with simple regression models and proceed sequentially to more complex models. There are three possible models to be considered in this study:

Model (1): Regression of each geomorphic variable on each uplift variable using all points in a pooled manner. This yields a single regression equation.

Model (2): This is a more complex model in which the data set consists of two or more distinct subsets. The qualitative factor of the transect to which each datum belongs is hypothesised to affect the relationship. The different transects are represented by dummy variables in an additive manner to account for the possible different signals contributed by different transects. This model yields equations that differ in response (constant term) between transects, but which have the same regression slope (coefficient).

Model (3): This is an even more complex model that adds interaction terms to model 2. Regression equations yielded by this model differ in both response and slope between transects and are the same equations that would be produced if the data from each transect had been analysed separately.

To choose the most appropriate regression model, we use extra sums of squares tests to establish whether a more complex model provides a significant increase in the sums of squares explained by regression over the simpler model(s) (e.g. Draper and Smith, 1981).

Example: regression of mean surface elevation on rock uplift

Model 1: $y = b_0 + b_1x$

mean surface elevation = -0.67 + 0.39 rock uplift

The regression is significant at the $\alpha = 0.001$ level. The residuals are unsatisfactory as they are clumped by transect (Fig. 4A). Now we move on to model 2, which uses dummy variables to represent the different transects.

Table 2: Analysis of variance for regressions of mean surface elevation on rock uplift for locations to the east of the Main Divide.

Regression Model	Source	DF	SS	MS	P
Model 1	Regression	1	2.95	2.95	0.000
	Error	43	1.75	0.041	
	Total	44	4.70		
Model 2	Regression	7	3.92	0.560	0.000
	Error	37	0.78	0.021	
	Total	44	4.70		
Model 3	Regression	13	4.11	0.316	0.000
	Error	31	0.59	0.019	
	Total	44	4.70		

DF is degrees of freedom; SS is sums of squares; MS is mean square error; P is significance.

There are 7 transects so that 6 dummy variables (z_1 to z_6) appear in the model (as the 7th is defined in terms of the other 6).

Model 2: $y = b_0 + b_1x + a_1z_1 + ...+ g_1z_6$

There are 7 equations (1 for each transect) that differ in response but have the same slope.

e.g. Haast: mean surface elevation = -1.07 + 0.42 rock uplift + $0.79z_1$ + $0.86z_2$ + $0.80z_3$ + $0.72z_4$ + $0.60z_5$ + $0.41z_6$

The full set of equations is given in Appendix 1.

The regression is significant at the $\alpha = 0.001$ level. We now test if model 2 provides significant extra sums of squares explained by regression over model 1. We test the general proposition that H_0: extra sums of squares not significant versus H_1: H_0 not true, by using an F-test:

$$Fcalc = \frac{(SS_2\text{-}SS_1)/(dfSS_2\text{-}dfSS_1)}{s^2}$$

where $(SS_2\text{-}SS_1)$ is extra sums of squares provided by the new model;
$(dfSS_2\text{-}dfSS_1)$ is degrees of freedom associated with introduction of the additional terms; and
s^2 is the mean square of the error.

When Fcalc<Fcrit, H_0 cannot be rejected, hence the extra sums of squares are not significant and we retain model 1. If Fcalc>Fcrit we reject H_0, and hence the extra sums of squares provided by model 2 are significant. We are testing H_0: $a_1=c_1=d_1=e_1=f_1=g_1$ versus H_1: H_0 not true; that is, for equation 1, H_0: 0.79=0.86=0.80=0.73=0.60=0.41=0 versus H_1: H_0 not true. The extra sums of squares for a_1,c_1,d_1,e_1,f_1,g_1 is given by $SS(a_1,c_1,d_1,e_1,f_1,g_1,b_1 \mid b_0) - SS(b_1 \mid b_0)$ = 3.92 - 2.95 = 0.97 (Table 2). The appropriate F statistic is F = (0.97/6)/0.0209 = 7.74 which exceeds $F_{crit}(6,37,0.95) = 2.38$.

H_0 is rejected and we conclude that model 2 provides significant additional sums of squares explanation by regression. Hence, model 2 is preferred over model 1. Model 2 shows no lack of fit which suggests that the model is adequate and the relationship linear, and r^2 has increased from 0.63 to 0.84. Inspection of residuals shows that the clustering of residuals by transect has disappeared (Fig. 4B).

Table 3: Extra sums of squares tests for regression analysis of geomorphic variables on rock uplift for locations to the east of the Main Divide.

	Model 1 → Model 2	Model 2 → Model 3
Surface elevation	Fcalc=7.74>Fcrit=2.38	Fcalc=1.67<Fcrit=2.42
Summit elevation	Fcalc=3.86>Fcrit=2.38	Fcalc=1.85<Fcrit=2.42
Valley elevation	Fcalc=13.70>Fcrit=2.38	Fcalc=1.98<Fcrit=2.42

(i) F-test at α=0.05 level. (ii) Model 1 uses pooled data set; model 2 introduces dummy variables; model 3 introduces interaction terms. (iii) All regressions significant at α=0.001 level.

Table 4: Relationships between geomorphic variables and rock uplift for locations to the east of the Main Divide.

Equation	$b_1 \pm 2\sigma$	r^2
Surface elevation = b_0 + 0.42 rock uplift	0.42 ± 0.07	0.84
Summit elevation = b_0 + 0.67 rock uplift	0.67 ± 0.12	0.81
Valley elevation = b_0 + 0.25 rock uplift	0.25 ± 0.04	0.83
Relief = b_0 + 0.52 rock uplift		
Denudation = b_0 + 0.58 rock uplift		
Summit denudation = b_0 + 0.33 rock uplift		
Valley denudation = b_0 + 0.75 rock uplift		

It is of interest now to examine the extra sums of squares provided by model 3 over model 2.

Model 3: $y = b_0 + b_1x_1 + a_1z_1 + a_2z_1 + \ldots\ldots\ldots + g_1z_6 + g_2z_6x$

Each transect has a different equation differing in response and slope.

e.g. Haast: mean surface elevation = $-0.31 + 0.25$ rock uplift $- 0.81z_1 + 0.21z_1x + 0.52z_2 - 0.04z_2x - 1.08z_3 + 0.34z_3x - 0.51z_4 + 0.23z_4x - 0.81z_5 + 0.27z_5x + 0.11z_6x$

For the sake of brevity the remaining equations are not given. The regression is significant at the $\alpha = 0.001$ level.

The extra sums of squares for a_2,c_2,d_2,e_2,f_2,g_2 are given by $SS(a_1,c_1,d_1,e_1,f_1,g_1,a_2,c_2,d_2,e_2,f_2,g_2,b_1 \mid b_0) - SS(a_1,c_1,d_1,e_1,f_1,g_1,b_1 \mid b_0) = 4.11 - 3.92 = 0.19$ (Table 2). The appropriate F statistic is $F = (0.19/6)/0.019 = 1.67$ which is less than $F_{crit}(6,31,0.95) = 2.42$. H_0 cannot be rejected so we conclude that model 3 does not provide significant additional explained sums of squares, and model 2 is retained.

RESULTS: REGRESSION OF GEOMORPHIC VARIABLES ON ROCK UPLIFT AND UPLIFT AGE (EAST OF MAIN DIVIDE)

Regressions on rock uplift

Table 3 shows the results of extra sums of squares tests for regression analyses of the geomorphic variables on rock uplift. Model 2 is preferred for all regressions. The relationships between mean surface/summit/valley elevation and rock uplift are given in general equation form in Table 4, and the full sets of equations in Appendix 1. Also given in Table 4 are equations obtained by subtraction that relate relief (summit elevation - valley elevation), denudation (rock uplift - mean surface elevation), summit denudation (rock uplift - summit elevation), and valley denudation (rock uplift - valley elevation), to rock uplift. These variables are of use (below) in examining landscape evolution. Subtraction is an appropriate manipulation when ordinary least squares regression has been used (Williams and Troutman, 1987).

Regressions on uplift age

The estimates of rock uplift are directly estimated values, whereas uplift age estimates have been derived by prediction from a linear trend

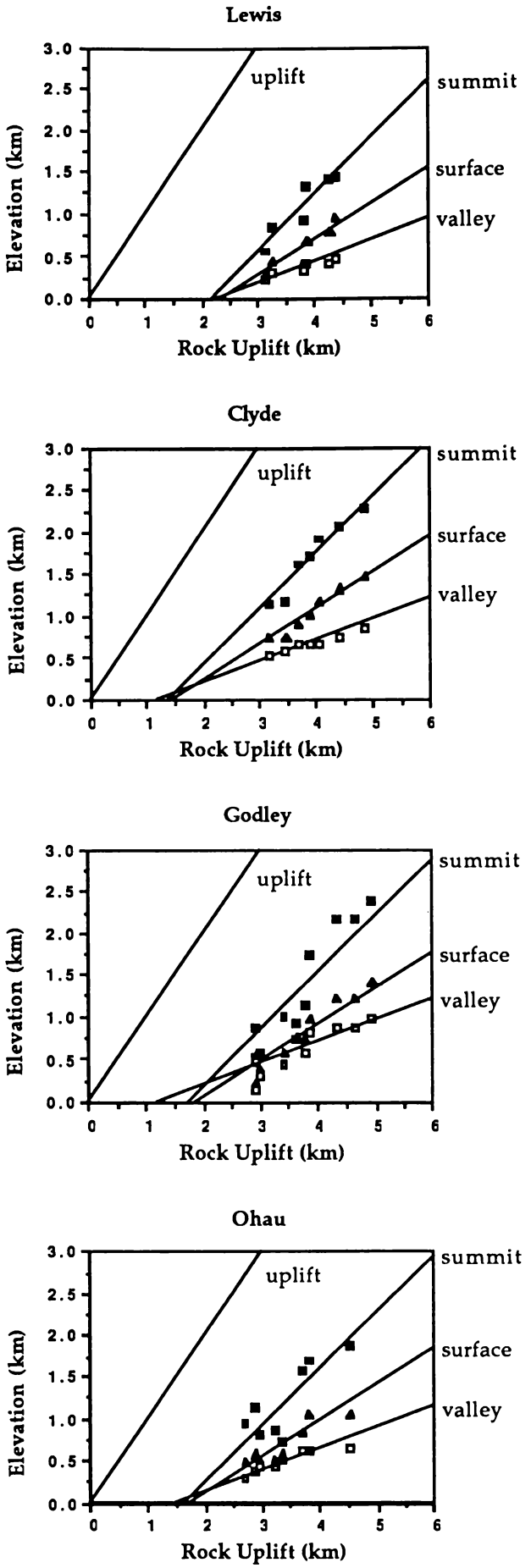


Fig. 5. Bivariate scatter plots of surface, summit, and valley elevation versus rock uplift for selected transects located to the east of the Main Divide in the Southern Alps. Regression lines are those reported in Appendix 1.

surface model (Tippett and Kamp, in press), as there are no direct measurements of uplift age for the sample points for which rock uplift estimates exist. Although the uplift age estimates are therefore to some extent a function of the type of model fitted to the data, it is important to analyse the relations between uplift age and geomorphology, in a manner identical to that for rock uplift. The results of the extra sums of squares tests for these regression analyses are reported in Table 5.

Model 2 is preferred for the regression of both rock uplift and summit elevation on uplift age. Model 3 provides very marginally significant extra sums of squares explained for mean surface elevation on uplift age, and we conservatively retain model 2. Also, as rock uplift and uplift age are so closely related, it is difficult to see why the regression models should not be similar to regressions on rock uplift. Model 2 is also preferred for the regression of valley elevation on uplift age for this reason. Table 6 presents the general equations for the regressions on uplift age, and the equations (obtained by subtraction) that relate uplift age to relief, denudation, and summit and valley denudation.

DISCUSSION: AREA TO THE EAST OF THE MAIN DIVIDE

Description of regressions

Rock uplift accounts for 84% of the variation in mean surface elevation. The repetition of the pattern of the relationship as indicated by the bivariate plots for all transects, is good evidence that there is a strong and consistent association between elevation and rock uplift. The regression slope of 0.4 ± 0.1 (2σ) km/km represents the amount of elevation increase with respect to the amount of rock uplift (Fig. 5). Responses range from -0.6 to -1.1 km, and for all transects are significantly different from zero, implying that there are significant x-intercepts that range from 1.4-2.6 km. There are no areas in the S. Alps that have had less than ~3 km of rock uplift, and all areas have been uplifted more recently than ~3 Ma ago (Tippett and Kamp, in press). Therefore the x-intercepts of 1.4-2.6 km are not physically meaningful in a spatial sense, but instead describe a temporal lag between the start of rock uplift and the start of mean surface uplift.

Uplift age accounts for 83% of the variation in rock uplift. The regression slope of 0.8 ± 0.1 km/Ma represents the rock uplift rate of the sample points (Table 6 and Fig. 6). There is a systematic increase in the

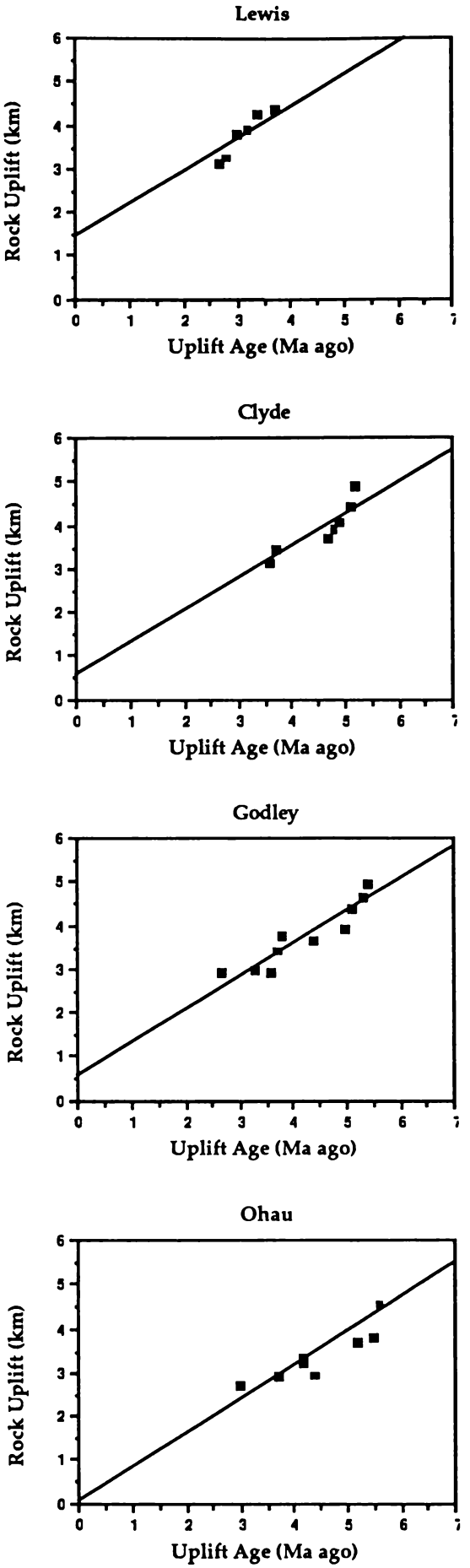


Fig. 6. Bivariate scatter plots of rock uplift versus uplift age for selected transects located to the east of the Main Divide in the Southern Alps. Regression lines are those reported in Appendix 1.

Table 5: Extra sums of squares tests for regression analysis of rock uplift/geomorphic variables on uplift age for locations to the east of the Main Divide.

	Model 1 → Model 2	Model 2 → Model 3
Rock uplift	Fcalc=13.27>Fcrit=2.38	Fcalc=1.93<Fcrit=2.42
Surface elevation	Fcalc=18.90>Fcrit=2.38	Fcalc=2.44>Fcrit=2.42
Summit elevation	Fcalc=11.83>Fcrit=2.38	Fcalc=2.38<Fcrit=2.42
Valley elevation	Fcalc=29.71>Fcrit=2.38	Fcalc=8.17>Fcrit=2.42

(i) F-test at α=0.05 level. (ii) Model 1 uses pooled data set; model 2 introduces dummy variables; model 3 introduces interaction terms. (iii) All regressions significant at α=0.001 level.

Table 6: Relationships between rock uplift/geomorphic variables and uplift age for locations to the east of the Main Divide.

Equation	$b_1 \pm 2\sigma$	r^2
Rock uplift = b_0 + 0.75 uplift age	0.75 ± 0.13	0.83
Surface elevation = b_0 + 0.36 uplift age	0.36 ± 0.06	0.86
Summit elevation = b_0 + 0.57 uplift age	0.57 ± 0.10	0.83
Valley elevation = b_0 + 0.22 uplift age	0.22 ± 0.03	0.90
Relief = b_0 + 0.35 uplift age		
Denudation = b_0 + 0.39 uplift age		
Summit denudation = b_0 + 0.18 uplift age		
Valley denudation = b_0 + 0.53 uplift age		

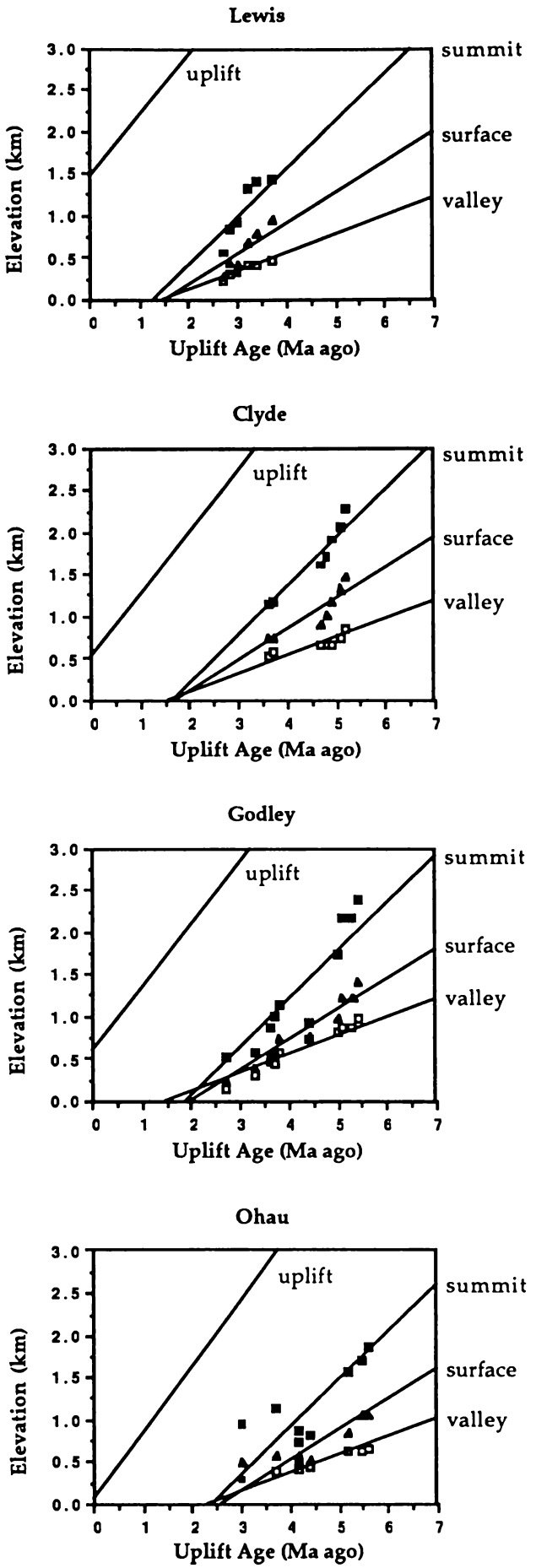


Fig. 7. Bivariate scatter plots of surface, summit, and valley elevation versus uplift age for selected transects located to the east of the Main Divide in the Southern Alps. Regression lines are those reported in Appendix 1.

elevation response from Haast in the south (0.1 km) to Lewis in the north (1.5 km) (Appendix 1). This is a function of the fact that all the transects have been uplifted by similar amounts, but the northern transects have younger uplift ages than those in the south (Table 1).

Uplift age accounts for 86% of the variation in mean surface elevation. The regression slope of 0.4 ± 0.1 km/Ma represents the rate of increase in mean surface elevation with respect to rock uplift (Fig. 7). Response terms range from -0.5 to -1.3 km (Appendix 1) and for all transects are significantly different from zero, implying that there are significant x-intercepts that range from 1.3 to 3.7 Ma. These intercepts are interpreted in the same way as for the regressions of mean surface elevation on rock uplift discussed above; that is, they describe the lag between the start of rock uplift and the start of mean surface uplift.

The regression equations describing the relationships between summit/valley elevation and rock uplift/uplift age are given in Appendix 1, and bivariate line plots are shown in Figs 5 and 7. For regressions on rock uplift, the regression slope for summit elevation is steeper than that for mean surface elevation and the response lower, whereas the regression slope for valley elevation is lower and the response higher; however, the x-intercept is the same for the three variables (Appendix 1). The common x-intercepts suggest that it is they that are physically meaningful rather than the response terms, an important constraint on interpretation of the data (below). Both relief and elevation increase with rock uplift. The significant x-intercepts for regressions of summit elevation and valley elevation on rock uplift/uplift age (Appendix 1), of 1.2-2.5 km and 1.3-3.8 Ma, respectively, again indicate the temporal lag between the start of rock uplift and the start of mean surface uplift.

Substitution of space for time

The data from which the regression equations and bivariate plots have been constructed have different spatial locations, which means that we can legitimately infer conclusions concerning the spatial point to point association between geomorphology and uplift. We suggest that in this situation it is possible to substitute space for time, by assuming that probabilities of sampling a property of the landscape through time and over space are interchangeable. For the S. Alps we have derived the spatial pattern of the age of uplift initiation (Fig. 12, Tippett and Kamp, in press),

which allows a space for time substitution to be made. Uplift propagated southeastward from the Alpine Fault across the trend of South Island, implying that a spatial sequence of forms from the southeast to the northwest will describe an evolutionary sequence of forms through time at a particular site.

Landscape evolution east of the Main Divide

With space for time substitution, the equations of Tables 4 and 6 and plots of Figs 5 and 7 can be seen as evolutionary sequences of topography with respect to increasing uplift and time. The x-intercepts represent the amount of rock uplift that had taken place, or the amount of time since rock uplift began, before topography began to develop. The slopes of the relationships represent the subsequent rate of development of topography per kilometre or per million years of rock uplift.

The plots of Figs 5 and 7 show several features of interest. Mountain elevation is directly proportional to the amount of rock uplift and uplift age. However, topography did not start to develop significantly until 1.4-2.6 km and 1.3-3.7 Ma of rock uplift (depending on transect), which means that the amount and rate of denudation initially matched the amount and rate of rock uplift. The subsequent increase in mean surfce elevation was then linear with respect to both the amount of rock uplift and time, with values of 0.4 km/km, and 0.4 km/Ma; more than half of the amount of rock uplift has been removed subsequently by erosion. Once topographic development had started, the summits rose at 0.7 km/km of rock uplift, and the valley floors increased in elevation at 0.3 km/km of rock uplift. One third of the crustal column uplifted has been lost off the top of the mountains, while denudation of the valleys has involved removing three quarters of the rock column. The increase in mean surface elevation has taken place at 0.4 km/Ma compared with the rate of rock uplift at 0.8 km/Ma. The summits, mean surface, and valleys have increased in elevation at different rates (0.6 km/Ma, 0.4 km/Ma, and 0.2 km/Ma respectively), with corresponding rates of denudation of 0.2 km/Ma, 0.4 km/Ma and 0.6 km/Ma. Both elevation and relative relief have consequently increased over time.

The diverging slopes of the regression lines relating mean surface/summit/valley elevation to rock uplift show that as rock uplift has proceeded, the form of the landscape has changed and relief has increased because the elevation differences between summits, mean surface, and

valley floors have increased. The form of the landscape is therefore dependent on the age of uplift, the amount of rock uplift, and the distribution of erosional downcutting across the landscape. The elevation and form of the landscape can be related to stages of development defined by the age and amount of uplift. The mountains to the east of the Main Divide have evolved in form over time.

All transects have exhibited similar late Cenozoic mean rock uplift rates of 0.8-1.0 km/Ma, and within any one transect there is minimal variation in the rate (Table 1). Therefore the regression of geomorphic variables on late Cenozoic mean rock uplift rate yielded equations with low r^2 values (0.25 to 0.36) indicating a poor degree of association. The linear nature of the relationship between rock uplift and uplift age suggests that contemporary rock uplift rates probably equal 0.8-1.0 km/Ma (Table 1 and Fig. 6); that is, the rates are similar to the late Cenozoic mean rock uplift rates. Mountain elevation therefore shows little relationship to either late Cenozoic mean rates of rock uplift or contemporary rates of rock uplift; this implies that the mountain elevations are not in a stable equilibrium with respect to rock uplift rate, but are related to the age and amount of rock uplift as already concluded.

The rejection of a single relationship between uplift and geomorphic expression for the S. Alps, and the variation in geomorphic expression remaining unexplained by uplift, imply the existence of other factors that contribute to variation in geomorphic expression. However, although there are inter-transect differences in response, regression slopes relating elevation to uplift are the same between transects. Therefore once the response level is reached, the interaction between uplift and geomorphology is universal. The regression x-intercepts have been identified (above) as being physically meaningful. We need therefore to be able to explain the inter-transect differences in response, the significant x-intercepts for all transects, and the similar regression slope between transects. Possible factors include inter-transect differences in climate, in initial rock uplift rate, and in lithology.

Inter-transect differences in climate cannot explain satisfactorily the variation in the uplift/geomorphology relationship between transects, as regression slopes for all transects are the same. If climatic variations affected response levels, then the same variations maintained over time would also be expected to produce differences in regression slopes, which

has been demonstrated not to be the case. For instance, a stormier climate may lead to increased erosion and a more subdued topography yielding a shallower regression slope.

Although all transects exhibit a rock uplift rate (regression slope) of 0.8 km/Ma, responses are all positive and increase from south to north (Fig. 6) which gives rise to the recognition that the late Cenozoic mean rock uplift rates (~1 km/Ma) exceed slightly the 0.8 km/Ma value. The northward increase in response may explain the decreasing time lag between the start of rock uplift and the start of mean surface uplift from the Haast transect in the south (3.7 Ma) northward through to the Lewis (1.3 Ma) transect (Appendix 1). The positive responses suggest that there was probably an initial period of slightly more rapid rock uplift of >1 km/Ma. This higher rock uplift rate lasted until mean surface uplift started, after which point the rock uplift rate reduced to 0.8 km/Ma.

Present differences in rock type between the transects are probably minimal as the rock type is shattered greywacke, which Augustinus (1988) has demonstrated is almost uniform in both intact strength and resistance to erosion. However, a Tertiary cover rock sequence deposited over the greywacke basement between the late Eocene and mid-Miocene, would have been initially stripped after rock uplift began. The cover rocks were sedimentary rocks of limited depth of burial and low mass strength, as indicated by surviving outcrops. It is probable therefore that the cover rocks would have been stripped easily from the landscape and would not have formed appreciable topography. Only when the more erodible greywacke was subsequently exposed would topography have started to form (i.e. would mean surface uplift have started). Remnants of the cover rocks are preserved in fault-angle depressions in the eastern parts of the S. Alps, and along the margins of the Canterbury Plains. The full extent of the Tertiary transgression is not known, but Stevens and Suggate (1978) and Field and Browne et al. (1989) show that marine depositional environments probably covered most of the present site of the S. Alps in the late Oligocene.

Variations in the original thickness of the cover rock succession would therefore influence regression response levels but not regression slopes. The regular regression slope is controlled by the nature of the consistent interaction between rock uplift and the resistance of greywacke to erosion. This assists in explaining why mean surface uplift started only after 1.4-2.6 km and 1.3-3.7 Ma of rock uplift (depending on transect), and

then increased at a linear rate (0.4 km/Ma) that was common to all transects. The higher initial rate of erosion would have led to a higher initial rate of rock uplift (>1 km/Ma) by isostatic rebound, particularly over the northern transects where the cover rock succession may have been thicker, an idea supported by the positive responses of regression of rock uplift on uplift age. The rock uplift rate decreased to 0.8 km/Ma when greywacke was exposed, as the denudation rate was reduced thereby reducing the rate of isostatic uplift.

The hypothesis that the varying thicknesses of the Cenozoic succession influenced regression response levels and x-intercept values is supported by the thicknesses of the cover rock succession that remain (Gair, 1978; Gregg, 1978). Near the Lewis transect, the preserved thickness of the Cenozoic succession is >1.4 km. To the south the thickness reduces to >0.8 km (Arthur's), >0.6 km (Wilberforce), and >0.3 km (Clyde). Further to the southwest, thicknesses increase to >0.7 km (Godley) and >0.6 km (Ohau). The succession thicknesses are minima due to late Cenozoic erosion. The pattern of a thick Cenozoic succession at Lewis, thinning towards the southwest, and then thickening further to the south, mirrors the trend of the x-intercept of mean surface elevation versus rock uplift between the Lewis and the Ohau transects (Appendix 1 and Fig. 5). The larger x-intercept of the Haast transect appears to be unrelated however to the thickness of Cenozoic cover; it may be a function of the difference between the basement lithologies of schist (which underlies the Haast transect) and greywacke (which underlies the remaining transects), which is not significant enough to alter the regular regression slope between transects but is manifest in the response value.

The significant x-intercepts and differences in response between transects can therefore be seen as a result of the varying thicknesses of cover rocks, and increased initial rock uplift rates in response to rapid denudation. The regular regression slope on the other hand is the result of the consistent nature of the interaction between rock uplift and the erodibility of greywacke.

REGRESSION OF GEOMORPHIC VARIABLES ON TECTONIC UPLIFT (EAST OF THE MAIN DIVIDE)

Only tectonic uplift can contribute to a rise in mean surface elevation. However, even under pure isostatic uplift, summits and uneroded parts of

Table 7: Relationships between geomorphic variables and tectonic uplift for locations to the east of the Main Divide.

Equation	$b_1 \pm 2\sigma$	r^2
Surface elevation = -0.36 + 0.87 tectonic uplift	0.87 ± 0.05	0.96
Summit elevation = -0.38 + 1.29 tectonic uplift	1.29 ± 0.12	0.92
Valley elevation = -0.07 + 0.45 tectonic uplift	0.45 ± 0.08	0.74

Table 8: Extra sums of squares tests for regression analysis of geomorphic variables on uplift rate for locations to the west of the Main Divide.

	Model 1 → Model 2	Model 2 → Model 3
Surface elevation	Fcalc=12.66>Fcrit=2.31	Fcalc=0.54<Fcrit=2.48
Summit elevation	Fcalc=14.95>Fcrit=2.31	Fcalc=0.67<Fcrit=2.48
Valley elevation	Fcalc=13.75>Fcrit=2.31	Fcalc=0.45<Fcrit=2.48

(i) F-test at α=0.05 level. (ii) Model 1 uses pooled data set; model 2 introduces dummy variables; model 3 introduces interaction terms. (iii) All regressions significant at α=0.001 level.

Table 9: Relationships between geomorphic variables and rock uplift rate for locations to the west of the Main Divide.

Equation	$b_1 \pm 2\sigma$	r^2
Surface elevation = b_0 - 0.056 rock uplift rate	0.056 ± 0.027	0.80
Summit elevation = b_0 - 0.054 rock uplift rate	0.054 ± 0.025	0.83
Valley elevation = b_0 - 0.046 rock uplift rate	0.046 ± 0.018	0.81

the landscape can rise substantially, although the mean surface elevation decreases (see England and Molnar, 1990, for discussion). The mean surface elevation of the S. Alps, which has developed from sea level, indicates that there is a major component of tectonic uplift in South Island.

As the calculation of the amount of tectonic uplift for the S. Alps involves the use of mean surface elevation, regression with geomorphic variables will create self-correlations. However here we are not so much interested in r^2 values, but in the parameters of the regression equations. Model 1 is preferred for the regressions (Table 7), because the use of mean surface elevation in calculating tectonic uplift has eliminated inter-transect differences in response. Of most significance are the slopes of the relationships. Once topography started to develop, the rate of increase in elevation of the summits exceeded the amount of tectonic uplift (by a factor of 1.3); this 'excess' is the result of isostatic uplift that has raised the summits above the elevation contributed by tectonic uplift alone. This is in contrast to mean surface elevation, which has increased as a proportion (0.9) of the tectonic uplift since mean surface uplift started; indeed, it would be disturbing if this were not the case.

The important conclusions to be drawn are that both tectonic and isostatic uplift are required to explain the height of the summits; and that a small proportion of the tectonic uplift is lost by erosion during mean surface uplift.

REGRESSION OF GEOMORPHIC VARIABLES ON ROCK UPLIFT RATE (WEST OF THE MAIN DIVIDE)

Table 8 shows the results of extra sums of squares tests for regression analyses of the geomorphic variables on rock uplift rate for west of the Main Divide. Model 2 is preferred for all regressions. The relationships between mean surface/summit/valley elevation and rock uplift rate are given in general equation form in Table 9.

Regression of elevation on rock uplift rate and the dummy variables yields equations that differ in response between transects but have the same regression slope (Appendix 1), and in this respect are similar to the regressions for the area east of the Main Divide. Rock uplift rate accounts for 80% of the variation in mean surface elevation. The regression slope of -0.06 ± 0.03 (2σ) Ma represents the amount of elevation decrease with respect

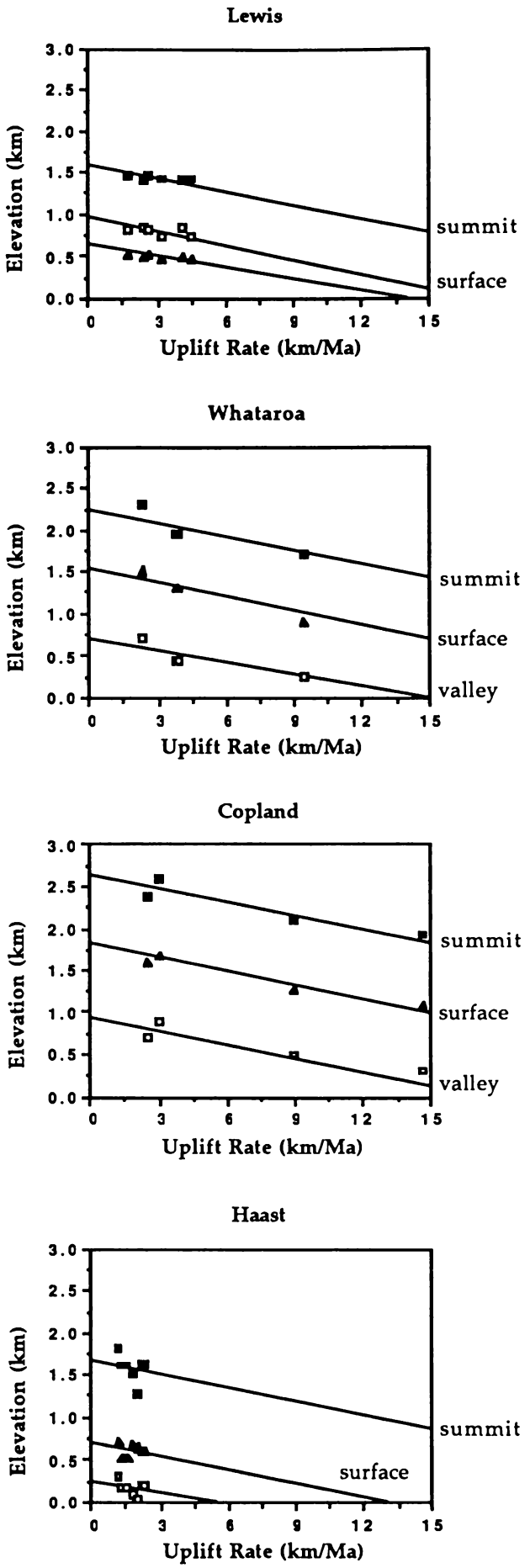


Fig. 8. Bivariate scatter plots of surface, summit, and valley elevation versus uplift rate for selected transects located to the west of the Main Divide in the Southern Alps. Regression lines are those reported in Appendix 1.

to increasing rock uplift rate (Table 9 and Fig. 8). The slopes for mean surface/summit/valley elevation are statistically the same (Table 9), but responses differ.

The high r^2 values (0.80-0.83) for the regression of elevation on rock uplift rate west of the Main Divide contrast with the poor relationship (r^2=0.25-0.36) for the regression of elevation on rock uplift rate for the area east of the Main Divide. Although regression slopes are uniform between transects, responses differ and therefore for any given rock uplift rate the elevation is different for different transects for the area west of the Main Divide (Fig. 8). The elevation response increases from the north and south to reach a maximum in the central region. The reason for this is the variation in rock uplift rate between transects. Fig. 8 shows that the northern and southern transects have rock uplift rates in the order of 1-4 km/Ma and mean surface elevation responses of 0.75-1.0 km. The transects in the central parts of the western Alps however have rock uplift rates of up to 8-10 km/Ma and mean surface elevation responses of 1.5-2.0 km. The transects with higher rock uplift rates also exhibit greater relief. The observed dependence of elevation on rock uplift rate implies that the mountains to the west of the Main Divide are in a stable equilibrium with respect to rock uplift rate. There is a balance between the rates of rock uplift and erosion, a conclusion reached by Koons (1989) who numerically modelled simultaneous (rock) uplift and denudation for an problem domain representing an area adjacent to the Alpine Fault in the central S. Alps, by applying the two dimensional diffusion equation for a moving medium. Under Koons' (1989) assumed uplift rate model, topography increased in elevation until 0.25 - 0.5 Ma after the start of (rock) uplift, after which time the erosion rate equalled the (rock) uplift rate.

The elevation attained by the stable equilibrium topography depends on the rate of rock uplift. A more rapid rate of rock uplift will produce higher topography because a greater potential energy is needed to provide sufficient erosional energy to balance the uplift (Hack, 1960). A corollary of the nature of the relationships established here is that the variation in resistance to erosion of the rocks between transects does not play an important role in the variation in elevation along the transects; indeed, the pattern of lithological variation within the schists along the strike of the Alpine Fault does not reflect at all the observed pattern of variation in elevation response between transects (Figs 1 and 8).

The stable equilibrium that exists between rock uplift rate and elevation/relief to the west of the Main Divide contrasts with the region to the east, where mountains have continued to increase in elevation/relief since the start of uplift and which are related to the age of initiation of rock uplift and the amount of rock uplift.

SUMMARY AND CONCLUSIONS

The Southern Alps (S. Alps) of New Zealand have been uplifted as a consequence of late Cenozoic tectonic collision of the Pacific and Australia plates. Fission track analysis has provided estimates of the amount, age, and rate of late Cenozoic (<8 Ma ago) uplift for 82 rock samples from the S. Alps. The mean surface, summit, and valley elevations in the vicinity of each of the rock sample sites have also been measured. We have used this uplift and geomorphic information to quantitatively analyse the nature of the relationship between uplift and geomorphology in the S. Alps. This has provided insights into long-term landscape evolution in a continental collision setting.

Regression of the geomorphic variables on the uplift variables has enabled quantitative relationships to be established, and shows that there are strong and consistent associations between uplift and the elevations of the mean surface, summits, and valleys. The relationships are linear, and uplift explains 80-90% of the variation in elevation. The relationships are best described by regression models having uniform slope but varying elevation response between transects. A well constrained pattern of rock uplift propagation southeastwards across the S. Alps has meant that spatial position can be confidently substituted for time, allowing the evolution of landforms over time to the east of the Main Divide to be studied.

To the east of the Main Divide, estimates of the amount of rock uplift range from 2.8 to 5.5 km, and estimates of the age of the start of uplift range from 2.7 to 6.4 Ma ago. Mountain elevation is proportional to the age and amount of rock uplift. Elevation and relief have increased with increasing amounts of rock uplift and over time. Uplift of the mean surface was delayed for 1.3-3.7 Ma (1.4-2.6 km of rock uplift), depending on transect, after the start of rock uplift. This was probably a result of the stripping of soft Cenozoic rocks that originally overlaid a harder greywacke basement, which gave rise to an initial period of rapid erosion and rock uplift. The regular regression slope for elevation versus rock uplift for the eastern transects,

reflects the consistent nature of the interaction between rock uplift and greywacke erodiblilty in the absence of significant climate differences between transects. Variations in response and hence in x-intercept reflect primarily the erosion of variable thicknesses of soft cover rocks, during which the rock uplift rate was >1.0 km/Ma. Once greywacke was exposed, mean surface elevation increased at a constant rate of 0.4 km/km and 0.4 km/Ma of rock uplift, and the rate of rock uplift was 0.8 km/Ma. Summits have increased in elevation at 0.7 km/km and 0.6 km/Ma, and valleys at 0.3 km/km and 0.2 km/Ma of rock uplift. Mean surface elevation has increased as a proportion (0.9) of tectonic uplift, whereas the height of the summits is a function of both tectonic and isostatic uplift. The divergence from common x-intercepts of the regression lines relating mean surface, summit, and valley elevations to rock uplift and uplift age, implies that the mountains to the east of the Main Divide have continued to increase in relief and evolve in form over time since uplift started. Mountain elevation and relief have little relationship with late Cenozoic mean rock uplift rates of 0.8-1.0 km/Ma and inferred contemporary rock uplift rates of 0.8-1.0 km/Ma (r^2~0.3).

To the west of the Main Divide, elevation is closely related (r^2>0.8) to rock uplift rate, which varies from 1-10 km/Ma; transects where the rock uplift rate is higher (central S. Alps) support higher topography, and have greater relief. Topography is in a stable equilibrium with rock uplift rate, and the landscape therefore contains no residual evidence of the total amount of rock uplift, or the age of uplift. Lithological variation in the schist rocks along the strike of the S. Alps to the west of the Main Divide is not related to elevation, which implies that these rocks effectively have uniform strength.

The findings of this study provide constraints for a model of the evolution of the Southern Alps which is outlined in a companion paper (Tippett and Kamp, submitted). This study also shows the contribution fission track analysis can make to quantifying landscape evolution in a collisional tectonic setting, particularly where the amount, age, and rate of uplift, and geomorphology, vary spatially.

APPENDIX 1: Regression Equations

(a) Regressions on rock uplift (east of Main Divide)

Transect	Mean surface elevation	response	x-intercept (km)
Haast	y=-1.07+0.42x	<0	2.6
Ohau	y=-0.72+0.42x	<0	1.7
Godley	y=-0.77+0.42x	<0	1.8
Clyde	y=-0.60+0.42x	<0	1.4
Wilberforce	y=-0.68+0.42x	<0	1.6
Arthur's	y=-0.73+0.42x	<0	1.7
Lewis	y=-0.99+0.42x	<0	2.4
	Summit elevation		
Haast	y=-1.45+0.67x	<0	2.2
Ohau	y=-1.07+0.67x	<0	1.6
Godley	y=-1.15+0.67x	<0	1.7
Clyde	y=-0.94+0.67x	<0	1.4
Wilberforce	y=-1.09+0.67x	<0	1.6
Arthur's	y=-1.17+0.67x	<0	1.8
Lewis	y=-1.44+0.67x	<0	2.2
	Valley floor elevation		
Haast	y=-0.63+0.25x	<0	2.5
Ohau	y=-0.35+0.25x	<0	1.4
Godley	y=-0.30+0.25x	<0	1.2
Clyde	y=-0.30+0.25x	<0	1.2
Wilberforce	y=-0.41+0.25x	<0	1.6
Arthur's	y=-0.44+0.25x	<0	1.8
Lewis	y=-0.57+0.25x	<0	2.3

(b) Regressions on uplift age (east of Main Divide)

Transect	Mean surface elevation	response	x-intercept (Ma)
Haast	y=-1.32+0.36x	<0	3.7
Ohau	y=-0.92+0.36x	<0	2.6
Godley	y=-0.72+0.36x	<0	2.0
Clyde	y=-0.60+0.36x	<0	1.7
Wilberforce	y=-0.52+0.36x	<0	1.4
Arthur's	y=-0.46+0.36x	<0	1.3
Lewis	y=-0.54+0.36x	<0	1.5
	Summit elevation		
Haast	y=-1.83+0.57x	<0	3.2
Ohau	y=-1.36+0.57x	<0	2.4
Godley	y=-1.07+0.57x	<0	1.9
Clyde	y=-0.93+0.57x	<0	1.6
Wilberforce	y=-0.82+0.57x	<0	1.4
Arthur's	y=-0.74+0.57x	<0	1.3
Lewis	y=-0.71+0.57x	<0	1.3

Valley floor elevation

Haast	y=-0.83+0.22x	<0	3.8
Ohau	y=-0.50+0.22x	<0	2.3
Godley	y=-0.31+0.22x	<0	1.4
Clyde	y=-0.34+0.22x	<0	1.6
Wilberforce	y=-0.35+0.22x	<0	1.6
Arthur's	y=-0.32+0.22x	<0	1.5
Lewis	y=-0.32+0.22x	<0	1.5

Rock uplift

Haast	y=0.08+0.75x	=0
Ohau	y=0.07+0.75x	=0
Godley	y=0.60+0.75x	=0
Clyde	y=0.53+0.75x	=0
Wilberforce	y=0.90+0.75x	>0
Arthur's	y=1.13+0.75x	>0
Lewis	y=1.45+0.75x	>0

(C) Regressions on uplift rate (west of Main Divide)

Transect	Mean surface elevation	response
Haast	y=0.72-0.056x	>0
Paringa	y=1.07-0.056x	>0
Copland	y=1.82-0.056x	>0
Fox-Franz Josef	y=1.59-0.056x	>0
Whataroa	y=1.53-0.056x	>0
Whitcombe	y=1.23-0.056x	>0
Arthur's	y=0.71-0.056x	>0
Robinson	y=1.06-0.056x	>0
Lewis	y=0.97-0.056x	>0

Summit elevation

Haast	y=1.68-0.054x	>0
Paringa	y=1.77-0.054x	>0
Copland	y=2.65-0.054x	>0
Fox-Franz Josef	y=2.45-0.054x	>0
Whataroa	y=2.24-0.054x	>0
Whitcombe	y=1.94-0.054x	>0
Arthur's	y=1.64-0.054x	>0
Robinson	y=1.64-0.054x	>0
Lewis	y=1.60-0.054x	>0

Valley floor elevation

Haast	y=0.26-0.046x	>0
Paringa	y=0.32-0.046x	>0
Copland	y=0.95-0.046x	>0
Fox-Franz Josef	y=0.92-0.046x	>0
Whataroa	y=0.69-0.046x	>0

Whitcombe	y=0.57-0.046x	>0
Arthur's	y=0.36-0.046x	>0
Robinson	y=0.49-0.046x	>0
Lewis	y=0.65-0.046x	>0

(i) Note that precisions in the text are quoted usually to one decimal place.

REFERENCES

Adams, J. 1980. 'Contemporary uplift and erosion of the Southern Alps, New Zealand', *Geol. Soc. Am. Bull.,* **91**, 1-114.

Adams, J. 1985. 'Large-scale tectonic geomorphology of the Southern Alps, New Zealand', in *Tectonic Geomorphology*, editors M. Morisawa and J. T. Hack, Proc. 15th Ann. Binghamton Geomorphology Symposium, Allen and Unwin, 105-128.

Augustinus, P.C. 1988. 'The influence of the lithological and geotechnical properties of rocks on the morphology of glacial valleys', *Unpublished D. Phil. thesis,* University of Waikato, 257 pp.

Brunsden, D. 1980. 'Applicable models of long term landform evolution', *Zeitschrift fur Geomorphologie Supplementband,* **36**, 16-26.

Brunsden, D. and J.B. Thornes 1979. 'Landscape sensitivity and change', *Transactions of the Institute of British Geographers,* **4**, 463-484.

Davis, W.M. 1899. 'The geographical cycle', *Geographical Journal,* **14**, 481-504.

Draper, N.R., and H. Smith 1981. *Applied regression analysis, second edition*, Wiley, New York, 709 pp.

England, P., and P. Molnar 1990. 'Surface uplift, uplift of rocks, and exhumation of rocks', *Geology,* **18**, 1173-1177.

Gair, H.S. 1978. 'The late mobile phase: Tertiary. Stratigraphy - Mid and South Canterbury and North Otago', in *The geology of New Zealand*, chief editor R.P. Suggate, Government Printer, Wellington, 510-516.

Gleadow, A.J.W. and I.R. Duddy 1981. 'A natural long-term track annealing experiment for apatite', *Nuclear Tracks*, **5**, 169-174.

Gleadow, A.J.W. and P.G. Fitzgerald 1987. 'Uplift history and structure of the Transantarctic Mountains: new evidence from fission track dating of basement apatites in the Dry Valleys area, southern Victoria Land', *Earth and Planetary Science Letters*, **82**, 1-14.

Green, P.F. 1986. 'On the thermo-tectonic evolution of Northern England: evidence from fission track analysis', *Geological Magazine,* **123**, 493-506.

Green, P.F., I.R. Duddy, G.M. Laslett, K.A. Hegarty, A.J.W. Gleadow, and J.F. Lovering 1989. 'Thermal annealing of fission tracks in apatite 4', *Chemical Geology,* **79**, 155-182.

Gregg, D. R. 1978. 'The late mobile phase: Tertiary. Stratigraphy - North Canterbury', in *The geology of New Zealand*, chief editor R.P. Suggate, Government Printer, Wellington, 503-510.

Hack, J.T. 1960. 'Interpretation of erosional topography in humid temperate regions', *American Journal of Science, Bradley Volume,* **258-A**, 80-97.

Hubert, L.J., R.G. Golledge, C.M. Costanzo, and N. Gale 1985. 'Measuring association between spatially defined variables: an alternative procedure', *Geographical Analysis*, **17/1**, 36-46.

Hurford, A.J. 1986. 'Cooling and uplift patterns in the Lepontine Alps, South Central Switzerland, and an age of vertical movement of the Insubric fault line', *Contributions to Mineralogy and Petrology,* **92**, 413-427.

Kamp, P.J.J., P.F. Green, and S.H. White 1989. 'Fission track analysis reveals character of collisional tectonics in New Zealand', *Tectonics,* **8**, 169-195.

Kamp, P.J.J. and J.M. Tippett 'Dynamics of Pacific plate continental crust in the South Island collision zone (New Zealand)', *Journal of Geophysical Research*, (submitted).

King, L.C. 1953. 'Canons of landscape evolution', *Bulletin of the Geological Society of America,* **64**, 721-752.

Koons, P.O. 1989. 'The topographic evolution of collisional mountain belts: a numerical look at the Southern Alps, New Zealand', *American Journal of Science,* **289**, 1041-1069.

Penck, W. 1953. *Morphological analysis of landforms* (translated by H. Czech and K.C. Boswell), Macmillan.

Stevens, G.R. and R.P. Suggate 1978. 'Atlas of paleogeographic maps', in *The geology of New Zealand*, chief editor R.P. Suggate, Government Printer, Wellington, 727-743.

Tippett, J.M. and P.J.J. Kamp 'Fission track analysis of the late Cenozoic vertical kinematics of continental Pacific crust, South Island, New Zealand', *Journal of Geophysical Research*, (in press).

Tippett, J.M. and P.J.J. Kamp 'Geomorphic evolution of the Southern Alps, New Zealand', *Earth Surface Processes and Landforms* (submitted).

Wellman, H.W. 1979. 'An uplift map for the South Island of New Zealand, and a model for the uplift of the Southern Alps', *Bulletin of the Royal Society of New Zealand,* **18**, 13-20.

Whitehouse, I.E. 1987. 'Geomorphology of a compressional plate boundary, Southern Alps, New Zealand', in *International Geomorphology*, chief editor V. Gardiner, John Wiley and Sons Ltd, Part 1, 897-924.

Williams, G.P. and B.M. Troutman 1987. 'Algebraic manipulation of best-fit straight lines', in *Use and abuse of statistical methods in the Earth Sciences*, editor W. B. Size, Oxford University Press, 129-141.

Yoshikawa, T. 1985. 'Landform development by tectonics and denudation', in *Themes in Geomorphology*, editor A. Pitty, Croom Helm, 194-210.

CHAPTER 7

Geomorphic evolution of the Southern Alps, New Zealand

(Manuscript submitted to *Earth Surface Processes and Landforms*)

J. Mark Tippett
Peter J.J. Kamp

Geochronology Research Unit,
Department of Earth Sciences,
University of Waikato,
Private Bag 3105,
Hamilton 2001, New Zealand.

ABSTRACT

The Southern Alps are the topographic expression of late Cenozoic (<8 Ma ago) uplift of the crust of the leading edge of the Pacific plate in South Island, New Zealand. New fission track data on the basement exposed in the Southern Alps quantify the age, amount, and rate of rock uplift, and in combination with geomorphic parameters permit the construction of a new model of the geomorphic evolution of the Southern Alps. The model emphasises the development over time and space of rock uplift, mean surface elevation, exhumation of crustal section, and relief. The earliest indications of mean surface uplift are between 4 and 5 Ma ago at the Alpine Fault. Mean surface uplift, which lagged the start of rock uplift, propagated southeastward from the Alpine Fault at a rate of 30 km/Ma. By about 4 Ma ago, exhumation had exposed greywacke basement adjacent to and east of the entire 300 km-long central section of the Alpine Fault. At 3 Ma ago greenschist was exposed in the southern parts of the Southern Alps near Lake Wanaka, and since then has become exhumed along a narrow strip east of the Alpine Fault. The model infers that amphibolite grade schist has been exhumed adjacent to the Alpine Fault only in the last 0.3 Ma. The age of the start of rock uplift, and the amount and rate of rock uplift, all of which vary spatially, are considered to be the dominant influences on the development of the landscape in the Southern Alps.

The Southern Alps have been studied in terms of domains of different rock uplift rate. At present the rate of rock uplift varies from up to 8-10 mm/a adjacent to the Alpine Fault to 0.8-1.0 mm/a along the southeastern margin of the Southern Alps. This spectrum can be divided into two domains, one northwest of the Main Divide where the present rock uplift rates are very high (up to 8-10 mm/a) and exceed the long-term value of 0.8-1.0 mm/a, and another to the southeast of the Main Divide where the long-term rate is 0.8-1.0 mm/a. A domain of no uplift lies immediately to the east of the Southern Alps, and is separated from them by a 1.0 to 1.5 km step in the basement topography. We argue that this spatial sequence of uplift rate domains represents a temporal one.

The existing models of the geomorphic development of the Southern Alps - the dynamic cuesta model of J. Adams and the numerical model of P. Koons - are compared with the new data and evolutionary model. Particular constraints unrealised by these two earlier models include the following: the earlier timing of the start of rock uplift of the Southern Alps (8 Ma ago); the

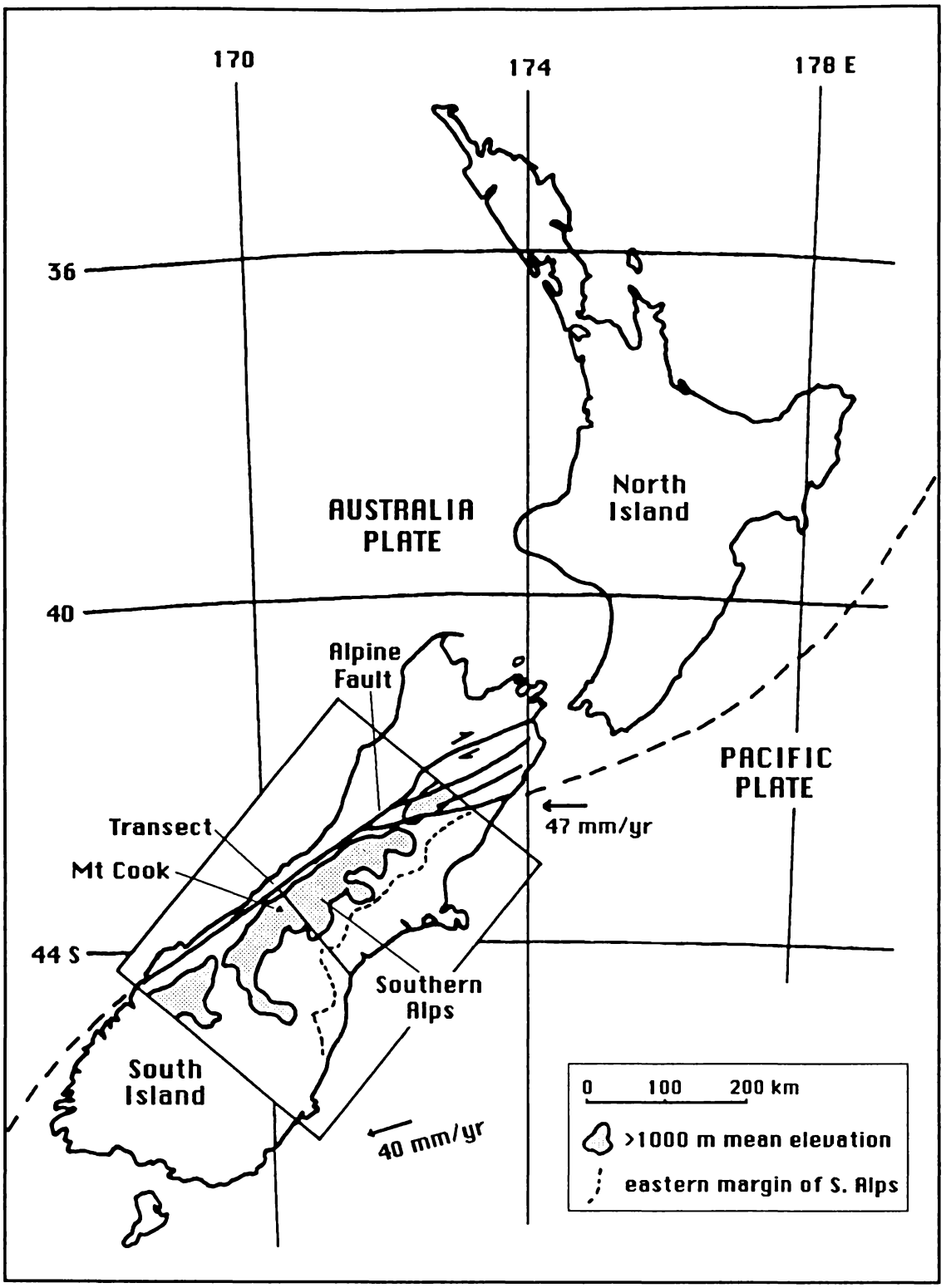


Fig. 1. Tectonic setting of the Southern Alps, New Zealand. The box shows the area covered by maps in Figs 2, 4, 5, and 7. The transect line is for Figs 6, 8, and 9.

spatial variation in the timing of the start of rock uplift (8 Ma ago to 3 Ma ago); the lower long-term rock uplift rate (0.8-1.0 mm/a) of the Southern Alps for most of the late Cenozoic; the lag between the start of rock uplift and the start of mean surface uplift; and the patterns of the amounts of late Cenozoic rock uplift and erosion across the Southern Alps.

INTRODUCTION

The Southern Alps of South Island, New Zealand, have been formed by widespread uplift of crust due to late Cenozoic collision of the Pacific and Australian plates (Fig. 1). The Alpine Fault is the plate boundary in South Island; the Southern Alps are located on the edge of the Pacific plate immediately to the southeast of the Fault. The central sector of the Southern Alps (S. Alps) is about 300 km long and up to 120 km wide, with summit elevations reaching >3000 m. The recent timing of rock uplift (<8 Ma ago), the large amount of rock uplift (up to 19 km), and the high rock uplift rates (0.8-10 mm/a), make the S. Alps a good example of an actively forming mountain range.

Two models have been proposed recently to explain the simultaneous tectonic and geomorphic development of the S. Alps: the dynamic cuesta model of Adams (1980, 1985), and the numerical model of Koons (1989). Since the publication of these models, new data bearing on the kinematics (rock uplift amount, age and rate), dynamics, and tectonic geomorphology of the S. Alps have been established by application of fission track analysis to apatite and zircon separates from basement rocks exposed in the S. Alps (Kamp et al., 1989; Tippett and Kamp, in press; Kamp and Tippett, submitted; Tippett and Kamp, submitted). These data provide new constraints that allow us to evaluate the existing models of the geomorphic evolution of the S. Alps and to outline a new one. Here we examine particularly the evolutionary interaction of rock uplift and landscape (mean surface elevation and relief).

EXISTING MODELS FOR THE EVOLUTION OF THE SOUTHERN ALPS

Dynamic cuesta model (Adams 1980, 1985)

Adams (1980, 1985) proposed that the contemporary rate of erosion of the S. Alps is equal to the rate of (rock) uplift. The uplift data were derived from displaced and deformed surfaces of known or inferred age. At the Alpine Fault, displaced and deformed river terraces, and upthrown marine

shell beds, yielded rock uplift rates of 2-12 mm/a. To the east of the Main Divide (the major drainage divide in the S. Alps), tilted post-glacial stranded lake shorelines yielded (rock) uplift rates of ~0.5-2.0 mm/a (Wellman, 1979).

Adams (1980) described in detail the pattern of uplift across a NW-SE oriented transect in the central S. Alps that started at the Alpine Fault. A curve was fitted to the uplift data, with the constraint that the area under the uplift rate curve balanced the current 22 mm/a component of compression (Walcott, 1979) across the Australia-Pacific plate boundary. The uplift pattern was considered to be the difference between 'unconstrained uplift,' and 'fault drag' on the Alpine Fault. The resulting apparent (rock) uplift rates increased from 15 mm/a at the Alpine Fault to 22 mm/a some 7 km southeast of the Fault, then declined exponentially to reach zero about 70 km southeast of the Fault.

Adams (1980) synthesised published information on sedimentation rates offshore, and found that the rate of deposition equalled the average (rock) uplift rate of the S. Alps. River sediment loads also appeared to be in balance with the uplift rate. Adams (1980) also modelled the geomorphic evolution (growth to 'steady state') of the S. Alps, by establishing empirical relationships between present mountain height, present runoff, and present (rock) uplift rate. The uplift pattern described was assumed to develop rapidly and was maintained for the nominal 2.5 Ma age of the S. Alps. In his model, erosion started to lower the crests when the 'flat-topped' ('non-steady state') mountains attained a height of 2 km, at which point they became 'spiky' (i.e. with steep peaks) 'steady state' mountains. At that point the erosion rate was calculated from the relationship between uplift rate, mountain height, and runoff, assuming that the erosion rate equals the uplift rate (i.e. 'steady state' equilibrium). The spiky mountains appeared to reach their present state after about 1.5 Ma of uplift. It was recognised that the state of balance was achieved only over a period of >0.1 Ma because of climate changes and periodicity in the erosion-causing processes.

Mountains in the far east of the S. Alps were viewed by Adams (1980, 1985) as flat-topped time-dependent landforms that represent an uplifted peneplain. They were noted to change further inland to spiky time-independent landforms at about the 0.5 mm/a post-glacial uplift rate contour of Wellman (1979). The type, lithology, and height of the mountains at any one location were considered to stay constant, as the mountain range was said to behave like a cuesta that is constantly being renewed by uplift.

Adams' (1980, 1985) model is an inadequate description of the geomorphic development of the S. Alps because a minimum of 1.5 to 2.0 km of rock has been removed from the whole of the S. Alps, including the eastern margin where there are so-called 'flat-topped' mountains (Kamp and Tippett, submitted). The smooth increase in summit heights inland from the east is therefore the result of the pattern of uplift and erosion (Tippett and Kamp, submitted), rather than being due to differential uplift of a peneplained surface. We have shown that the mountains to the east of the Main Divide have increased in elevation and relief and changed in form with respect to time and rock uplift, and therefore they are not 'steady state' landforms (Tippett and Kamp, submitted). Another problem with the model is that the 2.5 Ma time frame is too short, and the timing of the start of rock uplift is now known to vary across the S. Alps. Also, it is clearly unrealistic to apply rock uplift rates of >10 mm/a from the start of uplift, as shown by the results of our fission track studies (Kamp et al., 1989; Tippett and Kamp, in press). For most of the period of uplift the S. Alps have been uplifted at a rate of 0.8-1.0 mm/a. We have also shown (Kamp et al., 1989) that the highest uplift amounts and rates occur at the Alpine Fault, rather than to the southeast as inferred by Adams (1980, 1985).

Numerical model (Koons, 1989)

Koons (1989) numerically modelled the simultaneous (rock) uplift and erosion of the S. Alps using the diffusion equation for a moving medium. In doing so he examined the relative importance to morphology of uplift rates, drainage density, and variations in diffusivity (material transport parameter).

One-dimensional modelling (transport normal to the Alpine Fault) was considered appropriate by Koons (1989) for the region east of the Main Divide where drainage density and diffusivity were assumed to be low. Koons (1989) inferred from the results that pre-uplift surfaces are likely to be preserved in this region.

One-dimensional modelling for the area to the west of the Main Divide was rejected by Koons (1989), however, as the models apparently did not approximate the topography of the S. Alps. Two-dimensional modelling was applied to this area, and modern uplift data were used to constrain the model, and east-west rainfall variations were assumed to represent major

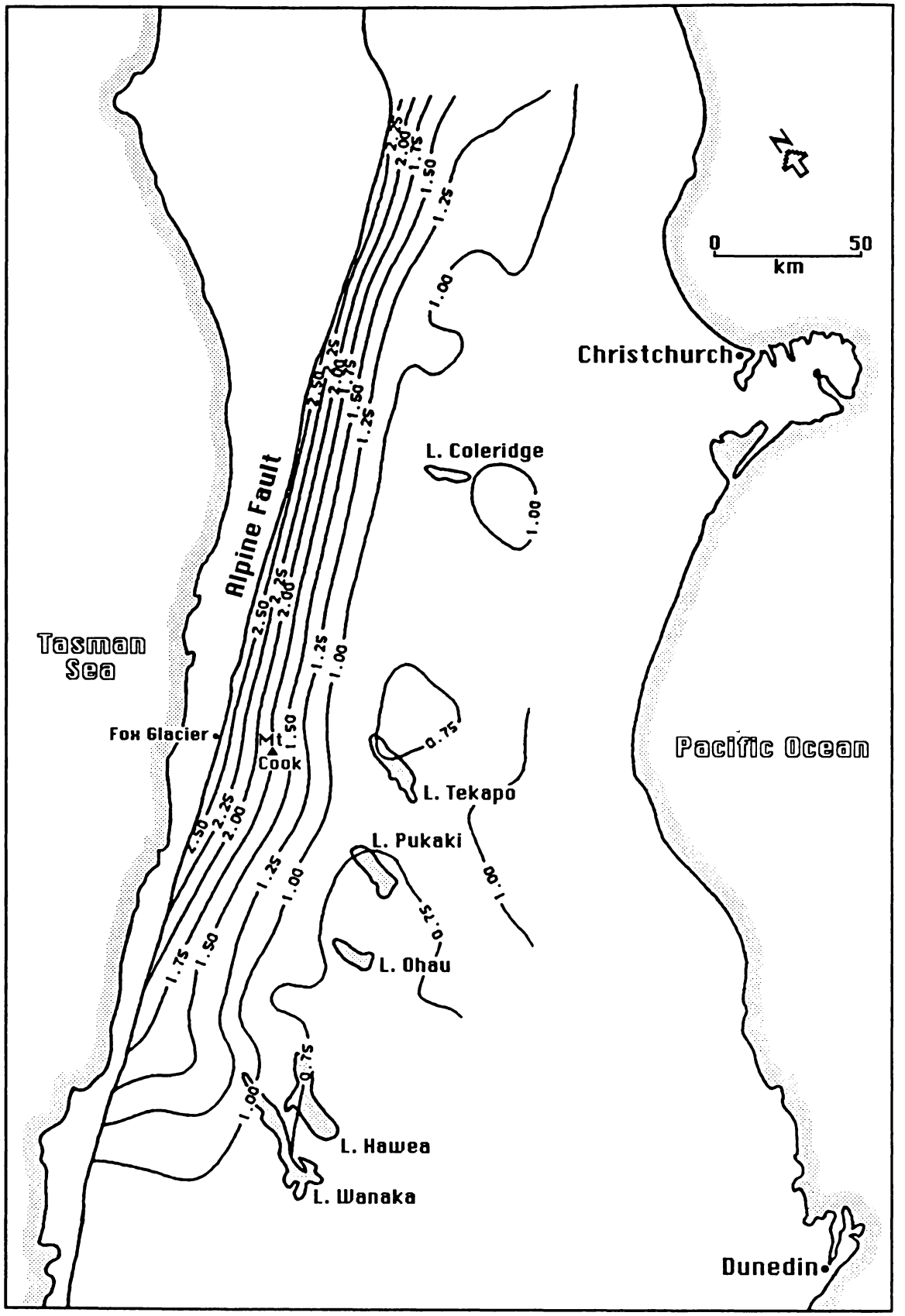


Fig. 2. Map of the late Cenozoic mean rock uplift rate (in mm/a) in the 300-km long central sector of the Southern Alps (from Tippett and Kamp, in press).

trends in diffusivity. The problem domain measured x=40 km and y=25 km, and the stream spacings adopted within the problem domain were maintained throughout uplift. The initial elevation was taken as sea level, and the eastern and western boundaries were fixed at sea level throughout the interval of uplift (5 Ma), with the Main Divide fixed at x=25 km. Models were run with an uplift rate pattern of 10 mm/a adjacent to the (Alpine) Fault and decreasing linearly away from the Fault to 1 mm/a at x=30 km; from x=33 km to the eastern boundary at x=40 km, a uniform uplift rate of 0.5 mm/a was adopted. This uplift rate pattern is compatible with the modern uplift pattern in the S. Alps as proposed by Wellman (1979). All points were modelled to start being uplifted simultaneously. The development of topography at intervals up to 5 Ma after the start of uplift was simulated. The numerical models predicted that near-'steady state' elevations would be reached in the region to the west of the Main Divide within 0.25 to 0.5 Ma of the start of (rock) uplift.

Koons' numerical model (1989), like that of Adams (1980, 1985), applies Wellman's (1979) contemporary uplift rates (10 mm/a) from the beginning of rock uplift. These rates exceed enormously the late Cenozoic mean rock uplift rates for the region of interest (Fig. 2). That the rock uplift age varies spatially across the S. Alps has also not been taken into account in the numerical model. The model does not predict or account for the lag between the start of rock uplift and the start of mean surface uplift. The mountains to the east of the Main Divide have had a minimum of 1.5-2.0 km of erosion, and therefore no pre-uplift surfaces are preserved in that region. This is contrary to the predictions of the numerical model (Koons, 1989).

CONSTRAINTS ON A NEW MODEL

Initial conditions

Prior to late Cenozoic uplift, the mean surface elevation was at or close to sea level. At the end of the late Cretaceous to late Oligocene New Zealand-wide marine transgression, the sea almost completely covered the New Zealand landmass (e.g. Kamp, 1986). Up to 1000 m of cover rocks accumulated during the transgression in South Island, and widespread late Miocene regressive facies occur in successions around the margin of the S. Alps (Field and Browne et al., 1989).

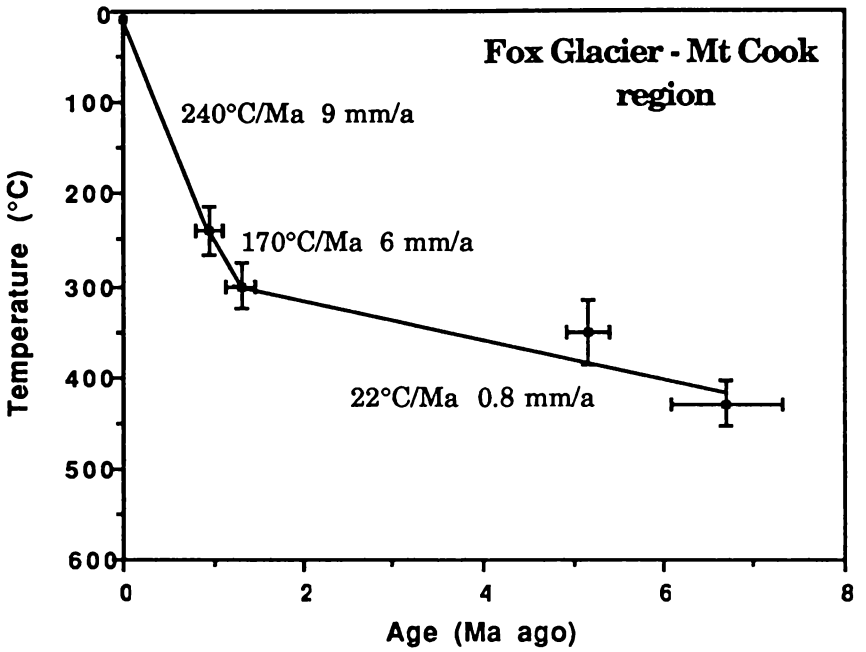


Fig. 3. Cooling history of rocks adjacent to the Alpine Fault in the Fox Glacier - Mt Cook region (from Tippett and Kamp, in press). The rock uplift rates quoted have been calculated assuming a 27.5° C geothermal gradient. Errors are 1σ.

Rock uplift amount

The amount of late Cenozoic rock uplift adjacent to the Alpine Fault in the Fox Glacier - Mt Cook region of the S. Alps has reached a maximum of ~19 km, with lesser amounts at the northern (~10 km) and southern (~8 km) margins of the S. Alps. From the Alpine Fault, rock uplift decreases almost exponentially to values of 3 km along the southeastern margin of the S. Alps. (Fig. 10 of Tippett and Kamp, in press).

Rock uplift age

There is significant spatial variation across the S. Alps in the age of the start of rock uplift. Rock uplift at the Alpine Fault began at about 8 Ma ago in the southern parts of the S. Alps, compared with about 5 Ma ago in the northern parts. The eastern margin of the S. Alps started to be uplifted at about 3 Ma ago. The eastward propagation of rock uplift initiation occurred at a rate of 30 km/Ma (Fig. 12 of Tippett and Kamp, in press).

Rock uplift rate

Fig. 2 shows the pattern of late Cenozoic mean rock uplift rate ('long-term' rock uplift rate) for the S. Alps. These uplift rates range from a minimum of 0.8 mm/a in the east, to a maximum of 2.7 mm/a adjacent to the Alpine Fault in the Fox Glacier - Mt Cook region (Fig. 2). The long-term rock uplift rate is 2.3 mm/a adjacent to the Alpine Fault in the northern part of the S. Alps and is 1.0 mm/a against the Fault at the southern end of the S. Alps.

Fig. 3 shows a cooling/rock uplift curve for samples from rocks presently exposed adjacent to the Alpine Fault in the Fox Glacier - Mt Cook region. The rocks in this area started to be uplifted at 6.7 ± 1.2 (2σ) Ma ago and until 1.3 ± 0.3 Ma ago were uplifted at a rate of about 0.8 mm/a; this increased to about 6 mm/a between 1.3 and 0.9 Ma ago, and increased again to about 9 mm/a after 0.9 Ma ago.

Rock uplift rates derived from reset zircon fission track ages for rocks from within 5 km of the Alpine Fault range from 8-10 mm/a in the Fox Glacier - Mt Cook region to ~4 mm/a at the northern end of the S. Alps, and ~2.5 mm/a at the southern end of the S. Alps (Fig. 18 of Tippett and Kamp, in press).

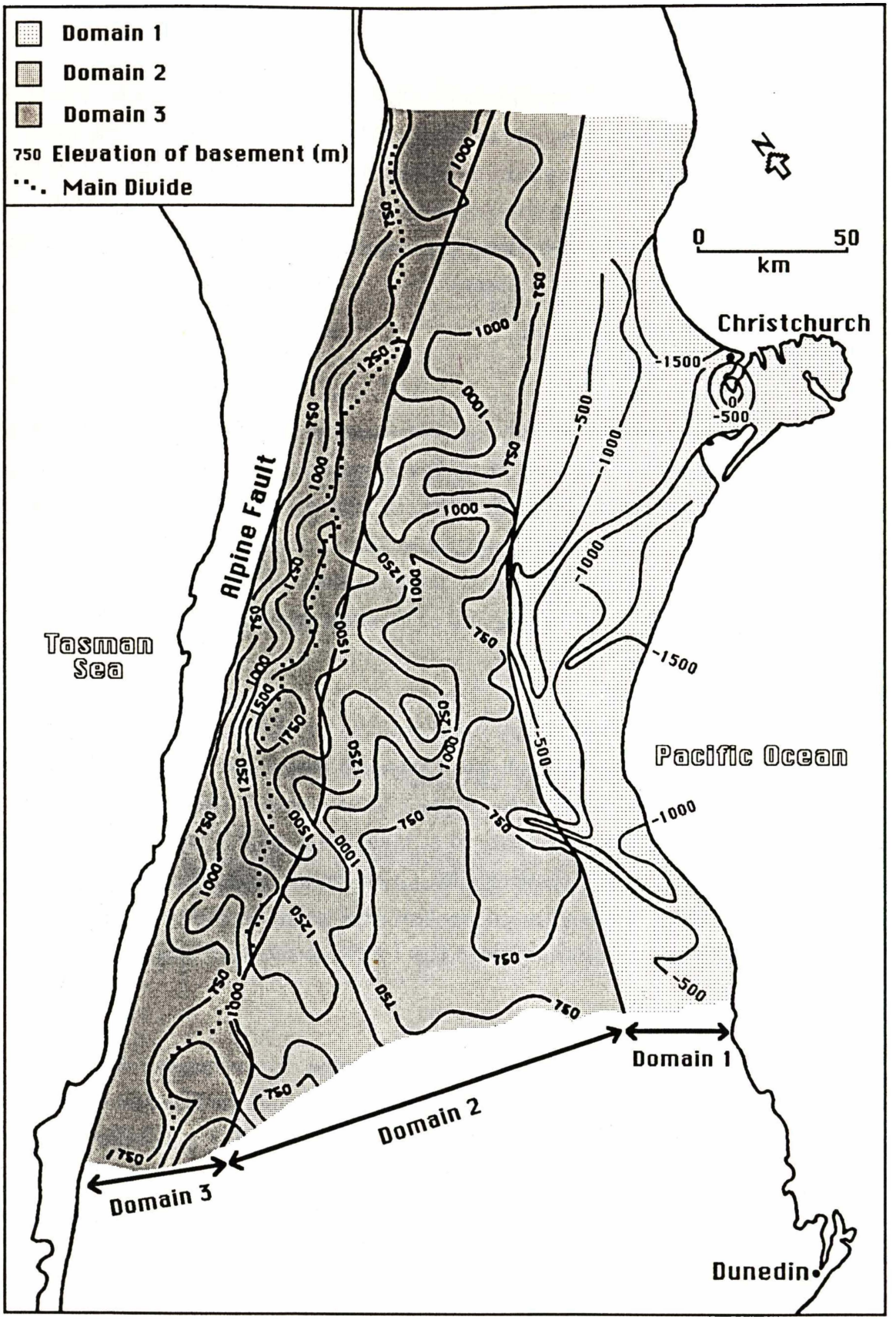


Fig. 4. Map showing the 3 domains of rock uplift rate in the vicinity of the Southern Alps, and the elevation (in m) of the basement rock. Elevation data in domain 1 are from the gravity survey of Hicks (1989).

Final conditions

The present mean surface elevation and relief, and the rock outcrop pattern define the final conditions that constrain any model of the geomorphic evolution of the S. Alps. The spatial variation in mean surface elevation of the S. Alps is shown in Fig. 4. The mean surface elevation is greatest along a zone 20-30 km to the southeast of, and subparallel to, the Alpine Fault. Mean surface elevation reaches almost 2000 m above mean sea level in the central S. Alps, and decreases gently to ~750 m at the northern and southern ends of the S. Alps. Mean surface elevation decreases more rapidly to the west of the Main Divide than it does to the east, and therefore the mountain elevations of the S. Alps define an elongate asymmetric dome.

Schist crops out in a narrow belt immediately to the southeast of the Alpine Fault. A narrow belt of amphibolite grade schist passes southeastward into greenschist facies rocks, which then give way further east to Torlesse greywacke of pumpellyite-actinolite and then prehnite-pumpellyite metamorphic grade. This metamorphic succession indicates decreasing depth of burial to the southeast away from the Alpine Fault, exhumed by the asymmetric pattern of late Cenozoic uplift (Kamp et al., 1989). Cenozoic cover rocks are preserved around the southeast margins of the S. Alps, and under the alluvial plains to the east.

A MODEL FOR THE GEOMORPHIC EVOLUTION OF THE SOUTHERN ALPS

Uplift domains and regimes

We have divided the area of the 300 km-long central sector of the S. Alps into 3 domains based upon long-term rates of rock uplift (Fig. 4). Domain 1 is an area of no uplift that lies to the east of the S. Alps. Domain 2 has been uplifted at relatively uniform long-term rates of 0.8-1.0 mm/a. Domain 3 lies adjacent to the Alpine Fault and has undergone long-term rock uplift rates of 1.0 to 2.7 mm/a, with shorter-term (1.3 Ma ago to present) rates of 6-9 mm/a, and modern rates of 8-10 mm/a.

In the model we substitute space for time. Domain 2 is viewed as describing the first stage of development of Domain 3. Initially (between 6.7 ± 1.2 and 1.3 ± 0.3 Ma ago), Domain 3 rocks were inferred to have been

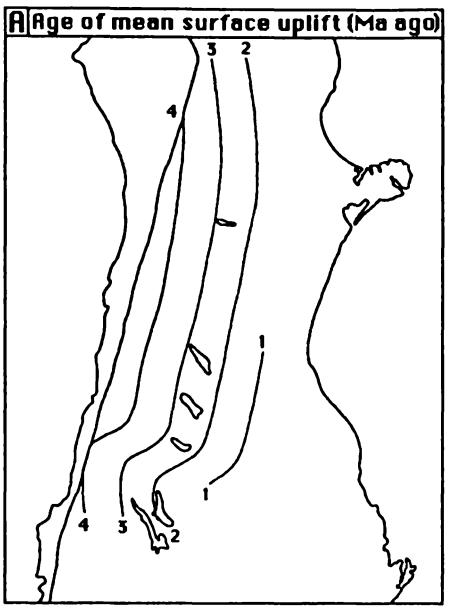
uplifted at a rate of ~0.8 mm/a, which subsequently increased to values in the range 6 to 9 mm/a. These later rates have been derived from the Fox Glacier - Mt Cook region of Domain 3, which currently has the highest uplift rates, and therefore the northern and southern parts of Domain 3 will have been uplifted at slightly lower rates. The timing (1.3 ± 0.3 Ma ago) of the rapid increase in rock uplift rate is based on the cooling curve in Fig. 3. The boundary between Domains 2 and 3 is located where the long-term rock uplift rate changes dramatically, mapped approximately by the 1 mm/a contour in Fig 2.

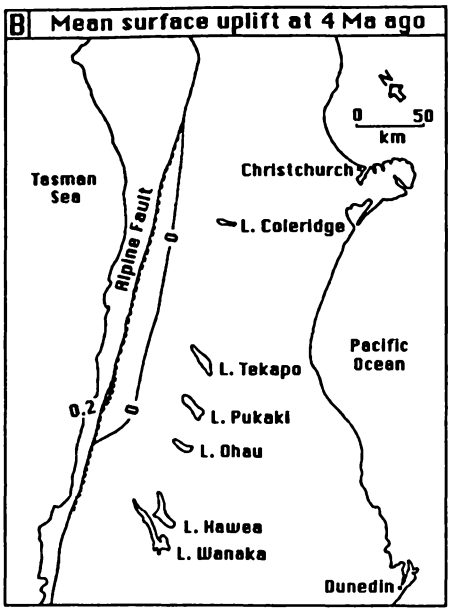
The rocks exposed along the eastern margin of the S. Alps have been uplifted about 3 km, and started to be uplifted at ~3 Ma ago (Tippett and Kamp, in press). Along this margin there is a 1.0 to 1.5 km difference in the elevation of the basement between that exposed in the S. Alps and that buried beneath the Canterbury Plains (Fig 4). This stepped topography together with the covering of Pleistocene gravels, suggests that the Plains have not been uplifted during the late Cenozoic. Hence areas with less than 3 km of rock uplift, uplifted less than 3 Ma ago, probably do not exist in the 300 km-long central sector of the S. Alps.

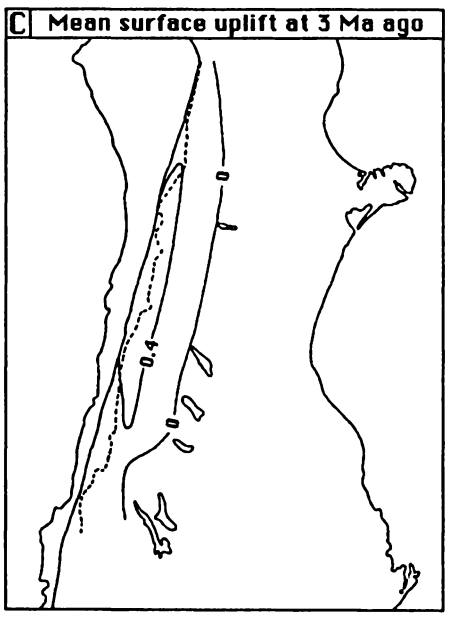
In summary, mean surface elevation prior to the start of rock uplift lay at, or close to, sea level. At times starting between 8 and 5 Ma ago, depending on location in the S. Alps, and continuing until 3 Ma ago, rock uplift propagated eastward at a rate of 30 km/Ma. Domain 1, an area of no uplift, lies to the east of the S. Alps. The eastern parts of the S. Alps now comprise Domain 2 where the long-term rock uplift rate is 0.8-1.0 mm/a. Domain 3 extends southeastward from the Alpine Fault to just east of the Main Divide, and it has had a long-term rock uplift rate of 2.7 mm/a. From 1.3 ± 0.3 Ma ago, average rates of rock uplift have been 6-9 mm/a in the Fox Glacier - Mt Cook region, ~2.5 mm/a in the south, and ~4 mm/a in the north.

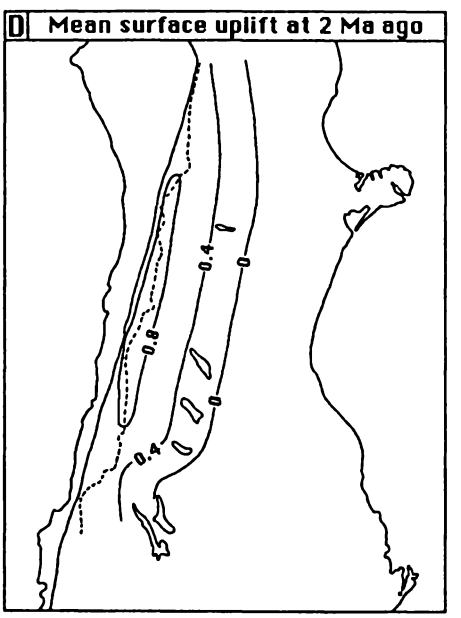
Increase in elevation of the mean surface

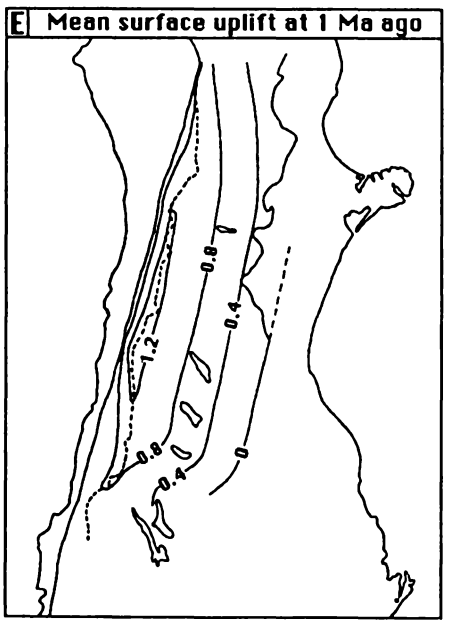
Tippett and Kamp (submitted) showed that mean surface uplift was delayed for 1.3-3.7 Ma (depending on location in the S. Alps) after rock uplift started, due to the initial stripping of a succession of soft Cenozoic cover rock. Fig. 5A shows the time (in Ma ago) of initiation of mean surface uplift for rocks presently exposed in the S. Alps, calculated by subtracting for each transect the appropriate interval of delay from the age of the start of rock


A Age of mean surface uplift (Ma ago)
3
2
4
1
4
3
2
1


B Mean surface uplift at 4 Ma ago
0 50
km
Tasman Sea
Alpine Fault
Christchurch
L. Coleridge
Pacific Ocean
L. Tekapo
L. Pukaki
L. Ohau
L. Hawea
L. Wanaka
Dunedin
0
0.2
0


C Mean surface uplift at 3 Ma ago
0
0.4
0


D Mean surface uplift at 2 Ma ago
0.4
0
0.8
0
0.4


E Mean surface uplift at 1 Ma ago
0.8
0.4
1.2
0.8
0.4
0

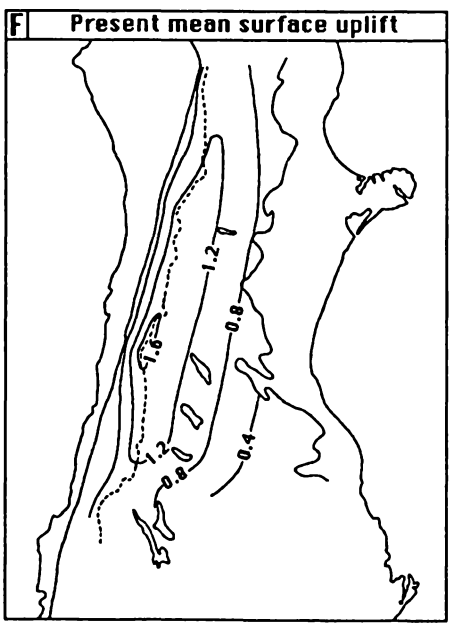

F Present mean surface uplift
1.2
0.8
1.6
1.2
0.8
0.4

Fig. 5. **(A)** Map of the spatial variation in the age of the start of mean surface uplift (in Ma ago), with respect to the present geographical configuration of South Island. The map was constructed by subtracting from the age of rock uplift initiation the time for which the start of mean surface uplift lagged the start of rock uplift (from Tippett and Kamp, submitted). **(B-F)** Maps showing the amount of mean surface uplift (in km) through the last 4 Ma. The rate of mean surface uplift of 0.4 km/Ma is from Table 6 of Tippett and Kamp (submitted), and is derived from relationships between the age of rock uplift and present mean surface elevation. Summit elevations would have been half as high again at any stage. The broken line shows the inferred position of the Main Divide.

uplift established by fission track analysis. The earliest indications of mean surface uplift at the Alpine Fault are between 4 and 5 Ma ago. The start of mean surface uplift propagated eastward from the Alpine Fault at about 30 km/Ma. Fig. 5B-F shows a model of the evolutionary increase in the elevation of the topography (amount of uplift of the mean surface) for the S. Alps. At 1.0 to 1.5 Ma ago, topography at the eastern margin of the S. Alps started to be established (Fig 5E). In the model the Main Divide is assumed to have migrated southeastward from the Alpine Fault between 4 Ma ago and the present at a constant rate. Mountains to the west of the Main Divide reached stable equilibrium elevations quickly.

Progressive exposure of lithology

Fig. 6 shows the pattern of rock exhumation and of mean surface uplift for a transect (shown on Fig. 1) across the central S. Alps. In the first 5 Ma of rock uplift, cover rocks were removed progressively eastward across the growing range, thereby exposing greywacke basement. Four million years after the start of rock uplift (~3 Ma ago), a step started to develop in the basement because the eastward propagation of rock uplift stopped. After 5 Ma of rock uplift (1.7 Ma ago) greywacke was exposed across the whole transect. After 5.7 Ma of rock uplift (1.0 Ma ago), greenschist was exposed adjacent to the Alpine Fault, and biotite and amphibolite schists were exposed shortly thereafter.

Fig. 7 shows now for the whole of the central sector of the S. Alps the proposed progressive rock exposure since 7 Ma ago. Prior to 7 Ma ago, an assumed uniform, 1 km-thick layer of cover rock overlay the basement. At 5 Ma ago, greywacke was exposed in a narrow zone east of, and for almost the whole length of, the 300 km-long central section of the Alpine Fault. By 3 Ma ago, greywacke was exposed across most of the modern S. Alps, and greenschist was exposed between Lakes Wanaka/Hawea and the Alpine Fault. By about 1.5 Ma ago, the present range front started to form, and Quaternary gravels started to accumulate to the southeast of the S. Alps, forming the Canterbury Plains. By 1 Ma ago, the cover rock succession was almost completely stripped. Also by 1 Ma ago, greenschist was exposed adjacent to the Alpine Fault in the Fox Glacier - Mt Cook region, and by ~0.5 Ma ago it was exposed further to the north. Biotite schist was first exposed at 0.5 Ma ago adjacent to the Fault in the south, and amphibolite grade schist was first exposed at about 0.3 Ma ago.

Southern Alps

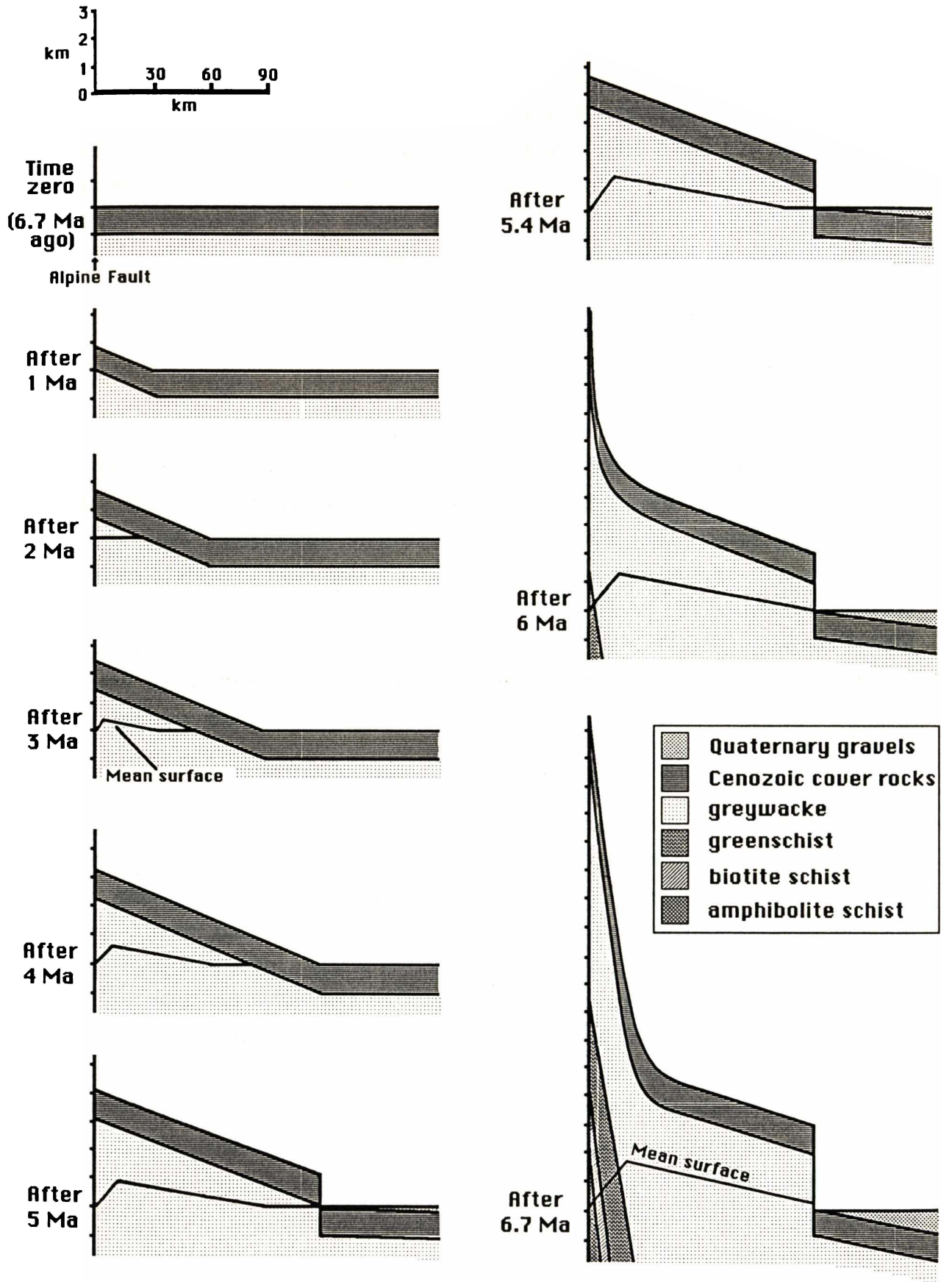


Fig. 6. Simplified history of rock exposure and elevation of the mean topographic surface for a transect across the central S. Alps located on Fig. 1. For simplicity, it is assumed that a uniform 1 km thickness of Cenozoic cover rock formerly overlaid the basement. Exposure of greenschist occurs after 10.5 km of total rock uplift from a formation temperature of 300° C (e.g. Essene, 1989); biotite schist is exposed after 14 km of total rock uplift from a formation temperature of 400° C (e.g. Yardley, 1982; Jamieson and Craw, 1987); amphibolite schist is exposed after 16.5 km of total rock uplift from a formation temperature of 460° C (interpolated between the 400° C biotite isotherm and the 520° C of the Oligoclase zone adjacent to the Alpine Fault determined by Grapes and Otsuki (1983), Johnstone and White (1983), and Findlay (1985)). Three kilometres of Mesozoic rock uplift in the vicinity of this transect (Fig. 11, Tippett and Kamp, in press) reduce the amount of late Cenozoic rock uplift required to produce exposure of the schists.

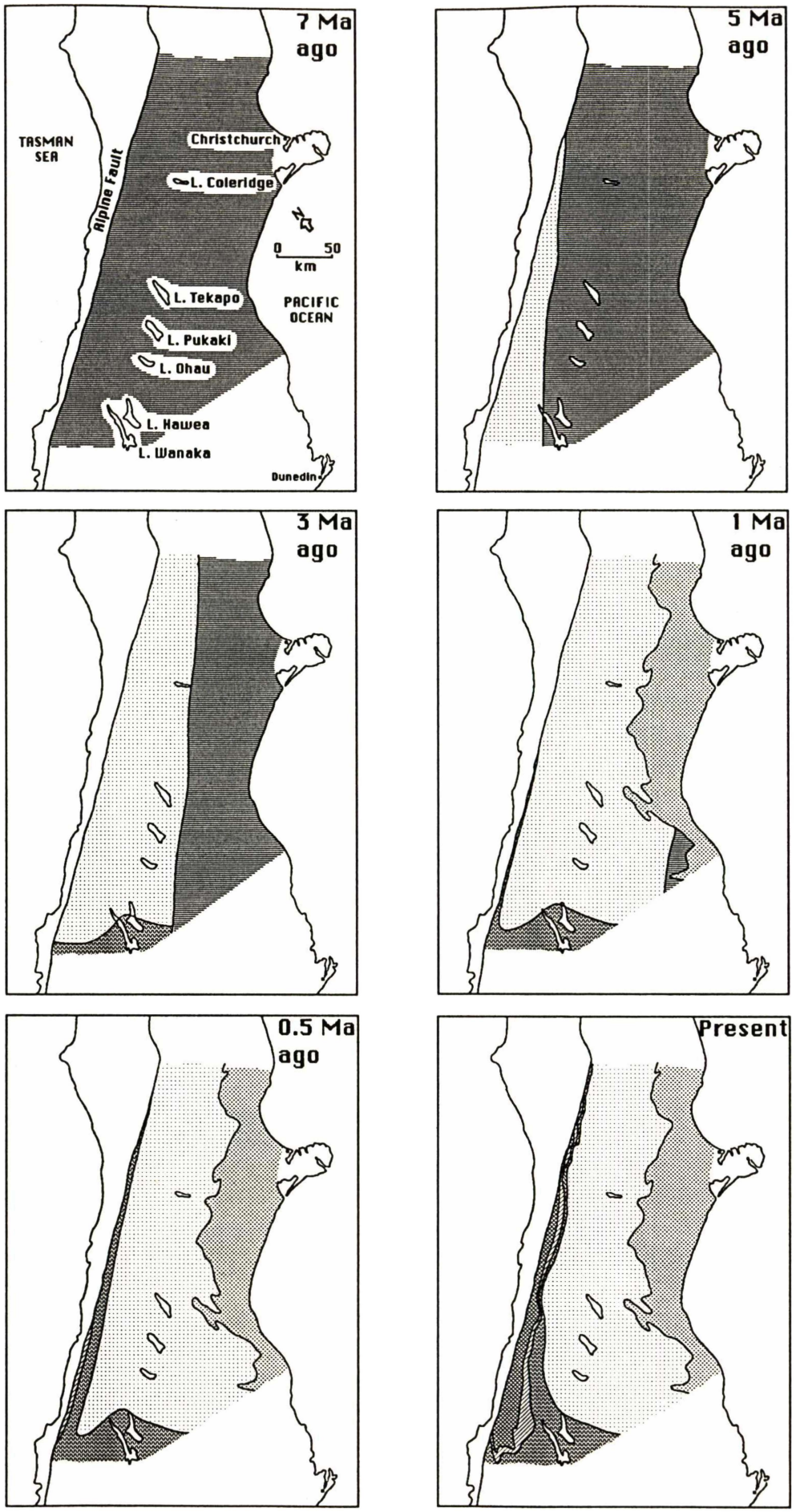

7 Ma ago
TASMAN SEA
Alpine Fault
Christchurch
L. Coleridge
0 50
km
PACIFIC OCEAN
L. Tekapo
L. Pukaki
L. Ohau
L. Hawea
L. Wanaka
Dunedin
5 Ma ago
3 Ma ago
1 Ma ago
0.5 Ma ago
Present

Fig. 7. Maps proposing the history of exhumation of the Southern Alps since 7 Ma ago, with respect to the present geographical configuration of South Island. Shading patterns are the same as for the key in Fig. 6. The map for 7 Ma ago assumes for simplicity that a uniform 1 km thickness of Cenozoic cover rock formerly overlaid the basement. The subsequent pattern of rock exposure is a function of Mesozoic rock uplift, late Cenozoic rock uplift, and mean surface uplift. The mean surface uplift corrections are 0 km for 7 Ma ago and 5 Ma ago, 0.25 km at 3 Ma ago, 0.5 km at 2 Ma ago, 0.75 km at 1 Ma ago and 0.5 Ma ago, and 1 km at the present.

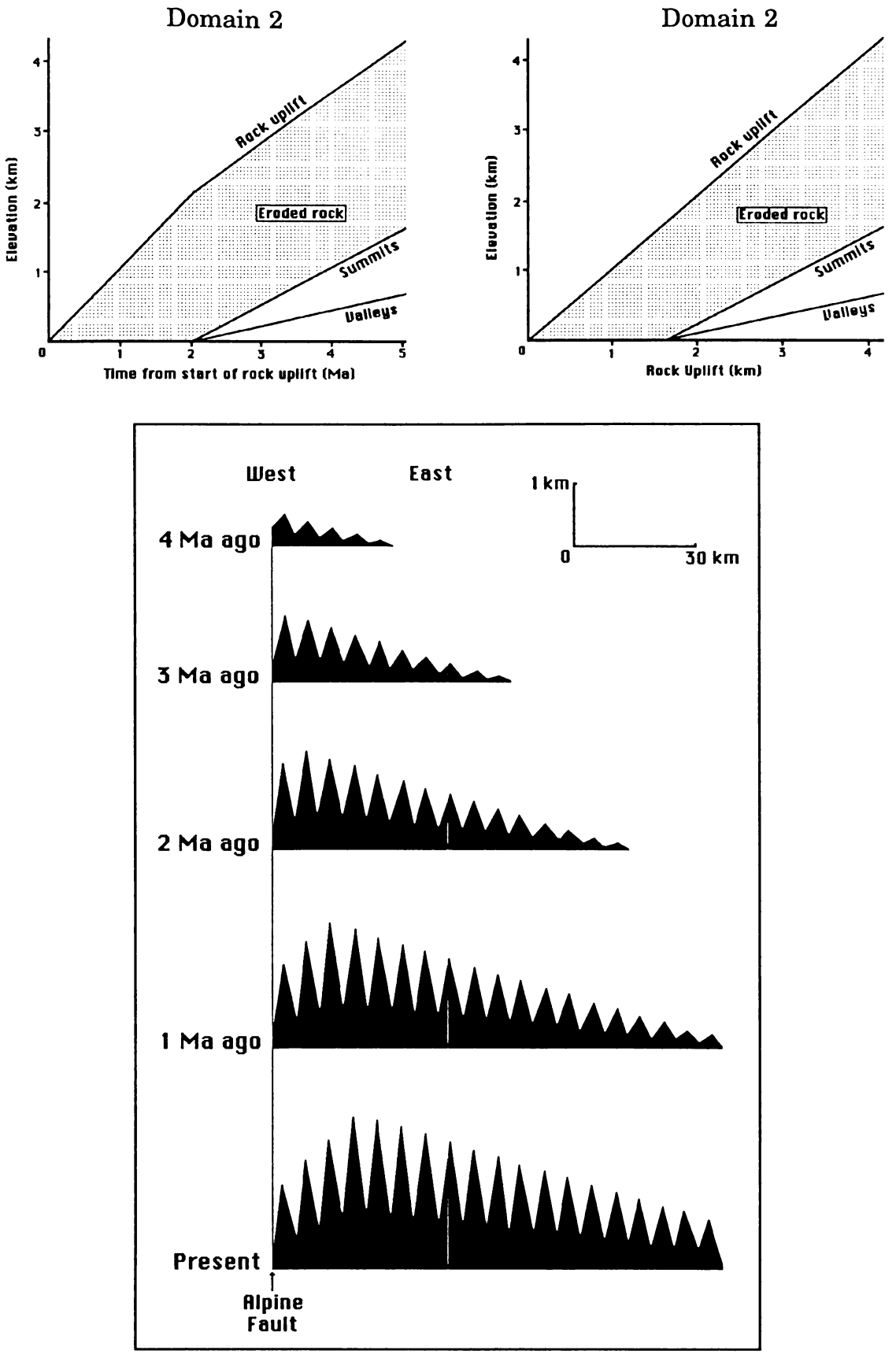


Fig. 8. (Top diagrams) Increase in relief of mountains to the east of the Main Divide with respect to time and the amount of rock uplift, for a transect across the central S. Alps (located on Fig. 1). The volume of eroded rock and the relief of the mountains are shown. The relationships between rock uplift, elevation and relief are from the Godley transect of Tippett and Kamp (submitted). (Bottom diagram) A schematic diagram showing the evolution of the relief of the S. Alps across the same transect.

Landform and relief development

Fig. 8 (top diagrams) shows the increase in the average elevations of the summits and valleys of the mountains in the central region of Domain 2, where the long-term rock uplift rate is 0.8-1.0 mm/a. Almost 2 km of erosion occurred before mean surface uplift began, and erosion has continued during uplift of the mean surface. Mountain elevation and relief have changed with respect to time and the amount of rock uplift, and the mountains are therefore not stable equilibrium forms. The mountains have continued to increase in elevation and evolve in form since the start of uplift. In contrast, in Domain 3 (west of Main Divide) mountain elevations are in a stable equilibrium with respect to rock uplift rate (Tippett and Kamp, submitted).

Fig. 8 (bottom diagram) shows a schematic representation of the evolution of relief for a transect (located on Fig. 1) across the S. Alps, constructed using the constraints described above. The relief diagram assumes that drainage density is constant over time and that incision, rather than rock resistance, controls hillslope inclinations. Features of the diagram include the eastward migration of the Main Divide over time; the evolving relief for any one location to the east of the Main Divide and the quickly-developed constant relief for any one location to the west of the Main Divide; and the cessation of the propagation of surface uplift to the east at about 1 Ma ago.

DISCUSSION

There are strong and consistent relationships between the rock uplift parameters (amount, age, and rate) and elevation/relief parameters in the S. Alps. Therefore the pattern of rock uplift is the primary influence on the landscape development of the S. Alps. Fig. 9 illustrates for a transect (located on Fig. 1) across the central S. Alps, data on the rock uplift amount, age of the start of rock uplift ('uplift age'), late Cenozoic mean rock uplift rate, inferred present rock uplift rate, precipitation, mean surface elevation, and rock type.

There are factors other than uplift that contribute to the nature of landscape development, chiefly those that affect the magnitude and style of erosion. Denudation rates appear to be influenced by climate, elevation, and relief. McSaveney (1978) and Griffiths (1979) suggested that rainfall is the

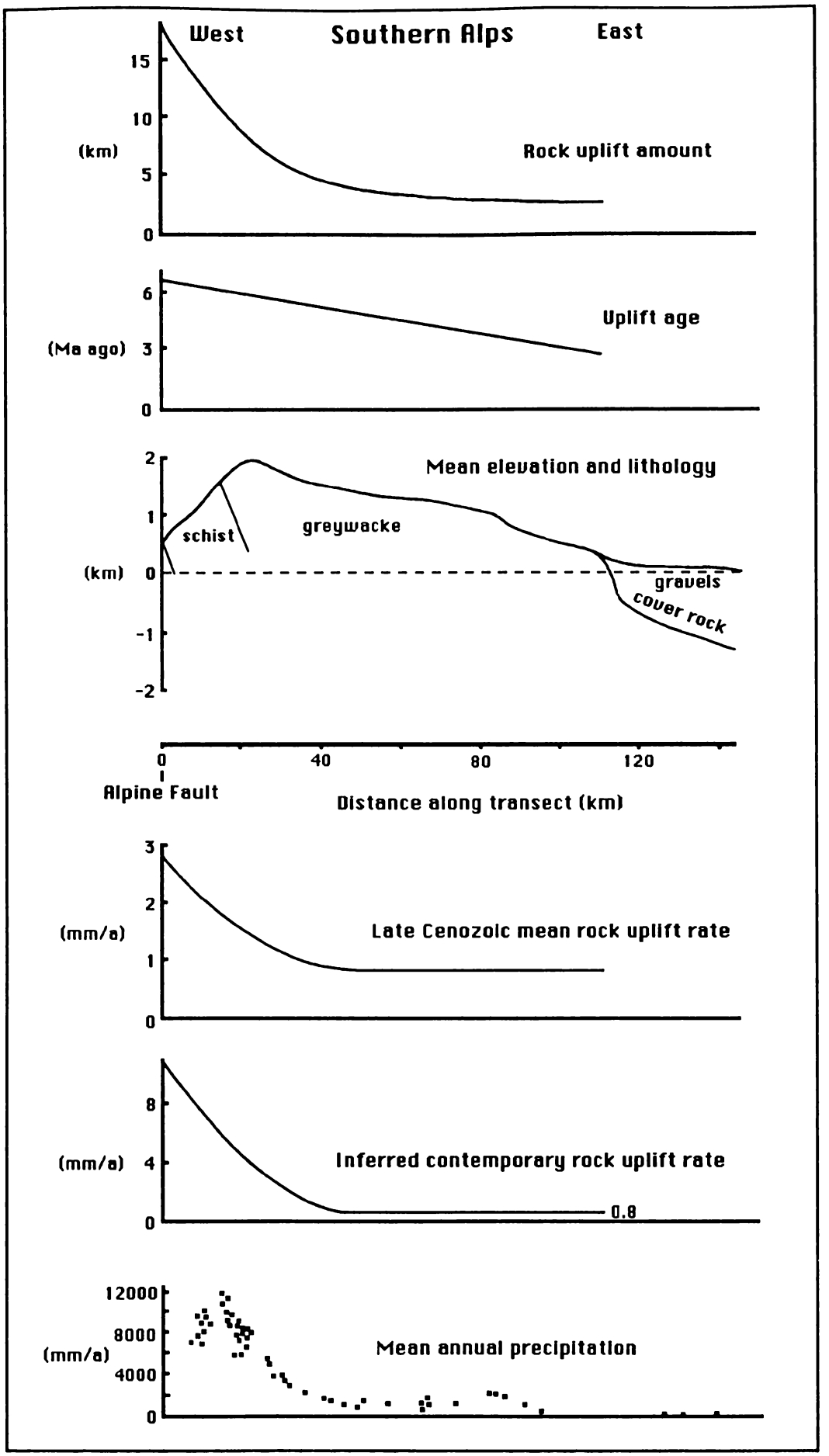


Fig. 9. Variation in rock uplift variables and landscape for a transect across the central S. Alps (located on Fig. 1). Precipitation data are from a transect across the S. Alps ~70 km to the north (Griffiths and McSaveney, 1983).

major influence on contemporary rates of erosion in the S. Alps, although other variables that may affect the erosion rate (rock uplift, relief, vegetation, and geology) were ignored. In contrast, Anhert (1970) showed for 20 mid-latitude river basins from various countries that denudation rate was directly proportional and strongly related to basin relief (range), but was unrelated to mean annual precipitation. Pinet and Souriau (1988) showed in a world-wide study of large drainage basins that mechanical denudation rates are correlated with mean basin elevation, and not with mean annual precipitation. For the S. Alps, Whitehouse (1987) inferred from the river sediment yield data of Griffiths (1979, 1981) that contemporary erosion rates in glaciated and non-glaciated basins are not significantly different.

Oscillatory glacial-interglacial climate changes have occurred in the New Zealand region since ~2.4 Ma ago (e.g. Suggate, 1990). Sea level fluctuations in the order of ~100 m have provided an oscillating base level for landscape-forming processes, and rainfall patterns and rates of weathering have also varied. As the lag times between changes in base level or climate and changes in landscape morphology for mountain ranges are probably large, the nett result may be that, since the onset of glaciations, the landforms of the S. Alps have developed with only small perturbations of form attributable to these fluctuating influences.

The nature of the rock type being eroded may contribute to variation in landscape morphology. Griffiths (1981) suggested that geology has little influence on sediment yield, based on the similarity of suspended sediment concentration ratings for basins of different rock type in the S. Alps. On the other hand, Augustinus (1988) emphasised the contribution of the rock mass strength of the bedrock to the erosion morphology of the S. Alps. Augustinus (1988) found that glaciers exploit structural weaknesses as shown by the correspondence of the orientations of vertical fractures and the trends of glacial valleys in the S. Alps.

In areas of high elevation and relief such as the S. Alps, the climatic parameters of precipitation, temperature, and wind vary as functions of elevation. Uplift, through the development of topography, controls the precipitation pattern, which in turn influences erosion. Elevation and relief, which are dependent on rock uplift, also directly influence the erosion rate through the provision of potential energy. In the S. Alps, the pattern of rock exposure is closely related to the pattern of uplift. Therefore uplift has a fundamental control on landscape development in the S. Alps.

SUMMARY

The Southern Alps (S. Alps) are the topographic manifestation of late Cenozoic uplift of Pacific plate crust in South Island, New Zealand. New data derived by fission track analysis have provided new constraints for the geomorphic evolution of the S. Alps and these have been used to construct a new model. This model emphasises the evolution of rock uplift, rock exposure, and topographic development of the S. Alps. The S. Alps have been studied in terms of domains of differing rock uplift rate. There are 3 domains in the vicinity of the 300 km-long central section of the S. Alps. A high uplift rate domain extends southeastward from the Alpine Fault to just east of the Main Divide. A 0.8-1.0 mm/a uplift rate domain contains the eastern area of the S. Alps. A domain of no uplift lies immediately to the east of the S. Alps, separated from the uplifted parts by a conspicuous 1.0 to 1.5 km step in the basement topography.

The earliest indications of mean surface uplift at the Alpine Fault are inferred at between 4 and 5 Ma ago. The initiation of surface uplift propagated southeastward from the Alpine Fault at a rate of 30 km/Ma. At 5 Ma ago, greywacke was exposed in a narrow zone east of, and for almost the whole length of, the 300 km-long central section of the Alpine Fault. At 3 Ma ago greywacke was exposed across most of the modern S. Alps, and greenschist was exposed in the southern parts of the S. Alps at Lake Wanaka. Greenschist exposure has since propagated northeastward along the Alpine Fault due to continued uplift and associated denudation. Topography at the eastern margin of the S. Alps started to be established between 1.0 and 1.5 Ma ago. For only the last 0.3 Ma does the model predict exposure of amphibolite grade schist. The mountains to the east of the Main Divide have continued to increase in elevation and relief and evolve in form since the start of uplift; the elevation and form of these mountains are related to the age of initiation of rock uplift and the amount of rock uplift. Mountain elevations to the west of the Main Divide are related to the rate of rock uplift.

The age of the start of rock uplift, the amount of rock uplift, and the rate of rock uplift, are considered to be the primary influences on the geomorphic evolution of the Southern Alps of New Zealand.

REFERENCES

Adams, J. 1980. 'Contemporary uplift and erosion of the Southern Alps, New Zealand', *Geol. Soc. Amer. Bull.*, **91**, 1-114.

Adams, J. 1985. 'Large-scale tectonic geomorphology of the Southern Alps, New Zealand', in *Tectonic Geomorphology*, editors M. Morisawa and J. T. Hack, Proc. 15th Ann. Binghamton Geomorphology Symposium, Allen and Unwin, 105-128.

Anhert, F. 1970. 'Functional relationships between denudation, relief, and uplift in large mid-latitude drainage basins', *Amer. J. Sci.*, **268**, 243-263.

Augustinus, P.C. 1988. 'The influence of the lithological and geotechnical properties of rocks on the morphology of glacial valleys', *Unpublished D. Phil. thesis,* University of Waikato, 257 pp.

Essene, E.J. 1989. 'The current status of thermobarometry in metamorphic rocks', in *Evolution of metamorphic belts*, editors J.S. Daly, R.A. Cliff, and B.W.D. Yardley, *Geol. Soc. Spec. Publ.*, **43**, 1-44.

Field, B.D., G.H. Browne and others 1989. 'Cretaceous and Cenozoic sedimentary basins and geological evolution of the Canterbury region, South Island, New Zealand', *N.Z. Geol. Surv. Basin Studies* **2**, 94pp.

Findlay, R.H. 1985. 'Metamorphic low to high 2Vx K-feldspar in kyanite zone rocks within the Alpine schists of Copland Valley, South Westland, New Zealand', *N. Z. J. Geol. Geophys.*, **28**, 77-83.

Grapes, R., and H. Otsuki 1983. 'Peristerite compositions in quartzofeldspathic schists, Franz Josef - Fox Glacier area, New Zealand', *J. Metamorph. Geol.*, **1**, 47-61.

Griffiths, G.A. 1979. 'High sediment yields from major rivers of the Western Southern Alps, New Zealand', *Nature,* **282**, 61-63.

Griffiths, G.A. 1981. 'Some suspended sediment yields from South Island catchments, New Zealand', *Water Res.Bull.*, **17/4**, 662-671.

Griffiths, G.A., and M.J. McSaveney 1983. 'Distribution of mean annual precipitation across some steepland regions of New Zealand', *N.Z. J. Sci.*,**26**, 197-209.

Hicks, S.R. 1989. 'Structure of the Canterbury Plains, New Zealand, from gravity modelling', *New Zealand D.S.I.R. Geophysics Division Research Report* **222**.

Jamieson, R.A., and D. Craw 1987. 'Sphalerite geobarometry in metamorphic terranes: an appraisal with implications for metamorphic pressure in the Otago Schist', *J. Metamorph. Geol.*, **5**, 87-99.

Johnstone, D.C., and S.H. White 1983. 'Shear heating associated with movement along the Alpine fault, New Zealand', *Tectonophysics,* **92,** 241-252.

Kamp, P.J.J. 1986. 'Mid-Cenozoic Challenger Rift System of western New Zealand and its implications for the age of Alpine fault inception', *Geol. Soc. Amer. Bull.,* **97,** 255-281.

Kamp, P.J.J., P.F. Green, and S.H. White 1989. 'Fission track analysis reveals character of collisional tectonics in New Zealand', *Tectonics,* **8,** 169-195.

Kamp, P.J.J. and J.M. Tippett 'Dynamics of Pacific plate continental crust in the South Island collision zone (New Zealand)', *Journal of Geophysical Research,* (submitted).

Koons, P.O. 1989. 'The topographic evolution of collisional mountain belts: a numerical look at the Southern Alps, New Zealand', *American Journal of Science,* **289,** 1041-1069.

McSaveney, M.J. 1978. 'The magnitude of erosion across the Southern Alps', in *Proceedings of a Conference on Erosion Assessment and Control in New Zealand,* New Zealand Association of Soil Conservators, 7-24.

Pinet, P., and M. Souriau 1988. 'Continental erosion and large-scale relief', *Tectonics,* **7/3,** 563-582.

Suggate, R.P., Late Pliocene and Quaternary glaciations of New Zealand, *Quat. Sci. Rev., 9,* 175-197, 1990.

Tippett, J.M. and P.J.J. Kamp 'Fission track analysis of the late Cenozoic vertical kinematics of continental Pacific crust, South Island, New Zealand', *Journal of Geophysical Research,* (in press).

Tippett, J.M., and P.J.J. Kamp 'Fission track analysis enables determination of quantitative relationships between uplift and geomorphology of the Southern Alps, New Zealand', *Earth Surface Processes and Landforms,* (submitted).

Walcott, R.I. 1979. 'Plate motion and shear strain rates in the vicinity of the Southern Alps', *Bull. R. Soc. N. Z.,* **18,**5-12.

Wellman, H.W. 1979. 'An uplift map for the South Island of New Zealand, and a model for the uplift of the Southern Alps', *Bull. R. Soc. N. Z.,* **18,** 13-20.

Whitehouse, I.E. 1986. 'Geomorphology of a compressional plate boundary, Southern Alps, New Zealand', in *International Geomorphology,* chief editor V. Gardiner, John Wiley and Sons Ltd, Part 1, 897-924.

Yardley, B.W.D. 1982. 'The early metamorphic history of the Haast Schists and related rocks of New Zealand', *Contrib. Mineral. Petrol.,* **81,** 317-327.

CHAPTER 8: Summary

This study has quantified the uplift history and geomorphic development of the Southern Alps, New Zealand, using fission track analysis in combination with information on the geomorphology of the Southern Alps.

Vertical kinematics of Pacific plate continental crust in South Island

Fission track analysis of apatite and zircon has been used to investigate the late Cenozoic vertical kinematics of the Pacific continental crust in South Island, New Zealand. New data have been presented that constrain the spatial variations in the amount, age and rate of late Cenozoic rock uplift across the leading edge of the Pacific plate presently in collision with the Australia plate.

The pattern of late Cenozoic uplift is strongly asymmetrical with respect to the Alpine Fault, and varies from a maximum of ~19 km at the Alpine Fault near Fox Glacier, to ~3 km along the eastern margin of the Southern Alps. To the north at Lewis Pass, the maximum uplift is 10 km, and it reaches 8 km at Arawata in the south.

There are major differences along the 300-km long central sector of the Southern Alps in the age of the start of late Cenozoic rock uplift. Uplift started earlier in the southern part of the central Southern Alps (at about 8 Ma ago) than the northern part (5 Ma ago). The uplift age also youngs to the southeast, and the rate of uplift propagation is 30 mm/a in that direction, which exceeds the late Cenozoic average rate of convergence normal to the Alpine Fault of ~8 mm/a. The 8 Ma ago estimate of uplift initiation lags the predicted age (by plate rotation data) of the start of compression across the Alpine Fault by about 2 Ma.

Late Cenozoic uplift rates have averaged no more than 2.8 mm/a right at the Alpine Fault near Fox Glacier, but have been sufficient in 5 - 8 Ma to expose amphibolite grade schist near the Fault. The lowest mean rates of 1 mm/a occur in the southern and eastern parts of the Southern Alps. The mean rates have been sustained for periods of 3 - 8 Ma. Uplift has accelerated over time to reach ~7-10 mm/a at Fox Glacier, with lower rates to the north, south and east. Significant acceleration of cooling and uplift has

occurred only since 1.3 ± 0.3 Ma ago in the Fox Glacier region, which has the highest uplift rates.

From 6.7 to 1.3 Ma ago, cooling rates were in the order of 22°C/Ma, and inferred uplift rates of 0.8 mm/a are too low to have significantly perturbed the geotherms. Geotherms have however been perturbed in areas adjacent to the Alpine Fault in the period of accelerated uplift since 1.3 ± 0.3 Ma ago, as evidenced by the contemporary geothermal gradient of 60° ± 10°C/km [*Allis*, 1981]. The fission track data derived from within the zircon and apatite exhumed annealing zones are unaffected by geotherm perturbation as the uplift of geotherms must have postdated the setting of ages in the respective exhumed annealing zones. Also, the timing of significant perturbation (1.3 Ma ago) even post-dates the uplift of most of the rocks now exposed at the surface that contain reset zircons.

The pattern of increasing uplift rate with increasing proximity to the Alpine Fault suggests that uplift has not been constrained by vertical drag on the Alpine Fault during the late Cenozoic.

Differences between the peak metamorphic temperatures of the host rocks, and the ambient temperatures just prior to late Cenozoic uplift, allow estimates to be made of the amount of Mesozoic uplift across the Southern Alps. These estimates range from negligible uplift north of Arthur's Pass, increasing to ~3 km at Mt Cook, to a maximum of 10 km at Lakes Wanaka and Hawea.

Dynamics of the South Island collision zone

Two claims have been examined in respect of the dynamics of the South Island Pacific plate crust and the dynamics of mountain ranges in general: the claim by *England and Molnar* [1990] that no one to date has produced reliable quantitative estimates of rates of surface uplift in mountain ranges that place useful constraints on tectonic processes, and the assertion by *Koons* [1990] that the South Island collision zone is an example of a two-sided orogen with erosional-mechanical coupling of the two wedges.

England and Molnar [1990] underestimated the potential of fission track thermochronology to quantitatively estimate rates of surface uplift in mountain ranges. This information has been successfully derived in this thesis, including a rigorous estimation of the associated uncertainties, for

the Southern Alps from a combination of topographic data and an extensive fission track data base. The late Cenozoic rate of mean surface uplift in the Southern Alps ranges from <0.1 mm/a adjacent to the Alpine Fault to >0.3 mm/a over most of the area east of the Main Divide. The highest rates of mean surface uplift do not coincide spatially with the regions of highest mean elevation. The rate of work done in elevating the mean surface ranges from ~2.5 mWm^{-2} to ~10 mWm^{-2}, although most areas have experienced similar rates of energy input of ~7.5 mWm^{-2}.

From the fission track data information has been derived about the amounts and rates of denudation, and the isostatic and tectonic components of uplift that are important in better understanding the dynamics of the crust in the continental collision zone. The essential contribution of fission track analysis to estimation of the rates of mean surface uplift lies in estimation of the ages of the start of uplift. The geological setting was favourable to the extent that the initial mean surface elevation was at or near sea level. Resolution of the amounts and rates of denudation and isostatic uplift, and of the amount of tectonic uplift is due largely to the very strong rock uplift signal, and the fact that the uplift has been so recent. The amount of denudation ranges from ~18 km adjacent to the Alpine Fault to ~2 km along the southeast margin of the Southern Alps; the late Cenozoic mean rate of denudation ranges from ~2.5 mm/a at the Fault to ~0.5 mm/a in the southeast parts of the Southern Alps. The amount of tectonic uplift decreases from ~4 km at the Alpine Fault to ~1 km along the Southern Alps' eastern margin. Despite the constraints on the amount and timing of uplift, precise estimates of the rates of tectonic uplift could not be made.

For there to be substantial erosional-mechanical coupling between the two wedges in a two-sided orogen, most of the denudation must occur in the inboard wedge, and be strongly concentrated at its toe [*Koons*, 1990]. This condition is not satisfied in the Southern Alps as half of the total denudation over the 300 km-long central section of the Southern Alps has occurred in the outboard wedge. In addition, it has been shown elsewhere [*Kamp et al.*, 1992] that there has been substantial subsidence and rock uplift of the indentor (Australia plate) during the period of uplift of the Pacific plate; the collision zone throughout its history has not been characterised by a stationary indentor near sealevel.

The nature of the deformation within the Southern Alps

In a comparison of short- and long-term kinematics of the plate boundary zone through New Zealand, *Walcott* [1984] concluded that while at a scale of a few hundred metres faulting is important and the deformation is continuous, at scale lengths of a few tens of kilometres the deformation is continuous and regular, and the effects of faulting can be ignored. Moreover, the plate boundary could be treated as if it were a continuum, with a ductile deformation. The results of this present work, which has been concerned with establishing the long-term uplift (dilatational strain) in central South Island, support and extend this conclusion. The principal conclusions of this study are (i) that the amount of vertical offset on the more major faults within the Pacific plate is a minor proportion of the total amount of surrounding uplift, and (ii) that no major fault displacements occur within the ~50 km wide zone of the central Southern Alps where most of the uplift takes place. The amount of uplift within central South Island increases nearly exponentially with increasing proximity to the Alpine Fault, in a very clear continuum. This pattern is maintained with little variation over 300 km of the Southern Alps parallel to the Alpine Fault. This pattern in itself is indicative of the important role of ductile deformation within the Pacific plate and the role of the Alpine Fault as a major discontinuity.

The relationship between uplift and geomorphology in the Southern Alps

Fission track analysis has provided estimates of the amount, age, and rate of late Cenozoic (<8 Ma ago) uplift for 82 rock samples from the Southern Alps. The mean surface, summit, and valley elevations in the vicinity of each of the rock sample sites have also been measured. This uplift and geomorphic information has been used to quantitatively analyse the nature of the relationship between uplift and geomorphology in the Southern Alps. This has provided insights into long-term landscape evolution in a continental collision setting.

Regression of the geomorphic variables on the uplift variables has enabled quantitative relationships to be established, and shows that there are strong and consistent associations between uplift and the elevations of the mean surface, summits, and valleys. The relationships are linear, and uplift explains 80-90% of the variation in elevation. The relationships are best described by regression models having uniform slope but varying

elevation response between transects. A well constrained pattern of rock uplift propogation southeastwards across the Southern Alps has meant that spatial position can be confidently substituted for time, allowing the evolution of landforms over time to the east of the Main Divide to be studied.

To the east of the Main Divide, estimates of the amount of rock uplift range from 2.8 to 5.5 km, and estimates of the age of the start of uplift range from 2.7 to 6.4 Ma ago. Elevation and relief have increased with increasing amounts of rock uplift and over time. Uplift of the mean surface was delayed for 1.3-3.7 Ma (1.4-2.6 km of rock uplift), depending on transect, after the start of rock uplift. This was probably a result of the stripping of soft Cenozoic rocks that originally overlaid a harder greywacke basement, which gave rise to an initial period of rapid erosion and rock uplift. The regular regression slope for elevation versus rock uplift for the eastern transects, reflects the consistent nature of the interaction between rock uplift and greywacke erodiblilty in the absence of significant climate differences between transects. Variations in response and hence in x-intercept reflect primarily the erosion of variable thicknesses of soft cover rocks, during which the rock uplift rate was >1.0 km/Ma. Once greywacke was exposed, mean surface elevation increased at a constant rate of 0.4 km/km and 0.4 km/Ma of rock uplift, and the rate of rock uplift was 0.8 km/Ma. Summits have increased in elevation at 0.7 km/km and 0.6 km/Ma, and valleys at 0.3 km/km and 0.2 km/Ma of rock uplift. Mean surface elevation has increased as a proportion (0.9) of tectonic uplift, whereas the height of the summits is a function of both tectonic and isostatic uplift. The divergence from common x-intercepts of the regression lines relating mean surface, summit, and valley elevations to rock uplift and uplift age, implies that the mountains to the east of the Main Divide have continued to increase in relief and evolve over time since uplift started. Mountain elevation and relief have little relationship with late Cenozoic mean rock uplift rates of 0.8-1.0 km/Ma and inferred contemporary rock uplift rates of 0.8-1.0 km/Ma (r^2~0.3).

To the west of the Main Divide, elevation is closely related (r^2>0.8) to rock uplift rate, which varies from 1-10 km/Ma; transects where the rock uplift rate is higher (central Southern Alps) support higher topography, and have greater relief. Topography is in a stable equilibrium with rock uplift rate, and the landscape therefore contains no residual evidence of the total amount of rock uplift, or the age of uplift. Lithological variation in the schist rocks along the strike of the Southern Alps to the west of the Main Divide is

not related to elevation, which implies that these rocks effectively have uniform strength.

These results provide constraints for a model of the evolution of the Southern Alps. This study also shows the contribution fission track analysis can make to quantifying landscape evolution in a collisional tectonic setting, particularly where the amount, age, and rate of uplift, and geomorphology, vary spatially.

Geomorphic evolution of the Southern Alps

The new data derived by fission track analysis have provided new constraints for the geomorphic evolution of the Southern Alps and these have been used to construct a new model of the geomorphic evolution of the Southern Alps. In Chapter 3, the patterns of the amount, age of initiation, and rate of rock uplift across the Southern Alps were quantified. This gave information about the history of exhumation of the rocks in the vicinity of the Southern Alps. In Chapter 4, the spatial patterns of the variation in mean surface uplift, rock uplift, and denudation were used to show that the two-sided orogen model of the Southern Alps proposed by Koons [1990] is an inadequate analysis of the development of the Southern Alps. Chapter 5 showed that vertical deformation in the Southern Alps can be treated as ductile and continuous, which suggests that there is probably a smooth continuum of landforms across the Southern Alps. Chapter 6 showed quantitatively that there are strong relationships between the uplift pattern and the present elevation/relief of the Southern Alps. This analysis provided information about the timing and rates of the development of mean surface elevation and relief.

The existing models of the geomorphic development of the Southern Alps - the dynamic cuesta model of *J. Adams* [1980 and 1985] and the numerical model of *Koons* [1989] - are compared with the new data. Particular constraints unrealised by these two earlier models include the following: the earlier timing of the start of rock uplift of the Southern Alps (8 Ma ago); the spatial variation in the timing of the start of rock uplift (8 Ma ago to 3 Ma ago); the lower long-term rock uplift rate (0.8-1.0 mm/a) of the Southern Alps for most of the late Cenozoic; the lag between the start of rock uplift and the start of mean surface uplift; and the patterns of the amounts of late Cenozoic rock uplift and erosion across the Southern Alps.

The new model proposed of the evolution of the Southern Alps emphasises the evolution of rock uplift, rock exposure, and topographic development of the Southern Alps. The Southern Alps have been studied in terms of domains of differing rock uplift rate. There are 3 domains in the vicinity of the 300 km-long central sector of the Southern Alps. A high uplift rate domain extends southeastward from the Alpine Fault to just east of the Main Divide. A 0.8-1.0 mm/a uplift rate domain contains the eastern area of the Southern Alps. A domain of no uplift lies immediately to the east of the Southern Alps, separated from the uplifted parts by a conspicuous 1.0 to 1.5 km step in the basement topography.

The earliest indications of mean surface uplift at the Alpine Fault are inferred at between 4 and 5 Ma ago. The initiation of surface uplift propagated southeastward from the Alpine Fault at a rate of 30 km/Ma. At 5 Ma ago, greywacke was exposed in a narrow zone east of, and for almost the whole length of, the 300 km-long central section of the Alpine Fault. At 3 Ma ago greywacke was exposed across most of the modern Southern Alps, and greenschist was exposed in the southern parts of the Southern Alps at Lake Wanaka. Greenschist exposure has since propagated northeastward along the Alpine Fault due to continued uplift and associated denudation. Topography at the eastern margin of the Southern Alps started to be established between 1.0 and 1.5 Ma ago. For only the last 0.3 Ma does the model predict exposure of amphibolite grade schist. The mountains to the east of the Main Divide have continued to increase in elevation and relief and evolve in form since the start of uplift; the elevation and form of these mountains are related to the age of initiation of rock uplift and the amount of rock uplift. Mountain elevations to the west of the Main Divide are related to the rate of rock uplift.

The age of the start of rock uplift, the amount of rock uplift, and the rate of rock uplift, are considered to be the primary influences on the geomorphic evolution of the Southern Alps.

REFERENCES

Adams, J., Contemporary uplift and erosion of the Southern Alps, New Zealand, *Geol. Soc. Am. Bull., 91,* 1-114, 1980.

Adams, J., Large-scale tectonic geomorphology of the Southern Alps, New Zealand, in *Tectonic Geomorphology*, editors M. Morisawa and J. T. Hack, Proc. 15th Ann. Binghamton Geomorphology Symposium, Allen and Unwin, 105-128, 1985.

England, P., and P. Molnar, Surface uplift, uplift of rocks, and exhumation of rocks, *Geology, 18,* 1173-1177, 1990.

Kamp, P.J.J., P.F. Green and J.M. Tippett, Tectonic architecture of the mountain front-foreland basin transition, South Island, New Zealand, assessed by fission track analysis, *Tectonics, 11*, 98-113, 1992.

Koons, P.O., The topographic evolution of collisional mountain belts: A numerical look at the Southern Alps, New Zealand, *American Journal of Science, 289*, 1041-1069, 1989.

Koons, P.O., Two-sided orogen: Collision and erosion from the sandbox to the Southern Alps, New Zealand, *Geology, 18*, 679-682, 1990.

Walcott, R.I., The kinematics of the plate boundary zone through New Zealand: a comparison of short- and long-term deformations, *Geophysical Journal of the Royal Astronomical Society, 79*, 613-633, 1984.

Data Appendix

Apatite single grain fission track age data
Apatite horizontally confined fission track length data
Zircon single grain fission track age data

8902-20 APATITE matukituki s106/537424 535m

IRRADIATION jmt data:jmt apatite data:matukituki apatites:wk018/15
SLIDE NUMBER 1
COUNTED BY: jmt

No.	Ns	Ni	Na	RATIO	U (ppm)	RHOs (E+06)	RHOi (E+06)	F.TAGE (Ma)
1	0	0	48	0.000	0.0	0.000	0.000	0.0 ± 0.0
2	0	0	49	0.000	0.0	0.000	0.000	0.0 ± 0.0
3	0	0	25	0.000	0.0	0.000	0.000	0.0 ± 0.0
4	0	0	70	0.000	0.0	0.000	0.000	0.0 ± 0.0
5	0	2	49	0.000	0.1	0.000	0.041	0.0 ± 0.0
6	0	2	80	0.000	0.1	0.000	0.025	0.0 ± 0.0
7	0	16	100	0.000	0.5	0.000	0.162	0.0 ± 0.0
8	0	1	100	0.000	0.0	0.000	0.010	0.0 ± 0.0
9	0	1	100	0.000	0.0	0.000	0.010	0.0 ± 0.0
10	0	0	80	0.000	0.0	0.000	0.000	0.0 ± 0.0
11	0	0	80	0.000	0.0	0.000	0.000	0.0 ± 0.0
12	0	0	70	0.000	0.0	0.000	0.000	0.0 ± 0.0
13	0	1	60	0.000	0.0	0.000	0.017	0.0 ± 0.0
14	0	0	60	0.000	0.0	0.000	0.000	0.0 ± 0.0
15	0	3	100	0.000	0.1	0.000	0.030	0.0 ± 0.0
	0	26			0.1	0.000	0.025	

AREA OF BASIC UNIT = 9.89E-07 cm
CHI SQUARED = 6.250499E-07 WITH 14 DEGREES OF FREEDOM
P(chi squared) = 100.0 %
CORRELATION COEFFICIENT = 0.972
VARIANCE OF SQR(Ns) = 0.00
VARIANCE OF SQR(Ni) = 1.21

Ns/Ni = 0.000 ± 0.000
MEAN RATIO = 0.000 ± 0.000

Ages calculated using a zeta of 354.9 ± 4.3 for SRM612 glass
RHO D = 4.580E+06 ; ND = 3623

POOLED AGE = 0.0 ± 0.0 Ma
MEAN AGE = 0.0 ± 0.0 Ma

8902-20 ZIRCON matukituki s106/537424 535m

IRRADIATION jmt data:jmt zircon data:matukituki zircons:wk022/18
SLIDE NUMBER 1
COUNTED BY: jmt

No.	Ns	Ni	Na	RATIO	U (ppm)	RHOs (E+06)	RHOi (E+06)	F.TAGE (Ma)
1	31	68	6	0.456	0.0	5.224	11.459	30.3 ± 6.6
2	13	34	4	0.382	0.0	3.286	8.595	25.5 ± 8.3
	44	102			0.0	4.449	10.313	

AREA OF BASIC UNIT = 9.89E-07 cm
CHI SQUARED = .202053 WITH 1 DEGREES OF FREEDOM
P(chi squared) = 65.3 %
CORRELATION COEFFICIENT = 1.000
VARIANCE OF SQR(Ns) = 1.93
VARIANCE OF SQR(Ni) = 2.92

Ns/Ni = 0.431 ± 0.078
MEAN RATIO = 0.419 ± 0.037

Ages calculated using a zeta of 133.9 ± 1.4 for CN1 glass
RHO D = 9.966E+05 ; ND = 4929

POOLED AGE = 28.7 ± 5.2 Ma
MEAN AGE = 27.9 ± 2.5 Ma

8902-21 APATITE matukituki s106/532411 520m

IRRADIATION jmt data:jmt apatite data:matukituki apatites:wk018/14
SLIDE NUMBER 1
COUNTED BY: jmt

No.	Ns	Ni	Na	RATIO	U (ppm)	RHOs (E+06)	RHOi (E+06)	F.TAGE (Ma)
1	0	8	36	0.000	0.6	0.000	0.225	0.0 ± 0.0
2	0	0	70	0.000	0.0	0.000	0.000	0.0 ± 0.0
3	0	0	60	0.000	0.0	0.000	0.000	0.0 ± 0.0
4	0	8	49	0.000	0.5	0.000	0.165	0.0 ± 0.0
5	0	6	60	0.000	0.3	0.000	0.101	0.0 ± 0.0
6	0	0	24	0.000	0.0	0.000	0.000	0.0 ± 0.0
7	0	1	49	0.000	0.1	0.000	0.021	0.0 ± 0.0
8	0	0	25	0.000	0.0	0.000	0.000	0.0 ± 0.0
9	0	62	49	0.000	3.7	0.000	1.279	0.0 ± 0.0
10	0	0	20	0.000	0.0	0.000	0.000	0.0 ± 0.0
11	0	0	60	0.000	0.0	0.000	0.000	0.0 ± 0.0
12	0	0	42	0.000	0.0	0.000	0.000	0.0 ± 0.0
13	0	0	35	0.000	0.0	0.000	0.000	0.0 ± 0.0
14	0	0	100	0.000	0.0	0.000	0.000	0.0 ± 0.0
15	0	2	40	0.000	0.1	0.000	0.051	0.0 ± 0.0
	0	87			0.4	0.000	0.122	

AREA OF BASIC UNIT = 9.89E-07 cm
CHI SQUARED = 9.875109E-06 WITH 14 DEGREES OF FREEDOM
P(chi squared) = 100.0 %
CORRELATION COEFFICIENT = 0.038
VARIANCE OF SQR(Ns) = 0.00
VARIANCE OF SQR(Ni) = 4.59

Ns/Ni = 0.000 ± 0.000
MEAN RATIO = 0.000 ± 0.000

Ages calculated using a zeta of 354.9 ± 4.3 for SRM612 glass
RHO D = 4.539E+06 ; ND = 3591

POOLED AGE = 0.0 ± 0.0 Ma
MEAN AGE = 0.0 ± 0.0 Ma

8902-21 ZIRCON matukituki s106/532411 520m

IRRADIATION jmt data:jmt zircon data:matukituki zircons:wk022/17
SLIDE NUMBER 1
COUNTED BY: jmt

No.	Ns	Ni	Na	RATIO	U (ppm)	RHOs (E+06)	RHOi (E+06)	F.TAGE (Ma)
1	13	45	3	0.289	0.0	4.382	15.167	19.1 ± 6.0
2	30	49	9	0.612	0.0	3.370	5.505	40.4 ± 9.4
	43	94			0.0	3.623	7.920	

AREA OF BASIC UNIT = 9.89E-07 cm
CHI SQUARED = 3.760524 WITH 1 DEGREES OF FREEDOM
P(chi squared) = 5.2 %
CORRELATION COEFFICIENT = 1.000
VARIANCE OF SQR(Ns) = 1.75
VARIANCE OF SQR(Ni) = 0.04

Ns/Ni = 0.457 ± 0.084
MEAN RATIO = 0.451 ± 0.162

Ages calculated using a zeta of 133.9 ± 1.4 for CN1 glass
RHO D = 9.889E+05 ; ND = 4891

POOLED AGE = 30.2 ± 5.6 Ma
MEAN AGE = 29.8 ± 10.7 Ma

8902-22 APATITE matukituki s114/544348 490m

IRRADIATION jmt data:jmt apatite data:matukituki apatites:wk018/13
SLIDE NUMBER 1
COUNTED BY: jmt

No.	Ns	Ni	Na	RATIO	U (ppm)	RHOs (E+06)	RHOi (E+06)	F.T.AGE (Ma)
1	0	1	12	0.000	0.2	0.000	0.084	0.0 ± 0.0
2	0	0	24	0.000	0.0	0.000	0.000	0.0 ± 0.0
3	0	1	18	0.000	0.2	0.000	0.056	0.0 ± 0.0
4	0	0	18	0.000	0.0	0.000	0.000	0.0 ± 0.0
5	0	0	18	0.000	0.0	0.000	0.000	0.0 ± 0.0
6	0	0	8	0.000	0.0	0.000	0.000	0.0 ± 0.0
7	0	1	16	0.000	0.2	0.000	0.063	0.0 ± 0.0
8	0	0	15	0.000	0.0	0.000	0.000	0.0 ± 0.0
9	0	2	30	0.000	0.2	0.000	0.067	0.0 ± 0.0
10	0	0	9	0.000	0.0	0.000	0.000	0.0 ± 0.0
11	0	0	16	0.000	0.0	0.000	0.000	0.0 ± 0.0
12	0	3	16	0.000	0.6	0.000	0.190	0.0 ± 0.0
13	0	1	28	0.000	0.1	0.000	0.036	0.0 ± 0.0
14	0	0	12	0.000	0.0	0.000	0.000	0.0 ± 0.0
15	0	0	9	0.000	0.0	0.000	0.000	0.0 ± 0.0
	0	9			0.1	0.000	0.037	

AREA OF BASIC UNIT = 9.89E-07 cm
CHI SQUARED = 2.0003E-06 WITH 14 DEGREES OF FREEDOM
P(chi squared) = 100.0 %
CORRELATION COEFFICIENT = 0.729
VARIANCE OF SQR(Ns) = 0.00
VARIANCE OF SQR(Ni) = 0.39

Ns/Ni = 0.000 ± 0.000
MEAN RATIO = 0.000 ± 0.000

Ages calculated using a zeta of 354.9 ± 4.3 for SRM612 glass
RHO D = 4.497E+06 ; ND = 3558

POOLED AGE = 0.0 ± 0.0 Ma
MEAN AGE = 0.0 ± 0.0 Ma

8902-23 APATITE matukituki s114/579341 395m

IRRADIATION jmt data:jmt apatite data:matukituki apatites:wk018/12
SLIDE NUMBER 1
COUNTED BY: jmt

No.	Ns	Ni	Na	RATIO	U (ppm)	RHOs (E+06)	RHOi (E+06)	F.T.AGE (Ma)
1	0	0	100	0.000	0.0	0.000	0.000	0.0 ± 0.0
2	0	0	48	0.000	0.0	0.000	0.000	0.0 ± 0.0
3	0	2	12	0.000	0.5	0.000	0.169	0.0 ± 0.0
4	0	3	30	0.000	0.3	0.000	0.101	0.0 ± 0.0
5	0	7	36	0.000	0.6	0.000	0.197	0.0 ± 0.0
6	0	1	24	0.000	0.1	0.000	0.042	0.0 ± 0.0
7	0	4	30	0.000	0.4	0.000	0.135	0.0 ± 0.0
8	0	1	20	0.000	0.1	0.000	0.051	0.0 ± 0.0
9	0	1	12	0.000	0.2	0.000	0.084	0.0 ± 0.0
10	0	6	30	0.000	0.6	0.000	0.202	0.0 ± 0.0
11	0	2	60	0.000	0.1	0.000	0.034	0.0 ± 0.0
12	0	3	35	0.000	0.3	0.000	0.087	0.0 ± 0.0
13	0	3	48	0.000	0.2	0.000	0.063	0.0 ± 0.0
14	0	18	25	0.000	2.1	0.000	0.728	0.0 ± 0.0
15	0	1	48	0.000	0.1	0.000	0.021	0.0 ± 0.0
	0	52			0.3	0.000	0.094	

AREA OF BASIC UNIT = 9.89E-07 cm
CHI SQUARED = 1.8889E-06 WITH 14 DEGREES OF FREEDOM
P(chi squared) = 100.0 %
CORRELATION COEFFICIENT = 0.893
VARIANCE OF SQR(Ns) = 0.00
VARIANCE OF SQR(Ni) = 1.11

Ns/Ni = 0.000 ± 0.000
MEAN RATIO = 0.000 ± 0.000

Ages calculated using a zeta of 354.9 ± 4.3 for SRM612 glass
RHO D = 4.456E+06 ; ND = 3526

POOLED AGE = 0.0 ± 0.0 Ma
MEAN AGE = 0.0 ± 0.0 Ma

8902-23 ZIRCON matukituki s114/579341 395m

IRRADIATION jmt data:jmt zircon data:matukituki zircons:wk022/16
SLIDE NUMBER 1
COUNTED BY: jmt

No.	Ns	Ni	Na	RATIO	U (ppm)	RHOs (E+06)	RHOi (E+06)	F.T.AGE (Ma)
1	39	39	6	1.000	0.0	6.572	6.572	65.4 ± 14.8
2	30	45	5	0.667	0.0	6.067	9.100	43.6 ± 10.3
3	19	39	14	0.487	0.0	1.372	2.817	31.9 ± 8.9
	88	123			0.0	3.559	4.975	

AREA OF BASIC UNIT = 9.89E-07 cm
CHI SQUARED = 4.20661 WITH 2 DEGREES OF FREEDOM
P(chi squared) = 12.2 %
CORRELATION COEFFICIENT = 0.058
VARIANCE OF SQR(Ns) = 0.90
VARIANCE OF SQR(Ni) = 0.07

Ns/Ni = 0.715 ± 0.100
MEAN RATIO = 0.718 ± 0.150

Ages calculated using a zeta of 133.9 ± 1.4 for CN1 glass
RHO D = 9.812E+05 ; ND = 4853

POOLED AGE = 46.8 ± 6.6 Ma
MEAN AGE = 47.0 ± 9.9 Ma

8902-24 APATITE matukituki s114/590344 455m

IRRADIATION jmt data:jmt apatite data:matukituki apatites:wk018/11
SLIDE NUMBER 1
COUNTED BY: jmt

No.	Ns	Ni	Na	RATIO	U (ppm)	RHOs (E+06)	RHOi (E+06)	F.T.AGE (Ma)
1	0	0	8	0.000	0.0	0.000	0.000	0.0 ± 0.0
2	0	0	35	0.000	0.0	0.000	0.000	0.0 ± 0.0
3	0	4	35	0.000	0.3	0.000	0.116	0.0 ± 0.0
4	0	0	100	0.000	0.0	0.000	0.000	0.0 ± 0.0
5	0	5	18	0.000	0.8	0.000	0.281	0.0 ± 0.0
6	0	0	9	0.000	0.0	0.000	0.000	0.0 ± 0.0
7	0	2	20	0.000	0.3	0.000	0.101	0.0 ± 0.0
8	0	0	16	0.000	0.0	0.000	0.000	0.0 ± 0.0
9	0	0	16	0.000	0.0	0.000	0.000	0.0 ± 0.0
10	0	1	60	0.000	0.1	0.000	0.017	0.0 ± 0.0
11	0	1	16	0.000	0.2	0.000	0.063	0.0 ± 0.0
12	0	0	12	0.000	0.0	0.000	0.000	0.0 ± 0.0
13	0	0	12	0.000	0.0	0.000	0.000	0.0 ± 0.0
14	0	0	20	0.000	0.0	0.000	0.000	0.0 ± 0.0
15	0	0	12	0.000	0.0	0.000	0.000	0.0 ± 0.0
	0	13			0.1	0.000	0.034	

AREA OF BASIC UNIT = 9.89E-07 cm
CHI SQUARED = 1.6002E-06 WITH 14 DEGREES OF FREEDOM
P(chi squared) = 100.0 %
CORRELATION COEFFICIENT = 0.716
VARIANCE OF SQR(Ns) = 0.00
VARIANCE OF SQR(Ni) = 0.64

Ns/Ni = 0.000 ± 0.000
MEAN RATIO = 0.000 ± 0.000

Ages calculated using a zeta of 354.9 ± 4.3 for SRM612 glass
RHO D = 4.415E+06 ; ND = 3493

POOLED AGE = 0.0 ± 0.0 Ma
MEAN AGE = 0.0 ± 0.0 Ma

8902-25 APATITE matukituki s114/629342 365m

IRRADIATION jmt data:jmt apatite data:matukituki apatites:wk018/10
SLIDE NUMBER 1
COUNTED BY: jmt

No.	Ns	Ni	Na	RATIO	U (ppm)	RHOs (E+06)	RHOi (E+06)	F.T.AGE (Ma)
1	0	18	16	0.000	3.4	0.000	1.138	0.0 ± 0.0
2	0	31	16	0.000	5.9	0.000	1.959	0.0 ± 0.0
3	0	14	20	0.000	2.1	0.000	0.708	0.0 ± 0.0
4	0	79	20	0.000	12.0	0.000	3.994	0.0 ± 0.0
5	0	0	12	0.000	0.0	0.000	0.000	0.0 ± 0.0
6	0	1	20	0.000	0.2	0.000	0.051	0.0 ± 0.0
7	0	1	20	0.000	0.2	0.000	0.051	0.0 ± 0.0
8	0	0	36	0.000	0.0	0.000	0.000	0.0 ± 0.0
9	0	10	24	0.000	1.3	0.000	0.421	0.0 ± 0.0
10	0	22	36	0.000	1.8	0.000	0.618	0.0 ± 0.0
11	0	0	30	0.000	0.0	0.000	0.000	0.0 ± 0.0
12	0	13	16	0.000	2.5	0.000	0.822	0.0 ± 0.0
13	0	28	28	0.000	3.0	0.000	1.011	0.0 ± 0.0
14	0	1	16	0.000	0.2	0.000	0.063	0.0 ± 0.0
15	0	1	16	0.000	0.2	0.000	0.063	0.0 ± 0.0
	0	219			2.0	0.000	0.679	

AREA OF BASIC UNIT = 9.89E-07 cm
CHI SQUARED = 1.116668E-05 WITH 14 DEGREES OF FREEDOM
P(chi squared) = 100.0 %
CORRELATION COEFFICIENT = 0.045
VARIANCE OF SQR(Ns) = 0.00
VARIANCE OF SQR(Ni) = 6.75

Ns/Ni = 0.000 ± 0.000
MEAN RATIO = 0.000 ± 0.000

Ages calculated using a zeta of 354.9 ± 4.3 for SRM612 glass
RHO D = 4.374E+06 ; ND = 3460

POOLED AGE = 0.0 ± 0.0 Ma
MEAN AGE = 0.0 ± 0.0 Ma

8902-25 ZIRCON matukituki s114/629342 365m

IRRADIATION jmt data:jmt zircon data:matukituki zircons:wk022/15
SLIDE NUMBER 1
COUNTED BY: jmt

No.	Ns	Ni	Na	RATIO	U (ppm)	RHOs (E+06)	RHOi (E+06)	F.T.AGE (Ma)
1	25	34	4	0.735	0.0	6.320	8.595	47.7 ± 12.6
2	56	55	4	1.018	0.0	14.156	13.903	66.0 ± 12.6
3	40	52	5	0.769	0.0	8.089	10.516	49.9 ± 10.5
4	123	127	15	0.968	0.0	8.291	8.561	62.8 ± 8.0
5	79	82	12	0.963	0.0	6.657	6.909	62.5 ± 9.9
6	64	100	10	0.640	0.0	6.471	10.111	41.6 ± 6.7
7	97	87	10	1.115	0.0	9.808	8.797	72.3 ± 10.7
8	77	55	8	1.400	0.0	9.732	6.951	90.6 ± 16.1
9	12	18	2	0.667	0.0	6.067	9.100	43.3 ± 16.2
10	101	128	15	0.789	0.0	6.808	8.628	51.2 ± 6.9
11	24	36	4	0.667	0.0	6.067	9.100	43.3 ± 11.4
	698	774			0.0	7.930	8.793	

AREA OF BASIC UNIT = 9.89E-07 cm
CHI SQUARED = 18.0873 WITH 10 DEGREES OF FREEDOM
P(chi squared) = 5.4 %
CORRELATION COEFFICIENT = 0.906
VARIANCE OF SQR(Ns) = 5.92
VARIANCE OF SQR(Ni) = 5.26

Ns/Ni = 0.902 ± 0.047
MEAN RATIO = 0.885 ± 0.071

Ages calculated using a zeta of 133.9 ± 1.4 for CN1 glass
RHO D = 9.735E+05 ; ND = 4815

POOLED AGE = 58.5 ± 3.2 Ma
MEAN AGE = 57.4 ± 4.7 Ma

8902-26 APATITE matukituki s114/675363 365m

IRRADIATION jmt data:jmt apatite data:matukituki apatites:wk018/9
SLIDE NUMBER 1
COUNTED BY: jmt

No.	Ns	NI	Na	RATIO	U (ppm)	RHOs (E+06)	RHOi (E+06)	F.T.AGE (Ma)
1	0	3	70	0.000	0.1	0.000	0.043	0.0 ± 0.0
2	0	1	100	0.000	0.0	0.000	0.010	0.0 ± 0.0
3	0	11	100	0.000	0.3	0.000	0.111	0.0 ± 0.0
4	0	0	80	0.000	0.0	0.000	0.000	0.0 ± 0.0
5	0	7	80	0.000	0.3	0.000	0.088	0.0 ± 0.0
6	0	4	80	0.000	0.2	0.000	0.051	0.0 ± 0.0
7	0	2	50	0.000	0.1	0.000	0.040	0.0 ± 0.0
8	0	22	100	0.000	0.7	0.000	0.222	0.0 ± 0.0
9	0	2	100	0.000	0.1	0.000	0.020	0.0 ± 0.0
10	0	6	50	0.000	0.4	0.000	0.121	0.0 ± 0.0
11	0	3	36	0.000	0.3	0.000	0.084	0.0 ± 0.0
12	0	3	100	0.000	0.1	0.000	0.030	0.0 ± 0.0
13	0	3	100	0.000	0.1	0.000	0.030	0.0 ± 0.0
14	0	9	100	0.000	0.3	0.000	0.091	0.0 ± 0.0
15	0	11	100	0.000	0.3	0.000	0.111	0.0 ± 0.0
	0	87			0.2	0.000	0.071	

AREA OF BASIC UNIT = 9.89E-07 cm
CHI SQUARED = 2.954549E-06 WITH 14 DEGREES OF FREEDOM
P(chi squared) = 100.0 %
CORRELATION COEFFICIENT = 0.792
VARIANCE OF SQR(Ns) = 0.00
VARIANCE OF SQR(Ni) = 1.28

Ns/Ni = 0.000 ± 0.000
MEAN RATIO = 0.000 ± 0.000

Ages calculated using a zeta of 354.9 ± 4.3 for SRM612 glass
RHO D = 4.333E+06 ; ND = 3428

POOLED AGE = 0.0 ± 0.0 Ma
MEAN AGE = 0.0 ± 0.0 Ma

8902-27 APATITE matukituki s115/813171 335m

IRRADIATION jmt data:jmt apatite data:matukituki apatites:wk021/1
SLIDE NUMBER 1
COUNTED BY: jmt

No.	Ns	Ni	Na	RATIO	U (ppm)	RHOs (E+06)	RHOi (E+06)	F.T.AGE (Ma)
1	4	110	16	0.036	21.4	0.253	6.951	27.4 ± 14.0
2	6	61	12	0.098	15.8	0.506	5.140	73.9 ± 31.7
3	25	303	20	0.082	47.1	1.264	15.318	62.1 ± 13.0
4	0	1	36	0.000	0.1	0.000	0.028	0.0 ± 0.0
5	4	54	14	0.074	12.0	0.289	3.900	55.8 ± 28.9
6	0	4	35	0.000	0.4	0.000	0.116	0.0 ± 0.0
7	1	38	18	0.026	6.6	0.056	2.135	19.9 ± 20.1
8	7	69	24	0.101	8.9	0.295	2.907	76.3 ± 30.3
9	16	242	24	0.066	31.3	0.674	10.195	49.8 ± 12.9
10	0	1	30	0.000	0.1	0.000	0.034	0.0 ± 0.0
11	15	113	15	0.133	23.4	1.011	7.617	99.6 ± 27.4
12	0	2	32	0.000	0.2	0.000	0.063	0.0 ± 0.0
13	9	139	18	0.065	24.0	0.506	7.808	48.8 ± 16.8
14	0	0	32	0.000	0.0	0.000	0.000	0.0 ± 0.0
15	0	3	16	0.000	0.6	0.000	0.190	0.0 ± 0.0
16	0	5	25	0.000	0.6	0.000	0.202	0.0 ± 0.0
17	0	1	25	0.000	0.1	0.000	0.040	0.0 ± 0.0
18	6	48	28	0.125	5.3	0.217	1.733	93.8 ± 40.7
19	0	21	48	0.000	1.4	0.000	0.442	0.0 ± 0.0
20	0	2	20	0.000	0.3	0.000	0.101	0.0 ± 0.0
	93	1217			7.8	0.193	2.522	

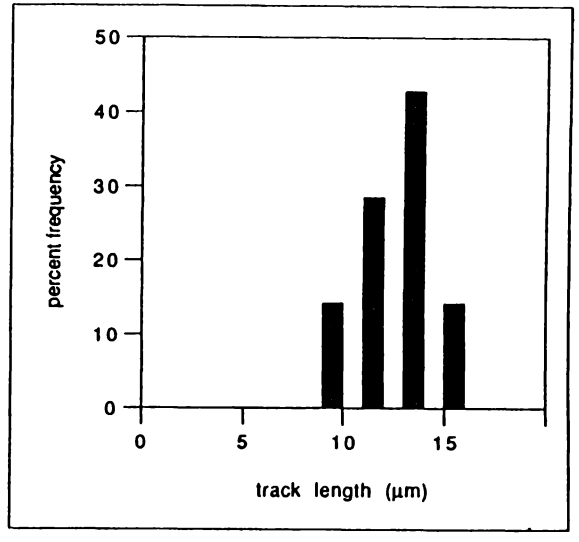
AREA OF BASIC UNIT = 9.89E-07 cm
CHI SQUARED = 13.51166 WITH 19 DEGREES OF FREEDOM
P(chi squared) = 81.1 %
CORRELATION COEFFICIENT = 0.950
VARIANCE OF SQR(Ns) = 2.77
VARIANCE OF SQR(Ni) = 26.90

Ns/Ni = 0.076 ± 0.008
MEAN RATIO = 0.040 ± 0.011

Ages calculated using a zeta of 354.9 ± 4.3 for SRM612 glass
RHO D = 4.261E+06 ; ND = 3371

POOLED AGE = 57.5 ± 6.3 Ma
MEAN AGE = 30.5 ± 8.1 Ma

8902-27



n = 7
Mean = 12.64 µm
Sample std. dev. = 1.64 µm

8902-27 ZIRCON matukituki s115/813171 335m

IRRADIATION jmt data:jmt zircon data:matukituki zircons:wk038/1
SLIDE NUMBER 1
COUNTED BY: jmt

No.	Ns	Ni	Na	RATIO	U (ppm)	RHOs (E+06)	RHOi (E+06)	F.T.AGE (Ma)
1	17	22	3	0.773	0.0	5.730	7.415	54.9 ± 17.7
2	5	4	2	1.250	0.0	2.528	2.022	88.5 ± 59.4
3	30	39	6	0.769	0.0	5.056	6.572	54.6 ± 13.3
4	11	13	2	0.846	0.0	5.561	6.572	60.1 ± 24.6
5	27	19	6	1.421	0.0	4.550	3.202	100.5 ± 30.2
6	20	20	8	1.000	0.0	2.528	2.528	70.9 ± 22.5
7	118	91	24	1.297	0.0	4.971	3.834	91.8 ± 12.9
8	76	59	9	1.288	0.0	8.538	6.628	91.2 ± 15.9
9	35	30	6	1.167	0.0	5.898	5.056	82.7 ± 20.6
10	33	35	9	0.943	0.0	3.707	3.932	66.9 ± 16.3
11	84	47	12	1.787	0.0	7.078	3.960	126.2 ± 23.1
	456	379			0.0	5.300	4.405	

AREA OF BASIC UNIT = 9.89E-07 cm
CHI SQUARED = 13.01671 WITH 10 DEGREES OF FREEDOM
P(chi squared) = 22.3 %
CORRELATION COEFFICIENT = 0.952
VARIANCE OF SQR(Ns) = 6.92
VARIANCE OF SQR(Ni) = 4.25

Ns/Ni = 1.203 ± 0.084
MEAN RATIO = 1.140 ± 0.094

Ages calculated using a zeta of 133.9 ± 1.4 for CN1 glass
RHO D = 1.065E+06 ; ND = 5265

POOLED AGE = 85.2 ± 6.1 Ma
MEAN AGE = 80.8 ± 6.8 Ma

8902-28 APATITE matukituki s124/994072 120m

IRRADIATION jmt data:jmt apatite data:matukituki apatites:wk018/8
SLIDE NUMBER 1
COUNTED BY: jmt

No.	Ns	Ni	Na	RATIO	U (ppm)	RHOs (E+06)	RHOi (E+06)	F.T.AGE (Ma)
1	71	826	30	0.086	85.0	2.393	27.840	65.1 ± 8.2
2	0	0	30	0.000	0.0	0.000	0.000	0.0 ± 0.0
3	0	3	50	0.000	0.2	0.000	0.061	0.0 ± 0.0
4	0	0	30	0.000	0.0	0.000	0.000	0.0 ± 0.0
5	0	0	36	0.000	0.0	0.000	0.000	0.0 ± 0.0
6	14	229	36	0.061	19.6	0.393	6.432	46.4 ± 12.8
7	0	0	45	0.000	0.0	0.000	0.000	0.0 ± 0.0
8	0	0	36	0.000	0.0	0.000	0.000	0.0 ± 0.0
9	0	25	60	0.000	1.3	0.000	0.421	0.0 ± 0.0
10	0	37	40	0.000	2.9	0.000	0.935	0.0 ± 0.0
11	0	14	16	0.000	2.7	0.000	0.885	0.0 ± 0.0
12	0	5	80	0.000	0.2	0.000	0.063	0.0 ± 0.0
13	0	1	15	0.000	0.2	0.000	0.067	0.0 ± 0.0
14	0	12	24	0.000	1.5	0.000	0.506	0.0 ± 0.0
15	0	0	25	0.000	0.0	0.000	0.000	0.0 ± 0.0
16	0	4	36	0.000	0.3	0.000	0.112	0.0 ± 0.0
17	2	56	49	0.036	3.5	0.041	1.156	27.1 ± 19.5
18	0	0	28	0.000	0.0	0.000	0.000	0.0 ± 0.0
19	1	50	18	0.020	8.6	0.056	2.809	15.2 ± 15.4
20	0	1	40	0.000	0.1	0.000	0.025	0.0 ± 0.0
	88	1263			5.4	0.123	1.764	

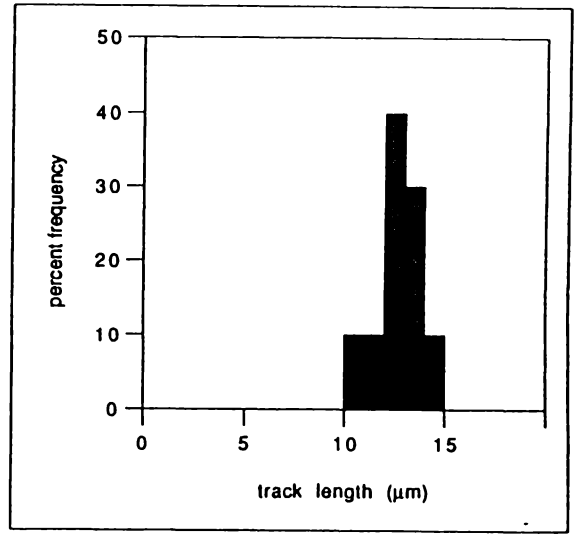
AREA OF BASIC UNIT = 9.89E-07 cm
CHI SQUARED = 12.85759 WITH 19 DEGREES OF FREEDOM
P(chi squared) = 84.6 %
CORRELATION COEFFICIENT = 0.995
VARIANCE OF SQR(Ns) = 4.07
VARIANCE OF SQR(Ni) = 47.59

Ns/Ni = 0.070 ± 0.008
MEAN RATIO = 0.010 ± 0.005

Ages calculated using a zeta of 354.9 ± 4.3 for SRM612 glass
RHO D = 4.291E+06 ; ND = 3395

POOLED AGE = 52.8 ± 5.9 Ma
MEAN AGE = 7.7 ± 4.0 Ma

8902-28



n = 10
Mean = 12.91 µm
Sample std. dev. = 0.98 µm

8902-28 ZIRCON matukituki s124/994072 120m

IRRADIATION jmt data:jmt zircon data:matukituki zircons:wk038/2
SLIDE NUMBER 1
COUNTED BY: jmt

No.	Ns	Ni	Na	RATIO	U (ppm)	RHOs (E+06)	RHOi (E+06)	F.TAGE (Ma)
1	30	13	2	2.308	0.0	15.167	6.572	162.5 ± 54.0
2	81	54	6	1.500	0.0	13.650	9.100	106.1 ± 18.7
3	9	6	3	1.500	0.0	3.033	2.022	106.1 ± 55.9
4	204	107	12	1.907	0.0	17.189	9.016	134.5 ± 16.2
5	90	66	6	1.364	0.0	15.167	11.122	96.5 ± 15.7
6	32	15	2	2.133	0.0	16.178	7.583	150.3 ± 47.1
7	21	19	3	1.105	0.0	7.078	6.404	78.3 ± 24.8
8	72	67	6	1.075	0.0	12.133	11.291	76.2 ± 13.0
9	49	50	4	0.980	0.0	12.386	12.639	69.5 ± 14.0
	588	397			0.0	13.512	9.123	

AREA OF BASIC UNIT = 9.89E-07 cm
CHI SQUARED = 16.69743 WITH 8 DEGREES OF FREEDOM
P(chi squared) = 3.3 %
CORRELATION COEFFICIENT = 0.935
VARIANCE OF SQR(Ns) = 11.21
VARIANCE OF SQR(Ni) = 7.06

Ns/Ni = 1.481 ± 0.096
MEAN RATIO = 1.541 ± 0.159

Ages calculated using a zeta of 133.9 ± 1.4 for CN1 glass
RHO D = 1.065E+06 ; ND = 5265

POOLED AGE = 104.8 ± 7.0 Ma
MEAN AGE = 109.0 ± 11.4 Ma

8902-29 APATITE matukituki s124/110934 290m

IRRADIATION jmt data:jmt apatite data:matukituki apatites:wk018/7
SLIDE NUMBER 1
COUNTED BY: jmt

No.	Ns	Ni	Na	RATIO	U (ppm)	RHOs (E+06)	RHOi (E+06)	F.T.AGE (Ma)
1	3	62	28	0.048	6.9	0.108	2.239	36.4 ± 21.5
2	22	228	35	0.096	20.3	0.636	6.587	72.4 ± 16.2
3	0	0	16	0.000	0.0	0.000	0.000	0.0 ± 0.0
4	4	228	35	0.018	20.3	0.116	6.587	13.2 ± 6.7
5	0	0	49	0.000	0.0	0.000	0.000	0.0 ± 0.0
6	8	127	15	0.063	26.4	0.539	8.561	47.3 ± 17.3
7	9	188	25	0.048	23.4	0.364	7.604	36.0 ± 12.3
8	0	1	40	0.000	0.1	0.000	0.025	0.0 ± 0.0
9	8	98	8	0.082	38.2	1.011	12.386	61.3 ± 22.6
10	3	32	12	0.094	8.3	0.253	2.696	70.3 ± 42.5
11	7	50	12	0.140	13.0	0.590	4.213	104.7 ± 42.3
12	3	80	30	0.038	8.3	0.101	2.696	28.2 ± 16.6
13	0	1	25	0.000	0.1	0.000	0.040	0.0 ± 0.0
14	10	115	8	0.087	44.8	1.264	14.535	65.2 ± 21.6
15	34	633	28	0.054	70.5	1.228	22.859	40.4 ± 7.2
16	0	1	16	0.000	0.2	0.000	0.063	0.0 ± 0.0
17	0	0	50	0.000	0.0	0.000	0.000	0.0 ± 0.0
18	0	1	25	0.000	0.1	0.000	0.040	0.0 ± 0.0
19	0	0	20	0.000	0.0	0.000	0.000	0.0 ± 0.0
20	0	2	20	0.000	0.3	0.000	0.101	0.0 ± 0.0
21	0	0	12	0.000	0.0	0.000	0.000	0.0 ± 0.0
22	0	3	70	0.000	0.1	0.000	0.043	0.0 ± 0.0
23	5	93	16	0.054	18.1	0.316	5.877	40.4 ± 18.6
24	2	72	30	0.028	7.5	0.067	2.427	20.9 ± 15.0
25	0	0	9	0.000	0.0	0.000	0.000	0.0 ± 0.0
26	0	0	16	0.000	0.0	0.000	0.000	0.0 ± 0.0
27	0	0	25	0.000	0.0	0.000	0.000	0.0 ± 0.0
28	0	1	14	0.000	0.2	0.000	0.072	0.0 ± 0.0
29	0	1	36	0.000	0.1	0.000	0.028	0.0 ± 0.0
30	2	58	12	0.034	15.1	0.169	4.887	26.0 ± 18.7
31	9	63	6	0.143	32.7	1.517	10.617	106.8 ± 38.1
32	0	0	80	0.000	0.0	0.000	0.000	0.0 ± 0.0
33	6	108	30	0.056	11.2	0.202	3.640	41.8 ± 17.5
34	7	197	20	0.036	30.7	0.354	9.960	26.7 ± 10.3
35	8	104	30	0.077	10.8	0.270	3.505	57.8 ± 21.2
36	6	111	24	0.054	14.4	0.253	4.676	40.6 ± 17.1
37	4	93	8	0.043	36.2	0.506	11.754	32.4 ± 16.5
38	27	228	24	0.118	29.6	1.138	9.606	88.7 ± 18.1
39	15	176	20	0.085	27.4	0.758	8.898	64.0 ± 17.3
40	0	0	32	0.000	0.0	0.000	0.000	0.0 ± 0.0
	202	3155			9.7	0.202	3.155	

AREA OF BASIC UNIT = 9.89E-07 cm
CHI SQUARED = 41.97227 WITH 39 DEGREES OF FREEDOM
P(chi squared) = 34.3 %
CORRELATION COEFFICIENT = 0.890

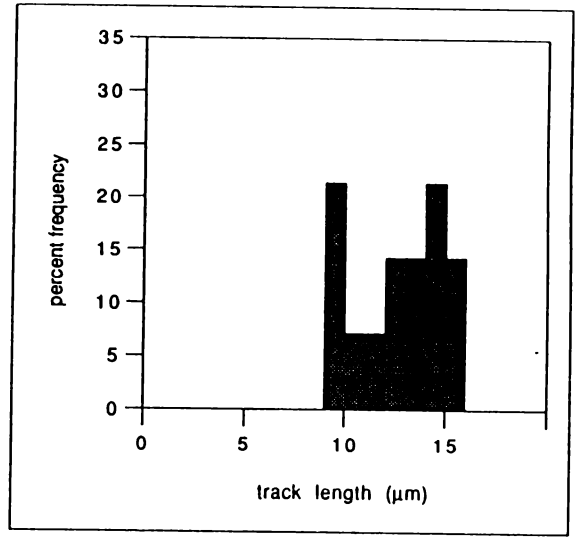
VARIANCE OF SQR(Ns) = 2.74
VARIANCE OF SQR(Ni) = 38.69

Ns/Ni = 0.064 ± 0.005
MEAN RATIO = 0.037 ± 0.007

Ages calculated using a zeta of 354.9 ± 4.3 for SRM612 glass
RHO D = 4.250E+06 ; ND = 3363

POOLED AGE = 48.1 ± 3.6 Ma
MEAN AGE = 28.1 ± 5.1 Ma

8902-29



n = 14
Mean = 12.66 µm
Sample std. dev. = 2.11 µm

8902-29 ZIRCON matukituki s124/110934 290m

IRRADIATION jmt data:jmt zircon data:matukituki zircons:wk022/12
SLIDE NUMBER 1
COUNTED BY: jmt

No.	Ns	Ni	Na	RATIO	U (ppm)	RHOs (E+06)	RHOi (E+06)	F.T.AGE (Ma)
1	124	78	27	1.590	0.0	4.644	2.921	100.4 ± 14.6
2	38	28	6	1.357	0.0	6.404	4.719	85.8 ± 21.4
3	52	38	9	1.368	0.0	5.842	4.269	86.5 ± 18.5
4	44	32	6	1.375	0.0	7.415	5.393	86.9 ± 20.2
5	58	53	15	1.094	0.0	3.910	3.573	69.3 ± 13.2
6	133	121	28	1.099	0.0	4.803	4.369	69.6 ± 8.8
7	105	60	9	1.750	0.0	11.796	6.741	110.4 ± 18.0
8	78	72	9	1.083	0.0	8.763	8.089	68.6 ± 11.3
9	95	70	12	1.357	0.0	8.005	5.898	85.8 ± 13.6
10	116	87	15	1.333	0.0	7.819	5.865	84.3 ± 12.0
11	103	67	9	1.537	0.0	11.572	7.527	97.1 ± 15.3
12	241	136	30	1.772	0.0	8.123	4.584	111.8 ± 12.2
13	131	102	16	1.284	0.0	8.279	6.446	81.2 ± 10.8
	1318	944			0.0	6.977	4.997	

AREA OF BASIC UNIT = 9.89E-07 cm
CHI SQUARED = 16.38617 WITH 12 DEGREES OF FREEDOM
P(chi squared) = 17.4 %
CORRELATION COEFFICIENT = 0.917
VARIANCE OF SQR(Ns) = 6.43
VARIANCE OF SQR(Ni) = 3.76

Ns/Ni = 1.396 ± 0.060
MEAN RATIO = 1.385 ± 0.063

Ages calculated using a zeta of 133.9 ± 1.4 for CN1 glass
RHO D = 9.504E+05 ; ND = 4700

POOLED AGE = 88.2 ± 4.1 Ma
MEAN AGE = 87.5 ± 4.3 Ma

8902-30 APATITE matukituki s124/043885 610m

IRRADIATION jmt data:jmt apatite data:matukituki apatites:wk018/6
SLIDE NUMBER 1
COUNTED BY: jmt

No.	Ns	Ni	Na	RATIO	U (ppm)	RHOs (E+06)	RHOi (E+06)	F.T.AGE (Ma)
1	0	0	80	0.000	0.0	0.000	0.000	0.0 ± 0.0
2	0	0	35	0.000	0.0	0.000	0.000	0.0 ± 0.0
3	0	0	15	0.000	0.0	0.000	0.000	0.0 ± 0.0
4	0	0	49	0.000	0.0	0.000	0.000	0.0 ± 0.0
5	0	0	30	0.000	0.0	0.000	0.000	0.0 ± 0.0
6	0	0	27	0.000	0.0	0.000	0.000	0.0 ± 0.0
7	0	0	32	0.000	0.0	0.000	0.000	0.0 ± 0.0
8	0	0	25	0.000	0.0	0.000	0.000	0.0 ± 0.0
9	0	1	36	0.000	0.1	0.000	0.028	0.0 ± 0.0
10	0	0	36	0.000	0.0	0.000	0.000	0.0 ± 0.0
11	0	10	80	0.000	0.4	0.000	0.126	0.0 ± 0.0
12	0	0	49	0.000	0.0	0.000	0.000	0.0 ± 0.0
13	0	1	24	0.000	0.1	0.000	0.042	0.0 ± 0.0
14	0	4	16	0.000	0.8	0.000	0.253	0.0 ± 0.0
15	0	1	80	0.000	0.0	0.000	0.013	0.0 ± 0.0
	0	17			0.1	0.000	0.028	

AREA OF BASIC UNIT = 9.89E-07 cm
CHI SQUARED = 7.000099E-07 WITH 14 DEGREES OF FREEDOM
P(chi squared) = 100.0 %
CORRELATION COEFFICIENT = 0.919
VARIANCE OF SQR(Ns) = 0.00
VARIANCE OF SQR(Ni) = 0.89

Ns/Ni = 0.000 ± 0.000
MEAN RATIO = 0.000 ± 0.000

Ages calculated using a zeta of 354.9 ± 4.3 for SRM612 glass
RHO D = 4.209E+06 ; ND = 3330

POOLED AGE = 0.0 ± 0.0 Ma
MEAN AGE = 0.0 ± 0.0 Ma

8902-30 ZIRCON matukituki s124/043885 610m

IRRADIATION jmt data:jmt zircon data:matukituki zircons:wk038/3
SLIDE NUMBER 1
COUNTED BY: jmt

No.	Ns	Ni	Na	RATIO	U (ppm)	RHOs (E+06)	RHOi (E+06)	F.T.AGE (Ma)
1	28	21	4	1.333	0.0	7.078	5.308	94.4 ± 27.3
2	88	69	7	1.275	0.0	12.711	9.967	90.3 ± 14.6
3	18	14	2	1.286	0.0	9.100	7.078	91.0 ± 32.5
4	28	18	4	1.556	0.0	7.078	4.550	110.0 ± 33.3
	162	122			0.0	9.635	7.256	

AREA OF BASIC UNIT = 9.89E-07 cm
CHI SQUARED = .3463438 WITH 3 DEGREES OF FREEDOM
P(chi squared) = 95.1 %
CORRELATION COEFFICIENT = 0.998
VARIANCE OF SQR(Ns) = 5.17
VARIANCE OF SQR(Ni) = 4.36

Ns/Ni = 1.328 ± 0.159
MEAN RATIO = 1.362 ± 0.066

Ages calculated using a zeta of 133.9 ± 1.4 for CN1 glass
RHO D = 1.065E+06 ; ND = 5265

POOLED AGE = 94.0 ± 11.4 Ma
MEAN AGE = 96.4 ± 4.9 Ma

8902-31 APATITE matukituki s124/026895 870m

IRRADIATION jmt data:jmt apatite data:matukituki apatites:wk018/5
SLIDE NUMBER 1
COUNTED BY: jmt

No.	Ns	Ni	Na	RATIO	U (ppm)	RHOs (E+06)	RHOi (E+06)	F.T.AGE (Ma)
1	0	1	50	0.000	0.1	0.000	0.020	0.0 ± 0.0
2	5	88	12	0.057	23.3	0.421	7.415	41.9 ± 19.3
3	0	0	16	0.000	0.0	0.000	0.000	0.0 ± 0.0
4	0	0	12	0.000	0.0	0.000	0.000	0.0 ± 0.0
5	0	32	20	0.000	5.1	0.000	1.618	0.0 ± 0.0
6	0	2	24	0.000	0.3	0.000	0.084	0.0 ± 0.0
7	0	0	40	0.000	0.0	0.000	0.000	0.0 ± 0.0
8	0	0	48	0.000	0.0	0.000	0.000	0.0 ± 0.0
9	0	2	50	0.000	0.1	0.000	0.040	0.0 ± 0.0
10	0	2	30	0.000	0.2	0.000	0.067	0.0 ± 0.0
11	0	1	18	0.000	0.2	0.000	0.056	0.0 ± 0.0
12	0	0	42	0.000	0.0	0.000	0.000	0.0 ± 0.0
13	0	0	30	0.000	0.0	0.000	0.000	0.0 ± 0.0
14	0	0	20	0.000	0.0	0.000	0.000	0.0 ± 0.0
15	0	0	15	0.000	0.0	0.000	0.000	0.0 ± 0.0
16	0	0	30	0.000	0.0	0.000	0.000	0.0 ± 0.0
17	0	1	50	0.000	0.1	0.000	0.020	0.0 ± 0.0
18	0	2	30	0.000	0.2	0.000	0.067	0.0 ± 0.0
19	3	89	16	0.034	17.7	0.190	5.624	24.9 ± 14.6
20	0	0	20	0.000	0.0	0.000	0.000	0.0 ± 0.0
	8	220			1.2	0.014	0.388	

AREA OF BASIC UNIT = 9.89E-07 cm
CHI SQUARED = 2.538404 WITH 19 DEGREES OF FREEDOM
P(chi squared) = 100.0 %
CORRELATION COEFFICIENT = 0.933
VARIANCE OF SQR(Ns) = 0.38
VARIANCE OF SQR(Ni) = 8.69

Ns/Ni = 0.036 ± 0.013
MEAN RATIO = 0.005 ± 0.003

Ages calculated using a zeta of 354.9 ± 4.3 for SRM612 glass
RHO D = 4.168E+06 ; ND = 3297

POOLED AGE = 26.8 ± 9.7 Ma
MEAN AGE = 3.3 ± 2.4 Ma

8902-31 ZIRCON matukituki s124/026895 870m

IRRADIATION jmt data:jmt zircon data:matukituki zircons:wk022/10
SLIDE NUMBER 1
COUNTED BY: jmt

No.	Ns	Ni	Na	RATIO	U (ppm)	RHOs (E+06)	RHOi (E+06)	F.T.AGE (Ma)
1	102	74	18	1.378	0.0	5.730	4.157	85.7 ± 13.2
2	128	87	20	1.471	0.0	6.471	4.398	91.4 ± 12.8
3	59	48	10	1.229	0.0	5.966	4.853	76.5 ± 14.9
4	98	69	12	1.420	0.0	8.257	5.814	88.3 ± 14.0
5	106	83	18	1.277	0.0	5.954	4.662	79.5 ± 11.7
6	91	48	21	1.896	0.0	4.382	2.311	117.6 ± 21.1
7	30	20	3	1.500	0.0	10.111	6.741	93.2 ± 27.0
8	57	41	9	1.390	0.0	6.404	4.606	86.4 ± 17.8
9	88	49	10	1.796	0.0	8.898	4.954	111.5 ± 20.0
10	36	29	6	1.241	0.0	6.067	4.887	77.2 ± 19.3
	795	548			0.0	6.329	4.363	

AREA OF BASIC UNIT = 9.89E-07 cm
CHI SQUARED = 5.77732 WITH 9 DEGREES OF FREEDOM
P(chi squared) = 76.2 %
CORRELATION COEFFICIENT = 0.940
VARIANCE OF SQR(Ns) = 3.77
VARIANCE OF SQR(Ni) = 2.54

Ns/Ni = 1.451 ± 0.081
MEAN RATIO = 1.460 ± 0.071

Ages calculated using a zeta of 133.9 ± 1.4 for CN1 glass
RHO D = 9.350E+05 ; ND = 4624

POOLED AGE = 90.2 ± 5.3 Ma
MEAN AGE = 90.7 ± 4.7 Ma

8902-32 APATITE matukituki s124/017905 1400m

IRRADIATION jmt data:jmt apatite data:matukituki apatites:wk018/4
SLIDE NUMBER 1
COUNTED BY: jmt

No.	Ns	Ni	Na	RATIO	U (ppm)	RHOs (E+06)	RHOi (E+06)	F.T.AGE (Ma)
1	0	0	70	0.000	0.0	0.000	0.000	0.0 ± 0.0
2	0	0	36	0.000	0.0	0.000	0.000	0.0 ± 0.0
3	0	0	49	0.000	0.0	0.000	0.000	0.0 ± 0.0
4	0	1	60	0.000	0.1	0.000	0.017	0.0 ± 0.0
5	0	18	48	0.000	1.2	0.000	0.379	0.0 ± 0.0
6	0	1	28	0.000	0.1	0.000	0.036	0.0 ± 0.0
7	0	1	25	0.000	0.1	0.000	0.040	0.0 ± 0.0
8	0	0	24	0.000	0.0	0.000	0.000	0.0 ± 0.0
9	0	0	20	0.000	0.0	0.000	0.000	0.0 ± 0.0
10	0	0	40	0.000	0.0	0.000	0.000	0.0 ± 0.0
11	0	0	49	0.000	0.0	0.000	0.000	0.0 ± 0.0
12	0	2	49	0.000	0.1	0.000	0.041	0.0 ± 0.0
13	0	0	60	0.000	0.0	0.000	0.000	0.0 ± 0.0
14	0	2	36	0.000	0.2	0.000	0.056	0.0 ± 0.0
15	0	0	25	0.000	0.0	0.000	0.000	0.0 ± 0.0
	0	25			0.1	0.000	0.041	

AREA OF BASIC UNIT = 9.89E-07 cm
CHI SQUARED = 3.888937E-07 WITH 14 DEGREES OF FREEDOM
P(chi squared) = 100.0 %
CORRELATION COEFFICIENT = 0.987
VARIANCE OF SQR(Ns) = 0.00
VARIANCE OF SQR(Ni) = 1.30

Ns/Ni = 0.000 ± 0.000
MEAN RATIO = 0.000 ± 0.000

Ages calculated using a zeta of 354.9 ± 4.3 for SRM612 glass
RHO D = 4.127E+06 ; ND = 3265

POOLED AGE = 0.0 ± 0.0 Ma
MEAN AGE = 0.0 ± 0.0 Ma

8902-33 APATITE matukituki s124/011909 1630m

IRRADIATION jmt data:jmt apatite data:matukituki apatites:wk018/3
SLIDE NUMBER 1
COUNTED BY: jmt

No.	Ns	Ni	Na	RATIO	U (ppm)	RHOs (E+06)	RHOi (E+06)	F.TAGE (Ma)
1	0	2	48	0.000	0.1	0.000	0.042	0.0 ± 0.0
2	0	3	80	0.000	0.1	0.000	0.038	0.0 ± 0.0
3	0	0	80	0.000	0.0	0.000	0.000	0.0 ± 0.0
4	0	15	50	0.000	1.0	0.000	0.303	0.0 ± 0.0
5	0	3	70	0.000	0.1	0.000	0.043	0.0 ± 0.0
6	0	0	100	0.000	0.0	0.000	0.000	0.0 ± 0.0
7	0	1	100	0.000	0.0	0.000	0.010	0.0 ± 0.0
8	0	27	49	0.000	1.8	0.000	0.557	0.0 ± 0.0
9	0	0	50	0.000	0.0	0.000	0.000	0.0 ± 0.0
10	0	1	100	0.000	0.0	0.000	0.010	0.0 ± 0.0
11	0	8	90	0.000	0.3	0.000	0.090	0.0 ± 0.0
12	0	3	50	0.000	0.2	0.000	0.061	0.0 ± 0.0
13	0	1	48	0.000	0.1	0.000	0.021	0.0 ± 0.0
14	0	4	50	0.000	0.3	0.000	0.081	0.0 ± 0.0
15	0	2	80	0.000	0.1	0.000	0.025	0.0 ± 0.0
	0	70			0.2	0.000	0.068	

AREA OF BASIC UNIT = 9.89E-07 cm
CHI SQUARED = 1.592594E-06 WITH 14 DEGREES OF FREEDOM
P(chi squared) = 100.0 %
CORRELATION COEFFICIENT = 0.847
VARIANCE OF SQR(Ns) = 0.00
VARIANCE OF SQR(Ni) = 2.04

Ns/Ni = 0.000 ± 0.000
MEAN RATIO = 0.000 ± 0.000

Ages calculated using a zeta of 354.9 ± 4.3 for SRM612 glass
RHO D = 4.085E+06 ; ND = 3232

POOLED AGE = 0.0 ± 0.0 Ma
MEAN AGE = 0.0 ± 0.0 Ma

8902-33 ZIRCON matukituki s124/011909 1630m

IRRADIATION jmt data:jmt zircon data:matukituki zircons:wk022/9
SLIDE NUMBER 1
COUNTED BY: jmt

No.	Ns	Ni	Na	RATIO	U (ppm)	RHOs (E+06)	RHOi (E+06)	F.TAGE (Ma)
1	39	34	6	1.147	0.0	6.572	5.730	70.8 ± 16.7
2	51	36	4	1.417	0.0	12.892	9.100	87.4 ± 19.1
3	24	14	3	1.714	0.0	8.089	4.719	105.6 ± 35.6
4	23	16	3	1.438	0.0	7.752	5.393	88.6 ± 28.9
	137	100			0.0	8.658	6.320	

AREA OF BASIC UNIT = 9.89E-07 cm
CHI SQUARED = 1.066279 WITH 3 DEGREES OF FREEDOM
P(chi squared) = 78.5 %
CORRELATION COEFFICIENT = 0.949
VARIANCE OF SQR(Ns) = 1.27
VARIANCE OF SQR(Ni) = 1.41

Ns/Ni = 1.370 ± 0.180
MEAN RATIO = 1.429 ± 0.116

Ages calculated using a zeta of 133.9 ± 1.4 for CN1 glass
RHO D = 9.273E+05 ; ND = 4586

POOLED AGE = 84.5 ± 11.2 Ma
MEAN AGE = 88.1 ± 7.3 Ma

8902-34 APATITE matukituki s124/004910 1965m

IRRADIATION jmt data:jmt apatite data:matukituki apatites:wk018/2
SLIDE NUMBER 1
COUNTED BY: jmt

No.	Ns	Ni	Na	RATIO	U (ppm)	RHOs (E+06)	RHOi (E+06)	F.T.AGE (Ma)
1	0	0	70	0.000	0.0	0.000	0.000	0.0 ± 0.0
2	0	0	100	0.000	0.0	0.000	0.000	0.0 ± 0.0
3	0	0	50	0.000	0.0	0.000	0.000	0.0 ± 0.0
4	0	0	32	0.000	0.0	0.000	0.000	0.0 ± 0.0
5	0	0	60	0.000	0.0	0.000	0.000	0.0 ± 0.0
6	0	1	80	0.000	0.0	0.000	0.013	0.0 ± 0.0
7	0	0	21	0.000	0.0	0.000	0.000	0.0 ± 0.0
8	0	2	50	0.000	0.1	0.000	0.040	0.0 ± 0.0
9	0	1	40	0.000	0.1	0.000	0.025	0.0 ± 0.0
10	0	2	49	0.000	0.1	0.000	0.041	0.0 ± 0.0
11	0	0	50	0.000	0.0	0.000	0.000	0.0 ± 0.0
12	0	0	60	0.000	0.0	0.000	0.000	0.0 ± 0.0
13	0	0	80	0.000	0.0	0.000	0.000	0.0 ± 0.0
14	0	0	48	0.000	0.0	0.000	0.000	0.0 ± 0.0
15	0	0	64	0.000	0.0	0.000	0.000	0.0 ± 0.0
	0	6			0.0	0.000	0.007	

AREA OF BASIC UNIT = 9.89E-07 cm
CHI SQUARED = 2.000549E-06 WITH 14 DEGREES OF FREEDOM
P(chi squared) = 100.0 %
CORRELATION COEFFICIENT = 0.601
VARIANCE OF SQR(Ns) = 0.00
VARIANCE OF SQR(Ni) = 0.31

Ns/Ni = 0.000 ± 0.000
MEAN RATIO = 0.000 ± 0.000

Ages calculated using a zeta of 354.9 ± 4.3 for SRM612 glass
RHO D = 4.044E+06 ; ND = 3200

POOLED AGE = 0.0 ± 0.0 Ma
MEAN AGE = 0.0 ± 0.0 Ma

8902-34 ZIRCON matukituki s124/004910 1965m

IRRADIATION jmt data:jmt zircon data:matukituki zircons:wk038/4
SLIDE NUMBER 1
COUNTED BY: jmt

No.	Ns	Ni	Na	RATIO	U (ppm)	RHOs (E+06)	RHOi (E+06)	F.T.AGE (Ma)
1	47	35	5	1.343	0.0	9.505	7.078	95.0 ± 21.3
2	31	27	4	1.148	0.0	7.836	6.825	81.3 ± 21.5
3	107	79	20	1.354	0.0	5.410	3.994	95.9 ± 14.3
	185	141			0.0	6.450	4.916	

AREA OF BASIC UNIT = 9.89E-07 cm
CHI SQUARED = .3140847 WITH 2 DEGREES OF FREEDOM
P(chi squared) = 85.5 %
CORRELATION COEFFICIENT = 0.998
VARIANCE OF SQR(Ns) = 6.11
VARIANCE OF SQR(Ni) = 3.83

Ns/Ni = 1.312 ± 0.147
MEAN RATIO = 1.282 ± 0.067

Ages calculated using a zeta of 133.9 ± 1.4 for CN1 glass
RHO D = 1.065E+06 ; ND = 5265

POOLED AGE = 92.9 ± 10.5 Ma
MEAN AGE = 90.8 ± 5.0 Ma

8902-35 APATITE matukituki s133/092638 185m

IRRADIATION jmt data:jmt apatite data:matukituki apatites:wk018/1
SLIDE NUMBER 1
COUNTED BY: jmt

No.	Ns	Ni	Na	RATIO	U (ppm)	RHOs (E+06)	RHOi (E+06)	F.T.AGE (Ma)
1	0	0	30	0.000	0.0	0.000	0.000	0.0 ± 0.0
2	0	0	24	0.000	0.0	0.000	0.000	0.0 ± 0.0
3	0	1	50	0.000	0.1	0.000	0.020	0.0 ± 0.0
4	0	1	90	0.000	0.0	0.000	0.011	0.0 ± 0.0
5	0	7	35	0.000	0.7	0.000	0.202	0.0 ± 0.0
6	0	30	60	0.000	1.7	0.000	0.506	0.0 ± 0.0
7	18	332	50	0.054	22.0	0.364	6.714	38.4 ± 9.3
8	5	191	100	0.026	6.3	0.051	1.931	18.6 ± 8.4
9	0	1	24	0.000	0.1	0.000	0.042	0.0 ± 0.0
10	0	0	24	0.000	0.0	0.000	0.000	0.0 ± 0.0
11	0	1	48	0.000	0.1	0.000	0.021	0.0 ± 0.0
12	0	0	42	0.000	0.0	0.000	0.000	0.0 ± 0.0
13	2	82	60	0.024	4.5	0.034	1.382	17.3 ± 12.4
14	0	25	50	0.000	1.7	0.000	0.506	0.0 ± 0.0
15	0	4	32	0.000	0.4	0.000	0.126	0.0 ± 0.0
16	0	7	40	0.000	0.6	0.000	0.177	0.0 ± 0.0
17	0	7	100	0.000	0.2	0.000	0.071	0.0 ± 0.0
18	0	2	48	0.000	0.1	0.000	0.042	0.0 ± 0.0
19	0	11	60	0.000	0.6	0.000	0.185	0.0 ± 0.0
20	6	101	48	0.059	7.0	0.126	2.128	42.1 ± 17.7
21	1	65	100	0.015	2.2	0.010	0.657	10.9 ± 11.0
22	3	59	36	0.051	5.4	0.084	1.657	36.0 ± 21.3
23	18	306	50	0.059	20.2	0.364	6.188	41.6 ± 10.1
24	0	0	30	0.000	0.0	0.000	0.000	0.0 ± 0.0
25	4	158	48	0.025	10.9	0.084	3.328	18.0 ± 9.1
26	18	221	24	0.081	30.5	0.758	9.311	57.6 ± 14.2
27	0	6	100	0.000	0.2	0.000	0.061	0.0 ± 0.0
28	0	0	80	0.000	0.0	0.000	0.000	0.0 ± 0.0
29	0	0	30	0.000	0.0	0.000	0.000	0.0 ± 0.0
30	0	0	30	0.000	0.0	0.000	0.000	0.0 ± 0.0
	75	1618			3.5	0.049	1.060	

AREA OF BASIC UNIT = 9.89E-07 cm
CHI SQUARED = 17.23191 WITH 29 DEGREES OF FREEDOM
P(chi squared) = 95.8 %
CORRELATION COEFFICIENT = 0.941
VARIANCE OF SQR(Ns) = 1.95
VARIANCE OF SQR(Ni) = 32.13

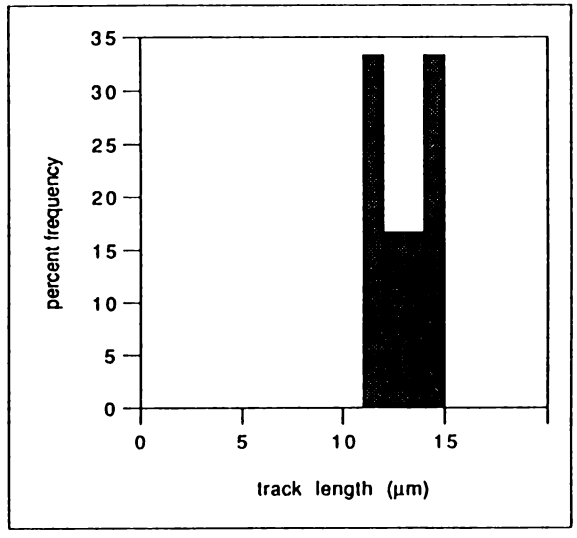
Ns/Ni = 0.046 ± 0.005
MEAN RATIO = 0.013 ± 0.004

Ages calculated using a zeta of 354.9 ± 4.3 for SRM612 glass
RHO D = 4.003E+06 ; ND = 3167

POOLED AGE = 32.8 ± 3.9 Ma

MEAN AGE = 9.4 ± 3.1 Ma

8902-35



n = 6
Mean = 13.06 µm
Sample std. dev. = 1.43 µm

8902-35 ZIRCON matukituki s133/092638 185m

IRRADIATION jmt data:jmt zircon data:matukituki zircons:wk038/5
SLIDE NUMBER 1
COUNTED BY: jmt

No.	Ns	Ni	Na	RATIO	U (ppm)	RHOs (E+06)	RHOi (E+06)	F.T.AGE (Ma)
1	26	21	4	1.238	0.0	6.572	5.308	87.7 ± 25.8
2	90	75	9	1.200	0.0	10.111	8.426	85.0 ± 13.4
3	25	17	3	1.471	0.0	8.426	5.730	104.0 ± 32.7
4	30	19	3	1.579	0.0	10.111	6.404	111.6 ± 32.8
5	80	47	10	1.702	0.0	8.089	4.752	120.2 ± 22.2
6	37	29	3	1.276	0.0	12.471	9.774	90.3 ± 22.5
7	43	40	6	1.075	0.0	7.246	6.741	76.2 ± 16.8
8	61	57	8	1.070	0.0	7.710	7.204	75.9 ± 14.0
9	55	46	9	1.196	0.0	6.179	5.168	84.7 ± 17.0
10	70	45	8	1.556	0.0	8.847	5.688	110.0 ± 21.1
11	91	89	12	1.022	0.0	7.668	7.499	72.5 ± 10.9
12	60	49	6	1.224	0.0	10.111	8.257	86.7 ± 16.8
13	67	42	6	1.595	0.0	11.291	7.078	112.8 ± 22.3
	735	576			0.0	8.542	6.694	

AREA OF BASIC UNIT = 9.89E-07 cm
CHI SQUARED = 9.638316 WITH 12 DEGREES OF FREEDOM
P(chi squared) = 64.8 %
CORRELATION COEFFICIENT = 0.908
VARIANCE OF SQR(Ns) = 2.53
VARIANCE OF SQR(Ni) = 2.50

Ns/Ni = 1.276 ± 0.071
MEAN RATIO = 1.323 ± 0.063

Ages calculated using a zeta of 133.9 ± 1.4 for CN1 glass
RHO D = 1.065E+06 ; ND = 5265

POOLED AGE = 90.3 ± 5.3 Ma
MEAN AGE = 93.7 ± 4.8 Ma

8902-36 APATITE arawata s97/543763 90m

IRRADIATION jmt data:jmt apatite data:arawata apatite:wk019/14
SLIDE NUMBER 1
COUNTED BY: jmt

No.	Ns	Ni	Na	RATIO	U (ppm)	RHOs (E+06)	RHOi (E+06)	F.T.AGE (Ma)
1	0	4	36	0.000	0.3	0.000	0.112	0.0 ± 0.0
2	0	2	50	0.000	0.1	0.000	0.040	0.0 ± 0.0
3	0	0	16	0.000	0.0	0.000	0.000	0.0 ± 0.0
4	0	0	24	0.000	0.0	0.000	0.000	0.0 ± 0.0
5	0	7	48	0.000	0.4	0.000	0.147	0.0 ± 0.0
6	0	0	30	0.000	0.0	0.000	0.000	0.0 ± 0.0
7	0	2	70	0.000	0.1	0.000	0.029	0.0 ± 0.0
8	0	2	40	0.000	0.1	0.000	0.051	0.0 ± 0.0
9	0	0	30	0.000	0.0	0.000	0.000	0.0 ± 0.0
10	0	2	40	0.000	0.1	0.000	0.051	0.0 ± 0.0
11	0	4	20	0.000	0.6	0.000	0.202	0.0 ± 0.0
12	0	1	24	0.000	0.1	0.000	0.042	0.0 ± 0.0
13	0	0	49	0.000	0.0	0.000	0.000	0.0 ± 0.0
14	0	3	28	0.000	0.3	0.000	0.108	0.0 ± 0.0
15	0	2	42	0.000	0.1	0.000	0.048	0.0 ± 0.0
	0	29			0.2	0.000	0.054	

AREA OF BASIC UNIT = 9.89E-07 cm
CHI SQUARED = 6.250124E-06 WITH 14 DEGREES OF FREEDOM
P(chi squared) = 100.0 %
CORRELATION COEFFICIENT = 0.289
VARIANCE OF SQR(Ns) = 0.00
VARIANCE OF SQR(Ni) = 0.78

Ns/Ni = 0.000 ± 0.000
MEAN RATIO = 0.000 ± 0.000

Ages calculated using a zeta of 354.9 ± 4.3 for SRM612 glass
RHO D = 4.674E+06 ; ND = 3698

POOLED AGE = 0.0 ± 0.0 Ma
MEAN AGE = 0.0 ± 0.0 Ma

8902-36 ZIRCON arawata s97/543763 90m

IRRADIATION jmt data:jmt zircon data:arawata zircons:wk038/6
SLIDE NUMBER 1
COUNTED BY: jmt

No.	Ns	Ni	Na	RATIO	U (ppm)	RHOs (E+06)	RHOi (E+06)	F.T.AGE (Ma)
1	8	91	6	0.088	0.0	1.348	15.335	6.3 ± 2.3
2	2	39	3	0.051	0.0	0.674	13.145	3.7 ± 2.6
3	12	125	18	0.096	0.0	0.674	7.022	6.8 ± 2.1
4	16	178	12	0.090	0.0	1.348	14.998	6.4 ± 1.7
5	12	244	20	0.049	0.0	0.607	12.336	3.5 ± 1.0
6	1	39	24	0.026	0.0	0.042	1.643	1.8 ± 1.9
7	23	364	12	0.063	0.0	1.938	30.671	4.5 ± 1.0
8	7	74	4	0.095	0.0	1.769	18.706	6.7 ± 2.7
9	4	27	4	0.148	0.0	1.011	6.825	10.6 ± 5.7
10	9	86	9	0.105	0.0	1.011	9.662	7.5 ± 2.6
11	20	134	10	0.149	0.0	2.022	13.549	10.6 ± 2.6
12	10	146	20	0.068	0.0	0.506	7.381	4.9 ± 1.6
13	11	174	12	0.063	0.0	0.927	14.661	4.5 ± 1.4
14	12	160	10	0.075	0.0	1.213	16.178	5.3 ± 1.6
	147	1881			0.0	0.906	11.597	

AREA OF BASIC UNIT = 9.89E-07 cm
CHI SQUARED = 16.61728 WITH 13 DEGREES OF FREEDOM
P(chi squared) = 21.7 %
CORRELATION COEFFICIENT = 0.830
VARIANCE OF SQR(Ns) = 1.14
VARIANCE OF SQR(Ni) = 14.69

Ns/Ni = 0.078 ± 0.007
MEAN RATIO = 0.083 ± 0.009

Ages calculated using a zeta of 133.9 ± 1.4 for CN1 glass
RHO D = 1.065E+06 ; ND = 5265

POOLED AGE = 5.6 ± 0.5 Ma
MEAN AGE = 5.9 ± 0.7 Ma

8902-37 APATITE wilkin s98/855745 610m

IRRADIATION jmt data:jmt apatite data:wilkin apatites:wk019/13
SLIDE NUMBER 1
COUNTED BY: jmt

No.	Ns	Ni	Na	RATIO	U (ppm)	RHOs (E+06)	RHOi (E+06)	F.T.AGE (Ma)
1	0	0	16	0.000	0.0	0.000	0.000	0.0 ± 0.0
2	0	0	16	0.000	0.0	0.000	0.000	0.0 ± 0.0
3	0	1	25	0.000	0.1	0.000	0.040	0.0 ± 0.0
4	0	0	16	0.000	0.0	0.000	0.000	0.0 ± 0.0
5	0	0	60	0.000	0.0	0.000	0.000	0.0 ± 0.0
6	0	0	25	0.000	0.0	0.000	0.000	0.0 ± 0.0
7	0	1	35	0.000	0.1	0.000	0.029	0.0 ± 0.0
8	0	0	36	0.000	0.0	0.000	0.000	0.0 ± 0.0
9	0	2	36	0.000	0.2	0.000	0.056	0.0 ± 0.0
10	0	0	32	0.000	0.0	0.000	0.000	0.0 ± 0.0
11	0	0	16	0.000	0.0	0.000	0.000	0.0 ± 0.0
12	0	0	25	0.000	0.0	0.000	0.000	0.0 ± 0.0
13	0	1	24	0.000	0.1	0.000	0.042	0.0 ± 0.0
14	0	1	20	0.000	0.1	0.000	0.051	0.0 ± 0.0
15	0	0	20	0.000	0.0	0.000	0.000	0.0 ± 0.0
	0	6			0.0	0.000	0.015	

AREA OF BASIC UNIT = 9.89E-07 cm
CHI SQUARED = 2.000499E-06 WITH 14 DEGREES OF FREEDOM
P(chi squared) = 100.0 %
CORRELATION COEFFICIENT = 0.700
VARIANCE OF SQR(Ns) = 0.00
VARIANCE OF SQR(Ni) = 0.28

Ns/Ni = 0.000 ± 0.000
MEAN RATIO = 0.000 ± 0.000

Ages calculated using a zeta of 354.9 ± 4.3 for SRM612 glass
RHO D = 4.640E+06 ; ND = 3671

POOLED AGE = 0.0 ± 0.0 Ma
MEAN AGE = 0.0 ± 0.0 Ma

8902-37 ZIRCON wilkin s98/869718 610m

IRRADIATION jmt data:jmt zircon data:wilkin zircons :wk022/5
SLIDE NUMBER 1
COUNTED BY: jmt

No.	Ns	Ni	Na	RATIO	U (ppm)	RHOs (E+06)	RHOi (E+06)	F.T.AGE (Ma)
1	47	169	9	0.278	0.0	5.280	18.987	16.7 ± 2.8
2	40	133	9	0.301	0.0	4.494	14.942	18.0 ± 3.3
3	5	35	6	0.143	0.0	0.843	5.898	8.6 ± 4.1
4	9	55	6	0.164	0.0	1.517	9.269	9.8 ± 3.5
5	38	119	12	0.319	0.0	3.202	10.027	19.1 ± 3.6
6	12	44	4	0.273	0.0	3.033	11.122	16.3 ± 5.3
7	23	138	15	0.167	0.0	1.550	9.302	10.0 ± 2.3
8	25	78	6	0.321	0.0	4.213	13.145	19.2 ± 4.4
9	21	85	8	0.247	0.0	2.654	10.743	14.8 ± 3.6
10	17	67	4	0.254	0.0	4.297	16.936	15.2 ± 4.1
	237	923			0.0	3.033	11.813	

AREA OF BASIC UNIT = 9.89E-07 cm
CHI SQUARED = 10.25967 WITH 9 DEGREES OF FREEDOM
P(chi squared) = 33.0 %
CORRELATION COEFFICIENT = 0.907
VARIANCE OF SQR(Ns) = 2.26
VARIANCE OF SQR(Ni) = 5.65

Ns/Ni = 0.257 ± 0.019
MEAN RATIO = 0.247 ± 0.021

Ages calculated using a zeta of 133.9 ± 1.4 for CN1 glass
RHO D = 8.965E+05 ; ND = 4433

POOLED AGE = 15.4 ± 1.2 Ma
MEAN AGE = 14.8 ± 1.3 Ma

8902-38 APATITE wilkin s98/857740 610m

IRRADIATION jmt data:jmt apatite data:wilkin apatites:wk019/12
SLIDE NUMBER 1
COUNTED BY: jmt

No.	Ns	Ni	Na	RATIO	U (ppm)	RHOs (E+06)	RHOi (E+06)	F.T AGE (Ma)
1	0	0	28	0.000	0.0	0.000	0.000	0.0 ± 0.0
2	0	2	100	0.000	0.1	0.000	0.020	0.0 ± 0.0
3	0	49	100	0.000	1.4	0.000	0.495	0.0 ± 0.0
4	0	2	36	0.000	0.2	0.000	0.056	0.0 ± 0.0
5	0	0	12	0.000	0.0	0.000	0.000	0.0 ± 0.0
6	0	16	35	0.000	1.3	0.000	0.462	0.0 ± 0.0
7	0	0	16	0.000	0.0	0.000	0.000	0.0 ± 0.0
8	0	0	36	0.000	0.0	0.000	0.000	0.0 ± 0.0
9	0	0	24	0.000	0.0	0.000	0.000	0.0 ± 0.0
10	0	1	24	0.000	0.1	0.000	0.042	0.0 ± 0.0
11	0	0	35	0.000	0.0	0.000	0.000	0.0 ± 0.0
12	0	1	50	0.000	0.1	0.000	0.020	0.0 ± 0.0
13	0	0	21	0.000	0.0	0.000	0.000	0.0 ± 0.0
14	0	0	40	0.000	0.0	0.000	0.000	0.0 ± 0.0
15	0	0	49	0.000	0.0	0.000	0.000	0.0 ± 0.0
	0	71			0.3	0.000	0.118	

AREA OF BASIC UNIT = 9.89E-07 cm
CHI SQUARED = 4.489979E-07 WITH 14 DEGREES OF FREEDOM
P(chi squared) = 100.0 %
CORRELATION COEFFICIENT = 0.949
VARIANCE OF SQR(Ns) = 0.00
VARIANCE OF SQR(Ni) = 3.86

Ns/Ni = 0.000 ± 0.000
MEAN RATIO = 0.000 ± 0.000

Ages calculated using a zeta of 354.9 ± 4.3 for SRM612 glass
RHO D = 4.607E+06 ; ND = 3645

POOLED AGE = 0.0 ± 0.0 Ma
MEAN AGE = 0.0 ± 0.0 Ma

8902-38 ZIRCON wilkin s98/857740 610m

IRRADIATION jmt data:jmt zircon data:wilkin zircons :wk022/4
SLIDE NUMBER 1
COUNTED BY: jmt

No.	Ns	Ni	Na	RATIO	U (ppm)	RHOs (E+06)	RHOi (E+06)	F.T AGE (Ma)
1	8	77	6	0.104	0.0	1.348	12.976	6.2 ± 2.3
2	8	30	3	0.267	0.0	2.696	10.111	15.8 ± 6.3
3	3	25	4	0.120	0.0	0.758	6.320	7.1 ± 4.4
4	3	35	6	0.086	0.0	0.506	5.898	5.1 ± 3.1
	22	167			0.0	1.171	8.887	

AREA OF BASIC UNIT = 9.89E-07 cm
CHI SQUARED = 4.225226 WITH 3 DEGREES OF FREEDOM
P(chi squared) = 23.8 %
CORRELATION COEFFICIENT = 0.569
VARIANCE OF SQR(Ns) = 0.40
VARIANCE OF SQR(Ni) = 2.88

Ns/Ni = 0.132 ± 0.030
MEAN RATIO = 0.144 ± 0.041

Ages calculated using a zeta of 133.9 ± 1.4 for CN1 glass
RHO D = 8.888E+05 ; ND = 4395

POOLED AGE = 7.8 ± 1.8 Ma
MEAN AGE = 8.6 ± 2.5 Ma

8902-39 APATITE wilkin s98/869718 610m

IRRADIATION jmt data:jmt apatite data:wilkin apatites:wk019/11
SLIDE NUMBER 1
COUNTED BY: jmt

No.	Ns	Ni	Na	RATIO	U (ppm)	RHOs (E+06)	RHOi (E+06)	F.T.AGE (Ma)
1	0	2	10	0.000	0.6	0.000	0.202	0.0 ± 0.0
2	0	0	25	0.000	0.0	0.000	0.000	0.0 ± 0.0
3	0	1	12	0.000	0.2	0.000	0.084	0.0 ± 0.0
4	0	0	12	0.000	0.0	0.000	0.000	0.0 ± 0.0
5	0	4	12	0.000	1.0	0.000	0.337	0.0 ± 0.0
6	0	0	25	0.000	0.0	0.000	0.000	0.0 ± 0.0
7	0	0	10	0.000	0.0	0.000	0.000	0.0 ± 0.0
8	0	0	21	0.000	0.0	0.000	0.000	0.0 ± 0.0
9	0	0	9	0.000	0.0	0.000	0.000	0.0 ± 0.0
10	0	0	12	0.000	0.0	0.000	0.000	0.0 ± 0.0
11	0	5	9	0.000	1.6	0.000	0.562	0.0 ± 0.0
12	0	10	12	0.000	2.4	0.000	0.843	0.0 ± 0.0
13	0	1	9	0.000	0.3	0.000	0.112	0.0 ± 0.0
14	0	19	12	0.000	4.6	0.000	1.601	0.0 ± 0.0
15	0	0	12	0.000	0.0	0.000	0.000	0.0 ± 0.0
	0	42			0.6	0.000	0.210	

AREA OF BASIC UNIT = 9.89E-07 cm
CHI SQUARED = 3.20008E-06 WITH 14 DEGREES OF FREEDOM
P(chi squared) = 100.0 %
CORRELATION COEFFICIENT = 0.377
VARIANCE OF SQR(Ns) = 0.00
VARIANCE OF SQR(Ni) = 1.89

Ns/Ni = 0.000 ± 0.000
MEAN RATIO = 0.000 ± 0.000

Ages calculated using a zeta of 354.9 ± 4.3 for SRM612 glass
RHO D = 4.573E+06 ; ND = 3618

POOLED AGE = 0.0 ± 0.0 Ma
MEAN AGE = 0.0 ± 0.0 Ma

8902-39 ZIRCON wilkin s98/869718 610m

IRRADIATION jmt data:jmt zircon data:wilkin zircons :wk022/3
SLIDE NUMBER 1
COUNTED BY: jmt

No.	Ns	Ni	Na	RATIO	U (ppm)	RHOs (E+06)	RHOi (E+06)	F.T.AGE (Ma)
1	98	247	24	0.397	0.0	4.129	10.406	23.4 ± 2.8
2	27	68	6	0.397	0.0	4.550	11.459	23.4 ± 5.3
3	53	141	18	0.376	0.0	2.977	7.920	22.1 ± 3.6
4	8	25	12	0.320	0.0	0.674	2.106	18.8 ± 7.7
5	8	22	3	0.364	0.0	2.696	7.415	21.4 ± 8.8
6	12	36	4	0.333	0.0	3.033	9.100	19.6 ± 6.6
7	13	43	6	0.302	0.0	2.191	7.246	17.8 ± 5.6
	219	582			0.0	3.033	8.061	

AREA OF BASIC UNIT = 9.89E-07 cm
CHI SQUARED = 1.031565 WITH 6 DEGREES OF FREEDOM
P(chi squared) = 98.4 %
CORRELATION COEFFICIENT = 0.999
VARIANCE OF SQR(Ns) = 7.16
VARIANCE OF SQR(Ni) = 16.67

Ns/Ni = 0.376 ± 0.030
MEAN RATIO = 0.356 ± 0.014

Ages calculated using a zeta of 133.9 ± 1.4 for CN1 glass
RHO D = 8.811E+05 ; ND = 4357

POOLED AGE = 22.2 ± 1.8 Ma
MEAN AGE = 20.9 ± 0.9 Ma

8902-40 APATITE wilkin s107/844675 335m

IRRADIATION jmt data:jmt apatite data:wilkin apatites:wk019/10
SLIDE NUMBER 1
COUNTED BY: jmt

No.	Ns	Ni	Na	RATIO	U (ppm)	RHOs (E+06)	RHOi (E+06)	F.T.AGE (Ma)
1	0	0	30	0.000	0.0	0.000	0.000	0.0 ± 0.0
2	0	1	49	0.000	0.1	0.000	0.021	0.0 ± 0.0
3	0	8	36	0.000	0.6	0.000	0.225	0.0 ± 0.0
4	0	0	24	0.000	0.0	0.000	0.000	0.0 ± 0.0
5	0	6	36	0.000	0.5	0.000	0.169	0.0 ± 0.0
6	0	1	25	0.000	0.1	0.000	0.040	0.0 ± 0.0
7	0	15	25	0.000	1.8	0.000	0.607	0.0 ± 0.0
8	0	1	60	0.000	0.0	0.000	0.017	0.0 ± 0.0
9	0	1	35	0.000	0.1	0.000	0.029	0.0 ± 0.0
10	0	11	100	0.000	0.3	0.000	0.111	0.0 ± 0.0
11	0	0	16	0.000	0.0	0.000	0.000	0.0 ± 0.0
12	0	25	40	0.000	1.8	0.000	0.632	0.0 ± 0.0
13	0	2	50	0.000	0.1	0.000	0.040	0.0 ± 0.0
14	0	4	35	0.000	0.3	0.000	0.116	0.0 ± 0.0
15	0	17	60	0.000	0.8	0.000	0.286	0.0 ± 0.0
	0	92			0.4	0.000	0.150	

AREA OF BASIC UNIT = 9.89E-07 cm
CHI SQUARED = 5.133352E-06 WITH 14 DEGREES OF FREEDOM
P(chi squared) = 100.0 %
CORRELATION COEFFICIENT = 0.321
VARIANCE OF SQR(Ns) = 0.00
VARIANCE OF SQR(Ni) = 2.56

Ns/Ni = 0.000 ± 0.000
MEAN RATIO = 0.000 ± 0.000

Ages calculated using a zeta of 354.9 ± 4.3 for SRM612 glass
RHO D = 4.540E+06 ; ND = 3592

POOLED AGE = 0.0 ± 0.0 Ma
MEAN AGE = 0.0 ± 0.0 Ma

8902-40 ZIRCON wilkin s107/844675 335m

IRRADIATION jmt data:jmt zircon data:wilkin zircons :wk022/2
SLIDE NUMBER 1
COUNTED BY: jmt

No.	Ns	Ni	Na	RATIO	U (ppm)	RHOs (E+06)	RHOi (E+06)	F.T.AGE (Ma)
1	23	52	5	0.442	0.0	4.651	10.516	25.8 ± 6.5
2	13	29	3	0.448	0.0	4.382	9.774	26.2 ± 8.7
3	41	98	10	0.418	0.0	4.146	9.909	24.4 ± 4.6
4	22	61	12	0.361	0.0	1.854	5.140	21.1 ± 5.2
5	14	22	2	0.636	0.0	7.078	11.122	37.1 ± 12.7
6	54	91	9	0.593	0.0	6.067	10.224	34.6 ± 6.0
	167	353			0.0	4.118	8.706	

AREA OF BASIC UNIT = 9.89E-07 cm
CHI SQUARED = 4.238674 WITH 5 DEGREES OF FREEDOM
P(chi squared) = 51.6 %
CORRELATION COEFFICIENT = 0.917
VARIANCE OF SQR(Ns) = 2.22
VARIANCE OF SQR(Ni) = 4.49

Ns/Ni = 0.473 ± 0.044
MEAN RATIO = 0.483 ± 0.044

Ages calculated using a zeta of 133.9 ± 1.4 for CN1 glass
RHO D = 8.734E+05 ; ND = 4319

POOLED AGE = 27.6 ± 2.6 Ma
MEAN AGE = 28.2 ± 2.6 Ma

8902-41 APATITE wilkin s107/010665 305m

IRRADIATION jmt data:jmt apatite data:wilkin apatites:wk019/9
SLIDE NUMBER 1
COUNTED BY: jmt

No.	Ns	Ni	Na	RATIO	U (ppm)	RHOs (E+06)	RHOi (E+06)	F.T.AGE (Ma)
1	0	70	24	0.000	8.6	0.000	2.949	0.0 ± 0.0
2	0	34	9	0.000	11.1	0.000	3.820	0.0 ± 0.0
3	0	0	9	0.000	0.0	0.000	0.000	0.0 ± 0.0
4	0	39	10	0.000	11.5	0.000	3.943	0.0 ± 0.0
5	0	88	8	0.000	32.3	0.000	11.122	0.0 ± 0.0
6	0	0	18	0.000	0.0	0.000	0.000	0.0 ± 0.0
7	0	41	6	0.000	20.1	0.000	6.909	0.0 ± 0.0
8	0	63	36	0.000	5.1	0.000	1.769	0.0 ± 0.0
9	0	144	12	0.000	35.3	0.000	12.133	0.0 ± 0.0
10	0	16	6	0.000	7.8	0.000	2.696	0.0 ± 0.0
11	0	0	6	0.000	0.0	0.000	0.000	0.0 ± 0.0
12	0	62	9	0.000	20.2	0.000	6.966	0.0 ± 0.0
13	0	32	6	0.000	15.7	0.000	5.393	0.0 ± 0.0
14	0	58	9	0.000	18.9	0.000	6.516	0.0 ± 0.0
15	0	20	10	0.000	5.9	0.000	2.022	0.0 ± 0.0
	0	667			11.0	0.000	3.789	

AREA OF BASIC UNIT = 9.89E-07 cm
CHI SQUARED = 8.528573E-06 WITH 14 DEGREES OF FREEDOM
P(chi squared) = 100.0 %
CORRELATION COEFFICIENT = 0.183
VARIANCE OF SQR(Ns) = 0.00
VARIANCE OF SQR(Ni) = 12.58

Ns/Ni = 0.000 ± 0.000
MEAN RATIO = 0.000 ± 0.000

Ages calculated using a zeta of 354.9 ± 4.3 for SRM612 glass
RHO D = 4.506E+06 ; ND = 3565

POOLED AGE = 0.0 ± 0.0 Ma
MEAN AGE = 0.0 ± 0.0 Ma

8902-41 ZIRCON wilkin s107/010665 305m

IRRADIATION jmt data:jmt zircon data:wilkin zircons :wk038/7
SLIDE NUMBER 1
COUNTED BY: jmt

No.	Ns	Ni	Na	RATIO	U (ppm)	RHOs (E+06)	RHOi (E+06)	F.T.AGE (Ma)
1	42	52	20	0.808	0.0	2.123	2.629	57.3 ± 11.9
2	35	34	24	1.029	0.0	1.475	1.432	73.0 ± 17.6
3	64	69	18	0.928	0.0	3.595	3.876	65.8 ± 11.5
4	92	97	12	0.948	0.0	7.752	8.173	67.3 ± 9.9
	233	252			0.0	3.184	3.443	

AREA OF BASIC UNIT = 9.89E-07 cm
CHI SQUARED = .6552433 WITH 3 DEGREES OF FREEDOM
P(chi squared) = 88.4 %
CORRELATION COEFFICIENT = 0.986
VARIANCE OF SQR(Ns) = 2.72
VARIANCE OF SQR(Ni) = 2.89

Ns/Ni = 0.925 ± 0.084
MEAN RATIO = 0.928 ± 0.046

Ages calculated using a zeta of 133.9 ± 1.4 for CN1 glass
RHO D = 1.065E+06 ; ND = 5265

POOLED AGE = 65.6 ± 6.1 Ma
MEAN AGE = 65.8 ± 3.4 Ma

8902-42 APATITE wilkin s107/986487 305m

IRRADIATION jmt data:jmt apatite data:wilkin apatites:wk019/8
SLIDE NUMBER 1
COUNTED BY: jmt

No.	Ns	Ni	Na	RATIO	U (ppm)	RHOs (E+06)	RHOi (E+06)	F.T AGE (Ma)
1	0	2	20	0.000	0.3	0.000	0.101	0.0 ± 0.0
2	1	537	24	0.002	66.3	0.042	22.624	1.5 ± 1.5
3	0	0	16	0.000	0.0	0.000	0.000	0.0 ± 0.0
4	0	25	30	0.000	2.5	0.000	0.843	0.0 ± 0.0
5	0	140	16	0.000	25.9	0.000	8.847	0.0 ± 0.0
6	0	0	20	0.000	0.0	0.000	0.000	0.0 ± 0.0
7	0	1	24	0.000	0.1	0.000	0.042	0.0 ± 0.0
8	0	1	24	0.000	0.1	0.000	0.042	0.0 ± 0.0
9	0	7	20	0.000	1.0	0.000	0.354	0.0 ± 0.0
10	0	0	9	0.000	0.0	0.000	0.000	0.0 ± 0.0
11	0	0	24	0.000	0.0	0.000	0.000	0.0 ± 0.0
12	0	0	14	0.000	0.0	0.000	0.000	0.0 ± 0.0
13	0	1	16	0.000	0.2	0.000	0.063	0.0 ± 0.0
14	0	0	28	0.000	0.0	0.000	0.000	0.0 ± 0.0
15	0	0	20	0.000	0.0	0.000	0.000	0.0 ± 0.0
16	0	1	12	0.000	0.2	0.000	0.084	0.0 ± 0.0
17	0	8	20	0.000	1.2	0.000	0.404	0.0 ± 0.0
18	0	9	20	0.000	1.3	0.000	0.455	0.0 ± 0.0
19	0	1	40	0.000	0.1	0.000	0.025	0.0 ± 0.0
20	0	57	25	0.000	6.8	0.000	2.305	0.0 ± 0.0
	1	790			5.5	0.002	1.893	

AREA OF BASIC UNIT = 9.89E-07 cm
CHI SQUARED = .4708568 WITH 19 DEGREES OF FREEDOM
P(chi squared) = 100.0 %
CORRELATION COEFFICIENT = 0.963
VARIANCE OF SQR(Ns) = 0.05
VARIANCE OF SQR(Ni) = 31.29

Ns/Ni = 0.001 ± 0.001
MEAN RATIO = 0.000 ± 0.000

Ages calculated using a zeta of 354.9 ± 4.3 for SRM612 glass
RHO D = 4.473E+06 ; ND = 3539

POOLED AGE = 1.0 ± 1.0 Ma
MEAN AGE = 0.1 ± 0.1 Ma

8902-42 ZIRCON wilkin s107/986487 305m

IRRADIATION jmt data:jmt zircon data:wilkin zircons :wk023/18
SLIDE NUMBER 1
COUNTED BY: jmt

No.	Ns	Ni	Na	RATIO	U (ppm)	RHOs (E+06)	RHOi (E+06)	F.T AGE (Ma)
1	24	30	4	0.800	0.0	6.067	7.583	54.7 ± 15.0
2	41	53	6	0.774	0.0	6.909	8.932	52.9 ± 11.0
3	53	61	8	0.869	0.0	6.699	7.710	59.4 ± 11.2
4	34	53	6	0.642	0.0	5.730	8.932	43.9 ± 9.7
5	90	90	9	1.000	0.0	10.111	10.111	68.3 ± 10.2
6	49	75	8	0.653	0.0	6.193	9.479	44.7 ± 8.2
7	44	50	9	0.880	0.0	4.943	5.617	60.1 ± 12.5
8	41	49	8	0.837	0.0	5.182	6.193	57.2 ± 12.1
9	148	176	24	0.841	0.0	6.235	7.415	57.4 ± 6.5
10	46	52	6	0.885	0.0	7.752	8.763	60.4 ± 12.3
11	122	172	15	0.709	0.0	8.224	11.594	48.5 ± 5.8
12	74	90	9	0.822	0.0	8.314	10.111	56.2 ± 8.9
13	78	99	15	0.788	0.0	5.258	6.673	53.8 ± 8.2
	844	1050			0.0	6.720	8.360	

AREA OF BASIC UNIT = 9.89E-07 cm
CHI SQUARED = 6.469151 WITH 12 DEGREES OF FREEDOM
P(chi squared) = 89.1 %
CORRELATION COEFFICIENT = 0.973
VARIANCE OF SQR(Ns) = 4.47
VARIANCE OF SQR(Ni) = 5.51

Ns/Ni = 0.804 ± 0.037
MEAN RATIO = 0.808 ± 0.027

Ages calculated using a zeta of 133.9 ± 1.4 for CN1 glass
RHO D = 1.025E+06 ; ND = 5064

POOLED AGE = 54.9 ± 2.7 Ma
MEAN AGE = 55.2 ± 2.1 Ma

8902-43 APATITE hunter s107/991438 395m

IRRADIATION jmt data:jmt apatite data:hunter apatites:wk019/7
SLIDE NUMBER 1
COUNTED BY: jmt

No.	Ns	Ni	Na	RATIO	U (ppm)	RHOs (E+06)	RHOi (E+06)	F.T.AGE (Ma)
1	0	0	20	0.000	0.0	0.000	0.000	0.0 ± 0.0
2	0	0	20	0.000	0.0	0.000	0.000	0.0 ± 0.0
3	0	0	24	0.000	0.0	0.000	0.000	0.0 ± 0.0
4	0	0	25	0.000	0.0	0.000	0.000	0.0 ± 0.0
5	0	0	16	0.000	0.0	0.000	0.000	0.0 ± 0.0
6	0	0	25	0.000	0.0	0.000	0.000	0.0 ± 0.0
7	0	124	32	0.000	11.6	0.000	3.918	0.0 ± 0.0
8	0	0	9	0.000	0.0	0.000	0.000	0.0 ± 0.0
9	0	2	30	0.000	0.2	0.000	0.067	0.0 ± 0.0
10	0	0	21	0.000	0.0	0.000	0.000	0.0 ± 0.0
11	0	0	12	0.000	0.0	0.000	0.000	0.0 ± 0.0
12	0	0	28	0.000	0.0	0.000	0.000	0.0 ± 0.0
13	0	0	15	0.000	0.0	0.000	0.000	0.0 ± 0.0
14	0	6	49	0.000	0.4	0.000	0.124	0.0 ± 0.0
15	0	0	20	0.000	0.0	0.000	0.000	0.0 ± 0.0
	0	132			1.1	0.000	0.386	

AREA OF BASIC UNIT = 9.89E-07 cm
CHI SQUARED = 6.452579E-08 WITH 14 DEGREES OF FREEDOM
P(chi squared) = 100.0 %
CORRELATION COEFFICIENT = 0.999
VARIANCE OF SQR(Ns) = 0.00
VARIANCE OF SQR(Ni) = 8.34

Ns/Ni = 0.000 ± 0.000
MEAN RATIO = 0.000 ± 0.000

Ages calculated using a zeta of 354.9 ± 4.3 for SRM612 glass
RHO D = 4.439E+06 ; ND = 3512

POOLED AGE = 0.0 ± 0.0 Ma
MEAN AGE = 0.0 ± 0.0 Ma

8902-43 ZIRCON hunter s107/991438 395m

IRRADIATION jmt data:jmt zircon data:hunter zircons:wk038/8
SLIDE NUMBER 1
COUNTED BY: PFG

No.	Ns	Ni	Na	RATIO	U (ppm)	RHOs (E+06)	RHOi (E+06)	F.T.AGE (Ma)
1	34	33	6	1.030	0.0	5.730	5.561	73.0 ± 17.9
2	50	46	5	1.087	0.0	10.111	9.302	77.0 ± 15.8
3	51	57	8	0.895	0.0	6.446	7.204	63.5 ± 12.3
4	11	11	4	1.000	0.0	2.781	2.781	70.9 ± 30.3
5	82	84	12	0.976	0.0	6.909	7.078	69.2 ± 10.8
	228	231			0.0	6.587	6.673	

AREA OF BASIC UNIT = 9.89E-07 cm
CHI SQUARED = .5194359 WITH 4 DEGREES OF FREEDOM
P(chi squared) = 97.2 %
CORRELATION COEFFICIENT = 0.991
VARIANCE OF SQR(Ns) = 4.46
VARIANCE OF SQR(Ni) = 4.75

Ns/Ni = 0.987 ± 0.092
MEAN RATIO = 0.998 ± 0.032

Ages calculated using a zeta of 133.9 ± 1.4 for CN1 glass
RHO D = 1.065E+06 ; ND = 5265

POOLED AGE = 70.0 ± 6.6 Ma
MEAN AGE = 70.7 ± 2.6 Ma

8902-44 APATITE hunter s107/006436 365m

IRRADIATION jmt data:jmt apatite data:hunter apatites:wk019/6
SLIDE NUMBER 1
COUNTED BY: jmt

No.	Ns	Ni	Na	RATIO	U (ppm)	RHOs (E+06)	RHOi (E+06)	F.T.AGE (Ma)
1	0	0	20	0.000	0.0	0.000	0.000	0.0 ± 0.0
2	0	0	9	0.000	0.0	0.000	0.000	0.0 ± 0.0
3	0	0	12	0.000	0.0	0.000	0.000	0.0 ± 0.0
4	0	2	28	0.000	0.2	0.000	0.072	0.0 ± 0.0
5	0	0	20	0.000	0.0	0.000	0.000	0.0 ± 0.0
6	0	1	12	0.000	0.2	0.000	0.084	0.0 ± 0.0
7	0	0	6	0.000	0.0	0.000	0.000	0.0 ± 0.0
8	0	0	12	0.000	0.0	0.000	0.000	0.0 ± 0.0
9	0	0	30	0.000	0.0	0.000	0.000	0.0 ± 0.0
10	0	0	6	0.000	0.0	0.000	0.000	0.0 ± 0.0
11	1	58	12	0.017	14.5	0.084	4.887	13.5 ± 13.6
12	0	1	9	0.000	0.3	0.000	0.112	0.0 ± 0.0
13	0	0	9	0.000	0.0	0.000	0.000	0.0 ± 0.0
14	0	0	18	0.000	0.0	0.000	0.000	0.0 ± 0.0
15	0	0	12	0.000	0.0	0.000	0.000	0.0 ± 0.0
	1	62			0.9	0.005	0.292	

AREA OF BASIC UNIT = 9.89E-07 cm
CHI SQUARED = 6.890902E-02 WITH 14 DEGREES OF FREEDOM
P(chi squared) = 100.0 %
CORRELATION COEFFICIENT = 0.999
VARIANCE OF SQR(Ns) = 0.07
VARIANCE OF SQR(Ni) = 3.84

Ns/Ni = 0.016 ± 0.016
MEAN RATIO = 0.001 ± 0.001

Ages calculated using a zeta of 354.9 ± 4.3 for SRM612 glass
RHO D = 4.406E+06 ; ND = 3486

POOLED AGE = 12.6 ± 12.7 Ma
MEAN AGE = 0.9 ± 0.9 Ma

8902-44 ZIRCON hunter s107/006436 365m

IRRADIATION jmt data:jmt zircon data:hunter zircons:wk023/16
SLIDE NUMBER 1
COUNTED BY: jmt

No.	Ns	Ni	Na	RATIO	U (ppm)	RHOs (E+06)	RHOi (E+06)	F.T.AGE (Ma)
1	37	28	6	1.321	0.0	6.235	4.719	88.5 ± 22.2
2	27	21	4	1.286	0.0	6.825	5.308	86.1 ± 25.1
3	46	36	4	1.278	0.0	11.628	9.100	85.6 ± 19.1
4	32	21	8	1.524	0.0	4.044	2.654	101.9 ± 28.7
5	44	32	9	1.375	0.0	4.943	3.595	92.0 ± 21.4
6	15	19	3	0.789	0.0	5.056	6.404	53.0 ± 18.3
7	44	39	4	1.128	0.0	11.122	9.858	75.6 ± 16.7
8	40	34	4	1.176	0.0	10.111	8.595	78.8 ± 18.4
9	517	432	48	1.197	0.0	10.891	9.100	80.2 ± 5.4
	802	662			0.0	9.010	7.437	

AREA OF BASIC UNIT = 9.89E-07 cm
CHI SQUARED = 2.903553 WITH 8 DEGREES OF FREEDOM
P(chi squared) = 94.0 %
CORRELATION COEFFICIENT = 1.000
VARIANCE OF SQR(Ns) = 32.35
VARIANCE OF SQR(Ni) = 27.04

Ns/Ni = 1.211 ± 0.064
MEAN RATIO = 1.231 ± 0.068

Ages calculated using a zeta of 133.9 ± 1.4 for CN1 glass
RHO D = 1.007E+06 ; ND = 4979

POOLED AGE = 81.2 ± 4.5 Ma
MEAN AGE = 82.4 ± 4.8 Ma

8902-45 APATITE hunter s107/015436 395m

IRRADIATION jmt data:jmt apatite data:hunter apatites:wk019/4
SLIDE NUMBER 1
COUNTED BY: jmt

No.	Ns	Ni	Na	RATIO	U (ppm)	RHOs (E+06)	RHOi (E+06)	F.T.AGE (Ma)
1	0	1	8	0.000	0.4	0.000	0.126	0.0 ± 0.0
2	0	3	12	0.000	0.8	0.000	0.253	0.0 ± 0.0
3	0	0	12	0.000	0.0	0.000	0.000	0.0 ± 0.0
4	0	1	10	0.000	0.3	0.000	0.101	0.0 ± 0.0
5	0	3	9	0.000	1.0	0.000	0.337	0.0 ± 0.0
6	0	2	9	0.000	0.7	0.000	0.225	0.0 ± 0.0
7	0	3	9	0.000	1.0	0.000	0.337	0.0 ± 0.0
8	0	2	18	0.000	0.3	0.000	0.112	0.0 ± 0.0
9	0	17	16	0.000	3.2	0.000	1.074	0.0 ± 0.0
10	0	18	30	0.000	1.8	0.000	0.607	0.0 ± 0.0
11	0	14	15	0.000	2.8	0.000	0.944	0.0 ± 0.0
12	0	0	8	0.000	0.0	0.000	0.000	0.0 ± 0.0
13	0	5	9	0.000	1.7	0.000	0.562	0.0 ± 0.0
14	0	0	15	0.000	0.0	0.000	0.000	0.0 ± 0.0
15	0	0	4	0.000	0.0	0.000	0.000	0.0 ± 0.0
	0	69			1.1	0.000	0.379	

AREA OF BASIC UNIT = 9.89E-07 cm
CHI SQUARED = 3.058846E-06 WITH 14 DEGREES OF FREEDOM
P(chi squared) = 100.0 %
CORRELATION COEFFICIENT = 0.546
VARIANCE OF SQR(Ns) = 0.00
VARIANCE OF SQR(Ni) = 2.09

Ns/Ni = 0.000 ± 0.000
MEAN RATIO = 0.000 ± 0.000

Ages calculated using a zeta of 354.9 ± 4.3 for SRM612 glass
RHO D = 4.339E+06 ; ND = 3433

POOLED AGE = 0.0 ± 0.0 Ma
MEAN AGE = 0.0 ± 0.0 Ma

8902-45 ZIRCON hunter s107/015436 395m

IRRADIATION jmt data:jmt zircon data:hunter zircons:wk038/9
SLIDE NUMBER 1
COUNTED BY: jmt

No.	Ns	Ni	Na	RATIO	U (ppm)	RHOs (E+06)	RHOi (E+06)	F.T.AGE (Ma)
1	87	60	9	1.450	0.0	9.774	6.741	102.6 ± 17.3
2	61	54	18	1.130	0.0	3.427	3.033	80.0 ± 15.0
3	19	19	4	1.000	0.0	4.803	4.803	70.9 ± 23.0
4	28	17	3	1.647	0.0	9.437	5.730	116.4 ± 35.8
5	60	41	4	1.463	0.0	15.167	10.364	103.5 ± 21.0
6	80	58	14	1.379	0.0	5.778	4.189	97.6 ± 16.9
7	24	20	6	1.200	0.0	4.044	3.370	85.0 ± 25.8
	359	269			0.0	6.258	4.690	

AREA OF BASIC UNIT = 9.89E-07 cm
CHI SQUARED = 2.676176 WITH 6 DEGREES OF FREEDOM
P(chi squared) = 84.8 %
CORRELATION COEFFICIENT = 0.969
VARIANCE OF SQR(Ns) = 4.11
VARIANCE OF SQR(Ni) = 2.70

Ns/Ni = 1.335 ± 0.108
MEAN RATIO = 1.324 ± 0.085

Ages calculated using a zeta of 133.9 ± 1.4 for CN1 glass
RHO D = 1.065E+06 ; ND = 5265

POOLED AGE = 94.5 ± 7.8 Ma
MEAN AGE = 93.7 ± 6.2 Ma

8902-46 APATITE hunter s107/032435 425m

IRRADIATION jmt data:jmt apatite data:hunter apatites:wk019/3
SLIDE NUMBER 1
COUNTED BY: jmt

No.	Ns	Ni	Na	RATIO	U (ppm)	RHOs (E+06)	RHOi (E+06)	F.T.AGE (Ma)
1	0	45	70	0.000	2.0	0.000	0.650	0.0 ± 0.0
2	0	0	12	0.000	0.0	0.000	0.000	0.0 ± 0.0
3	0	0	20	0.000	0.0	0.000	0.000	0.0 ± 0.0
4	0	0	16	0.000	0.0	0.000	0.000	0.0 ± 0.0
5	0	0	60	0.000	0.0	0.000	0.000	0.0 ± 0.0
6	0	0	24	0.000	0.0	0.000	0.000	0.0 ± 0.0
7	0	0	20	0.000	0.0	0.000	0.000	0.0 ± 0.0
8	0	1	12	0.000	0.3	0.000	0.084	0.0 ± 0.0
9	0	0	24	0.000	0.0	0.000	0.000	0.0 ± 0.0
10	0	0	24	0.000	0.0	0.000	0.000	0.0 ± 0.0
11	0	0	9	0.000	0.0	0.000	0.000	0.0 ± 0.0
12	0	1	12	0.000	0.3	0.000	0.084	0.0 ± 0.0
13	0	0	20	0.000	0.0	0.000	0.000	0.0 ± 0.0
14	0	0	20	0.000	0.0	0.000	0.000	0.0 ± 0.0
15	0	2	30	0.000	0.2	0.000	0.067	0.0 ± 0.0
	0	49			0.4	0.000	0.133	

AREA OF BASIC UNIT = 9.89E-07 cm
CHI SQUARED = 8.891332E-08 WITH 14 DEGREES OF FREEDOM
P(chi squared) = 100.0 %
CORRELATION COEFFICIENT = 0.999
VARIANCE OF SQR(Ns) = 0.00
VARIANCE OF SQR(Ni) = 3.00

Ns/Ni = 0.000 ± 0.000
MEAN RATIO = 0.000 ± 0.000

Ages calculated using a zeta of 354.9 ± 4.3 for SRM612 glass
RHO D = 4.305E+06 ; ND = 3406

POOLED AGE = 0.0 ± 0.0 Ma
MEAN AGE = 0.0 ± 0.0 Ma

8902-46 ZIRCON hunter s107/032435 425m

IRRADIATION jmt data:jmt zircon data:hunter zircons:wk023/14
SLIDE NUMBER 1
COUNTED BY: jmt

No.	Ns	Ni	Na	RATIO	U (ppm)	RHOs (E+06)	RHOi (E+06)	F.T.AGE (Ma)
1	132	77	14	1.714	0.0	9.533	5.561	112.6 ± 16.3
2	124	89	12	1.393	0.0	10.448	7.499	91.7 ± 12.8
3	63	36	6	1.750	0.0	10.617	6.067	115.0 ± 24.1
4	56	44	6	1.273	0.0	9.437	7.415	83.8 ± 17.0
5	54	42	6	1.286	0.0	9.100	7.078	84.7 ± 17.5
6	260	164	24	1.585	0.0	10.954	6.909	104.2 ± 10.6
	689	452			0.0	10.245	6.721	

AREA OF BASIC UNIT = 9.89E-07 cm
CHI SQUARED = 3.173387 WITH 5 DEGREES OF FREEDOM
P(chi squared) = 67.3 %
CORRELATION COEFFICIENT = 0.990
VARIANCE OF SQR(Ns) = 11.65
VARIANCE OF SQR(Ni) = 6.64

Ns/Ni = 1.524 ± 0.092
MEAN RATIO = 1.500 ± 0.087

Ages calculated using a zeta of 133.9 ± 1.4 for CN1 glass
RHO D = 9.901E+05 ; ND = 4894

POOLED AGE = 100.3 ± 6.3 Ma
MEAN AGE = 98.7 ± 6.0 Ma

8902-47 APATITE hunter s107/042435 380m

IRRADIATION jmt data:jmt apatite data:hunter apatites:wk010/7
SLIDE NUMBER 1
COUNTED BY: jmt

No.	Ns	Ni	Na	RATIO	U (ppm)	RHOs (E+06)	RHOi (E+06)	F.T.AGE (Ma)
1	0	6	4	0.000	18.4	0.000	1.517	0.0 ± 0.0
2	0	27	6	0.000	55.2	0.000	4.550	0.0 ± 0.0
3	0	3	9	0.000	4.1	0.000	0.337	0.0 ± 0.0
4	0	4	12	0.000	4.1	0.000	0.337	0.0 ± 0.0
5	0	2	6	0.000	4.1	0.000	0.337	0.0 ± 0.0
6	0	5	9	0.000	6.8	0.000	0.562	0.0 ± 0.0
7	0	19	4	0.000	58.3	0.000	4.803	0.0 ± 0.0
8	0	2	6	0.000	4.1	0.000	0.337	0.0 ± 0.0
9	0	3	4	0.000	9.2	0.000	0.758	0.0 ± 0.0
10	0	20	9	0.000	27.3	0.000	2.247	0.0 ± 0.0
	0	91			16.2	0.000	1.334	

AREA OF BASIC UNIT = 9.89E-07 cm
CHI SQUARED = 2.37037E-06 WITH 9 DEGREES OF FREEDOM
P(chi squared) = 100.0 %
CORRELATION COEFFICIENT = 0.682
VARIANCE OF SQR(Ns) = 0.00
VARIANCE OF SQR(Ni) = 2.01

Ns/Ni = 0.000 ± 0.000
MEAN RATIO = 0.000 ± 0.000

Ages calculated using a zeta of 354.9 ± 4.3 for SRM612 glass
RHO D = 1.080E+06 ; ND = 2136

POOLED AGE = 0.0 ± 0.0 Ma
MEAN AGE = 0.0 ± 0.0 Ma

8902-47 ZIRCON hunter s107/042435 380m

IRRADIATION jmt data:jmt zircon data:hunter zircons:wk023/13
SLIDE NUMBER 1
COUNTED BY: jmt

No.	Ns	Ni	Na	RATIO	U (ppm)	RHOs (E+06)	RHOi (E+06)	F.T.AGE (Ma)
1	41	28	4	1.464	0.0	10.364	7.078	95.5 ± 23.5
2	169	104	15	1.625	0.0	11.392	7.010	105.9 ± 13.3
3	62	52	4	1.192	0.0	15.672	13.145	77.9 ± 14.7
4	135	65	12	2.077	0.0	11.375	5.477	135.1 ± 20.5
5	35	30	4	1.167	0.0	8.847	7.583	76.2 ± 19.0
6	42	43	6	0.977	0.0	7.078	7.246	63.9 ± 13.9
7	97	70	10	1.386	0.0	9.808	7.078	90.4 ± 14.3
	581	392			0.0	10.681	7.207	

AREA OF BASIC UNIT = 9.89E-07 cm
CHI SQUARED = 11.7972 WITH 6 DEGREES OF FREEDOM
P(chi squared) = 6.7 %
CORRELATION COEFFICIENT = 0.938
VARIANCE OF SQR(Ns) = 7.83
VARIANCE OF SQR(Ni) = 3.01

Ns/Ni = 1.482 ± 0.097
MEAN RATIO = 1.413 ± 0.137

Ages calculated using a zeta of 133.9 ± 1.4 for CN1 glass
RHO D = 9.815E+05 ; ND = 4852

POOLED AGE = 96.7 ± 6.5 Ma
MEAN AGE = 92.2 ± 9.1 Ma

8902-48 APATITE hunter s107/057439 410m

IRRADIATION jmt data:jmt apatite data:hunter apatites:wk010/6
SLIDE NUMBER 1
COUNTED BY: jmt

No.	Ns	Ni	Na	RATIO	U (ppm)	RHOs (E+06)	RHOi (E+06)	F.T AGE (Ma)
1	0	7	10	0.000	8.6	0.000	0.708	0.0 ± 0.0
2	0	9	6	0.000	18.5	0.000	1.517	0.0 ± 0.0
3	0	6	9	0.000	8.2	0.000	0.674	0.0 ± 0.0
4	2	5	8	0.400	7.7	0.253	0.632	75.6 ± 63.3
5	1	33	12	0.030	34.0	0.084	2.781	5.8 ± 5.8
6	0	1	25	0.000	0.5	0.000	0.040	0.0 ± 0.0
7	0	3	6	0.000	6.2	0.000	0.506	0.0 ± 0.0
8	1	11	6	0.091	22.7	0.169	1.854	17.3 ± 18.0
9	0	3	4	0.000	9.3	0.000	0.758	0.0 ± 0.0
10	2	62	16	0.032	47.9	0.126	3.918	6.1 ± 4.4
11	0	103	10	0.000	127.3	0.000	10.415	0.0 ± 0.0
12	1	3	6	0.333	6.2	0.169	0.506	63.1 ± 72.9
13	2	62	9	0.032	85.1	0.225	6.966	6.1 ± 4.4
14	0	18	8	0.000	27.8	0.000	2.275	0.0 ± 0.0
15	0	11	12	0.000	11.3	0.000	0.927	0.0 ± 0.0
16	1	3	6	0.333	6.2	0.169	0.506	63.1 ± 72.9
17	0	7	6	0.000	14.4	0.000	1.180	0.0 ± 0.0
18	3	22	4	0.136	68.0	0.758	5.561	25.9 ± 15.9
19	1	3	9	0.333	4.1	0.112	0.337	63.1 ± 72.9
20	2	33	6	0.061	68.0	0.337	5.561	11.5 ± 8.4
21	0	3	6	0.000	6.2	0.000	0.506	0.0 ± 0.0
22	0	3	6	0.000	6.2	0.000	0.506	0.0 ± 0.0
23	0	18	12	0.000	18.5	0.000	1.517	0.0 ± 0.0
24	1	119	15	0.008	98.0	0.067	8.022	1.6 ± 1.6
25	3	213	40	0.014	65.8	0.076	5.384	2.7 ± 1.6
	20	761			36.6	0.079	2.994	

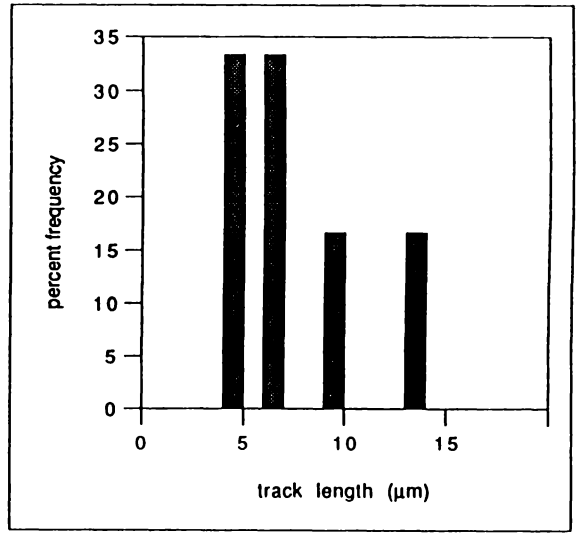
AREA OF BASIC UNIT = 9.89E-07 cm
CHI SQUARED = 62.97167 WITH 24 DEGREES OF FREEDOM
P(chi squared) = < 0.1 %
CORRELATION COEFFICIENT = 0.500
VARIANCE OF SQR(Ns) = 0.45
VARIANCE OF SQR(Ni) = 11.98

Ns/Ni = 0.026 ± 0.006
MEAN RATIO = 0.072 ± 0.026

Ages calculated using a zeta of 354.9 ± 4.3 for SRM612 glass
RHO D = 1.072E+06 ; ND = 2120

POOLED AGE = 5.0 ± 1.1 Ma
MEAN AGE = 13.7 ± 4.9 Ma

8902-48



n = 6
Mean = 7.50 µm
Sample std. dev. = 2.98 µm

8902-48 ZIRCON hunter s107/057439 410m

IRRADIATION jmt data:jmt zircon data:hunter zircons:wk023/12
SLIDE NUMBER 1
COUNTED BY: jmt

No.	Ns	Ni	Na	RATIO	U (ppm)	RHOs (E+06)	RHOi (E+06)	F.T.AGE (Ma)
1	12	7	4	1.714	0.0	3.033	1.769	110.7 ± 52.7
2	61	35	12	1.743	0.0	5.140	2.949	112.5 ± 23.9
3	32	20	4	1.600	0.0	8.089	5.056	103.4 ± 29.5
4	72	31	6	2.323	0.0	12.133	5.224	149.5 ± 32.2
5	60	37	6	1.622	0.0	10.111	6.235	104.8 ± 22.0
6	103	70	9	1.471	0.0	11.572	7.864	95.1 ± 14.8
7	110	65	16	1.692	0.0	6.951	4.108	109.3 ± 17.2
8	42	17	6	2.471	0.0	7.078	2.865	158.9 ± 45.8
9	49	28	4	1.750	0.0	12.386	7.078	113.0 ± 26.8
10	177	72	15	2.458	0.0	11.931	4.853	158.2 ± 22.3
11	132	80	15	1.650	0.0	8.898	5.393	106.6 ± 15.2
12	42	36	4	1.167	0.0	10.617	9.100	75.5 ± 17.2
	892	498			0.0	8.930	4.986	

AREA OF BASIC UNIT = 9.89E-07 cm
CHI SQUARED = 14.02722 WITH 11 DEGREES OF FREEDOM
P(chi squared) = 23.1 %
CORRELATION COEFFICIENT = 0.917
VARIANCE OF SQR(Ns) = 7.51
VARIANCE OF SQR(Ni) = 3.84

Ns/Ni = 1.791 ± 0.100
MEAN RATIO = 1.805 ± 0.116

Ages calculated using a zeta of 133.9 ± 1.4 for CN1 glass
RHO D = 9.729E+05 ; ND = 4809

POOLED AGE = 115.6 ± 6.8 Ma
MEAN AGE = 116.5 ± 7.8 Ma

8902-49 APATITE hunter s107/084443 380m

IRRADIATION jmt data:jmt apatite data:hunter apatites:wk043/8
SLIDE NUMBER 1
COUNTED BY: jmt

No.	Ns	Ni	Na	RATIO	U (ppm)	RHOs (E+06)	RHOi (E+06)	F.T.AGE (Ma)
1	2	45	4	0.044	167.9	0.506	11.375	7.0 ± 5.1
2	1	13	12	0.077	16.2	0.084	1.095	12.1 ± 12.6
3	0	7	9	0.000	11.6	0.000	0.786	0.0 ± 0.0
4	0	2	6	0.000	5.0	0.000	0.337	0.0 ± 0.0
5	1	14	12	0.071	17.4	0.084	1.180	11.2 ± 11.6
6	0	14	15	0.000	13.9	0.000	0.944	0.0 ± 0.0
7	0	7	12	0.000	8.7	0.000	0.590	0.0 ± 0.0
8	2	41	12	0.049	51.0	0.169	3.455	7.7 ± 5.6
9	0	1	20	0.000	0.7	0.000	0.051	0.0 ± 0.0
10	1	13	30	0.077	6.5	0.034	0.438	12.1 ± 12.6
11	0	5	18	0.000	4.1	0.000	0.281	0.0 ± 0.0
12	2	39	12	0.051	48.5	0.169	3.286	8.1 ± 5.9
13	0	52	20	0.000	38.8	0.000	2.629	0.0 ± 0.0
14	1	18	9	0.056	29.8	0.112	2.022	8.7 ± 9.0
15	0	9	14	0.000	9.6	0.000	0.650	0.0 ± 0.0
16	3	129	12	0.023	160.4	0.253	10.870	3.7 ± 2.1
17	1	12	20	0.083	9.0	0.051	0.607	13.1 ± 13.6
18	0	4	9	0.000	6.6	0.000	0.449	0.0 ± 0.0
19	0	14	12	0.000	17.4	0.000	1.180	0.0 ± 0.0
20	1	33	12	0.030	41.0	0.084	2.781	4.8 ± 4.8
	15	472			26.1	0.056	1.768	

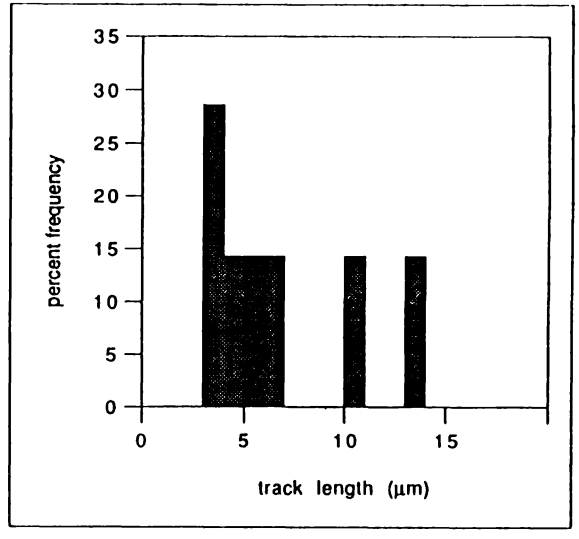
AREA OF BASIC UNIT = 9.89E-07 cm
CHI SQUARED = 8.386346 WITH 19 DEGREES OF FREEDOM
P(chi squared) = 98.2 %
CORRELATION COEFFICIENT = 0.766
VARIANCE OF SQR(Ns) = 0.41
VARIANCE OF SQR(Ni) = 5.94

Ns/Ni = 0.032 ± 0.008
MEAN RATIO = 0.028 ± 0.007

Ages calculated using a zeta of 354.9 ± 4.3 for SRM612 glass
RHO D = 8.876E+05 ; ND = 5267

POOLED AGE = 5.0 ± 1.3 Ma
MEAN AGE = 4.4 ± 1.1 Ma

8902-49



n = 7
Mean = 6.55 µm
Sample std. dev. = 3.69 µm

8902-49 ZIRCON hunter s107/084443 380m

IRRADIATION jmt data:jmt zircon data:hunter zircons:wk038/10
SLIDE NUMBER 1
COUNTED BY: jmt

No.	Ns	Ni	Na	RATIO	U (ppm)	RHOs (E+06)	RHOi (E+06)	F.T.AGE (Ma)
1	92	58	24	1.586	0.0	3.876	2.444	112.1 ± 18.9
2	45	21	10	2.143	0.0	4.550	2.123	151.0 ± 40.0
3	135	106	14	1.274	0.0	9.750	7.656	90.2 ± 11.8
4	58	28	6	2.071	0.0	9.774	4.719	146.0 ± 33.7
5	155	84	25	1.845	0.0	6.269	3.397	130.2 ± 17.8
6	199	84	40	2.369	0.0	5.030	2.123	166.7 ± 21.9
	684	381			0.0	5.812	3.237	

AREA OF BASIC UNIT = 9.89E-07 cm
CHI SQUARED = 13.064 WITH 5 DEGREES OF FREEDOM
P(chi squared) = 2.3 %
CORRELATION COEFFICIENT = 0.844
VARIANCE OF SQR(Ns) = 8.29
VARIANCE OF SQR(Ni) = 5.31

Ns/Ni = 1.795 ± 0.115
MEAN RATIO = 1.881 ± 0.163

Ages calculated using a zeta of 133.9 ± 1.4 for CN1 glass
RHO D = 1.065E+06 ; ND = 5265

POOLED AGE = 126.8 ± 8.4 Ma
MEAN AGE = 132.8 ± 11.8 Ma

8902-50 APATITE hunter s107/090452 395m

IRRADIATION jmt data:jmt apatite data:hunter apatites:wk010/4
SLIDE NUMBER 1
COUNTED BY: jmt

No.	Ns	NI	Na	RATIO	U (ppm)	RHOs (E+06)	RHOi (E+06)	F.TAGE (Ma)
1	2	147	60	0.014	30.8	0.034	2.477	2.5 ± 1.8
2	1	6	15	0.167	5.0	0.067	0.404	31.1 ± 33.6
3	0	11	9	0.000	15.3	0.000	1.236	0.0 ± 0.0
4	1	32	18	0.031	22.3	0.056	1.798	5.8 ± 5.9
5	0	148	40	0.000	46.5	0.000	3.741	0.0 ± 0.0
6	3	45	3	0.067	188.3	1.011	15.167	12.5 ± 7.4
7	0	5	12	0.000	5.2	0.000	0.421	0.0 ± 0.0
8	0	19	16	0.000	14.9	0.000	1.201	0.0 ± 0.0
9	0	9	15	0.000	7.5	0.000	0.607	0.0 ± 0.0
10	1	15	12	0.067	15.7	0.084	1.264	12.5 ± 12.9
11	1	9	4	0.111	28.2	0.253	2.275	20.8 ± 21.9
12	8	292	18	0.027	203.7	0.449	16.403	5.1 ± 1.8
13	1	177	50	0.006	44.4	0.020	3.579	1.1 ± 1.1
14	7	125	18	0.056	87.2	0.393	7.022	10.5 ± 4.1
15	0	3	9	0.000	4.2	0.000	0.337	0.0 ± 0.0
16	2	32	24	0.062	16.7	0.084	1.348	11.7 ± 8.5
17	0	10	30	0.000	4.2	0.000	0.337	0.0 ± 0.0
18	4	35	36	0.114	12.2	0.112	0.983	21.4 ± 11.3
19	0	5	9	0.000	7.0	0.000	0.562	0.0 ± 0.0
20	1	17	6	0.059	35.6	0.169	2.865	11.0 ± 11.3
	32	1142			35.5	0.080	2.858	

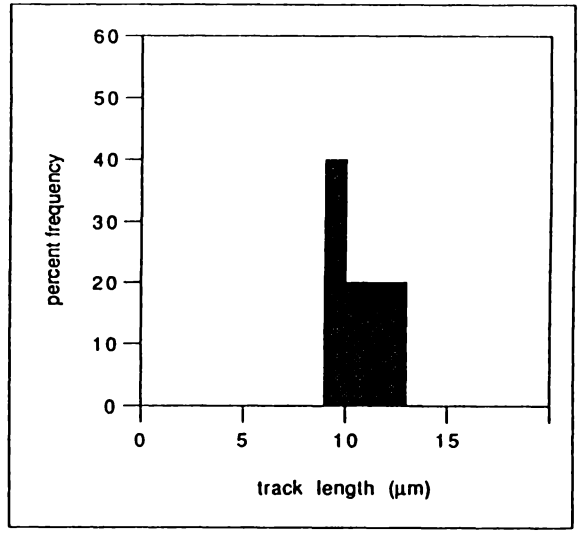
AREA OF BASIC UNIT = 9.89E-07 cm
CHI SQUARED = 32.11086 WITH 19 DEGREES OF FREEDOM
P(chi squared) = 3.0 %
CORRELATION COEFFICIENT = 0.661
VARIANCE OF SQR(Ns) = 0.83
VARIANCE OF SQR(Ni) = 20.11

Ns/Ni = 0.028 ± 0.005
MEAN RATIO = 0.039 ± 0.011

Ages calculated using a zeta of 354.9 ± 4.3 for SRM612 glass
RHO D = 1.055E+06 ; ND = 2088

POOLED AGE = 5.2 ± 0.9 Ma
MEAN AGE = 7.3 ± 2.0 Ma

8902-50



n = 5
Mean = 10.74 µm
Sample std. dev. = 1.05 µm

8902-50 ZIRCON hunter s107/090452 395m

IRRADIATION jmt data:jmt zircon data:hunter zircons:wk038/11
SLIDE NUMBER 1
COUNTED BY: jmt

No.	Ns	Ni	Na	RATIO	U (ppm)	RHOs (E+06)	RHOi (E+06)	F.T.AGE (Ma)
1	64	41	10	1.561	0.0	6.471	4.146	110.4 ± 22.2
2	139	71	12	1.958	0.0	11.712	5.982	138.1 ± 20.3
3	133	68	14	1.956	0.0	9.606	4.911	138.0 ± 20.7
4	32	13	3	2.462	0.0	10.785	4.382	173.2 ± 57.0
5	114	63	12	1.810	0.0	9.606	5.308	127.7 ± 20.2
6	113	67	9	1.687	0.0	12.695	7.527	119.1 ± 18.5
7	232	154	18	1.506	0.0	13.032	8.651	106.5 ± 11.2
	827	477			0.0	10.720	6.183	

AREA OF BASIC UNIT = 9.89E-07 cm
CHI SQUARED = 4.708913 WITH 6 DEGREES OF FREEDOM
P(chi squared) = 58.2 %
CORRELATION COEFFICIENT = 0.981
VARIANCE OF SQR(Ns) = 9.15
VARIANCE OF SQR(Ni) = 6.92

Ns/Ni = 1.734 ± 0.100
MEAN RATIO = 1.848 ± 0.122

Ages calculated using a zeta of 133.9 ± 1.4 for CN1 glass
RHO D = 1.065E+06 ; ND = 5265

POOLED AGE = 122.4 ± 7.4 Ma
MEAN AGE = 130.5 ± 8.9 Ma

8902-51 APATITE haast s87/098028 75m

IRRADIATION jmt data:jmt apatite data:haast apatites:wk019/1
SLIDE NUMBER 1
COUNTED BY: jmt

No.	Ns	Ni	Na	RATIO	U (ppm)	RHOs (E+06)	RHOi (E+06)	F.T.AGE (Ma)
1	0	2	48	0.000	0.1	0.000	0.042	0.0 ± 0.0
2	0	1	15	0.000	0.2	0.000	0.067	0.0 ± 0.0
3	0	5	36	0.000	0.4	0.000	0.140	0.0 ± 0.0
4	0	13	30	0.000	1.4	0.000	0.438	0.0 ± 0.0
5	0	1	16	0.000	0.2	0.000	0.063	0.0 ± 0.0
6	0	1	30	0.000	0.1	0.000	0.034	0.0 ± 0.0
7	0	2	70	0.000	0.1	0.000	0.029	0.0 ± 0.0
8	0	1	20	0.000	0.2	0.000	0.051	0.0 ± 0.0
9	0	3	24	0.000	0.4	0.000	0.126	0.0 ± 0.0
10	0	2	18	0.000	0.3	0.000	0.112	0.0 ± 0.0
11	0	0	30	0.000	0.0	0.000	0.000	0.0 ± 0.0
12	0	3	36	0.000	0.3	0.000	0.084	0.0 ± 0.0
13	0	2	16	0.000	0.4	0.000	0.126	0.0 ± 0.0
14	0	0	24	0.000	0.0	0.000	0.000	0.0 ± 0.0
15	0	1	25	0.000	0.1	0.000	0.040	0.0 ± 0.0
	0	37			0.3	0.000	0.085	

AREA OF BASIC UNIT = 9.89E-07 cm
CHI SQUARED = 1.846169E-06 WITH 14 DEGREES OF FREEDOM
P(chi squared) = 100.0 %
CORRELATION COEFFICIENT = 0.916
VARIANCE OF SQR(Ns) = 0.00
VARIANCE OF SQR(Ni) = 0.74

Ns/Ni = 0.000 ± 0.000
MEAN RATIO = 0.000 ± 0.000

Ages calculated using a zeta of 354.9 ± 4.3 for SRM612 glass
RHO D = 4.238E+06 ; ND = 3353

POOLED AGE = 0.0 ± 0.0 Ma
MEAN AGE = 0.0 ± 0.0 Ma

8902-51 ZIRCON haast s87/098028 75m

IRRADIATION jmt data:jmt zircon data:haast zircons:wk023/9
SLIDE NUMBER 1
COUNTED BY: jmt

No.	Ns	Ni	Na	RATIO	U (ppm)	RHOs (E+06)	RHOi (E+06)	F.T.AGE (Ma)
1	3	77	12	0.039	0.0	0.253	6.488	2.5 ± 1.5
2	2	48	6	0.042	0.0	0.337	8.089	2.6 ± 1.9
3	3	82	6	0.037	0.0	0.506	13.819	2.3 ± 1.4
4	4	44	4	0.091	0.0	1.011	11.122	5.8 ± 3.0
5	10	133	12	0.075	0.0	0.843	11.207	4.8 ± 1.6
	22	384			0.0	0.556	9.707	

AREA OF BASIC UNIT = 9.89E-07 cm
CHI SQUARED = 2.710159 WITH 4 DEGREES OF FREEDOM
P(chi squared) = 60.7 %
CORRELATION COEFFICIENT = 0.850
VARIANCE OF SQR(Ns) = 0.46
VARIANCE OF SQR(Ni) = 3.87

Ns/Ni = 0.057 ± 0.013
MEAN RATIO = 0.057 ± 0.011

Ages calculated using a zeta of 133.9 ± 1.4 for CN1 glass
RHO D = 9.471E+05 ; ND = 4682

POOLED AGE = 3.6 ± 0.8 Ma
MEAN AGE = 3.6 ± 0.7 Ma

8902-52 APATITE haast s87/117031 90m

IRRADIATION jmt data:jmt apatite data:haast apatites:wk020/14
SLIDE NUMBER 1
COUNTED BY: jmt

No.	Ns	Ni	Na	RATIO	U (ppm)	RHOs (E+06)	RHOi (E+06)	F.T.AGE (Ma)
1	0	1	42	0.000	0.1	0.000	0.024	0.0 ± 0.0
2	0	16	24	0.000	1.9	0.000	0.674	0.0 ± 0.0
3	0	1	16	0.000	0.2	0.000	0.063	0.0 ± 0.0
4	0	18	24	0.000	2.2	0.000	0.758	0.0 ± 0.0
5	0	0	24	0.000	0.0	0.000	0.000	0.0 ± 0.0
6	0	0	20	0.000	0.0	0.000	0.000	0.0 ± 0.0
7	0	4	70	0.000	0.2	0.000	0.058	0.0 ± 0.0
8	0	2	12	0.000	0.5	0.000	0.169	0.0 ± 0.0
9	0	0	24	0.000	0.0	0.000	0.000	0.0 ± 0.0
10	0	1	20	0.000	0.1	0.000	0.051	0.0 ± 0.0
11	0	0	6	0.000	0.0	0.000	0.000	0.0 ± 0.0
12	0	1	18	0.000	0.2	0.000	0.056	0.0 ± 0.0
13	0	1	24	0.000	0.1	0.000	0.042	0.0 ± 0.0
14	0	1	21	0.000	0.1	0.000	0.048	0.0 ± 0.0
15	0	1	12	0.000	0.2	0.000	0.084	0.0 ± 0.0
	0	47			0.4	0.000	0.133	

AREA OF BASIC UNIT = 9.89E-07 cm
CHI SQUARED = 1.611133E-06 WITH 14 DEGREES OF FREEDOM
P(chi squared) = 100.0 %
CORRELATION COEFFICIENT = 0.718
VARIANCE OF SQR(Ns) = 0.00
VARIANCE OF SQR(Ni) = 1.69

Ns/Ni = 0.000 ± 0.000
MEAN RATIO = 0.000 ± 0.000

Ages calculated using a zeta of 354.9 ± 4.3 for SRM612 glass
RHO D = 4.533E+06 ; ND = 3586

POOLED AGE = 0.0 ± 0.0 Ma
MEAN AGE = 0.0 ± 0.0 Ma

8902-52 ZIRCON haast s87/117031 90m

IRRADIATION jmt data:jmt zircon data:haast zircons:wk023/8
SLIDE NUMBER 1
COUNTED BY: jmt

No.	Ns	Ni	Na	RATIO	U (ppm)	RHOs (E+06)	RHOi (E+06)	F.T.AGE (Ma)
1	4	62	10	0.065	0.0	0.404	6.269	4.1 ± 2.1
2	5	76	5	0.066	0.0	1.011	15.369	4.1 ± 1.9
3	15	242	16	0.062	0.0	0.948	15.293	3.9 ± 1.0
4	24	228	15	0.105	0.0	1.618	15.369	6.6 ± 1.4
5	7	103	16	0.068	0.0	0.442	6.509	4.3 ± 1.7
6	31	256	30	0.121	0.0	1.045	8.628	7.6 ± 1.5
	86	967			0.0	0.945	10.628	

AREA OF BASIC UNIT = 9.89E-07 cm
CHI SQUARED = 6.432055 WITH 5 DEGREES OF FREEDOM
P(chi squared) = 26.6 %
CORRELATION COEFFICIENT = 0.904
VARIANCE OF SQR(Ns) = 2.19
VARIANCE OF SQR(Ni) = 13.83

Ns/Ni = 0.089 ± 0.010
MEAN RATIO = 0.081 ± 0.010

Ages calculated using a zeta of 133.9 ± 1.4 for CN1 glass
RHO D = 9.385E+05 ; ND = 4640

POOLED AGE = 5.6 ± 0.6 Ma
MEAN AGE = 5.1 ± 0.7 Ma

8902-53 APATITE haast s87/130023 90m

IRRADIATION jmt data:jmt apatite data:haast apatites:wk020/13
SLIDE NUMBER 1
COUNTED BY: jmt

No.	Ns	Ni	Na	RATIO	U (ppm)	RHOs (E+06)	RHOi (E+06)	F.T AGE (Ma)
1	0	0	15	0.000	0.0	0.000	0.000	0.0 ± 0.0
2	0	1	20	0.000	0.1	0.000	0.051	0.0 ± 0.0
3	0	1	32	0.000	0.1	0.000	0.032	0.0 ± 0.0
4	0	2	36	0.000	0.2	0.000	0.056	0.0 ± 0.0
5	0	0	15	0.000	0.0	0.000	0.000	0.0 ± 0.0
6	0	0	28	0.000	0.0	0.000	0.000	0.0 ± 0.0
7	0	4	40	0.000	0.3	0.000	0.101	0.0 ± 0.0
8	0	1	20	0.000	0.1	0.000	0.051	0.0 ± 0.0
9	0	0	20	0.000	0.0	0.000	0.000	0.0 ± 0.0
10	0	8	40	0.000	0.6	0.000	0.202	0.0 ± 0.0
11	0	1	48	0.000	0.1	0.000	0.021	0.0 ± 0.0
12	0	1	25	0.000	0.1	0.000	0.040	0.0 ± 0.0
13	0	5	50	0.000	0.3	0.000	0.101	0.0 ± 0.0
14	0	0	28	0.000	0.0	0.000	0.000	0.0 ± 0.0
15	0	1	30	0.000	0.1	0.000	0.034	0.0 ± 0.0
	0	25			0.2	0.000	0.057	

AREA OF BASIC UNIT = 9.89E-07 cm
CHI SQUARED = 2.125062E-06 WITH 14 DEGREES OF FREEDOM
P(chi squared) = 100.0 %
CORRELATION COEFFICIENT = 0.766
VARIANCE OF SQR(Ns) = 0.00
VARIANCE OF SQR(Ni) = 0.78

Ns/Ni = 0.000 ± 0.000
MEAN RATIO = 0.000 ± 0.000

Ages calculated using a zeta of 354.9 ± 4.3 for SRM612 glass
RHO D = 4.497E+06 ; ND = 3558

POOLED AGE = 0.0 ± 0.0 Ma
MEAN AGE = 0.0 ± 0.0 Ma

8902-54 APATITE haast s98/126935 135m

IRRADIATION jmt data:jmt apatite data:haast apatites:wk021/2
SLIDE NUMBER 1
COUNTED BY: jmt

No.	Ns	Ni	Na	RATIO	U (ppm)	RHOs (E+06)	RHOi (E+06)	F.T.AGE (Ma)
1	0	0	100	0.000	0.0	0.000	0.000	0.0 ± 0.0
2	0	1	36	0.000	0.1	0.000	0.028	0.0 ± 0.0
3	0	1	36	0.000	0.1	0.000	0.028	0.0 ± 0.0
4	3	%1060	50	0.003	65.5	0.061	21.436	2.2 ± 1.2
5	0	0	30	0.000	0.0	0.000	0.000	0.0 ± 0.0
6	0	0	50	0.000	0.0	0.000	0.000	0.0 ± 0.0
7	0	60	40	0.000	4.6	0.000	1.517	0.0 ± 0.0
8	0	0	12	0.000	0.0	0.000	0.000	0.0 ± 0.0
9	0	1	50	0.000	0.1	0.000	0.020	0.0 ± 0.0
10	0	142	25	0.000	17.5	0.000	5.743	0.0 ± 0.0
11	0	1	25	0.000	0.1	0.000	0.040	0.0 ± 0.0
12	1	159	24	0.006	20.5	0.042	6.699	4.8 ± 4.8
13	1	344	24	0.003	44.3	0.042	14.493	2.2 ± 2.2
14	0	0	100	0.000	0.0	0.000	0.000	0.0 ± 0.0
15	2	840	50	0.002	51.9	0.040	16.987	1.8 ± 1.3
	7	2609			12.4	0.011	4.046	

AREA OF BASIC UNIT = 9.89E-07 cm
CHI SQUARED = 1.362046 WITH 14 DEGREES OF FREEDOM
P(chi squared) = 100.0 %
CORRELATION COEFFICIENT = 0.974
VARIANCE OF SQR(Ns) = 0.37
VARIANCE OF SQR(Ni) = %121.83

Ns/Ni = 0.003 ± 0.001
MEAN RATIO = 0.001 ± 0.000

Ages calculated using a zeta of 354.9 ± 4.3 for SRM612 glass
RHO D = 4.288E+06 ; ND = 3393

POOLED AGE = 2.0 ± 0.8 Ma
MEAN AGE = 0.7 ± 0.4 Ma

8902-54 ZIRCON haast s98/126935 135m

IRRADIATION jmt data:jmt zircon data:haast zircons:wk023/6
SLIDE NUMBER 1
COUNTED BY: jmt

No.	Ns	Ni	Na	RATIO	U (ppm)	RHOs (E+06)	RHOi (E+06)	F.T.AGE (Ma)
1	8	57	12	0.140	0.0	0.674	4.803	8.7 ± 3.3
2	12	101	32	0.119	0.0	0.379	3.191	7.3 ± 2.2
3	11	97	12	0.113	0.0	0.927	8.173	7.0 ± 2.2
4	8	94	12	0.085	0.0	0.674	7.920	5.2 ± 1.9
5	3	41	6	0.073	0.0	0.506	6.909	4.5 ± 2.7
6	6	66	6	0.091	0.0	1.011	11.122	5.6 ± 2.4
7	42	356	60	0.118	0.0	0.708	5.999	7.3 ± 1.2
8	13	91	15	0.143	0.0	0.876	6.134	8.8 ± 2.6
9	22	136	12	0.162	0.0	1.854	11.459	10.0 ± 2.3
	125	1039			0.0	0.757	6.291	

AREA OF BASIC UNIT = 9.89E-07 cm
CHI SQUARED = 4.25879 WITH 8 DEGREES OF FREEDOM
P(chi squared) = 83.3 %
CORRELATION COEFFICIENT = 0.974
VARIANCE OF SQR(Ns) = 1.93
VARIANCE OF SQR(Ni) = 12.98

Ns/Ni = 0.120 ± 0.011
MEAN RATIO = 0.116 ± 0.010

Ages calculated using a zeta of 133.9 ± 1.4 for CN1 glass
RHO D = 9.213E+05 ; ND = 4555

POOLED AGE = 7.4 ± 0.7 Ma
MEAN AGE = 7.2 ± 0.6 Ma

8902-55 APATITE haast s98/135928 170m

IRRADIATION jmt data:jmt apatite data:haast apatites:wk020/12
SLIDE NUMBER 1
COUNTED BY: jmt

No.	Ns	Ni	Na	RATIO	U (ppm)	RHOs (E+06)	RHOi (E+06)	F.T.AGE (Ma)
1	0	5	24	0.000	0.6	0.000	0.211	0.0 ± 0.0
2	0	0	21	0.000	0.0	0.000	0.000	0.0 ± 0.0
3	0	17	8	0.000	6.3	0.000	2.149	0.0 ± 0.0
4	0	0	18	0.000	0.0	0.000	0.000	0.0 ± 0.0
5	0	1	18	0.000	0.2	0.000	0.056	0.0 ± 0.0
6	0	2	24	0.000	0.2	0.000	0.084	0.0 ± 0.0
7	0	0	24	0.000	0.0	0.000	0.000	0.0 ± 0.0
8	0	3	48	0.000	0.2	0.000	0.063	0.0 ± 0.0
9	0	0	12	0.000	0.0	0.000	0.000	0.0 ± 0.0
10	0	1	35	0.000	0.1	0.000	0.029	0.0 ± 0.0
11	0	4	8	0.000	1.5	0.000	0.506	0.0 ± 0.0
12	0	0	20	0.000	0.0	0.000	0.000	0.0 ± 0.0
13	0	515	28	0.000	54.6	0.000	18.597	0.0 ± 0.0
14	0	72	12	0.000	17.8	0.000	6.067	0.0 ± 0.0
15	0	1	35	0.000	0.1	0.000	0.029	0.0 ± 0.0
	0	621			5.5	0.000	1.874	

AREA OF BASIC UNIT = 9.89E-07 cm
CHI SQUARED = 2.058262E-07 WITH 14 DEGREES OF FREEDOM
P(chi squared) = 100.0 %
CORRELATION COEFFICIENT = 0.990
VARIANCE OF SQR(Ns) = 0.00
VARIANCE OF SQR(Ni) = 34.40

Ns/Ni = 0.000 ± 0.000
MEAN RATIO = 0.000 ± 0.000

Ages calculated using a zeta of 354.9 ± 4.3 for SRM612 glass
RHO D = 4.460E+06 ; ND = 3529

POOLED AGE = 0.0 ± 0.0 Ma
MEAN AGE = 0.0 ± 0.0 Ma

8902-56 APATITE haast s98/146919 290m

IRRADIATION jmt data:jmt apatite data:haast apatites:wk011/15
SLIDE NUMBER 1
COUNTED BY: jmt

No.	Ns	Ni	Na	RATIO	U (ppm)	RHOs (E+06)	RHOi (E+06)	F.T.AGE (Ma)
1	0	0	80	0.000	0.0	0.000	0.000	0.0 ± 0.0
2	0	0	25	0.000	0.0	0.000	0.000	0.0 ± 0.0
3	0	1	100	0.000	0.1	0.000	0.010	0.0 ± 0.0
4	0	1	42	0.000	0.3	0.000	0.024	0.0 ± 0.0
5	0	0	70	0.000	0.0	0.000	0.000	0.0 ± 0.0
6	0	1	49	0.000	0.2	0.000	0.021	0.0 ± 0.0
7	0	0	49	0.000	0.0	0.000	0.000	0.0 ± 0.0
8	0	0	49	0.000	0.0	0.000	0.000	0.0 ± 0.0
9	0	0	80	0.000	0.0	0.000	0.000	0.0 ± 0.0
10	0	0	60	0.000	0.0	0.000	0.000	0.0 ± 0.0
11	0	0	49	0.000	0.0	0.000	0.000	0.0 ± 0.0
12	0	0	60	0.000	0.0	0.000	0.000	0.0 ± 0.0
13	0	0	24	0.000	0.0	0.000	0.000	0.0 ± 0.0
14	0	0	70	0.000	0.0	0.000	0.000	0.0 ± 0.0
15	0	0	60	0.000	0.0	0.000	0.000	0.0 ± 0.0
	0	3			0.0	0.000	0.004	

AREA OF BASIC UNIT = 9.89E-07 cm
CHI SQUARED = 2.001197E-06 WITH 14 DEGREES OF FREEDOM
P(chi squared) = 100.0 %
CORRELATION COEFFICIENT = 0.535
VARIANCE OF SQR(Ns) = 0.00
VARIANCE OF SQR(Ni) = 0.17

Ns/Ni = 0.000 ± 0.000
MEAN RATIO = 0.000 ± 0.000

Ages calculated using a zeta of 354.9 ± 4.3 for SRM612 glass
RHO D = 1.207E+06 ; ND = 2984

POOLED AGE = 0.0 ± 0.0 Ma
MEAN AGE = 0.0 ± 0.0 Ma

8902-56 ZIRCON haast s98/146919 290m

IRRADIATION jmt data:jmt zircon data:haast zircons:wk038/13
SLIDE NUMBER 1
COUNTED BY: jmt

No.	Ns	Ni	Na	RATIO	U (ppm)	RHOs (E+06)	RHOi (E+06)	F.T.AGE (Ma)
1	8	33	3	0.242	0.0	2.696	11.122	17.3 ± 6.8
2	49	155	12	0.316	0.0	4.129	13.060	22.5 ± 3.7
3	12	45	3	0.267	0.0	4.044	15.167	19.0 ± 6.2
4	8	8	2	1.000	0.0	4.044	4.044	70.9 ± 35.5
5	17	41	3	0.415	0.0	5.730	13.819	29.5 ± 8.5
6	33	98	4	0.337	0.0	8.342	24.772	24.0 ± 4.8
7	29	69	6	0.420	0.0	4.887	11.628	29.9 ± 6.6
	156	449			0.0	4.780	13.757	

AREA OF BASIC UNIT = 9.89E-07 cm
CHI SQUARED = 7.887976 WITH 6 DEGREES OF FREEDOM
P(chi squared) = 24.6 %
CORRELATION COEFFICIENT = 0.970
VARIANCE OF SQR(Ns) = 2.56
VARIANCE OF SQR(Ni) = 9.61

Ns/Ni = 0.347 ± 0.032
MEAN RATIO = 0.428 ± 0.099

Ages calculated using a zeta of 133.9 ± 1.4 for CN1 glass
RHO D = 1.065E+06 ; ND = 5265

POOLED AGE = 24.7 ± 2.3 Ma
MEAN AGE = 30.5 ± 7.0 Ma

8902-57 APATITE haast s98/148878 455m

IRRADIATION jmt data:jmt apatite data:haast apatites:wk020/10
SLIDE NUMBER 1
COUNTED BY: jmt

No.	Ns	Ni	Na	RATIO	U (ppm)	RHOs (E+06)	RHOi (E+06)	F.T.AGE (Ma)
1	1	128	9	0.008	42.9	0.112	14.380	6.1 ± 6.1
2	0	13	3	0.000	13.1	0.000	4.382	0.0 ± 0.0
3	0	13	9	0.000	4.4	0.000	1.461	0.0 ± 0.0
4	0	6	6	0.000	3.0	0.000	1.011	0.0 ± 0.0
5	0	8	4	0.000	6.0	0.000	2.022	0.0 ± 0.0
6	0	7	4	0.000	5.3	0.000	1.769	0.0 ± 0.0
7	0	8	4	0.000	6.0	0.000	2.022	0.0 ± 0.0
8	0	8	4	0.000	6.0	0.000	2.022	0.0 ± 0.0
9	0	2	4	0.000	1.5	0.000	0.506	0.0 ± 0.0
10	0	7	4	0.000	5.3	0.000	1.769	0.0 ± 0.0
11	0	25	6	0.000	12.6	0.000	4.213	0.0 ± 0.0
12	0	2	9	0.000	0.7	0.000	0.225	0.0 ± 0.0
13	0	17	2	0.000	25.7	0.000	8.595	0.0 ± 0.0
14	0	2	8	0.000	0.8	0.000	0.253	0.0 ± 0.0
15	0	10	4	0.000	7.5	0.000	2.528	0.0 ± 0.0
16	1	91	6	0.011	45.8	0.169	15.335	8.6 ± 8.6
17	1	9	6	0.111	4.5	0.169	1.517	85.9 ± 90.6
18	0	4	12	0.000	1.0	0.000	0.337	0.0 ± 0.0
19	0	7	6	0.000	3.5	0.000	1.180	0.0 ± 0.0
20	0	6	4	0.000	4.5	0.000	1.517	0.0 ± 0.0
21	0	2	4	0.000	1.5	0.000	0.506	0.0 ± 0.0
22	0	7	4	0.000	5.3	0.000	1.769	0.0 ± 0.0
23	0	9	6	0.000	4.5	0.000	1.517	0.0 ± 0.0
24	0	2	6	0.000	1.0	0.000	0.337	0.0 ± 0.0
25	0	13	3	0.000	13.1	0.000	4.382	0.0 ± 0.0
	3	406			8.9	0.022	2.996	

AREA OF BASIC UNIT = 9.89E-07 cm
CHI SQUARED = 13.26939 WITH 24 DEGREES OF FREEDOM
P(chi squared) = 96.1 %
CORRELATION COEFFICIENT = 0.775
VARIANCE OF SQR(Ns) = 0.11
VARIANCE OF SQR(Ni) = 5.44

Ns/Ni = 0.007 ± 0.004
MEAN RATIO = 0.005 ± 0.004

Ages calculated using a zeta of 354.9 ± 4.3 for SRM612 glass
RHO D = 4.388E+06 ; ND = 3471

POOLED AGE = 5.8 ± 3.3 Ma
MEAN AGE = 4.0 ± 3.5 Ma

8902-57 ZIRCON haast s98/148878 455m

IRRADIATION jmt data:jmt zircon data:haast zircons:wk023/3
SLIDE NUMBER 1
COUNTED BY: jmt

No.	Ns	Ni	Na	RATIO	U (ppm)	RHOs (E+06)	RHOi (E+06)	F.T.AGE (Ma)
1	84	39	9	2.154	0.0	9.437	4.382	127.9 ± 24.9
2	148	91	30	1.626	0.0	4.988	3.067	96.8 ± 13.0
3	82	33	9	2.485	0.0	9.212	3.707	147.3 ± 30.5
4	19	8	2	2.375	0.0	9.606	4.044	140.8 ± 59.4
5	100	52	8	1.923	0.0	12.639	6.572	114.3 ± 19.6
6	41	16	4	2.562	0.0	10.364	4.044	151.8 ± 44.8
7	60	40	10	1.500	0.0	6.067	4.044	89.3 ± 18.3
8	28	56	10	0.500	0.0	2.831	5.662	29.9 ± 6.9
	562	335			0.0	6.930	4.131	

AREA OF BASIC UNIT = 9.89E-07 cm
CHI SQUARED = 39.98846 WITH 7 DEGREES OF FREEDOM
P(chi squared) = < 0.1 %
CORRELATION COEFFICIENT = 0.771
VARIANCE OF SQR(Ns) = 6.72
VARIANCE OF SQR(Ni) = 4.32

Ns/Ni = 1.678 ± 0.116
MEAN RATIO = 1.891 ± 0.241

Ages calculated using a zeta of 133.9 ± 1.4 for CN1 glass
RHO D = 8.955E+05 ; ND = 4428

POOLED AGE = 99.8 ± 7.1 Ma
MEAN AGE = 112.4 ± 14.5 Ma

8902-58 APATITE haast s98/167868 1310m

IRRADIATION jmt data:jmt apatite data:haast apatites:wk043/9
SLIDE NUMBER 1
COUNTED BY: jmt

No.	Ns	Ni	Na	RATIO	U (ppm)	RHOs (E+06)	RHOi (E+06)	F.T AGE (Ma)
1	0	93	16	0.000	86.7	0.000	5.877	0.0 ± 0.0
2	1	2	12	0.500	2.5	0.084	0.169	78.3 ± 95.9
3	3	47	8	0.064	87.7	0.379	5.940	10.0 ± 6.0
4	0	1	8	0.000	1.9	0.000	0.126	0.0 ± 0.0
5	4	89	18	0.045	73.8	0.225	4.999	7.1 ± 3.6
6	0	25	12	0.000	31.1	0.000	2.106	0.0 ± 0.0
7	0	17	9	0.000	28.2	0.000	1.910	0.0 ± 0.0
8	4	20	20	0.200	14.9	0.202	1.011	31.4 ± 17.2
9	1	20	12	0.050	24.9	0.084	1.685	7.9 ± 8.1
10	1	33	9	0.030	54.7	0.112	3.707	4.8 ± 4.8
11	0	34	8	0.000	63.4	0.000	4.297	0.0 ± 0.0
12	2	244	28	0.008	130.0	0.072	8.811	1.3 ± 0.9
13	0	8	6	0.000	19.9	0.000	1.348	0.0 ± 0.0
14	0	17	9	0.000	28.2	0.000	1.910	0.0 ± 0.0
15	1	8	12	0.125	9.9	0.084	0.674	19.7 ± 20.9
16	0	9	18	0.000	7.5	0.000	0.506	0.0 ± 0.0
17	2	113	20	0.018	84.3	0.101	5.713	2.8 ± 2.0
18	0	3	9	0.000	5.0	0.000	0.337	0.0 ± 0.0
19	0	18	15	0.000	17.9	0.000	1.213	0.0 ± 0.0
20	0	5	8	0.000	9.3	0.000	0.632	0.0 ± 0.0
21	1	18	18	0.056	14.9	0.056	1.011	8.7 ± 9.0
22	0	9	20	0.000	6.7	0.000	0.455	0.0 ± 0.0
	20	833			42.1	0.069	2.855	

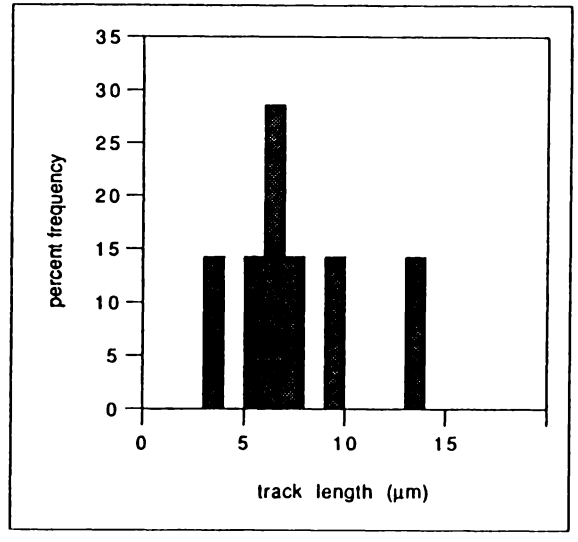
AREA OF BASIC UNIT = 9.89E-07 cm
CHI SQUARED = 51.31371 WITH 21 DEGREES OF FREEDOM
P(chi squared) = < 0.1 %
CORRELATION COEFFICIENT = 0.404
VARIANCE OF SQR(Ns) = 0.55
VARIANCE OF SQR(Ni) = 12.28

Ns/Ni = 0.024 ± 0.005
MEAN RATIO = 0.050 ± 0.024

Ages calculated using a zeta of 354.9 ± 4.3 for SRM612 glass
RHO D = 8.876E+05 ; ND = 5267

POOLED AGE = 3.8 ± 0.9 Ma
MEAN AGE = 7.8 ± 3.8 Ma

8902-58



n = 7
Mean = 7.50 µm
Sample std. dev. = 2.94 µm

8902-58 ZIRCON haast s98/167868 1310m

IRRADIATION jmt data:jmt zircon data:haast zircons:wk023/2
SLIDE NUMBER 1
COUNTED BY: jmt

No.	Ns	Ni	Na	RATIO	U (ppm)	RHOs (E+06)	RHOi (E+06)	F.T.AGE (Ma)
1	116	73	12	1.589	0.0	9.774	6.151	93.7 ± 14.1
2	386	216	30	1.787	0.0	13.010	7.280	105.2 ± 9.1
3	310	172	48	1.802	0.0	6.530	3.623	106.1 ± 10.3
4	166	112	30	1.482	0.0	5.595	3.775	87.4 ± 10.8
5	95	63	9	1.508	0.0	10.673	7.078	88.9 ± 14.5
6	415	274	40	1.515	0.0	10.490	6.926	89.3 ± 7.1
7	270	141	24	1.915	0.0	11.375	5.940	112.7 ± 11.9
	1758	1051			0.0	9.210	5.506	

AREA OF BASIC UNIT = 9.89E-07 cm
CHI SQUARED = 6.052077 WITH 6 DEGREES OF FREEDOM
P(chi squared) = 41.7 %
CORRELATION COEFFICIENT = 0.976
VARIANCE OF SQR(Ns) = 18.07
VARIANCE OF SQR(Ni) = 9.94

Ns/Ni = 1.673 ± 0.065
MEAN RATIO = 1.657 ± 0.066

Ages calculated using a zeta of 133.9 ± 1.4 for CN1 glass
RHO D = 8.869E+05 ; ND = 4385

POOLED AGE = 98.6 ± 4.2 Ma
MEAN AGE = 97.6 ± 4.3 Ma

8902-59 APATITE lindis s125/226926 305m

IRRADIATION jmt data:jmt apatite data:lindis apatites:wk020/9
SLIDE NUMBER 1
COUNTED BY: jmt

No.	Ns	Ni	Na	RATIO	U (ppm)	RHOs (E+06)	RHOi (E+06)	F.T.AGE (Ma)
1	0	0	20	0.000	0.0	0.000	0.000	0.0 ± 0.0
2	0	5	20	0.000	0.8	0.000	0.253	0.0 ± 0.0
3	0	0	15	0.000	0.0	0.000	0.000	0.0 ± 0.0
4	7	217	12	0.032	55.0	0.590	18.284	24.9 ± 9.6
5	2	22	12	0.091	5.6	0.169	1.854	69.8 ± 51.6
6	0	1	60	0.000	0.1	0.000	0.017	0.0 ± 0.0
7	7	130	12	0.054	33.0	0.590	10.954	41.4 ± 16.1
8	4	68	15	0.059	13.8	0.270	4.584	45.3 ± 23.3
9	1	13	4	0.077	9.9	0.253	3.286	59.1 ± 61.4
10	0	0	15	0.000	0.0	0.000	0.000	0.0 ± 0.0
11	0	0	18	0.000	0.0	0.000	0.000	0.0 ± 0.0
12	0	0	16	0.000	0.0	0.000	0.000	0.0 ± 0.0
13	0	2	50	0.000	0.1	0.000	0.040	0.0 ± 0.0
14	0	0	12	0.000	0.0	0.000	0.000	0.0 ± 0.0
15	0	0	16	0.000	0.0	0.000	0.000	0.0 ± 0.0
	21	458			4.7	0.071	1.559	

AREA OF BASIC UNIT = 9.89E-07 cm
CHI SQUARED = 2.768776 WITH 14 DEGREES OF FREEDOM
P(chi squared) = 99.9 %
CORRELATION COEFFICIENT = 0.951
VARIANCE OF SQR(Ns) = 1.05
VARIANCE OF SQR(Ni) = 22.02

Ns/Ni = 0.046 ± 0.010
MEAN RATIO = 0.021 ± 0.008

Ages calculated using a zeta of 354.9 ± 4.3 for SRM612 glass
RHO D = 4.351E+06 ; ND = 3443

POOLED AGE = 35.3 ± 7.9 Ma
MEAN AGE = 16.1 ± 6.5 Ma

8902-59 ZIRCON lindis s125/221926 305m

IRRADIATION jmt data:jmt zircon data:lindis zircons:wk023/1
SLIDE NUMBER 1
COUNTED BY: jmt

No.	Ns	Ni	Na	RATIO	U (ppm)	RHOs (E+06)	RHOi (E+06)	F.T.AGE (Ma)
1	32	18	4	1.778	0.0	8.089	4.550	103.7 ± 30.6
2	64	54	6	1.185	0.0	10.785	9.100	69.3 ± 12.9
3	270	233	24	1.159	0.0	11.375	9.816	67.8 ± 6.2
4	73	58	6	1.259	0.0	12.302	9.774	73.6 ± 13.0
5	56	37	8	1.514	0.0	7.078	4.676	88.4 ± 18.8
6	107	72	8	1.486	0.0	13.524	9.100	86.8 ± 13.3
7	72	66	8	1.091	0.0	9.100	8.342	63.8 ± 10.9
8	99	90	8	1.100	0.0	12.513	11.375	64.4 ± 9.4
9	45	41	5	1.098	0.0	9.100	8.291	64.2 ± 13.9
10	370	251	32	1.474	0.0	11.691	7.931	86.1 ± 7.2
	1188	920			0.0	11.020	8.534	

AREA OF BASIC UNIT = 9.89E-07 cm
CHI SQUARED = 9.695617 WITH 9 DEGREES OF FREEDOM
P(chi squared) = 37.6 %
CORRELATION COEFFICIENT = 0.982
VARIANCE OF SQR(Ns) = 19.02
VARIANCE OF SQR(Ni) = 14.42

Ns/Ni = 1.291 ± 0.057
MEAN RATIO = 1.314 ± 0.074

Ages calculated using a zeta of 133.9 ± 1.4 for CN1 glass
RHO D = 8.783E+05 ; ND = 4343

POOLED AGE = 75.5 ± 3.6 Ma
MEAN AGE = 76.8 ± 4.6 Ma

8902-60 APATITE lindis s125/276078 395m

IRRADIATION jmt data:jmt apatite data:lindis apatites:wk020/8
SLIDE NUMBER 1
COUNTED BY: jmt

No.	Ns	Ni	Na	RATIO	U (ppm)	RHOs (E+06)	RHOi (E+06)	F.T AGE (Ma)
1	0	1	16	0.000	0.2	0.000	0.063	0.0 ± 0.0
2	11	115	15	0.096	23.5	0.741	7.752	72.8 ± 23.0
3	13	150	9	0.087	51.2	1.461	16.852	66.0 ± 19.1
4	0	1	32	0.000	0.1	0.000	0.032	0.0 ± 0.0
5	0	1	18	0.000	0.2	0.000	0.056	0.0 ± 0.0
6	2	16	9	0.125	5.5	0.225	1.798	95.0 ± 71.3
7	0	1	12	0.000	0.3	0.000	0.084	0.0 ± 0.0
8	11	139	12	0.079	35.6	0.927	11.712	60.3 ± 18.9
9	8	61	12	0.131	15.6	0.674	5.140	99.6 ± 37.5
10	0	1	12	0.000	0.3	0.000	0.084	0.0 ± 0.0
11	9	87	12	0.103	22.3	0.758	7.331	78.7 ± 27.6
12	0	1	20	0.000	0.2	0.000	0.051	0.0 ± 0.0
13	0	1	20	0.000	0.2	0.000	0.051	0.0 ± 0.0
14	0	1	40	0.000	0.1	0.000	0.025	0.0 ± 0.0
15	0	1	36	0.000	0.1	0.000	0.028	0.0 ± 0.0
16	45	465	30	0.097	47.6	1.517	15.672	73.7 ± 11.6
17	5	68	9	0.074	23.2	0.562	7.640	56.1 ± 26.0
18	8	52	12	0.154	13.3	0.674	4.382	116.7 ± 44.4
19	0	1	30	0.000	0.1	0.000	0.034	0.0 ± 0.0
20	5	115	12	0.043	29.4	0.421	9.690	33.2 ± 15.2
21	0	1	16	0.000	0.2	0.000	0.063	0.0 ± 0.0
22	3	21	10	0.143	6.4	0.303	2.123	108.5 ± 67.0
23	3	59	12	0.051	15.1	0.253	4.971	38.8 ± 23.0
24	0	1	16	0.000	0.2	0.000	0.063	0.0 ± 0.0
25	12	97	9	0.124	33.1	1.348	10.898	94.0 ± 28.8
26	0	1	28	0.000	0.1	0.000	0.036	0.0 ± 0.0
27	8	132	24	0.061	16.9	0.337	5.561	46.2 ± 16.9
28	14	142	16	0.099	27.2	0.885	8.974	75.1 ± 21.1
29	5	73	12	0.068	18.7	0.421	6.151	52.2 ± 24.2
	162	1805			10.8	0.321	3.572	

AREA OF BASIC UNIT = 9.89E-07 cm
CHI SQUARED = 12.15386 WITH 28 DEGREES OF FREEDOM
P(chi squared) = 99.6 %
CORRELATION COEFFICIENT = 0.978
VARIANCE OF SQR(Ns) = 3.04
VARIANCE OF SQR(Ni) = 28.58

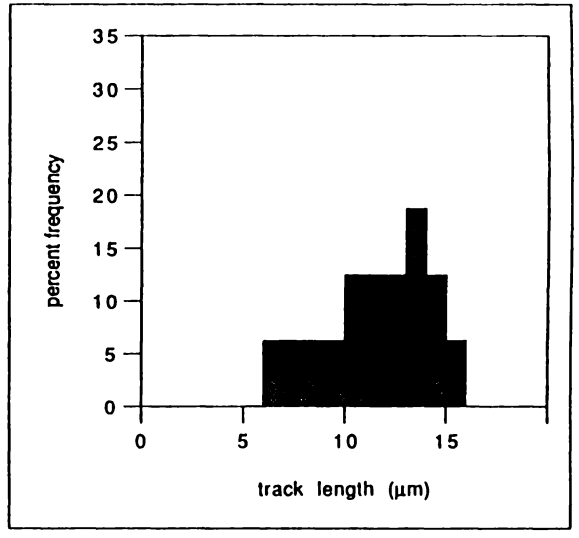
Ns/Ni = 0.090 ± 0.007
MEAN RATIO = 0.053 ± 0.010

Ages calculated using a zeta of 354.9 ± 4.3 for SRM612 glass
RHO D = 4.315E+06 ; ND = 3414

POOLED AGE = 68.4 ± 5.8 Ma

MEAN AGE = 40.4 ± 7.7 Ma

8902-60



n = 16
Mean = 11.56 µm
Sample std. dev. = 2.46 µm

8902-61 APATITE lindis s116/256140 470m

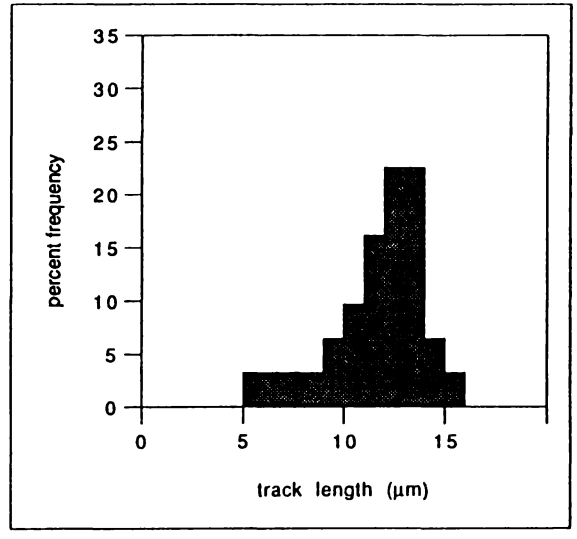
IRRADIATION jmt data:jmt apatite data:lindis apatites:wk043/4
SLIDE NUMBER 1
COUNTED BY: jmt

No.	Ns	Ni	Na	RATIO	U (ppm)	RHOs (E+06)	RHOi (E+06)	F.T.AGE (Ma)
1	0	2	6	0.000	5.0	0.000	0.337	0.0 ± 0.0
2	12	35	16	0.343	32.6	0.758	2.212	53.8 ± 18.0
3	8	21	12	0.381	26.1	0.674	1.769	59.7 ± 24.8
4	7	20	6	0.350	49.7	1.180	3.370	54.9 ± 24.1
5	1	3	6	0.333	7.5	0.169	0.506	52.3 ± 60.4
6	2	5	9	0.400	8.3	0.225	0.562	62.7 ± 52.5
7	1	5	16	0.200	4.7	0.063	0.316	31.4 ± 34.4
8	2	5	9	0.400	8.3	0.225	0.562	62.7 ± 52.5
9	21	68	12	0.309	84.6	1.769	5.730	48.5 ± 12.1
10	28	65	24	0.431	40.4	1.180	2.738	67.5 ± 15.3
11	2	7	12	0.286	8.7	0.169	0.590	44.8 ± 36.0
12	10	40	9	0.250	66.3	1.123	4.494	39.3 ± 13.9
13	0	4	6	0.000	9.9	0.000	0.674	0.0 ± 0.0
14	2	5	8	0.400	9.3	0.253	0.632	62.7 ± 52.5
15	23	59	24	0.390	36.7	0.969	2.486	61.1 ± 15.1
16	1	9	15	0.111	9.0	0.067	0.607	17.5 ± 18.4
17	2	5	15	0.400	5.0	0.135	0.337	62.7 ± 52.5
18	15	35	15	0.429	34.8	1.011	2.359	67.2 ± 20.8
19	1	4	8	0.250	7.5	0.126	0.506	39.3 ± 43.9
20	0	2	6	0.000	5.0	0.000	0.337	0.0 ± 0.0
21	10	30	8	0.333	56.0	1.264	3.792	52.3 ± 19.1
22	33	77	21	0.429	54.7	1.589	3.707	67.2 ± 14.0
23	2	5	4	0.400	18.7	0.506	1.264	62.7 ± 52.5
24	1	7	8	0.143	13.1	0.126	0.885	22.5 ± 24.0
25	24	53	12	0.453	65.9	2.022	4.466	70.9 ± 17.5
26	4	11	6	0.364	27.4	0.674	1.854	57.0 ± 33.3
27	17	45	18	0.378	37.3	0.955	2.528	59.2 ± 16.9
28	3	9	6	0.333	22.4	0.506	1.517	52.3 ± 34.9
29	1	5	12	0.200	6.2	0.084	0.421	31.4 ± 34.4
30	6	17	12	0.353	21.1	0.506	1.432	55.4 ± 26.3
	239	658			28.8	0.709	1.951	

AREA OF BASIC UNIT = 9.89E-07 cm
CHI SQUARED = 10.10734 WITH 29 DEGREES OF FREEDOM
P(chi squared) = 100.0 %
CORRELATION COEFFICIENT = 0.980

MEAN AGE = 47.3 ± 3.9 Ma

8902-61



n = 31
Mean = 11.78 µm
Sample std. dev. = 2.18 µm

8902-61 ZIRCON lindis s116/256140 470m

IRRADIATION jmt data:jmt zircon data:lindis zircons:wk024/18
SLIDE NUMBER 1
COUNTED BY: jmt

No.	Ns	Ni	Na	RATIO	U (ppm)	RHOs (E+06)	RHOi (E+06)	F.T AGE (Ma)
1	90	73	12	1.233	0.0	7.583	6.151	74.4 ± 11.8
2	92	73	12	1.260	0.0	7.752	6.151	76.1 ± 12.0
3	36	34	6	1.059	0.0	6.067	5.730	64.0 ± 15.3
4	87	64	9	1.359	0.0	9.774	7.190	82.0 ± 13.6
5	34	30	4	1.133	0.0	8.595	7.583	68.5 ± 17.2
6	56	44	9	1.273	0.0	6.291	4.943	76.8 ± 15.5
7	107	85	12	1.259	0.0	9.016	7.162	76.0 ± 11.1
8	24	19	4	1.263	0.0	6.067	4.803	76.2 ± 23.5
	526	422			0.0	7.821	6.275	

AREA OF BASIC UNIT = 9.89E-07 cm
CHI SQUARED = .9153011 WITH 7 DEGREES OF FREEDOM
P(chi squared) = 99.6 %
CORRELATION COEFFICIENT = 0.994
VARIANCE OF SQR(Ns) = 4.35
VARIANCE OF SQR(Ni) = 3.06

Ns/Ni = 1.246 ± 0.081
MEAN RATIO = 1.230 ± 0.033

Ages calculated using a zeta of 133.9 ± 1.4 for CN1 glass
RHO D = 9.070E+05 ; ND = 4485

POOLED AGE = 75.2 ± 5.1 Ma
MEAN AGE = 74.3 ± 2.4 Ma

8902-62 APATITE lindis s116/287218 520m

IRRADIATION jmt data:jmt apatite data:lindis apatites:wk020/7
SLIDE NUMBER 1
COUNTED BY: jmt

No.	Ns	Ni	Na	RATIO	U (ppm)	RHOs (E+06)	RHOi (E+06)	F.T.AGE (Ma)
1	0	1	25	0.000	0.1	0.000	0.040	0.0 ± 0.0
2	8	147	12	0.054	37.9	0.674	12.386	41.2 ± 15.0
3	0	0	36	0.000	0.0	0.000	0.000	0.0 ± 0.0
4	0	2	28	0.000	0.2	0.000	0.072	0.0 ± 0.0
5	7	88	16	0.080	17.0	0.442	5.561	60.1 ± 23.6
6	0	0	20	0.000	0.0	0.000	0.000	0.0 ± 0.0
7	1	15	6	0.067	7.7	0.169	2.528	50.4 ± 52.1
8	11	148	15	0.074	30.5	0.741	9.976	56.2 ± 17.6
9	0	0	36	0.000	0.0	0.000	0.000	0.0 ± 0.0
10	10	213	20	0.047	33.0	0.506	10.768	35.5 ± 11.5
11	31	344	20	0.090	53.2	1.567	17.391	68.1 ± 12.8
12	18	220	10	0.082	68.1	1.820	22.245	61.8 ± 15.2
13	0	0	30	0.000	0.0	0.000	0.000	0.0 ± 0.0
14	5	79	9	0.063	27.2	0.562	8.875	47.9 ± 22.1
15	12	128	16	0.094	24.8	0.758	8.089	70.8 ± 21.4
16	0	0	25	0.000	0.0	0.000	0.000	0.0 ± 0.0
17	2	26	9	0.077	8.9	0.225	2.921	58.1 ± 42.7
18	0	0	16	0.000	0.0	0.000	0.000	0.0 ± 0.0
19	0	0	16	0.000	0.0	0.000	0.000	0.0 ± 0.0
20	5	71	15	0.070	14.7	0.337	4.786	53.3 ± 24.7
21	0	0	9	0.000	0.0	0.000	0.000	0.0 ± 0.0
22	3	129	12	0.023	33.3	0.253	10.870	17.6 ± 10.3
23	3	30	16	0.100	5.8	0.190	1.896	75.5 ± 45.7
24	7	61	9	0.115	21.0	0.786	6.853	86.6 ± 34.6
25	0	0	18	0.000	0.0	0.000	0.000	0.0 ± 0.0
26	9	58	6	0.155	29.9	1.517	9.774	116.8 ± 41.9
27	0	0	70	0.000	0.0	0.000	0.000	0.0 ± 0.0
28	13	213	24	0.061	27.5	0.548	8.974	46.2 ± 13.2
29	4	74	15	0.054	15.3	0.270	4.988	40.9 ± 21.0
30	16	207	24	0.077	26.7	0.674	8.721	58.4 ± 15.2
	165	2254			12.0	0.286	3.909	

AREA OF BASIC UNIT = 9.89E-07 cm
CHI SQUARED = 16.35278 WITH 29 DEGREES OF FREEDOM
P(chi squared) = 97.1 %
CORRELATION COEFFICIENT = 0.944
VARIANCE OF SQR(Ns) = 2.72
VARIANCE OF SQR(Ni) = 35.53

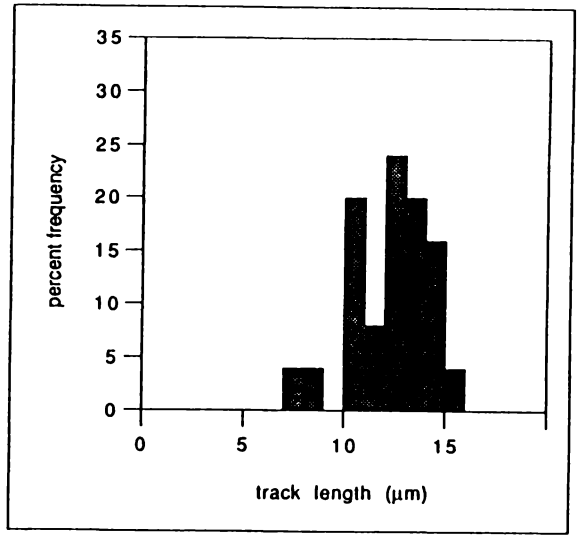
Ns/Ni = 0.073 ± 0.006
MEAN RATIO = 0.046 ± 0.008

Ages calculated using a zeta of 354.9 ± 4.3 for SRM612 glass
RHO D = 4.279E+06 ; ND = 3385

POOLED AGE = 55.3 ± 4.6 Ma

MEAN AGE = 34.9 ± 6.1 Ma

8902-62



n = 25
Mean = 12.38 µm
Sample std. dev. = 1.91 µm

8902-62 ZIRCON lindis s116/287218 520m

IRRADIATION jmt data:jmt zircon data:lindis zircons:wk024/17
SLIDE NUMBER 1
COUNTED BY: jmt

No.	Ns	Ni	Na	RATIO	U (ppm)	RHOs (E+06)	RHOi (E+06)	F.T AGE (Ma)
1	45	36	6	1.250	0.0	7.583	6.067	74.7 ± 16.8
2	63	54	12	1.167	0.0	5.308	4.550	69.8 ± 13.0
3	129	116	24	1.112	0.0	5.435	4.887	66.5 ± 8.6
4	31	25	8	1.240	0.0	3.918	3.160	74.1 ± 20.0
5	12	12	2	1.000	0.0	6.067	6.067	59.9 ± 24.5
6	34	29	6	1.172	0.0	5.730	4.887	70.1 ± 17.8
7	92	62	16	1.484	0.0	5.814	3.918	88.6 ± 14.7
	406	334			0.0	5.548	4.564	

AREA OF BASIC UNIT = 9.89E-07 cm
CHI SQUARED = 2.282141 WITH 6 DEGREES OF FREEDOM
P(chi squared) = 89.2 %
CORRELATION COEFFICIENT = 0.979
VARIANCE OF SQR(Ns) = 7.05
VARIANCE OF SQR(Ni) = 5.63

Ns/Ni = 1.216 ± 0.090
MEAN RATIO = 1.204 ± 0.057

Ages calculated using a zeta of 133.9 ± 1.4 for CN1 glass
RHO D = 8.983E+05 ; ND = 4441

POOLED AGE = 72.7 ± 5.5 Ma
MEAN AGE = 72.0 ± 3.6 Ma

8902-63 APATITE lindis s116/335265 715m

IRRADIATION jmt data:jmt apatite data:lindis apatites:wk043/5
SLIDE NUMBER 1
COUNTED BY: jmt

No.	Ns	Ni	Na	RATIO	U (ppm)	RHOs (E+06)	RHOi (E+06)	F.T.AGE (Ma)
1	21	33	15	0.636	32.8	1.416	2.224	99.5 ± 27.8
2	8	23	24	0.348	14.3	0.337	0.969	54.6 ± 22.4
3	66	138	40	0.478	51.5	1.668	3.488	74.9 ± 11.3
4	15	26	12	0.577	32.3	1.264	2.191	90.2 ± 29.3
5	2	13	30	0.154	6.5	0.067	0.438	24.2 ± 18.4
6	1	3	12	0.333	3.7	0.084	0.253	52.3 ± 60.4
7	12	23	48	0.522	7.2	0.253	0.484	81.7 ± 29.1
8	19	31	25	0.613	18.5	0.768	1.254	95.8 ± 28.0
9	9	18	12	0.500	22.4	0.758	1.517	78.3 ± 32.0
10	5	12	16	0.417	11.2	0.316	0.758	65.3 ± 34.8
11	16	33	15	0.485	32.8	1.079	2.224	75.9 ± 23.2
12	9	23	16	0.391	21.5	0.569	1.453	61.3 ± 24.1
13	23	63	28	0.365	33.6	0.831	2.275	57.2 ± 14.0
14	11	30	12	0.367	37.3	0.927	2.528	57.5 ± 20.3
15	3	8	30	0.375	4.0	0.101	0.270	58.8 ± 39.8
16	25	74	32	0.338	34.5	0.790	2.338	53.0 ± 12.3
17	19	44	12	0.432	54.7	1.601	3.707	67.7 ± 18.6
18	5	10	9	0.500	16.6	0.562	1.123	78.3 ± 42.9
19	8	23	9	0.348	38.1	0.899	2.584	54.6 ± 22.4
20	2	14	16	0.143	13.1	0.126	0.885	22.5 ± 17.0
21	8	18	12	0.444	22.4	0.674	1.517	69.6 ± 29.6
22	4	25	9	0.160	41.5	0.449	2.809	25.2 ± 13.6
23	28	51	16	0.549	47.6	1.769	3.223	85.9 ± 20.3
	319	736			24.4	0.717	1.654	

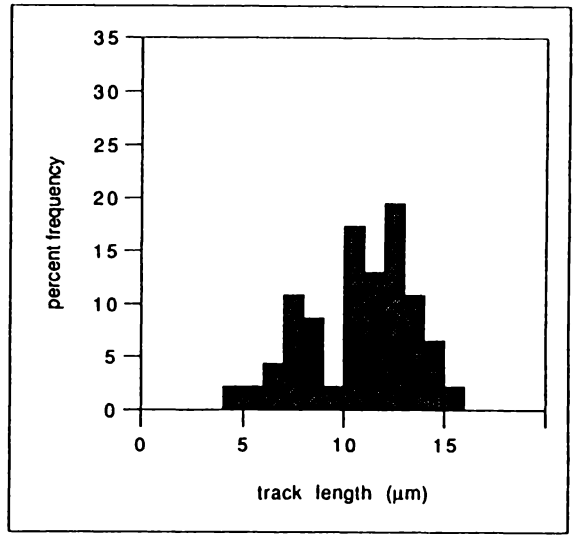
AREA OF BASIC UNIT = 9.89E-07 cm
CHI SQUARED = 16.95078 WITH 22 DEGREES OF FREEDOM
P(chi squared) = 76.6 %
CORRELATION COEFFICIENT = 0.962
VARIANCE OF SQR(Ns) = 2.57
VARIANCE OF SQR(Ni) = 4.57

Ns/Ni = 0.433 ± 0.029
MEAN RATIO = 0.412 ± 0.028

Ages calculated using a zeta of 354.9 ± 4.3 for SRM612 glass
RHO D = 8.876E+05 ; ND = 5267

POOLED AGE = 67.9 ± 4.7 Ma
MEAN AGE = 64.6 ± 4.6 Ma

8902-63



n = 46
Mean = 10.83 µm
Sample std. dev. = 2.67 µm

8902-63 ZIRCON lindis s116/335265 715m

IRRADIATION jmt data:jmt zircon data:lindis zircons:wk024/16
SLIDE NUMBER 1
COUNTED BY: jmt

No.	Ns	Ni	Na	RATIO	U (ppm)	RHOs (E+06)	RHOi (E+06)	F.TAGE (Ma)
1	86	46	12	1.870	0.0	7.246	3.876	110.4 ± 20.3
2	209	98	25	2.133	0.0	8.453	3.964	125.8 ± 15.6
3	63	40	6	1.575	0.0	10.617	6.741	93.1 ± 18.9
4	104	43	8	2.419	0.0	13.145	5.435	142.5 ± 26.0
5	42	17	5	2.471	0.0	8.493	3.438	145.5 ± 41.9
6	86	46	12	1.870	0.0	7.246	3.876	110.4 ± 20.3
7	372	159	28	2.340	0.0	13.433	5.742	137.9 ± 13.3
8	128	48	12	2.667	0.0	10.785	4.044	156.9 ± 26.7
9	121	58	12	2.086	0.0	10.195	4.887	123.1 ± 19.8
	1211	555			0.0	10.204	4.676	

AREA OF BASIC UNIT = 9.89E-07 cm
CHI SQUARED = 6.632319 WITH 8 DEGREES OF FREEDOM
P(chi squared) = 57.7 %
CORRELATION COEFFICIENT = 0.988
VARIANCE OF SQR(Ns) = 14.64
VARIANCE OF SQR(Ni) = 5.86

Ns/Ni = 2.182 ± 0.112
MEAN RATIO = 2.159 ± 0.116

Ages calculated using a zeta of 133.9 ± 1.4 for CN1 glass
RHO D = 8.896E+05 ; ND = 4398

POOLED AGE = 128.7 ± 7.0 Ma
MEAN AGE = 127.3 ± 7.2 Ma

8902-64 APATITE lindis s116/412298 775m

IRRADIATION jmt data:jmt apatite data:lindis apatites:wk011/7
SLIDE NUMBER 1
COUNTED BY: jmt

No.	Ns	Ni	Na	RATIO	U (ppm)	RHOs (E+06)	RHOi (E+06)	F.T.AGE (Ma)
1	15	22	12	0.682	21.9	1.264	1.854	133.0 ± 44.6
2	8	14	4	0.571	41.7	2.022	3.539	111.7 ± 49.6
3	5	10	4	0.500	29.8	1.264	2.528	97.8 ± 53.6
4	3	4	3	0.750	15.9	1.011	1.348	146.2 ± 111.7
5	4	8	8	0.500	11.9	0.506	1.011	97.8 ± 59.9
6	1	5	9	0.200	6.6	0.112	0.562	39.3 ± 43.1
7	12	13	8	0.923	19.4	1.517	1.643	179.5 ± 72.0
8	12	44	9	0.273	58.3	1.348	4.943	53.5 ± 17.5
9	4	9	4	0.444	26.8	1.011	2.275	87.0 ± 52.3
10	6	13	8	0.462	19.4	0.758	1.643	90.4 ± 44.6
11	14	27	4	0.519	80.5	3.539	6.825	101.4 ± 33.5
12	10	24	6	0.417	47.7	1.685	4.044	81.6 ± 30.8
13	8	27	9	0.296	35.8	0.899	3.033	58.2 ± 23.4
14	4	10	8	0.400	14.9	0.506	1.264	78.4 ± 46.4
15	8	25	9	0.320	33.1	0.899	2.809	62.8 ± 25.5
16	24	93	12	0.258	92.4	2.022	7.836	50.7 ± 11.7
17	9	30	18	0.300	19.9	0.506	1.685	58.9 ± 22.4
18	22	84	8	0.262	125.2	2.781	10.617	51.4 ± 12.4
19	5	29	6	0.172	57.6	0.843	4.887	33.9 ± 16.4
20	1	2	16	0.500	1.5	0.063	0.126	97.8 ± 119.8
21	3	5	6	0.600	9.9	0.506	0.843	117.2 ± 85.6
22	4	16	9	0.250	21.2	0.449	1.798	49.1 ± 27.5
23	4	9	3	0.444	35.8	1.348	3.033	87.0 ± 52.3
24	4	19	9	0.211	25.2	0.449	2.135	41.4 ± 22.8
	190	542			33.7	1.001	2.854	

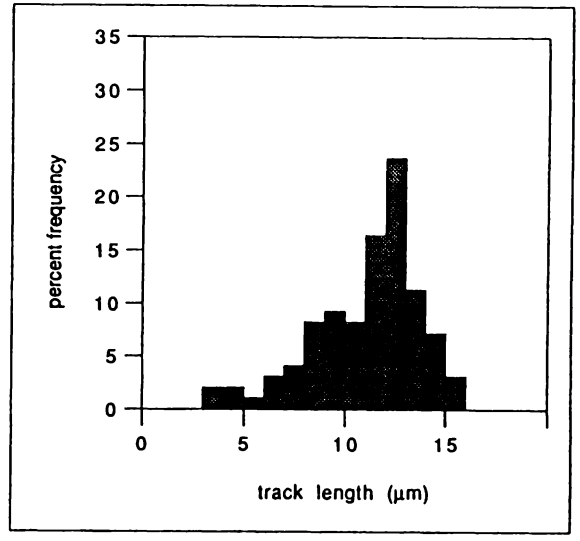
AREA OF BASIC UNIT = 9.89E-07 cm
CHI SQUARED = 24.4608 WITH 23 DEGREES OF FREEDOM
P(chi squared) = 37.9 %
CORRELATION COEFFICIENT = 0.888
VARIANCE OF SQR(Ns) = 1.03
VARIANCE OF SQR(Ni) = 4.11

Ns/Ni = 0.351 ± 0.030
MEAN RATIO = 0.427 ± 0.038

Ages calculated using a zeta of 354.9 ± 4.3 for SRM612 glass
RHO D = 1.111E+06 ; ND = 2746

POOLED AGE = 68.7 ± 6.0 Ma
MEAN AGE = 83.7 ± 7.7 Ma

8902-64



n = 97
Mean = 11.17 µm
Sample std. dev. = 2.66 µm

8902-64 ZIRCON lindis s116/412298 775m

IRRADIATION jmt data:jmt zircon data:lindis zircons:wk024/15
SLIDE NUMBER 1
COUNTED BY: jmt

No.	Ns	Ni	Na	RATIO	U (ppm)	RHOs (E+06)	RHOi (E+06)	F.T.AGE (Ma)
1	29	18	3	1.611	0.0	9.774	6.067	94.3 ± 28.3
2	35	28	5	1.250	0.0	7.078	5.662	73.3 ± 18.6
3	41	32	6	1.281	0.0	6.909	5.393	75.1 ± 17.8
	105	78			0.0	7.583	5.633	

AREA OF BASIC UNIT = 9.89E-07 cm
CHI SQUARED = .48887 WITH 2 DEGREES OF FREEDOM
P(chi squared) = 78.3 %
CORRELATION COEFFICIENT = 0.971
VARIANCE OF SQR(Ns) = 0.26
VARIANCE OF SQR(Ni) = 0.54

Ns/Ni = 1.346 ± 0.201
MEAN RATIO = 1.381 ± 0.116

Ages calculated using a zeta of 133.9 ± 1.4 for CN1 glass
RHO D = 8.807E+05 ; ND = 4355

POOLED AGE = 78.9 ± 11.9 Ma
MEAN AGE = 80.9 ± 6.9 Ma

8902-65 APATITE lindis s116/459351 640m

IRRADIATION jmt data:jmt apatite data:lindis apatites:wk011/6
SLIDE NUMBER 1
COUNTED BY: jmt

No.	Ns	Ni	Na	RATIO	U (ppm)	RHOs (E+06)	RHOi (E+06)	F.T.AGE (Ma)
1	3	4	4	0.750	12.1	0.758	1.011	144.6 ± 110.5
2	2	8	6	0.250	16.1	0.337	1.348	48.6 ± 38.4
3	3	14	9	0.214	18.7	0.337	1.573	41.7 ± 26.5
4	6	44	4	0.136	132.6	1.517	11.122	26.5 ± 11.6
5	6	11	6	0.545	22.1	1.011	1.854	105.5 ± 53.6
6	10	21	4	0.476	63.3	2.528	5.308	92.2 ± 35.5
7	2	12	6	0.167	24.1	0.337	2.022	32.4 ± 24.8
8	4	10	3	0.400	40.2	1.348	3.370	77.5 ± 45.9
9	7	45	10	0.156	54.2	0.708	4.550	30.3 ± 12.3
10	8	15	9	0.533	20.1	0.899	1.685	103.2 ± 45.2
11	0	4	9	0.000	5.4	0.000	0.449	0.0 ± 0.0
12	2	15	6	0.133	30.1	0.337	2.528	25.9 ± 19.5
13	3	18	8	0.167	27.1	0.379	2.275	32.4 ± 20.2
14	7	8	6	0.875	16.1	1.180	1.348	168.4 ± 87.2
15	30	110	12	0.273	110.5	2.528	9.269	53.0 ± 11.0
16	6	8	6	0.750	16.1	1.011	1.348	144.6 ± 78.2
17	6	18	6	0.333	36.2	1.011	3.033	64.7 ± 30.5
18	3	7	4	0.429	21.1	0.758	1.769	83.0 ± 57.3
19	4	11	4	0.364	33.1	1.011	2.781	70.5 ± 41.2
20	4	13	6	0.308	26.1	0.674	2.191	59.7 ± 34.2
	116	396			37.3	0.916	3.128	

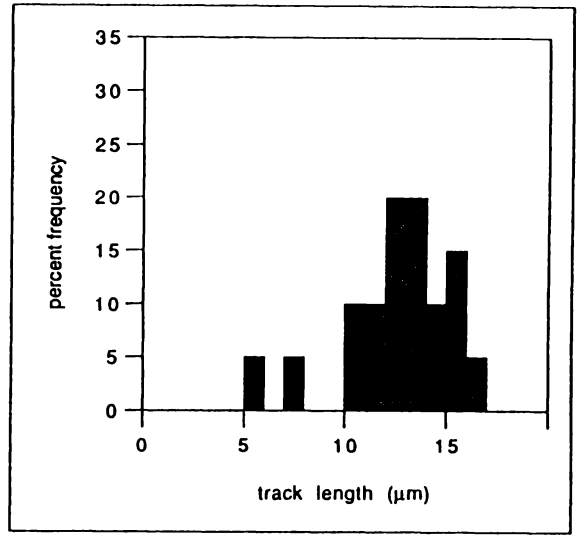
AREA OF BASIC UNIT = 9.89E-07 cm
CHI SQUARED = 25.61857 WITH 19 DEGREES OF FREEDOM
P(chi squared) = 14.1 %
CORRELATION COEFFICIENT = 0.896
VARIANCE OF SQR(Ns) = 1.07
VARIANCE OF SQR(Ni) = 3.84

Ns/Ni = 0.293 ± 0.031
MEAN RATIO = 0.363 ± 0.052

Ages calculated using a zeta of 354.9 ± 4.3 for SRM612 glass
RHO D = 1.099E+06 ; ND = 2716

POOLED AGE = 56.9 ± 6.1 Ma
MEAN AGE = 70.4 ± 10.3 Ma

8902-65



n = 20
Mean = 12.60 µm
Sample std. dev. = 2.52 µm

8902-65 ZIRCON lindis s116/459351 640m

IRRADIATION jmt data:jmt zircon data:lindis zircons:wk024/14
SLIDE NUMBER 1
COUNTED BY: jmt

No.	Ns	Ni	Na	RATIO	U (ppm)	RHOs (E+06)	RHOi (E+06)	F.TAGE (Ma)
1	107	54	7	1.981	0.0	15.456	7.800	114.7 ± 19.3
2	0	0	20	0.000	0.0	0.000	0.000	0.0 ± 0.0
	107	54			0.0	4.007	2.022	

AREA OF BASIC UNIT = 9.89E-07 cm
CHI SQUARED = 1.981481E-05 WITH 1 DEGREES OF FREEDOM
P(chi squared) = 99.6 %
CORRELATION COEFFICIENT = 1.000
VARIANCE OF SQR(Ns) = 53.50
VARIANCE OF SQR(Ni) = 26.98

Ns/Ni = 1.981 ± 0.331
MEAN RATIO = 0.991 ± 0.991

Ages calculated using a zeta of 133.9 ± 1.4 for CN1 glass
RHO D = 8.720E+05 ; ND = 4312

POOLED AGE = 114.7 ± 19.3 Ma
MEAN AGE = 57.6 ± 57.6 Ma

8902-66 APATITE paringa s78/230301 30m

IRRADIATION jmt data:jmt apatite data:paringa apatites:wk011/5
SLIDE NUMBER 1
COUNTED BY: jmt

No.	Ns	Ni	Na	RATIO	U (ppm)	RHOs (E+06)	RHOi (E+06)	F.T.AGE (Ma)
1	0	85	100	0.000	10.4	0.000	0.859	0.0 ± 0.0
2	0	61	60	0.000	12.4	0.000	1.028	0.0 ± 0.0
3	0	18	30	0.000	7.3	0.000	0.607	0.0 ± 0.0
4	0	49	48	0.000	12.4	0.000	1.032	0.0 ± 0.0
5	0	35	70	0.000	6.1	0.000	0.506	0.0 ± 0.0
6	0	41	50	0.000	10.0	0.000	0.829	0.0 ± 0.0
7	0	30	28	0.000	13.1	0.000	1.083	0.0 ± 0.0
8	0	162	100	0.000	19.8	0.000	1.638	0.0 ± 0.0
9	0	9	30	0.000	3.7	0.000	0.303	0.0 ± 0.0
10	0	52	60	0.000	10.6	0.000	0.876	0.0 ± 0.0
11	0	23	25	0.000	11.2	0.000	0.930	0.0 ± 0.0
12	0	12	24	0.000	6.1	0.000	0.506	0.0 ± 0.0
13	0	67	80	0.000	10.2	0.000	0.847	0.0 ± 0.0
14	0	19	25	0.000	9.3	0.000	0.768	0.0 ± 0.0
15	0	156	100	0.000	19.0	0.000	1.577	0.0 ± 0.0
	0	819			12.0	0.000	0.998	

AREA OF BASIC UNIT = 9.89E-07 cm
CHI SQUARED = 8.635295E-06 WITH 14 DEGREES OF FREEDOM
P(chi squared) = 100.0 %
CORRELATION COEFFICIENT = 0.177
VARIANCE OF SQR(Ns) = 0.00
VARIANCE OF SQR(Ni) = 8.66

Ns/Ni = 0.000 ± 0.000
MEAN RATIO = 0.000 ± 0.000

Ages calculated using a zeta of 354.9 ± 4.3 for SRM612 glass
RHO D = 1.086E+06 ; ND = 2686

POOLED AGE = 0.0 ± 0.0 Ma
MEAN AGE = 0.0 ± 0.0 Ma

8902-66 ZIRCON paringa s78/230301 30m

IRRADIATION jmt data:jmt zircon data:paringa zircons:wk038/14
SLIDE NUMBER 1
COUNTED BY: jmt

No.	Ns	Ni	Na	RATIO	U (ppm)	RHOs (E+06)	RHOi (E+06)	F.T.AGE (Ma)
1	2	34	4	0.059	0.0	0.506	8.595	4.2 ± 3.1
2	1	132	6	0.008	0.0	0.169	22.245	0.5 ± 0.5
3	2	118	6	0.017	0.0	0.337	19.885	1.2 ± 0.9
4	2	37	5	0.054	0.0	0.404	7.482	3.9 ± 2.8
5	2	87	3	0.023	0.0	0.674	29.323	1.6 ± 1.2
6	1	37	2	0.027	0.0	0.506	18.706	1.9 ± 2.0
7	2	38	3	0.053	0.0	0.674	12.808	3.8 ± 2.7
8	3	70	5	0.043	0.0	0.607	14.156	3.1 ± 1.8
	15	553			0.0	0.446	16.446	

AREA OF BASIC UNIT = 9.89E-07 cm
CHI SQUARED = 5.948722 WITH 7 DEGREES OF FREEDOM
P(chi squared) = 54.6 %
CORRELATION COEFFICIENT = -0.169
VARIANCE OF SQR(Ns) = 0.06
VARIANCE OF SQR(Ni) = 5.38

Ns/Ni = 0.027 ± 0.007
MEAN RATIO = 0.035 ± 0.007

Ages calculated using a zeta of 133.9 ± 1.4 for CN1 glass
RHO D = 1.065E+06 ; ND = 5265

POOLED AGE = 1.9 ± 0.5 Ma
MEAN AGE = 2.5 ± 0.5 Ma

8902-67 APATITE paringa s88/248258 60m

IRRADIATION jmt data:jmt apatite data:paringa apatites:wk020/6
SLIDE NUMBER 1
COUNTED BY: jmt

No.	Ns	Ni	Na	RATIO	U (ppm)	RHOs (E+06)	RHOi (E+06)	F.TAGE (Ma)
1	0	2	100	0.000	0.1	0.000	0.020	0.0 ± 0.0
2	0	18	200	0.000	0.3	0.000	0.091	0.0 ± 0.0
3	0	2	100	0.000	0.1	0.000	0.020	0.0 ± 0.0
4	0	8	200	0.000	0.1	0.000	0.040	0.0 ± 0.0
5	0	3	70	0.000	0.1	0.000	0.043	0.0 ± 0.0
6	0	0	48	0.000	0.0	0.000	0.000	0.0 ± 0.0
7	0	3	80	0.000	0.1	0.000	0.038	0.0 ± 0.0
8	0	3	60	0.000	0.2	0.000	0.051	0.0 ± 0.0
9	0	1	60	0.000	0.1	0.000	0.017	0.0 ± 0.0
10	0	5	90	0.000	0.2	0.000	0.056	0.0 ± 0.0
11	0	2	100	0.000	0.1	0.000	0.020	0.0 ± 0.0
12	0	1	100	0.000	0.0	0.000	0.010	0.0 ± 0.0
13	0	9	100	0.000	0.3	0.000	0.091	0.0 ± 0.0
14	0	1	36	0.000	0.1	0.000	0.028	0.0 ± 0.0
15	0	7	200	0.000	0.1	0.000	0.035	0.0 ± 0.0
	0	65			0.1	0.000	0.043	

AREA OF BASIC UNIT = 9.89E-07 cm
CHI SQUARED = 2.611116E-06 WITH 14 DEGREES OF FREEDOM
P(chi squared) = 100.0 %
CORRELATION COEFFICIENT = 0.812
VARIANCE OF SQR(Ns) = 0.00
VARIANCE OF SQR(Ni) = 1.07

Ns/Ni = 0.000 ± 0.000
MEAN RATIO = 0.000 ± 0.000

Ages calculated using a zeta of 354.9 ± 4.3 for SRM612 glass
RHO D = 4.243E+06 ; ND = 3357

POOLED AGE = 0.0 ± 0.0 Ma
MEAN AGE = 0.0 ± 0.0 Ma

8902-68 APATITE paringa s88/279196 170m

IRRADIATION jmt data:jmt apatite data:paringa apatites:wk011/3
SLIDE NUMBER 1
COUNTED BY: jmt

No.	Ns	Ni	Na	RATIO	U (ppm)	RHOs (E+06)	RHOi (E+06)	F.T.AGE (Ma)
1	0	0	36	0.000	0.0	0.000	0.000	0.0 ± 0.0
2	0	0	10	0.000	0.0	0.000	0.000	0.0 ± 0.0
3	0	0	20	0.000	0.0	0.000	0.000	0.0 ± 0.0
4	0	2	12	0.000	2.1	0.000	0.169	0.0 ± 0.0
5	0	0	8	0.000	0.0	0.000	0.000	0.0 ± 0.0
6	0	0	8	0.000	0.0	0.000	0.000	0.0 ± 0.0
7	0	0	6	0.000	0.0	0.000	0.000	0.0 ± 0.0
8	0	0	12	0.000	0.0	0.000	0.000	0.0 ± 0.0
9	0	1	10	0.000	1.2	0.000	0.101	0.0 ± 0.0
10	0	0	12	0.000	0.0	0.000	0.000	0.0 ± 0.0
11	0	1	12	0.000	1.0	0.000	0.084	0.0 ± 0.0
12	0	1	12	0.000	1.0	0.000	0.084	0.0 ± 0.0
13	0	1	100	0.000	0.1	0.000	0.010	0.0 ± 0.0
14	0	0	6	0.000	0.0	0.000	0.000	0.0 ± 0.0
15	0	1	24	0.000	0.5	0.000	0.042	0.0 ± 0.0
	0	7			0.3	0.000	0.025	

AREA OF BASIC UNIT = 9.89E-07 cm
CHI SQUARED = 2.500449E-06 WITH 14 DEGREES OF FREEDOM
P(chi squared) = 100.0 %
CORRELATION COEFFICIENT = 0.663
VARIANCE OF SQR(Ns) = 0.00
VARIANCE OF SQR(Ni) = 0.30

Ns/Ni = 0.000 ± 0.000
MEAN RATIO = 0.000 ± 0.000

Ages calculated using a zeta of 354.9 ± 4.3 for SRM612 glass
RHO D = 1.062E+06 ; ND = 2627

POOLED AGE = 0.0 ± 0.0 Ma
MEAN AGE = 0.0 ± 0.0 Ma

8902-68 ZIRCON paringa s88/279196 170m

IRRADIATION jmt data:jmt zircon data:paringa zircons:wk038/15
SLIDE NUMBER 1
COUNTED BY: jmt

No.	Ns	Ni	Na	RATIO	U (ppm)	RHOs (E+06)	RHOi (E+06)	F.T.AGE (Ma)
1	6	194	6	0.031	0.0	1.011	32.693	2.2 ± 0.9
2	4	62	10	0.065	0.0	0.404	6.269	4.6 ± 2.4
3	8	215	21	0.037	0.0	0.385	10.352	2.7 ± 1.0
4	9	180	21	0.050	0.0	0.433	8.667	3.6 ± 1.2
5	3	129	8	0.023	0.0	0.379	16.304	1.7 ± 1.0
6	9	178	21	0.051	0.0	0.433	8.570	3.6 ± 1.2
7	6	107	12	0.056	0.0	0.506	9.016	4.0 ± 1.7
8	3	35	10	0.086	0.0	0.303	3.539	6.1 ± 3.7
	48	1100			0.0	0.445	10.204	

AREA OF BASIC UNIT = 9.89E-07 cm
CHI SQUARED = 4.687186 WITH 7 DEGREES OF FREEDOM
P(chi squared) = 69.8 %
CORRELATION COEFFICIENT = 0.775
VARIANCE OF SQR(Ns) = 0.28
VARIANCE OF SQR(Ni) = 9.78

Ns/Ni = 0.044 ± 0.006
MEAN RATIO = 0.050 ± 0.007

Ages calculated using a zeta of 133.9 ± 1.4 for CN1 glass
RHO D = 1.065E+06 ; ND = 5265

POOLED AGE = 3.1 ± 0.5 Ma
MEAN AGE = 3.5 ± 0.5 Ma

8902-69 APATITE ohau s99/456974 760m

IRRADIATION jmt data:jmt apatite data:ohau apatites:wk011/2
SLIDE NUMBER 1
COUNTED BY: jmt

No.	Ns	NI	Na	RATIO	U (ppm)	RHOs (E+06)	RHOi (E+06)	F.T.AGE (Ma)
1	1	107	30	0.009	45.0	0.034	3.606	1.7 ± 1.7
2	1	9	12	0.111	9.5	0.084	0.758	20.7 ± 21.8
3	0	3	16	0.000	2.4	0.000	0.190	0.0 ± 0.0
4	0	7	12	0.000	7.4	0.000	0.590	0.0 ± 0.0
5	0	45	9	0.000	63.1	0.000	5.056	0.0 ± 0.0
6	0	37	28	0.000	16.7	0.000	1.336	0.0 ± 0.0
7	0	21	24	0.000	11.0	0.000	0.885	0.0 ± 0.0
8	0	59	16	0.000	46.5	0.000	3.729	0.0 ± 0.0
9	1	130	18	0.008	91.1	0.056	7.303	1.4 ± 1.4
10	0	2	15	0.000	1.7	0.000	0.135	0.0 ± 0.0
11	0	71	28	0.000	32.0	0.000	2.564	0.0 ± 0.0
12	0	28	28	0.000	12.6	0.000	1.011	0.0 ± 0.0
13	0	61	12	0.000	64.1	0.000	5.140	0.0 ± 0.0
14	0	60	18	0.000	42.0	0.000	3.370	0.0 ± 0.0
15	0	35	64	0.000	6.9	0.000	0.553	0.0 ± 0.0
16	0	5	8	0.000	7.9	0.000	0.632	0.0 ± 0.0
17	0	93	18	0.000	65.2	0.000	5.224	0.0 ± 0.0
18	1	33	16	0.030	26.0	0.063	2.085	5.6 ± 5.7
19	1	41	16	0.024	32.3	0.063	2.591	4.5 ± 4.6
20	0	37	24	0.000	19.4	0.000	1.559	0.0 ± 0.0
	5	884			27.1	0.012	2.169	

AREA OF BASIC UNIT = 9.89E-07 cm
CHI SQUARED = 25.38908 WITH 19 DEGREES OF FREEDOM
P(chi squared) = 14.8 %
CORRELATION COEFFICIENT = 0.331
VARIANCE OF SQR(Ns) = 0.20
VARIANCE OF SQR(Ni) = 8.07

Ns/Ni = 0.006 ± 0.003
MEAN RATIO = 0.009 ± 0.006

Ages calculated using a zeta of 354.9 ± 4.3 for SRM612 glass
RHO D = 1.050E+06 ; ND = 2597

POOLED AGE = 1.1 ± 0.5 Ma
MEAN AGE = 1.7 ± 1.1 Ma

8902-69 ZIRCON ohau s99/456974 760m

IRRADIATION jmt data:jmt zircon data:ohau zircons:wk024/11
SLIDE NUMBER 1
COUNTED BY: jmt

No.	Ns	NI	Na	RATIO	U (ppm)	RHOs (E+06)	RHOi (E+06)	F.T.AGE (Ma)
1	83	43	10	1.930	0.0	8.392	4.348	108.4 ± 20.5
2	83	49	9	1.694	0.0	9.325	5.505	95.2 ± 17.2
3	172	96	12	1.792	0.0	14.493	8.089	100.7 ± 13.0
4	119	89	12	1.337	0.0	10.027	7.499	75.3 ± 10.6
5	417	205	35	2.034	0.0	12.047	5.922	114.2 ± 10.0
6	155	65	15	2.385	0.0	10.448	4.382	133.6 ± 19.9
7	79	53	8	1.491	0.0	9.985	6.699	83.8 ± 15.0
8	153	87	16	1.759	0.0	9.669	5.498	98.8 ± 13.4
9	49	20	6	2.450	0.0	8.257	3.370	137.2 ± 36.5
10	299	141	30	2.121	0.0	10.078	4.752	119.0 ± 12.4
11	56	27	8	2.074	0.0	7.078	3.413	116.4 ± 27.4
	1665	875			0.0	10.457	5.495	

AREA OF BASIC UNIT = 9.89E-07 cm
CHI SQUARED = 14.42592 WITH 10 DEGREES OF FREEDOM
P(chi squared) = 15.4 %
CORRELATION COEFFICIENT = 0.978
VARIANCE OF SQR(Ns) = 17.21
VARIANCE OF SQR(Ni) = 8.33

Ns/Ni = 1.903 ± 0.079
MEAN RATIO = 1.915 ± 0.104

Ages calculated using a zeta of 133.9 ± 1.4 for CN1 glass
RHO D = 8.457E+05 ; ND = 4182

POOLED AGE = 106.8 ± 4.9 Ma
MEAN AGE = 107.5 ± 6.2 Ma

8902-70 APATITE ohau s99/516983 640m

IRRADIATION jmt data:jmt apatite data:ohau apatites:wk011/1
SLIDE NUMBER 1
COUNTED BY: jmt

No.	Ns	Ni	Na	RATIO	U (ppm)	RHOs (E+06)	RHOi (E+06)	F.T AGE (Ma)
1	0	8	6	0.000	17.0	0.000	1.348	0.0 ± 0.0
2	0	10	9	0.000	14.2	0.000	1.123	0.0 ± 0.0
3	0	16	16	0.000	12.8	0.000	1.011	0.0 ± 0.0
4	0	32	16	0.000	25.5	0.000	2.022	0.0 ± 0.0
5	0	6	6	0.000	12.8	0.000	1.011	0.0 ± 0.0
6	0	14	10	0.000	17.9	0.000	1.416	0.0 ± 0.0
7	0	6	8	0.000	9.6	0.000	0.758	0.0 ± 0.0
8	0	15	4	0.000	47.9	0.000	3.792	0.0 ± 0.0
9	0	70	16	0.000	55.8	0.000	4.424	0.0 ± 0.0
10	0	43	12	0.000	45.7	0.000	3.623	0.0 ± 0.0
11	0	47	20	0.000	30.0	0.000	2.376	0.0 ± 0.0
12	0	14	16	0.000	11.2	0.000	0.885	0.0 ± 0.0
13	0	12	10	0.000	15.3	0.000	1.213	0.0 ± 0.0
14	0	29	15	0.000	24.7	0.000	1.955	0.0 ± 0.0
15	0	5	4	0.000	16.0	0.000	1.264	0.0 ± 0.0
16	0	9	4	0.000	28.7	0.000	2.275	0.0 ± 0.0
17	0	3	9	0.000	4.3	0.000	0.337	0.0 ± 0.0
18	0	7	6	0.000	14.9	0.000	1.180	0.0 ± 0.0
19	0	14	15	0.000	11.9	0.000	0.944	0.0 ± 0.0
	0	360			22.7	0.000	1.802	

AREA OF BASIC UNIT = 9.89E-07 cm
CHI SQUARED = 1.025E-05 WITH 18 DEGREES OF FREEDOM
P(chi squared) = 100.0 %
CORRELATION COEFFICIENT = 0.179
VARIANCE OF SQR(Ns) = 0.00
VARIANCE OF SQR(Ni) = 3.16

Ns/Ni = 0.000 ± 0.000
MEAN RATIO = 0.000 ± 0.000

Ages calculated using a zeta of 354.9 ± 4.3 for SRM612 glass
RHO D = 1.038E+06 ; ND = 2567

POOLED AGE = 0.0 ± 0.0 Ma
MEAN AGE = 0.0 ± 0.0 Ma

8902-70 ZIRCON ohau s99/516983 640m

IRRADIATION jmt data:jmt zircon data:ohau zircons:wk024/10
SLIDE NUMBER 1
COUNTED BY: jmt

No.	Ns	NI	Na	RATIO	U (ppm)	RHOs (E+06)	RHOi (E+06)	F.T AGE (Ma)
1	18	10	2	1.800	0.0	9.100	5.056	100.1 ± 39.5
2	140	67	16	2.090	0.0	8.847	4.234	116.0 ± 17.4
3	94	65	12	1.446	0.0	7.920	5.477	80.5 ± 13.1
4	144	58	20	2.483	0.0	7.280	2.932	137.6 ± 21.6
5	44	30	6	1.467	0.0	7.415	5.056	81.7 ± 19.4
6	100	35	8	2.857	0.0	12.639	4.424	158.1 ± 31.2
	540	265			0.0	8.531	4.187	

AREA OF BASIC UNIT = 9.89E-07 cm
CHI SQUARED = 11.24612 WITH 5 DEGREES OF FREEDOM
P(chi squared) = 4.7 %
CORRELATION COEFFICIENT = 0.864
VARIANCE OF SQR(Ns) = 9.34
VARIANCE OF SQR(Ni) = 3.80

Ns/NI = 2.038 ± 0.153
MEAN RATIO = 2.024 ± 0.231

Ages calculated using a zeta of 133.9 ± 1.4 for CN1 glass
RHO D = 8.369E+05 ; ND = 4139

POOLED AGE = 113.2 ± 8.7 Ma
MEAN AGE = 112.4 ± 13.0 Ma

8902-71 APATITE ohau s99/521914 640m

IRRADIATION jmt data:jmt apatite data:ohau apatites:wk012/17
SLIDE NUMBER 1
COUNTED BY: jmt

No.	Ns	Ni	Na	RATIO	U (ppm)	RHOs (E+06)	RHOi (E+06)	F.T.AGE (Ma)
1	1	65	16	0.015	42.9	0.063	4.108	3.4 ± 3.4
2	2	46	24	0.043	20.3	0.084	1.938	9.7 ± 7.0
3	2	63	16	0.032	41.6	0.126	3.981	7.1 ± 5.1
4	0	6	12	0.000	5.3	0.000	0.506	0.0 ± 0.0
5	0	28	18	0.000	16.4	0.000	1.573	0.0 ± 0.0
6	0	3	30	0.000	1.1	0.000	0.101	0.0 ± 0.0
7	0	13	25	0.000	5.5	0.000	0.526	0.0 ± 0.0
8	1	21	21	0.048	10.6	0.048	1.011	10.6 ± 10.8
9	2	88	42	0.023	22.1	0.048	2.119	5.1 ± 3.6
10	3	148	30	0.020	52.2	0.101	4.988	4.5 ± 2.6
11	8	243	30	0.033	85.6	0.270	8.190	7.3 ± 2.6
12	2	48	16	0.042	31.7	0.126	3.033	9.3 ± 6.7
13	2	147	24	0.014	64.7	0.084	6.193	3.0 ± 2.2
14	1	79	25	0.013	33.4	0.040	3.195	2.8 ± 2.8
15	1	156	21	0.006	78.5	0.048	7.511	1.4 ± 1.4
16	0	13	50	0.000	2.7	0.000	0.263	0.0 ± 0.0
17	0	29	12	0.000	25.5	0.000	2.444	0.0 ± 0.0
18	0	26	25	0.000	11.0	0.000	1.052	0.0 ± 0.0
19	0	16	16	0.000	10.6	0.000	1.011	0.0 ± 0.0
20	0	22	36	0.000	6.5	0.000	0.618	0.0 ± 0.0
21	2	97	30	0.021	34.2	0.067	3.269	4.6 ± 3.3
22	1	36	15	0.028	25.4	0.067	2.427	6.2 ± 6.3
23	0	7	15	0.000	4.9	0.000	0.472	0.0 ± 0.0
24	2	28	16	0.071	18.5	0.126	1.769	15.9 ± 11.6
25	2	104	30	0.019	36.6	0.067	3.505	4.3 ± 3.1
26	5	159	40	0.031	42.0	0.126	4.019	7.0 ± 3.2
	37	1691			28.2	0.059	2.693	

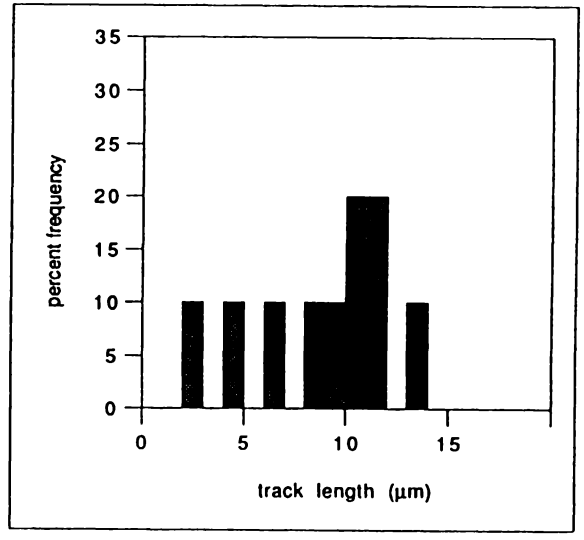
AREA OF BASIC UNIT = 9.89E-07 cm
CHI SQUARED = 13.7883 WITH 25 DEGREES OF FREEDOM
P(chi squared) = 96.5 %
CORRELATION COEFFICIENT = 0.849
VARIANCE OF SQR(Ns) = 0.66
VARIANCE OF SQR(Ni) = 13.62

Ns/Ni = 0.022 ± 0.004
MEAN RATIO = 0.018 ± 0.004

Ages calculated using a zeta of 354.9 ± 4.3 for SRM612 glass
RHO D = 1.253E+06 ; ND = 3100

POOLED AGE = 4.9 ± 0.8 Ma
MEAN AGE = 3.9 ± 0.8 Ma

8902-71



n = 10
Mean = 8.99 µm
Sample std. dev. = 3.28 µm

8902-71 ZIRCON ohau s99/521914 640m

IRRADIATION jmt data:jmt zircon data:ohau zircons:wk024/9
SLIDE NUMBER 1
COUNTED BY: jmt

No.	Ns	Ni	Na	RATIO	U (ppm)	RHOs (E+06)	RHOi (E+06)	F.T.AGE (Ma)
1	102	39	10	2.615	0.0	10.313	3.943	143.4 ± 27.1
2	113	36	9	3.139	0.0	12.695	4.044	171.7 ± 33.0
3	107	41	9	2.610	0.0	12.021	4.606	143.1 ± 26.4
4	401	149	40	2.691	0.0	10.136	3.766	147.5 ± 14.4
5	165	76	16	2.171	0.0	10.427	4.803	119.3 ± 16.7
6	131	58	9	2.259	0.0	14.717	6.516	124.0 ± 19.7
7	203	88	12	2.307	0.0	17.105	7.415	126.7 ± 16.3
8	217	107	16	2.028	0.0	13.713	6.762	111.5 ± 13.3
9	101	43	14	2.349	0.0	7.295	3.106	128.9 ± 23.6
10	294	148	20	1.986	0.0	14.864	7.482	109.2 ± 11.2
	1834	785			0.0	11.964	5.121	

AREA OF BASIC UNIT = 9.89E-07 cm
CHI SQUARED = 9.668192 WITH 9 DEGREES OF FREEDOM
P(chi squared) = 37.8 %
CORRELATION COEFFICIENT = 0.957
VARIANCE OF SQR(Ns) = 11.45
VARIANCE OF SQR(Ni) = 5.74

Ns/Ni = 2.336 ± 0.100
MEAN RATIO = 2.416 ± 0.111

Ages calculated using a zeta of 133.9 ± 1.4 for CN1 glass
RHO D = 8.282E+05 ; ND = 4095

POOLED AGE = 128.3 ± 6.0 Ma
MEAN AGE = 132.6 ± 6.6 Ma

8902-72 APATITE ohau s99/544877 550m

IRRADIATION jmt data:jmt apatite data:ohau apatites:wk012/16
SLIDE NUMBER 1
COUNTED BY: jmt

No.	Ns	NI	Na	RATIO	U (ppm)	RHOs (E+06)	RHOi (E+06)	F.T AGE (Ma)
1	20	131	24	0.153	58.1	0.843	5.519	33.6 ± 8.1
2	6	22	16	0.273	14.6	0.379	1.390	59.9 ± 27.6
3	5	14	8	0.357	18.6	0.632	1.769	78.4 ± 40.9
4	6	40	24	0.150	17.7	0.253	1.685	33.0 ± 14.5
5	2	11	18	0.182	6.5	0.112	0.618	40.0 ± 30.8
6	4	19	12	0.211	16.9	0.337	1.601	46.3 ± 25.5
7	4	22	35	0.182	6.7	0.116	0.636	40.0 ± 21.8
8	5	37	20	0.135	19.7	0.253	1.871	29.8 ± 14.2
9	18	122	24	0.148	54.1	0.758	5.140	32.5 ± 8.2
10	29	157	24	0.185	69.7	1.222	6.614	40.6 ± 8.3
11	2	14	35	0.143	4.3	0.058	0.404	31.5 ± 23.8
12	19	44	24	0.432	19.5	0.800	1.854	94.6 ± 26.1
13	4	14	24	0.286	6.2	0.169	0.590	62.8 ± 35.6
14	1	7	12	0.143	6.2	0.084	0.590	31.5 ± 33.6
15	21	78	12	0.269	69.2	1.769	6.572	59.2 ± 14.6
16	0	38	20	0.000	20.2	0.000	1.921	0.0 ± 0.0
17	33	160	25	0.206	68.1	1.335	6.471	45.4 ± 8.7
18	5	74	16	0.068	49.2	0.316	4.676	14.9 ± 6.9
19	0	8	12	0.000	7.1	0.000	0.674	0.0 ± 0.0
20	4	24	20	0.167	12.8	0.202	1.213	36.7 ± 19.8
21	37	149	28	0.248	56.7	1.336	5.381	54.6 ± 10.1
	225	1185			29.1	0.525	2.767	

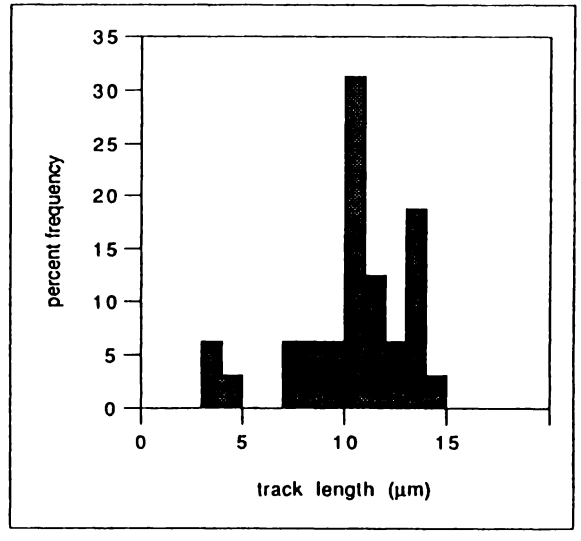
AREA OF BASIC UNIT = 9.89E-07 cm
CHI SQUARED = 33.68716 WITH 20 DEGREES OF FREEDOM
P(chi squared) = 2.8 %
CORRELATION COEFFICIENT = 0.913
VARIANCE OF SQR(Ns) = 3.16
VARIANCE OF SQR(Ni) = 11.80

Ns/Ni = 0.190 ± 0.014
MEAN RATIO = 0.187 ± 0.022

Ages calculated using a zeta of 354.9 ± 4.3 for SRM612 glass
RHO D = 1.244E+06 ; ND = 3076

POOLED AGE = 41.8 ± 3.2 Ma
MEAN AGE = 41.2 ± 5.0 Ma

8902-72



n = 32
Mean = 10.47 µm
Sample std. dev. = 2.74 µm

8902-72 ZIRCON ohau s99/544877 550m

IRRADIATION jmt data:jmt zircon data:ohau zircons:wk024/8
SLIDE NUMBER 1
COUNTED BY: jmt

No.	Ns	Ni	Na	RATIO	U (ppm)	RHOs (E+06)	RHOi (E+06)	F.T.AGE (Ma)
1	163	50	30	3.260	0.0	5.494	1.685	176.4 ± 28.7
2	205	48	20	4.271	0.0	10.364	2.427	230.1 ± 37.2
3	119	26	15	4.577	0.0	8.022	1.753	246.3 ± 53.5
4	280	77	20	3.636	0.0	14.156	3.893	196.5 ± 25.6
5	85	33	8	2.576	0.0	10.743	4.171	139.8 ± 28.8
6	374	80	24	4.675	0.0	15.757	3.370	251.5 ± 31.3
7	520	111	36	4.685	0.0	14.605	3.118	252.0 ± 26.8
8	76	23	9	3.304	0.0	8.538	2.584	178.8 ± 42.7
	1822	448			0.0	11.372	2.796	

AREA OF BASIC UNIT = 9.89E-07 cm
CHI SQUARED = 11.95132 WITH 7 DEGREES OF FREEDOM
P(chi squared) = 10.2 %
CORRELATION COEFFICIENT = 0.976
VARIANCE OF SQR(Ns) = 24.92
VARIANCE OF SQR(Ni) = 4.15

Ns/Ni = 4.067 ± 0.214
MEAN RATIO = 3.873 ± 0.280

Ages calculated using a zeta of 133.9 ± 1.4 for CN1 glass
RHO D = 8.194E+05 ; ND = 4052

POOLED AGE = 219.3 ± 12.3 Ma
MEAN AGE = 209.0 ± 15.6 Ma

8902-73 APATITE ohau s99/526711 565m

IRRADIATION jmt data:jmt apatite data:ohau apatites:wk033/11
SLIDE NUMBER 1
COUNTED BY: jmt

No.	Ns	Ni	Na	RATIO	U (ppm)	RHOs (E+06)	RHOi (E+06)	F.T.AGE (Ma)
1	13	21	12	0.619	28.5	1.095	1.769	88.8 ± 31.4
2	4	22	20	0.182	17.9	0.202	1.112	26.2 ± 14.3
3	6	11	8	0.545	22.4	0.758	1.390	78.3 ± 39.8
4	10	13	9	0.769	23.5	1.123	1.461	110.2 ± 46.4
5	9	14	12	0.643	19.0	0.758	1.180	92.2 ± 39.5
6	14	43	16	0.326	43.7	0.885	2.717	46.9 ± 14.5
7	0	4	15	0.000	4.3	0.000	0.270	0.0 ± 0.0
8	6	13	8	0.462	26.4	0.758	1.643	66.4 ± 32.8
9	0	2	6	0.000	5.4	0.000	0.337	0.0 ± 0.0
10	14	23	20	0.609	18.7	0.708	1.163	87.4 ± 29.7
11	1	6	12	0.167	8.1	0.084	0.506	24.0 ± 26.0
12	16	20	12	0.800	27.1	1.348	1.685	114.6 ± 38.5
13	1	7	12	0.143	9.5	0.084	0.590	20.6 ± 22.0
14	2	4	12	0.500	5.4	0.169	0.337	71.9 ± 62.3
15	1	4	16	0.250	4.1	0.063	0.253	36.0 ± 40.3
16	6	17	16	0.353	17.3	0.379	1.074	50.8 ± 24.2
17	2	10	12	0.200	13.6	0.169	0.843	28.8 ± 22.4
18	1	2	9	0.500	3.6	0.112	0.225	71.9 ± 88.0
19	4	5	12	0.800	6.8	0.337	0.421	114.6 ± 76.9
20	13	17	14	0.765	19.7	0.939	1.228	109.6 ± 40.5
21	1	4	15	0.250	4.3	0.067	0.270	36.0 ± 40.3
22	8	14	12	0.571	19.0	0.674	1.180	82.1 ± 36.4
23	69	185	25	0.373	120.4	2.791	7.482	53.7 ± 7.7
	201	461			24.6	0.666	1.528	

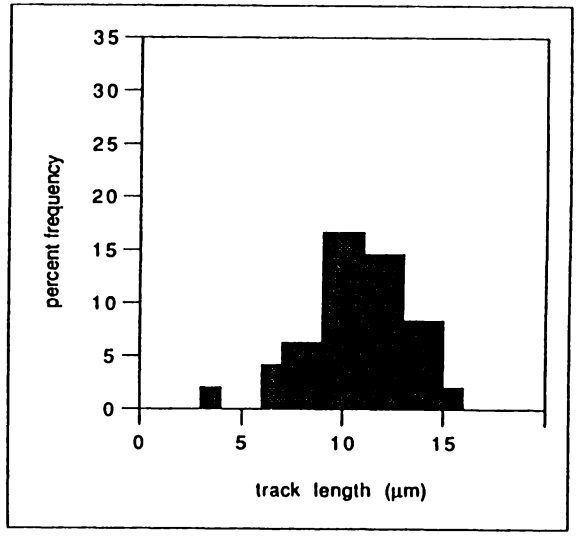
AREA OF BASIC UNIT = 9.89E-07 cm
CHI SQUARED = 23.25482 WITH 22 DEGREES OF FREEDOM
P(chi squared) = 38.7 %
CORRELATION COEFFICIENT = 0.974
VARIANCE OF SQR(Ns) = 3.12
VARIANCE OF SQR(Ni) = 6.24

Ns/Ni = 0.436 ± 0.037
MEAN RATIO = 0.427 ± 0.052

Ages calculated using a zeta of 354.9 ± 4.3 for SRM612 glass
RHO D = 8.144E+05 ; ND = 2014

POOLED AGE = 62.7 ± 5.5 Ma
MEAN AGE = 61.4 ± 7.7 Ma

8902-73



n = 48
Mean = 10.76 µm
Sample std. dev. = 2.49 µm

8902-73 ZIRCON ohau s99/526711 565m

IRRADIATION jmt data:jmt zircon data:ohau zircons:wk024/7
SLIDE NUMBER 1
COUNTED BY: jmt

No.	Ns	Ni	Na	RATIO	U (ppm)	RHOs (E+06)	RHOi (E+06)	F.T.AGE (Ma)
1	92	22	10	4.182	0.0	9.302	2.224	223.1 ± 53.1
2	145	32	12	4.531	0.0	12.218	2.696	241.4 ± 47.4
3	81	18	6	4.500	0.0	13.650	3.033	239.7 ± 62.6
4	55	14	4	3.929	0.0	13.903	3.539	209.8 ± 62.9
5	51	20	6	2.550	0.0	8.595	3.370	136.9 ± 36.2
6	207	69	16	3.000	0.0	13.081	4.360	160.8 ± 22.6
7	113	50	12	2.260	0.0	9.521	4.213	121.5 ± 20.8
8	187	39	18	4.795	0.0	10.504	2.191	255.1 ± 45.2
9	190	63	21	3.016	0.0	9.148	3.033	161.6 ± 23.7
10	86	25	14	3.440	0.0	6.211	1.806	184.1 ± 42.0
11	42	9	3	4.667	0.0	14.156	3.033	248.4 ± 91.4
12	311	121	24	2.570	0.0	13.102	5.098	138.0 ± 15.0
13	129	33	14	3.909	0.0	9.317	2.383	208.8 ± 40.9
14	82	35	10	2.343	0.0	8.291	3.539	125.9 ± 25.5
15	134	61	12	2.197	0.0	11.291	5.140	118.1 ± 18.4
16	82	37	8	2.216	0.0	10.364	4.676	119.2 ± 23.7
17	267	73	18	3.658	0.0	14.998	4.101	195.5 ± 26.1
	2254	721			0.0	10.957	3.505	

AREA OF BASIC UNIT = 9.89E-07 cm
CHI SQUARED = 35.99311 WITH 16 DEGREES OF FREEDOM
P(chi squared) = 0.3 %
CORRELATION COEFFICIENT = 0.909
VARIANCE OF SQR(Ns) = 10.32
VARIANCE OF SQR(Ni) = 4.17

Ns/Ni = 3.126 ± 0.134
MEAN RATIO = 3.398 ± 0.229

Ages calculated using a zeta of 133.9 ± 1.4 for CN1 glass
RHO D = 8.107E+05 ; ND = 4009

POOLED AGE = 167.5 ± 7.8 Ma
MEAN AGE = 181.8 ± 12.7 Ma

8902-74 APATITE ohau s109/673431 425m

IRRADIATION jmt data:jmt apatite data:ohau apatites:wk012/14
SLIDE NUMBER 1
COUNTED BY: jmt

No.	Ns	Ni	Na	RATIO	U (ppm)	RHOs (E+06)	RHOi (E+06)	F.TAGE (Ma)
1	1	7	8	0.143	9.5	0.126	0.885	31.0 ± 33.1
2	2	18	18	0.111	10.8	0.112	1.011	24.1 ± 18.0
3	1	14	12	0.071	12.6	0.084	1.180	15.5 ± 16.0
4	8	43	24	0.186	19.4	0.337	1.812	40.3 ± 15.5
5	0	5	4	0.000	13.5	0.000	1.264	0.0 ± 0.0
6	5	18	9	0.278	21.6	0.562	2.022	60.1 ± 30.4
7	30	92	12	0.326	83.0	2.528	7.752	70.4 ± 14.9
8	4	7	6	0.571	12.6	0.674	1.180	122.9 ± 77.1
9	20	74	12	0.270	66.7	1.685	6.235	58.4 ± 14.8
10	2	6	6	0.333	10.8	0.337	1.011	72.0 ± 58.8
11	0	3	4	0.000	8.1	0.000	0.758	0.0 ± 0.0
12	0	7	12	0.000	6.3	0.000	0.590	0.0 ± 0.0
13	3	10	8	0.300	13.5	0.379	1.264	64.8 ± 42.7
14	15	54	12	0.278	48.7	1.264	4.550	60.1 ± 17.6
15	8	22	12	0.364	19.8	0.674	1.854	78.5 ± 32.5
16	12	25	9	0.480	30.1	1.348	2.809	103.4 ± 36.4
17	4	14	12	0.286	12.6	0.337	1.180	61.8 ± 35.0
18	18	40	18	0.450	24.0	1.011	2.247	97.0 ± 27.6
19	1	27	16	0.037	18.3	0.063	1.706	8.0 ± 8.2
20	8	16	6	0.500	28.9	1.348	2.696	107.7 ± 46.7
	142	502			24.7	0.653	2.307	

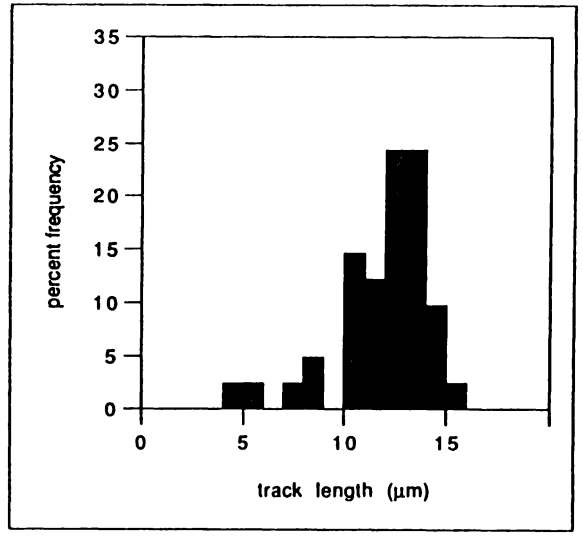
AREA OF BASIC UNIT = 9.89E-07 cm
CHI SQUARED = 24.23671 WITH 19 DEGREES OF FREEDOM
P(chi squared) = 18.7 %
CORRELATION COEFFICIENT = 0.923
VARIANCE OF SQR(Ns) = 2.42
VARIANCE OF SQR(Ni) = 4.73

Ns/Ni = 0.283 ± 0.027
MEAN RATIO = 0.249 ± 0.039

Ages calculated using a zeta of 354.9 ± 4.3 for SRM612 glass
RHO D = 1.224E+06 ; ND = 3027

POOLED AGE = 61.1 ± 6.0 Ma
MEAN AGE = 53.9 ± 8.6 Ma

8902-74



n = 41
Mean = 11.87 µm
Sample std. dev. = 2.27 µm

8902-74 ZIRCON ohau s109/673431 425m

IRRADIATION jmt data:jmt zircon data:ohau zircons:wk024/6
SLIDE NUMBER 1
COUNTED BY: jmt

No.	Ns	Ni	Na	RATIO	U (ppm)	RHOs (E+06)	RHOi (E+06)	F.T AGE (Ma)
1	571	118	48	4.839	0.0	12.028	2.486	254.7 ± 26.2
2	101	19	8	5.316	0.0	12.765	2.401	279.3 ± 70.0
3	155	53	20	2.925	0.0	7.836	2.679	155.1 ± 24.9
4	182	51	16	3.569	0.0	11.502	3.223	188.8 ± 30.1
5	140	30	12	4.667	0.0	11.796	2.528	245.8 ± 49.7
6	387	119	42	3.252	0.0	9.317	2.865	172.3 ± 18.4
7	321	77	24	4.169	0.0	13.524	3.244	220.0 ± 28.2
8	289	48	18	6.021	0.0	16.234	2.696	315.4 ± 49.5
9	334	85	32	3.929	0.0	10.554	2.686	207.6 ± 25.5
	2480	600			0.0	11.398	2.758	

AREA OF BASIC UNIT = 9.89E-07 cm
CHI SQUARED = 20.78091 WITH 8 DEGREES OF FREEDOM
P(chi squared) = 0.8 %
CORRELATION COEFFICIENT = 0.909
VARIANCE OF SQR(Ns) = 19.66
VARIANCE OF SQR(Ni) = 5.08

Ns/Ni = 4.133 ± 0.188
MEAN RATIO = 4.298 ± 0.335

Ages calculated using a zeta of 133.9 ± 1.4 for CN1 glass
RHO D = 8.020E+05 ; ND = 3965

POOLED AGE = 218.2 ± 10.8 Ma
MEAN AGE = 226.8 ± 18.2 Ma

8902-75 APATITE ohau s117/7 66333 410m

IRRADIATION jmt data:jmt apatite data:ohau apatites:wk012/13
SLIDE NUMBER 1
COUNTED BY: jmt

No.	Ns	NI	Na	RATIO	U (ppm)	RHOs (E+06)	RHOi (E+06)	F.T.AGE (Ma)
1	9	30	50	0.300	6.5	0.182	0.607	64.3 ± 24.5
2	34	70	12	0.486	63.6	2.865	5.898	103.8 ± 21.8
3	87	164	30	0.530	59.6	2.932	5.527	113.3 ± 15.2
4	9	45	16	0.200	30.7	0.569	2.844	42.9 ± 15.7
5	24	44	15	0.545	32.0	1.618	2.966	116.4 ± 29.7
6	3	16	24	0.188	7.3	0.126	0.674	40.3 ± 25.3
7	1	11	12	0.091	10.0	0.084	0.927	19.6 ± 20.4
8	4	16	12	0.250	14.5	0.337	1.348	53.6 ± 30.0
9	8	35	28	0.229	13.6	0.289	1.264	49.1 ± 19.3
10	16	37	12	0.432	33.6	1.348	3.118	92.5 ± 27.7
11	6	25	30	0.240	9.1	0.202	0.843	51.5 ± 23.4
12	15	53	16	0.283	36.1	0.948	3.349	60.7 ± 17.8
13	1	11	24	0.091	5.0	0.042	0.463	19.6 ± 20.4
14	20	44	16	0.455	30.0	1.264	2.781	97.2 ± 26.3
15	56	127	21	0.441	66.0	2.696	6.115	94.3 ± 15.3
16	65	137	36	0.474	41.5	1.826	3.848	101.4 ± 15.4
17	25	43	12	0.581	39.1	2.106	3.623	124.0 ± 31.3
18	18	27	12	0.667	24.5	1.517	2.275	142.0 ± 43.3
19	20	60	16	0.333	40.9	1.264	3.792	71.4 ± 18.5
20	3	20	30	0.150	7.3	0.101	0.674	32.2 ± 20.0
	424	1015			26.1	1.011	2.420	

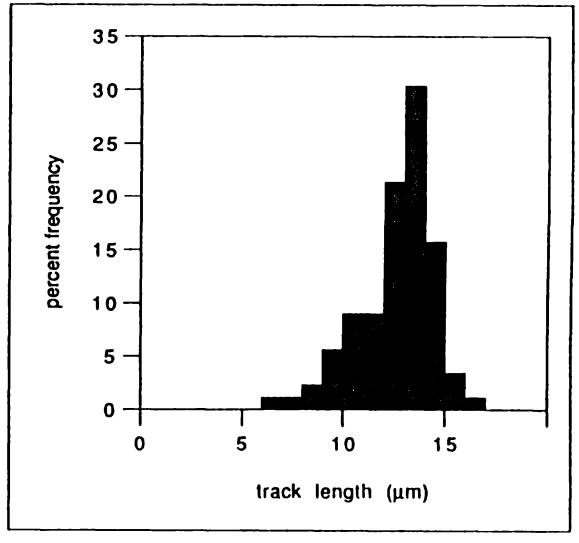
AREA OF BASIC UNIT = 9.89E-07 cm
CHI SQUARED = 32.24269 WITH 19 DEGREES OF FREEDOM
P(chi squared) = 2.9 %
CORRELATION COEFFICIENT = 0.976
VARIANCE OF SQR(Ns) = 5.30
VARIANCE OF SQR(Ni) = 7.23

Ns/Ni = 0.418 ± 0.024
MEAN RATIO = 0.348 ± 0.038

Ages calculated using a zeta of 354.9 ± 4.3 for SRM612 glass
RHO D = 1.214E+06 ; ND = 3002

POOLED AGE = 89.4 ± 5.5 Ma
MEAN AGE = 74.6 ± 8.3 Ma

8902-75



n = 89
Mean = 12.64 μm
Sample std. dev. = 1.84 μm

8902-75 ZIRCON ohau s117/766333 410m

IRRADIATION jmt data:jmt zircon data:ohau zircons:wk038/17
SLIDE NUMBER 1
COUNTED BY: jmt

No.	Ns	Ni	Na	RATIO	U (ppm)	RHOs (E+06)	RHOi (E+06)	F.T.AGE (Ma)
1	363	139	40	2.612	0.0	9.176	3.514	183.6 ± 18.6
2	67	16	6	4.188	0.0	11.291	2.696	291.9 ± 81.4
3	147	50	18	2.940	0.0	8.257	2.809	206.3 ± 34.0
	577	205			0.0	9.116	3.239	

AREA OF BASIC UNIT = 9.89E-07 cm
CHI SQUARED = 2.700412 WITH 2 DEGREES OF FREEDOM
P(chi squared) = 25.9 %
CORRELATION COEFFICIENT = 1.000
VARIANCE OF SQR(Ns) = 30.27
VARIANCE OF SQR(Ni) = 15.40

Ns/Ni = 2.815 ± 0.229
MEAN RATIO = 3.246 ± 0.480

Ages calculated using a zeta of 133.9 ± 1.4 for CN1 glass
RHO D = 1.065E+06 ; ND = 5265

POOLED AGE = 197.6 ± 16.4 Ma
MEAN AGE = 227.4 ± 33.9 Ma

8902-76 APATITE ohau s117/951217 320m

IRRADIATION jmt data:jmt apatite data:ohau apatites:wk043/7
SLIDE NUMBER 1
COUNTED BY: jmt

No.	Ns	Ni	Na	RATIO	U (ppm)	RHOs (E+06)	RHOi (E+06)	F.T AGE (Ma)
1	33	34	12	0.971	42.3	2.781	2.865	151.1 ± 37.0
2	32	52	21	0.615	37.0	1.541	2.504	96.2 ± 21.7
3	20	30	30	0.667	14.9	0.674	1.011	104.2 ± 30.1
4	4	10	9	0.400	16.6	0.449	1.123	62.7 ± 37.1
5	24	30	9	0.800	49.7	2.696	3.370	124.8 ± 34.3
6	33	27	12	1.222	33.6	2.781	2.275	189.7 ± 49.3
7	34	43	8	0.791	80.2	4.297	5.435	123.4 ± 28.4
8	1	5	16	0.200	4.7	0.063	0.316	31.4 ± 34.4
9	11	10	9	1.100	16.6	1.236	1.123	171.0 ± 74.8
10	30	46	9	0.652	76.3	3.370	5.168	101.9 ± 24.0
11	7	5	16	1.400	4.7	0.442	0.316	216.8 ± 127.0
12	13	15	16	0.867	14.0	0.822	0.948	135.1 ± 51.2
13	10	12	6	0.833	29.8	1.685	2.022	129.9 ± 55.7
14	31	49	15	0.633	48.7	2.090	3.303	98.9 ± 22.8
15	18	43	30	0.419	21.4	0.607	1.449	65.6 ± 18.5
16	22	33	18	0.667	27.4	1.236	1.854	104.2 ± 28.7
17	12	22	15	0.545	21.9	0.809	1.483	85.3 ± 30.7
18	48	68	24	0.706	42.3	2.022	2.865	110.2 ± 20.9
19	11	24	30	0.458	11.9	0.371	0.809	71.8 ± 26.2
20	16	37	20	0.432	27.6	0.809	1.871	67.8 ± 20.3
	410	595			27.3	1.276	1.851	

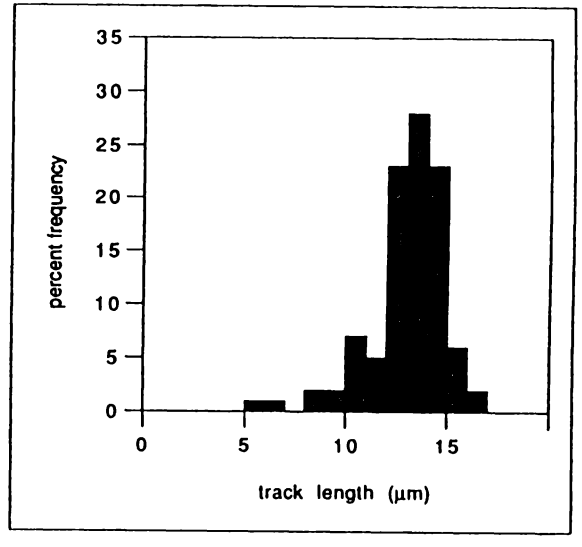
AREA OF BASIC UNIT = 9.89E-07 cm
CHI SQUARED = 21.10261 WITH 19 DEGREES OF FREEDOM
P(chi squared) = 33.1 %
CORRELATION COEFFICIENT = 0.879
VARIANCE OF SQR(Ns) = 2.22
VARIANCE OF SQR(Ni) = 2.91

Ns/Ni = 0.689 ± 0.044
MEAN RATIO = 0.719 ± 0.066

Ages calculated using a zeta of 354.9 ± 4.3 for SRM612 glass
RHO D = 8.876E+05 ; ND = 5267

POOLED AGE = 107.6 ± 7.2 Ma
MEAN AGE = 112.2 ± 10.5 Ma

8902-76



n = 100
Mean = 13.03 µm
Sample std. dev. = 1.84 µm

8902-76 ZIRCON ohau s117/951217 320m

IRRADIATION jmt data:jmt zircon data:ohau zircons:wk038/18
SLIDE NUMBER 1
COUNTED BY: jmt

No.	Ns	Ni	Na	RATIO	U (ppm)	RHOs (E+06)	RHOi (E+06)	F.T AGE (Ma)
1	97	30	6	3.233	0.0	16.346	5.056	226.5 ± 47.5
2	78	21	12	3.714	0.0	6.572	1.769	259.5 ± 64.0
3	21	10	2	2.100	0.0	10.617	5.056	148.0 ± 56.9
4	52	23	9	2.261	0.0	5.842	2.584	159.2 ± 40.0
5	87	23	8	3.783	0.0	10.996	2.907	264.2 ± 62.1
6	181	56	14	3.232	0.0	13.072	4.044	226.4 ± 34.8
	516	163			0.0	10.230	3.232	

AREA OF BASIC UNIT = 9.89E-07 cm
CHI SQUARED = 4.011693 WITH 5 DEGREES OF FREEDOM
P(chi squared) = 54.8 %
CORRELATION COEFFICIENT = 0.971
VARIANCE OF SQR(Ns) = 8.66
VARIANCE OF SQR(Ni) = 2.00

Ns/Ni = 3.166 ± 0.284
MEAN RATIO = 3.054 ± 0.293

Ages calculated using a zeta of 133.9 ± 1.4 for CN1 glass
RHO D = 1.065E+06 ; ND = 5265

POOLED AGE = 221.9 ± 20.3 Ma
MEAN AGE = 214.1 ± 20.9 Ma

8902-77 APATITE ohau s127/403911 120m

IRRADIATION jmt data:jmt apatite data:ohau apatites:wk012/11
SLIDE NUMBER 1
COUNTED BY: jmt

No.	Ns	Ni	Na	RATIO	U (ppm)	RHOs (E+06)	RHOi (E+06)	F.T AGE (Ma)
1	0	4	30	0.000	1.5	0.000	0.135	0.0 ± 0.0
2	0	1	8	0.000	1.4	0.000	0.126	0.0 ± 0.0
3	0	1	8	0.000	1.4	0.000	0.126	0.0 ± 0.0
4	10	9	4	1.111	25.0	2.528	2.275	231.2 ± 106.4
5	4	10	6	0.400	18.5	0.674	1.685	84.2 ± 49.8
6	0	1	8	0.000	1.4	0.000	0.126	0.0 ± 0.0
7	0	1	14	0.000	0.8	0.000	0.072	0.0 ± 0.0
8	0	1	12	0.000	0.9	0.000	0.084	0.0 ± 0.0
9	0	1	6	0.000	1.8	0.000	0.169	0.0 ± 0.0
10	0	2	9	0.000	2.5	0.000	0.225	0.0 ± 0.0
11	3	4	2	0.750	22.2	1.517	2.022	157.0 ± 119.9
12	0	1	15	0.000	0.7	0.000	0.067	0.0 ± 0.0
13	8	10	9	0.800	12.3	0.899	1.123	167.3 ± 79.4
14	0	1	36	0.000	0.3	0.000	0.028	0.0 ± 0.0
	25	47			3.1	0.151	0.285	

AREA OF BASIC UNIT = 9.89E-07 cm
CHI SQUARED = 11.32419 WITH 13 DEGREES OF FREEDOM
P(chi squared) = 58.4 %
CORRELATION COEFFICIENT = 0.889
VARIANCE OF SQR(Ns) = 1.40
VARIANCE OF SQR(Ni) = 0.77

Ns/Ni = 0.532 ± 0.132
MEAN RATIO = 0.219 ± 0.103

Ages calculated using a zeta of 354.9 ± 4.3 for SRM612 glass
RHO D = 1.194E+06 ; ND = 2953

POOLED AGE = 111.7 ± 27.8 Ma
MEAN AGE = 46.2 ± 21.8 Ma

8902-77 ZIRCON ohau s127/403911 120m

IRRADIATION jmt data:jmt zircon data:ohau zircons:wk037/1
SLIDE NUMBER 1
COUNTED BY: jmt

No.	Ns	Ni	Na	RATIO	U (ppm)	RHOs (E+06)	RHOi (E+06)	F.T AGE (Ma)
1	52	18	4	2.889	0.0	13.145	4.550	203.1 ± 55.6
2	38	20	4	1.900	0.0	9.606	5.056	134.3 ± 37.2
3	50	21	4	2.381	0.0	12.639	5.308	167.9 ± 43.7
4	68	26	6	2.615	0.0	11.459	4.382	184.2 ± 42.6
	208	85			0.0	11.684	4.775	

AREA OF BASIC UNIT = 9.89E-07 cm
CHI SQUARED = 1.307046 WITH 3 DEGREES OF FREEDOM
P(chi squared) = 72.7 %
CORRELATION COEFFICIENT = 0.747
VARIANCE OF SQR(Ns) = 0.73
VARIANCE OF SQR(Ni) = 0.13

Ns/Ni = 2.447 ± 0.315
MEAN RATIO = 2.446 ± 0.210

Ages calculated using a zeta of 133.9 ± 1.4 for CN1 glass
RHO D = 1.067E+06 ; ND = 6342

POOLED AGE = 172.5 ± 22.4 Ma
MEAN AGE = 172.4 ± 15.0 Ma

8902-78 APATITE copland s78/586461 260m

IRRADIATION jmt data:jmt apatite data:copland apatites:wk020/5
SLIDE NUMBER 1
COUNTED BY: jmt

No.	Ns	Ni	Na	RATIO	U (ppm)	RHOs (E+06)	RHOi (E+06)	F.T.AGE (Ma)
1	0	9	36	0.000	0.8	0.000	0.253	0.0 ± 0.0
2	0	75	100	0.000	2.4	0.000	0.758	0.0 ± 0.0
3	0	14	20	0.000	2.2	0.000	0.708	0.0 ± 0.0
4	0	17	40	0.000	1.3	0.000	0.430	0.0 ± 0.0
5	0	9	30	0.000	0.9	0.000	0.303	0.0 ± 0.0
6	0	13	100	0.000	0.4	0.000	0.131	0.0 ± 0.0
7	0	52	49	0.000	3.3	0.000	1.073	0.0 ± 0.0
8	0	7	60	0.000	0.4	0.000	0.118	0.0 ± 0.0
9	0	12	64	0.000	0.6	0.000	0.190	0.0 ± 0.0
10	0	91	100	0.000	2.9	0.000	0.920	0.0 ± 0.0
11	0	19	100	0.000	0.6	0.000	0.192	0.0 ± 0.0
12	0	140	100	0.000	4.4	0.000	1.416	0.0 ± 0.0
13	0	23	100	0.000	0.7	0.000	0.233	0.0 ± 0.0
14	0	41	100	0.000	1.3	0.000	0.415	0.0 ± 0.0
15	0	11	20	0.000	1.7	0.000	0.556	0.0 ± 0.0
	0	533			1.6	0.000	0.529	

AREA OF BASIC UNIT = 9.89E-07 cm
CHI SQUARED = 9.249999E-06 WITH 14 DEGREES OF FREEDOM
P(chi squared) = 100.0 %
CORRELATION COEFFICIENT = 0.118
VARIANCE OF SQR(Ns) = 0.00
VARIANCE OF SQR(Ni) = 7.83

Ns/Ni = 0.000 ± 0.000
MEAN RATIO = 0.000 ± 0.000

Ages calculated using a zeta of 354.9 ± 4.3 for SRM612 glass
RHO D = 4.206E+06 ; ND = 3328

POOLED AGE = 0.0 ± 0.0 Ma
MEAN AGE = 0.0 ± 0.0 Ma

8902-78 ZIRCON copland s78/586461 260m

IRRADIATION jmt data:jmt zircon data:copland zircons:wk037/2
SLIDE NUMBER 1
COUNTED BY: jmt

No.	Ns	Ni	Na	RATIO	U (ppm)	RHOs (E+06)	RHOi (E+06)	F.T.AGE (Ma)
1	1	74	8	0.014	0.0	0.126	9.353	1.0 ± 1.0
2	0	191	16	0.000	0.0	0.000	12.070	0.0 ± 0.0
3	0	198	16	0.000	0.0	0.000	12.513	0.0 ± 0.0
4	0	282	20	0.000	0.0	0.000	14.257	0.0 ± 0.0
5	0	50	7	0.000	0.0	0.000	7.222	0.0 ± 0.0
	1	795			0.0	0.015	11.998	

AREA OF BASIC UNIT = 9.89E-07 cm
CHI SQUARED = 9.625424 WITH 4 DEGREES OF FREEDOM
P(chi squared) = 4.7 %
CORRELATION COEFFICIENT = -0.496
VARIANCE OF SQR(Ns) = 0.20
VARIANCE OF SQR(Ni) = 16.60

Ns/Ni = 0.001 ± 0.001
MEAN RATIO = 0.003 ± 0.003

Ages calculated using a zeta of 133.9 ± 1.4 for CN1 glass
RHO D = 1.067E+06 ; ND = 6342

POOLED AGE = 0.1 ± 0.1 Ma
MEAN AGE = 0.2 ± 0.2 Ma

8902-79 APATITE copland s78/612451 410m

IRRADIATION jmt data:jmt apatite data:copland apatites:wk020/4
SLIDE NUMBER 1
COUNTED BY: jmt

No.	Ns	Ni	Na	RATIO	U (ppm)	RHOs (E+06)	RHOi (E+06)	F.TAGE (Ma)
1	0	7	40	0.000	0.6	0.000	0.177	0.0 ± 0.0
2	0	29	24	0.000	3.8	0.000	1.222	0.0 ± 0.0
3	0	8	24	0.000	1.1	0.000	0.337	0.0 ± 0.0
4	0	4	24	0.000	0.5	0.000	0.169	0.0 ± 0.0
5	0	54	15	0.000	11.4	0.000	3.640	0.0 ± 0.0
6	0	11	21	0.000	1.7	0.000	0.530	0.0 ± 0.0
7	0	17	32	0.000	1.7	0.000	0.537	0.0 ± 0.0
8	0	7	32	0.000	0.7	0.000	0.221	0.0 ± 0.0
9	0	4	16	0.000	0.8	0.000	0.253	0.0 ± 0.0
10	0	8	16	0.000	1.6	0.000	0.506	0.0 ± 0.0
11	0	2	9	0.000	0.7	0.000	0.225	0.0 ± 0.0
12	0	5	12	0.000	1.3	0.000	0.421	0.0 ± 0.0
13	0	5	18	0.000	0.9	0.000	0.281	0.0 ± 0.0
14	0	69	50	0.000	4.4	0.000	1.395	0.0 ± 0.0
15	0	2	25	0.000	0.3	0.000	0.081	0.0 ± 0.0
	0	232			2.1	0.000	0.655	

AREA OF BASIC UNIT = 9.89E-07 cm
CHI SQUARED = 3.296296E-06 WITH 14 DEGREES OF FREEDOM
P(chi squared) = 100.0 %
CORRELATION COEFFICIENT = 0.530
VARIANCE OF SQR(Ns) = 0.00
VARIANCE OF SQR(Ni) = 4.32

Ns/Ni = 0.000 ± 0.000
MEAN RATIO = 0.000 ± 0.000

Ages calculated using a zeta of 354.9 ± 4.3 for SRM612 glass
RHO D = 4.170E+06 ; ND = 3299

POOLED AGE = 0.0 ± 0.0 Ma
MEAN AGE = 0.0 ± 0.0 Ma

8902-79 ZIRCON copland s78/612450 410m

IRRADIATION jmt data:jmt zircon data:copland zircons:wk024/1
SLIDE NUMBER 1
COUNTED BY: jmt

No.	Ns	Ni	Na	RATIO	U (ppm)	RHOs (E+06)	RHOi (E+06)	F.TAGE (Ma)
1	1	98	12	0.010	0.0	0.084	8.257	0.5 ± 0.5
2	1	108	20	0.009	0.0	0.051	5.460	0.5 ± 0.5
3	1	11	15	0.091	0.0	0.067	0.741	4.6 ± 4.8
4	1	61	5	0.016	0.0	0.202	12.336	0.8 ± 0.8
5	1	84	6	0.012	0.0	0.169	14.156	0.6 ± 0.6
6	0	25	9	0.000	0.0	0.000	2.809	0.0 ± 0.0
7	1	140	24	0.007	0.0	0.042	5.898	0.4 ± 0.4
8	0	24	16	0.000	0.0	0.000	1.517	0.0 ± 0.0
	6	551			0.0	0.057	5.207	

AREA OF BASIC UNIT = 9.89E-07 cm
CHI SQUARED = 6.847122 WITH 7 DEGREES OF FREEDOM
P(chi squared) = 44.5 %
CORRELATION COEFFICIENT = 0.591
VARIANCE OF SQR(Ns) = 0.21
VARIANCE OF SQR(Ni) = 9.37

Ns/Ni = 0.011 ± 0.004
MEAN RATIO = 0.018 ± 0.011

Ages calculated using a zeta of 133.9 ± 1.4 for CN1 glass
RHO D = 7.581E+05 ; ND = 3749

POOLED AGE = 0.6 ± 0.2 Ma
MEAN AGE = 0.9 ± 0.5 Ma

8902-80 APATITE copland s78/629439 595m

IRRADIATION jmt data:jmt apatite data:copland apatites:wk020/3
SLIDE NUMBER 1
COUNTED BY: jmt

No.	Ns	Ni	Na	RATIO	U (ppm)	RHOs (E+06)	RHOi (E+06)	F.T.AGE (Ma)
1	0	3	60	0.000	0.2	0.000	0.051	0.0 ± 0.0
2	0	13	28	0.000	1.5	0.000	0.469	0.0 ± 0.0
3	0	42	70	0.000	1.9	0.000	0.607	0.0 ± 0.0
4	0	2	24	0.000	0.3	0.000	0.084	0.0 ± 0.0
5	0	2	24	0.000	0.3	0.000	0.084	0.0 ± 0.0
6	0	31	50	0.000	2.0	0.000	0.627	0.0 ± 0.0
7	0	13	25	0.000	1.7	0.000	0.526	0.0 ± 0.0
8	0	2	48	0.000	0.1	0.000	0.042	0.0 ± 0.0
9	0	9	40	0.000	0.7	0.000	0.228	0.0 ± 0.0
10	0	20	70	0.000	0.9	0.000	0.289	0.0 ± 0.0
11	0	17	60	0.000	0.9	0.000	0.286	0.0 ± 0.0
12	0	9	80	0.000	0.4	0.000	0.114	0.0 ± 0.0
13	0	1	50	0.000	0.1	0.000	0.020	0.0 ± 0.0
14	0	3	16	0.000	0.6	0.000	0.190	0.0 ± 0.0
15	0	12	40	0.000	1.0	0.000	0.303	0.0 ± 0.0
	0	179			0.8	0.000	0.264	

AREA OF BASIC UNIT = 9.89E-07 cm
CHI SQUARED = 4.774193E-06 WITH 14 DEGREES OF FREEDOM
P(chi squared) = 100.0 %
CORRELATION COEFFICIENT = 0.447
VARIANCE OF SQR(Ns) = 0.00
VARIANCE OF SQR(Ni) = 2.70

Ns/Ni = 0.000 ± 0.000
MEAN RATIO = 0.000 ± 0.000

Ages calculated using a zeta of 354.9 ± 4.3 for SRM612 glass
RHO D = 4.134E+06 ; ND = 3270

POOLED AGE = 0.0 ± 0.0 Ma
MEAN AGE = 0.0 ± 0.0 Ma

8902-80 ZIRCON copland s78/629439 595m

IRRADIATION jmt data:jmt zircon data:copland zircons:wk025/18
SLIDE NUMBER 1
COUNTED BY: jmt

No.	Ns	Ni	Na	RATIO	U (ppm)	RHOs (E+06)	RHOi (E+06)	F.T.AGE (Ma)
1	1	170	12	0.006	0.0	0.084	14.324	0.4 ± 0.4
2	2	117	15	0.017	0.0	0.135	7.887	1.1 ± 0.8
3	1	96	20	0.010	0.0	0.051	4.853	0.6 ± 0.7
4	1	126	35	0.008	0.0	0.029	3.640	0.5 ± 0.5
5	3	198	9	0.015	0.0	0.337	22.245	0.9 ± 0.5
6	1	85	18	0.012	0.0	0.056	4.775	0.7 ± 0.7
7	28	%1800	112	0.016	0.0	0.253	16.250	1.0 ± 0.2
8	1	70	24	0.014	0.0	0.042	2.949	0.9 ± 0.9
9	4	112	25	0.036	0.0	0.162	4.530	2.2 ± 1.1
10	4	179	15	0.022	0.0	0.270	12.066	1.4 ± 0.7
11	5	170	40	0.029	0.0	0.126	4.297	1.8 ± 0.8
	51	3123			0.0	0.159	9.716	

AREA OF BASIC UNIT = 9.89E-07 cm
CHI SQUARED = 6.689898 WITH 10 DEGREES OF FREEDOM
P(chi squared) = 75.4 %
CORRELATION COEFFICIENT = 0.987
VARIANCE OF SQR(Ns) = 1.58
VARIANCE OF SQR(Ni) = 91.17

Ns/Ni = 0.016 ± 0.002
MEAN RATIO = 0.017 ± 0.003

Ages calculated using a zeta of 133.9 ± 1.4 for CN1 glass
RHO D = 9.295E+05 ; ND = 4596

POOLED AGE = 1.0 ± 0.1 Ma
MEAN AGE = 1.0 ± 0.2 Ma

8902-81 APATITE copland s79/695403 775m

IRRADIATION jmt data:jmt apatite data:copland apatites:wk020/2
SLIDE NUMBER 1
COUNTED BY: jmt

No.	Ns	Ni	Na	RATIO	U (ppm)	RHOs (E+06)	RHOi (E+06)	F.T.AGE (Ma)
1	0	187	20	0.000	30.2	0.000	9.454	0.0 ± 0.0
2	0	313	36	0.000	28.1	0.000	8.791	0.0 ± 0.0
3	0	64	24	0.000	8.6	0.000	2.696	0.0 ± 0.0
4	0	85	16	0.000	17.2	0.000	5.372	0.0 ± 0.0
5	0	406	30	0.000	43.8	0.000	13.684	0.0 ± 0.0
6	0	93	50	0.000	6.0	0.000	1.881	0.0 ± 0.0
7	0	42	6	0.000	22.6	0.000	7.078	0.0 ± 0.0
8	0	113	25	0.000	14.6	0.000	4.570	0.0 ± 0.0
9	0	118	12	0.000	31.8	0.000	9.943	0.0 ± 0.0
10	0	224	20	0.000	36.2	0.000	11.325	0.0 ± 0.0
11	0	65	28	0.000	7.5	0.000	2.347	0.0 ± 0.0
12	0	58	15	0.000	12.5	0.000	3.910	0.0 ± 0.0
13	0	16	15	0.000	3.4	0.000	1.079	0.0 ± 0.0
14	0	75	24	0.000	10.1	0.000	3.160	0.0 ± 0.0
15	0	46	12	0.000	12.4	0.000	3.876	0.0 ± 0.0
	0	1905			18.5	0.000	5.784	

AREA OF BASIC UNIT = 9.89E-07 cm
CHI SQUARED = 9.187164E-06 WITH 14 DEGREES OF FREEDOM
P(chi squared) = 100.0 %
CORRELATION COEFFICIENT = 0.151
VARIANCE OF SQR(Ns) = 0.00
VARIANCE OF SQR(Ni) = 19.53

Ns/Ni = 0.000 ± 0.000
MEAN RATIO = 0.000 ± 0.000

Ages calculated using a zeta of 354.9 ± 4.3 for SRM612 glass
RHO D = 4.097E+06 ; ND = 3242

POOLED AGE = 0.0 ± 0.0 Ma
MEAN AGE = 0.0 ± 0.0 Ma

8902-81 ZIRCON copland s79/695403 775m

IRRADIATION jmt data:jmt zircon data:copland zircons:wk025/17
SLIDE NUMBER 1
COUNTED BY: jmt

No.	Ns	Ni	Na	RATIO	U (ppm)	RHOs (E+06)	RHOi (E+06)	F.T.AGE (Ma)
1	3	99	9	0.030	0.0	0.337	11.122	1.9 ± 1.1
2	3	33	12	0.091	0.0	0.253	2.781	5.6 ± 3.4
3	2	56	24	0.036	0.0	0.084	2.359	2.2 ± 1.6
4	2	34	9	0.059	0.0	0.225	3.820	3.6 ± 2.6
5	7	59	9	0.119	0.0	0.786	6.628	7.3 ± 2.9
6	10	105	15	0.095	0.0	0.674	7.078	5.9 ± 1.9
7	10	204	16	0.049	0.0	0.632	12.892	3.0 ± 1.0
8	13	124	18	0.105	0.0	0.730	6.966	6.5 ± 1.9
9	10	321	24	0.031	0.0	0.421	13.524	1.9 ± 0.6
10	2	46	9	0.043	0.0	0.225	5.168	2.7 ± 1.9
11	10	121	20	0.083	0.0	0.506	6.117	5.1 ± 1.7
	72	1202			0.0	0.441	7.366	

AREA OF BASIC UNIT = 9.89E-07 cm
CHI SQUARED = 17.08335 WITH 10 DEGREES OF FREEDOM
P(chi squared) = 7.3 %
CORRELATION COEFFICIENT = 0.641
VARIANCE OF SQR(Ns) = 0.76
VARIANCE OF SQR(Ni) = 14.06

Ns/Ni = 0.060 ± 0.007
MEAN RATIO = 0.067 ± 0.010

Ages calculated using a zeta of 133.9 ± 1.4 for CN1 glass
RHO D = 9.218E+05 ; ND = 4558

POOLED AGE = 3.7 ± 0.5 Ma
MEAN AGE = 4.2 ± 0.6 Ma

8902-82 APATITE copland s79/734411 1080m

IRRADIATION jmt data:jmt apatite data:copland apatites:wk012/6
SLIDE NUMBER 1
COUNTED BY: jmt

No.	Ns	NI	Na	RATIO	U (ppm)	RHOs (E+06)	RHOi (E+06)	F.T.AGE (Ma)
1	0	28	9	0.000	36.0	0.000	3.146	0.0 ± 0.0
2	0	32	6	0.000	61.7	0.000	5.393	0.0 ± 0.0
3	0	18	10	0.000	20.8	0.000	1.820	0.0 ± 0.0
4	0	3	6	0.000	5.8	0.000	0.506	0.0 ± 0.0
5	0	14	9	0.000	18.0	0.000	1.573	0.0 ± 0.0
6	0	29	9	0.000	37.3	0.000	3.258	0.0 ± 0.0
7	0	66	12	0.000	63.6	0.000	5.561	0.0 ± 0.0
8	0	62	15	0.000	47.8	0.000	4.179	0.0 ± 0.0
9	0	43	12	0.000	41.5	0.000	3.623	0.0 ± 0.0
10	0	47	12	0.000	45.3	0.000	3.960	0.0 ± 0.0
11	0	43	20	0.000	24.9	0.000	2.174	0.0 ± 0.0
12	0	14	9	0.000	18.0	0.000	1.573	0.0 ± 0.0
13	0	23	9	0.000	29.6	0.000	2.584	0.0 ± 0.0
14	0	6	15	0.000	4.6	0.000	0.404	0.0 ± 0.0
15	0	55	16	0.000	39.8	0.000	3.476	0.0 ± 0.0
	0	483			33.1	0.000	2.890	

AREA OF BASIC UNIT = 9.89E-07 cm
CHI SQUARED = 1.625E-05 WITH 14 DEGREES OF FREEDOM
P(chi squared) = 100.0 %
CORRELATION COEFFICIENT = -0.059
VARIANCE OF SQR(Ns) = 0.00
VARIANCE OF SQR(Ni) = 3.70

Ns/Ni = 0.000 ± 0.000
MEAN RATIO = 0.000 ± 0.000

Ages calculated using a zeta of 354.9 ± 4.3 for SRM612 glass
RHO D = 1.145E+06 ; ND = 2830

POOLED AGE = 0.0 ± 0.0 Ma
MEAN AGE = 0.0 ± 0.0 Ma

8902-82 ZIRCON copland s79/734411 1080m

IRRADIATION jmt data:jmt zircon data:copland zircons:wk025/16
SLIDE NUMBER 1
COUNTED BY: jmt

No.	Ns	NI	Na	RATIO	U (ppm)	RHOs (E+06)	RHOi (E+06)	F.T.AGE (Ma)
1	1	28	4	0.036	0.0	0.253	7.078	2.2 ± 2.2
2	9	171	10	0.053	0.0	0.910	17.290	3.2 ± 1.1
	10	199			0.0	0.722	14.372	

AREA OF BASIC UNIT = 9.89E-07 cm
CHI SQUARED = .1320058 WITH 1 DEGREES OF FREEDOM
P(chi squared) = 71.6 %
CORRELATION COEFFICIENT = 1.000
VARIANCE OF SQR(Ns) = 2.00
VARIANCE OF SQR(Ni) = 30.30

Ns/NI = 0.050 ± 0.016
MEAN RATIO = 0.044 ± 0.008

Ages calculated using a zeta of 133.9 ± 1.4 for CN1 glass
RHO D = 9.142E+05 ; ND = 4520

POOLED AGE = 3.1 ± 1.0 Ma
MEAN AGE = 2.7 ± 0.5 Ma

8902-83 APATITE hooker s79/766406 1830m

IRRADIATION jmt data:jmt apatite data:hooker apatites:wk017/6
SLIDE NUMBER 1
COUNTED BY: jmt

No.	Ns	NI	Na	RATIO	U (ppm)	RHOs (E+06)	RHOi (E+06)	F.T.AGE (Ma)
1	0	14	8	0.000	18.6	0.000	1.769	0.0 ± 0.0
2	0	7	4	0.000	18.6	0.000	1.769	0.0 ± 0.0
3	0	4	3	0.000	14.2	0.000	1.348	0.0 ± 0.0
4	0	63	12	0.000	55.9	0.000	5.308	0.0 ± 0.0
5	0	7	4	0.000	18.6	0.000	1.769	0.0 ± 0.0
6	0	65	36	0.000	19.2	0.000	1.826	0.0 ± 0.0
7	0	23	8	0.000	30.6	0.000	2.907	0.0 ± 0.0
8	0	2	12	0.000	1.8	0.000	0.169	0.0 ± 0.0
9	0	5	6	0.000	8.9	0.000	0.843	0.0 ± 0.0
10	0	25	6	0.000	44.4	0.000	4.213	0.0 ± 0.0
	0	215			23.1	0.000	2.196	

AREA OF BASIC UNIT = 9.89E-07 cm
CHI SQUARED = 2.412698E-06 WITH 9 DEGREES OF FREEDOM
P(chi squared) = 100.0 %
CORRELATION COEFFICIENT = 0.615
VARIANCE OF SQR(Ns) = 0.00
VARIANCE OF SQR(Ni) = 5.68

Ns/Ni = 0.000 ± 0.000
MEAN RATIO = 0.000 ± 0.000

Ages calculated using a zeta of 354.9 ± 4.3 for SRM612 glass
RHO D = 1.243E+06 ; ND = 3074

POOLED AGE = 0.0 ± 0.0 Ma
MEAN AGE = 0.0 ± 0.0 Ma

8902-83 ZIRCON hooker s79/766406 1830m

IRRADIATION jmt data:jmt zircon data:hooker zircons:wk025/15
SLIDE NUMBER 1
COUNTED BY: jmt

No.	Ns	NI	Na	RATIO	U (ppm)	RHOs (E+06)	RHOi (E+06)	F.T.AGE (Ma)
1	83	61	6	1.361	0.0	13.987	10.280	82.1 ± 13.9
2	85	66	8	1.288	0.0	10.743	8.342	77.7 ± 12.8
3	96	78	8	1.231	0.0	12.133	9.858	74.3 ± 11.4
4	107	50	8	2.140	0.0	13.524	6.320	128.6 ± 22.2
5	135	114	12	1.184	0.0	11.375	9.606	71.5 ± 9.2
6	135	102	8	1.324	0.0	17.063	12.892	79.8 ± 10.6
7	213	141	12	1.511	0.0	17.947	11.881	91.0 ± 10.0
8	124	107	8	1.159	0.0	15.672	13.524	70.0 ± 9.3
9	75	32	5	2.344	0.0	15.167	6.471	140.7 ± 29.8
10	65	50	5	1.300	0.0	13.145	10.111	78.4 ± 14.8
11	187	122	12	1.533	0.0	15.757	10.280	92.4 ± 10.9
12	473	354	36	1.336	0.0	13.285	9.943	80.6 ± 5.8
13	130	83	8	1.566	0.0	16.431	10.490	94.4 ± 13.4
	1908	1360			0.0	14.185	10.111	

AREA OF BASIC UNIT = 9.89E-07 cm
CHI SQUARED = 19.63338 WITH 12 DEGREES OF FREEDOM
P(chi squared) = 7.4 %
CORRELATION COEFFICIENT = 0.985
VARIANCE OF SQR(Ns) = 12.86
VARIANCE OF SQR(Ni) = 10.70

Ns/Ni = 1.403 ± 0.050
MEAN RATIO = 1.483 ± 0.100

Ages calculated using a zeta of 133.9 ± 1.4 for CN1 glass
RHO D = 9.065E+05 ; ND = 4483

POOLED AGE = 84.6 ± 3.4 Ma
MEAN AGE = 89.4 ± 6.3 Ma

8902-84 APATITE hooker s79/769405 1575m

IRRADIATION jmt data:jmt apatite data:hooker apatites:wk012/4
SLIDE NUMBER 1
COUNTED BY: jmt

No.	Ns	Ni	Na	RATIO	U (ppm)	RHOs (E+06)	RHOi (E+06)	F.T.AGE (Ma)
1	0	9	16	0.000	6.6	0.000	0.569	0.0 ± 0.0
2	0	14	24	0.000	6.9	0.000	0.590	0.0 ± 0.0
3	0	81	30	0.000	31.8	0.000	2.730	0.0 ± 0.0
4	0	11	24	0.000	5.4	0.000	0.463	0.0 ± 0.0
5	0	28	16	0.000	20.6	0.000	1.769	0.0 ± 0.0
6	0	7	12	0.000	6.9	0.000	0.590	0.0 ± 0.0
7	0	18	20	0.000	10.6	0.000	0.910	0.0 ± 0.0
8	0	13	32	0.000	4.8	0.000	0.411	0.0 ± 0.0
9	0	28	18	0.000	18.3	0.000	1.573	0.0 ± 0.0
10	0	43	16	0.000	31.6	0.000	2.717	0.0 ± 0.0
11	0	15	24	0.000	7.4	0.000	0.632	0.0 ± 0.0
12	0	102	35	0.000	34.3	0.000	2.947	0.0 ± 0.0
13	0	14	32	0.000	5.2	0.000	0.442	0.0 ± 0.0
14	0	17	24	0.000	8.3	0.000	0.716	0.0 ± 0.0
15	0	35	48	0.000	8.6	0.000	0.737	0.0 ± 0.0
	0	435			13.8	0.000	1.186	

AREA OF BASIC UNIT = 9.89E-07 cm
CHI SQUARED = 4.37037E-06 WITH 14 DEGREES OF FREEDOM
P(chi squared) = 100.0 %
CORRELATION COEFFICIENT = 0.522
VARIANCE OF SQR(Ns) = 0.00
VARIANCE OF SQR(Ni) = 4.68

Ns/Ni = 0.000 ± 0.000
MEAN RATIO = 0.000 ± 0.000

Ages calculated using a zeta of 354.9 ± 4.3 for SRM612 glass
RHO D = 1.125E+06 ; ND = 2781

POOLED AGE = 0.0 ± 0.0 Ma
MEAN AGE = 0.0 ± 0.0 Ma

8902-84 ZIRCON hooker s79/769405 1575m

IRRADIATION jmt data:jmt zircon data:hooker zircons:wk025/14
SLIDE NUMBER 1
COUNTED BY: jmt

No.	Ns	Ni	Na	RATIO	U (ppm)	RHOs (E+06)	RHOi (E+06)	F.T.AGE (Ma)
1	120	42	18	2.857	0.0	6.741	2.359	169.7 ± 30.6
2	93	30	12	3.100	0.0	7.836	2.528	183.9 ± 38.8
3	251	121	20	2.074	0.0	12.690	6.117	123.6 ± 13.9
4	68	30	8	2.267	0.0	8.595	3.792	135.0 ± 29.7
5	71	34	24	2.088	0.0	2.991	1.432	124.5 ± 26.1
6	574	273	50	2.103	0.0	11.608	5.521	125.3 ± 9.5
7	29	17	4	1.706	0.0	7.331	4.297	101.9 ± 31.2
8	290	110	28	2.636	0.0	10.472	3.972	156.7 ± 17.8
9	125	33	10	3.788	0.0	12.639	3.337	224.0 ± 44.0
10	87	31	24	2.806	0.0	3.665	1.306	166.7 ± 35.0
11	53	23	12	2.304	0.0	4.466	1.938	137.2 ± 34.4
12	149	62	14	2.403	0.0	10.761	4.478	143.0 ± 21.8
13	423	192	28	2.203	0.0	15.275	6.933	131.2 ± 11.7
	2333	998			0.0	9.361	4.004	

AREA OF BASIC UNIT = 9.89E-07 cm
CHI SQUARED = 16.33117 WITH 12 DEGREES OF FREEDOM
P(chi squared) = 17.7 %
CORRELATION COEFFICIENT = 0.991
VARIANCE OF SQR(Ns) = 30.22
VARIANCE OF SQR(Ni) = 14.84

Ns/Ni = 2.338 ± 0.088
MEAN RATIO = 2.487 ± 0.152

Ages calculated using a zeta of 133.9 ± 1.4 for CN1 glass
RHO D = 8.989E+05 ; ND = 4445

POOLED AGE = 139.2 ± 5.8 Ma
MEAN AGE = 148.0 ± 9.4 Ma

8902-85 APATITE hooker s79/773404 1320m

IRRADIATION jmt data:jmt apatite data:hooker apatites:wk012/3
SLIDE NUMBER 1
COUNTED BY: jmt

No.	Ns	Ni	Na	RATIO	U (ppm)	RHOs (E+06)	RHOi (E+06)	F.T AGE (Ma)
1	0	4	15	0.000	3.2	0.000	0.270	0.0 ± 0.0
2	1	38	16	0.026	28.2	0.063	2.401	5.2 ± 5.3
3	0	27	18	0.000	17.8	0.000	1.517	0.0 ± 0.0
4	0	42	18	0.000	27.7	0.000	2.359	0.0 ± 0.0
5	0	7	18	0.000	4.6	0.000	0.393	0.0 ± 0.0
6	1	40	15	0.025	31.7	0.067	2.696	4.9 ± 5.0
7	0	58	36	0.000	19.1	0.000	1.629	0.0 ± 0.0
8	0	13	20	0.000	7.7	0.000	0.657	0.0 ± 0.0
9	0	101	30	0.000	40.0	0.000	3.404	0.0 ± 0.0
10	0	25	25	0.000	11.9	0.000	1.011	0.0 ± 0.0
11	0	20	35	0.000	6.8	0.000	0.578	0.0 ± 0.0
12	0	10	16	0.000	7.4	0.000	0.632	0.0 ± 0.0
13	0	38	32	0.000	14.1	0.000	1.201	0.0 ± 0.0
14	0	7	28	0.000	3.0	0.000	0.253	0.0 ± 0.0
15	0	12	24	0.000	5.9	0.000	0.506	0.0 ± 0.0
	2	442			15.2	0.006	1.292	

AREA OF BASIC UNIT = 9.89E-07 cm
CHI SQUARED = 9.148146 WITH 14 DEGREES OF FREEDOM
P(chi squared) = 82.1 %
CORRELATION COEFFICIENT = 0.152
VARIANCE OF SQR(Ns) = 0.12
VARIANCE OF SQR(Ni) = 4.79

Ns/Ni = 0.005 ± 0.003
MEAN RATIO = 0.003 ± 0.002

Ages calculated using a zeta of 354.9 ± 4.3 for SRM612 glass
RHO D = 1.115E+06 ; ND = 2756

POOLED AGE = 0.9 ± 0.6 Ma
MEAN AGE = 0.7 ± 0.5 Ma

8902-85 ZIRCON hooker s79/773404 1320m

IRRADIATION jmt data:jmt zircon data:hooker zircons:wk025/13
SLIDE NUMBER 1
COUNTED BY: jmt

No.	Ns	Ni	Na	RATIO	U (ppm)	RHOs (E+06)	RHOi (E+06)	F.T AGE (Ma)
1	175	64	12	2.734	0.0	14.746	5.393	161.1 ± 23.7
2	182	81	12	2.247	0.0	15.335	6.825	132.7 ± 17.9
3	105	54	9	1.944	0.0	11.796	6.067	115.0 ± 19.4
4	201	91	18	2.209	0.0	11.291	5.112	130.5 ± 16.7
5	334	132	20	2.530	0.0	16.886	6.673	149.2 ± 15.6
6	160	38	9	4.211	0.0	17.976	4.269	246.5 ± 44.7
7	206	91	15	2.264	0.0	13.886	6.134	133.7 ± 17.0
8	235	100	21	2.350	0.0	11.315	4.815	138.7 ± 16.8
9	224	99	14	2.263	0.0	16.178	7.150	133.6 ± 16.3
10	252	104	15	2.423	0.0	16.987	7.010	143.0 ± 16.9
11	995	342	70	2.909	0.0	14.372	4.940	171.3 ± 11.2
12	99	38	6	2.605	0.0	16.684	6.404	153.6 ± 29.4
13	103	49	6	2.102	0.0	17.358	8.257	124.2 ± 21.7
14	148	61	9	2.426	0.0	16.627	6.853	143.2 ± 21.9
15	200	75	12	2.667	0.0	16.852	6.320	157.2 ± 21.5
	3619	1419			0.0	14.755	5.785	

AREA OF BASIC UNIT = 9.89E-07 cm
CHI SQUARED = 21.39325 WITH 14 DEGREES OF FREEDOM
P(chi squared) = 9.2 %
CORRELATION COEFFICIENT = 0.990
VARIANCE OF SQR(Ns) = 26.89
VARIANCE OF SQR(Ni) = 8.88

Ns/Ni = 2.550 ± 0.080
MEAN RATIO = 2.526 ± 0.137

Ages calculated using a zeta of 133.9 ± 1.4 for CN1 glass
RHO D = 8.913E+05 ; ND = 4407

POOLED AGE = 150.4 ± 5.5 Ma
MEAN AGE = 149.0 ± 8.5 Ma

8902-86 APATITE hooker s79/775399 1140m

IRRADIATION jmt data:jmt apatite data:hooker apatites:wk012/2
SLIDE NUMBER 1
COUNTED BY: jmt

No.	Ns	Ni	Na	RATIO	U (ppm)	RHOs (E+06)	RHOi (E+06)	F.T.AGE (Ma)
1	0	6	6	0.000	12.0	0.000	1.011	0.0 ± 0.0
2	0	23	16	0.000	17.2	0.000	1.453	0.0 ± 0.0
3	0	18	12	0.000	18.0	0.000	1.517	0.0 ± 0.0
4	0	6	16	0.000	4.5	0.000	0.379	0.0 ± 0.0
5	0	87	20	0.000	52.1	0.000	4.398	0.0 ± 0.0
6	0	40	40	0.000	12.0	0.000	1.011	0.0 ± 0.0
7	0	4	8	0.000	6.0	0.000	0.506	0.0 ± 0.0
8	0	22	24	0.000	11.0	0.000	0.927	0.0 ± 0.0
9	0	12	12	0.000	12.0	0.000	1.011	0.0 ± 0.0
10	0	31	6	0.000	61.9	0.000	5.224	0.0 ± 0.0
11	0	6	12	0.000	6.0	0.000	0.506	0.0 ± 0.0
12	1	50	24	0.020	25.0	0.042	2.106	3.9 ± 4.0
13	0	10	16	0.000	7.5	0.000	0.632	0.0 ± 0.0
14	0	90	50	0.000	21.6	0.000	1.820	0.0 ± 0.0
15	0	16	8	0.000	24.0	0.000	2.022	0.0 ± 0.0
	1	421			18.7	0.004	1.577	

AREA OF BASIC UNIT = 9.89E-07 cm
CHI SQUARED = 7.291788 WITH 14 DEGREES OF FREEDOM
P(chi squared) = 92.3 %
CORRELATION COEFFICIENT = 0.218
VARIANCE OF SQR(Ns) = 0.07
VARIANCE OF SQR(Ni) = 5.74

Ns/Ni = 0.002 ± 0.002
MEAN RATIO = 0.001 ± 0.001

Ages calculated using a zeta of 354.9 ± 4.3 for SRM612 glass
RHO D = 1.105E+06 ; ND = 2732

POOLED AGE = 0.5 ± 0.5 Ma
MEAN AGE = 0.3 ± 0.3 Ma

8902-86 ZIRCON hooker s79/775399 1140m

IRRADIATION jmt data:jmt zircon data:hooker zircons:wk025/12
SLIDE NUMBER 1
COUNTED BY: jmt

No.	Ns	Ni	Na	RATIO	U (ppm)	RHOs (E+06)	RHOi (E+06)	F.T.AGE (Ma)
1	72	30	9	2.400	0.0	8.089	3.370	140.4 ± 30.6
2	64	25	6	2.560	0.0	10.785	4.213	149.7 ± 35.4
3	226	66	25	3.424	0.0	9.141	2.669	199.4 ± 28.1
4	124	50	30	2.480	0.0	4.179	1.685	145.1 ± 24.4
5	315	101	21	3.119	0.0	15.167	4.863	181.9 ± 21.1
6	316	73	24	4.329	0.0	13.313	3.075	251.1 ± 32.9
7	318	93	25	3.419	0.0	12.861	3.761	199.2 ± 23.8
8	74	31	9	2.387	0.0	8.314	3.483	139.7 ± 30.0
9	162	56	12	2.893	0.0	13.650	4.719	168.9 ± 26.4
10	138	45	12	3.067	0.0	11.628	3.792	178.9 ± 30.9
	1809	570			0.0	10.573	3.331	

AREA OF BASIC UNIT = 9.89E-07 cm
CHI SQUARED = 13.33538 WITH 9 DEGREES OF FREEDOM
P(chi squared) = 14.8 %
CORRELATION COEFFICIENT = 0.959
VARIANCE OF SQR(Ns) = 15.85
VARIANCE OF SQR(Ni) = 3.03

Ns/Ni = 3.174 ± 0.152
MEAN RATIO = 3.008 ± 0.193

Ages calculated using a zeta of 133.9 ± 1.4 for CN1 glass
RHO D = 8.836E+05 ; ND = 4369

POOLED AGE = 185.1 ± 9.5 Ma
MEAN AGE = 175.5 ± 11.7 Ma

8902-87 APATITE hooker s79/766347 825m

IRRADIATION jmt data:jmt apatite data:hooker apatites:wk012/1
SLIDE NUMBER 1
COUNTED BY: jmt

No.	Ns	Ni	Na	RATIO	U (ppm)	RHOs (E+06)	RHOi (E+06)	F.T.AGE (Ma)
1	0	7	9	0.000	9.4	0.000	0.786	0.0 ± 0.0
2	0	40	12	0.000	40.3	0.000	3.370	0.0 ± 0.0
3	0	48	16	0.000	36.3	0.000	3.033	0.0 ± 0.0
4	0	4	5	0.000	9.7	0.000	0.809	0.0 ± 0.0
5	1	51	6	0.020	102.8	0.169	8.595	3.8 ± 3.8
6	0	3	4	0.000	9.1	0.000	0.758	0.0 ± 0.0
7	0	7	9	0.000	9.4	0.000	0.786	0.0 ± 0.0
8	1	73	8	0.014	110.4	0.126	9.226	2.7 ± 2.7
9	0	24	12	0.000	24.2	0.000	2.022	0.0 ± 0.0
10	0	25	25	0.000	12.1	0.000	1.011	0.0 ± 0.0
11	0	6	9	0.000	8.1	0.000	0.674	0.0 ± 0.0
12	0	3	4	0.000	9.1	0.000	0.758	0.0 ± 0.0
13	0	31	8	0.000	46.9	0.000	3.918	0.0 ± 0.0
14	0	36	10	0.000	43.5	0.000	3.640	0.0 ± 0.0
15	0	18	12	0.000	18.1	0.000	1.517	0.0 ± 0.0
	2	376			30.5	0.014	2.552	

AREA OF BASIC UNIT = 9.89E-07 cm
CHI SQUARED = 4.210948 WITH 14 DEGREES OF FREEDOM
P(chi squared) = 99.4 %
CORRELATION COEFFICIENT = 0.704
VARIANCE OF SQR(Ns) = 0.12
VARIANCE OF SQR(Ni) = 4.93

Ns/Ni = 0.005 ± 0.004
MEAN RATIO = 0.002 ± 0.002

Ages calculated using a zeta of 354.9 ± 4.3 for SRM612 glass
RHO D = 1.095E+06 ; ND = 2707

POOLED AGE = 1.0 ± 0.7 Ma
MEAN AGE = 0.4 ± 0.3 Ma

8902-87 ZIRCON hooker s79/766347 825m

IRRADIATION jmt data:jmt zircon data:hooker zircons:wk025/11
SLIDE NUMBER 1
COUNTED BY: jmt

No.	Ns	Ni	Na	RATIO	U (ppm)	RHOs (E+06)	RHOi (E+06)	F.T.AGE (Ma)
1	61	29	4	2.103	0.0	15.420	7.331	122.2 ± 27.7
2	135	55	12	2.455	0.0	11.375	4.634	142.4 ± 22.9
3	19	8	2	2.375	0.0	9.606	4.044	137.8 ± 58.1
4	41	20	4	2.050	0.0	10.364	5.056	119.1 ± 32.6
5	96	29	9	3.310	0.0	10.785	3.258	191.3 ± 40.7
6	131	46	8	2.848	0.0	16.557	5.814	164.9 ± 28.4
7	314	103	24	3.049	0.0	13.229	4.339	176.4 ± 20.3
8	129	48	15	2.688	0.0	8.696	3.236	155.7 ± 26.5
9	130	55	9	2.364	0.0	14.605	6.179	137.2 ± 22.2
10	102	24	10	4.250	0.0	10.313	2.427	244.6 ± 55.7
	1158	417			0.0	12.071	4.347	

AREA OF BASIC UNIT = 9.89E-07 cm
CHI SQUARED = 9.510325 WITH 9 DEGREES OF FREEDOM
P(chi squared) = 39.2 %
CORRELATION COEFFICIENT = 0.969
VARIANCE OF SQR(Ns) = 13.04
VARIANCE OF SQR(Ni) = 4.09

Ns/Ni = 2.777 ± 0.159
MEAN RATIO = 2.749 ± 0.210

Ages calculated using a zeta of 133.9 ± 1.4 for CN1 glass
RHO D = 8.760E+05 ; ND = 4331

POOLED AGE = 160.8 ± 9.7 Ma
MEAN AGE = 159.2 ± 12.5 Ma

8902-88 APATITE hooker s79/786307 715m

IRRADIATION jmt data:jmt apatite data:hooker apatites:wk013/17
SLIDE NUMBER 1
COUNTED BY: jmt

No.	Ns	Ni	Na	RATIO	U (ppm)	RHOs (E+06)	RHOi (E+06)	F.T.AGE (Ma)
1	0	32	16	0.000	21.4	0.000	2.022	0.0 ± 0.0
2	0	26	18	0.000	15.5	0.000	1.461	0.0 ± 0.0
3	0	54	36	0.000	16.1	0.000	1.517	0.0 ± 0.0
4	0	9	24	0.000	4.0	0.000	0.379	0.0 ± 0.0
5	0	78	36	0.000	23.2	0.000	2.191	0.0 ± 0.0
6	0	43	24	0.000	19.2	0.000	1.812	0.0 ± 0.0
7	0	65	40	0.000	17.4	0.000	1.643	0.0 ± 0.0
8	0	34	9	0.000	40.5	0.000	3.820	0.0 ± 0.0
9	0	16	12	0.000	14.3	0.000	1.348	0.0 ± 0.0
10	0	12	12	0.000	10.7	0.000	1.011	0.0 ± 0.0
11	2	368	28	0.005	141.0	0.072	13.289	1.2 ± 0.8
12	2	36	20	0.056	19.3	0.101	1.820	12.2 ± 8.8
13	0	151	49	0.000	33.1	0.000	3.116	0.0 ± 0.0
14	0	43	30	0.000	15.4	0.000	1.449	0.0 ± 0.0
15	2	119	20	0.017	63.8	0.101	6.016	3.7 ± 2.6
16	0	7	20	0.000	3.8	0.000	0.354	0.0 ± 0.0
17	0	78	20	0.000	41.8	0.000	3.943	0.0 ± 0.0
18	1	52	42	0.019	13.3	0.024	1.252	4.2 ± 4.3
19	1	57	15	0.018	40.8	0.067	3.842	3.8 ± 3.9
20	0	7	15	0.000	5.0	0.000	0.472	0.0 ± 0.0
21	1	31	12	0.032	27.7	0.084	2.612	7.1 ± 7.2
22	0	102	15	0.000	72.9	0.000	6.876	0.0 ± 0.0
	9	1420			29.7	0.018	2.799	

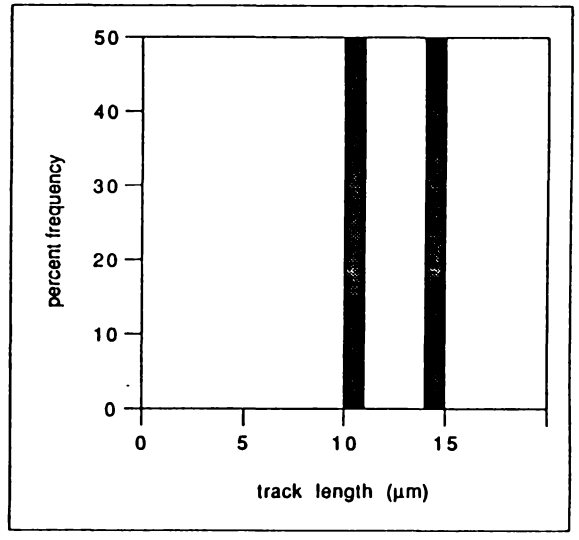
AREA OF BASIC UNIT = 9.89E-07 cm
CHI SQUARED = 25.53479 WITH 21 DEGREES OF FREEDOM
P(chi squared) = 22.5 %
CORRELATION COEFFICIENT = 0.507
VARIANCE OF SQR(Ns) = 0.32
VARIANCE OF SQR(Ni) = 14.03

Ns/Ni = 0.006 ± 0.002
MEAN RATIO = 0.007 ± 0.003

Ages calculated using a zeta of 354.9 ± 4.3 for SRM612 glass
RHO D = 1.235E+06 ; ND = 3055

POOLED AGE = 1.4 ± 0.5 Ma
MEAN AGE = 1.5 ± 0.7 Ma

8902-88



n = 2
Mean = 12.84 µm
Sample std. dev. = 2.07 µm

8902-88 ZIRCON hooker s79/786307 715m

IRRADIATION jmt data:jmt zircon data:hooker zircons:wk025/10
SLIDE NUMBER 1
COUNTED BY: jmt

No.	Ns	Ni	Na	RATIO	U (ppm)	RHOs (E+06)	RHOi (E+06)	F.TAGE (Ma)
1	50	18	3	2.778	0.0	16.852	6.067	159.5 ± 43.9
2	58	22	6	2.636	0.0	9.774	3.707	151.5 ± 38.0
3	184	76	14	2.421	0.0	13.289	5.489	139.2 ± 19.2
4	153	82	14	1.866	0.0	11.050	5.922	107.6 ± 14.9
5	85	40	5	2.125	0.0	17.189	8.089	122.4 ± 23.6
6	53	16	3	3.312	0.0	17.863	5.393	189.7 ± 54.2
7	152	67	15	2.269	0.0	10.246	4.516	130.6 ± 19.3
	735	321			0.0	12.386	5.410	

AREA OF BASIC UNIT = 9.89E-07 cm
CHI SQUARED = 5.076277 WITH 6 DEGREES OF FREEDOM
P(chi squared) = 53.4 %
CORRELATION COEFFICIENT = 0.972
VARIANCE OF SQR(Ns) = 7.66
VARIANCE OF SQR(Ni) = 4.82

Ns/Ni = 2.290 ± 0.153
MEAN RATIO = 2.487 ± 0.180

Ages calculated using a zeta of 133.9 ± 1.4 for CN1 glass
RHO D = 8.683E+05 ; ND = 4393

POOLED AGE = 131.8 ± 9.1 Ma
MEAN AGE = 143.0 ± 10.7 Ma

8902-89 APATITE hooker s100/937753 550m

IRRADIATION jmt data:jmt apatite data:hooker apatites:wk013/16
SLIDE NUMBER 1
COUNTED BY: jmt

No.	Ns	NI	Na	RATIO	U (ppm)	RHOs (E+06)	RHOI (E+06)	F.T.AGE (Ma)
1	33	98	21	0.337	50.5	1.589	4.719	72.7 ± 14.7
2	10	50	16	0.200	33.8	0.632	3.160	43.3 ± 15.0
3	2	26	16	0.077	17.6	0.126	1.643	16.7 ± 12.2
4	0	6	12	0.000	5.4	0.000	0.506	0.0 ± 0.0
5	4	19	12	0.211	17.1	0.337	1.601	45.5 ± 25.1
6	9	23	16	0.391	15.6	0.569	1.453	84.4 ± 33.2
7	24	81	20	0.296	43.9	1.213	4.095	64.0 ± 14.9
8	3	18	9	0.167	21.7	0.337	2.022	36.1 ± 22.5
9	4	22	15	0.182	15.9	0.270	1.483	39.3 ± 21.4
10	10	36	8	0.278	48.7	1.264	4.550	60.0 ± 21.5
11	25	61	8	0.410	82.6	3.160	7.710	88.3 ± 21.1
12	3	9	8	0.333	12.2	0.379	1.138	71.9 ± 48.0
13	28	44	10	0.636	47.7	2.831	4.449	136.6 ± 33.2
14	11	31	9	0.355	37.3	1.236	3.483	76.6 ± 26.9
15	8	39	24	0.205	17.6	0.337	1.643	44.4 ± 17.2
16	7	31	15	0.226	22.4	0.472	2.090	48.8 ± 20.5
17	7	36	6	0.194	65.0	1.180	6.067	42.1 ± 17.4
18	8	41	16	0.195	27.8	0.506	2.591	42.2 ± 16.3
19	19	68	18	0.279	40.9	1.067	3.820	60.4 ± 15.7
20	0	4	15	0.000	2.9	0.000	0.270	0.0 ± 0.0
	215	743			29.4	0.793	2.742	

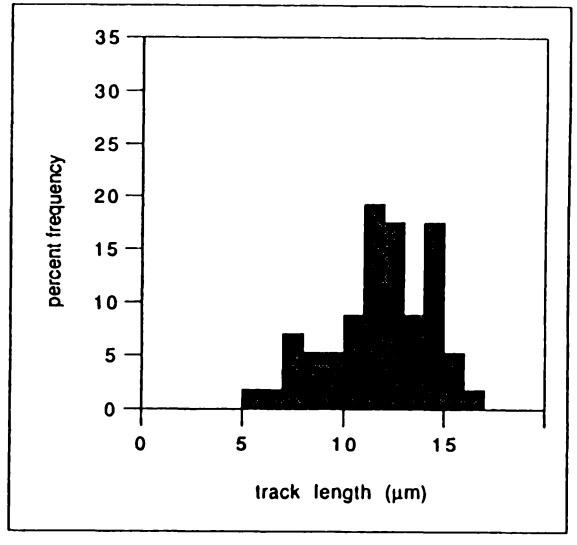
AREA OF BASIC UNIT = 9.89E-07 cm
CHI SQUARED = 27.77773 WITH 19 DEGREES OF FREEDOM
P(chi squared) = 8.8 %
CORRELATION COEFFICIENT = 0.887
VARIANCE OF SQR(Ns) = 2.54
VARIANCE OF SQR(Ni) = 4.25

Ns/Ni = 0.289 ± 0.022
MEAN RATIO = 0.249 ± 0.033

Ages calculated using a zeta of 354.9 ± 4.3 for SRM612 glass
RHO D = 1.223E+06 ; ND = 3025

POOLED AGE = 62.5 ± 5.0 Ma
MEAN AGE = 53.7 ± 7.1 Ma

8902-89



n = 57
Mean = 11.86 µm
Sample std. dev. = 2.47 µm

8902-89 ZIRCON hooker s100/937753 550m

IRRADIATION jmt data:jmt zircon data:hooker zircons:wk025/9
SLIDE NUMBER 1
COUNTED BY: jmt

No.	Ns	Ni	Na	RATIO	U (ppm)	RHOs (E+06)	RHOi (E+06)	F.T.AGE (Ma)
1	57	21	4	2.714	0.0	14.408	5.308	154.5 ± 39.5
2	148	60	18	2.467	0.0	8.314	3.370	140.6 ± 21.7
3	109	36	10	3.028	0.0	11.021	3.640	172.1 ± 33.2
4	25	6	12	4.167	0.0	2.106	0.506	235.7 ± 107.2
5	32	17	10	1.882	0.0	3.236	1.719	107.6 ± 32.3
6	117	39	12	3.000	0.0	9.858	3.286	170.6 ± 31.7
7	393	134	32	2.933	0.0	12.418	4.234	166.8 ± 17.0
8	46	21	10	2.190	0.0	4.651	2.123	125.0 ± 33.0
9	116	33	21	3.515	0.0	5.585	1.589	199.4 ± 39.5
10	66	18	8	3.667	0.0	8.342	2.275	207.9 ± 55.4
11	104	44	10	2.364	0.0	10.516	4.449	134.8 ± 24.4
12	179	43	28	4.163	0.0	6.464	1.553	235.5 ± 40.2
13	145	56	15	2.589	0.0	9.774	3.775	147.5 ± 23.4
14	108	26	18	4.154	0.0	6.067	1.461	235.0 ± 51.5
	1645	554			0.0	7.997	2.693	

AREA OF BASIC UNIT = 9.89E-07 cm
CHI SQUARED = 15.99651 WITH 13 DEGREES OF FREEDOM
P(chi squared) = 24.9 %
CORRELATION COEFFICIENT = 0.969
VARIANCE OF SQR(Ns) = 13.96
VARIANCE OF SQR(Ni) = 4.70

Ns/Ni = 2.969 ± 0.146
MEAN RATIO = 3.059 ± 0.204

Ages calculated using a zeta of 133.9 ± 1.4 for CN1 glass
RHO D = 8.606E+05 ; ND = 4256

POOLED AGE = 168.9 ± 8.9 Ma
MEAN AGE = 173.9 ± 12.0 Ma

8902-90 APATITE hooker s109/763642 425m

IRRADIATION jmt data:jmt apatite data:hooker apatites:wk013/15
SLIDE NUMBER 1
COUNTED BY: jmt

No.	Ns	Ni	Na	RATIO	U (ppm)	RHOs (E+06)	RHOi (E+06)	F.T.AGE (Ma)
1	8	23	18	0.348	14.0	0.449	1.292	74.3 ± 30.5
2	51	87	42	0.586	22.7	1.228	2.094	124.8 ± 22.2
3	9	18	12	0.500	16.4	0.758	1.517	106.6 ± 43.6
4	6	24	24	0.250	10.9	0.253	1.011	53.5 ± 24.4
5	122	221	40	0.552	60.4	3.084	5.586	117.5 ± 13.5
6	13	49	35	0.265	15.3	0.376	1.416	56.8 ± 17.8
7	21	82	48	0.256	18.7	0.442	1.727	54.8 ± 13.5
8	37	67	30	0.552	24.4	1.247	2.258	117.6 ± 24.2
9	23	98	25	0.235	42.9	0.930	3.964	50.2 ± 11.7
10	76	200	60	0.380	36.5	1.281	3.370	81.1 ± 11.1
11	116	217	40	0.535	59.3	2.932	5.485	113.9 ± 13.3
12	24	65	15	0.369	47.4	1.618	4.382	78.9 ± 18.9
13	69	137	60	0.504	25.0	1.163	2.309	107.3 ± 16.0
14	30	73	24	0.411	33.3	1.264	3.075	87.7 ± 19.1
15	19	88	40	0.216	24.1	0.480	2.224	46.2 ± 11.7
16	25	63	32	0.397	21.5	0.790	1.991	84.7 ± 20.1
17	25	39	20	0.641	21.3	1.264	1.972	136.3 ± 35.0
18	10	14	24	0.714	6.4	0.421	0.590	151.7 ± 62.9
19	39	49	24	0.796	22.3	1.643	2.064	168.8 ± 36.4
20	23	43	24	0.535	19.6	0.969	1.812	113.9 ± 29.5
	746	1657			28.5	1.184	2.630	

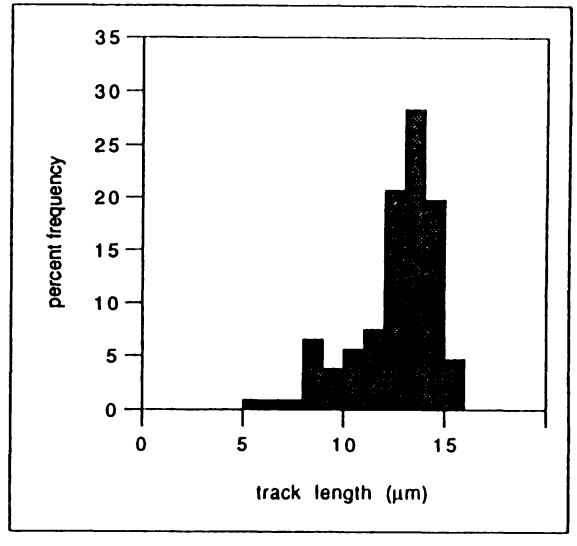
AREA OF BASIC UNIT = 9.89E-07 cm
CHI SQUARED = 50.55136 WITH 19 DEGREES OF FREEDOM
P(chi squared) = < 0.1 %
CORRELATION COEFFICIENT = 0.933
VARIANCE OF SQR(Ns) = 6.10
VARIANCE OF SQR(Ni) = 10.87

Ns/Ni = 0.450 ± 0.020
MEAN RATIO = 0.452 ± 0.037

Ages calculated using a zeta of 354.9 ± 4.3 for SRM612 glass
RHO D = 1.211E+06 ; ND = 2994

POOLED AGE = 96.0 ± 4.7 Ma
MEAN AGE = 96.4 ± 8.2 Ma

8902-90



n = 106
Mean = 12.60 µm
Sample std. dev. = 2.09 µm

8902-90 ZIRCON hooker s109/763642 425m

IRRADIATION jmt data:jmt zircon data:hooker zircons:wk025/8
SLIDE NUMBER 1
COUNTED BY: jmt

No.	Ns	Ni	Na	RATIO	U (ppm)	RHOs (E+06)	RHOi (E+06)	F.T.AGE (Ma)
1	186	95	18	1.958	0.0	10.448	5.336	110.5 ± 14.1
2	56	18	7	3.111	0.0	8.089	2.600	174.7 ± 47.5
3	108	55	16	1.964	0.0	6.825	3.476	110.8 ± 18.5
4	187	60	24	3.117	0.0	7.878	2.528	175.0 ± 26.2
5	37	15	4	2.467	0.0	9.353	3.792	138.9 ± 42.6
6	142	44	15	3.227	0.0	9.572	2.966	181.2 ± 31.4
7	127	36	10	3.528	0.0	12.841	3.640	197.8 ± 37.5
8	99	32	15	3.094	0.0	6.673	2.157	173.8 ± 35.5
9	121	45	40	2.689	0.0	3.059	1.138	151.3 ± 26.6
10	37	15	6	2.467	0.0	6.235	2.528	138.9 ± 42.6
11	37	18	4	2.056	0.0	9.353	4.550	116.0 ± 33.4
12	41	17	4	2.412	0.0	10.364	4.297	135.9 ± 39.3
13	159	46	12	3.457	0.0	13.397	3.876	193.8 ± 32.6
14	41	17	8	2.412	0.0	5.182	2.149	135.9 ± 39.3
15	59	25	8	2.360	0.0	7.457	3.160	133.0 ± 31.8
16	144	30	18	4.800	0.0	8.089	1.685	267.6 ± 53.9
17	111	29	16	3.828	0.0	7.015	1.833	214.3 ± 44.9
18	179	39	12	4.590	0.0	15.083	3.286	256.1 ± 45.5
	1871	636			0.0	7.982	2.713	

AREA OF BASIC UNIT = 9.89E-07 cm
CHI SQUARED = 37.4307 WITH 17 DEGREES OF FREEDOM
P(chi squared) = 0.3 %
CORRELATION COEFFICIENT = 0.812
VARIANCE OF SQR(Ns) = 8.16
VARIANCE OF SQR(Ni) = 2.56

Ns/Ni = 2.942 ± 0.135
MEAN RATIO = 2.974 ± 0.197

Ages calculated using a zeta of 133.9 ± 1.4 for CN1 glass
RHO D = 8.503E+05 ; ND = 4218

POOLED AGE = 165.3 ± 8.2 Ma
MEAN AGE = 167.1 ± 11.5 Ma

8902-91 APATITE fox s71/703607 230m

IRRADIATION jmt data:jmt apatite data:fox apatites:wk020/1
SLIDE NUMBER 1
COUNTED BY: jmt

No.	Ns	Ni	Na	RATIO	U (ppm)	RHOs (E+06)	RHOi (E+06)	F.TAGE (Ma)
1	0	7	20	0.000	1.1	0.000	0.354	0.0 ± 0.0
2	0	12	40	0.000	1.0	0.000	0.303	0.0 ± 0.0
3	0	9	25	0.000	1.2	0.000	0.364	0.0 ± 0.0
4	0	15	36	0.000	1.4	0.000	0.421	0.0 ± 0.0
5	0	3	12	0.000	0.8	0.000	0.253	0.0 ± 0.0
6	0	12	40	0.000	1.0	0.000	0.303	0.0 ± 0.0
7	0	34	60	0.000	1.8	0.000	0.573	0.0 ± 0.0
8	0	10	25	0.000	1.3	0.000	0.404	0.0 ± 0.0
9	0	15	36	0.000	1.4	0.000	0.421	0.0 ± 0.0
10	0	7	16	0.000	1.4	0.000	0.442	0.0 ± 0.0
	0	124			1.3	0.000	0.404	

AREA OF BASIC UNIT = 9.89E-07 cm
CHI SQUARED = 2.647059E-06 WITH 9 DEGREES OF FREEDOM
P(chi squared) = 100.0 %
CORRELATION COEFFICIENT = 0.897
VARIANCE OF SQR(Ns) = 0.00
VARIANCE OF SQR(Ni) = 1.17

Ns/Ni = 0.000 ± 0.000
MEAN RATIO = 0.000 ± 0.000

Ages calculated using a zeta of 354.9 ± 4.3 for SRM612 glass
RHO D = 4.061E+06 ; ND = 3213

POOLED AGE = 0.0 ± 0.0 Ma
MEAN AGE = 0.0 ± 0.0 Ma

8902-92 APATITE fox s79/725595 380m

IRRADIATION jmt data:jmt apatite data:fox apatites:wk021/15
SLIDE NUMBER 1
COUNTED BY: jmt

No.	Ns	Ni	Na	RATIO	U (ppm)	RHOs (E+06)	RHOi (E+06)	F.TAGE (Ma)
1	0	3	9	0.000	1.0	0.000	0.337	0.0 ± 0.0
2	0	4	12	0.000	1.0	0.000	0.337	0.0 ± 0.0
3	0	12	36	0.000	1.0	0.000	0.337	0.0 ± 0.0
4	0	0	16	0.000	0.0	0.000	0.000	0.0 ± 0.0
5	0	10	50	0.000	0.6	0.000	0.202	0.0 ± 0.0
6	0	4	8	0.000	1.4	0.000	0.506	0.0 ± 0.0
7	0	14	25	0.000	1.6	0.000	0.566	0.0 ± 0.0
8	0	0	12	0.000	0.0	0.000	0.000	0.0 ± 0.0
	0	47			0.8	0.000	0.283	

AREA OF BASIC UNIT = 9.89E-07 cm
CHI SQUARED = 2.357157E-06 WITH 7 DEGREES OF FREEDOM
P(chi squared) = 100.0 %
CORRELATION COEFFICIENT = 0.607
VARIANCE OF SQR(Ns) = 0.00
VARIANCE OF SQR(Ni) = 2.07

Ns/Ni = 0.000 ± 0.000
MEAN RATIO = 0.000 ± 0.000

Ages calculated using a zeta of 354.9 ± 4.3 for SRM612 glass
RHO D = 4.643E+06 ; ND = 3673

POOLED AGE = 0.0 ± 0.0 Ma
MEAN AGE = 0.0 ± 0.0 Ma

9001-5 APATITE cook s79/802476 3660m

IRRADIATION jmt data:jmt apatite data:cook apatites:wk033/10
SLIDE NUMBER 1
COUNTED BY: jmt

No.	Ns	Ni	Na	RATIO	U (ppm)	RHOs (E+06)	RHOi (E+06)	F.T AGE (Ma)
1	0	9	20	0.000	7.3	0.000	0.455	0.0 ± 0.0
2	0	24	21	0.000	18.5	0.000	1.156	0.0 ± 0.0
3	0	9	12	0.000	12.1	0.000	0.758	0.0 ± 0.0
4	0	54	6	0.000	145.4	0.000	9.100	0.0 ± 0.0
5	0	5	10	0.000	8.1	0.000	0.506	0.0 ± 0.0
6	0	7	8	0.000	14.1	0.000	0.885	0.0 ± 0.0
7	0	21	12	0.000	28.3	0.000	1.769	0.0 ± 0.0
8	0	9	12	0.000	12.1	0.000	0.758	0.0 ± 0.0
9	0	140	30	0.000	75.4	0.000	4.719	0.0 ± 0.0
10	0	32	21	0.000	24.6	0.000	1.541	0.0 ± 0.0
11	0	8	12	0.000	10.8	0.000	0.674	0.0 ± 0.0
	0	318			31.3	0.000	1.961	

AREA OF BASIC UNIT = 9.89E-07 cm
CHI SQUARED = 4.888888E-06 WITH 10 DEGREES OF FREEDOM
P(chi squared) = 100.0 %
CORRELATION COEFFICIENT = 0.210
VARIANCE OF SQR(Ns) = 0.00
VARIANCE OF SQR(Ni) = 8.13

Ns/Ni = 0.000 ± 0.000
MEAN RATIO = 0.000 ± 0.000

Ages calculated using a zeta of 354.9 ± 4.3 for SRM612 glass
RHO D = 8.201E+05 ; ND = 2027

POOLED AGE = 0.0 ± 0.0 Ma
MEAN AGE = 0.0 ± 0.0 Ma

9001-5 ZIRCON cook s79/802476 3660m

IRRADIATION jmt data:jmt zircon data:cook zircons:wk037/13
SLIDE NUMBER 1
COUNTED BY: jmt

No.	Ns	Ni	Na	RATIO	U (ppm)	RHOs (E+06)	RHOi (E+06)	F.T AGE (Ma)
1	122	76	12	1.605	0.0	10.280	6.404	113.7 ± 16.7
2	66	24	6	2.750	0.0	11.122	4.044	193.5 ± 46.2
3	24	10	4	2.400	0.0	6.067	2.528	169.2 ± 63.7
4	86	43	10	2.000	0.0	8.696	4.348	141.3 ± 26.5
5	63	35	4	1.800	0.0	15.925	8.847	127.3 ± 26.9
6	83	47	8	1.766	0.0	10.490	5.940	124.9 ± 22.9
	444	235			0.0	10.203	5.400	

AREA OF BASIC UNIT = 9.89E-07 cm
CHI SQUARED = 4.443792 WITH 5 DEGREES OF FREEDOM
P(chi squared) = 48.7 %
CORRELATION COEFFICIENT = 0.966
VARIANCE OF SQR(Ns) = 4.16
VARIANCE OF SQR(Ni) = 3.54

Ns/Ni = 1.889 ± 0.152
MEAN RATIO = 2.054 ± 0.178

Ages calculated using a zeta of 133.9 ± 1.4 for CN1 glass
RHO D = 1.067E+06 ; ND = 6342

POOLED AGE = 133.6 ± 11.0 Ma
MEAN AGE = 145.1 ± 12.8 Ma

9001-6 APATITE cook s79/797474 3230m

IRRADIATION jmt data:jmt apatite data:cook apatites:wk033/8
SLIDE NUMBER 1
COUNTED BY: jmt

No.	Ns	Ni	Na	RATIO	U (ppm)	RHOs (E+06)	RHOi (E+06)	F.T.AGE (Ma)
1	0	47	42	0.000	17.8	0.000	1.131	0.0 ± 0.0
2	0	10	18	0.000	8.9	0.000	0.562	0.0 ± 0.0
3	0	32	16	0.000	31.9	0.000	2.022	0.0 ± 0.0
4	0	9	24	0.000	6.0	0.000	0.379	0.0 ± 0.0
5	0	21	20	0.000	16.7	0.000	1.062	0.0 ± 0.0
6	0	12	9	0.000	21.2	0.000	1.348	0.0 ± 0.0
7	0	32	12	0.000	42.5	0.000	2.696	0.0 ± 0.0
8	1	12	12	0.083	15.9	0.084	1.011	12.3 ± 12.8
9	0	13	9	0.000	23.0	0.000	1.461	0.0 ± 0.0
10	0	35	16	0.000	34.9	0.000	2.212	0.0 ± 0.0
	1	223			20.0	0.006	1.267	

AREA OF BASIC UNIT = 9.89E-07 cm
CHI SQUARED = 16.30353 WITH 9 DEGREES OF FREEDOM
P(chi squared) = 6.1 %
CORRELATION COEFFICIENT = -0.272
VARIANCE OF SQR(Ns) = 0.10
VARIANCE OF SQR(Ni) = 1.91

Ns/Ni = 0.004 ± 0.004
MEAN RATIO = 0.008 ± 0.008

Ages calculated using a zeta of 354.9 ± 4.3 for SRM612 glass
RHO D = 8.313E+05 ; ND = 2055

POOLED AGE = 0.7 ± 0.7 Ma
MEAN AGE = 1.2 ± 1.2 Ma

9001-6 ZIRCON cook s79/797474 3230m

IRRADIATION jmt data:jmt zircon data:cook zircons:wk037/14
SLIDE NUMBER 1
COUNTED BY: jmt

No.	Ns	Ni	Na	RATIO	U (ppm)	RHOs (E+06)	RHOi (E+06)	F.T.AGE (Ma)
1	53	16	6	3.312	0.0	8.932	2.696	232.4 ± 66.4
2	47	21	6	2.238	0.0	7.920	3.539	157.9 ± 41.5
3	64	49	8	1.306	0.0	8.089	6.193	92.6 ± 17.6
4	63	28	6	2.250	0.0	10.617	4.719	158.8 ± 36.2
5	54	20	6	2.700	0.0	9.100	3.370	190.0 ± 49.8
6	62	35	9	1.771	0.0	6.966	3.932	125.3 ± 26.6
7	29	19	6	1.526	0.0	4.887	3.202	108.1 ± 32.0
8	127	53	3	2.396	0.0	42.804	17.863	168.9 ± 27.8
9	53	31	6	1.710	0.0	8.932	5.224	121.0 ± 27.4
	552	272			0.0	9.967	4.911	

AREA OF BASIC UNIT = 9.89E-07 cm
CHI SQUARED = 12.99372 WITH 8 DEGREES OF FREEDOM
P(chi squared) = 11.2 %
CORRELATION COEFFICIENT = 0.779
VARIANCE OF SQR(Ns) = 2.43
VARIANCE OF SQR(Ni) = 1.37

Ns/Ni = 2.029 ± 0.150
MEAN RATIO = 2.134 ± 0.210

Ages calculated using a zeta of 133.9 ± 1.4 for CN1 glass
RHO D = 1.067E+06 ; ND = 6342

POOLED AGE = 143.4 ± 10.9 Ma
MEAN AGE = 150.7 ± 15.0 Ma

9001-7 ZIRCON cook s79/774478 2530m

IRRADIATION jmt data:jmt zircon data:cook zircons:wk037/15
SLIDE NUMBER 1
COUNTED BY: jmt

No.	Ns	Ni	Na	RATIO	U (ppm)	RHOs (E+06)	RHOi (E+06)	F.T.AGE (Ma)
1	51	24	6	2.125	0.0	8.595	4.044	150.0 ± 37.2
2	31	10	4	3.100	0.0	7.836	2.528	217.7 ± 79.3
3	122	54	9	2.259	0.0	13.706	6.067	159.4 ± 26.2
4	28	19	4	1.474	0.0	7.078	4.803	104.4 ± 31.1
5	48	20	4	2.400	0.0	12.133	5.056	169.2 ± 45.1
6	128	86	24	1.488	0.0	5.393	3.623	105.5 ± 14.8
	408	213			0.0	8.089	4.223	

AREA OF BASIC UNIT = 9.89E-07 cm
CHI SQUARED = 7.779857 WITH 5 DEGREES OF FREEDOM
P(chi squared) = 16.9 %
CORRELATION COEFFICIENT = 0.940
VARIANCE OF SQR(Ns) = 7.06
VARIANCE OF SQR(Ni) = 5.16

Ns/Ni = 1.915 ± 0.162
MEAN RATIO = 2.141 ± 0.250

Ages calculated using a zeta of 133.9 ± 1.4 for CN1 glass
RHO D = 1.067E+06 ; ND = 6342

POOLED AGE = 135.4 ± 11.7 Ma
MEAN AGE = 151.2 ± 17.8 Ma

8902-93 APATITE whataroa s71/058791 150m

IRRADIATION jmt data:jmt apatite data:whataroa apatites:wk021/14
SLIDE NUMBER 1
COUNTED BY: jmt

No.	Ns	Ni	Na	RATIO	U (ppm)	RHOs (E+06)	RHOi (E+06)	F.T.AGE (Ma)
1	0	66	20	0.000	9.5	0.000	3.337	0.0 ± 0.0
2	0	2	20	0.000	0.3	0.000	0.101	0.0 ± 0.0
3	0	8	28	0.000	0.8	0.000	0.289	0.0 ± 0.0
4	0	4	20	0.000	0.6	0.000	0.202	0.0 ± 0.0
5	0	27	21	0.000	3.7	0.000	1.300	0.0 ± 0.0
6	0	19	12	0.000	4.5	0.000	1.601	0.0 ± 0.0
7	0	4	25	0.000	0.5	0.000	0.162	0.0 ± 0.0
8	0	25	20	0.000	3.6	0.000	1.264	0.0 ± 0.0
9	0	136	28	0.000	13.9	0.000	4.911	0.0 ± 0.0
10	0	9	16	0.000	1.6	0.000	0.569	0.0 ± 0.0
11	0	45	50	0.000	2.6	0.000	0.910	0.0 ± 0.0
12	0	2	16	0.000	0.4	0.000	0.126	0.0 ± 0.0
13	0	1	25	0.000	0.1	0.000	0.040	0.0 ± 0.0
14	0	19	30	0.000	1.8	0.000	0.640	0.0 ± 0.0
15	0	83	28	0.000	8.5	0.000	2.997	0.0 ± 0.0
	0	450			3.6	0.000	1.267	

AREA OF BASIC UNIT = 9.89E-07 cm
CHI SQUARED = 5.818181E-06 WITH 14 DEGREES OF FREEDOM
P(chi squared) = 100.0 %
CORRELATION COEFFICIENT = 0.260
VARIANCE OF SQR(Ns) = 0.00
VARIANCE OF SQR(Ni) = 10.01

Ns/Ni = 0.000 ± 0.000
MEAN RATIO = 0.000 ± 0.000

Ages calculated using a zeta of 354.9 ± 4.3 for SRM612 glass
RHO D = 4.616E+06 ; ND = 3652

POOLED AGE = 0.0 ± 0.0 Ma
MEAN AGE = 0.0 ± 0.0 Ma

8902-93 ZIRCON whataroa s71/058791 150m

IRRADIATION jmt data:jmt zircon data:whataroa zircons:wk025/5
SLIDE NUMBER 1
COUNTED BY: jmt

No.	Ns	Ni	Na	RATIO	U (ppm)	RHOs (E+06)	RHOi (E+06)	F.T.AGE (Ma)
1	2	159	12	0.013	0.0	0.169	13.397	0.7 ± 0.5
2	3	86	15	0.035	0.0	0.202	5.797	1.9 ± 1.1
3	3	147	15	0.020	0.0	0.202	9.909	1.1 ± 0.7
4	2	78	6	0.026	0.0	0.337	13.145	1.4 ± 1.0
5	1	84	8	0.012	0.0	0.126	10.617	0.7 ± 0.7
6	2	158	15	0.013	0.0	0.135	10.650	0.7 ± 0.5
7	1	111	14	0.009	0.0	0.072	8.017	0.5 ± 0.5
8	13	741	52	0.018	0.0	0.253	14.408	1.0 ± 0.3
9	1	52	8	0.019	0.0	0.126	6.572	1.1 ± 1.1
10	1	127	15	0.008	0.0	0.067	8.561	0.4 ± 0.4
11	4	194	16	0.021	0.0	0.253	12.260	1.1 ± 0.6
	33	1937			0.0	0.190	11.128	

AREA OF BASIC UNIT = 9.89E-07 cm
CHI SQUARED = 3.672964 WITH 10 DEGREES OF FREEDOM
P(chi squared) = 96.1 %
CORRELATION COEFFICIENT = 0.971
VARIANCE OF SQR(Ns) = 0.58
VARIANCE OF SQR(Ni) = 28.66

Ns/Ni = 0.017 ± 0.003
MEAN RATIO = 0.017 ± 0.002

Ages calculated using a zeta of 133.9 ± 1.4 for CN1 glass
RHO D = 8.300E+05 ; ND = 4104

POOLED AGE = 0.9 ± 0.2 Ma
MEAN AGE = 1.0 ± 0.1 Ma

8902-94 APATITE whataroa s71/044745 200m

IRRADIATION jmt data:jmt apatite data:whataroa apatites:wk021/13
SLIDE NUMBER 1
COUNTED BY: jmt

No.	Ns	Ni	Na	RATIO	U (ppm)	RHOs (E+06)	RHOi (E+06)	F.T.AGE (Ma)
1	0	71	9	0.000	22.8	0.000	7.977	0.0 ± 0.0
2	0	43	12	0.000	10.3	0.000	3.623	0.0 ± 0.0
3	0	29	9	0.000	9.3	0.000	3.258	0.0 ± 0.0
4	0	0	10	0.000	0.0	0.000	0.000	0.0 ± 0.0
5	0	1	4	0.000	0.7	0.000	0.253	0.0 ± 0.0
6	0	42	6	0.000	20.2	0.000	7.078	0.0 ± 0.0
7	0	31	9	0.000	9.9	0.000	3.483	0.0 ± 0.0
8	0	0	12	0.000	0.0	0.000	0.000	0.0 ± 0.0
9	0	2	25	0.000	0.2	0.000	0.081	0.0 ± 0.0
10	0	153	24	0.000	18.4	0.000	6.446	0.0 ± 0.0
11	0	54	12	0.000	13.0	0.000	4.550	0.0 ± 0.0
12	0	44	20	0.000	6.4	0.000	2.224	0.0 ± 0.0
	0	470			8.9	0.000	3.126	

AREA OF BASIC UNIT = 9.89E-07 cm
CHI SQUARED = 2.071897E-06 WITH 11 DEGREES OF FREEDOM
P(chi squared) = 100.0 %
CORRELATION COEFFICIENT = 0.834
VARIANCE OF SQR(Ns) = 0.00
VARIANCE OF SQR(Ni) = 14.35

Ns/Ni = 0.000 ± 0.000
MEAN RATIO = 0.000 ± 0.000

Ages calculated using a zeta of 354.9 ± 4.3 for SRM612 glass
RHO D = 4.589E+06 ; ND = 3630

POOLED AGE = 0.0 ± 0.0 Ma
MEAN AGE = 0.0 ± 0.0 Ma

8902-94 ZIRCON whataroa s71/044745 200m

IRRADIATION jmt data:jmt zircon data:whataroa zircons:wk025/4
SLIDE NUMBER 1
COUNTED BY: jmt

No.	Ns	Ni	Na	RATIO	U (ppm)	RHOs (E+06)	RHOi (E+06)	F.T.AGE (Ma)
1	7	391	30	0.018	0.0	0.236	13.178	1.0 ± 0.4
2	2	16	12	0.125	0.0	0.169	1.348	6.9 ± 5.2
3	1	65	9	0.015	0.0	0.112	7.303	0.8 ± 0.9
4	1	51	7	0.020	0.0	0.144	7.367	1.1 ± 1.1
5	13	273	30	0.048	0.0	0.438	9.201	2.6 ± 0.7
6	3	148	36	0.020	0.0	0.084	4.157	1.1 ± 0.7
7	2	100	8	0.020	0.0	0.253	12.639	1.1 ± 0.8
8	9	78	15	0.115	0.0	0.607	5.258	6.3 ± 2.2
9	26	351	28	0.074	0.0	0.939	12.675	4.1 ± 0.8
10	3	87	12	0.034	0.0	0.253	7.331	1.9 ± 1.1
11	1	69	8	0.014	0.0	0.126	8.721	0.8 ± 0.8
12	2	136	12	0.015	0.0	0.169	11.459	0.8 ± 0.6
13	1	35	15	0.029	0.0	0.067	2.359	1.6 ± 1.6
14	2	125	18	0.016	0.0	0.112	7.022	0.9 ± 0.6
15	15	674	45	0.022	0.0	0.337	15.144	1.2 ± 0.3
16	5	42	7	0.119	0.0	0.722	6.067	6.6 ± 3.1
17	3	112	16	0.027	0.0	0.190	7.078	1.5 ± 0.9
18	2	113	12	0.018	0.0	0.169	9.521	1.0 ± 0.7
19	6	115	24	0.052	0.0	0.253	4.845	2.9 ± 1.2
20	3	54	18	0.056	0.0	0.169	3.033	3.1 ± 1.8
21	2	77	8	0.026	0.0	0.253	9.732	1.4 ± 1.0
22	6	103	10	0.058	0.0	0.607	10.415	3.2 ± 1.3
23	6	131	8	0.046	0.0	0.758	16.557	2.5 ± 1.1
24	6	92	10	0.065	0.0	0.607	9.302	3.6 ± 1.5
25	20	484	40	0.041	0.0	0.506	12.235	2.3 ± 0.5
26	4	135	15	0.030	0.0	0.270	9.100	1.6 ± 0.8
27	10	354	108	0.028	0.0	0.094	3.314	1.6 ± 0.5
28	4	241	40	0.017	0.0	0.101	6.092	0.9 ± 0.5
29	2	162	40	0.012	0.0	0.051	4.095	0.7 ± 0.5
	167	4814			0.0	0.263	7.594	

AREA OF BASIC UNIT = 9.89E-07 cm
CHI SQUARED = 65.06113 WITH 28 DEGREES OF FREEDOM
P(chi squared) = < 0.1 %
CORRELATION COEFFICIENT = 0.743
VARIANCE OF SQR(Ns) = 1.12
VARIANCE OF SQR(Ni) = 26.20

Ns/Ni = 0.035 ± 0.003
MEAN RATIO = 0.041 ± 0.006

Ages calculated using a zeta of 133.9 ± 1.4 for CN1 glass
RHO D = 8.224E+05 ; ND = 4066

POOLED AGE = 1.9 ± 0.2 Ma

8902-95 APATITE whataroa s71/039709 350m

IRRADIATION jmt data:jmt apatite data:whataroa apatites:wk013/10
SLIDE NUMBER 1
COUNTED BY: jmt

No.	Ns	Ni	Na	RATIO	U (ppm)	RHOs (E+06)	RHOi (E+06)	F.T.AGE (Ma)
1	0	75	48	0.000	18.0	0.000	1.580	0.0 ± 0.0
2	0	15	35	0.000	4.9	0.000	0.433	0.0 ± 0.0
3	0	33	18	0.000	21.1	0.000	1.854	0.0 ± 0.0
4	0	82	36	0.000	26.2	0.000	2.303	0.0 ± 0.0
5	0	96	36	0.000	30.7	0.000	2.696	0.0 ± 0.0
6	0	21	16	0.000	15.1	0.000	1.327	0.0 ± 0.0
7	0	47	64	0.000	8.5	0.000	0.743	0.0 ± 0.0
8	0	1	25	0.000	0.5	0.000	0.040	0.0 ± 0.0
9	0	165	40	0.000	47.5	0.000	4.171	0.0 ± 0.0
10	0	39	25	0.000	18.0	0.000	1.577	0.0 ± 0.0
11	0	50	36	0.000	16.0	0.000	1.404	0.0 ± 0.0
12	0	30	36	0.000	9.6	0.000	0.843	0.0 ± 0.0
13	0	13	32	0.000	4.2	0.000	0.365	0.0 ± 0.0
14	0	60	36	0.000	19.2	0.000	1.685	0.0 ± 0.0
15	0	335	200	0.000	19.3	0.000	1.694	0.0 ± 0.0
	0	1062			17.8	0.000	1.563	

AREA OF BASIC UNIT = 9.89E-07 cm
CHI SQUARED = 1.316E-05 WITH 14 DEGREES OF FREEDOM
P(chi squared) = 100.0 %
CORRELATION COEFFICIENT = 0.014
VARIANCE OF SQR(Ns) = 0.00
VARIANCE OF SQR(Ni) = 17.33

Ns/Ni = 0.000 ± 0.000
MEAN RATIO = 0.000 ± 0.000

Ages calculated using a zeta of 354.9 ± 4.3 for SRM612 glass
RHO D = 1.150E+06 ; ND = 2843

POOLED AGE = 0.0 ± 0.0 Ma
MEAN AGE = 0.0 ± 0.0 Ma

8902-95 ZIRCON whataroa s71/039709 350m

IRRADIATION jmt data:jmt zircon data:whataroa zircons:wk025/3
SLIDE NUMBER 1
COUNTED BY: jmt

No.	Ns	Ni	Na	RATIO	U (ppm)	RHOs (E+06)	RHOi (E+06)	F.T.AGE (Ma)
1	12	331	40	0.036	0.0	0.303	8.367	2.0 ± 0.6
2	8	235	30	0.034	0.0	0.270	7.920	1.9 ± 0.7
3	20	288	80	0.069	0.0	0.253	3.640	3.8 ± 0.9
4	3	77	14	0.039	0.0	0.217	5.561	2.1 ± 1.2
5	3	38	10	0.079	0.0	0.303	3.842	4.3 ± 2.6
6	5	163	32	0.031	0.0	0.158	5.150	1.7 ± 0.8
7	16	479	100	0.033	0.0	0.162	4.843	1.8 ± 0.5
8	5	142	15	0.035	0.0	0.337	9.572	1.9 ± 0.9
9	8	136	35	0.059	0.0	0.231	3.929	3.2 ± 1.2
10	8	197	56	0.041	0.0	0.144	3.557	2.2 ± 0.8
11	14	356	50	0.039	0.0	0.283	7.199	2.1 ± 0.6
12	5	127	30	0.039	0.0	0.169	4.280	2.1 ± 1.0
	107	2569			0.0	0.220	5.280	

AREA OF BASIC UNIT = 9.89E-07 cm
CHI SQUARED = 9.048161 WITH 11 DEGREES OF FREEDOM
P(chi squared) = 61.7 %
CORRELATION COEFFICIENT = 0.847
VARIANCE OF SQR(Ns) = 0.80
VARIANCE OF SQR(Ni) = 20.14

Ns/Ni = 0.042 ± 0.004
MEAN RATIO = 0.045 ± 0.005

Ages calculated using a zeta of 133.9 ± 1.4 for CN1 glass
RHO D = 8.147E+05 ; ND = 4029

POOLED AGE = 2.3 ± 0.2 Ma
MEAN AGE = 2.4 ± 0.2 Ma

8902-96 APATITE whataroa s71/061695 655m

IRRADIATION jmt data:jmt apatite data:whataroa apatites:wk021/12
SLIDE NUMBER 1
COUNTED BY: jmt

No.	Ns	Ni	Na	RATIO	U (ppm)	RHOs (E+06)	RHOi (E+06)	F.TAGE (Ma)
1	0	27	6	0.000	13.1	0.000	4.550	0.0 ± 0.0
2	0	11	20	0.000	1.6	0.000	0.556	0.0 ± 0.0
3	0	2	9	0.000	0.6	0.000	0.225	0.0 ± 0.0
4	0	535	25	0.000	62.1	0.000	21.638	0.0 ± 0.0
5	0	109	32	0.000	9.9	0.000	3.444	0.0 ± 0.0
6	0	153	16	0.000	27.8	0.000	9.669	0.0 ± 0.0
7	0	149	24	0.000	18.0	0.000	6.277	0.0 ± 0.0
8	0	42	12	0.000	10.2	0.000	3.539	0.0 ± 0.0
9	0	51	12	0.000	12.3	0.000	4.297	0.0 ± 0.0
10	0	83	6	0.000	40.2	0.000	13.987	0.0 ± 0.0
	0	1162			20.8	0.000	7.253	

AREA OF BASIC UNIT = 9.89E-07 cm
CHI SQUARED = 1.171963E-06 WITH 9 DEGREES OF FREEDOM
P(chi squared) = 100.0 %
CORRELATION COEFFICIENT = 0.939
VARIANCE OF SQR(Ns) = 0.00
VARIANCE OF SQR(Ni) = 37.49

Ns/Ni = 0.000 ± 0.000
MEAN RATIO = 0.000 ± 0.000

Ages calculated using a zeta of 354.9 ± 4.3 for SRM612 glass
RHO D = 4.561E+06 ; ND = 3609

POOLED AGE = 0.0 ± 0.0 Ma
MEAN AGE = 0.0 ± 0.0 Ma

8902-96 ZIRCON whataroa s71/061695

IRRADIATION jmt data:jmt zircon data:whataroa zircons:wk037/3
SLIDE NUMBER 1
COUNTED BY: jmt

No.	Ns	Ni	Na	RATIO	U (ppm)	RHOs (E+06)	RHOi (E+06)	F.TAGE (Ma)
1	4	40	5	0.100	0.0	0.809	8.089	7.1 ± 3.7
2	3	42	6	0.071	0.0	0.506	7.078	5.1 ± 3.0
3	2	57	6	0.035	0.0	0.337	9.606	2.5 ± 1.8
4	3	99	9	0.030	0.0	0.337	11.122	2.2 ± 1.3
5	9	124	12	0.073	0.0	0.758	10.448	5.2 ± 1.8
6	1	14	4	0.071	0.0	0.253	3.539	5.1 ± 5.3
7	1	49	4	0.020	0.0	0.253	12.386	1.5 ± 1.5
8	7	139	8	0.050	0.0	0.885	17.568	3.6 ± 1.4
9	2	95	12	0.021	0.0	0.169	8.005	1.5 ± 1.1
10	3	41	6	0.073	0.0	0.506	6.909	5.2 ± 3.1
11	3	31	2	0.097	0.0	1.517	15.672	6.9 ± 4.2
12	48	812	40	0.059	0.0	1.213	20.526	4.2 ± 0.6
13	11	242	16	0.045	0.0	0.695	15.293	3.2 ± 1.0
14	18	198	18	0.091	0.0	1.011	11.122	6.5 ± 1.6
15	1	25	3	0.040	0.0	0.337	8.426	2.9 ± 2.9
16	13	350	30	0.037	0.0	0.438	11.796	2.7 ± 0.8
17	7	113	8	0.062	0.0	0.885	14.282	4.4 ± 1.7
	136	2471			0.0	0.728	13.219	

AREA OF BASIC UNIT = 9.89E-07 cm
CHI SQUARED = 14.89322 WITH 16 DEGREES OF FREEDOM
P(chi squared) = 53.2 %
CORRELATION COEFFICIENT = 0.966
VARIANCE OF SQR(Ns) = 2.28
VARIANCE OF SQR(Ni) = 37.75

Ns/Ni = 0.055 ± 0.005
MEAN RATIO = 0.057 ± 0.006

Ages calculated using a zeta of 133.9 ± 1.4 for CN1 glass
RHO D = 1.067E+06 ; ND = 6342

POOLED AGE = 3.9 ± 0.4 Ma
MEAN AGE = 4.1 ± 0.4 Ma

8902-97 APATITE godley s80/120599 1065m

IRRADIATION jmt data:jmt apatite data:godley apatites:wk013/8
SLIDE NUMBER 1
COUNTED BY: jmt

No.	Ns	Ni	Na	RATIO	U (ppm)	RHOs (E+06)	RHOi (E+06)	F.T.AGE (Ma)
1	0	9	20	0.000	5.3	0.000	0.455	0.0 ± 0.0
2	0	78	60	0.000	15.3	0.000	1.314	0.0 ± 0.0
3	0	3	24	0.000	1.5	0.000	0.126	0.0 ± 0.0
4	0	9	20	0.000	5.3	0.000	0.455	0.0 ± 0.0
5	0	5	15	0.000	3.9	0.000	0.337	0.0 ± 0.0
6	0	8	12	0.000	7.8	0.000	0.674	0.0 ± 0.0
7	0	41	60	0.000	8.0	0.000	0.691	0.0 ± 0.0
8	0	5	12	0.000	4.9	0.000	0.421	0.0 ± 0.0
9	0	1	9	0.000	1.3	0.000	0.112	0.0 ± 0.0
10	0	15	15	0.000	11.8	0.000	1.011	0.0 ± 0.0
11	0	6	12	0.000	5.9	0.000	0.506	0.0 ± 0.0
12	0	33	16	0.000	24.3	0.000	2.085	0.0 ± 0.0
13	0	23	10	0.000	27.1	0.000	2.326	0.0 ± 0.0
14	0	33	15	0.000	25.9	0.000	2.224	0.0 ± 0.0
15	0	58	24	0.000	28.5	0.000	2.444	0.0 ± 0.0
	0	327			11.9	0.000	1.020	

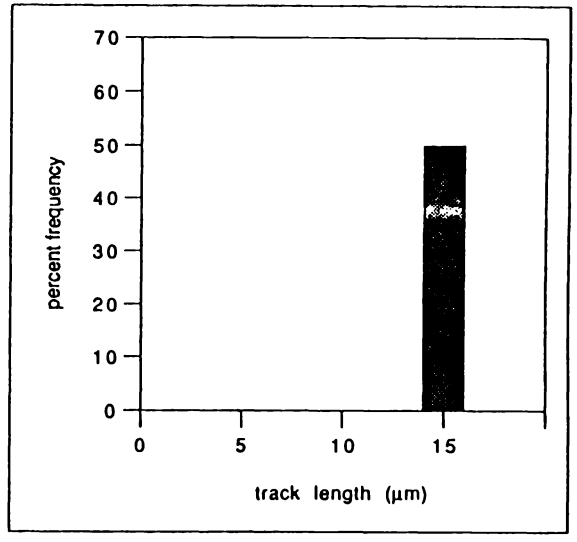
AREA OF BASIC UNIT = 9.89E-07 cm
CHI SQUARED = 4.637931E-06 WITH 14 DEGREES OF FREEDOM
P(chi squared) = 100.0 %
CORRELATION COEFFICIENT = 0.440
VARIANCE OF SQR(Ns) = 0.00
VARIANCE OF SQR(Ni) = 5.35

Ns/Ni = 0.000 ± 0.000
MEAN RATIO = 0.000 ± 0.000

Ages calculated using a zeta of 354.9 ± 4.3 for SRM612 glass
RHO D = 1.125E+06 ; ND = 2783

POOLED AGE = 0.0 ± 0.0 Ma
MEAN AGE = 0.0 ± 0.0 Ma

8902-97



n = 2
Mean = 14.69 µm
Sample std. dev. = 0.44 µm

8902-97 ZIRCON godley s80/120599 1065m

IRRADIATION jmt data:jmt zircon data:godley zircons:wk025/1
SLIDE NUMBER 1
COUNTED BY: jmt

No.	Ns	Ni	Na	RATIO	U (ppm)	RHOs (E+06)	RHOi (E+06)	F.TAGE (Ma)
1	67	23	6	2.913	0.0	11.291	3.876	154.0 ± 37.3
2	139	46	12	3.022	0.0	11.712	3.876	159.7 ± 27.3
3	59	22	6	2.682	0.0	9.943	3.707	142.0 ± 35.6
4	588	116	40	5.069	0.0	14.864	2.932	265.7 ± 27.5
5	72	11	6	6.545	0.0	12.133	1.854	341.1 ± 110.6
6	364	102	20	3.569	0.0	18.402	5.157	188.2 ± 21.4
7	189	77	20	2.455	0.0	9.555	3.893	130.0 ± 17.8
8	112	38	10	2.947	0.0	11.325	3.842	155.8 ± 29.4
9	177	47	12	3.766	0.0	14.914	3.960	198.5 ± 32.8
10	83	33	9	2.515	0.0	9.325	3.707	133.2 ± 27.5
11	170	50	20	3.400	0.0	8.595	2.528	179.4 ± 29.1
12	468	153	30	3.059	0.0	15.774	5.157	161.7 ± 15.4
13	50	16	6	3.125	0.0	8.426	2.696	165.1 ± 47.5
14	59	13	4	4.538	0.0	14.914	3.286	238.4 ± 73.2
15	121	44	12	2.750	0.0	10.195	3.707	145.5 ± 25.8
16	64	24	4	2.667	0.0	16.178	6.067	141.2 ± 33.9
17	122	38	12	3.211	0.0	10.280	3.202	169.6 ± 31.7
18	637	191	50	3.335	0.0	12.882	3.862	176.1 ± 14.9
19	57	17	6	3.353	0.0	9.606	2.865	177.0 ± 49.0
20	134	41	9	3.268	0.0	15.054	4.606	172.6 ± 31.0
	3732	1102			0.0	12.835	3.790	

AREA OF BASIC UNIT = 9.89E-07 cm
CHI SQUARED = 35.75184 WITH 19 DEGREES OF FREEDOM
P(chi squared) = 1.1 %
CORRELATION COEFFICIENT = 0.958
VARIANCE OF SQR(Ns) = 31.88
VARIANCE OF SQR(Ni) = 8.55

Ns/Ni = 3.387 ± 0.116
MEAN RATIO = 3.409 ± 0.218

Ages calculated using a zeta of 133.9 ± 1.4 for CN1 glass
RHO D = 7.994E+05 ; ND = 3953

POOLED AGE = 178.7 ± 7.0 Ma
MEAN AGE = 179.9 ± 12.0 Ma

8902-98 APATITE godley s80/117573 1005m

IRRADIATION jmt data:jmt apatite data:godley apatites:wk013/7
SLIDE NUMBER 1
COUNTED BY: jmt

No.	Ns	NI	Na	RATIO	U (ppm)	RHOs (E+06)	RHOi (E+06)	F.T.AGE (Ma)
1	0	9	6	0.000	17.9	0.000	1.517	0.0 ± 0.0
2	0	9	4	0.000	26.8	0.000	2.275	0.0 ± 0.0
3	0	20	4	0.000	59.5	0.000	5.056	0.0 ± 0.0
4	0	14	6	0.000	27.8	0.000	2.359	0.0 ± 0.0
5	0	16	3	0.000	63.5	0.000	5.393	0.0 ± 0.0
6	0	4	8	0.000	6.0	0.000	0.506	0.0 ± 0.0
7	0	2	9	0.000	2.6	0.000	0.225	0.0 ± 0.0
8	0	2	6	0.000	4.0	0.000	0.337	0.0 ± 0.0
9	0	3	12	0.000	3.0	0.000	0.253	0.0 ± 0.0
10	0	11	20	0.000	6.5	0.000	0.556	0.0 ± 0.0
11	0	11	24	0.000	5.5	0.000	0.463	0.0 ± 0.0
12	0	9	12	0.000	8.9	0.000	0.758	0.0 ± 0.0
13	0	11	12	0.000	10.9	0.000	0.927	0.0 ± 0.0
14	0	7	9	0.000	9.3	0.000	0.786	0.0 ± 0.0
15	0	19	15	0.000	15.1	0.000	1.281	0.0 ± 0.0
	0	147			11.7	0.000	0.991	

AREA OF BASIC UNIT = 9.89E-07 cm
CHI SQUARED = 6.349999E-06 WITH 14 DEGREES OF FREEDOM
P(chi squared) = 100.0 %
CORRELATION COEFFICIENT = 0.492
VARIANCE OF SQR(Ns) = 0.00
VARIANCE OF SQR(Ni) = 0.97

Ns/Ni = 0.000 ± 0.000
MEAN RATIO = 0.000 ± 0.000

Ages calculated using a zeta of 354.9 ± 4.3 for SRM612 glass
RHO D = 1.113E+06 ; ND = 2752

POOLED AGE = 0.0 ± 0.0 Ma
MEAN AGE = 0.0 ± 0.0 Ma

8902-98 ZIRCON godley s80/117573 1005m

IRRADIATION jmt data:jmt zircon data:godley zircons:wk026/18
SLIDE NUMBER 1
COUNTED BY: jmt

No.	Ns	NI	Na	RATIO	U (ppm)	RHOs (E+06)	RHOi (E+06)	F.T.AGE (Ma)
1	40	10	4	4.000	0.0	10.111	2.528	260.6 ± 92.3
2	103	23	8	4.478	0.0	13.018	2.907	291.1 ± 67.3
3	69	17	5	4.059	0.0	13.953	3.438	264.4 ± 71.7
4	96	33	6	2.909	0.0	16.178	5.561	190.6 ± 38.6
5	85	22	12	3.864	0.0	7.162	1.854	251.9 ± 60.4
6	152	50	8	3.040	0.0	19.211	6.320	199.0 ± 32.6
7	114	39	9	2.923	0.0	12.808	4.382	191.5 ± 35.7
8	44	21	6	2.095	0.0	7.415	3.539	137.8 ± 36.6
9	59	16	5	3.688	0.0	11.931	3.236	240.7 ± 68.0
10	86	30	8	2.867	0.0	10.870	3.792	187.9 ± 40.0
11	63	25	8	2.520	0.0	7.963	3.160	165.4 ± 39.2
12	142	47	12	3.021	0.0	11.965	3.960	197.8 ± 33.5
13	92	46	9	2.000	0.0	10.336	5.168	131.6 ± 23.9
14	101	42	8	2.405	0.0	12.765	5.308	158.0 ± 29.1
15	371	119	24	3.118	0.0	15.630	5.013	204.0 ± 21.8
16	44	15	6	2.933	0.0	7.415	2.528	192.2 ± 57.6
17	70	27	9	2.593	0.0	7.864	3.033	170.1 ± 38.7
18	133	64	10	2.078	0.0	13.448	6.471	136.7 ± 20.9
19	112	38	12	2.947	0.0	9.437	3.202	193.1 ± 36.4
20	550	175	40	3.143	0.0	13.903	4.424	205.7 ± 18.2
21	61	25	8	2.440	0.0	7.710	3.160	160.2 ± 38.2
22	229	52	30	4.404	0.0	7.718	1.753	286.4 ± 44.3
	2816	936			0.0	11.528	3.832	

AREA OF BASIC UNIT = 9.89E-07 cm
CHI SQUARED = 29.56359 WITH 21 DEGREES OF FREEDOM
P(chi squared) = 10.1 %
CORRELATION COEFFICIENT = 0.974
VARIANCE OF SQR(Ns) = 16.93
VARIANCE OF SQR(Ni) = 5.36

Ns/Ni = 3.009 ± 0.114
MEAN RATIO = 3.069 ± 0.156

Ages calculated using a zeta of 133.9 ± 1.4 for CN1 glass
RHO D = 9.932E+05 ; ND = 4912

POOLED AGE = 197.0 ± 8.2 Ma
MEAN AGE = 200.9 ± 10.8 Ma

8902-99 APATITE godley s80/118554 960m

IRRADIATION jmt data:jmt apatite data:godley apatites:wk013/6
SLIDE NUMBER 1
COUNTED BY: jmt

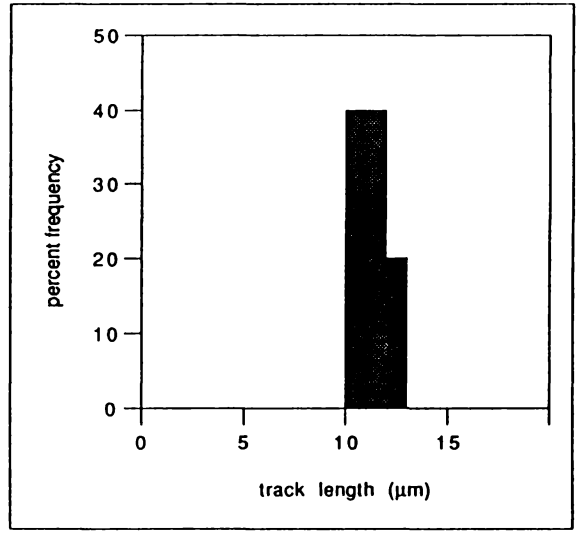
No.	Ns	NI	Na	RATIO	U (ppm)	RHOs (E+06)	RHOi (E+06)	F.T.AGE (Ma)
1	0	66	36	0.000	22.1	0.000	1.854	0.0 ± 0.0
2	0	16	12	0.000	16.0	0.000	1.348	0.0 ± 0.0
3	1	47	36	0.021	15.7	0.028	1.320	4.2 ± 4.2
4	1	58	30	0.017	23.3	0.034	1.955	3.4 ± 3.4
5	0	8	36	0.000	2.7	0.000	0.225	0.0 ± 0.0
6	0	238	25	0.000	114.5	0.000	9.626	0.0 ± 0.0
7	0	12	40	0.000	3.6	0.000	0.303	0.0 ± 0.0
8	1	41	5	0.024	98.7	0.202	8.291	4.8 ± 4.8
9	0	8	25	0.000	3.8	0.000	0.324	0.0 ± 0.0
10	0	18	15	0.000	14.4	0.000	1.213	0.0 ± 0.0
11	1	18	12	0.056	18.0	0.084	1.517	10.8 ± 11.1
12	0	31	9	0.000	41.4	0.000	3.483	0.0 ± 0.0
13	0	81	16	0.000	60.9	0.000	5.119	0.0 ± 0.0
14	0	66	36	0.000	22.1	0.000	1.854	0.0 ± 0.0
15	0	19	24	0.000	9.5	0.000	0.800	0.0 ± 0.0
16	0	20	24	0.000	10.0	0.000	0.843	0.0 ± 0.0
17	0	10	24	0.000	5.0	0.000	0.421	0.0 ± 0.0
18	2	139	16	0.014	104.5	0.126	8.784	2.8 ± 2.0
19	0	124	24	0.000	62.2	0.000	5.224	0.0 ± 0.0
20	0	32	15	0.000	25.7	0.000	2.157	0.0 ± 0.0
	6	1052			27.5	0.013	2.312	

AREA OF BASIC UNIT = 9.89E-07 cm
CHI SQUARED = 19.25297 WITH 19 DEGREES OF FREEDOM
P(chi squared) = 44.1 %
CORRELATION COEFFICIENT = 0.203
VARIANCE OF SQR(Ns) = 0.24
VARIANCE OF SQR(Ni) = 11.37

Ns/Ni = 0.006 ± 0.002
MEAN RATIO = 0.007 ± 0.003

Ages calculated using a zeta of 354.9 ± 4.3 for SRM612 glass
RHO D = 1.101E+06 ; ND = 2722

POOLED AGE = 1.1 ± 0.5 Ma
MEAN AGE = 1.3 ± 0.6 Ma



n = 5
Mean = 11.32 µm
Sample std. dev. = 0.94 µm

8902-99 ZIRCON godley s80/118554 960m

IRRADIATION jmt data:jmt zircon data:godley zircons:wk026/17
SLIDE NUMBER 1
COUNTED BY: jmt

No.	Ns	Ni	Na	RATIO	U (ppm)	RHOs (E+06)	RHOi (E+06)	F.TAGE (Ma)
1	191	50	16	3.820	0.0	12.070	3.160	246.9 ± 39.5
2	369	93	24	3.968	0.0	15.546	3.918	256.3 ± 30.1
3	45	23	4	1.957	0.0	11.375	5.814	127.7 ± 32.8
4	44	11	4	4.000	0.0	11.122	2.781	258.3 ± 87.2
5	162	38	8	4.263	0.0	20.475	4.803	275.0 ± 49.8
6	93	33	8	2.818	0.0	11.754	4.171	183.1 ± 37.2
7	80	20	8	4.000	0.0	10.111	2.528	258.3 ± 64.7
	984	268			0.0	13.819	3.764	

AREA OF BASIC UNIT = 9.89E-07 cm
CHI SQUARED = 9.326609 WITH 6 DEGREES OF FREEDOM
P(chi squared) = 15.6 %
CORRELATION COEFFICIENT = 0.983
VARIANCE OF SQR(Ns) = 20.30
VARIANCE OF SQR(Ni) = 4.24

Ns/Ni = 3.672 ± 0.253
MEAN RATIO = 3.547 ± 0.318

Ages calculated using a zeta of 133.9 ± 1.4 for CN1 glass
RHO D = 9.843E+05 ; ND = 4868

POOLED AGE = 237.5 ± 16.9 Ma
MEAN AGE = 229.6 ± 21.0 Ma

8902-100 APATITE godley s80/118506 915m

IRRADIATION jmt data:jmt apatite data:godley apatites:wk043/6
SLIDE NUMBER 1
COUNTED BY: jmt

No.	Ns	NI	Na	RATIO	U (ppm)	RHOs (E+06)	RHOi (E+06)	F.T.AGE (Ma)
1	1	51	21	0.020	36.2	0.048	2.456	3.1 ± 3.1
2	2	37	9	0.054	61.4	0.225	4.157	8.5 ± 6.2
3	0	50	16	0.000	46.6	0.000	3.160	0.0 ± 0.0
4	1	85	20	0.012	63.4	0.051	4.297	1.9 ± 1.9
5	0	28	6	0.000	69.6	0.000	4.719	0.0 ± 0.0
6	1	11	4	0.091	41.0	0.253	2.781	14.3 ± 14.9
7	0	6	12	0.000	7.5	0.000	0.506	0.0 ± 0.0
8	1	47	30	0.021	23.4	0.034	1.584	3.4 ± 3.4
9	2	45	18	0.044	37.3	0.112	2.528	7.0 ± 5.1
10	1	23	12	0.043	28.6	0.084	1.938	6.8 ± 7.0
11	0	17	9	0.000	28.2	0.000	1.910	0.0 ± 0.0
12	0	5	9	0.000	8.3	0.000	0.562	0.0 ± 0.0
13	0	25	18	0.000	20.7	0.000	1.404	0.0 ± 0.0
14	6	39	6	0.154	97.0	1.011	6.572	24.2 ± 10.6
15	0	16	12	0.000	19.9	0.000	1.348	0.0 ± 0.0
16	0	17	8	0.000	31.7	0.000	2.149	0.0 ± 0.0
17	0	5	9	0.000	8.3	0.000	0.562	0.0 ± 0.0
18	0	10	15	0.000	9.9	0.000	0.674	0.0 ± 0.0
19	1	40	18	0.025	33.2	0.056	2.247	3.9 ± 4.0
20	1	20	6	0.050	49.7	0.169	3.370	7.9 ± 8.1
21	0	18	12	0.000	22.4	0.000	1.517	0.0 ± 0.0
22	0	7	6	0.000	17.4	0.000	1.180	0.0 ± 0.0
23	7	153	28	0.046	81.5	0.253	5.525	7.2 ± 2.8
24	0	7	12	0.000	8.7	0.000	0.590	0.0 ± 0.0
25	0	32	15	0.000	31.8	0.000	2.157	0.0 ± 0.0
	24	794			35.8	0.073	2.425	

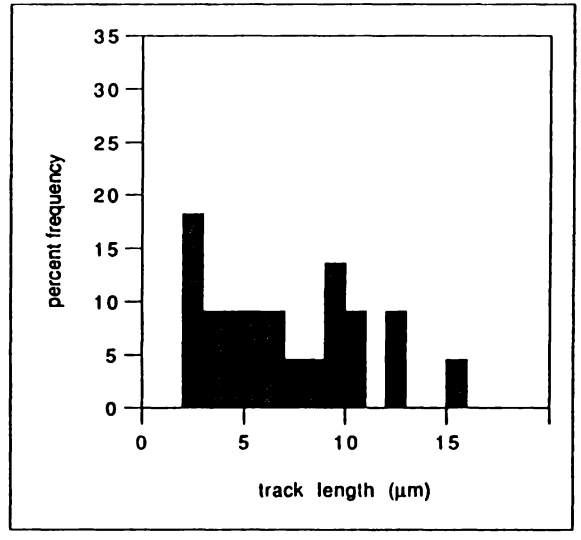
AREA OF BASIC UNIT = 9.89E-07 cm
CHI SQUARED = 29.44149 WITH 24 DEGREES OF FREEDOM
P(chi squared) = 20.4 %
CORRELATION COEFFICIENT = 0.721
VARIANCE OF SQR(Ns) = 0.63
VARIANCE OF SQR(Ni) = 5.60

Ns/NI = 0.030 ± 0.006
MEAN RATIO = 0.022 ± 0.007

Ages calculated using a zeta of 354.9 ± 4.3 for SRM612 glass
RHO D = 8.876E+05 ; ND = 5267

POOLED AGE = 4.8 ± 1.0 Ma
MEAN AGE = 3.5 ± 1.2 Ma

8902-100



n = 22
Mean = 7.17 µm
Sample std. dev. = 3.72 µm

8902-100 ZIRCON godley s80/118506 915m

IRRADIATION jmt data:jmt zircon data:godley zircons:wk026/16
SLIDE NUMBER 1
COUNTED BY: jmt

No.	Ns	Ni	Na	RATIO	U (ppm)	RHOs (E+06)	RHOi (E+06)	F.T AGE (Ma)
1	44	21	6	2.095	0.0	7.415	3.539	135.4 ± 36.0
2	153	34	12	4.500	0.0	12.892	2.865	287.4 ± 54.7
3	207	62	18	3.339	0.0	11.628	3.483	214.4 ± 31.3
4	43	16	4	2.688	0.0	10.870	4.044	173.2 ± 50.8
5	89	29	6	3.069	0.0	14.998	4.887	197.4 ± 42.3
6	140	54	16	2.593	0.0	8.847	3.413	167.1 ± 26.9
7	413	133	28	3.105	0.0	14.914	4.803	199.7 ± 20.2
8	248	97	30	2.557	0.0	8.359	3.269	164.8 ± 20.0
9	189	56	12	3.375	0.0	15.925	4.719	216.7 ± 33.2
10	495	123	40	4.024	0.0	12.513	3.109	257.6 ± 26.4
11	734	183	60	4.011	0.0	12.369	3.084	256.7 ± 21.7
	2755	808			0.0	12.007	3.521	

AREA OF BASIC UNIT = 9.89E-07 cm
CHI SQUARED = 22.75318 WITH 10 DEGREES OF FREEDOM
P(chi squared) = 1.2 %
CORRELATION COEFFICIENT = 0.973
VARIANCE OF SQR(Ns) = 41.69
VARIANCE OF SQR(Ni) = 9.59

Ns/Ni = 3.410 ± 0.136
MEAN RATIO = 3.214 ± 0.221

Ages calculated using a zeta of 133.9 ± 1.4 for CN1 glass
RHO D = 9.754E+05 ; ND = 4824

POOLED AGE = 218.9 ± 9.6 Ma
MEAN AGE = 206.5 ± 14.7 Ma

8902-101 APATITE godley s80/122443 825m

IRRADIATION jmt data:jmt apatite data:godley apatites:wk013/4
SLIDE NUMBER 1
COUNTED BY: jmt

No.	Ns	NI	Na	RATIO	U (ppm)	RHOs (E+06)	RHOi (E+06)	F.T.AGE (Ma)
1	2	64	80	0.031	9.8	0.025	0.809	6.0 ± 4.3
2	0	36	20	0.000	22.1	0.000	1.820	0.0 ± 0.0
3	1	23	24	0.043	11.8	0.042	0.969	8.3 ± 8.5
4	1	26	30	0.038	10.7	0.034	0.876	7.3 ± 7.5
5	4	21	12	0.190	21.5	0.337	1.769	36.3 ± 19.8
6	2	33	24	0.061	16.9	0.084	1.390	11.6 ± 8.4
7	5	31	12	0.161	31.8	0.421	2.612	30.8 ± 14.8
8	10	138	18	0.072	94.3	0.562	7.752	13.8 ± 4.5
9	9	25	15	0.360	20.5	0.607	1.685	68.4 ± 26.6
10	0	37	50	0.000	9.1	0.000	0.748	0.0 ± 0.0
11	0	57	36	0.000	19.5	0.000	1.601	0.0 ± 0.0
12	16	83	24	0.193	42.5	0.674	3.497	36.7 ± 10.1
13	0	69	24	0.000	35.4	0.000	2.907	0.0 ± 0.0
14	1	19	20	0.053	11.7	0.051	0.961	10.0 ± 10.3
15	2	67	24	0.030	34.3	0.084	2.823	5.7 ± 4.1
16	5	30	60	0.167	6.1	0.084	0.506	31.8 ± 15.4
17	0	52	49	0.000	13.1	0.000	1.073	0.0 ± 0.0
18	11	343	60	0.032	70.3	0.185	5.780	6.1 ± 1.9
19	2	34	24	0.059	17.4	0.084	1.432	11.2 ± 8.2
20	2	87	25	0.023	42.8	0.081	3.519	4.4 ± 3.1
	73	1275			24.8	0.117	2.043	

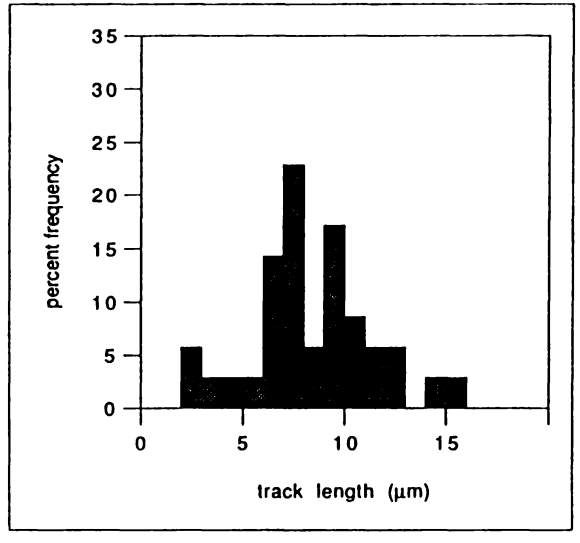
AREA OF BASIC UNIT = 9.89E-07 cm
CHI SQUARED = 89.78206 WITH 19 DEGREES OF FREEDOM
P(chi squared) = < 0.1 %
CORRELATION COEFFICIENT = 0.503
VARIANCE OF SQR(Ns) = 1.47
VARIANCE OF SQR(Ni) = 10.63

Ns/Ni = 0.057 ± 0.007
MEAN RATIO = 0.076 ± 0.021

Ages calculated using a zeta of 354.9 ± 4.3 for SRM612 glass
RHO D = 1.077E+06 ; ND = 2662

POOLED AGE = 10.9 ± 1.3 Ma
MEAN AGE = 14.4 ± 4.0 Ma

8902-101



n = 35
Mean = 8.40 µm
Sample std. dev. = 2.90 µm

8902-101 ZIRCON godley s80/122443 825m

IRRADIATION jmt data:jmt zircon data:godley zircons:wk026/15
SLIDE NUMBER 1
COUNTED BY: jmt

No.	Ns	Ni	Na	RATIO	U (ppm)	RHOs (E+06)	RHOi (E+06)	F.T.AGE (Ma)
1	163	39	15	4.179	0.0	10.988	2.629	264.9 ± 47.5
2	350	127	50	2.756	0.0	7.078	2.568	175.9 ± 18.5
3	78	25	6	3.120	0.0	13.145	4.213	198.8 ± 45.8
4	100	54	8	1.852	0.0	12.639	6.825	118.7 ± 20.2
5	93	35	6	2.657	0.0	15.672	5.898	169.7 ± 33.8
6	98	45	16	2.178	0.0	6.193	2.844	139.4 ± 25.2
7	62	18	4	3.444	0.0	15.672	4.550	219.1 ± 58.8
8	117	51	8	2.294	0.0	14.788	6.446	146.7 ± 24.8
9	69	21	6	3.286	0.0	11.628	3.539	209.2 ± 52.3
10	534	124	35	4.306	0.0	15.427	3.582	272.8 ± 27.6
11	120	41	8	2.927	0.0	15.167	5.182	186.6 ± 33.9
12	259	99	20	2.616	0.0	13.094	5.005	167.1 ± 20.0
13	74	28	6	2.643	0.0	12.471	4.719	168.8 ± 37.6
14	438	180	32	2.433	0.0	13.840	5.688	155.5 ± 14.0
	2555	887			0.0	11.743	4.077	

AREA OF BASIC UNIT = 9.89E-07 cm
CHI SQUARED = 37.79463 WITH 13 DEGREES OF FREEDOM
P(chi squared) = < 0.1 %
CORRELATION COEFFICIENT = 0.920
VARIANCE OF SQR(Ns) = 25.30
VARIANCE OF SQR(Ni) = 8.06

Ns/Ni = 2.880 ± 0.112
MEAN RATIO = 2.907 ± 0.190

Ages calculated using a zeta of 133.9 ± 1.4 for CN1 glass
RHO D = 9.664E+05 ; ND = 4779

POOLED AGE = 183.7 ± 7.9 Ma
MEAN AGE = 185.4 ± 12.5 Ma

8902-102 APATITE godley s80/133401 790m

IRRADIATION jmt data:jmt apatite data:godley apatites:wk013/3
SLIDE NUMBER 1
COUNTED BY: jmt

No.	Ns	NI	Na	RATIO	U (ppm)	RHOs (E+06)	RHOI (E+06)	F.T AGE (Ma)
1	6	13	9	0.462	18.0	0.674	1.461	86.6 ± 42.8
2	23	83	12	0.277	86.1	1.938	6.994	52.1 ± 12.3
3	0	3	4	0.000	9.3	0.000	0.758	0.0 ± 0.0
4	1	4	12	0.250	4.1	0.084	0.337	47.0 ± 52.6
5	1	10	12	0.100	10.4	0.084	0.843	18.9 ± 19.8
6	1	3	3	0.333	12.4	0.337	1.011	62.6 ± 72.3
7	1	6	6	0.167	12.4	0.169	1.011	31.4 ± 33.9
8	1	11	9	0.091	15.2	0.112	1.236	17.1 ± 17.9
9	0	4	6	0.000	8.3	0.000	0.674	0.0 ± 0.0
10	1	12	9	0.083	16.6	0.112	1.348	15.7 ± 16.4
11	0	9	15	0.000	7.5	0.000	0.607	0.0 ± 0.0
12	0	3	8	0.000	4.7	0.000	0.379	0.0 ± 0.0
13	0	2	20	0.000	1.2	0.000	0.101	0.0 ± 0.0
14	2	6	8	0.333	9.3	0.253	0.758	62.6 ± 51.2
15	9	70	9	0.129	96.8	1.011	7.864	24.2 ± 8.6
16	1	22	20	0.045	13.7	0.051	1.112	8.6 ± 8.8
17	4	56	15	0.071	46.5	0.270	3.775	13.5 ± 7.0
18	1	5	6	0.200	10.4	0.169	0.843	37.7 ± 41.3
19	6	51	12	0.118	52.9	0.506	4.297	22.2 ± 9.6
20	0	13	10	0.000	16.2	0.000	1.314	0.0 ± 0.0
	58	386			23.4	0.286	1.904	

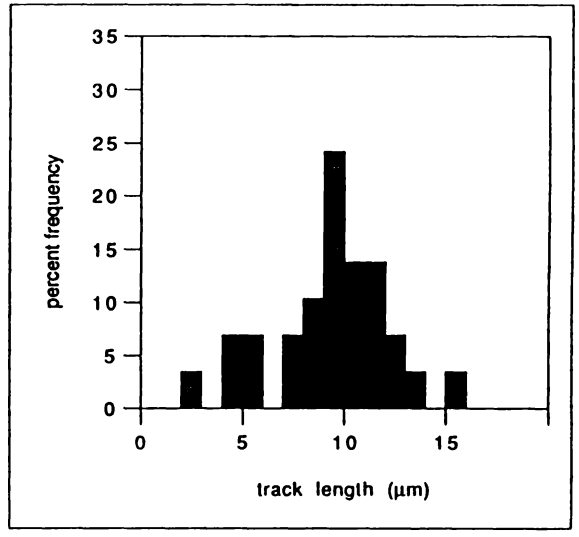
AREA OF BASIC UNIT = 9.89E-07 cm
CHI SQUARED = 24.53594 WITH 19 DEGREES OF FREEDOM
P(chi squared) = 17.6 %
CORRELATION COEFFICIENT = 0.846
VARIANCE OF SQR(Ns) = 1.52
VARIANCE OF SQR(Ni) = 5.63

Ns/Ni = 0.150 ± 0.021
MEAN RATIO = 0.133 ± 0.030

Ages calculated using a zeta of 354.9 ± 4.3 for SRM612 glass
RHO D = 1.064E+06 ; ND = 2631

POOLED AGE = 28.3 ± 4.0 Ma
MEAN AGE = 25.1 ± 5.8 Ma

8902-102



n = 29
Mean = 9.37 µm
Sample std. dev. = 2.74 µm

8902-102 ZIRCON godley s80/133401 790m

IRRADIATION jmt data:jmt zircon data:godley zircons:wk026/14
SLIDE NUMBER 1
COUNTED BY: jmt

No.	Ns	Ni	Na	RATIO	U (ppm)	RHOs (E+06)	RHOi (E+06)	F.T.AGE (Ma)
1	98	23	12	4.261	0.0	8.257	1.938	267.5 ± 62.2
2	72	24	8	3.000	0.0	9.100	3.033	189.5 ± 44.8
3	36	11	4	3.273	0.0	9.100	2.781	206.5 ± 71.2
4	36	11	3	3.273	0.0	12.133	3.707	206.5 ± 71.2
5	173	72	21	2.403	0.0	8.330	3.467	152.2 ± 21.5
	415	141			0.0	8.742	2.970	

AREA OF BASIC UNIT = 9.89E-07 cm
CHI SQUARED = 4.875312 WITH 4 DEGREES OF FREEDOM
P(chi squared) = 30.0 %
CORRELATION COEFFICIENT = 0.964
VARIANCE OF SQR(Ns) = 8.97
VARIANCE OF SQR(Ni) = 4.46

Ns/Ni = 2.943 ± 0.287
MEAN RATIO = 3.242 ± 0.300

Ages calculated using a zeta of 133.9 ± 1.4 for CN1 glass
RHO D = 9.575E+05 ; ND = 4735

POOLED AGE = 186.0 ± 18.4 Ma
MEAN AGE = 204.5 ± 19.3 Ma

8902-103 APATITE godley s80/155371 760m

IRRADIATION jmt data:jmt apatite data:godley apatites:wk013/2
SLIDE NUMBER 1
COUNTED BY: jmt

No.	Ns	Ni	Na	RATIO	U (ppm)	RHOs (E+06)	RHOi (E+06)	F.T.AGE (Ma)
1	11	63	35	0.175	22.7	0.318	1.820	32.5 ± 10.6
2	2	7	30	0.286	2.9	0.067	0.236	53.1 ± 42.6
3	5	54	16	0.093	42.5	0.316	3.413	17.3 ± 8.1
4	1	27	40	0.037	8.5	0.025	0.682	6.9 ± 7.0
5	13	19	30	0.684	8.0	0.438	0.640	126.5 ± 45.6
6	1	32	20	0.031	20.1	0.051	1.618	5.8 ± 5.9
7	8	20	9	0.400	28.0	0.899	2.247	74.2 ± 31.1
8	24	84	42	0.286	25.2	0.578	2.022	53.1 ± 12.4
9	21	51	12	0.412	53.5	1.769	4.297	76.4 ± 19.9
10	4	37	30	0.108	15.5	0.135	1.247	20.2 ± 10.6
11	2	12	15	0.167	10.1	0.135	0.809	31.0 ± 23.7
12	34	122	48	0.279	32.0	0.716	2.570	51.8 ± 10.1
13	19	42	35	0.452	15.1	0.549	1.213	83.9 ± 23.3
14	1	30	16	0.033	23.6	0.063	1.896	6.2 ± 6.3
15	16	91	48	0.176	23.9	0.337	1.917	32.7 ± 8.9
16	15	43	25	0.349	21.7	0.607	1.739	64.8 ± 19.5
17	1	10	12	0.100	10.5	0.084	0.843	18.6 ± 19.6
18	1	4	14	0.250	3.6	0.072	0.289	46.5 ± 52.0
19	16	61	21	0.262	36.6	0.770	2.937	48.8 ± 13.7
20	0	9	18	0.000	6.3	0.000	0.506	0.0 ± 0.0
	195	818			20.0	0.382	1.603	

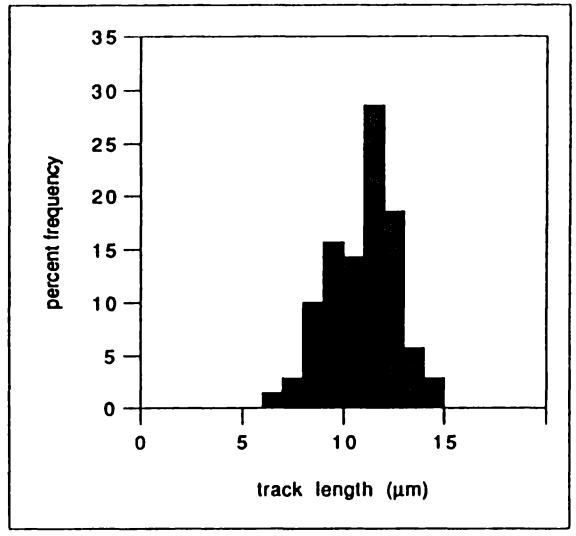
AREA OF BASIC UNIT = 9.89E-07 cm
CHI SQUARED = 51.34721 WITH 19 DEGREES OF FREEDOM
P(chi squared) = < 0.1 %
CORRELATION COEFFICIENT = 0.830
VARIANCE OF SQR(Ns) = 2.77
VARIANCE OF SQR(Ni) = 6.07

Ns/Ni = 0.238 ± 0.019
MEAN RATIO = 0.229 ± 0.039

Ages calculated using a zeta of 354.9 ± 4.3 for SRM612 glass
RHO D = 1.052E+06 ; ND = 2601

POOLED AGE = 44.3 ± 3.7 Ma
MEAN AGE = 42.6 ± 7.3 Ma

8902-103



n = 70
Mean = 10.97 µm
Sample std. dev. = 1.70 µm

8902-103 ZIRCON godley s80/155371 760m

IRRADIATION jmt data:jmt zircon data:godley zircons:wk026/13
SLIDE NUMBER 1
COUNTED BY: jmt

No.	Ns	Ni	Na	RATIO	U (ppm)	RHOs (E+06)	RHOi (E+06)	F.TAGE (Ma)
1	385	98	30	3.929	0.0	12.976	3.303	244.8 ± 28.0
2	114	25	9	4.560	0.0	12.808	2.809	283.3 ± 62.8
3	250	87	24	2.874	0.0	10.533	3.665	180.0 ± 22.6
4	32	8	8	4.000	0.0	4.044	1.011	249.2 ± 98.6
5	77	29	8	2.655	0.0	9.732	3.665	166.5 ± 36.4
6	423	117	30	3.615	0.0	14.257	3.943	225.6 ± 23.9
7	230	93	21	2.473	0.0	11.074	4.478	155.2 ± 19.3
8	212	74	14	2.865	0.0	15.311	5.344	179.4 ± 24.4
9	124	37	12	3.351	0.0	10.448	3.118	209.4 ± 39.4
10	147	52	16	2.827	0.0	9.290	3.286	177.1 ± 28.7
	1994	620			0.0	11.722	3.645	

AREA OF BASIC UNIT = 9.89E-07 cm
CHI SQUARED = 14.84032 WITH 9 DEGREES OF FREEDOM
P(chi squared) = 9.5 %
CORRELATION COEFFICIENT = 0.947
VARIANCE OF SQR(Ns) = 21.76
VARIANCE OF SQR(Ni) = 6.73

Ns/Ni = 3.216 ± 0.148
MEAN RATIO = 3.315 ± 0.218

Ages calculated using a zeta of 133.9 ± 1.4 for CN1 glass
RHO D = 9.486E+05 ; ND = 4691

POOLED AGE = 201.1 ± 9.9 Ma
MEAN AGE = 207.2 ± 14.1 Ma

8902-105 APATITE godley s89/085008 810m

IRRADIATION jmt data:jmt apatite data:godley apatites:wk014/16
SLIDE NUMBER 1
COUNTED BY: jmt

No.	Ns	NI	Na	RATIO	U (ppm)	RHOs (E+06)	RHOI (E+06)	F.T.AGE (Ma)
1	10	22	4	0.455	61.4	2.528	5.561	95.0 ± 36.3
2	2	10	6	0.200	18.6	0.337	1.685	42.0 ± 32.5
3	6	56	16	0.107	39.1	0.379	3.539	22.5 ± 9.7
4	14	46	20	0.304	25.7	0.708	2.326	63.8 ± 19.5
5	8	37	12	0.216	34.4	0.674	3.118	45.4 ± 17.7
6	10	28	16	0.357	19.5	0.632	1.769	74.8 ± 27.6
7	1	18	12	0.056	16.7	0.084	1.517	11.7 ± 12.0
8	8	45	14	0.178	35.9	0.578	3.250	37.3 ± 14.4
9	4	31	12	0.129	28.8	0.337	2.612	27.1 ± 14.4
10	28	79	8	0.354	110.2	3.539	9.985	74.2 ± 16.4
11	5	58	28	0.086	23.1	0.181	2.094	18.1 ± 8.5
12	1	6	12	0.167	5.6	0.084	0.506	35.0 ± 37.8
13	8	36	12	0.222	33.5	0.674	3.033	46.6 ± 18.3
14	9	44	15	0.205	32.7	0.607	2.966	42.9 ± 15.7
15	2	20	12	0.100	18.6	0.169	1.685	21.0 ± 15.6
16	11	80	28	0.138	31.9	0.397	2.889	28.9 ± 9.3
17	9	18	8	0.500	25.1	1.138	2.275	104.5 ± 42.7
18	13	31	12	0.419	28.8	1.095	2.612	87.7 ± 29.1
19	6	32	4	0.188	89.3	1.517	8.089	39.4 ± 17.5
20	14	35	12	0.400	32.5	1.180	2.949	83.7 ± 26.5
	169	732			31.1	0.650	2.814	

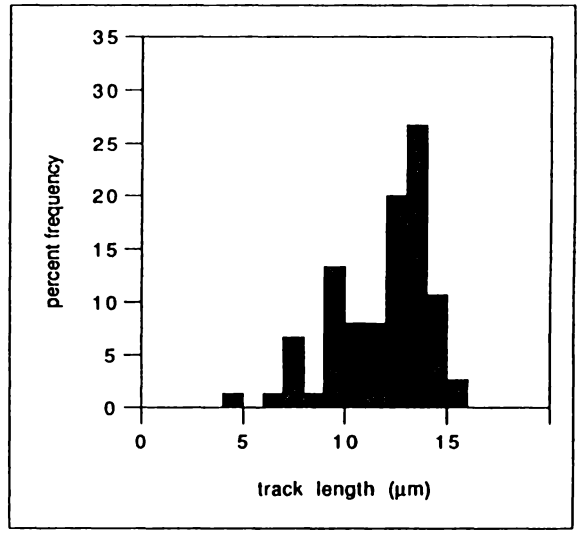
AREA OF BASIC UNIT = 9.89E-07 cm
CHI SQUARED = 36.2691 WITH 19 DEGREES OF FREEDOM
P(chi squared) = 1.0 %
CORRELATION COEFFICIENT = 0.627
VARIANCE OF SQR(Ns) = 1.09
VARIANCE OF SQR(Ni) = 2.87

Ns/Ni = 0.231 ± 0.020
MEAN RATIO = 0.239 ± 0.030

Ages calculated using a zeta of 354.9 ± 4.3 for SRM612 glass
RHO D = 1.187E+06 ; ND = 2936

POOLED AGE = 48.4 ± 4.3 Ma
MEAN AGE = 50.1 ± 6.3 Ma

8902-105



n = 75
Mean = 11.88 µm
Sample std. dev. = 2.31 µm

8902-105 ZIRCON godley s89/085008 810m

IRRADIATION jmt data:jmt zircon data:godley zircons:wk026/11
SLIDE NUMBER 1
COUNTED BY: jmt

No.	Ns	Ni	Na	RATIO	U (ppm)	RHOs (E+06)	RHOi (E+06)	F.T.AGE (Ma)
1	150	32	20	4.688	0.0	7.583	1.618	285.7 ± 55.9
2	701	273	50	2.568	0.0	14.176	5.521	158.1 ± 11.6
3	57	23	9	2.478	0.0	6.404	2.584	152.6 ± 37.8
4	219	74	20	2.959	0.0	11.072	3.741	181.8 ± 24.7
5	76	31	9	2.452	0.0	8.538	3.483	151.0 ± 32.3
6	134	34	20	3.941	0.0	6.775	1.719	241.0 ± 46.5
7	156	63	12	2.476	0.0	13.145	5.308	152.5 ± 22.9
8	153	91	20	1.681	0.0	7.735	4.601	103.9 ± 13.9
9	109	48	8	2.271	0.0	13.777	6.067	140.0 ± 24.4
10	63	24	8	2.625	0.0	7.963	3.033	161.5 ± 38.9
11	194	91	16	2.132	0.0	12.260	5.751	131.5 ± 16.9
12	127	45	18	2.822	0.0	7.134	2.528	173.5 ± 30.3
13	202	75	24	2.693	0.0	8.510	3.160	165.7 ± 22.6
14	373	126	30	2.960	0.0	12.572	4.247	181.9 ± 19.0
15	106	39	9	2.718	0.0	11.909	4.382	167.2 ± 31.5
16	179	65	18	2.754	0.0	10.055	3.651	169.4 ± 24.7
17	190	64	15	2.969	0.0	12.808	4.314	182.4 ± 26.6
18	171	63	24	2.714	0.0	7.204	2.654	167.0 ± 24.8
	3360	1261			0.0	10.295	3.864	

AREA OF BASIC UNIT = 9.89E-07 cm
CHI SQUARED = 32.27409 WITH 17 DEGREES OF FREEDOM
P(chi squared) = 1.4 %
CORRELATION COEFFICIENT = 0.975
VARIANCE OF SQR(Ns) = 18.92
VARIANCE OF SQR(Ni) = 7.67

Ns/Ni = 2.665 ± 0.088
MEAN RATIO = 2.772 ± 0.155

Ages calculated using a zeta of 133.9 ± 1.4 for CN1 glass
RHO D = 9.308E+05 ; ND = 4603

POOLED AGE = 163.9 ± 6.2 Ma
MEAN AGE = 170.5 ± 10.0 Ma

8902-106 APATITE godley s101/208884 715m

IRRADIATION jmt data:jmt apatite data:godley apatites:wk014/15
SLIDE NUMBER 1
COUNTED BY: jmt

No.	Ns	NI	Na	RATIO	U (ppm)	RHOs (E+06)	RHOi (E+06)	F.TAGE (Ma)
1	50	133	25	0.376	59.8	2.022	5.379	78.1 ± 13.1
2	1	5	8	0.200	7.0	0.126	0.632	41.7 ± 45.7
3	1	6	8	0.167	8.4	0.126	0.758	34.7 ± 37.5
4	25	44	10	0.568	49.5	2.528	4.449	117.7 ± 29.6
5	1	13	20	0.077	7.3	0.051	0.657	16.1 ± 16.7
6	2	18	12	0.111	16.9	0.169	1.517	23.2 ± 17.3
7	4	47	16	0.085	33.0	0.253	2.970	17.8 ± 9.3
8	10	17	25	0.588	7.6	0.404	0.688	121.8 ± 48.6
9	2	6	8	0.333	8.4	0.253	0.758	69.3 ± 56.6
10	9	23	8	0.391	32.3	1.138	2.907	81.3 ± 32.0
11	6	17	8	0.353	23.9	0.758	2.149	73.4 ± 34.9
12	1	6	16	0.167	4.2	0.063	0.379	34.7 ± 37.5
13	16	159	25	0.101	71.5	0.647	6.431	21.0 ± 5.5
14	11	27	15	0.407	20.2	0.741	1.820	84.6 ± 30.3
15	2	19	8	0.105	26.7	0.253	2.401	22.0 ± 16.3
16	10	38	12	0.263	35.6	0.843	3.202	54.8 ± 19.5
17	2	11	9	0.182	13.7	0.225	1.236	37.9 ± 29.1
18	7	42	10	0.167	47.2	0.708	4.247	34.7 ± 14.2
19	2	32	15	0.062	24.0	0.135	2.157	13.1 ± 9.5
20	6	39	16	0.154	27.4	0.379	2.465	32.1 ± 14.1
	168	702			28.8	0.620	2.591	

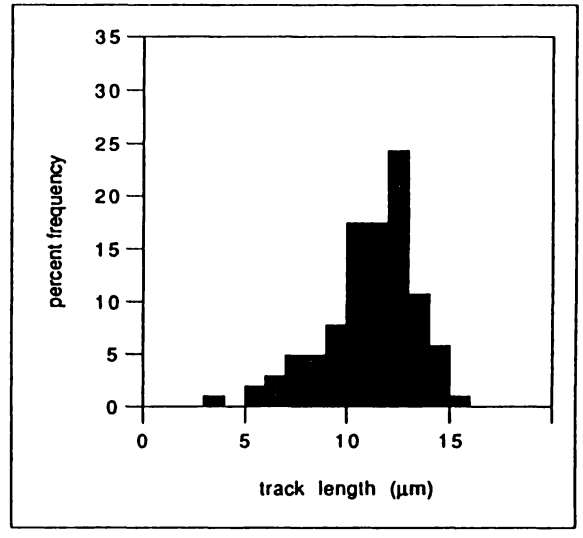
AREA OF BASIC UNIT = 9.89E-07 cm
CHI SQUARED = 56.23171 WITH 19 DEGREES OF FREEDOM
P(chi squared) = < 0.1 %
CORRELATION COEFFICIENT = 0.728
VARIANCE OF SQR(Ns) = 2.44
VARIANCE OF SQR(Ni) = 7.64

Ns/Ni = 0.239 ± 0.021
MEAN RATIO = 0.243 ± 0.036

Ages calculated using a zeta of 354.9 ± 4.3 for SRM612 glass
RHO D = 1.178E+06 ; ND = 2912

POOLED AGE = 49.8 ± 4.4 Ma
MEAN AGE = 50.6 ± 7.5 Ma

8902-106



n = 103
Mean = 11.16 µm
Sample std. dev. = 2.26 µm

8902-106 ZIRCON godley s101/208884 715m

IRRADIATION jmt data:jmt zircon data:godley zircons:wk026/10
SLIDE NUMBER 1
COUNTED BY: jmt

No.	Ns	Ni	Na	RATIO	U (ppm)	RHOs (E+06)	RHOi (E+06)	F.T AGE (Ma)
1	54	15	6	3.600	0.0	9.100	2.528	218.5 ± 63.9
2	40	23	6	1.739	0.0	6.741	3.876	106.5 ± 27.9
3	64	31	6	2.065	0.0	10.785	5.224	126.2 ± 27.7
4	67	20	6	3.350	0.0	11.291	3.370	203.5 ± 52.0
5	147	62	15	2.371	0.0	9.909	4.179	144.7 ± 22.1
6	72	23	9	3.130	0.0	8.089	2.584	190.4 ± 45.7
7	39	30	3	1.300	0.0	13.145	10.111	79.7 ± 19.4
8	95	22	6	4.318	0.0	16.009	3.707	261.2 ± 62.0
9	68	47	9	1.447	0.0	7.640	5.280	88.7 ± 16.9
10	109	54	12	2.019	0.0	9.184	4.550	123.4 ± 20.7
11	54	17	5	3.176	0.0	10.920	3.438	193.1 ± 53.8
12	149	51	10	2.922	0.0	15.066	5.157	177.8 ± 29.0
13	71	38	12	1.868	0.0	5.982	3.202	114.3 ± 23.1
14	150	36	15	4.167	0.0	10.111	2.427	252.2 ± 47.0
15	57	23	6	2.478	0.0	9.606	3.876	151.2 ± 37.4
16	196	86	8	2.279	0.0	24.772	10.870	139.2 ± 18.2
	1432	578			0.0	10.805	4.361	

AREA OF BASIC UNIT = 9.89E-07 cm
CHI SQUARED = 41.63525 WITH 15 DEGREES OF FREEDOM
P(chi squared) = < 0.1 %
CORRELATION COEFFICIENT = 0.819
VARIANCE OF SQR(Ns) = 5.52
VARIANCE OF SQR(Ni) = 2.30

Ns/Ni = 2.478 ± 0.122
MEAN RATIO = 2.639 ± 0.231

Ages calculated using a zeta of 133.9 ± 1.4 for CN1 glass
RHO D = 9.219E+05 ; ND = 4559

POOLED AGE = 151.1 ± 7.9 Ma
MEAN AGE = 160.9 ± 14.4 Ma

8902-107 APATITE godley s101/312958 440m

IRRADIATION jmt data:jmt apatite data:godley apatites:wk014/14
SLIDE NUMBER 1
COUNTED BY: jmt

No.	Ns	Ni	Na	RATIO	U (ppm)	RHOs (E+06)	RHOi (E+06)	F.T.AGE (Ma)
1	0	1	4	0.000	2.8	0.000	0.253	0.0 ± 0.0
2	1	10	4	0.100	28.4	0.253	2.528	20.7 ± 21.7
3	0	1	15	0.000	0.8	0.000	0.067	0.0 ± 0.0
4	0	1	12	0.000	0.9	0.000	0.084	0.0 ± 0.0
5	0	1	4	0.000	2.8	0.000	0.253	0.0 ± 0.0
6	6	17	6	0.353	32.1	1.011	2.865	72.7 ± 34.6
7	11	34	12	0.324	32.1	0.927	2.865	66.7 ± 23.2
8	0	1	15	0.000	0.8	0.000	0.067	0.0 ± 0.0
9	1	13	4	0.077	36.9	0.253	3.286	15.9 ± 16.5
10	0	1	5	0.000	2.3	0.000	0.202	0.0 ± 0.0
11	10	36	12	0.278	34.0	0.843	3.033	57.3 ± 20.5
12	1	4	6	0.250	7.6	0.169	0.674	51.6 ± 57.7
13	1	4	6	0.250	7.6	0.169	0.674	51.6 ± 57.7
14	0	4	10	0.000	4.5	0.000	0.404	0.0 ± 0.0
15	0	1	25	0.000	0.5	0.000	0.040	0.0 ± 0.0
	31	129			10.4	0.224	0.932	

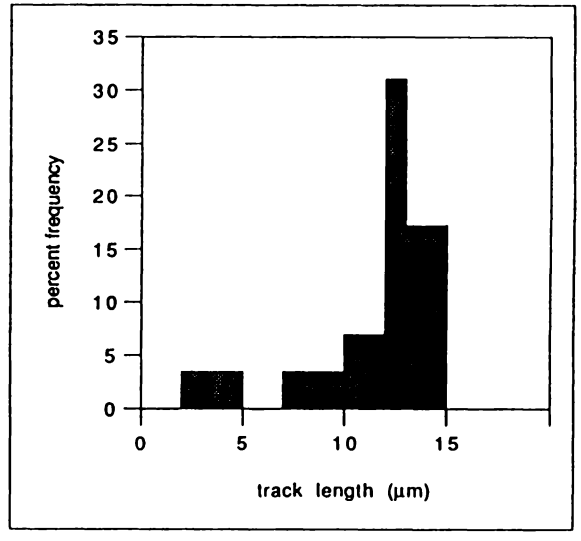
AREA OF BASIC UNIT = 9.89E-07 cm
CHI SQUARED = 6.299858 WITH 14 DEGREES OF FREEDOM
P(chi squared) = 95.8 %
CORRELATION COEFFICIENT = 0.967
VARIANCE OF SQR(Ns) = 1.42
VARIANCE OF SQR(Ni) = 3.14

Ns/Ni = 0.240 ± 0.048
MEAN RATIO = 0.109 ± 0.036

Ages calculated using a zeta of 354.9 ± 4.3 for SRM612 glass
RHO D = 1.168E+06 ; ND = 2888

POOLED AGE = 49.6 ± 10.0 Ma
MEAN AGE = 22.5 ± 7.4 Ma

8902-107



n = 29
Mean = 11.44 µm
Sample std. dev. = 3.13 µm

8902-107 ZIRCON godley s101/312958 440m

IRRADIATION jmt data:jmt zircon data:godley zircons:wk026/9
SLIDE NUMBER 1
COUNTED BY: jmt

No.	Ns	Ni	Na	RATIO	U (ppm)	RHOs (E+06)	RHOi (E+06)	F.T.AGE (Ma)
1	18	11	3	1.636	0.0	6.067	3.707	99.3 ± 38.0
2	37	27	12	1.370	0.0	3.118	2.275	83.2 ± 21.1
3	27	14	4	1.929	0.0	6.825	3.539	116.8 ± 38.5
	82	52			0.0	4.364	2.767	

AREA OF BASIC UNIT = 9.89E-07 cm
CHI SQUARED = .6923931 WITH 2 DEGREES OF FREEDOM
P(chi squared) = 70.7 %
CORRELATION COEFFICIENT = 0.950
VARIANCE OF SQR(Ns) = 0.85
VARIANCE OF SQR(Ni) = 0.97

Ns/Ni = 1.577 ± 0.280
MEAN RATIO = 1.645 ± 0.161

Ages calculated using a zeta of 133.9 ± 1.4 for CN1 glass
RHO D = 9.130E+05 ; ND = 4515

POOLED AGE = 95.7 ± 17.0 Ma
MEAN AGE = 99.8 ± 9.9 Ma

8902-108 APATITE godley s90/461093 490m

IRRADIATION jmt data:jmt apatite data:godley apatites:wk014/13
SLIDE NUMBER 1
COUNTED BY: jmt

No.	Ns	Ni	Na	RATIO	U (ppm)	RHOs (E+06)	RHOi (E+06)	F.T.AGE (Ma)
1	10	16	20	0.625	9.2	0.506	0.809	127.2 ± 51.3
2	11	39	12	0.282	37.2	0.927	3.286	57.7 ± 19.7
3	0	1	12	0.000	1.0	0.000	0.084	0.0 ± 0.0
4	10	38	16	0.263	27.2	0.632	2.401	53.8 ± 19.2
5	0	11	15	0.000	8.4	0.000	0.741	0.0 ± 0.0
6	51	159	18	0.321	101.0	2.865	8.932	65.6 ± 10.6
7	16	77	15	0.208	58.7	1.079	5.190	42.6 ± 11.7
	98	341			36.1	0.917	3.193	

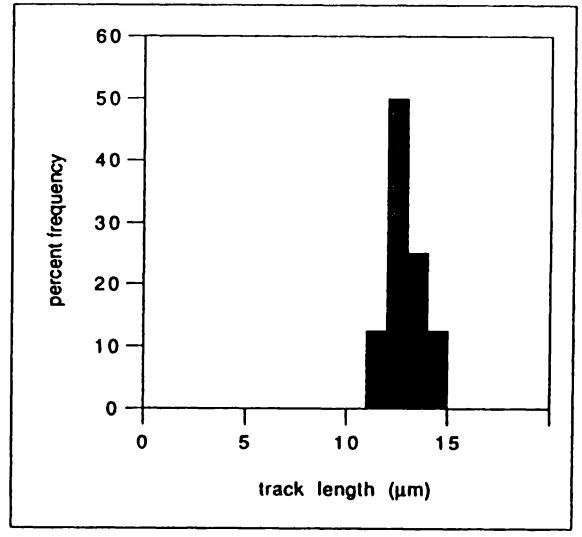
AREA OF BASIC UNIT = 9.89E-07 cm
CHI SQUARED = 9.290011 WITH 6 DEGREES OF FREEDOM
P(chi squared) = 15.8 %
CORRELATION COEFFICIENT = 0.973
VARIANCE OF SQR(Ns) = 6.05
VARIANCE OF SQR(Ni) = 14.61

Ns/Ni = 0.287 ± 0.033
MEAN RATIO = 0.243 ± 0.081

Ages calculated using a zeta of 354.9 ± 3.3 for SRM612 glass
RHO D = 1.158E+06 ; ND = 2864

POOLED AGE = 58.8 ± 6.8 Ma
MEAN AGE = 49.7 ± 16.5 Ma

8902-108



n = 8
Mean = 12.83 µm
Sample std. dev. = 0.85 µm

8902-108 ZIRCON godley s90/461093 490m

IRRADIATION jmt data:jmt zircon data:godley zircons:wk026/8
SLIDE NUMBER 1
COUNTED BY: jmt

No.	Ns	Ni	Na	RATIO	U (ppm)	RHOs (E+06)	RHOi (E+06)	F.T.AGE (Ma)
1	38	14	4	2.714	0.0	9.606	3.539	162.2 ± 50.8
2	81	22	9	3.682	0.0	9.100	2.472	219.1 ± 52.8
3	53	13	6	4.077	0.0	8.932	2.191	242.2 ± 75.1
4	45	9	6	5.000	0.0	7.583	1.517	295.8 ± 108.1
5	15	4	4	3.750	0.0	3.792	1.011	223.1 ± 125.6
6	308	71	28	4.338	0.0	11.122	2.564	257.4 ± 34.2
7	59	14	6	4.214	0.0	9.943	2.359	250.2 ± 74.5
	599	147			0.0	9.614	2.359	

AREA OF BASIC UNIT = 9.89E-07 cm
CHI SQUARED = 2.466196 WITH 6 DEGREES OF FREEDOM
P(chi squared) = 87.2 %
CORRELATION COEFFICIENT = 0.995
VARIANCE OF SQR(Ns) = 19.03
VARIANCE OF SQR(Ni) = 4.19

Ns/Ni = 4.075 ± 0.375
MEAN RATIO = 3.968 ± 0.266

Ages calculated using a zeta of 133.9 ± 1.4 for CN1 glass
RHO D = 9.041E+05 ; ND = 4471

POOLED AGE = 242.0 ± 22.7 Ma
MEAN AGE = 235.8 ± 16.4 Ma

8902-109 APATITE godley s101/472932 395m

IRRADIATION jmt data:jmt apatite data:godley apatites:wk014/12
SLIDE NUMBER 1
COUNTED BY: jmt

No.	Ns	Ni	Na	RATIO	U (ppm)	RHOs (E+06)	RHOi (E+06)	F.T.AGE (Ma)
1	4	14	6	0.286	26.9	0.674	2.359	57.9 ± 32.9
2	13	77	12	0.169	74.0	1.095	6.488	34.3 ± 10.3
3	8	17	6	0.471	32.7	1.348	2.865	95.2 ± 40.9
4	1	9	6	0.111	17.3	0.169	1.517	22.6 ± 23.8
5	5	21	20	0.238	12.1	0.253	1.062	48.3 ± 24.1
6	2	14	12	0.143	13.5	0.169	1.180	29.0 ± 22.0
7	14	39	16	0.359	28.1	0.885	2.465	72.7 ± 22.7
8	0	1	6	0.000	1.9	0.000	0.169	0.0 ± 0.0
9	1	19	12	0.053	18.3	0.084	1.601	10.7 ± 11.0
10	1	3	12	0.333	2.9	0.084	0.253	67.5 ± 78.0
11	16	80	12	0.200	76.9	1.348	6.741	40.6 ± 11.2
12	0	2	10	0.000	2.3	0.000	0.202	0.0 ± 0.0
13	4	47	20	0.085	27.1	0.202	2.376	17.3 ± 9.0
14	26	97	12	0.268	93.3	2.191	8.173	54.4 ± 12.1
15	9	47	12	0.191	45.2	0.758	3.960	38.9 ± 14.2
16	0	8	16	0.000	5.8	0.000	0.506	0.0 ± 0.0
17	11	43	8	0.256	62.0	1.390	5.435	51.9 ± 17.6
18	18	50	9	0.360	64.1	2.022	5.617	72.9 ± 20.1
19	8	20	9	0.400	25.6	0.899	2.247	81.0 ± 33.9
20	1	4	9	0.250	5.1	0.112	0.449	50.7 ± 56.7
	142	612			31.4	0.638	2.750	

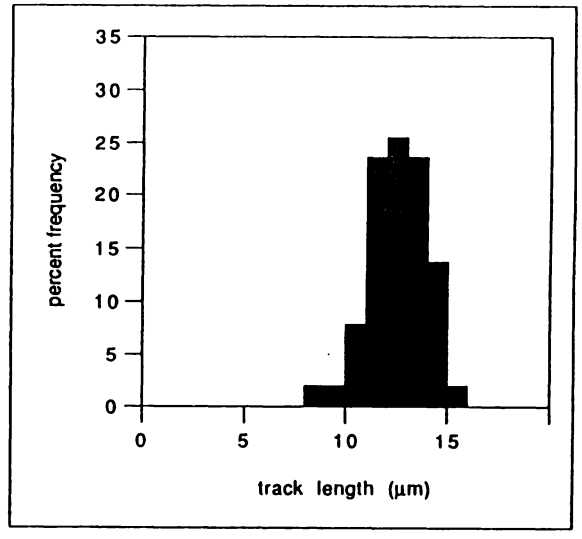
AREA OF BASIC UNIT = 9.89E-07 cm
CHI SQUARED = 21.63747 WITH 19 DEGREES OF FREEDOM
P(chi squared) = 30.3 %
CORRELATION COEFFICIENT = 0.892
VARIANCE OF SQR(Ns) = 2.31
VARIANCE OF SQR(Ni) = 6.86

Ns/Ni = 0.232 ± 0.022
MEAN RATIO = 0.209 ± 0.031

Ages calculated using a zeta of 354.9 ± 4.3 for SRM612 glass
RHO D = 1.148E+06 ; ND = 2839

POOLED AGE = 47.1 ± 4.5 Ma
MEAN AGE = 42.4 ± 6.4 Ma

8902-109



n = 51
Mean = 12.57 µm
Sample std. dev. = 1.38 µm

8902-109 ZIRCON godley s101/472932 395m

IRRADIATION jmt data:jmt zircon data:godley zircons:wk026/7
SLIDE NUMBER 1
COUNTED BY: jmt

No.	Ns	Ni	Na	RATIO	U (ppm)	RHOs (E+06)	RHOi (E+06)	F.T.AGE (Ma)
1	130	28	12	4.643	0.0	10.954	2.359	272.4 ± 57.0
2	17	6	2	2.833	0.0	8.595	3.033	167.6 ± 79.7
3	74	22	8	3.364	0.0	9.353	2.781	198.5 ± 48.3
4	66	52	6	1.269	0.0	11.122	8.763	75.6 ± 14.1
5	50	18	4	2.778	0.0	12.639	4.550	164.4 ± 45.3
6	56	26	5	2.154	0.0	11.325	5.258	127.8 ± 30.4
7	75	32	8	2.344	0.0	9.479	4.044	139.0 ± 29.5
8	70	23	6	3.043	0.0	11.796	3.876	179.9 ± 43.4
9	221	54	16	4.093	0.0	13.966	3.413	240.7 ± 36.8
10	117	20	9	5.850	0.0	13.145	2.247	341.4 ± 82.8
11	215	62	18	3.468	0.0	12.077	3.483	204.6 ± 29.7
	1091	343			0.0	11.735	3.690	

AREA OF BASIC UNIT = 9.89E-07 cm
CHI SQUARED = 44.56071 WITH 10 DEGREES OF FREEDOM
P(chi squared) = < 0.1 %
CORRELATION COEFFICIENT = 0.761
VARIANCE OF SQR(Ns) = 10.44
VARIANCE OF SQR(Ni) = 2.51

Ns/Ni = 3.181 ± 0.197
MEAN RATIO = 3.258 ± 0.380

Ages calculated using a zeta of 133.9 ± 1.4 for CN1 glass
RHO D = 8.952E+05 ; ND = 4427

POOLED AGE = 187.9 ± 12.1 Ma
MEAN AGE = 192.4 ± 22.7 Ma

8902-110 APATITE godley s102/636846 200m

IRRADIATION jmt data:jmt apatite data:godley apatites:wk014/11
SLIDE NUMBER 1
COUNTED BY: jmt

No.	Ns	NI	Na	RATIO	U (ppm)	RHOs (E+06)	RHOi (E+06)	F.T.AGE (Ma)
1	6	19	6	0.316	36.8	1.011	3.202	63.5 ± 29.8
2	13	43	15	0.302	33.3	0.876	2.899	60.8 ± 19.3
3	1	7	9	0.143	9.0	0.112	0.786	28.8 ± 30.8
4	8	23	6	0.348	44.6	1.348	3.876	69.9 ± 28.7
5	1	9	8	0.111	13.1	0.126	1.138	22.4 ± 23.6
6	5	19	8	0.263	27.6	0.632	2.401	53.0 ± 26.6
7	6	29	15	0.207	22.5	0.404	1.955	41.7 ± 18.7
8	11	65	12	0.169	63.0	0.927	5.477	34.1 ± 11.1
	51	214			31.5	0.653	2.739	

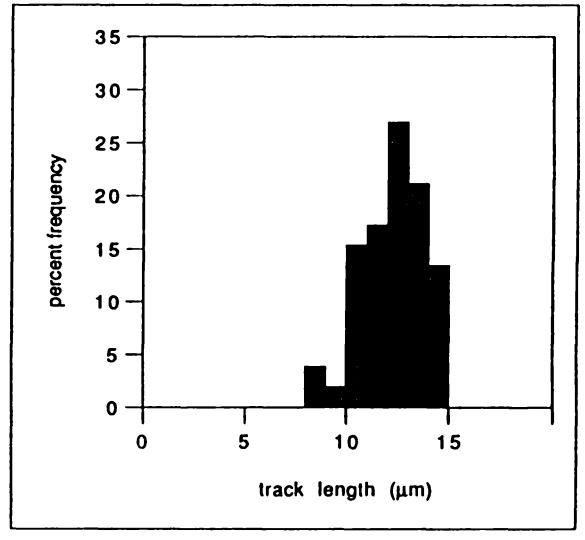
AREA OF BASIC UNIT = 9.89E-07 cm
CHI SQUARED = 3.826035 WITH 7 DEGREES OF FREEDOM
P(chi squared) = 80.0 %
CORRELATION COEFFICIENT = 0.859
VARIANCE OF SQR(Ns) = 0.92
VARIANCE OF SQR(Ni) = 3.18

Ns/Ni = 0.238 ± 0.037
MEAN RATIO = 0.232 ± 0.031

Ages calculated using a zeta of 354.9 ± 4.3 for SRM612 glass
RHO D = 1.139E+06 ; ND = 2815

POOLED AGE = 48.0 ± 7.6 Ma
MEAN AGE = 46.8 ± 6.3 Ma

8902-110



n = 52
Mean = 12.21 µm
Sample std. dev. = 1.50 µm

8902-110 ZIRCON godley s102/636846 200m

IRRADIATION jmt data:jmt zircon data:godley zircons:wk026/6
SLIDE NUMBER 1
COUNTED BY: jmt

No.	Ns	Ni	Na	RATIO	U (ppm)	RHOs (E+06)	RHOi (E+06)	F.T.AGE (Ma)
1	83	19	6	4.368	0.0	13.987	3.202	254.1 ± 64.8
2	79	39	9	2.026	0.0	8.875	4.382	119.1 ± 23.4
3	79	24	6	3.292	0.0	13.313	4.044	192.4 ± 45.0
4	104	43	14	2.419	0.0	7.511	3.106	141.9 ± 25.9
5	68	22	6	3.091	0.0	11.459	3.707	180.8 ± 44.5
6	36	10	3	3.600	0.0	12.133	3.370	210.2 ± 75.2
7	97	28	9	3.464	0.0	10.898	3.146	202.4 ± 43.6
8	99	43	9	2.302	0.0	11.122	4.831	135.2 ± 24.8
9	78	35	6	2.229	0.0	13.145	5.898	130.9 ± 26.7
10	160	59	12	2.712	0.0	13.482	4.971	158.9 ± 24.4
11	39	20	8	1.950	0.0	4.929	2.528	114.7 ± 31.6
12	105	61	12	1.721	0.0	8.847	5.140	101.3 ± 16.4
	1027	403			0.0	10.384	4.075	

AREA OF BASIC UNIT = 9.89E-07 cm
CHI SQUARED = 18.7879 WITH 11 DEGREES OF FREEDOM
P(chi squared) = 6.5 %
CORRELATION COEFFICIENT = 0.824
VARIANCE OF SQR(Ns) = 3.19
VARIANCE OF SQR(Ni) = 1.97

Ns/Ni = 2.548 ± 0.150
MEAN RATIO = 2.764 ± 0.231

Ages calculated using a zeta of 133.9 ± 1.4 for CN1 glass
RHO D = 8.863E+05 ; ND = 4383

POOLED AGE = 149.5 ± 9.2 Ma
MEAN AGE = 162.0 ± 13.9 Ma

8902-111 APATITE clyde s72/354753 915m

IRRADIATION jmt data:jmt apatite data:clyde apatites:wk014/10
SLIDE NUMBER 1
COUNTED BY: jmt

No.	Ns	Ni	Na	RATIO	U (ppm)	RHOs (E+06)	RHOi (E+06)	F.T.AGE (Ma)
1	0	62	24	0.000	30.3	0.000	2.612	0.0 ± 0.0
2	0	69	20	0.000	40.5	0.000	3.488	0.0 ± 0.0
3	0	77	35	0.000	25.8	0.000	2.224	0.0 ± 0.0
4	0	110	20	0.000	64.5	0.000	5.561	0.0 ± 0.0
5	0	32	35	0.000	10.7	0.000	0.924	0.0 ± 0.0
6	0	28	20	0.000	16.4	0.000	1.416	0.0 ± 0.0
7	0	57	20	0.000	33.4	0.000	2.882	0.0 ± 0.0
8	0	37	16	0.000	27.1	0.000	2.338	0.0 ± 0.0
9	0	22	24	0.000	10.8	0.000	0.927	0.0 ± 0.0
10	0	12	24	0.000	5.9	0.000	0.506	0.0 ± 0.0
11	0	26	18	0.000	16.9	0.000	1.461	0.0 ± 0.0
12	0	50	18	0.000	32.6	0.000	2.809	0.0 ± 0.0
13	0	107	25	0.000	50.2	0.000	4.328	0.0 ± 0.0
14	1	51	9	0.020	66.5	0.112	5.730	3.9 ± 4.0
15	0	81	48	0.000	19.8	0.000	1.706	0.0 ± 0.0
	1	821			27.1	0.003	2.332	

AREA OF BASIC UNIT = 9.89E-07 cm
CHI SQUARED = 14.82573 WITH 14 DEGREES OF FREEDOM
P(chi squared) = 39.0 %
CORRELATION COEFFICIENT = -0.035
VARIANCE OF SQR(Ns) = 0.07
VARIANCE OF SQR(Ni) = 4.29

Ns/Ni = 0.001 ± 0.001
MEAN RATIO = 0.001 ± 0.001

Ages calculated using a zeta of 354.9 ± 4.3 for SRM612 glass
RHO D = 1.129E+06 ; ND = 2791

POOLED AGE = 0.2 ± 0.2 Ma
MEAN AGE = 0.3 ± 0.3 Ma

8902-111 ZIRCON clyde s72/354753 915m

IRRADIATION jmt data:jmt zircon data:clyde zircons:wk026/5
SLIDE NUMBER 1
COUNTED BY: jmt

No.	Ns	Ni	Na	RATIO	U (ppm)	RHOs (E+06)	RHOi (E+06)	F.T.AGE (Ma)
1	420	132	36	3.182	0.0	11.796	3.707	184.2 ± 18.7
2	238	79	25	*3.013*	*0.0*	*9.626*	*3.195*	*174.6 ± 22.9*
3	907	398	75	2.279	0.0	12.228	5.366	132.5 ± 8.3
4	173	92	15	1.880	0.0	11.662	6.202	109.5 ± 14.3
5	82	22	9	3.727	0.0	9.212	2.472	215.3 ± 51.8
6	181	51	21	3.549	0.0	8.715	2.456	205.2 ± 32.7
7	415	158	30	2.627	0.0	13.987	5.325	152.5 ± 14.5
8	134	37	15	3.622	0.0	9.033	2.494	209.3 ± 39.1
9	282	96	30	2.938	0.0	9.505	3.236	170.3 ± 20.4
10	148	46	16	3.217	0.0	9.353	2.907	186.3 ± 31.6
11	211	51	20	4.137	0.0	10.667	2.578	238.5 ± 37.5
12	92	38	12	2.421	0.0	7.752	3.202	140.7 ± 27.2
13	74	40	9	1.850	0.0	8.314	4.494	107.8 ± 21.2
14	117	70	12	1.671	0.0	9.858	5.898	97.4 ± 14.8
15	167	43	15	3.884	0.0	11.257	2.899	224.2 ± 38.6
16	89	36	12	2.472	0.0	7.499	3.033	143.6 ± 28.5
17	363	106	25	3.425	0.0	14.682	4.287	198.1 ± 22.2
18	799	282	64	2.833	0.0	12.623	4.455	164.3 ± 11.8
19	185	73	20	2.534	0.0	9.353	3.691	147.2 ± 20.5
20	50	17	6	2.941	0.0	8.426	2.865	170.5 ± 48.0
21	35	16	9	2.188	0.0	3.932	1.798	127.2 ± 38.5
22	244	64	20	3.812	0.0	12.336	3.236	220.1 ± 31.2
23	47	18	6	2.611	0.0	7.920	3.033	151.6 ± 42.1
24	107	35	12	3.057	0.0	9.016	2.949	177.1 ± 34.6
25	208	80	15	2.600	0.0	14.021	5.393	150.9 ± 20.0
26	343	129	30	2.659	0.0	11.560	4.348	154.3 ± 16.2
27	93	51	15	1.824	0.0	6.269	3.438	106.2 ± 18.6
	6204	2260			0.0	10.929	3.981	

AREA OF BASIC UNIT = 9.89E-07 cm
CHI SQUARED = 72.8567 WITH 26 DEGREES OF FREEDOM
P(chi squared) = < 0.1 %
CORRELATION COEFFICIENT = 0.974
VARIANCE OF SQR(Ns) = 35.28
VARIANCE OF SQR(Ni) = 13.59

Ns/Ni = 2.745 ± 0.067
MEAN RATIO = 2.850 ± 0.130

Ages calculated using a zeta of 133.9 ± 1.4 for CN1 glass
RHO D = 8.773E+05 ; ND = 4338

POOLED AGE = 159.3 ± 4.9 Ma
MEAN AGE = 165.3 ± 8.2 Ma

8902-112 APATITE clyde s72/366735 855m

IRRADIATION jmt data:jmt apatite data:clyde apatites:wk014/9
SLIDE NUMBER 1
COUNTED BY: jmt

No.	Ns	Ni	Na	RATIO	U (ppm)	RHOs (E+06)	RHOi (E+06)	F.T.AGE (Ma)
1	0	11	9	0.000	14.5	0.000	1.236	0.0 ± 0.0
2	0	18	18	0.000	11.8	0.000	1.011	0.0 ± 0.0
3	0	30	16	0.000	22.2	0.000	1.896	0.0 ± 0.0
4	0	4	18	0.000	2.6	0.000	0.225	0.0 ± 0.0
5	0	13	6	0.000	25.6	0.000	2.191	0.0 ± 0.0
6	0	7	6	0.000	13.8	0.000	1.180	0.0 ± 0.0
7	0	31	9	0.000	40.8	0.000	3.483	0.0 ± 0.0
8	0	2	24	0.000	1.0	0.000	0.084	0.0 ± 0.0
9	0	3	9	0.000	3.9	0.000	0.337	0.0 ± 0.0
	0	119			12.2	0.000	1.046	

AREA OF BASIC UNIT = 9.89E-07 cm
CHI SQUARED = 2.966667E-06 WITH 8 DEGREES OF FREEDOM
P(chi squared) = 100.0 %
CORRELATION COEFFICIENT = 0.569
VARIANCE OF SQR(Ns) = 0.00
VARIANCE OF SQR(Ni) = 2.37

Ns/Ni = 0.000 ± 0.000
MEAN RATIO = 0.000 ± 0.000

Ages calculated using a zeta of 354.9 ± 4.3 for SRM612 glass
RHO D = 1.119E+06 ; ND = 2767

POOLED AGE = 0.0 ± 0.0 Ma
MEAN AGE = 0.0 ± 0.0 Ma

8902-112 ZIRCON clyde s72/366735 855m

IRRADIATION jmt data:jmt zircon data:clyde zircons:wk026/4
SLIDE NUMBER 1
COUNTED BY: jmt

No.	Ns	Ni	Na	RATIO	U (ppm)	RHOs (E+06)	RHOi (E+06)	F.T.AGE (Ma)
1	82	27	8	3.037	0.0	10.364	3.413	174.2 ± 38.8
2	149	80	12	1.862	0.0	12.555	6.741	107.4 ± 15.0
3	60	23	6	2.609	0.0	10.111	3.876	149.9 ± 36.9
4	103	33	9	3.121	0.0	11.572	3.707	179.0 ± 35.9
5	85	17	8	5.000	0.0	10.743	2.149	284.3 ± 75.7
6	446	118	24	3.780	0.0	18.790	4.971	216.1 ± 22.7
7	21	11	4	1.909	0.0	5.308	2.781	110.0 ± 41.0
8	55	21	12	2.619	0.0	4.634	1.769	150.5 ± 38.7
9	48	20	3	2.400	0.0	16.178	6.741	138.0 ± 36.8
10	53	42	8	1.262	0.0	6.699	5.308	73.0 ± 15.1
11	29	17	4	1.706	0.0	7.331	4.297	98.4 ± 30.1
12	122	31	10	3.935	0.0	12.336	3.134	224.8 ± 45.4
13	112	45	12	2.489	0.0	9.437	3.792	143.1 ± 25.4
14	121	48	12	2.521	0.0	10.195	4.044	144.9 ± 24.9
15	95	31	12	3.065	0.0	8.005	2.612	175.8 ± 36.5
16	56	45	8	1.244	0.0	7.078	5.688	71.9 ± 14.5
17	113	60	32	1.883	0.0	3.571	1.896	108.6 ± 17.5
	1750	669			0.0	9.617	3.676	

AREA OF BASIC UNIT = 9.89E-07 cm
CHI SQUARED = 65.64571 WITH 16 DEGREES OF FREEDOM
P(chi squared) = < 0.1 %
CORRELATION COEFFICIENT = 0.880
VARIANCE OF SQR(Ns) = 13.39
VARIANCE OF SQR(Ni) = 3.66

Ns/Ni = 2.616 ± 0.119
MEAN RATIO = 2.614 ± 0.240

Ages calculated using a zeta of 133.9 ± 1.4 for CN1 glass
RHO D = 8.684E+05 ; ND = 4294

POOLED AGE = 150.3 ± 7.4 Ma
MEAN AGE = 150.2 ± 14.1 Ma

8902-113 APATITE clyde s72/378711 810m

IRRADIATION jmt data:jmt apatite data:clyde apatites:wk014/8
SLIDE NUMBER 1
COUNTED BY: jmt

No.	Ns	NI	Na	RATIO	U (ppm)	RHOs (E+06)	RHOI (E+06)	F.T.AGE (Ma)
1	2	55	24	0.036	27.4	0.084	2.317	7.2 ± 5.2
2	2	121	15	0.017	96.3	0.135	8.156	3.3 ± 2.3
3	2	43	12	0.047	42.8	0.169	3.623	9.1 ± 6.6
4	0	63	20	0.000	37.6	0.000	3.185	0.0 ± 0.0
5	1	34	25	0.029	16.2	0.040	1.375	5.8 ± 5.9
6	3	53	24	0.057	26.4	0.126	2.233	11.1 ± 6.6
7	0	112	16	0.000	83.6	0.000	7.078	0.0 ± 0.0
8	0	29	25	0.000	13.9	0.000	1.173	0.0 ± 0.0
9	0	34	28	0.000	14.5	0.000	1.228	0.0 ± 0.0
10	1	41	49	0.024	10.0	0.021	0.846	4.8 ± 4.9
11	0	11	20	0.000	6.6	0.000	0.556	0.0 ± 0.0
12	0	10	16	0.000	7.5	0.000	0.632	0.0 ± 0.0
13	0	27	24	0.000	13.4	0.000	1.138	0.0 ± 0.0
14	0	19	25	0.000	9.1	0.000	0.768	0.0 ± 0.0
15	1	82	48	0.012	20.4	0.021	1.727	2.4 ± 2.4
16	1	101	60	0.010	20.1	0.017	1.702	1.9 ± 2.0
17	2	48	28	0.042	20.5	0.072	1.733	8.2 ± 5.9
18	1	64	25	0.016	30.6	0.040	2.588	3.1 ± 3.1
19	1	8	25	0.125	3.8	0.040	0.324	24.6 ± 26.0
20	1	18	20	0.056	10.7	0.051	0.910	10.9 ± 11.2
21	0	18	20	0.000	10.7	0.000	0.910	0.0 ± 0.0
22	0	7	16	0.000	5.2	0.000	0.442	0.0 ± 0.0
23	5	206	28	0.024	87.9	0.181	7.439	4.8 ± 2.2
24	2	107	49	0.019	26.1	0.041	2.208	3.7 ± 2.6
25	1	37	18	0.027	24.6	0.056	2.078	5.3 ± 5.4
26	2	52	8	0.038	77.6	0.253	6.572	7.6 ± 5.5
	28	1400			25.0	0.042	2.119	

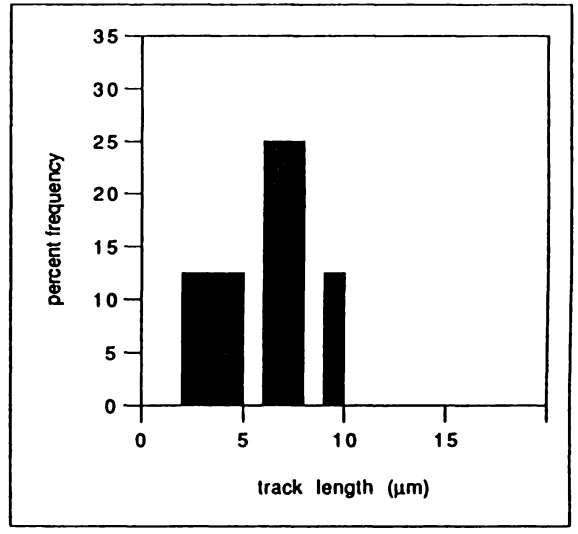
AREA OF BASIC UNIT = 9.89E-07 cm
CHI SQUARED = 20.40277 WITH 25 DEGREES OF FREEDOM
P(chi squared) = 72.5 %
CORRELATION COEFFICIENT = 0.675
VARIANCE OF SQR(Ns) = 0.48
VARIANCE OF SQR(Ni) = 8.21

Ns/NI = 0.020 ± 0.004
MEAN RATIO = 0.022 ± 0.005

Ages calculated using a zeta of 354.9 ± 4.3 for SRM612 glass
RHO D = 1.109E+06 ; ND = 2743

POOLED AGE = 3.9 ± 0.8 Ma
MEAN AGE = 4.4 ± 1.1 Ma

8902-113



n = 8
Mean = 6.11 µm
Sample std. dev. = 2.33 µm

8902-113 ZIRCON clyde s72/378711 810m

IRRADIATION jmt data:jmt zircon data:clyde zircons:wk026/3
SLIDE NUMBER 1
COUNTED BY: jmt

No.	Ns	Ni	Na	RATIO	U (ppm)	RHOs (E+06)	RHOi (E+06)	F.T AGE (Ma)
1	118	42	15	2.810	0.0	7.954	2.831	159.7 ± 28.8
2	103	51	10	2.020	0.0	10.415	5.157	115.2 ± 19.8
3	78	41	9	1.902	0.0	8.763	4.606	108.6 ± 21.0
4	186	80	18	2.325	0.0	10.448	4.494	132.4 ± 17.9
5	98	47	12	2.085	0.0	8.257	3.960	118.9 ± 21.2
6	26	10	3	2.600	0.0	8.763	3.370	147.9 ± 55.1
7	45	15	9	3.000	0.0	5.056	1.685	170.4 ± 50.9
	654	286			0.0	8.701	3.805	

AREA OF BASIC UNIT = 9.89E-07 cm
CHI SQUARED = 3.99676 WITH 6 DEGREES OF FREEDOM
P(chi squared) = 67.7 %
CORRELATION COEFFICIENT = 0.966
VARIANCE OF SQR(Ns) = 7.82
VARIANCE OF SQR(Ni) = 3.93

Ns/Ni = 2.287 ± 0.162
MEAN RATIO = 2.392 ± 0.159

Ages calculated using a zeta of 133.9 ± 1.4 for CN1 glass
RHO D = 8.595E+05 ; ND = 4250

POOLED AGE = 130.3 ± 9.5 Ma
MEAN AGE = 136.2 ± 9.4 Ma

8902-114 APATITE clyde s72/402683 715m

IRRADIATION jmt data:jmt apatite data:clyde apatites:wk014/7
SLIDE NUMBER 1
COUNTED BY: jmt

No.	Ns	NI	Na	RATIO	U (ppm)	RHOs (E+06)	RHOI (E+06)	F.T.AGE (Ma)
1	1	83	42	0.012	23.8	0.024	1.998	2.4 ± 2.4
2	0	9	10	0.000	10.8	0.000	0.910	0.0 ± 0.0
3	0	5	9	0.000	6.7	0.000	0.562	0.0 ± 0.0
4	0	103	48	0.000	25.8	0.000	2.170	0.0 ± 0.0
5	0	49	20	0.000	29.5	0.000	2.477	0.0 ± 0.0
6	0	24	16	0.000	18.1	0.000	1.517	0.0 ± 0.0
7	2	22	32	0.091	8.3	0.063	0.695	17.7 ± 13.1
8	1	10	32	0.100	3.8	0.032	0.316	19.5 ± 20.4
9	1	102	160	0.010	7.7	0.006	0.645	1.9 ± 1.9
10	0	21	20	0.000	12.6	0.000	1.062	0.0 ± 0.0
11	23	98	32	0.235	36.9	0.727	3.097	45.6 ± 10.6
12	1	41	25	0.024	19.7	0.040	1.658	4.8 ± 4.8
13	0	5	15	0.000	4.0	0.000	0.337	0.0 ± 0.0
14	0	9	15	0.000	7.2	0.000	0.607	0.0 ± 0.0
15	6	33	20	0.182	19.9	0.303	1.668	35.4 ± 15.7
16	8	40	8	0.200	60.2	1.011	5.056	38.9 ± 15.1
17	1	100	30	0.010	40.1	0.034	3.370	2.0 ± 2.0
18	0	13	24	0.000	6.5	0.000	0.548	0.0 ± 0.0
19	14	39	12	0.359	39.1	1.180	3.286	69.7 ± 21.8
20	5	53	15	0.094	42.5	0.337	3.573	18.4 ± 8.6
21	2	33	20	0.061	19.9	0.101	1.668	11.8 ± 8.6
22	1	12	20	0.083	7.2	0.051	0.607	16.2 ± 16.9
23	4	24	24	0.167	12.0	0.169	1.011	32.4 ± 17.5
24	0	22	16	0.000	16.6	0.000	1.390	0.0 ± 0.0
25	4	12	25	0.333	5.8	0.162	0.485	64.7 ± 37.4
	74	962			16.8	0.108	1.410	

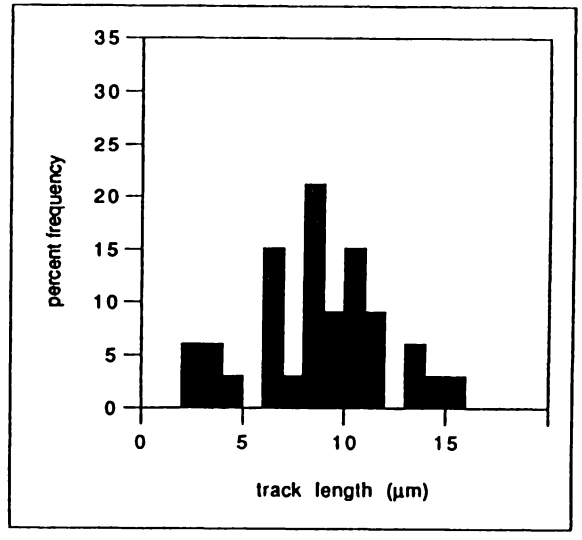
AREA OF BASIC UNIT = 9.89E-07 cm
CHI SQUARED = 113.7897 WITH 24 DEGREES OF FREEDOM
P(chi squared) = < 0.1 %
CORRELATION COEFFICIENT = 0.319
VARIANCE OF SQR(Ns) = 1.69
VARIANCE OF SQR(Ni) = 6.51

Ns/Ni = 0.077 ± 0.009
MEAN RATIO = 0.078 ± 0.022

Ages calculated using a zeta of 354.9 ± 4.3 for SRM612 glass
RHO D = 1.100E+06 ; ND = 2719

POOLED AGE = 15.0 ± 1.8 Ma
MEAN AGE = 15.3 ± 4.2 Ma

8902-114



n = 33
Mean = 8.73 µm
Sample std. dev. = 3.18 µm

8902-114 ZIRCON clyde s72/402683 715m

IRRADIATION jmt data:jmt zircon data:clyde zircons:wk026/2
SLIDE NUMBER 1
COUNTED BY: jmt

No.	Ns	Ni	Na	RATIO	U (ppm)	RHOs (E+06)	RHOi (E+06)	F.T.AGE (Ma)
1	95	39	15	2.436	0.0	6.404	2.629	137.2 ± 26.2
2	133	44	12	3.023	0.0	11.207	3.707	169.9 ± 29.7
3	25	10	4	2.500	0.0	6.320	2.528	140.8 ± 52.8
4	122	42	15	2.905	0.0	8.224	2.831	163.3 ± 29.4
5	214	52	60	4.115	0.0	3.606	0.876	230.2 ± 35.8
6	217	108	40	2.009	0.0	5.485	2.730	113.4 ± 13.5
7	109	45	12	2.422	0.0	9.184	3.792	136.5 ± 24.3
8	294	76	30	3.868	0.0	9.909	2.562	216.6 ± 28.2
9	89	47	16	1.894	0.0	5.624	2.970	106.9 ± 19.4
	1298	463			0.0	6.434	2.295	

AREA OF BASIC UNIT = 9.89E-07 cm
CHI SQUARED = 26.97674 WITH 8 DEGREES OF FREEDOM
P(chi squared) = < 0.1 %
CORRELATION COEFFICIENT = 0.793
VARIANCE OF SQR(Ns) = 12.88
VARIANCE OF SQR(Ni) = 3.78

Ns/Ni = 2.803 ± 0.152
MEAN RATIO = 2.797 ± 0.257

Ages calculated using a zeta of 133.9 ± 1.4 for CN1 glass
RHO D = 8.506E+05 ; ND = 4206

POOLED AGE = 157.7 ± 9.0 Ma
MEAN AGE = 157.3 ± 14.7 Ma

8902-115 APATITE clyde s72/433637 655m

IRRADIATION jmt data:jmt apatite data:clyde apatites:wk014/6
SLIDE NUMBER 1
COUNTED BY: jmt

No.	Ns	Ni	Na	RATIO	U (ppm)	RHOs (E+06)	RHOi (E+06)	F.T.AGE (Ma)
1	11	45	48	0.244	11.4	0.232	0.948	47.1 ± 15.9
2	5	30	18	0.167	20.3	0.281	1.685	32.2 ± 15.6
3	3	31	9	0.097	41.9	0.337	3.483	18.7 ± 11.3
4	2	6	25	0.333	2.9	0.081	0.243	64.2 ± 52.4
5	18	79	35	0.228	27.4	0.520	2.282	43.9 ± 11.5
6	2	14	21	0.143	8.1	0.096	0.674	27.6 ± 20.9
7	1	8	18	0.125	5.4	0.056	0.449	24.1 ± 25.6
8	6	36	16	0.167	27.3	0.379	2.275	32.2 ± 14.2
9	5	15	20	0.333	9.1	0.253	0.758	64.2 ± 33.2
10	6	21	6	0.286	42.5	1.011	3.539	55.0 ± 25.5
11	3	8	16	0.375	6.1	0.190	0.506	72.1 ± 48.9
12	5	33	18	0.152	22.3	0.281	1.854	29.2 ± 14.0
13	1	9	12	0.111	9.1	0.084	0.758	21.5 ± 22.6
14	0	6	9	0.000	8.1	0.000	0.674	0.0 ± 0.0
15	1	8	12	0.125	8.1	0.084	0.674	24.1 ± 25.6
16	1	4	12	0.250	4.0	0.084	0.337	48.2 ± 53.9
17	0	4	12	0.000	4.0	0.000	0.337	0.0 ± 0.0
18	1	12	8	0.083	18.2	0.126	1.517	16.1 ± 16.8
19	1	7	15	0.143	5.7	0.067	0.472	27.6 ± 29.5
20	10	54	20	0.185	32.8	0.506	2.730	35.7 ± 12.3
21	8	33	15	0.242	26.7	0.539	2.224	46.7 ± 18.4
	90	463			15.4	0.249	1.283	

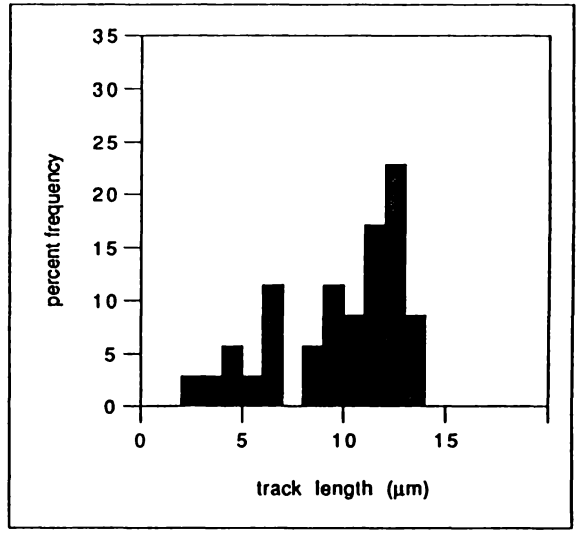
AREA OF BASIC UNIT = 9.89E-07 cm
CHI SQUARED = 9.883255 WITH 20 DEGREES OF FREEDOM
P(chi squared) = 97.0 %
CORRELATION COEFFICIENT = 0.948
VARIANCE OF SQR(Ns) = 1.16
VARIANCE OF SQR(Ni) = 3.79

Ns/Ni = 0.194 ± 0.022
MEAN RATIO = 0.180 ± 0.022

Ages calculated using a zeta of 354.9 ± 4.3 for SRM612 glass
RHO D = 1.090E+06 ; ND = 2695

POOLED AGE = 37.5 ± 4.4 Ma
MEAN AGE = 34.8 ± 4.4 Ma

8902-115



n = 35
Mean = 9.82 µm
Sample std. dev. = 3.11 µm

8902-115 ZIRCON clyde s72/433637 655m

IRRADIATION jmt data:jmt zircon data:clyde zircons:wk026/1
SLIDE NUMBER 1
COUNTED BY: jmt

No.	Ns	Ni	Na	RATIO	U (ppm)	RHOs (E+06)	RHOi (E+06)	F.T.AGE (Ma)
1	30	17	6	1.765	0.0	5.056	2.865	98.7 ± 30.0
2	38	13	4	2.923	0.0	9.606	3.286	162.7 ± 52.3
3	108	38	9	2.842	0.0	12.133	4.269	158.2 ± 30.0
4	47	16	9	2.938	0.0	5.280	1.798	163.4 ± 47.4
5	259	99	56	2.616	0.0	4.676	1.788	145.8 ± 17.4
6	53	16	8	3.312	0.0	6.699	2.022	184.0 ± 52.6
7	152	47	15	3.234	0.0	10.246	3.168	179.7 ± 30.2
8	14	6	4	2.333	0.0	3.539	1.517	130.2 ± 63.6
9	44	14	4	3.143	0.0	11.122	3.539	174.7 ± 53.7
10	66	20	6	3.300	0.0	11.122	3.370	183.3 ± 46.9
	811	286			0.0	6.777	2.390	

AREA OF BASIC UNIT = 9.89E-07 cm
CHI SQUARED = 4.521229 WITH 9 DEGREES OF FREEDOM
P(chi squared) = 87.4 %
CORRELATION COEFFICIENT = 0.989
VARIANCE OF SQR(Ns) = 13.40
VARIANCE OF SQR(Ni) = 4.70

Ns/Ni = 2.836 ± 0.195
MEAN RATIO = 2.841 ± 0.155

Ages calculated using a zeta of 133.9 ± 1.4 for CN1 glass
RHO D = 8.417E+05 ; ND = 4162

POOLED AGE = 157.8 ± 11.2 Ma
MEAN AGE = 158.1 ± 9.1 Ma

8902-116 APATITE clyde s80/428595 610m

IRRADIATION jmt data:jmt apatite data:clyde apatites:wk014/5
SLIDE NUMBER 1
COUNTED BY: jmt

No.	Ns	NI	Na	RATIO	U (ppm)	RHOs (E+06)	RHOI (E+06)	F.TAGE (Ma)
1	3	33	12	0.091	33.7	0.253	2.781	17.4 ± 10.5
2	14	40	36	0.350	13.6	0.393	1.123	66.7 ± 20.8
3	2	27	64	0.074	5.2	0.032	0.427	14.2 ± 10.4
4	2	21	25	0.095	10.3	0.081	0.849	18.2 ± 13.5
5	1	14	8	0.071	21.5	0.126	1.769	13.7 ± 14.2
6	1	6	12	0.167	6.1	0.084	0.506	31.9 ± 34.4
7	2	28	35	0.071	9.8	0.058	0.809	13.7 ± 10.0
8	1	24	35	0.042	8.4	0.029	0.693	8.0 ± 8.1
9	26	62	12	0.419	63.4	2.191	5.224	79.9 ± 18.8
10	4	19	20	0.211	11.7	0.202	0.961	40.2 ± 22.1
11	3	28	12	0.107	28.6	0.253	2.359	20.5 ± 12.5
12	5	20	20	0.250	12.3	0.253	1.011	47.7 ± 23.9
13	9	47	12	0.191	48.0	0.758	3.960	36.6 ± 13.3
14	11	45	12	0.244	46.0	0.927	3.792	46.7 ± 15.7
15	8	16	15	0.500	13.1	0.539	1.079	95.1 ± 41.2
16	11	40	16	0.275	30.7	0.695	2.528	52.5 ± 17.9
17	40	125	12	0.320	127.8	3.370	10.533	61.0 ± 11.2
18	5	10	12	0.500	10.2	0.421	0.843	95.1 ± 52.1
19	3	20	9	0.150	27.3	0.337	2.247	28.7 ± 17.8
20	9	36	15	0.250	29.4	0.607	2.427	47.7 ± 17.8
21	10	82	100	0.122	10.1	0.101	0.829	23.3 ± 7.8
	170	743			18.4	0.348	1.521	

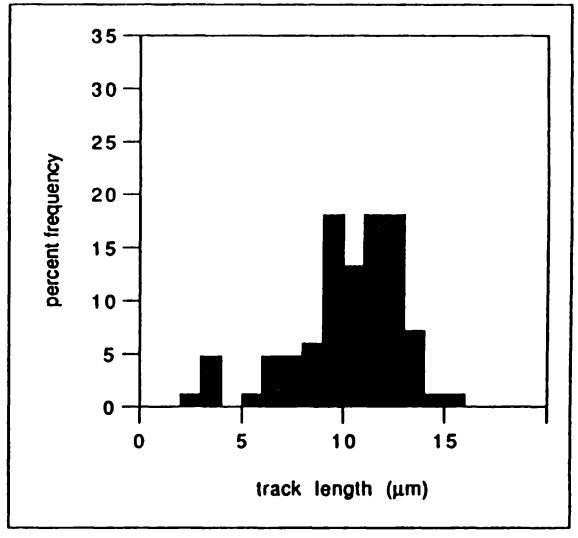
AREA OF BASIC UNIT = 9.89E-07 cm
CHI SQUARED = 38.78125 WITH 20 DEGREES OF FREEDOM
P(chi squared) = 0.7 %
CORRELATION COEFFICIENT = 0.870
VARIANCE OF SQR(Ns) = 1.89
VARIANCE OF SQR(Ni) = 4.01

Ns/Ni = 0.229 ± 0.019
MEAN RATIO = 0.214 ± 0.030

Ages calculated using a zeta of 354.9 ± 4.3 for SRM612 glass
RHO D = 1.080E+06 ; ND = 2671

POOLED AGE = 43.7 ± 3.8 Ma
MEAN AGE = 40.9 ± 5.9 Ma

8902-116



n = 83
Mean = 10.27 µm
Sample std. dev. = 2.68 µm

8902-116 ZIRCON clyde s80/428595 610m

IRRADIATION jmt data:jmt zircon data:clyde zircons:wk027/18
SLIDE NUMBER 1
COUNTED BY: jmt

No.	Ns	Ni	Na	RATIO	U (ppm)	RHOs (E+06)	RHOi (E+06)	F.T.AGE (Ma)
1	144	46	20	3.130	0.0	7.280	2.326	198.2 ± 33.8
2	130	41	15	3.171	0.0	8.763	2.764	200.8 ± 36.1
3	239	100	24	2.390	0.0	10.069	4.213	151.9 ± 18.3
4	108	50	15	2.160	0.0	7.280	3.370	137.4 ± 23.6
5	95	63	10	1.508	0.0	9.606	6.370	96.3 ± 15.7
6	181	56	30	3.232	0.0	6.100	1.887	204.6 ± 31.5
7	50	19	6	2.632	0.0	8.426	3.202	167.1 ± 45.1
	947	375			0.0	7.979	3.160	

AREA OF BASIC UNIT = 9.89E-07 cm
CHI SQUARED = 17.22387 WITH 6 DEGREES OF FREEDOM
P(chi squared) = 0.8 %
CORRELATION COEFFICIENT = 0.833
VARIANCE OF SQR(Ns) = 7.26
VARIANCE OF SQR(Ni) = 2.89

Ns/Ni = 2.525 ± 0.154
MEAN RATIO = 2.603 ± 0.241

Ages calculated using a zeta of 133.9 ± 1.4 for CN1 glass
RHO D = 9.606E+05 ; ND = 4750

POOLED AGE = 160.4 ± 10.2 Ma
MEAN AGE = 165.3 ± 15.6 Ma

8902-117 APATITE clyde s80/459566 595m

IRRADIATION jmt data:jmt apatite data:clyde apatites:wk014/4
SLIDE NUMBER 1
COUNTED BY: jmt

No.	Ns	NI	Na	RATIO	U (ppm)	RHOs (E+06)	RHOi (E+06)	F.T.AGE (Ma)
1	4	16	24	0.250	8.3	0.169	0.674	47.3 ± 26.5
2	15	36	9	0.417	49.5	1.685	4.044	78.6 ± 24.2
3	2	5	15	0.400	4.1	0.135	0.337	75.5 ± 63.2
4	20	63	25	0.317	31.2	0.809	2.548	60.0 ± 15.5
5	1	6	24	0.167	3.1	0.042	0.253	31.6 ± 34.1
6	56	395	70	0.142	69.9	0.809	5.706	26.9 ± 3.9
7	1	11	12	0.091	11.3	0.084	0.927	17.2 ± 18.0
8	4	14	6	0.286	28.9	0.674	2.359	54.0 ± 30.7
9	1	15	25	0.067	7.4	0.040	0.607	12.6 ± 13.1
10	3	6	12	0.500	6.2	0.253	0.506	94.2 ± 66.7
11	4	13	9	0.308	17.9	0.449	1.461	58.2 ± 33.3
12	11	30	8	0.367	46.4	1.390	3.792	69.2 ± 24.5
13	18	31	20	0.581	19.2	0.910	1.567	109.3 ± 32.5
14	3	23	9	0.130	31.6	0.337	2.584	24.7 ± 15.2
15	2	31	10	0.065	38.4	0.202	3.134	12.2 ± 8.9
16	11	55	12	0.200	56.7	0.927	4.634	37.9 ± 12.5
17	1	4	9	0.250	5.5	0.112	0.449	47.3 ± 52.9
18	4	11	24	0.364	5.7	0.169	0.463	68.7 ± 40.1
19	6	42	24	0.143	21.7	0.253	1.769	27.1 ± 11.8
20	1	8	20	0.125	5.0	0.051	0.404	23.7 ± 25.1
	168	815			27.5	0.463	2.245	

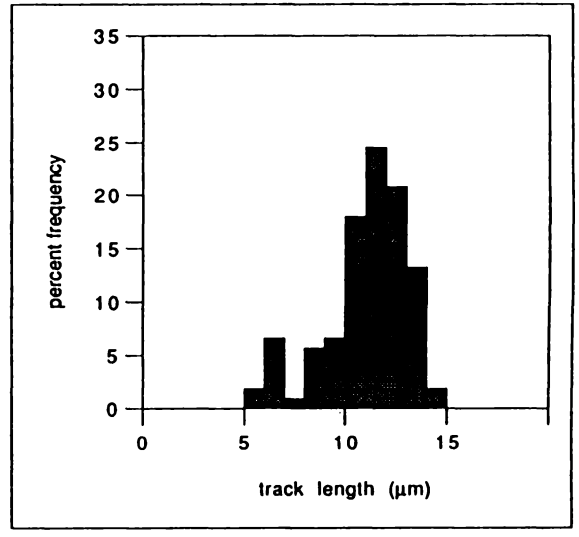
AREA OF BASIC UNIT = 9.89E-07 cm
CHI SQUARED = 42.02282 WITH 19 DEGREES OF FREEDOM
P(chi squared) = 0.2 %
CORRELATION COEFFICIENT = 0.940
VARIANCE OF SQR(Ns) = 2.67
VARIANCE OF SQR(Ni) = 15.01

Ns/Ni = 0.206 ± 0.017
MEAN RATIO = 0.258 ± 0.033

Ages calculated using a zeta of 354.9 ± 4.3 for SRM612 glass
RHO D = 1.070E+06 ; ND = 2649

POOLED AGE = 39.0 ± 3.4 Ma
MEAN AGE = 48.9 ± 6.3 Ma

8902-117



n = 106
Mean = 11.03 µm
Sample std. dev. = 2.01 µm

8902-117 ZIRCON clyde s80/459566 595m

IRRADIATION jmt data:jmt zircon data:clyde zircons:wk027/17
SLIDE NUMBER 1
COUNTED BY: jmt

No.	Ns	Ni	Na	RATIO	U (ppm)	RHOs (E+06)	RHOi (E+06)	F.T.AGE (Ma)
1	185	112	21	1.652	0.0	8.908	5.393	104.6 ± 12.7
2	92	34	9	2.706	0.0	10.336	3.820	170.5 ± 34.4
3	219	69	30	3.174	0.0	7.381	2.326	199.5 ± 27.8
4	298	113	35	2.637	0.0	8.609	3.264	166.2 ± 18.6
5	389	239	48	1.628	0.0	8.194	5.035	103.1 ± 8.7
6	261	145	24	1.800	0.0	10.996	6.109	113.9 ± 12.0
7	75	33	8	2.273	0.0	9.479	4.171	143.5 ± 30.1
8	128	47	12	2.723	0.0	10.785	3.960	171.6 ± 29.4
9	79	40	9	1.975	0.0	8.875	4.494	124.9 ± 24.3
10	55	20	6	2.750	0.0	9.269	3.370	173.2 ± 45.3
11	98	41	8	2.390	0.0	12.386	5.182	150.8 ± 28.2
12	107	43	12	2.488	0.0	9.016	3.623	157.0 ± 28.5
13	209	92	16	2.272	0.0	13.208	5.814	143.4 ± 18.1
14	136	89	14	1.528	0.0	9.822	6.428	96.8 ± 13.3
	2331	1117			0.0	9.353	4.482	

AREA OF BASIC UNIT = 9.89E-07 cm
CHI SQUARED = 41.65487 WITH 13 DEGREES OF FREEDOM
P(chi squared) = < 0.1 %
CORRELATION COEFFICIENT = 0.930
VARIANCE OF SQR(Ns) = 13.39
VARIANCE OF SQR(Ni) = 9.11

Ns/Ni = 2.087 ± 0.076
MEAN RATIO = 2.285 ± 0.134

Ages calculated using a zeta of 133.9 ± 1.4 for CN1 glass
RHO D = 9.537E+05 ; ND = 4716

POOLED AGE = 131.9 ± 5.4 Ma
MEAN AGE = 144.3 ± 8.9 Ma

8902-118 APATITE clyde s81/741436 550m

IRRADIATION jmt data:jmt apatite data:clyde apatites:wk014/3
SLIDE NUMBER 1
COUNTED BY: jmt

No.	Ns	NI	Na	RATIO	U (ppm)	RHOs (E+06)	RHOI (E+06)	F.T.AGE (Ma)
1	15	64	32	0.234	25.0	0.474	2.022	44.0 ± 12.7
2	19	59	12	0.322	61.4	1.601	4.971	60.3 ± 16.0
3	1	4	8	0.250	6.2	0.126	0.506	46.9 ± 52.4
4	5	13	12	0.385	13.5	0.421	1.095	72.0 ± 37.9
5	6	53	18	0.113	36.8	0.337	2.977	21.3 ± 9.2
6	20	53	9	0.377	73.5	2.247	5.954	70.7 ± 18.6
7	2	6	16	0.333	4.7	0.126	0.379	62.5 ± 51.0
8	5	23	12	0.217	23.9	0.421	1.938	40.8 ± 20.2
9	9	24	12	0.375	25.0	0.758	2.022	70.2 ± 27.5
10	6	38	25	0.158	19.0	0.243	1.537	29.7 ± 13.0
11	28	88	30	0.318	36.6	0.944	2.966	59.6 ± 13.0
12	2	7	6	0.286	14.6	0.337	1.180	53.6 ± 43.0
13	5	20	20	0.250	12.5	0.253	1.011	46.9 ± 23.5
14	14	17	16	0.824	13.3	0.885	1.074	153.2 ± 55.4
15	33	64	16	0.516	49.9	2.085	4.044	96.4 ± 20.8
16	10	17	12	0.588	17.7	0.843	1.432	109.8 ± 43.8
17	34	63	18	0.540	43.7	1.910	3.539	100.8 ± 21.6
18	21	56	12	0.375	58.3	1.769	4.719	70.2 ± 18.0
19	8	41	12	0.195	42.7	0.674	3.455	36.6 ± 14.2
20	30	112	24	0.268	58.3	1.264	4.719	50.2 ± 10.4
	273	822			31.9	0.857	2.581	

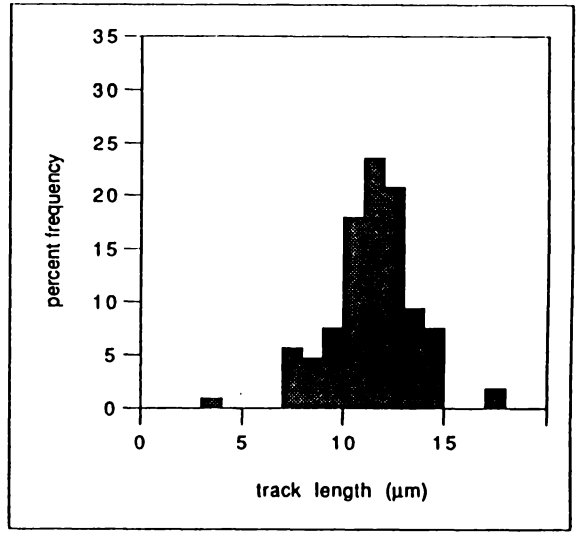
AREA OF BASIC UNIT = 9.89E-07 cm
CHI SQUARED = 34.74349 WITH 19 DEGREES OF FREEDOM
P(chi squared) = 1.5 %
CORRELATION COEFFICIENT = 0.825
VARIANCE OF SQR(Ns) = 2.27
VARIANCE OF SQR(NI) = 5.80

Ns/Ni = 0.332 ± 0.023
MEAN RATIO = 0.346 ± 0.037

Ages calculated using a zeta of 354.9 ± 4.3 for SRM612 glass
RHO D = 1.061E+06 ; ND = 2622

POOLED AGE = 62.2 ± 4.6 Ma
MEAN AGE = 64.9 ± 7.1 Ma

8902-118



n = 106
Mean = 11.51 µm
Sample std. dev. = 2.05 µm

8902-118 ZIRCON clyde s81/741436 550m

IRRADIATION jmt data:jmt zircon data:clyde zircons:wk027/16
SLIDE NUMBER 1
COUNTED BY: jmt

No.	Ns	Ni	Na	RATIO	U (ppm)	RHOs (E+06)	RHOi (E+06)	F.T.AGE (Ma)
1	93	31	6	3.000	0.0	15.672	5.224	187.4 ± 39.0
2	191	92	25	2.076	0.0	7.725	3.721	130.2 ± 16.7
3	82	43	6	1.907	0.0	13.819	7.246	119.7 ± 22.6
4	196	86	14	2.279	0.0	14.156	6.211	142.8 ± 18.7
5	86	40	8	2.150	0.0	10.870	5.056	134.8 ± 25.9
6	59	31	4	1.903	0.0	14.914	7.836	119.5 ± 26.6
7	116	51	6	2.275	0.0	19.548	8.595	142.6 ± 24.1
8	68	39	6	1.744	0.0	11.459	6.572	109.6 ± 22.1
9	103	40	8	2.575	0.0	13.018	5.056	161.2 ± 30.2
10	294	162	21	1.815	0.0	14.156	7.800	114.0 ± 11.3
11	101	57	9	1.772	0.0	11.347	6.404	111.3 ± 18.6
12	123	37	8	3.324	0.0	15.546	4.676	207.3 ± 39.0
	1512	709			0.0	12.635	5.925	

AREA OF BASIC UNIT = 9.89E-07 cm
CHI SQUARED = 15.52141 WITH 11 DEGREES OF FREEDOM
P(chi squared) = 16.0 %
CORRELATION COEFFICIENT = 0.960
VARIANCE OF SQR(Ns) = 7.59
VARIANCE OF SQR(Ni) = 4.51

Ns/Ni = 2.133 ± 0.097
MEAN RATIO = 2.235 ± 0.145

Ages calculated using a zeta of 133.9 ± 1.4 for CN1 glass
RHO D = 9.466E+05 ; ND = 4681

POOLED AGE = 133.8 ± 6.5 Ma
MEAN AGE = 140.1 ± 9.4 Ma

8902-119 APATITE clyde s81/762424 520m

IRRADIATION jmt data:jmt apatite data:clyde apatites:wk014/2
SLIDE NUMBER 1
COUNTED BY: jmt

No.	Ns	Ni	Na	RATIO	U (ppm)	RHOs (E+06)	RHOi (E+06)	F.T.AGE (Ma)
1	19	38	24	0.500	20.0	0.800	1.601	92.6 ± 26.1
2	173	297	24	0.582	156.0	7.288	12.513	107.7 ± 10.6
3	39	81	25	0.481	40.8	1.577	3.276	89.2 ± 17.5
4	23	27	24	0.852	14.2	0.969	1.138	156.9 ± 44.7
5	16	61	25	0.262	30.8	0.647	2.467	48.7 ± 13.7
6	70	125	24	0.560	65.6	2.949	5.266	103.6 ± 15.6
7	4	32	28	0.125	14.4	0.144	1.156	23.3 ± 12.4
8	11	20	8	0.550	31.5	1.390	2.528	101.8 ± 38.3
9	11	26	9	0.423	36.4	1.236	2.921	78.4 ± 28.3
10	80	201	24	0.398	105.5	3.370	8.468	73.8 ± 9.9
11	95	271	25	0.351	136.6	3.842	10.961	65.0 ± 7.9
12	24	30	12	0.800	31.5	2.022	2.528	147.5 ± 40.5
13	33	69	15	0.478	58.0	2.224	4.651	88.6 ± 18.9
14	16	31	20	0.516	19.5	0.809	1.567	95.5 ± 29.5
15	31	62	16	0.500	48.8	1.959	3.918	92.6 ± 20.5
16	9	55	25	0.164	27.7	0.364	2.224	30.4 ± 11.0
17	50	167	24	0.299	87.7	2.106	7.036	55.6 ± 9.1
18	13	68	16	0.191	53.6	0.822	4.297	35.6 ± 10.8
19	9	21	12	0.429	22.1	0.758	1.769	79.4 ± 31.7
20	108	134	12	0.806	140.7	9.100	11.291	148.6 ± 19.5
	834	1816			58.4	2.151	4.684	

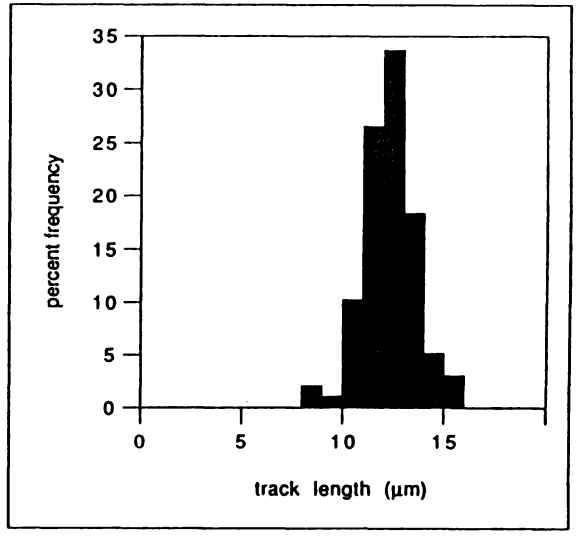
AREA OF BASIC UNIT = 9.89E-07 cm
CHI SQUARED = 79.71706 WITH 19 DEGREES OF FREEDOM
P(chi squared) = < 0.1 %
CORRELATION COEFFICIENT = 0.905
VARIANCE OF SQR(Ns) = 8.77
VARIANCE OF SQR(Ni) = 15.52

Ns/Ni = 0.459 ± 0.019
MEAN RATIO = 0.463 ± 0.045

Ages calculated using a zeta of 354.9 ± 4.3 for SRM612 glass
RHO D = 1.051E+06 ; ND = 2598

POOLED AGE = 85.1 ± 4.1 Ma
MEAN AGE = 85.8 ± 8.6 Ma

8902-119



n = 98
Mean = 12.27 μm
Sample std. dev. = 1.34 μm

8902-119 ZIRCON clyde s81/762424 520m

IRRADIATION jmt data:jmt zircon data:clyde zircons:wk027/15
SLIDE NUMBER 1
COUNTED BY: jmt

No.	Ns	Ni	Na	RATIO	U (ppm)	RHOs (E+06)	RHOi (E+06)	F.T.AGE (Ma)
1	142	53	18	2.679	0.0	7.977	2.977	166.4 ± 26.9
2	39	16	4	2.438	0.0	9.858	4.044	151.5 ± 45.1
3	26	19	2	1.368	0.0	13.145	9.606	85.5 ± 25.9
4	173	87	18	1.988	0.0	9.718	4.887	123.9 ± 16.4
5	89	62	12	1.435	0.0	7.499	5.224	89.7 ± 14.9
6	36	25	4	1.440	0.0	9.100	6.320	89.9 ± 23.5
	505	262			0.0	8.804	4.567	

AREA OF BASIC UNIT = 9.89E-07 cm
CHI SQUARED = 10.6691 WITH 5 DEGREES OF FREEDOM
P(chi squared) = 5.8 %
CORRELATION COEFFICIENT = 0.922
VARIANCE OF SQR(Ns) = 11.40
VARIANCE OF SQR(Ni) = 4.67

Ns/Ni = 1.927 ± 0.147
MEAN RATIO = 1.892 ± 0.232

Ages calculated using a zeta of 133.9 ± 1.4 for CN1 glass
RHO D = 9.395E+05 ; ND = 4646

POOLED AGE = 120.1 ± 9.4 Ma
MEAN AGE = 117.9 ± 14.6 Ma

8902-120 ZIRCON clyde s81/844396 440m

IRRADIATION jmt data:jmt zircon data:clyde zircons:wk027/14
SLIDE NUMBER 1
COUNTED BY: jmt

No.	Ns	NI	Na	RATIO	U (ppm)	RHOs (E+06)	RHOi (E+06)	F.T.AGE (Ma)
1	49	28	6	1.750	0.0	8.257	4.719	108.3 ± 25.7
2	120	76	12	1.579	0.0	10.111	6.404	97.8 ± 14.4
3	89	65	9	1.369	0.0	9.999	7.303	84.9 ± 13.9
4	165	106	16	1.557	0.0	10.427	6.699	96.5 ± 12.1
5	196	99	12	1.980	0.0	16.515	8.342	122.4 ± 15.3
6	37	37	4	1.000	0.0	9.353	9.353	62.1 ± 14.5
7	261	248	21	1.052	0.0	12.567	11.941	65.4 ± 5.9
8	96	74	8	1.297	0.0	12.133	9.353	80.5 ± 12.5
9	386	216	30	1.787	0.0	13.010	7.280	110.6 ± 9.6
10	84	38	6	2.211	0.0	14.156	6.404	136.5 ± 26.8
11	171	93	15	1.839	0.0	11.527	6.269	113.8 ± 14.8
12	184	155	20	1.187	0.0	9.302	7.836	73.7 ± 8.1
13	145	91	14	1.593	0.0	10.472	6.572	98.7 ± 13.3
14	188	137	16	1.372	0.0	11.881	8.658	85.1 ± 9.7
15	98	61	10	1.607	0.0	9.909	6.168	99.5 ± 16.3
	2269	1524			0.0	11.529	7.743	

AREA OF BASIC UNIT = 9.89E-07 cm
CHI SQUARED = 42.41803 WITH 14 DEGREES OF FREEDOM
P(chi squared) = < 0.1 %
CORRELATION COEFFICIENT = 0.903
VARIANCE OF SQR(Ns) = 12.25
VARIANCE OF SQR(Ni) = 9.07

Ns/NI = 1.489 ± 0.049
MEAN RATIO = 1.545 ± 0.088

Ages calculated using a zeta of 133.9 ± 1.4 for CN1 glass
RHO D = 9.325E+05 ; ND = 4611

POOLED AGE = 92.3 ± 3.5 Ma
MEAN AGE = 95.8 ± 5.7 Ma

8902-121 APATITE whitcombe s58/557208 105m

IRRADIATION jmt data:jmt apatite data:whitcombe apatites:wk015/16
SLIDE NUMBER 1
COUNTED BY: jmt

No.	Ns	Ni	Na	RATIO	U (ppm)	RHOs (E+06)	RHOi (E+06)	F.T.AGE (Ma)
1	0	11	9	0.000	13.8	0.000	1.236	0.0 ± 0.0
2	0	21	16	0.000	14.8	0.000	1.327	0.0 ± 0.0
3	0	7	16	0.000	4.9	0.000	0.442	0.0 ± 0.0
4	0	14	9	0.000	17.6	0.000	1.573	0.0 ± 0.0
5	0	5	9	0.000	6.3	0.000	0.562	0.0 ± 0.0
6	0	4	12	0.000	3.8	0.000	0.337	0.0 ± 0.0
7	0	18	16	0.000	12.7	0.000	1.138	0.0 ± 0.0
8	0	4	18	0.000	2.5	0.000	0.225	0.0 ± 0.0
9	0	8	12	0.000	7.5	0.000	0.674	0.0 ± 0.0
10	0	17	20	0.000	9.6	0.000	0.859	0.0 ± 0.0
	0	109			9.0	0.000	0.804	

AREA OF BASIC UNIT = 9.89E-07 cm
CHI SQUARED = 4.190476E-06 WITH 9 DEGREES OF FREEDOM
P(chi squared) = 100.0 %
CORRELATION COEFFICIENT = 0.567
VARIANCE OF SQR(Ns) = 0.00
VARIANCE OF SQR(Ni) = 0.93

Ns/Ni = 0.000 ± 0.000
MEAN RATIO = 0.000 ± 0.000

Ages calculated using a zeta of 354.9 ± 4.3 for SRM612 glass
RHO D = 1.171E+06 ; ND = 2895

POOLED AGE = 0.0 ± 0.0 Ma
MEAN AGE = 0.0 ± 0.0 Ma

8902-121 ZIRCON whitcombe s58/557208 105m

IRRADIATION jmt data:jmt zircon data:whitcombe zircons:wk027/13
SLIDE NUMBER 1
COUNTED BY: jmt

No.	Ns	Ni	Na	RATIO	U (ppm)	RHOs (E+06)	RHOi (E+06)	F.T.AGE (Ma)
1	4	91	8	0.044	0.0	0.506	11.502	2.7 ± 1.4
2	9	559	35	0.016	0.0	0.260	16.149	1.0 ± 0.3
3	2	84	10	0.024	0.0	0.202	8.493	1.5 ± 1.1
4	1	38	6	0.026	0.0	0.169	6.404	1.6 ± 1.7
5	3	136	12	0.022	0.0	0.253	11.459	1.4 ± 0.8
6	2	140	12	0.014	0.0	0.169	11.796	0.9 ± 0.6
7	1	58	6	0.017	0.0	0.169	9.774	1.1 ± 1.1
8	2	92	10	0.022	0.0	0.202	9.302	1.3 ± 1.0
9	6	261	12	0.023	0.0	0.506	21.992	1.4 ± 0.6
10	2	80	5	0.025	0.0	0.404	16.178	1.5 ± 1.1
	32	1539			0.0	0.279	13.415	

AREA OF BASIC UNIT = 9.89E-07 cm
CHI SQUARED = 3.377554 WITH 9 DEGREES OF FREEDOM
P(chi squared) = 94.7 %
CORRELATION COEFFICIENT = 0.943
VARIANCE OF SQR(Ns) = 0.41
VARIANCE OF SQR(Ni) = 25.80

Ns/Ni = 0.021 ± 0.004
MEAN RATIO = 0.023 ± 0.003

Ages calculated using a zeta of 133.9 ± 1.4 for CN1 glass
RHO D = 9.256E+05 ; ND = 4577

POOLED AGE = 1.3 ± 0.2 Ma
MEAN AGE = 1.4 ± 0.2 Ma

8902-122 APATITE whitcombe s65/591173 185m

IRRADIATION jmt data:jmt apatite data:whitcombe apatites:wk015/15
SLIDE NUMBER 1
COUNTED BY: jmt

No.	Ns	Ni	Na	RATIO	U (ppm)	RHOs (E+06)	RHOi (E+06)	F.T.AGE (Ma)
1	0	22	16	0.000	15.6	0.000	1.390	0.0 ± 0.0
2	0	12	20	0.000	6.8	0.000	0.607	0.0 ± 0.0
3	0	40	15	0.000	30.3	0.000	2.696	0.0 ± 0.0
4	0	4	15	0.000	3.0	0.000	0.270	0.0 ± 0.0
5	0	53	24	0.000	25.1	0.000	2.233	0.0 ± 0.0
6	0	6	16	0.000	4.3	0.000	0.379	0.0 ± 0.0
7	0	11	12	0.000	10.4	0.000	0.927	0.0 ± 0.0
8	0	10	9	0.000	12.6	0.000	1.123	0.0 ± 0.0
9	0	36	15	0.000	27.3	0.000	2.427	0.0 ± 0.0
10	0	10	9	0.000	12.6	0.000	1.123	0.0 ± 0.0
11	0	46	12	0.000	43.6	0.000	3.876	0.0 ± 0.0
12	0	105	50	0.000	23.9	0.000	2.123	0.0 ± 0.0
13	0	70	9	0.000	88.5	0.000	7.864	0.0 ± 0.0
14	0	18	12	0.000	17.1	0.000	1.517	0.0 ± 0.0
15	0	54	20	0.000	30.7	0.000	2.730	0.0 ± 0.0
	0	497			22.3	0.000	1.978	

AREA OF BASIC UNIT = 9.89E-07 cm
CHI SQUARED = 3.733333E-06 WITH 14 DEGREES OF FREEDOM
P(chi squared) = 100.0 %
CORRELATION COEFFICIENT = 0.693
VARIANCE OF SQR(Ns) = 0.00
VARIANCE OF SQR(Ni) = 5.90

Ns/Ni = 0.000 ± 0.000
MEAN RATIO = 0.000 ± 0.000

Ages calculated using a zeta of 354.9 ± 4.3 for SRM612 glass
RHO D = 1.164E+06 ; ND = 2876

POOLED AGE = 0.0 ± 0.0 Ma
MEAN AGE = 0.0 ± 0.0 Ma

8902-122 ZIRCON whitcombe s65/591173 185m

IRRADIATION jmt data:jmt zircon data:whitcombe zircons:wk027/12
SLIDE NUMBER 1
COUNTED BY: jmt

No.	Ns	Ni	Na	RATIO	U (ppm)	RHOs (E+06)	RHOi (E+06)	F.T.AGE (Ma)
1	2	131	12	0.015	0.0	0.169	11.038	0.9 ± 0.7
2	2	88	14	0.023	0.0	0.144	6.356	1.4 ± 1.0
3	2	60	4	0.033	0.0	0.506	15.167	2.0 ± 1.5
4	2	59	6	0.034	0.0	0.337	9.943	2.1 ± 1.5
5	4	97	6	0.041	0.0	0.674	16.346	2.5 ± 1.3
6	1	52	8	0.019	0.0	0.126	6.572	1.2 ± 1.2
7	2	291	12	0.007	0.0	0.169	24.520	0.4 ± 0.3
8	2	41	4	0.049	0.0	0.506	10.364	3.0 ± 2.2
9	2	70	6	0.029	0.0	0.337	11.796	1.8 ± 1.3
10	1	121	12	0.008	0.0	0.084	10.195	0.5 ± 0.5
	20	1010			0.0	0.241	12.158	

AREA OF BASIC UNIT = 9.89E-07 cm
CHI SQUARED = 8.611734 WITH 9 DEGREES OF FREEDOM
P(chi squared) = 47.4 %
CORRELATION COEFFICIENT = 0.039
VARIANCE OF SQR(Ns) = 0.08
VARIANCE OF SQR(Ni) = 9.52

Ns/Ni = 0.020 ± 0.004
MEAN RATIO = 0.026 ± 0.004

Ages calculated using a zeta of 133.9 ± 1.4 for CN1 glass
RHO D = 9.185E+05 ; ND = 4542

POOLED AGE = 1.2 ± 0.3 Ma
MEAN AGE = 1.6 ± 0.3 Ma

8902-123 APATITE whitcombe s65/606142 410m

IRRADIATION jmt data:jmt apatite data:whitcombe apatites:wk021/10
SLIDE NUMBER 1
COUNTED BY: jmt

No.	Ns	Ni	Na	RATIO	U (ppm)	RHOs (E+06)	RHOi (E+06)	F.T AGE (Ma)
1	0	1	30	0.000	0.1	0.000	0.034	0.0 ± 0.0
2	0	39	21	0.000	5.5	0.000	1.878	0.0 ± 0.0
3	0	2	20	0.000	0.3	0.000	0.101	0.0 ± 0.0
4	0	1	9	0.000	0.3	0.000	0.112	0.0 ± 0.0
5	0	0	8	0.000	0.0	0.000	0.000	0.0 ± 0.0
6	0	2	16	0.000	0.4	0.000	0.126	0.0 ± 0.0
7	0	1	9	0.000	0.3	0.000	0.112	0.0 ± 0.0
8	0	1	40	0.000	0.1	0.000	0.025	0.0 ± 0.0
9	0	1	40	0.000	0.1	0.000	0.025	0.0 ± 0.0
10	0	8	70	0.000	0.3	0.000	0.116	0.0 ± 0.0
11	0	0	20	0.000	0.0	0.000	0.000	0.0 ± 0.0
12	0	0	6	0.000	0.0	0.000	0.000	0.0 ± 0.0
13	0	12	25	0.000	1.4	0.000	0.485	0.0 ± 0.0
14	0	0	12	0.000	0.0	0.000	0.000	0.0 ± 0.0
15	0	4	48	0.000	0.2	0.000	0.084	0.0 ± 0.0
	0	72			0.6	0.000	0.195	

AREA OF BASIC UNIT = 9.89E-07 cm
CHI SQUARED = 8.461639E-07 WITH 14 DEGREES OF FREEDOM
P(chi squared) = 100.0 %
CORRELATION COEFFICIENT = 0.942
VARIANCE OF SQR(Ns) = 0.00
VARIANCE OF SQR(Ni) = 2.75

Ns/Ni = 0.000 ± 0.000
MEAN RATIO = 0.000 ± 0.000

Ages calculated using a zeta of 354.9 ± 4.3 for SRM612 glass
RHO D = 4.507E+06 ; ND = 3565

POOLED AGE = 0.0 ± 0.0 Ma
MEAN AGE = 0.0 ± 0.0 Ma

8902-123 ZIRCON whitcombe s65/606142 410m

IRRADIATION jmt data:jmt zircon data:whitcombe zircons:wk037/4
SLIDE NUMBER 1
COUNTED BY: jmt

No.	Ns	Ni	Na	RATIO	U (ppm)	RHOs (E+06)	RHOi (E+06)	F.T AGE (Ma)
1	5	111	8	0.045	0.0	0.632	14.029	3.2 ± 1.5
2	1	27	2	0.037	0.0	0.506	13.650	2.6 ± 2.7
3	2	59	6	0.034	0.0	0.337	9.943	2.4 ± 1.7
4	1	23	2	0.043	0.0	0.506	11.628	3.1 ± 3.2
5	3	54	5	0.056	0.0	0.607	10.920	4.0 ± 2.4
6	7	129	6	0.054	0.0	1.180	21.739	3.9 ± 1.5
	19	403			0.0	0.662	14.051	

AREA OF BASIC UNIT = 9.89E-07 cm
CHI SQUARED = .4933088 WITH 5 DEGREES OF FREEDOM
P(chi squared) = 99.2 %
CORRELATION COEFFICIENT = 0.975
VARIANCE OF SQR(Ns) = 0.45
VARIANCE OF SQR(Ni) = 7.23

Ns/Ni = 0.047 ± 0.011
MEAN RATIO = 0.045 ± 0.004

Ages calculated using a zeta of 133.9 ± 1.4 for CN1 glass
RHO D = 1.067E+06 ; ND = 6342

POOLED AGE = 3.4 ± 0.8 Ma
MEAN AGE = 3.2 ± 0.3 Ma

8902-124 APATITE wilberforce s65/855143 760m

IRRADIATION jmt data:jmt apatite data:wilberforce apatites:wk015/13
SLIDE NUMBER 1
COUNTED BY: jmt

No.	Ns	Ni	Na	RATIO	U (ppm)	RHOs (E+06)	RHOi (E+06)	F.T.AGE (Ma)
1	0	27	20	0.000	15.5	0.000	1.365	0.0 ± 0.0
2	0	99	12	0.000	95.0	0.000	8.342	0.0 ± 0.0
3	0	16	6	0.000	30.7	0.000	2.696	0.0 ± 0.0
4	0	12	18	0.000	7.7	0.000	0.674	0.0 ± 0.0
5	0	50	12	0.000	48.0	0.000	4.213	0.0 ± 0.0
6	0	27	35	0.000	8.9	0.000	0.780	0.0 ± 0.0
7	0	9	8	0.000	13.0	0.000	1.138	0.0 ± 0.0
8	0	9	9	0.000	11.5	0.000	1.011	0.0 ± 0.0
9	0	23	15	0.000	17.7	0.000	1.550	0.0 ± 0.0
10	0	70	20	0.000	40.3	0.000	3.539	0.0 ± 0.0
11	0	9	10	0.000	10.4	0.000	0.910	0.0 ± 0.0
12	0	24	24	0.000	11.5	0.000	1.011	0.0 ± 0.0
13	0	13	12	0.000	12.5	0.000	1.095	0.0 ± 0.0
14	0	21	16	0.000	15.1	0.000	1.327	0.0 ± 0.0
	0	409			21.7	0.000	1.906	

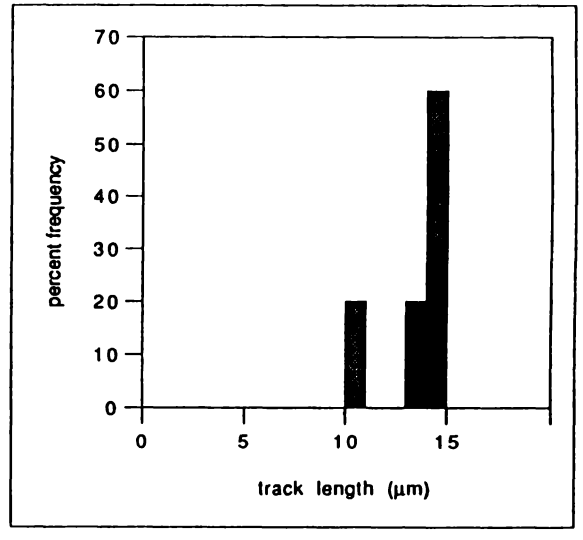
AREA OF BASIC UNIT = 9.89E-07 cm
CHI SQUARED = 3.131313E-06 WITH 13 DEGREES OF FREEDOM
P(chi squared) = 100.0 %
CORRELATION COEFFICIENT = 0.760
VARIANCE OF SQR(Ns) = 0.00
VARIANCE OF SQR(Ni) = 4.44

Ns/Ni = 0.000 ± 0.000
MEAN RATIO = 0.000 ± 0.000

Ages calculated using a zeta of 354.9 ± 4.3 for SRM612 glass
RHO D = 1.150E+06 ; ND = 2843

POOLED AGE = 0.0 ± 0.0 Ma
MEAN AGE = 0.0 ± 0.0 Ma

8902-124



n = 5
Mean = 13.63 µm
Sample std. dev. = 1.46 µm

8902-124 ZIRCON wilberforce s65/855143 760m

IRRADIATION jmt data:jmt zircon data:wilberforce zircons :wk027/10
SLIDE NUMBER 1
COUNTED BY: jmt

No.	Ns	Ni	Na	RATIO	U (ppm)	RHOs (E+06)	RHOi (E+06)	F.TAGE (Ma)
1	138	59	10	2.339	0.0	13.953	5.966	140.1 ± 21.9
2	82	28	6	2.929	0.0	13.819	4.719	174.9 ± 38.4
3	134	89	8	1.506	0.0	16.936	11.249	90.5 ± 12.5
4	81	36	6	2.250	0.0	13.650	6.067	134.8 ± 27.1
5	54	28	4	1.929	0.0	13.650	7.078	115.7 ± 27.0
6	92	33	6	2.788	0.0	15.504	5.561	166.6 ± 33.9
7	97	36	6	2.694	0.0	16.346	6.067	161.1 ± 31.6
8	74	33	4	2.242	0.0	18.706	8.342	134.4 ± 28.2
9	123	56	8	2.196	0.0	15.546	7.078	131.6 ± 21.4
10	49	18	4	2.722	0.0	12.386	4.550	162.7 ± 45.0
11	61	27	4	2.259	0.0	15.420	6.825	135.4 ± 31.4
12	41	22	3	1.864	0.0	13.819	7.415	111.9 ± 29.6
13	85	46	6	1.848	0.0	14.324	7.752	110.9 ± 20.4
14	558	212	30	2.632	0.0	18.807	7.145	157.4 ± 13.0
15	173	110	15	1.573	0.0	11.662	7.415	94.5 ± 11.7
16	281	125	24	2.248	0.0	11.839	5.266	134.7 ± 14.7
	2123	958			0.0	14.907	6.727	

AREA OF BASIC UNIT = 9.89E-07 cm
CHI SQUARED = 27.05009 WITH 15 DEGREES OF FREEDOM
P(chi squared) = 2.8 %
CORRELATION COEFFICIENT = 0.964
VARIANCE OF SQR(Ns) = 18.51
VARIANCE OF SQR(Ni) = 7.98

Ns/Ni = 2.216 ± 0.086
MEAN RATIO = 2.251 ± 0.107

Ages calculated using a zeta of 133.9 ± 1.4 for CN1 glass
RHO D = 9.043E+05 ; ND = 4472

POOLED AGE = 132.8 ± 5.7 Ma

MEAN AGE = 134.9 ± 6.9 Ma

8902-125 APATITE wilberforce s65/857110 670m

IRRADIATION jmt data:jmt apatite data:wilberforce apatites:wk015/12
SLIDE NUMBER 1
COUNTED BY: jmt

No.	Ns	Ni	Na	RATIO	U (ppm)	RHOs (E+06)	RHOi (E+06)	F.T.AGE (Ma)
1	1	22	8	0.045	31.9	0.126	2.781	9.2 ± 9.4
2	1	104	24	0.010	50.2	0.042	4.382	2.0 ± 2.0
3	3	56	12	0.054	54.1	0.253	4.719	10.9 ± 6.4
4	0	3	10	0.000	3.5	0.000	0.303	0.0 ± 0.0
5	0	18	16	0.000	13.0	0.000	1.138	0.0 ± 0.0
6	0	10	18	0.000	6.4	0.000	0.562	0.0 ± 0.0
7	0	47	15	0.000	36.3	0.000	3.168	0.0 ± 0.0
8	0	21	9	0.000	27.0	0.000	2.359	0.0 ± 0.0
9	0	5	6	0.000	9.7	0.000	0.843	0.0 ± 0.0
10	0	23	12	0.000	22.2	0.000	1.938	0.0 ± 0.0
11	0	78	25	0.000	36.2	0.000	3.155	0.0 ± 0.0
12	0	6	16	0.000	4.3	0.000	0.379	0.0 ± 0.0
13	0	2	6	0.000	3.9	0.000	0.337	0.0 ± 0.0
14	0	12	12	0.000	11.6	0.000	1.011	0.0 ± 0.0
15	1	34	9	0.029	43.8	0.112	3.820	6.0 ± 6.0
16	1	59	15	0.017	45.6	0.067	3.977	3.4 ± 3.5
17	1	47	24	0.021	22.7	0.042	1.980	4.3 ± 4.4
18	0	21	20	0.000	12.2	0.000	1.062	0.0 ± 0.0
19	1	36	20	0.028	20.9	0.051	1.820	5.6 ± 5.7
20	1	105	30	0.010	40.6	0.034	3.539	1.9 ± 1.9
21	0	23	9	0.000	29.6	0.000	2.584	0.0 ± 0.0
22	0	2	12	0.000	1.9	0.000	0.169	0.0 ± 0.0
23	2	53	12	0.038	51.2	0.169	4.466	7.6 ± 5.5
24	2	176	16	0.011	127.5	0.126	11.122	2.3 ± 1.6
25	2	29	6	0.069	56.0	0.337	4.887	14.0 ± 10.2
26	2	59	12	0.034	57.0	0.169	4.971	6.9 ± 4.9
27	4	44	12	0.091	42.5	0.337	3.707	18.4 ± 9.6
	22	1095			32.9	0.058	2.868	

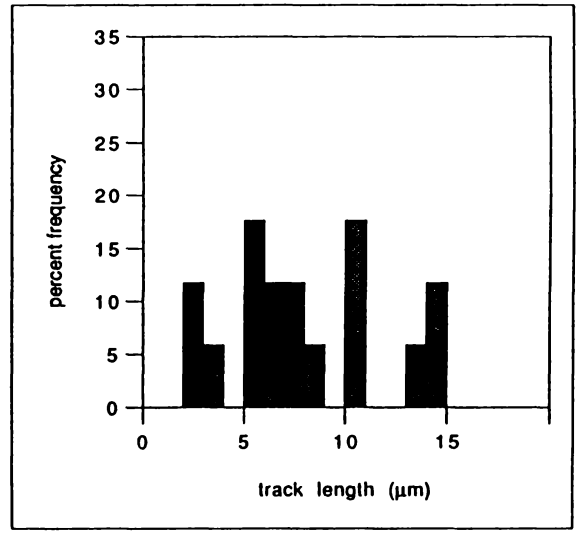
AREA OF BASIC UNIT = 9.89E-07 cm
CHI SQUARED = 25.78826 WITH 26 DEGREES OF FREEDOM
P(chi squared) = 47.5 %
CORRELATION COEFFICIENT = 0.449
VARIANCE OF SQR(Ns) = 0.46
VARIANCE OF SQR(Ni) = 8.42

Ns/Ni = 0.020 ± 0.004
MEAN RATIO = 0.017 ± 0.005

Ages calculated using a zeta of 354.9 ± 4.3 for SRM612 glass
RHO D = 1.143E+06 ; ND = 2825

POOLED AGE = 4.1 ± 0.9 Ma

8902-125



n = 17
Mean = 7.90 µm
Sample std. dev. = 3.63 µm

8902-125 ZIRCON wilberforce s65/857110 670m

IRRADIATION jmt data:jmt zircon data:wilberforce zircons :wk027/9
SLIDE NUMBER 1
COUNTED BY: jmt

No.	Ns	Ni	Na	RATIO	U (ppm)	RHOs (E+06)	RHOi (E+06)	F.T.AGE (Ma)
1	46	23	4	2.000	0.0	11.628	5.814	119.1 ± 30.5
2	27	22	3	1.227	0.0	9.100	7.415	73.3 ± 21.1
3	25	19	3	1.316	0.0	8.426	6.404	78.6 ± 24.0
4	37	18	3	2.056	0.0	12.471	6.067	122.3 ± 35.2
5	87	64	8	1.359	0.0	10.996	8.089	81.2 ± 13.4
6	28	14	2	2.000	0.0	14.156	7.078	119.1 ± 39.0
7	56	20	3	2.800	0.0	18.874	6.741	166.1 ± 43.4
8	51	25	3	2.040	0.0	17.189	8.426	121.4 ± 29.7
9	35	18	2	1.944	0.0	17.695	9.100	115.8 ± 33.7
10	37	21	3	1.762	0.0	12.471	7.078	105.0 ± 28.8
11	55	29	4	1.897	0.0	13.903	7.331	113.0 ± 26.0
12	84	28	4	3.000	0.0	21.234	7.078	177.8 ± 38.9
13	38	14	2	2.714	0.0	19.211	7.078	161.1 ± 50.4
14	24	10	2	2.400	0.0	12.133	5.056	142.6 ± 53.7
15	56	18	4	3.111	0.0	14.156	4.550	184.3 ± 50.0
	686	343			0.0	13.873	6.936	

AREA OF BASIC UNIT = 9.89E-07 cm
CHI SQUARED = 19.8136 WITH 14 DEGREES OF FREEDOM
P(chi squared) = 13.6 %
CORRELATION COEFFICIENT = 0.757
VARIANCE OF SQR(Ns) = 1.92
VARIANCE OF SQR(Ni) = 1.20

Ns/Ni = 2.000 ± 0.132
MEAN RATIO = 2.108 ± 0.153

Ages calculated using a zeta of 133.9 ± 1.4 for CN1 glass
RHO D = 8.975E+05 ; ND = 4438

POOLED AGE = 119.1 ± 8.2 Ma
MEAN AGE = 125.5 ± 9.4 Ma

8902-126 APATITE wilberforce s65/886057 700m

IRRADIATION jmt data:jmt apatite data:wilberforce apatites:wk015/11
SLIDE NUMBER 1
COUNTED BY: jmt

No.	Ns	NI	Na	RATIO	U (ppm)	RHOs (E+06)	RHOi (E+06)	F.T.AGE (Ma)
1	1	15	4	0.067	43.7	0.253	3.792	13.4 ± 13.9
2	2	31	15	0.065	24.1	0.135	2.090	13.0 ± 9.5
3	5	115	21	0.043	63.9	0.241	5.537	8.8 ± 4.0
4	2	7	6	0.286	13.6	0.337	1.180	57.3 ± 46.0
5	0	14	6	0.000	27.2	0.000	2.359	0.0 ± 0.0
6	2	30	6	0.067	58.3	0.337	5.056	13.4 ± 9.8
7	0	8	8	0.000	11.7	0.000	1.011	0.0 ± 0.0
8	0	6	6	0.000	11.7	0.000	1.011	0.0 ± 0.0
9	0	10	16	0.000	7.3	0.000	0.632	0.0 ± 0.0
10	1	63	40	0.016	18.4	0.025	1.593	3.2 ± 3.2
11	5	39	4	0.128	113.7	1.264	9.858	25.8 ± 12.3
12	0	22	12	0.000	21.4	0.000	1.854	0.0 ± 0.0
13	2	74	10	0.027	86.3	0.202	7.482	5.4 ± 3.9
14	0	11	6	0.000	21.4	0.000	1.854	0.0 ± 0.0
15	1	10	9	0.100	13.0	0.112	1.123	20.1 ± 21.1
16	0	37	10	0.000	43.1	0.000	3.741	0.0 ± 0.0
17	2	124	20	0.016	72.3	0.101	6.269	3.2 ± 2.3
18	0	3	12	0.000	2.9	0.000	0.253	0.0 ± 0.0
19	4	62	6	0.065	120.5	0.674	10.448	13.0 ± 6.7
20	1	18	12	0.056	17.5	0.084	1.517	11.2 ± 11.5
21	0	5	6	0.000	9.7	0.000	0.843	0.0 ± 0.0
22	14	104	12	0.135	101.1	1.180	8.763	27.1 ± 7.7
23	0	34	12	0.000	33.0	0.000	2.865	0.0 ± 0.0
24	1	12	4	0.083	35.0	0.253	3.033	16.8 ± 17.5
25	0	23	20	0.000	13.4	0.000	1.163	0.0 ± 0.0
26	2	89	12	0.022	86.5	0.169	7.499	4.5 ± 3.2
27	0	50	12	0.000	48.6	0.000	4.213	0.0 ± 0.0
28	2	56	8	0.036	81.6	0.253	7.078	7.2 ± 5.2
29	9	217	15	0.041	168.7	0.607	14.628	8.4 ± 2.8
30	0	17	9	0.000	22.0	0.000	1.910	0.0 ± 0.0
	56	1306			44.9	0.167	3.895	

AREA OF BASIC UNIT = 9.89E-07 cm
CHI SQUARED = 48.76064 WITH 29 DEGREES OF FREEDOM
P(chi squared) = 1.2 %
CORRELATION COEFFICIENT = 0.697
VARIANCE OF SQR(Ns) = 1.02
VARIANCE OF SQR(Ni) = 9.89

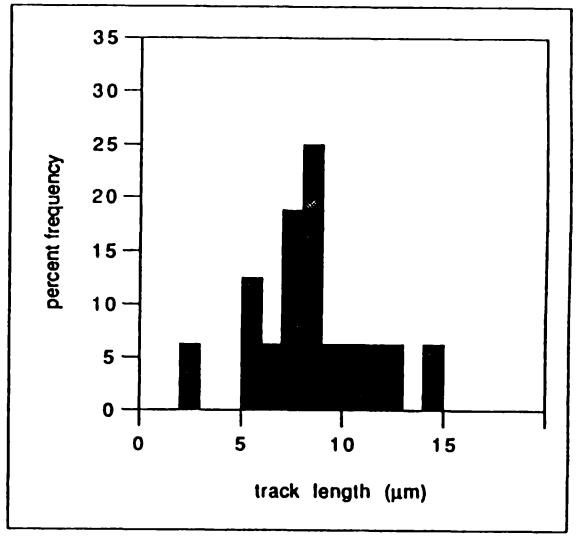
Ns/Ni = 0.043 ± 0.006
MEAN RATIO = 0.042 ± 0.011

Ages calculated using a zeta of 354.9 ± 4.3 for SRM612 glass
RHO D = 1.136E+06 ; ND = 2808

POOLED AGE = 8.6 ± 1.2 Ma

MEAN AGE = 8.4 ± 2.2 Ma

8902-126



n = 16
Mean = 8.49 µm
Sample std. dev. = 2.77 µm

8902-126 ZIRCON wilberforce s65/886057 700m

IRRADIATION jmt data:jmt zircon data:wilberforce zircons :wk027/8
SLIDE NUMBER 1
COUNTED BY: jmt

No.	Ns	Ni	Na	RATIO	U (ppm)	RHOs (E+06)	RHOi (E+06)	F.T.AGE (Ma)
1	34	20	3	1.700	0.0	11.459	6.741	100.6 ± 28.4
2	26	14	2	1.857	0.0	13.145	7.078	109.8 ± 36.4
3	48	15	4	3.200	0.0	12.133	3.792	188.0 ± 55.7
4	25	9	2	2.778	0.0	12.639	4.550	163.5 ± 63.6
5	43	14	3	3.071	0.0	14.493	4.719	180.5 ± 55.7
	176	72			0.0	12.711	5.200	

AREA OF BASIC UNIT = 9.89E-07 cm
CHI SQUARED = 3.86613 WITH 4 DEGREES OF FREEDOM
P(chi squared) = 42.4 %
CORRELATION COEFFICIENT = 0.355
VARIANCE OF SQR(Ns) = 0.74
VARIANCE OF SQR(Ni) = 0.27

Ns/Ni = 2.444 ± 0.342
MEAN RATIO = 2.521 ± 0.312

Ages calculated using a zeta of 133.9 ± 1.4 for CN1 glass
RHO D = 8.904E+05 ; ND = 4403

POOLED AGE = 144.1 ± 20.3 Ma
MEAN AGE = 148.6 ± 18.6 Ma

8902-127 APATITE wilberforce s65/933003 670m

IRRADIATION jmt data:jmt apatite data:wilberforce apatites:wk015/10
SLIDE NUMBER 1
COUNTED BY: jmt

No.	Ns	NI	Na	RATIO	U (ppm)	RHOs (E+06)	RHOI (E+06)	F.T.AGE (Ma)
1	16	93	15	0.172	72.7	1.079	6.269	34.4 ± 9.3
2	37	136	30	0.272	53.2	1.247	4.584	54.3 ± 10.1
3	0	12	25	0.000	5.6	0.000	0.485	0.0 ± 0.0
4	1	15	15	0.067	11.7	0.067	1.011	13.3 ± 13.8
5	5	19	30	0.263	7.4	0.169	0.640	52.5 ± 26.4
6	4	32	30	0.125	12.5	0.135	1.079	25.0 ± 13.3
7	9	35	20	0.257	20.5	0.455	1.769	51.3 ± 19.2
8	5	32	20	0.156	18.8	0.253	1.618	31.2 ± 15.0
9	56	201	25	0.279	94.3	2.265	8.129	55.6 ± 8.5
10	16	110	32	0.145	40.3	0.506	3.476	29.1 ± 7.8
11	72	243	32	0.296	89.1	2.275	7.678	59.1 ± 8.0
12	31	292	35	0.106	97.9	0.896	8.436	21.2 ± 4.0
13	4	24	25	0.167	11.3	0.162	0.971	33.3 ± 18.0
14	1	9	16	0.111	6.6	0.063	0.569	22.2 ± 23.4
15	15	42	24	0.357	20.5	0.632	1.769	71.2 ± 21.5
16	2	11	12	0.182	10.8	0.169	0.927	36.3 ± 27.9
17	5	99	20	0.050	58.1	0.253	5.005	10.1 ± 4.6
18	8	32	9	0.250	41.7	0.899	3.595	49.9 ± 19.8
19	11	25	12	0.440	24.4	0.927	2.106	87.6 ± 31.7
20	11	24	16	0.458	17.6	0.695	1.517	91.2 ± 33.3
21	15	92	24	0.163	45.0	0.632	3.876	32.6 ± 9.1
22	10	46	12	0.217	45.0	0.843	3.876	43.4 ± 15.2
23	5	34	24	0.147	16.6	0.211	1.432	29.4 ± 14.1
24	5	25	18	0.200	16.3	0.281	1.404	39.9 ± 19.6
25	11	61	40	0.180	17.9	0.278	1.542	36.0 ± 11.8
	355	1744			36.5	0.640	3.143	

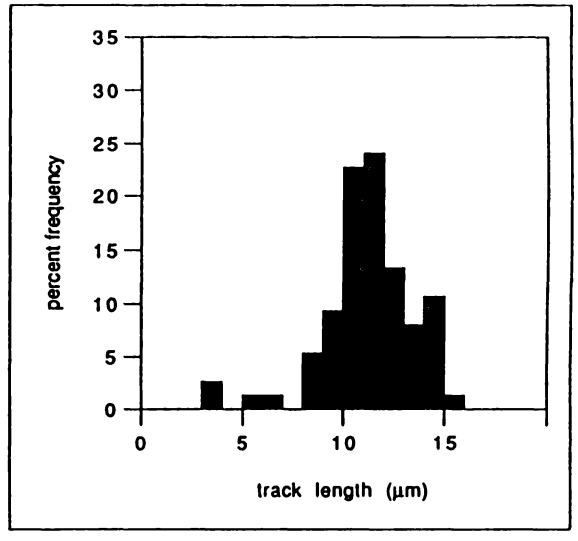
AREA OF BASIC UNIT = 9.89E-07 cm
CHI SQUARED = 61.06889 WITH 24 DEGREES OF FREEDOM
P(chi squared) = < 0.1 %
CORRELATION COEFFICIENT = 0.848
VARIANCE OF SQR(Ns) = 3.88
VARIANCE OF SQR(Ni) = 15.14

Ns/Ni = 0.204 ± 0.012
MEAN RATIO = 0.202 ± 0.022

Ages calculated using a zeta of 354.9 ± 4.3 for SRM612 glass
RHO D = 1.129E+06 ; ND = 2790

POOLED AGE = 40.7 ± 2.5 Ma
MEAN AGE = 40.4 ± 4.5 Ma

8902-127



n = 75
Mean = 11.27 µm
Sample std. dev. = 2.20 µm

8902-127 ZIRCON wilberforce s65/933003 670m

IRRADIATION jmt data:jmt zircon data:wilberforce zircons :wk027/7
SLIDE NUMBER 1
COUNTED BY: jmt

No.	Ns	Ni	Na	RATIO	U (ppm)	RHOs (E+06)	RHOi (E+06)	F.T.AGE (Ma)
1	171	86	12	1.988	0.0	14.408	7.246	116.5 ± 15.6
2	215	101	16	2.129	0.0	13.587	6.383	124.7 ± 15.2
3	86	43	9	2.000	0.0	9.662	4.831	117.2 ± 22.0
4	170	83	12	2.048	0.0	14.324	6.994	120.0 ± 16.2
5	56	23	5	2.435	0.0	11.325	4.651	142.4 ± 35.4
6	485	246	36	1.972	0.0	13.622	6.909	115.5 ± 9.3
7	156	75	12	2.080	0.0	13.145	6.320	121.8 ± 17.3
8	59	27	6	2.185	0.0	9.943	4.550	127.9 ± 29.8
9	54	23	4	2.348	0.0	13.650	5.814	137.4 ± 34.3
10	133	63	12	2.111	0.0	11.207	5.308	123.7 ± 19.0
11	120	46	8	2.609	0.0	15.167	5.814	152.5 ± 26.6
12	75	39	6	1.923	0.0	12.639	6.572	112.7 ± 22.4
13	383	141	24	2.716	0.0	16.136	5.940	158.7 ± 15.9
	2163	996			0.0	13.500	6.217	

AREA OF BASIC UNIT = 9.89E-07 cm
CHI SQUARED = 9.509047 WITH 12 DEGREES OF FREEDOM
P(chi squared) = 65.9 %
CORRELATION COEFFICIENT = 0.978
VARIANCE OF SQR(Ns) = 20.64
VARIANCE OF SQR(Ni) = 9.66

Ns/Ni = 2.172 ± 0.083
MEAN RATIO = 2.196 ± 0.070

Ages calculated using a zeta of 133.9 ± 1.4 for CN1 glass
RHO D = 8.833E+05 ; ND = 4368

POOLED AGE = 127.2 ± 5.4 Ma
MEAN AGE = 128.6 ± 4.8 Ma

8902-128 APATITE wilberforce s74/080783 520m

IRRADIATION jmt data:jmt apatite data:wilberforce apatites:wk015/9
SLIDE NUMBER 1
COUNTED BY: jmt

No.	Ns	NI	Na	RATIO	U (ppm)	RHOs (E+06)	RHOi (E+06)	F.T.AGE (Ma)
1	5	14	9	0.357	18.4	0.562	1.573	70.7 ± 36.9
2	2	44	15	0.045	34.6	0.135	2.966	9.0 ± 6.5
3	13	91	12	0.143	89.5	1.095	7.668	28.4 ± 8.4
4	8	37	6	0.216	72.8	1.348	6.235	42.9 ± 16.8
5	0	3	4	0.000	8.9	0.000	0.758	0.0 ± 0.0
6	6	13	12	0.462	12.8	0.506	1.095	91.2 ± 45.1
7	0	10	9	0.000	13.1	0.000	1.123	0.0 ± 0.0
8	0	4	9	0.000	5.2	0.000	0.449	0.0 ± 0.0
9	2	20	8	0.100	29.5	0.253	2.528	19.9 ± 14.7
10	2	9	9	0.222	11.8	0.225	1.011	44.1 ± 34.5
11	2	43	24	0.047	21.2	0.084	1.812	9.3 ± 6.7
12	5	14	9	0.357	18.4	0.562	1.573	70.7 ± 36.9
13	0	9	20	0.000	5.3	0.000	0.455	0.0 ± 0.0
14	7	26	12	0.269	25.6	0.590	2.191	53.4 ± 22.8
15	5	6	4	0.833	17.7	1.264	1.517	163.8 ± 99.3
16	6	38	20	0.158	22.4	0.303	1.921	31.4 ± 13.8
17	5	49	12	0.102	48.2	0.421	4.129	20.3 ± 9.5
18	6	29	10	0.207	34.2	0.607	2.932	41.1 ± 18.4
19	1	16	16	0.062	11.8	0.063	1.011	12.4 ± 12.8
20	26	47	12	0.553	46.2	2.191	3.960	109.2 ± 26.8
	101	522			26.6	0.440	2.275	

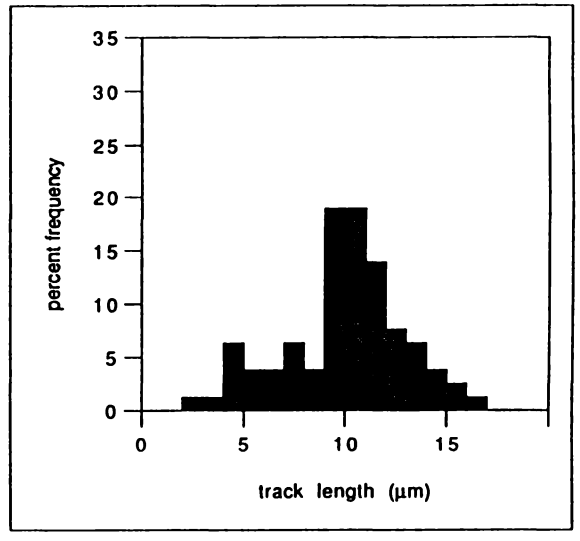
AREA OF BASIC UNIT = 9.89E-07 cm
CHI SQUARED = 53.79438 WITH 19 DEGREES OF FREEDOM
P(chi squared) = < 0.1 %
CORRELATION COEFFICIENT = 0.567
VARIANCE OF SQR(Ns) = 1.69
VARIANCE OF SQR(Ni) = 4.11

Ns/Ni = 0.193 ± 0.021
MEAN RATIO = 0.207 ± 0.049

Ages calculated using a zeta of 354.9 ± 4.3 for SRM612 glass
RHO D = 1.122E+06 ; ND = 2772

POOLED AGE = 38.4 ± 4.3 Ma
MEAN AGE = 41.0 ± 9.7 Ma

8902-128



n = 79
Mean = 9.98 µm
Sample std. dev. = 2.84 µm

8902-128 ZIRCON wilberforce s74/080783 520m

IRRADIATION jmt data:jmt zircon data:wilberforce zircons :wk027/6
SLIDE NUMBER 1
COUNTED BY: jmt

No.	Ns	Ni	Na	RATIO	U (ppm)	RHOs (E+06)	RHOi (E+06)	F.T.AGE (Ma)
1	328	104	30	3.154	0.0	11.055	3.505	182.4 ± 20.8
2	270	107	24	2.523	0.0	11.375	4.508	146.4 ± 16.9
3	68	35	12	1.943	0.0	5.730	2.949	113.0 ± 23.6
4	15	6	4	2.500	0.0	3.792	1.517	145.0 ± 70.1
5	218	102	21	2.137	0.0	10.496	4.911	124.2 ± 15.1
6	70	24	6	2.917	0.0	11.796	4.044	168.9 ± 40.1
7	295	97	24	3.041	0.0	12.428	4.087	176.0 ± 20.9
8	77	44	12	1.750	0.0	6.488	3.707	101.9 ± 19.3
9	288	115	24	2.504	0.0	12.133	4.845	145.3 ± 16.2
	1629	634			0.0	10.491	4.083	

AREA OF BASIC UNIT = 9.89E-07 cm
CHI SQUARED = 14.13923 WITH 8 DEGREES OF FREEDOM
P(chi squared) = 7.8 %
CORRELATION COEFFICIENT = 0.961
VARIANCE OF SQR(Ns) = 27.17
VARIANCE OF SQR(Ni) = 9.01

Ns/Ni = 2.569 ± 0.120
MEAN RATIO = 2.497 ± 0.162

Ages calculated using a zeta of 133.9 ± 1.4 for CN1 glass
RHO D = 8.764E+05 ; ND = 4334

POOLED AGE = 149.0 ± 7.5 Ma
MEAN AGE = 144.8 ± 9.8 Ma

8902-129 APATITE arthur's s51/980524 170m

IRRADIATION jmt data:jmt apatite data:arthur's apatites:wk015/8
SLIDE NUMBER 1
COUNTED BY: jmt

No.	Ns	Ni	Na	RATIO	U (ppm)	RHOs (E+06)	RHOi (E+06)	F.T.AGE (Ma)
1	0	21	8	0.000	31.2	0.000	2.654	0.0 ± 0.0
2	0	17	9	0.000	22.4	0.000	1.910	0.0 ± 0.0
3	0	53	12	0.000	52.5	0.000	4.466	0.0 ± 0.0
4	0	37	9	0.000	48.8	0.000	4.157	0.0 ± 0.0
5	0	5	4	0.000	14.8	0.000	1.264	0.0 ± 0.0
6	0	33	10	0.000	39.2	0.000	3.337	0.0 ± 0.0
7	0	6	6	0.000	11.9	0.000	1.011	0.0 ± 0.0
8	0	70	9	0.000	92.4	0.000	7.864	0.0 ± 0.0
9	0	11	6	0.000	21.8	0.000	1.854	0.0 ± 0.0
10	0	2	4	0.000	5.9	0.000	0.506	0.0 ± 0.0
11	0	20	9	0.000	26.4	0.000	2.247	0.0 ± 0.0
12	0	12	9	0.000	15.8	0.000	1.348	0.0 ± 0.0
13	0	1	12	0.000	1.0	0.000	0.084	0.0 ± 0.0
14	0	15	6	0.000	29.7	0.000	2.528	0.0 ± 0.0
15	0	1	20	0.000	0.6	0.000	0.051	0.0 ± 0.0
	0	304			27.2	0.000	2.311	

AREA OF BASIC UNIT = 9.89E-07 cm
CHI SQUARED = 1.347619E-05 WITH 14 DEGREES OF FREEDOM
P(chi squared) = 100.0 %
CORRELATION COEFFICIENT = 0.010
VARIANCE OF SQR(Ns) = 0.00
VARIANCE OF SQR(Ni) = 4.91

Ns/Ni = 0.000 ± 0.000
MEAN RATIO = 0.000 ± 0.000

Ages calculated using a zeta of 354.9 ± 4.3 for SRM612 glass
RHO D = 1.115E+06 ; ND = 2755

POOLED AGE = 0.0 ± 0.0 Ma
MEAN AGE = 0.0 ± 0.0 Ma

8902-129 ZIRCON arthur's s51/980524 170m

IRRADIATION jmt data:jmt zircon data:arthur's zircons:wk027/5
SLIDE NUMBER 1
COUNTED BY: jmt

No.	Ns	Ni	Na	RATIO	U (ppm)	RHOs (E+06)	RHOi (E+06)	F.T.AGE (Ma)
1	3	82	8	0.037	0.0	0.379	10.364	2.1 ± 1.3
2	3	97	10	0.031	0.0	0.303	9.808	1.8 ± 1.1
3	6	192	24	0.031	0.0	0.253	8.089	1.8 ± 0.8
4	0	43	6	0.000	0.0	0.000	7.246	0.0 ± 0.0
	12	414			0.0	0.253	8.721	

AREA OF BASIC UNIT = 9.89E-07 cm
CHI SQUARED = 1.449191 WITH 3 DEGREES OF FREEDOM
P(chi squared) = 69.4 %
CORRELATION COEFFICIENT = 0.962
VARIANCE OF SQR(Ns) = 1.09
VARIANCE OF SQR(Ni) = 9.17

Ns/Ni = 0.029 ± 0.008
MEAN RATIO = 0.025 ± 0.008

Ages calculated using a zeta of 133.9 ± 1.4 for CN1 glass
RHO D = 8.694E+05 ; ND = 4299

POOLED AGE = 1.7 ± 0.5 Ma
MEAN AGE = 1.4 ± 0.5 Ma

8902-130 APATITE arthur's s52/045506 245m

IRRADIATION jmt data:jmt apatite data:arthur's apatites:wk015/7
SLIDE NUMBER 1
COUNTED BY: jmt

No.	Ns	Ni	Na	RATIO	U (ppm)	RHOs (E+06)	RHOi (E+06)	F.T.AGE (Ma)
1	0	49	15	0.000	39.1	0.000	3.303	0.0 ± 0.0
2	0	14	12	0.000	13.9	0.000	1.180	0.0 ± 0.0
3	1	50	12	0.020	49.8	0.084	4.213	3.9 ± 4.0
4	0	42	49	0.000	10.2	0.000	0.867	0.0 ± 0.0
5	0	32	25	0.000	15.3	0.000	1.294	0.0 ± 0.0
6	0	60	24	0.000	29.9	0.000	2.528	0.0 ± 0.0
7	0	66	24	0.000	32.9	0.000	2.781	0.0 ± 0.0
8	0	5	12	0.000	5.0	0.000	0.421	0.0 ± 0.0
9	0	5	8	0.000	7.5	0.000	0.632	0.0 ± 0.0
10	0	18	24	0.000	9.0	0.000	0.758	0.0 ± 0.0
11	0	106	20	0.000	63.4	0.000	5.359	0.0 ± 0.0
12	1	125	28	0.008	53.4	0.036	4.514	1.6 ± 1.6
13	0	20	12	0.000	19.9	0.000	1.685	0.0 ± 0.0
14	0	25	15	0.000	19.9	0.000	1.685	0.0 ± 0.0
15	0	88	16	0.000	65.8	0.000	5.561	0.0 ± 0.0
	2	705			28.5	0.007	2.408	

AREA OF BASIC UNIT = 9.89E-07 cm
CHI SQUARED = 7.758876 WITH 14 DEGREES OF FREEDOM
P(chi squared) = 90.2 %
CORRELATION COEFFICIENT = 0.450
VARIANCE OF SQR(Ns) = 0.12
VARIANCE OF SQR(Ni) = 7.50

Ns/Ni = 0.003 ± 0.002
MEAN RATIO = 0.002 ± 0.001

Ages calculated using a zeta of 354.9 ± 4.3 for SRM612 glass
RHO D = 1.108E+06 ; ND = 2737

POOLED AGE = 0.6 ± 0.4 Ma
MEAN AGE = 0.4 ± 0.3 Ma

8902-130 ZIRCON arthur's s52/045506 245m

IRRADIATION jmt data:jmt zircon data:arthur's zircons:wk027/4
SLIDE NUMBER 1
COUNTED BY: jmt

No.	Ns	Ni	Na	RATIO	U (ppm)	RHOs (E+06)	RHOi (E+06)	F.T.AGE (Ma)
1	51	621	54	0.082	0.0	0.955	11.628	4.7 ± 0.7
2	48	661	50	0.073	0.0	0.971	13.367	4.2 ± 0.6
3	11	124	16	0.089	0.0	0.695	7.836	5.1 ± 1.6
4	26	274	30	0.095	0.0	0.876	9.235	5.5 ± 1.1
5	14	178	18	0.079	0.0	0.786	9.999	4.5 ± 1.3
6	2	14	4	0.143	0.0	0.506	3.539	8.2 ± 6.2
7	7	78	12	0.090	0.0	0.590	6.572	5.2 ± 2.0
8	4	40	9	0.100	0.0	0.449	4.494	5.8 ± 3.0
9	22	286	25	0.077	0.0	0.890	11.567	4.4 ± 1.0
10	10	147	18	0.068	0.0	0.562	8.257	3.9 ± 1.3
11	11	142	21	0.077	0.0	0.530	6.837	4.5 ± 1.4
12	17	204	21	0.083	0.0	0.819	9.822	4.8 ± 1.2
13	8	110	32	0.073	0.0	0.253	3.476	4.2 ± 1.5
14	17	130	18	0.131	0.0	0.955	7.303	7.5 ± 2.0
15	6	116	12	0.052	0.0	0.506	9.774	3.0 ± 1.3
16	5	55	10	0.091	0.0	0.506	5.561	5.2 ± 2.5
17	33	416	56	0.079	0.0	0.596	7.511	4.6 ± 0.8
18	23	310	48	0.074	0.0	0.484	6.530	4.3 ± 0.9
19	6	91	10	0.066	0.0	0.607	9.201	3.8 ± 1.6
	321	3997			0.0	0.700	8.710	

AREA OF BASIC UNIT = 9.89E-07 cm
CHI SQUARED = 7.698418 WITH 18 DEGREES OF FREEDOM
P(chi squared) = 98.3 %
CORRELATION COEFFICIENT = 0.986
VARIANCE OF SQR(Ns) = 2.59
VARIANCE OF SQR(Ni) = 34.29

Ns/Ni = 0.080 ± 0.005
MEAN RATIO = 0.085 ± 0.005

Ages calculated using a zeta of 133.9 ± 1.4 for CN1 glass
RHO D = 8.623E+05 ; ND = 4264

POOLED AGE = 4.6 ± 0.3 Ma
MEAN AGE = 4.9 ± 0.3 Ma

8902-132 APATITE arthur's s59/104498 290m

IRRADIATION jmt data:jmt apatite data:arthur's apatites:wk015/5
SLIDE NUMBER 1
COUNTED BY: jmt

No.	Ns	Ni	Na	RATIO	U (ppm)	RHOs (E+06)	RHOi (E+06)	F.T AGE (Ma)
1	0	21	6	0.000	42.4	0.000	3.539	0.0 ± 0.0
2	0	13	6	0.000	26.3	0.000	2.191	0.0 ± 0.0
3	0	4	8	0.000	6.1	0.000	0.506	0.0 ± 0.0
4	0	31	12	0.000	31.3	0.000	2.612	0.0 ± 0.0
5	0	15	9	0.000	20.2	0.000	1.685	0.0 ± 0.0
6	0	69	16	0.000	52.3	0.000	4.360	0.0 ± 0.0
7	0	23	12	0.000	23.2	0.000	1.938	0.0 ± 0.0
8	0	45	24	0.000	22.7	0.000	1.896	0.0 ± 0.0
9	0	4	6	0.000	8.1	0.000	0.674	0.0 ± 0.0
10	0	32	6	0.000	64.6	0.000	5.393	0.0 ± 0.0
11	0	18	9	0.000	24.2	0.000	2.022	0.0 ± 0.0
12	0	7	5	0.000	17.0	0.000	1.416	0.0 ± 0.0
13	0	11	6	0.000	22.2	0.000	1.854	0.0 ± 0.0
14	0	109	16	0.000	82.6	0.000	6.888	0.0 ± 0.0
15	0	49	9	0.000	66.0	0.000	5.505	0.0 ± 0.0
	0	451			36.4	0.000	3.040	

AREA OF BASIC UNIT = 9.89E-07 cm
CHI SQUARED = 3.137614E-05 WITH 14 DEGREES OF FREEDOM
P(chi squared) = 100.0 %
CORRELATION COEFFICIENT = 0.766
VARIANCE OF SQR(Ns) = 0.00
VARIANCE OF SQR(Ni) = 5.61

Ns/Ni = 0.000 ± 0.000
MEAN RATIO = 0.000 ± 0.000

Ages calculated using a zeta of 354.9 ± 4.3 for SRM612 glass
RHO D = 1.093E+06 ; ND = 2702

POOLED AGE = 0.0 ± 0.0 Ma
MEAN AGE = 0.0 ± 0.0 Ma

8902-132 ZIRCON arthur's s59/104498 290m

IRRADIATION jmt data:jmt zircon data:arthur's zircons:wk027/2
SLIDE NUMBER 1
COUNTED BY: jmt

No.	Ns	Ni	Na	RATIO	U (ppm)	RHOs (E+06)	RHOi (E+06)	F.T AGE (Ma)
1	3	12	2	0.250	0.0	1.517	6.067	14.2 ± 9.2
2	3	20	3	0.150	0.0	1.011	6.741	8.5 ± 5.3
3	5	15	2	0.333	0.0	2.528	7.583	18.9 ± 9.8
4	8	30	4	0.267	0.0	2.022	7.583	15.1 ± 6.0
5	15	19	4	0.789	0.0	3.792	4.803	44.7 ± 15.5
6	8	12	1	0.667	0.0	8.089	12.133	37.8 ± 17.2
	42	108			0.0	2.654	6.825	

AREA OF BASIC UNIT = 9.89E-07 cm
CHI SQUARED = 9.837111 WITH 5 DEGREES OF FREEDOM
P(chi squared) = 8.0 %
CORRELATION COEFFICIENT = 0.235
VARIANCE OF SQR(Ns) = 0.67
VARIANCE OF SQR(Ni) = 0.58

Ns/Ni = 0.389 ± 0.071
MEAN RATIO = 0.409 ± 0.105

Ages calculated using a zeta of 133.9 ± 1.4 for CN1 glass
RHO D = 8.483E+05 ; ND = 4195

POOLED AGE = 22.0 ± 4.0 Ma
MEAN AGE = 23.2 ± 6.0 Ma

8902-131 APATITE arthur's s52/082500 245m

IRRADIATION jmt data:jmt apatite data:arthur's apatites:wk021/9
SLIDE NUMBER 1
COUNTED BY: jmt

No.	Ns	Ni	Na	RATIO	U (ppm)	RHOs (E+06)	RHOi (E+06)	F.T.AGE (Ma)
1	0	201	16	0.000	37.2	0.000	12.702	0.0 ± 0.0
2	0	377	100	0.000	11.1	0.000	3.812	0.0 ± 0.0
3	0	22	8	0.000	8.1	0.000	2.781	0.0 ± 0.0
4	0	74	20	0.000	10.9	0.000	3.741	0.0 ± 0.0
5	0	203	24	0.000	25.0	0.000	8.552	0.0 ± 0.0
6	0	77	15	0.000	15.2	0.000	5.190	0.0 ± 0.0
7	0	378	60	0.000	18.6	0.000	6.370	0.0 ± 0.0
8	0	77	15	0.000	15.2	0.000	5.190	0.0 ± 0.0
9	0	304	25	0.000	36.0	0.000	12.295	0.0 ± 0.0
10	0	223	16	0.000	41.2	0.000	14.093	0.0 ± 0.0
11	0	360	36	0.000	29.6	0.000	10.111	0.0 ± 0.0
12	0	45	12	0.000	11.1	0.000	3.792	0.0 ± 0.0
13	0	31	16	0.000	5.7	0.000	1.959	0.0 ± 0.0
14	0	160	24	0.000	19.7	0.000	6.741	0.0 ± 0.0
15	0	153	16	0.000	28.3	0.000	9.669	0.0 ± 0.0
	0	2685			19.7	0.000	6.737	

AREA OF BASIC UNIT = 9.89E-07 cm
CHI SQUARED = 6.122015E-05 WITH 14 DEGREES OF FREEDOM
P(chi squared) = 100.0 %
CORRELATION COEFFICIENT = 0.430
VARIANCE OF SQR(Ns) = 0.00
VARIANCE OF SQR(Ni) = 25.69

Ns/Ni = 0.000 ± 0.000
MEAN RATIO = 0.000 ± 0.000

Ages calculated using a zeta of 354.9 ± 4.3 for SRM612 glass
RHO D = 4.479E+06 ; ND = 3544

POOLED AGE = 0.0 ± 0.0 Ma
MEAN AGE = 0.0 ± 0.0 Ma

8902-131 ZIRCON arthur's s52/082500 245m

IRRADIATION jmt data:jmt zircon data:arthur's zircons:wk027/3
SLIDE NUMBER 1
COUNTED BY: jmt

No.	Ns	Ni	Na	RATIO	U (ppm)	RHOs (E+06)	RHOi (E+06)	F.T.AGE (Ma)
1	46	253	28	0.182	0.0	1.661	9.136	10.4 ± 1.7
2	41	177	12	0.232	0.0	3.455	14.914	13.2 ± 2.3
3	22	110	20	0.200	0.0	1.112	5.561	11.4 ± 2.7
4	51	181	16	0.282	0.0	3.223	11.438	16.1 ± 2.6
5	23	68	10	0.338	0.0	2.326	6.876	19.3 ± 4.7
6	18	146	20	0.123	0.0	0.910	7.381	7.1 ± 1.8
7	127	438	56	0.290	0.0	2.293	7.908	16.6 ± 1.7
8	9	23	4	0.391	0.0	2.275	5.814	22.4 ± 8.8
9	39	161	12	0.242	0.0	3.286	13.566	13.9 ± 2.5
10	8	27	6	0.296	0.0	1.348	4.550	16.9 ± 6.8
11	24	139	9	0.173	0.0	2.696	15.616	9.9 ± 2.2
12	12	53	5	0.226	0.0	2.427	10.718	13.0 ± 4.1
13	5	25	4	0.200	0.0	1.264	6.320	11.4 ± 5.6
14	16	59	12	0.271	0.0	1.348	4.971	15.5 ± 4.4
15	28	127	9	0.220	0.0	3.146	14.268	12.6 ± 2.6
	469	1987			0.0	2.127	9.009	

AREA OF BASIC UNIT = 9.89E-07 cm
CHI SQUARED = 22.39244 WITH 14 DEGREES OF FREEDOM
P(chi squared) = 7.1 %
CORRELATION COEFFICIENT = 0.955
VARIANCE OF SQR(Ns) = 5.05
VARIANCE OF SQR(Ni) = 19.86

Ns/Ni = 0.236 ± 0.012
MEAN RATIO = 0.244 ± 0.018

Ages calculated using a zeta of 133.9 ± 1.4 for CN1 glass
RHO D = 8.552E+05 ; ND = 4229

POOLED AGE = 13.5 ± 0.7 Ma
MEAN AGE = 14.0 ± 1.0 Ma

8902-133 APATITE arthur's s59/053297 810m

IRRADIATION jmt data:jmt apatite data:arthur's apatites:wk021/8
SLIDE NUMBER 1
COUNTED BY: jmt

No.	Ns	Ni	Na	RATIO	U (ppm)	RHOs (E+06)	RHOi (E+06)	F.T.AGE (Ma)
1	0	39	6	0.000	19.3	0.000	6.572	0.0 ± 0.0
2	2	77	16	0.026	14.3	0.126	4.866	20.5 ± 14.7
3	0	63	6	0.000	31.2	0.000	10.617	0.0 ± 0.0
4	0	135	12	0.000	33.5	0.000	11.375	0.0 ± 0.0
5	0	110	12	0.000	27.3	0.000	9.269	0.0 ± 0.0
6	1	57	9	0.018	18.8	0.112	6.404	13.8 ± 14.0
7	0	33	16	0.000	6.1	0.000	2.085	0.0 ± 0.0
8	1	55	12	0.018	13.6	0.084	4.634	14.3 ± 14.5
9	0	47	16	0.000	8.7	0.000	2.970	0.0 ± 0.0
10	0	43	9	0.000	14.2	0.000	4.831	0.0 ± 0.0
11	1	151	16	0.007	28.1	0.063	9.542	5.2 ± 5.2
12	0	97	10	0.000	28.9	0.000	9.808	0.0 ± 0.0
13	0	80	20	0.000	11.9	0.000	4.044	0.0 ± 0.0
14	0	283	24	0.000	35.1	0.000	11.923	0.0 ± 0.0
15	0	40	12	0.000	9.9	0.000	3.370	0.0 ± 0.0
16	4	642	20	0.006	95.5	0.202	32.457	4.9 ± 2.5
	9	1952			26.9	0.042	9.138	

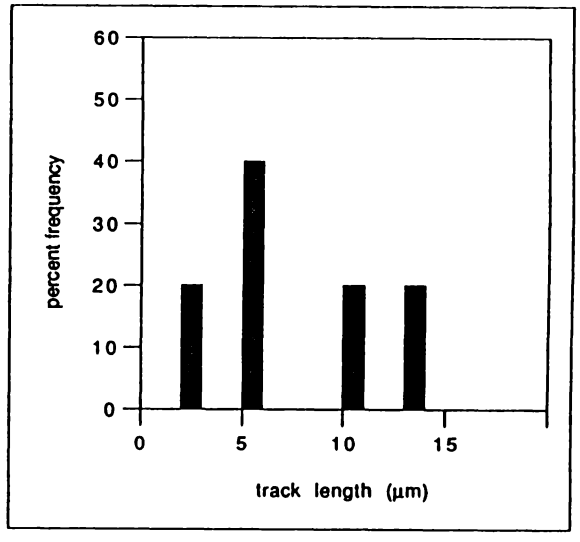
AREA OF BASIC UNIT = 9.89E-07 cm
CHI SQUARED = 16.58616 WITH 15 DEGREES OF FREEDOM
P(chi squared) = 34.4 %
CORRELATION COEFFICIENT = 0.756
VARIANCE OF SQR(Ns) = 0.43
VARIANCE OF SQR(Ni) = 25.12

Ns/Ni = 0.005 ± 0.002
MEAN RATIO = 0.005 ± 0.002

Ages calculated using a zeta of 354.9 ± 4.3 for SRM612 glass
RHO D = 4.452E+06 ; ND = 3522

POOLED AGE = 3.6 ± 1.2 Ma
MEAN AGE = 3.7 ± 1.7 Ma

8902-133



n = 5
Mean = 7.69 µm
Sample std. dev. = 3.86 µm

8902-133 ZIRCON arthur's s59/053297 810m

IRRADIATION jmt data:jmt zircon data:arthur's zircons:wk027/1
SLIDE NUMBER 1
COUNTED BY: jmt

No.	Ns	Ni	Na	RATIO	U (ppm)	RHOs (E+06)	RHOi (E+06)	F.T.AGE (Ma)
1	174	45	10	3.867	0.0	17.594	4.550	214.2 ± 36.0
2	149	56	12	2.661	0.0	12.555	4.719	148.1 ± 23.4
3	45	20	4	2.250	0.0	11.375	5.056	125.5 ± 33.8
4	63	19	8	3.316	0.0	7.963	2.401	184.1 ± 48.3
5	149	62	25	2.403	0.0	6.026	2.508	134.0 ± 20.4
6	38	19	4	2.000	0.0	9.606	4.803	111.7 ± 31.4
7	100	47	12	2.128	0.0	8.426	3.960	118.7 ± 21.1
8	182	61	12	2.984	0.0	15.335	5.140	165.9 ± 24.7
9	79	17	6	4.647	0.0	13.313	2.865	256.6 ± 68.8
10	118	32	15	3.688	0.0	7.954	2.157	204.4 ± 40.9
	1097	378			0.0	10.270	3.539	

AREA OF BASIC UNIT = 9.89E-07 cm
CHI SQUARED = 15.52132 WITH 9 DEGREES OF FREEDOM
P(chi squared) = 7.8 %
CORRELATION COEFFICIENT = 0.874
VARIANCE OF SQR(Ns) = 7.07
VARIANCE OF SQR(Ni) = 2.40

Ns/Ni = 2.902 ± 0.173
MEAN RATIO = 2.994 ± 0.275

Ages calculated using a zeta of 133.9 ± 1.4 for CN1 glass
RHO D = 8.413E+05 ; ND = 4160

POOLED AGE = 161.4 ± 10.1 Ma
MEAN AGE = 166.5 ± 15.6 Ma

8902-134 APATITE arthur's s59/064264 760m

IRRADIATION jmt data:jmt apatite data:arthur's apatites:wk015/3
SLIDE NUMBER 1
COUNTED BY: jmt

No.	Ns	NI	Na	RATIO	U (ppm)	RHOs (E+06)	RHOi (E+06)	F.TAGE (Ma)
1	1	25	16	0.040	19.2	0.063	1.580	7.7 ± 7.8
2	0	20	8	0.000	30.7	0.000	2.528	0.0 ± 0.0
3	0	59	16	0.000	45.3	0.000	3.729	0.0 ± 0.0
4	0	84	24	0.000	43.0	0.000	3.539	0.0 ± 0.0
5	0	32	70	0.000	5.6	0.000	0.462	0.0 ± 0.0
6	0	11	12	0.000	11.3	0.000	0.927	0.0 ± 0.0
7	2	34	12	0.059	34.8	0.169	2.865	11.3 ± 8.2
8	1	27	20	0.037	16.6	0.051	1.365	7.1 ± 7.2
9	0	11	12	0.000	11.3	0.000	0.927	0.0 ± 0.0
10	0	4	8	0.000	6.1	0.000	0.506	0.0 ± 0.0
11	0	40	12	0.000	40.9	0.000	3.370	0.0 ± 0.0
12	0	44	16	0.000	33.8	0.000	2.781	0.0 ± 0.0
13	0	5	12	0.000	5.1	0.000	0.421	0.0 ± 0.0
14	0	46	12	0.000	47.1	0.000	3.876	0.0 ± 0.0
15	2	224	28	0.009	98.2	0.072	8.089	1.7 ± 1.2
16	1	105	28	0.010	46.0	0.036	3.792	1.8 ± 1.8
17	2	68	12	0.029	69.6	0.169	5.730	5.6 ± 4.0
18	1	18	15	0.056	14.7	0.067	1.213	10.6 ± 10.9
19	1	31	6	0.032	63.4	0.169	5.224	6.2 ± 6.3
20	4	175	32	0.023	67.1	0.126	5.530	4.4 ± 2.2
21	1	18	6	0.056	36.8	0.169	3.033	10.6 ± 10.9
22	2	68	20	0.029	41.7	0.101	3.438	5.6 ± 4.0
23	2	19	8	0.105	29.2	0.253	2.401	20.1 ± 15.0
24	2	10	12	0.200	10.2	0.169	0.843	38.2 ± 29.6
	22	1178			34.7	0.053	2.856	

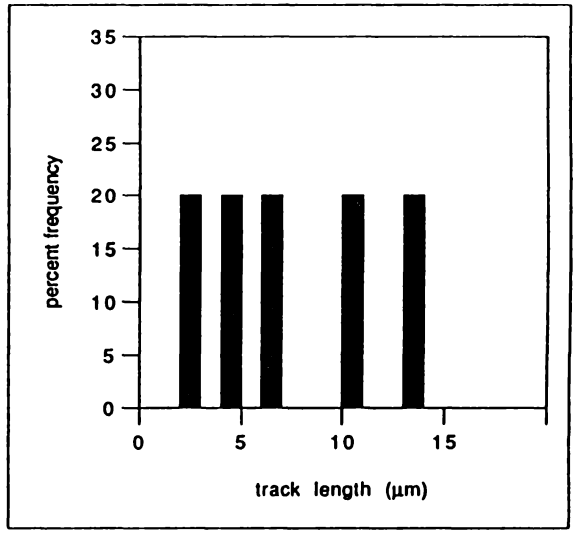
AREA OF BASIC UNIT = 9.89E-07 cm
CHI SQUARED = 37.39913 WITH 23 DEGREES OF FREEDOM
P(chi squared) = 3.0 %
CORRELATION COEFFICIENT = 0.530
VARIANCE OF SQR(Ns) = 0.46
VARIANCE OF SQR(Ni) = 10.39

Ns/Ni = 0.019 ± 0.004
MEAN RATIO = 0.029 ± 0.009

Ages calculated using a zeta of 354.9 ± 4.3 for SRM612 glass
RHO D = 1.079E+06 ; ND = 2667

POOLED AGE = 3.6 ± 0.8 Ma
MEAN AGE = 5.5 ± 1.8 Ma

8902-134



n = 5
Mean = 7.56 µm
Sample std. dev. = 4.26 µm

8902-134 ZIRCON arthur's s59/064264 760m

IRRADIATION jmt data:jmt zircon data:arthur's zircons:wk028/18
SLIDE NUMBER 1
COUNTED BY: jmt

No.	Ns	Ni	Na	RATIO	U (ppm)	RHOs (E+06)	RHOi (E+06)	F.T AGE (Ma)
1	152	43	12	3.535	0.0	12.808	3.623	225.1 ± 39.1
2	300	121	20	2.479	0.0	15.167	6.117	158.7 ± 17.3
3	94	36	8	2.611	0.0	11.881	4.550	167.0 ± 32.9
4	57	20	4	2.850	0.0	14.408	5.056	182.1 ± 47.4
5	126	25	20	5.040	0.0	6.370	1.264	318.6 ± 70.0
6	103	35	12	2.943	0.0	8.679	2.949	187.9 ± 36.9
7	319	120	28	2.658	0.0	11.520	4.333	170.0 ± 18.5
8	115	39	24	2.949	0.0	4.845	1.643	188.3 ± 35.0
9	169	56	10	3.018	0.0	17.088	5.662	192.6 ± 29.9
10	224	55	18	4.073	0.0	12.583	3.090	258.6 ± 39.2
11	70	29	10	2.414	0.0	7.078	2.932	154.5 ± 34.2
12	162	61	12	2.656	0.0	13.650	5.140	169.8 ± 25.7
13	73	39	6	1.872	0.0	12.302	6.572	120.2 ± 23.9
14	145	45	15	3.222	0.0	9.774	3.033	205.5 ± 35.3
15	143	57	9	2.509	0.0	16.066	6.404	160.5 ± 25.3
	2252	781			0.0	10.947	3.797	

AREA OF BASIC UNIT = 9.89E-07 cm
CHI SQUARED = 23.29238 WITH 14 DEGREES OF FREEDOM
P(chi squared) = 5.6 %
CORRELATION COEFFICIENT = 0.933
VARIANCE OF SQR(Ns) = 9.20
VARIANCE OF SQR(Ni) = 3.54

Ns/Ni = 2.883 ± 0.120
MEAN RATIO = 2.989 ± 0.197

Ages calculated using a zeta of 133.9 ± 1.4 for CN1 glass
RHO D = 9.678E+05 ; ND = 4786

POOLED AGE = 184.2 ± 8.3 Ma
MEAN AGE = 190.8 ± 13.1 Ma

8902-135 APATITE robinson s46/464844 335m

IRRADIATION jmt data:jmt apatite data:robinson apatites:wk021/7
SLIDE NUMBER 1
COUNTED BY: jmt

No.	Ns	Ni	Na	RATIO	U (ppm)	RHOs (E+06)	RHOi (E+06)	F.TAGE (Ma)
1	0	13	4	0.000	9.7	0.000	3.286	0.0 ± 0.0
2	0	52	9	0.000	17.3	0.000	5.842	0.0 ± 0.0
3	0	62	10	0.000	18.6	0.000	6.269	0.0 ± 0.0
4	0	20	6	0.000	10.0	0.000	3.370	0.0 ± 0.0
5	0	10	6	0.000	5.0	0.000	1.685	0.0 ± 0.0
6	0	155	15	0.000	30.9	0.000	10.448	0.0 ± 0.0
7	0	42	6	0.000	21.0	0.000	7.078	0.0 ± 0.0
8	0	58	12	0.000	14.5	0.000	4.887	0.0 ± 0.0
9	0	26	8	0.000	9.7	0.000	3.286	0.0 ± 0.0
10	0	34	15	0.000	6.8	0.000	2.292	0.0 ± 0.0
11	0	15	12	0.000	3.7	0.000	1.264	0.0 ± 0.0
12	0	30	6	0.000	15.0	0.000	5.056	0.0 ± 0.0
13	0	13	4	0.000	9.7	0.000	3.286	0.0 ± 0.0
14	0	41	9	0.000	13.6	0.000	4.606	0.0 ± 0.0
15	0	23	4	0.000	17.2	0.000	5.814	0.0 ± 0.0
	0	594			14.1	0.000	4.767	

AREA OF BASIC UNIT = 9.89E-07 cm
CHI SQUARED = 2.832258E-05 WITH 14 DEGREES OF FREEDOM
P(chi squared) = 100.0 %
CORRELATION COEFFICIENT = 0.886
VARIANCE OF SQR(Ns) = 0.00
VARIANCE OF SQR(Ni) = 5.59

Ns/Ni = 0.000 ± 0.000
MEAN RATIO = 0.000 ± 0.000

Ages calculated using a zeta of 354.9 ± 4.3 for SRM612 glass
RHO D = 4.425E+06 ; ND = 3501

POOLED AGE = 0.0 ± 0.0 Ma
MEAN AGE = 0.0 ± 0.0 Ma

8902-135 ZIRCON robinson s46/464844 335m

IRRADIATION jmt data:jmt zircon data:robinson zircons:wk037/5
SLIDE NUMBER 1
COUNTED BY: jmt

No.	Ns	Ni	Na	RATIO	U (ppm)	RHOs (E+06)	RHOi (E+06)	F.TAGE (Ma)
1	2	40	4	0.050	0.0	0.506	10.111	3.6 ± 2.6
2	1	25	2	0.040	0.0	0.506	12.639	2.9 ± 2.9
3	1	47	3	0.021	0.0	0.337	15.841	1.5 ± 1.5
	4	112			0.0	0.449	12.583	

AREA OF BASIC UNIT = 9.89E-07 cm
CHI SQUARED = .4986509 WITH 2 DEGREES OF FREEDOM
P(chi squared) = 77.9 %
CORRELATION COEFFICIENT = 0.205
VARIANCE OF SQR(Ns) = 0.06
VARIANCE OF SQR(Ni) = 0.91

Ns/Ni = 0.036 ± 0.018
MEAN RATIO = 0.037 ± 0.008

Ages calculated using a zeta of 133.9 ± 1.4 for CN1 glass
RHO D = 1.067E+06 ; ND = 6342

POOLED AGE = 2.6 ± 1.3 Ma
MEAN AGE = 2.6 ± 0.6 Ma

8902-137 APATITE robinson s46/500815 425m

IRRADIATION jmt data:jmt apatite data:robinson apatites:wk016/16
SLIDE NUMBER 1
COUNTED BY: jmt

No.	Ns	Ni	Na	RATIO	U (ppm)	RHOs (E+06)	RHOI (E+06)	F.T.AGE (Ma)
1	0	46	9	0.000	39.4	0.000	5.168	0.0 ± 0.0
2	0	18	6	0.000	23.1	0.000	3.033	0.0 ± 0.0
3	0	20	12	0.000	12.8	0.000	1.685	0.0 ± 0.0
4	0	69	36	0.000	14.8	0.000	1.938	0.0 ± 0.0
5	0	49	12	0.000	31.5	0.000	4.129	0.0 ± 0.0
6	0	91	12	0.000	58.5	0.000	7.668	0.0 ± 0.0
7	0	39	16	0.000	18.8	0.000	2.465	0.0 ± 0.0
8	0	103	12	0.000	66.2	0.000	8.679	0.0 ± 0.0
9	1	78	9	0.013	66.8	0.112	8.763	3.9 ± 3.9
10	0	21	6	0.000	27.0	0.000	3.539	0.0 ± 0.0
11	0	24	6	0.000	30.8	0.000	4.044	0.0 ± 0.0
12	0	10	3	0.000	25.7	0.000	3.370	0.0 ± 0.0
13	0	11	8	0.000	10.6	0.000	1.390	0.0 ± 0.0
14	0	24	16	0.000	11.6	0.000	1.517	0.0 ± 0.0
15	0	35	20	0.000	13.5	0.000	1.769	0.0 ± 0.0
	1	638			26.9	0.006	3.525	

AREA OF BASIC UNIT = 9.89E-07 cm
CHI SQUARED = 7.099717 WITH 14 DEGREES OF FREEDOM
P(chi squared) = 93.1 %
CORRELATION COEFFICIENT = 0.330
VARIANCE OF SQR(Ns) = 0.07
VARIANCE OF SQR(Ni) = 4.96

Ns/Ni = 0.002 ± 0.002
MEAN RATIO = 0.001 ± 0.001

Ages calculated using a zeta of 354.9 ± 4.3 for SRM612 glass
RHO D = 1.718E+06 ; ND = 3396

POOLED AGE = 0.5 ± 0.5 Ma
MEAN AGE = 0.3 ± 0.3 Ma

8902-137 ZIRCON robinson s46/500815 425m

IRRADIATION jmt data:jmt zircon data:robinson zircons:wk037/6
SLIDE NUMBER 1
COUNTED BY: jmt

No.	Ns	NI	Na	RATIO	U (ppm)	RHOs (E+06)	RHOI (E+06)	F.T.AGE (Ma)
1	12	185	12	0.065	0.0	1.011	15.588	4.6 ± 1.4
2	14	139	20	0.101	0.0	0.708	7.027	7.2 ± 2.0
	26	324			0.0	0.822	10.238	

AREA OF BASIC UNIT = 9.89E-07 cm
CHI SQUARED = 1.171801 WITH 1 DEGREES OF FREEDOM
P(chi squared) = 27.9 %
CORRELATION COEFFICIENT = -1.000
VARIANCE OF SQR(Ns) = 0.04
VARIANCE OF SQR(Ni) = 1.64

Ns/NI = 0.080 ± 0.016
MEAN RATIO = 0.083 ± 0.018

Ages calculated using a zeta of 133.9 ± 1.4 for CN1 glass
RHO D = 1.067E+06 ; ND = 6342

POOLED AGE = 5.7 ± 1.2 Ma
MEAN AGE = 5.9 ± 1.3 Ma

8902-138 APATITE robinson s46/505814 425m

IRRADIATION jmt data:jmt apatite data:robinson apatites:wk016/15
SLIDE NUMBER 1
COUNTED BY: jmt

No.	Ns	Ni	Na	RATIO	U (ppm)	RHOs (E+06)	RHOi (E+06)	F.T AGE (Ma)
1	0	111	10	0.000	86.2	0.000	11.223	0.0 ± 0.0
2	0	47	9	0.000	40.5	0.000	5.280	0.0 ± 0.0
3	0	78	8	0.000	75.7	0.000	9.858	0.0 ± 0.0
4	0	113	12	0.000	73.1	0.000	9.521	0.0 ± 0.0
5	0	52	16	0.000	25.2	0.000	3.286	0.0 ± 0.0
6	0	16	16	0.000	7.8	0.000	1.011	0.0 ± 0.0
7	0	39	6	0.000	50.5	0.000	6.572	0.0 ± 0.0
8	0	27	6	0.000	34.9	0.000	4.550	0.0 ± 0.0
9	0	41	15	0.000	21.2	0.000	2.764	0.0 ± 0.0
10	0	60	20	0.000	23.3	0.000	3.033	0.0 ± 0.0
11	0	41	8	0.000	39.8	0.000	5.182	0.0 ± 0.0
12	0	13	6	0.000	16.8	0.000	2.191	0.0 ± 0.0
13	0	13	6	0.000	16.8	0.000	2.191	0.0 ± 0.0
14	0	73	20	0.000	28.3	0.000	3.691	0.0 ± 0.0
15	0	22	12	0.000	14.2	0.000	1.854	0.0 ± 0.0
	0	746			34.1	0.000	4.437	

AREA OF BASIC UNIT = 9.89E-07 cm
CHI SQUARED = 5.72072E-05 WITH 14 DEGREES OF FREEDOM
P(chi squared) = 100.0 %
CORRELATION COEFFICIENT = 0.525
VARIANCE OF SQR(Ns) = 0.00
VARIANCE OF SQR(Ni) = 5.19

Ns/Ni = 0.000 ± 0.000
MEAN RATIO = 0.000 ± 0.000

Ages calculated using a zeta of 354.9 ± 4.3 for SRM612 glass
RHO D = 1.706E+06 ; ND = 3374

POOLED AGE = 0.0 ± 0.0 Ma
MEAN AGE = 0.0 ± 0.0 Ma

8902-138 ZIRCON robinson s46/505814 425m

IRRADIATION jmt data:jmt zircon data:robinson zircons:wk028/15
SLIDE NUMBER 1
COUNTED BY: jmt

No.	Ns	Ni	Na	RATIO	U (ppm)	RHOs (E+06)	RHOi (E+06)	F.T AGE (Ma)
1	17	186	18	0.091	0.0	0.955	10.448	5.8 ± 1.5
2	4	49	6	0.082	0.0	0.674	8.257	5.2 ± 2.7
3	11	122	6	0.090	0.0	1.854	20.559	5.7 ± 1.8
4	60	302	24	0.199	0.0	2.528	12.723	12.6 ± 1.8
5	14	104	15	0.135	0.0	0.944	7.010	8.5 ± 2.4
6	8	45	3	0.178	0.0	2.696	15.167	11.3 ± 4.3
7	14	175	12	0.080	0.0	1.180	14.746	5.1 ± 1.4
8	23	157	16	0.146	0.0	1.453	9.922	9.3 ± 2.1
9	18	227	10	0.079	0.0	1.820	22.952	5.0 ± 1.2
	169	1367			0.0	1.553	12.565	

AREA OF BASIC UNIT = 9.89E-07 cm
CHI SQUARED = 21.98314 WITH 8 DEGREES OF FREEDOM
P(chi squared) = 0.5 %
CORRELATION COEFFICIENT = 0.835
VARIANCE OF SQR(Ns) = 2.59
VARIANCE OF SQR(Ni) = 12.48

Ns/Ni = 0.124 ± 0.010
MEAN RATIO = 0.120 ± 0.015

Ages calculated using a zeta of 133.9 ± 1.4 for CN1 glass
RHO D = 9.468E+05 ; ND = 4682

POOLED AGE = 7.8 ± 0.7 Ma
MEAN AGE = 7.6 ± 1.0 Ma

8902-139 APATITE robinson s46/519816 455m

IRRADIATION jmt data:jmt apatite data:robinson apatites:wk016/14
SLIDE NUMBER 1
COUNTED BY: jmt

No.	Ns	Ni	Na	RATIO	U (ppm)	RHOs (E+06)	RHOi (E+06)	F.T AGE (Ma)
1	1	170	15	0.006	88.6	0.067	11.459	1.8 ± 1.8
2	0	25	20	0.000	9.8	0.000	1.264	0.0 ± 0.0
3	0	12	12	0.000	7.8	0.000	1.011	0.0 ± 0.0
4	0	26	12	0.000	16.9	0.000	2.191	0.0 ± 0.0
5	0	22	9	0.000	19.1	0.000	2.472	0.0 ± 0.0
6	0	27	6	0.000	35.2	0.000	4.550	0.0 ± 0.0
7	0	11	8	0.000	10.7	0.000	1.390	0.0 ± 0.0
8	0	8	6	0.000	10.4	0.000	1.348	0.0 ± 0.0
9	0	15	12	0.000	9.8	0.000	1.264	0.0 ± 0.0
10	0	17	9	0.000	14.8	0.000	1.910	0.0 ± 0.0
11	0	5	9	0.000	4.3	0.000	0.562	0.0 ± 0.0
12	0	22	9	0.000	19.1	0.000	2.472	0.0 ± 0.0
13	0	84	16	0.000	41.0	0.000	5.308	0.0 ± 0.0
14	1	94	24	0.011	30.6	0.042	3.960	3.2 ± 3.2
15	0	57	30	0.000	14.8	0.000	1.921	0.0 ± 0.0
16	1	20	12	0.050	13.0	0.084	1.685	15.0 ± 15.4
17	0	47	12	0.000	30.6	0.000	3.960	0.0 ± 0.0
18	0	69	12	0.000	44.9	0.000	5.814	0.0 ± 0.0
19	0	137	12	0.000	89.2	0.000	11.544	0.0 ± 0.0
20	0	17	9	0.000	14.8	0.000	1.910	0.0 ± 0.0
	3	885			27.2	0.012	3.523	

AREA OF BASIC UNIT = 9.89E-07 cm
CHI SQUARED = 15.99606 WITH 19 DEGREES OF FREEDOM
P(chi squared) = 65.8 %
CORRELATION COEFFICIENT = 0.479
VARIANCE OF SQR(Ns) = 0.13
VARIANCE OF SQR(Ni) = 9.04

Ns/Ni = 0.003 ± 0.002
MEAN RATIO = 0.003 ± 0.003

Ages calculated using a zeta of 354.9 ± 4.3 for SRM612 glass
RHO D = 1.695E+06 ; ND = 3351

POOLED AGE = 1.0 ± 0.6 Ma
MEAN AGE = 1.0 ± 0.8 Ma

8902-139 ZIRCON robinson s46/519816 455m

IRRADIATION jmt data:jmt zircon data:robinson zircons:wk028/14
SLIDE NUMBER 1
COUNTED BY: jmt

No.	Ns	Ni	Na	RATIO	U (ppm)	RHOs (E+06)	RHOi (E+06)	F.T AGE (Ma)
1	133	86	12	1.547	0.0	11.207	7.246	96.6 ± 13.5
2	69	40	4	1.725	0.0	17.442	10.111	107.7 ± 21.5
3	150	117	15	1.282	0.0	10.111	7.887	80.2 ± 10.0
4	20	16	4	1.250	0.0	5.056	4.044	78.2 ± 26.3
5	51	49	6	1.041	0.0	8.595	8.257	65.2 ± 13.1
6	162	101	12	1.604	0.0	13.650	8.510	100.2 ± 12.8
7	22	10	3	2.200	0.0	7.415	3.370	137.0 ± 52.3
8	34	28	6	1.214	0.0	5.730	4.719	76.0 ± 19.4
9	120	70	8	1.714	0.0	15.167	8.847	107.0 ± 16.2
	761	517			0.0	10.992	7.468	

AREA OF BASIC UNIT = 9.89E-07 cm
CHI SQUARED = 8.475951 WITH 8 DEGREES OF FREEDOM
P(chi squared) = 38.8 %
CORRELATION COEFFICIENT = 0.967
VARIANCE OF SQR(Ns) = 10.83
VARIANCE OF SQR(Ni) = 7.23

Ns/Ni = 1.472 ± 0.084
MEAN RATIO = 1.509 ± 0.118

Ages calculated using a zeta of 133.9 ± 1.4 for CN1 glass
RHO D = 9.400E+05 ; ND = 4648

POOLED AGE = 92.0 ± 5.5 Ma
MEAN AGE = 94.2 ± 7.6 Ma

8902-140 APATITE lewis s46/630972 1050m

IRRADIATION jmt data:jmt apatite data:lewis apatites:wk016/13
SLIDE NUMBER 1
COUNTED BY: jmt

No.	Ns	Ni	Na	RATIO	U (ppm)	RHOs (E+06)	RHOi (E+06)	F.T.AGE (Ma)
1	0	5	16	0.000	2.5	0.000	0.316	0.0 ± 0.0
2	0	1	12	0.000	0.7	0.000	0.084	0.0 ± 0.0
3	0	6	36	0.000	1.3	0.000	0.169	0.0 ± 0.0
4	0	5	12	0.000	3.3	0.000	0.421	0.0 ± 0.0
5	0	8	18	0.000	3.5	0.000	0.449	0.0 ± 0.0
6	0	11	15	0.000	5.8	0.000	0.741	0.0 ± 0.0
7	0	16	100	0.000	1.3	0.000	0.162	0.0 ± 0.0
8	0	12	25	0.000	3.8	0.000	0.485	0.0 ± 0.0
9	0	3	12	0.000	2.0	0.000	0.253	0.0 ± 0.0
10	0	8	50	0.000	1.3	0.000	0.162	0.0 ± 0.0
11	0	4	18	0.000	1.7	0.000	0.225	0.0 ± 0.0
12	0	15	54	0.000	2.2	0.000	0.281	0.0 ± 0.0
13	0	21	24	0.000	6.9	0.000	0.885	0.0 ± 0.0
14	0	5	24	0.000	1.6	0.000	0.211	0.0 ± 0.0
15	0	1	9	0.000	0.9	0.000	0.112	0.0 ± 0.0
	0	121			2.2	0.000	0.288	

AREA OF BASIC UNIT = 9.89E-07 cm
CHI SQUARED = 4.761903E-05 WITH 14 DEGREES OF FREEDOM
P(chi squared) = 100.0 %
CORRELATION COEFFICIENT = 0.613
VARIANCE OF SQR(Ns) = 0.00
VARIANCE OF SQR(Ni) = 1.11

Ns/Ni = 0.000 ± 0.000
MEAN RATIO = 0.000 ± 0.000

Ages calculated using a zeta of 354.9 ± 4.3 for SRM612 glass
RHO D = 1.683E+06 ; ND = 3328

POOLED AGE = 0.0 ± 0.0 Ma
MEAN AGE = 0.0 ± 0.0 Ma

8902-140 ZIRCON lewis s46/628974 1115m

IRRADIATION jmt data:jmt zircon data:lewis zircons:wk028/13
SLIDE NUMBER 1
COUNTED BY: jmt

No.	Ns	Ni	Na	RATIO	U (ppm)	RHOs (E+06)	RHOi (E+06)	F.T.AGE (Ma)
1	3	51	5	0.059	0.0	0.607	10.313	3.7 ± 2.2
2	2	102	12	0.020	0.0	0.169	8.595	1.2 ± 0.9
3	1	58	10	0.017	0.0	0.101	5.865	1.1 ± 1.1
4	1	42	4	0.024	0.0	0.253	10.617	1.5 ± 1.5
5	3	133	6	0.023	0.0	0.506	22.413	1.4 ± 0.8
6	2	57	3	0.035	0.0	0.674	19.211	2.2 ± 1.6
7	8	228	18	0.035	0.0	0.449	12.808	2.2 ± 0.8
8	3	52	10	0.058	0.0	0.303	5.258	3.6 ± 2.1
9	6	128	6	0.047	0.0	1.011	21.571	2.9 ± 1.2
	29	851			0.0	0.396	11.628	

AREA OF BASIC UNIT = 9.89E-07 cm
CHI SQUARED = 3.988383 WITH 8 DEGREES OF FREEDOM
P(chi squared) = 85.8 %
CORRELATION COEFFICIENT = 0.858
VARIANCE OF SQR(Ns) = 0.37
VARIANCE OF SQR(Ni) = 8.27

Ns/Ni = 0.034 ± 0.006
MEAN RATIO = 0.035 ± 0.005

Ages calculated using a zeta of 133.9 ± 1.4 for CN1 glass
RHO D = 9.329E+05 ; ND = 4613

POOLED AGE = 2.1 ± 0.4 Ma
MEAN AGE = 2.2 ± 0.3 Ma

8902-141 APATITE lewis s46/628974 1115m

IRRADIATION jmt data:jmt apatite data:lewis apatites:wk021/5
SLIDE NUMBER 1
COUNTED BY: jmt

No.	Ns	Ni	Na	RATIO	U (ppm)	RHOs (E+06)	RHOi (E+06)	F.T.AGE (Ma)
1	0	3	70	0.000	0.1	0.000	0.043	0.0 ± 0.0
2	0	3	25	0.000	0.4	0.000	0.121	0.0 ± 0.0
3	0	1	24	0.000	0.1	0.000	0.042	0.0 ± 0.0
4	0	8	18	0.000	1.3	0.000	0.449	0.0 ± 0.0
5	0	2	25	0.000	0.2	0.000	0.081	0.0 ± 0.0
6	0	0	36	0.000	0.0	0.000	0.000	0.0 ± 0.0
7	0	8	56	0.000	0.4	0.000	0.144	0.0 ± 0.0
8	0	0	24	0.000	0.0	0.000	0.000	0.0 ± 0.0
9	0	2	40	0.000	0.2	0.000	0.051	0.0 ± 0.0
10	0	8	36	0.000	0.7	0.000	0.225	0.0 ± 0.0
11	0	316	24	0.000	39.9	0.000	13.313	0.0 ± 0.0
12	0	4	50	0.000	0.2	0.000	0.081	0.0 ± 0.0
13	0	2	48	0.000	0.1	0.000	0.042	0.0 ± 0.0
14	0	2	40	0.000	0.2	0.000	0.051	0.0 ± 0.0
15	0	4	30	0.000	0.4	0.000	0.135	0.0 ± 0.0
	0	363			2.0	0.000	0.672	

AREA OF BASIC UNIT = 9.89E-07 cm
CHI SQUARED = 1.487405E-06 WITH 14 DEGREES OF FREEDOM
P(chi squared) = 100.0 %
CORRELATION COEFFICIENT = 0.999
VARIANCE OF SQR(Ns) = 0.00
VARIANCE OF SQR(Ni) = 18.14

Ns/Ni = 0.000 ± 0.000
MEAN RATIO = 0.000 ± 0.000

Ages calculated using a zeta of 354.9 ± 4.3 for SRM612 glass
RHO D = 4.370E+06 ; ND = 3457

POOLED AGE = 0.0 ± 0.0 Ma
MEAN AGE = 0.0 ± 0.0 Ma

8902-141 ZIRCON lewis s46/630972 1050m

IRRADIATION jmt data:jmt zircon data:lewis zircons:wk028/12
SLIDE NUMBER 1
COUNTED BY: jmt

No.	Ns	Ni	Na	RATIO	U (ppm)	RHOs (E+06)	RHOi (E+06)	F.T.AGE (Ma)
1	4	94	10	0.043	0.0	0.404	9.505	2.6 ± 1.3
2	3	124	24	0.024	0.0	0.126	5.224	1.5 ± 0.9
3	5	158	49	0.032	0.0	0.103	3.260	2.0 ± 0.9
4	62	%1242	60	0.050	0.0	1.045	20.930	3.1 ± 0.4
5	12	271	24	0.044	0.0	0.506	11.417	2.7 ± 0.8
6	24	383	24	0.063	0.0	1.011	16.136	3.9 ± 0.8
7	26	586	42	0.044	0.0	0.626	14.108	2.7 ± 0.6
8	16	374	20	0.043	0.0	0.809	18.908	2.7 ± 0.7
9	3	85	12	0.035	0.0	0.253	7.162	2.2 ± 1.3
10	23	563	50	0.041	0.0	0.465	11.385	2.5 ± 0.5
11	26	364	36	0.071	0.0	0.730	10.224	4.4 ± 0.9
12	17	324	24	0.052	0.0	0.716	13.650	3.3 ± 0.8
	221	4568			0.0	0.596	12.317	

AREA OF BASIC UNIT = 9.89E-07 cm
CHI SQUARED = 9.261585 WITH 11 DEGREES OF FREEDOM
P(chi squared) = 59.8 %
CORRELATION COEFFICIENT = 0.975
VARIANCE OF SQR(Ns) = 3.32
VARIANCE OF SQR(Ni) = 54.42

Ns/Ni = 0.048 ± 0.003
MEAN RATIO = 0.045 ± 0.004

Ages calculated using a zeta of 133.9 ± 1.4 for CN1 glass
RHO D = 9.260E+05 ; ND = 4579

POOLED AGE = 3.0 ± 0.2 Ma
MEAN AGE = 2.8 ± 0.2 Ma

8902-142 APATITE lewis s46/670004 610m

IRRADIATION jmt data:jmt apatite data:lewis apatites:wk021/4
SLIDE NUMBER 1
COUNTED BY: jmt

No.	Ns	Ni	Na	RATIO	U (ppm)	RHOs (E+06)	RHOi (E+06)	F.TAGE (Ma)
1	0	0	42	0.000	0.0	0.000	0.000	0.0 ± 0.0
2	0	3	70	0.000	0.1	0.000	0.043	0.0 ± 0.0
3	0	10	50	0.000	0.6	0.000	0.202	0.0 ± 0.0
4	0	0	25	0.000	0.0	0.000	0.000	0.0 ± 0.0
5	0	3	30	0.000	0.3	0.000	0.101	0.0 ± 0.0
6	0	55	20	0.000	8.4	0.000	2.781	0.0 ± 0.0
7	0	1	20	0.000	0.2	0.000	0.051	0.0 ± 0.0
8	0	1	36	0.000	0.1	0.000	0.028	0.0 ± 0.0
9	0	2	25	0.000	0.2	0.000	0.081	0.0 ± 0.0
10	0	8	80	0.000	0.3	0.000	0.101	0.0 ± 0.0
11	0	15	30	0.000	1.5	0.000	0.506	0.0 ± 0.0
12	0	15	40	0.000	1.1	0.000	0.379	0.0 ± 0.0
13	0	12	48	0.000	0.8	0.000	0.253	0.0 ± 0.0
14	0	19	28	0.000	2.1	0.000	0.686	0.0 ± 0.0
15	0	0	24	0.000	0.0	0.000	0.000	0.0 ± 0.0
	0	144			0.8	0.000	0.256	

AREA OF BASIC UNIT = 9.89E-07 cm
CHI SQUARED = 1.618236E-05 WITH 14 DEGREES OF FREEDOM
P(chi squared) = 100.0 %
CORRELATION COEFFICIENT = 0.890
VARIANCE OF SQR(Ns) = 0.00
VARIANCE OF SQR(Ni) = 4.13

Ns/Ni = 0.000 ± 0.000
MEAN RATIO = 0.000 ± 0.000

Ages calculated using a zeta of 354.9 ± 4.3 for SRM612 glass
RHO D = 4.343E+06 ; ND = 3436

POOLED AGE = 0.0 ± 0.0 Ma
MEAN AGE = 0.0 ± 0.0 Ma

8902-142 ZIRCON lewis s46/670004 610m

IRRADIATION jmt data:jmt zircon data:lewis zircons:wk037/7
SLIDE NUMBER 1
COUNTED BY: jmt

No.	Ns	Ni	Na	RATIO	U (ppm)	RHOs (E+06)	RHOi (E+06)	F.TAGE (Ma)
1	5	88	6	0.057	0.0	0.843	14.830	4.1 ± 1.9
2	2	32	6	0.062	0.0	0.337	5.393	4.5 ± 3.3
3	5	93	6	0.054	0.0	0.843	15.672	3.8 ± 1.8
4	4	51	4	0.078	0.0	1.011	12.892	5.6 ± 2.9
5	10	233	20	0.043	0.0	0.506	11.780	3.1 ± 1.0
	26	497			0.0	0.626	11.965	

AREA OF BASIC UNIT = 9.89E-07 cm
CHI SQUARED = 1.089184 WITH 4 DEGREES OF FREEDOM
P(chi squared) = 89.6 %
CORRELATION COEFFICIENT = 0.987
VARIANCE OF SQR(Ns) = 0.40
VARIANCE OF SQR(Ni) = 13.39

Ns/Ni = 0.052 ± 0.011
MEAN RATIO = 0.059 ± 0.006

Ages calculated using a zeta of 133.9 ± 1.4 for CN1 glass
RHO D = 1.067E+06 ; ND = 6342

POOLED AGE = 3.7 ± 0.8 Ma
MEAN AGE = 4.2 ± 0.4 Ma

8902-143 APATITE lewis s46/672004 655m

IRRADIATION jmt data:jmt apatite data:lewis apatites:wk021/3
SLIDE NUMBER 1
COUNTED BY: jmt

No.	Ns	Ni	Na	RATIO	U (ppm)	RHOs (E+06)	RHOi (E+06)	F.T.AGE (Ma)
1	0	2	12	0.000	0.5	0.000	0.169	0.0 ± 0.0
2	0	1	15	0.000	0.2	0.000	0.067	0.0 ± 0.0
3	0	3	18	0.000	0.5	0.000	0.169	0.0 ± 0.0
4	0	0	12	0.000	0.0	0.000	0.000	0.0 ± 0.0
5	0	1	10	0.000	0.3	0.000	0.101	0.0 ± 0.0
6	0	0	8	0.000	0.0	0.000	0.000	0.0 ± 0.0
7	0	0	3	0.000	0.0	0.000	0.000	0.0 ± 0.0
8	0	1	12	0.000	0.3	0.000	0.084	0.0 ± 0.0
9	0	2	32	0.000	0.2	0.000	0.063	0.0 ± 0.0
10	0	0	9	0.000	0.0	0.000	0.000	0.0 ± 0.0
11	0	1	16	0.000	0.2	0.000	0.063	0.0 ± 0.0
12	0	3	24	0.000	0.4	0.000	0.126	0.0 ± 0.0
13	0	6	18	0.000	1.0	0.000	0.337	0.0 ± 0.0
14	0	2	9	0.000	0.7	0.000	0.225	0.0 ± 0.0
15	0	0	6	0.000	0.0	0.000	0.000	0.0 ± 0.0
	0	22			0.3	0.000	0.109	

AREA OF BASIC UNIT = 9.89E-07 cm
CHI SQUARED = 2.66675E-06 WITH 14 DEGREES OF FREEDOM
P(chi squared) = 100.0 %
CORRELATION COEFFICIENT = 0.764
VARIANCE OF SQR(Ns) = 0.00
VARIANCE OF SQR(Ni) = 0.61

Ns/Ni = 0.000 ± 0.000
MEAN RATIO = 0.000 ± 0.000

Ages calculated using a zeta of 354.9 ± 4.3 for SRM612 glass
RHO D = 4.316E+06 ; ND = 3414

POOLED AGE = 0.0 ± 0.0 Ma
MEAN AGE = 0.0 ± 0.0 Ma

8902-143 ZIRCON lewis s46/672004 655m

IRRADIATION jmt data:jmt zircon data:lewis zircons:wk028/10
SLIDE NUMBER 1
COUNTED BY: jmt

No.	Ns	Ni	Na	RATIO	U (ppm)	RHOs (E+06)	RHOi (E+06)	F.T.AGE (Ma)
1	2	61	5	0.033	0.0	0.404	12.336	2.0 ± 1.4
2	1	39	4	0.026	0.0	0.253	9.858	1.6 ± 1.6
3	2	74	8	0.027	0.0	0.253	9.353	1.6 ± 1.2
4	3	90	6	0.033	0.0	0.506	15.167	2.0 ± 1.2
5	8	128	10	0.062	0.0	0.809	12.942	3.8 ± 1.4
6	0	45	12	0.000	0.0	0.000	3.792	0.0 ± 0.0
7	1	39	6	0.026	0.0	0.169	6.572	1.6 ± 1.6
	17	476			0.0	0.337	9.437	

AREA OF BASIC UNIT = 9.89E-07 cm
CHI SQUARED = 4.423634 WITH 6 DEGREES OF FREEDOM
P(chi squared) = 62.0 %
CORRELATION COEFFICIENT = 0.942
VARIANCE OF SQR(Ns) = 0.73
VARIANCE OF SQR(Ni) = 3.57

Ns/Ni = 0.036 ± 0.009
MEAN RATIO = 0.030 ± 0.007

Ages calculated using a zeta of 133.9 ± 1.4 for CN1 glass
RHO D = 9.120E+05 ; ND = 4510

POOLED AGE = 2.2 ± 0.5 Ma
MEAN AGE = 1.8 ± 0.4 Ma

8902-144 APATITE lewis s46/670993 490m

IRRADIATION jmt data:jmt apatite data:lewis apatites:wk016/9
SLIDE NUMBER 1
COUNTED BY: jmt

No.	Ns	Ni	Na	RATIO	U (ppm)	RHOs (E+06)	RHOi (E+06)	F.T.AGE (Ma)
1	0	6	16	0.000	3.0	0.000	0.379	0.0 ± 0.0
2	0	74	16	0.000	37.4	0.000	4.676	0.0 ± 0.0
3	0	8	7	0.000	9.2	0.000	1.156	0.0 ± 0.0
4	0	12	9	0.000	10.8	0.000	1.348	0.0 ± 0.0
5	0	62	24	0.000	20.9	0.000	2.612	0.0 ± 0.0
6	0	2	9	0.000	1.8	0.000	0.225	0.0 ± 0.0
7	0	5	9	0.000	4.5	0.000	0.562	0.0 ± 0.0
8	0	16	15	0.000	8.6	0.000	1.079	0.0 ± 0.0
9	0	47	25	0.000	15.2	0.000	1.901	0.0 ± 0.0
10	0	45	20	0.000	18.2	0.000	2.275	0.0 ± 0.0
11	0	63	20	0.000	25.5	0.000	3.185	0.0 ± 0.0
12	0	65	12	0.000	43.8	0.000	5.477	0.0 ± 0.0
13	0	49	12	0.000	33.0	0.000	4.129	0.0 ± 0.0
14	0	46	9	0.000	41.4	0.000	5.168	0.0 ± 0.0
15	0	8	8	0.000	8.1	0.000	1.011	0.0 ± 0.0
	0	508			19.5	0.000	2.434	

AREA OF BASIC UNIT = 9.89E-07 cm
CHI SQUARED = 5.864855E-04 WITH 14 DEGREES OF FREEDOM
P(chi squared) = 100.0 %
CORRELATION COEFFICIENT = 0.423
VARIANCE OF SQR(Ns) = 0.00
VARIANCE OF SQR(Ni) = 6.53

Ns/Ni = 0.000 ± 0.000
MEAN RATIO = 0.000 ± 0.000

Ages calculated using a zeta of 354.9 ± 4.3 for SRM612 glass
RHO D = 1.637E+06 ; ND = 3238

POOLED AGE = 0.0 ± 0.0 Ma
MEAN AGE = 0.0 ± 0.0 Ma

8902-144 ZIRCON lewis s46/670993 490m

IRRADIATION jmt data:jmt zircon data:lewis zircons:wk028/9
SLIDE NUMBER 1
COUNTED BY: jmt

No.	Ns	Ni	Na	RATIO	U (ppm)	RHOs (E+06)	RHOi (E+06)	F.T.AGE (Ma)
1	7	141	16	0.050	0.0	0.442	8.911	3.0 ± 1.2
2	4	110	12	0.036	0.0	0.337	9.269	2.2 ± 1.1
3	27	400	20	0.068	0.0	1.365	20.222	4.1 ± 0.8
4	8	167	14	0.048	0.0	0.578	12.061	2.9 ± 1.1
5	5	136	28	0.037	0.0	0.181	4.911	2.2 ± 1.0
6	20	279	40	0.072	0.0	0.506	7.053	4.3 ± 1.0
7	40	414	30	0.097	0.0	1.348	13.953	5.9 ± 1.0
8	7	130	24	0.054	0.0	0.295	5.477	3.3 ± 1.3
9	2	55	8	0.036	0.0	0.253	6.951	2.2 ± 1.6
10	7	94	8	0.074	0.0	0.885	11.881	4.5 ± 1.8
11	7	78	12	0.090	0.0	0.590	6.572	5.4 ± 2.1
12	21	331	24	0.063	0.0	0.885	13.945	3.8 ± 0.9
13	10	217	30	0.046	0.0	0.337	7.314	2.8 ± 0.9
14	14	368	40	0.038	0.0	0.354	9.302	2.3 ± 0.6
15	9	242	25	0.037	0.0	0.364	9.788	2.3 ± 0.8
16	23	378	35	0.061	0.0	0.664	10.920	3.7 ± 0.8
17	35	783	102	0.045	0.0	0.347	7.762	2.7 ± 0.5
	246	4323			0.0	0.531	9.340	

AREA OF BASIC UNIT = 9.89E-07 cm
CHI SQUARED = 23.04973 WITH 16 DEGREES OF FREEDOM
P(chi squared) = 11.2 %
CORRELATION COEFFICIENT = 0.869
VARIANCE OF SQR(Ns) = 2.03
VARIANCE OF SQR(Ni) = 28.43

Ns/Ni = 0.057 ± 0.004
MEAN RATIO = 0.056 ± 0.005

Ages calculated using a zeta of 133.9 ± 1.4 for CN1 glass
RHO D = 9.052E+05 ; ND = 4476

POOLED AGE = 3.4 ± 0.2 Ma
MEAN AGE = 3.4 ± 0.3 Ma

8902-145 APATITE lewis s46/678986 550m

IRRADIATION jmt data:jmt apatite data:lewis apatites:wk016/8
SLIDE NUMBER 1
COUNTED BY: jmt

No.	Ns	NI	Na	RATIO	U (ppm)	RHOs (E+06)	RHOi (E+06)	F.T.AGE (Ma)
1	0	101	12	0.000	68.6	0.000	8.510	0.0 ± 0.0
2	0	47	12	0.000	31.9	0.000	3.960	0.0 ± 0.0
3	1	70	9	0.014	63.4	0.112	7.864	4.1 ± 4.2
4	0	42	25	0.000	13.7	0.000	1.699	0.0 ± 0.0
5	0	44	8	0.000	44.8	0.000	5.561	0.0 ± 0.0
6	0	24	9	0.000	21.7	0.000	2.696	0.0 ± 0.0
7	1	154	28	0.006	44.8	0.036	5.561	1.9 ± 1.9
8	1	81	15	0.012	44.0	0.067	5.460	3.6 ± 3.6
9	0	7	16	0.000	3.6	0.000	0.442	0.0 ± 0.0
10	0	39	12	0.000	26.5	0.000	3.286	0.0 ± 0.0
11	0	37	9	0.000	33.5	0.000	4.157	0.0 ± 0.0
12	0	15	12	0.000	10.2	0.000	1.264	0.0 ± 0.0
13	0	39	16	0.000	19.9	0.000	2.465	0.0 ± 0.0
14	1	89	16	0.011	45.3	0.063	5.624	3.2 ± 3.3
15	0	15	12	0.000	10.2	0.000	1.264	0.0 ± 0.0
	4	804			31.0	0.019	3.853	

AREA OF BASIC UNIT = 9.89E-07 cm
CHI SQUARED = 4.880314 WITH 14 DEGREES OF FREEDOM
P(chi squared) = 98.7 %
CORRELATION COEFFICIENT = 0.714
VARIANCE OF SQR(Ns) = 0.21
VARIANCE OF SQR(Ni) = 6.82

Ns/Ni = 0.005 ± 0.002
MEAN RATIO = 0.003 ± 0.001

Ages calculated using a zeta of 354.9 ± 4.3 for SRM612 glass
RHO D = 1.626E+06 ; ND = 3215

POOLED AGE = 1.4 ± 0.7 Ma
MEAN AGE = 0.9 ± 0.4 Ma

8902-145 ZIRCON lewis s46/678986 550m

IRRADIATION jmt data:jmt zircon data:lewis zircons:wk028/8
SLIDE NUMBER 1
COUNTED BY: jmt

No.	Ns	NI	Na	RATIO	U (ppm)	RHOs (E+06)	RHOi (E+06)	F.T.AGE (Ma)
1	10	113	12	0.088	0.0	0.843	9.521	5.3 ± 1.8
2	11	111	25	0.099	0.0	0.445	4.489	6.0 ± 1.9
3	3	50	6	0.060	0.0	0.506	8.426	3.6 ± 2.1
4	6	56	5	0.107	0.0	1.213	11.325	6.4 ± 2.8
5	5	59	10	0.085	0.0	0.506	5.966	5.1 ± 2.4
6	20	321	28	0.062	0.0	0.722	11.592	3.7 ± 0.9
7	22	239	25	0.092	0.0	0.890	9.666	5.5 ± 1.2
8	9	72	6	0.125	0.0	1.517	12.133	7.5 ± 2.7
9	16	180	18	0.089	0.0	0.899	10.111	5.3 ± 1.4
10	15	88	16	0.170	0.0	0.948	5.561	10.2 ± 2.9
11	10	145	20	0.069	0.0	0.506	7.331	4.1 ± 1.4
12	3	86	20	0.035	0.0	0.152	4.348	2.1 ± 1.2
13	2	58	8	0.034	0.0	0.253	7.331	2.1 ± 1.5
14	9	74	6	0.122	0.0	1.517	12.471	7.3 ± 2.6
15	24	329	24	0.073	0.0	1.011	13.861	4.4 ± 0.9
16	46	421	40	0.109	0.0	1.163	10.642	6.6 ± 1.0
	211	2402			0.0	0.793	9.029	

AREA OF BASIC UNIT = 9.89E-07 cm
CHI SQUARED = 18.55421 WITH 15 DEGREES OF FREEDOM
P(chi squared) = 23.5 %
CORRELATION COEFFICIENT = 0.920
VARIANCE OF SQR(Ns) = 1.95
VARIANCE OF SQR(Ni) = 18.68

Ns/NI = 0.088 ± 0.006
MEAN RATIO = 0.089 ± 0.009

Ages calculated using a zeta of 133.9 ± 1.4 for CN1 glass
RHO D = 8.981E+05 ; ND = 4441

POOLED AGE = 5.3 ± 0.4 Ma
MEAN AGE = 5.3 ± 0.5 Ma

8902-146 APATITE lewis s46/699958 610m

IRRADIATION jmt data:jmt apatite data:lewis apatites:wk016/7
SLIDE NUMBER 1
COUNTED BY: jmt

No.	Ns	NI	Na	RATIO	U (ppm)	RHOs (E+06)	RHOI (E+06)	F.T.AGE (Ma)
1	0	13	8	0.000	13.3	0.000	1.643	0.0 ± 0.0
2	0	11	12	0.000	7.5	0.000	0.927	0.0 ± 0.0
3	0	40	9	0.000	36.5	0.000	4.494	0.0 ± 0.0
4	0	169	16	0.000	86.7	0.000	10.680	0.0 ± 0.0
5	0	42	6	0.000	57.4	0.000	7.078	0.0 ± 0.0
6	0	141	18	0.000	64.3	0.000	7.920	0.0 ± 0.0
7	0	61	28	0.000	17.9	0.000	2.203	0.0 ± 0.0
8	0	1	21	0.000	0.4	0.000	0.048	0.0 ± 0.0
9	0	13	12	0.000	8.9	0.000	1.095	0.0 ± 0.0
10	0	21	12	0.000	14.4	0.000	1.769	0.0 ± 0.0
11	0	89	20	0.000	36.5	0.000	4.499	0.0 ± 0.0
	0	601			30.4	0.000	3.751	

AREA OF BASIC UNIT = 9.89E-07 cm
CHI SQUARED = 2.556212E-04 WITH 10 DEGREES OF FREEDOM
P(chi squared) = 100.0 %
CORRELATION COEFFICIENT = 0.676
VARIANCE OF SQR(Ns) = 0.00
VARIANCE OF SQR(Ni) = 14.23

Ns/Ni = 0.000 ± 0.000
MEAN RATIO = 0.000 ± 0.000

Ages calculated using a zeta of 354.9 ± 4.3 for SRM612 glass
RHO D = 1.614E+06 ; ND = 3192

POOLED AGE = 0.0 ± 0.0 Ma
MEAN AGE = 0.0 ± 0.0 Ma

8902-146 ZIRCON lewis s46/699958 610m

IRRADIATION jmt data:jmt zircon data:lewis zircons:wk028/7
SLIDE NUMBER 1
COUNTED BY: jmt

No.	Ns	NI	Na	RATIO	U (ppm)	RHOs (E+06)	RHOI (E+06)	F.T.AGE (Ma)
1	154	137	16	1.124	0.0	9.732	8.658	66.7 ± 7.9
2	27	24	4	1.125	0.0	6.825	6.067	66.8 ± 18.8
3	44	25	9	1.760	0.0	4.943	2.809	104.2 ± 26.2
4	113	85	12	1.329	0.0	9.521	7.162	78.8 ± 11.4
5	162	76	12	2.132	0.0	13.650	6.404	125.9 ± 17.7
6	247	179	36	1.380	0.0	6.937	5.028	81.8 ± 8.2
7	123	100	12	1.230	0.0	10.364	8.426	73.0 ± 9.9
8	87	47	10	1.851	0.0	8.797	4.752	109.5 ± 19.9
9	136	105	12	1.295	0.0	11.459	8.847	76.8 ± 10.1
10	88	54	8	1.630	0.0	11.122	6.825	96.5 ± 16.8
11	64	51	8	1.255	0.0	8.089	6.446	74.4 ± 14.0
12	32	24	3	1.333	0.0	10.785	8.089	79.1 ± 21.4
13	88	64	8	1.375	0.0	11.122	8.089	81.5 ± 13.5
14	109	62	18	1.758	0.0	6.123	3.483	104.1 ± 16.7
15	106	95	12	1.116	0.0	8.932	8.005	66.2 ± 9.4
16	60	64	8	0.938	0.0	7.583	8.089	55.7 ± 10.1
17	68	45	6	1.511	0.0	11.459	7.583	89.5 ± 17.3
	1708	1237			0.0	8.902	6.447	

AREA OF BASIC UNIT = 9.89E-07 cm
CHI SQUARED = 28.87508 WITH 16 DEGREES OF FREEDOM
P(chi squared) = 2.5 %
CORRELATION COEFFICIENT = 0.924
VARIANCE OF SQR(Ns) = 7.22
VARIANCE OF SQR(Ni) = 5.52

Ns/Ni = 1.381 ± 0.052
MEAN RATIO = 1.420 ± 0.076

Ages calculated using a zeta of 133.9 ± 1.4 for CN1 glass
RHO D = 8.912E+05 ; ND = 4407

POOLED AGE = 81.9 ± 3.4 Ma
MEAN AGE = 84.2 ± 4.8 Ma

8902-147 APATITE lewis s46/723959 595m

IRRADIATION jmt data:jmt apatite data:lewis apatites:wk016/6
SLIDE NUMBER 1
COUNTED BY: jmt

No.	Ns	Ni	Na	RATIO	U (ppm)	RHOs (E+06)	RHOi (E+06)	F.T.AGE (Ma)
1	0	63	24	0.000	21.7	0.000	2.654	0.0 ± 0.0
2	0	17	16	0.000	8.8	0.000	1.074	0.0 ± 0.0
3	0	62	10	0.000	51.2	0.000	6.269	0.0 ± 0.0
4	0	25	6	0.000	34.4	0.000	4.213	0.0 ± 0.0
5	0	6	15	0.000	3.3	0.000	0.404	0.0 ± 0.0
6	0	6	6	0.000	8.3	0.000	1.011	0.0 ± 0.0
7	1	258	25	0.004	85.3	0.040	10.435	1.1 ± 1.1
8	0	20	25	0.000	6.6	0.000	0.809	0.0 ± 0.0
9	0	44	6	0.000	60.6	0.000	7.415	0.0 ± 0.0
10	0	15	36	0.000	3.4	0.000	0.421	0.0 ± 0.0
11	0	25	12	0.000	17.2	0.000	2.106	0.0 ± 0.0
12	0	15	6	0.000	20.7	0.000	2.528	0.0 ± 0.0
13	0	51	12	0.000	35.1	0.000	4.297	0.0 ± 0.0
14	0	52	12	0.000	35.8	0.000	4.382	0.0 ± 0.0
15	0	29	12	0.000	20.0	0.000	2.444	0.0 ± 0.0
	1	688			25.5	0.005	3.120	

AREA OF BASIC UNIT = 9.89E-07 cm
CHI SQUARED = 1.662644 WITH 14 DEGREES OF FREEDOM
P(chi squared) = 100.0 %
CORRELATION COEFFICIENT = 0.951
VARIANCE OF SQR(Ns) = 0.07
VARIANCE OF SQR(Ni) = 11.01

Ns/Ni = 0.001 ± 0.001
MEAN RATIO = 0.000 ± 0.000

Ages calculated using a zeta of 354.9 ± 4.3 for SRM612 glass
RHO D = 1.603E+06 ; ND = 3169

POOLED AGE = 0.4 ± 0.4 Ma
MEAN AGE = 0.1 ± 0.1 Ma

8902-147 ZIRCON lewis s46/723959 595m

IRRADIATION jmt data:jmt zircon data:lewis zircons:wk028/6
SLIDE NUMBER 1
COUNTED BY: jmt

No.	Ns	Ni	Na	RATIO	U (ppm)	RHOs (E+06)	RHOi (E+06)	F.T.AGE (Ma)
1	270	133	16	2.030	0.0	17.063	8.405	119.1 ± 12.8
2	120	47	12	2.553	0.0	10.111	3.960	149.4 ± 25.9
3	74	43	6	1.721	0.0	12.471	7.246	101.1 ± 19.5
4	68	27	6	2.519	0.0	11.459	4.550	147.4 ± 33.6
5	182	114	12	1.596	0.0	15.335	9.606	93.8 ± 11.3
6	88	55	6	1.600	0.0	14.830	9.269	94.0 ± 16.3
7	251	152	14	1.651	0.0	18.128	10.978	97.0 ± 10.1
8	125	60	8	2.083	0.0	15.799	7.583	122.1 ± 19.3
9	114	89	8	1.281	0.0	14.408	11.249	75.4 ± 10.8
10	60	47	5	1.277	0.0	12.133	9.505	75.1 ± 14.7
11	91	84	8	1.083	0.0	11.502	10.617	63.8 ± 9.7
12	156	90	18	1.733	0.0	8.763	5.056	101.8 ± 13.6
13	115	44	10	2.614	0.0	11.628	4.449	152.9 ± 27.2
14	164	71	16	2.310	0.0	10.364	4.487	135.3 ± 19.4
15	109	57	12	1.912	0.0	9.184	4.803	112.2 ± 18.5
	1987	1113			0.0	12.797	7.168	

AREA OF BASIC UNIT = 9.89E-07 cm
CHI SQUARED = 38.91148 WITH 14 DEGREES OF FREEDOM
P(chi squared) = < 0.1 %
CORRELATION COEFFICIENT = 0.886
VARIANCE OF SQR(Ns) = 6.64
VARIANCE OF SQR(Ni) = 4.07

Ns/Ni = 1.785 ± 0.067
MEAN RATIO = 1.864 ± 0.125

Ages calculated using a zeta of 133.9 ± 1.4 for CN1 glass
RHO D = 8.841E+05 ; ND = 4372

POOLED AGE = 104.8 ± 4.4 Ma
MEAN AGE = 109.4 ± 7.6 Ma

8902-148 APATITE lewis s46/784969 775m

IRRADIATION jmt data:jmt apatite data:lewis apatites:wk016/5
SLIDE NUMBER 1
COUNTED BY: jmt

No.	Ns	NI	Na	RATIO	U (ppm)	RHOs (E+06)	RHOI (E+06)	F.T.AGE (Ma)
1	0	121	25	0.000	40.3	0.000	4.894	0.0 ± 0.0
2	0	49	8	0.000	51.0	0.000	6.193	0.0 ± 0.0
3	0	16	9	0.000	14.8	0.000	1.798	0.0 ± 0.0
4	0	21	6	0.000	29.1	0.000	3.539	0.0 ± 0.0
5	0	76	20	0.000	31.6	0.000	3.842	0.0 ± 0.0
6	0	13	9	0.000	12.0	0.000	1.461	0.0 ± 0.0
7	0	8	12	0.000	5.6	0.000	0.674	0.0 ± 0.0
8	0	89	24	0.000	30.9	0.000	3.750	0.0 ± 0.0
9	0	56	12	0.000	38.9	0.000	4.719	0.0 ± 0.0
10	0	8	6	0.000	11.1	0.000	1.348	0.0 ± 0.0
11	0	32	28	0.000	9.5	0.000	1.156	0.0 ± 0.0
12	0	43	16	0.000	22.4	0.000	2.717	0.0 ± 0.0
13	0	41	25	0.000	13.7	0.000	1.658	0.0 ± 0.0
14	0	80	16	0.000	41.6	0.000	5.056	0.0 ± 0.0
15	0	88	12	0.000	61.1	0.000	7.415	0.0 ± 0.0
	0	741			27.1	0.000	3.286	

AREA OF BASIC UNIT = 9.89E-07 cm
CHI SQUARED = 5.123963E-04 WITH 14 DEGREES OF FREEDOM
P(chi squared) = 100.0 %
CORRELATION COEFFICIENT = 0.569
VARIANCE OF SQR(Ns) = 0.00
VARIANCE OF SQR(NI) = 6.80

Ns/NI = 0.000 ± 0.000
MEAN RATIO = 0.000 ± 0.000

Ages calculated using a zeta of 354.9 ± 4.3 for SRM612 glass
RHO D = 1.591E+06 ; ND = 3147

POOLED AGE = 0.0 ± 0.0 Ma
MEAN AGE = 0.0 ± 0.0 Ma

8902-148 ZIRCON lewis s46/784969 775m

IRRADIATION jmt data:jmt zircon data:lewis zircons:wk028/5
SLIDE NUMBER 1
COUNTED BY: jmt

No.	Ns	NI	Na	RATIO	U (ppm)	RHOs (E+06)	RHOI (E+06)	F.T.AGE (Ma)
1	107	42	9	2.548	0.0	12.021	4.719	147.9 ± 27.1
2	237	98	16	2.418	0.0	14.977	6.193	140.5 ± 17.1
3	155	64	9	2.422	0.0	17.414	7.190	140.7 ± 21.1
4	150	46	9	3.261	0.0	16.852	5.168	188.7 ± 32.0
5	124	61	12	2.033	0.0	10.448	5.140	118.3 ± 18.6
6	99	52	8	1.904	0.0	12.513	6.572	110.9 ± 19.1
7	185	105	14	1.762	0.0	13.361	7.583	102.7 ± 12.7
8	164	70	12	2.343	0.0	13.819	5.898	136.1 ± 19.6
9	254	122	24	2.082	0.0	10.701	5.140	121.1 ± 13.5
10	89	63	6	1.413	0.0	14.998	10.617	82.4 ± 13.7
11	35	18	3	1.944	0.0	11.796	6.067	113.2 ± 32.9
12	76	26	4	2.923	0.0	19.211	6.572	169.4 ± 38.6
13	91	28	8	3.250	0.0	11.502	3.539	188.1 ± 40.8
	1766	795			0.0	13.326	5.999	

AREA OF BASIC UNIT = 9.89E-07 cm
CHI SQUARED = 24.39666 WITH 12 DEGREES OF FREEDOM
P(chi squared) = 1.8 %
CORRELATION COEFFICIENT = 0.912
VARIANCE OF SQR(Ns) = 7.75
VARIANCE OF SQR(NI) = 4.17

Ns/NI = 2.221 ± 0.095
MEAN RATIO = 2.331 ± 0.156

Ages calculated using a zeta of 133.9 ± 1.4 for CN1 glass
RHO D = 8.772E+05 ; ND = 4338

POOLED AGE = 129.2 ± 6.0 Ma
MEAN AGE = 135.5 ± 9.4 Ma

8902-149 APATITE lewis s46/807969 915m

IRRADIATION jmt data:jmt apatite data:lewis apatites:wk016/4
SLIDE NUMBER 1
COUNTED BY: jmt

No.	Ns	Ni	Na	RATIO	U (ppm)	RHOs (E+06)	RHOi (E+06)	F.T.AGE (Ma)
1	0	11	4	0.000	23.1	0.000	2.781	0.0 ± 0.0
2	0	2	9	0.000	1.9	0.000	0.225	0.0 ± 0.0
3	0	68	9	0.000	63.3	0.000	7.640	0.0 ± 0.0
4	0	27	9	0.000	25.2	0.000	3.033	0.0 ± 0.0
5	0	2	6	0.000	2.8	0.000	0.337	0.0 ± 0.0
6	0	21	6	0.000	29.3	0.000	3.539	0.0 ± 0.0
7	0	30	12	0.000	21.0	0.000	2.528	0.0 ± 0.0
8	0	60	8	0.000	62.9	0.000	7.583	0.0 ± 0.0
9	0	44	12	0.000	30.7	0.000	3.707	0.0 ± 0.0
10	0	1	8	0.000	1.0	0.000	0.126	0.0 ± 0.0
11	0	7	10	0.000	5.9	0.000	0.708	0.0 ± 0.0
12	1	39	15	0.026	21.8	0.067	2.629	7.2 ± 7.3
13	0	21	9	0.000	19.6	0.000	2.359	0.0 ± 0.0
14	0	3	8	0.000	3.1	0.000	0.379	0.0 ± 0.0
15	0	8	12	0.000	5.6	0.000	0.674	0.0 ± 0.0
16	0	38	12	0.000	26.5	0.000	3.202	0.0 ± 0.0
17	0	16	6	0.000	22.4	0.000	2.696	0.0 ± 0.0
18	0	20	12	0.000	14.0	0.000	1.685	0.0 ± 0.0
19	0	6	4	0.000	12.6	0.000	1.517	0.0 ± 0.0
20	0	3	4	0.000	6.3	0.000	0.758	0.0 ± 0.0
	1	427			20.5	0.006	2.467	

AREA OF BASIC UNIT = 9.89E-07 cm
CHI SQUARED = 9.722716 WITH 19 DEGREES OF FREEDOM
P(chi squared) = 95.9 %
CORRELATION COEFFICIENT = 0.209
VARIANCE OF SQR(Ns) = 0.05
VARIANCE OF SQR(Ni) = 4.83

Ns/Ni = 0.002 ± 0.002
MEAN RATIO = 0.001 ± 0.001

Ages calculated using a zeta of 354.9 ± 4.3 for SRM612 glass
RHO D = 1.580E+06 ; ND = 3124

POOLED AGE = 0.7 ± 0.7 Ma
MEAN AGE = 0.4 ± 0.4 Ma

8902-149 ZIRCON lewis s46/807969 915m

IRRADIATION jmt data:jmt zircon data:lewis zircons:wk037/8
SLIDE NUMBER 1
COUNTED BY: jmt

No.	Ns	Ni	Na	RATIO	U (ppm)	RHOs (E+06)	RHOi (E+06)	F.T.AGE (Ma)
1	99	44	6	2.250	0.0	16.684	7.415	158.8 ± 28.9
2	34	15	4	2.267	0.0	8.595	3.792	159.9 ± 49.6
3	44	20	3	2.200	0.0	14.830	6.741	155.3 ± 42.0
4	16	6	2	2.667	0.0	8.089	3.033	187.7 ± 89.9
5	115	49	8	2.347	0.0	14.535	6.193	165.5 ± 28.4
6	69	28	6	2.464	0.0	11.628	4.719	173.7 ± 39.0
7	30	9	2	3.333	0.0	15.167	4.550	233.8 ± 88.9
8	54	29	4	1.862	0.0	13.650	7.331	131.7 ± 30.4
9	318	136	21	2.338	0.0	15.311	6.548	164.9 ± 17.1
	779	336			0.0	14.065	6.067	

AREA OF BASIC UNIT = 9.89E-07 cm
CHI SQUARED = 2.075193 WITH 8 DEGREES OF FREEDOM
P(chi squared) = 97.9 %
CORRELATION COEFFICIENT = 0.998
VARIANCE OF SQR(Ns) = 16.94
VARIANCE OF SQR(Ni) = 7.60

Ns/Ni = 2.318 ± 0.151
MEAN RATIO = 2.414 ± 0.135

Ages calculated using a zeta of 133.9 ± 1.4 for CN1 glass
RHO D = 1.067E+06 ; ND = 6342

POOLED AGE = 163.5 ± 11.0 Ma
MEAN AGE = 170.2 ± 9.9 Ma

8902-150 APATITE lewis s46/809939 825m

IRRADIATION jmt data:jmt apatite data:lewis apatites:wk016/3
SLIDE NUMBER 1
COUNTED BY: jmt

No.	Ns	Ni	Na	RATIO	U (ppm)	RHOs (E+06)	RHOi (E+06)	F.T AGE (Ma)
1	1	34	24	0.029	12.0	0.042	1.432	8.2 ± 8.3
2	0	11	8	0.000	11.6	0.000	1.390	0.0 ± 0.0
3	0	11	9	0.000	10.3	0.000	1.236	0.0 ± 0.0
4	0	22	6	0.000	31.0	0.000	3.707	0.0 ± 0.0
5	0	1	12	0.000	0.7	0.000	0.084	0.0 ± 0.0
6	0	8	4	0.000	16.9	0.000	2.022	0.0 ± 0.0
7	0	15	4	0.000	31.7	0.000	3.792	0.0 ± 0.0
8	0	45	24	0.000	15.8	0.000	1.896	0.0 ± 0.0
9	1	58	18	0.017	27.2	0.056	3.258	4.8 ± 4.8
10	0	54	12	0.000	38.0	0.000	4.550	0.0 ± 0.0
11	0	11	9	0.000	10.3	0.000	1.236	0.0 ± 0.0
12	0	30	24	0.000	10.6	0.000	1.264	0.0 ± 0.0
13	0	27	16	0.000	14.3	0.000	1.706	0.0 ± 0.0
14	0	80	36	0.000	18.8	0.000	2.247	0.0 ± 0.0
15	0	6	6	0.000	8.4	0.000	1.011	0.0 ± 0.0
16	0	55	12	0.000	38.7	0.000	4.634	0.0 ± 0.0
17	0	84	18	0.000	39.4	0.000	4.719	0.0 ± 0.0
18	0	8	4	0.000	16.9	0.000	2.022	0.0 ± 0.0
19	0	15	12	0.000	10.6	0.000	1.264	0.0 ± 0.0
20	1	117	20	0.009	49.4	0.051	5.915	2.4 ± 2.4
	3	692			21.0	0.011	2.517	

AREA OF BASIC UNIT = 9.89E-07 cm
CHI SQUARED = 9.550098 WITH 19 DEGREES OF FREEDOM
P(chi squared) = 96.3 %
CORRELATION COEFFICIENT = 0.481
VARIANCE OF SQR(Ns) = 0.13
VARIANCE OF SQR(Ni) = 6.85

Ns/Ni = 0.004 ± 0.002
MEAN RATIO = 0.003 ± 0.002

Ages calculated using a zeta of 354.9 ± 4.3 for SRM612 glass
RHO D = 1.568E+06 ; ND = 3101

POOLED AGE = 1.2 ± 0.7 Ma
MEAN AGE = 0.8 ± 0.5 Ma

8902-150 ZIRCON lewis s46/809939 825m

IRRADIATION jmt data:jmt zircon data:lewis zircons:wk028/3
SLIDE NUMBER 1
COUNTED BY: jmt

No.	Ns	Ni	Na	RATIO	U (ppm)	RHOs (E+06)	RHOi (E+06)	F.T AGE (Ma)
1	108	23	8	4.696	0.0	13.650	2.907	265.7 ± 61.2
2	296	97	30	3.052	0.0	9.976	3.269	173.9 ± 20.6
3	93	30	9	3.100	0.0	10.448	3.370	176.6 ± 37.2
4	325	74	20	4.392	0.0	16.431	3.741	248.9 ± 32.4
5	23	9	4	2.556	0.0	5.814	2.275	146.0 ± 57.5
6	86	19	8	4.526	0.0	10.870	2.401	256.3 ± 65.2
7	67	18	6	3.722	0.0	11.291	3.033	211.5 ± 56.3
8	281	93	20	3.022	0.0	14.206	4.702	172.2 ± 20.8
9	126	44	15	2.864	0.0	8.493	2.966	163.3 ± 28.8
10	79	20	6	3.950	0.0	13.313	3.370	224.2 ± 56.3
11	137	38	12	3.605	0.0	11.544	3.202	205.0 ± 37.8
	1621	465			0.0	11.877	3.407	

AREA OF BASIC UNIT = 9.89E-07 cm
CHI SQUARED = 11.27185 WITH 10 DEGREES OF FREEDOM
P(chi squared) = 33.7 %
CORRELATION COEFFICIENT = 0.956
VARIANCE OF SQR(Ns) = 17.53
VARIANCE OF SQR(Ni) = 5.40

Ns/Ni = 3.486 ± 0.183
MEAN RATIO = 3.589 ± 0.220

Ages calculated using a zeta of 133.9 ± 1.4 for CN1 glass
RHO D = 8.629E+05 ; ND = 4267

POOLED AGE = 198.3 ± 11.1 Ma
MEAN AGE = 204.1 ± 13.1 Ma

8902-151 APATITE lewis s46/812901 730m

IRRADIATION jmt data:jmt apatite data:lewis apatites:wk016/2
SLIDE NUMBER 1
COUNTED BY: jmt

No.	Ns	Ni	Na	RATIO	U (ppm)	RHOs (E+06)	RHOi (E+06)	F.T.AGE (Ma)
1	0	5	6	0.000	7.1	0.000	0.843	0.0 ± 0.0
2	0	24	9	0.000	22.7	0.000	2.696	0.0 ± 0.0
3	0	28	6	0.000	39.7	0.000	4.719	0.0 ± 0.0
4	0	67	9	0.000	63.3	0.000	7.527	0.0 ± 0.0
5	0	43	6	0.000	61.0	0.000	7.246	0.0 ± 0.0
6	0	5	12	0.000	3.5	0.000	0.421	0.0 ± 0.0
7	0	11	4	0.000	23.4	0.000	2.781	0.0 ± 0.0
8	0	70	9	0.000	66.2	0.000	7.864	0.0 ± 0.0
9	0	8	9	0.000	7.6	0.000	0.899	0.0 ± 0.0
10	0	88	8	0.000	93.6	0.000	11.122	0.0 ± 0.0
11	0	9	4	0.000	19.1	0.000	2.275	0.0 ± 0.0
12	0	4	4	0.000	8.5	0.000	1.011	0.0 ± 0.0
13	1	113	16	0.009	60.1	0.063	7.141	2.4 ± 2.5
14	0	37	20	0.000	15.7	0.000	1.871	0.0 ± 0.0
15	0	15	9	0.000	14.2	0.000	1.685	0.0 ± 0.0
16	0	16	4	0.000	34.0	0.000	4.044	0.0 ± 0.0
17	0	58	12	0.000	41.1	0.000	4.887	0.0 ± 0.0
18	0	6	4	0.000	12.8	0.000	1.517	0.0 ± 0.0
19	0	66	15	0.000	37.4	0.000	4.449	0.0 ± 0.0
20	1	52	6	0.019	73.7	0.169	8.763	5.3 ± 5.4
	2	725			35.9	0.012	4.262	

AREA OF BASIC UNIT = 9.89E-07 cm
CHI SQUARED = 8.069286 WITH 19 DEGREES OF FREEDOM
P(chi squared) = 98.6 %
CORRELATION COEFFICIENT = 0.494
VARIANCE OF SQR(Ns) = 0.09
VARIANCE OF SQR(Ni) = 7.30

Ns/Ni = 0.003 ± 0.002
MEAN RATIO = 0.001 ± 0.001

Ages calculated using a zeta of 354.9 ± 4.3 for SRM612 glass
RHO D = 1.557E+06 ; ND = 3079

POOLED AGE = 0.8 ± 0.5 Ma
MEAN AGE = 0.4 ± 0.3 Ma

8902-151 ZIRCON lewis s46/812901 730m

IRRADIATION jmt data:jmt zircon data:lewis zircons:wk028/2
SLIDE NUMBER 1
COUNTED BY: jmt

No.	Ns	Ni	Na	RATIO	U (ppm)	RHOs (E+06)	RHOi (E+06)	F.T.AGE (Ma)
1	298	104	20	2.865	0.0	15.066	5.258	162.2 ± 18.7
2	126	37	12	3.405	0.0	10.617	3.118	192.3 ± 36.1
3	226	80	12	2.825	0.0	19.043	6.741	159.9 ± 21.0
4	147	40	8	3.675	0.0	18.579	5.056	207.3 ± 37.2
5	230	83	14	2.771	0.0	16.611	5.995	156.9 ± 20.3
6	272	74	20	3.676	0.0	13.751	3.741	207.3 ± 27.5
7	146	54	12	2.704	0.0	12.302	4.550	153.1 ± 24.6
8	425	122	24	3.484	0.0	17.905	5.140	196.7 ± 20.5
9	244	68	18	3.588	0.0	13.706	3.820	202.5 ± 28.0
10	90	32	6	2.812	0.0	15.167	5.393	159.2 ± 32.9
11	329	109	24	3.018	0.0	13.861	4.592	170.7 ± 19.1
12	97	44	6	2.205	0.0	16.346	7.415	125.1 ± 22.9
13	88	20	8	4.400	0.0	11.122	2.528	247.4 ± 61.5
14	498	110	30	4.527	0.0	16.785	3.707	254.4 ± 27.2
15	223	47	10	4.745	0.0	22.548	4.752	266.4 ± 43.0
	3439	1024			0.0	15.523	4.622	

AREA OF BASIC UNIT = 9.89E-07 cm
CHI SQUARED = 30.03236 WITH 14 DEGREES OF FREEDOM
P(chi squared) = 0.8 %
CORRELATION COEFFICIENT = 0.913
VARIANCE OF SQR(Ns) = 15.74
VARIANCE OF SQR(Ni) = 4.06

Ns/Ni = 3.358 ± 0.120
MEAN RATIO = 3.380 ± 0.191

Ages calculated using a zeta of 133.9 ± 1.4 for CN1 glass
RHO D = 8.562E+05 ; ND = 4234

POOLED AGE = 189.7 ± 7.6 Ma
MEAN AGE = 190.9 ± 11.4 Ma

8902-152 APATITE lewis s53/764760 595m

IRRADIATION jmt data:jmt apatite data:lewis apatites:wk016/1
SLIDE NUMBER 1
COUNTED BY: jmt

No.	Ns	NI	Na	RATIO	U (ppm)	RHOs (E+06)	RHOi (E+06)	F.T.AGE (Ma)
1	1	98	8	0.010	105.0	0.126	12.386	2.8 ± 2.8
2	0	24	6	0.000	34.3	0.000	4.044	0.0 ± 0.0
3	0	3	4	0.000	6.4	0.000	0.758	0.0 ± 0.0
4	0	10	12	0.000	7.1	0.000	0.843	0.0 ± 0.0
5	0	53	21	0.000	21.6	0.000	2.552	0.0 ± 0.0
6	0	7	2	0.000	30.0	0.000	3.539	0.0 ± 0.0
7	2	126	8	0.016	135.0	0.253	15.925	4.4 ± 3.1
8	0	28	9	0.000	26.7	0.000	3.146	0.0 ± 0.0
9	0	4	4	0.000	8.6	0.000	1.011	0.0 ± 0.0
10	0	5	4	0.000	10.7	0.000	1.264	0.0 ± 0.0
11	0	9	4	0.000	19.3	0.000	2.275	0.0 ± 0.0
12	0	12	6	0.000	17.1	0.000	2.022	0.0 ± 0.0
13	0	3	6	0.000	4.3	0.000	0.506	0.0 ± 0.0
14	0	37	12	0.000	26.4	0.000	3.118	0.0 ± 0.0
15	0	15	6	0.000	21.4	0.000	2.528	0.0 ± 0.0
16	0	3	4	0.000	6.4	0.000	0.758	0.0 ± 0.0
17	0	27	24	0.000	9.6	0.000	1.138	0.0 ± 0.0
18	0	16	6	0.000	22.9	0.000	2.696	0.0 ± 0.0
19	0	5	6	0.000	7.1	0.000	0.843	0.0 ± 0.0
20	0	6	6	0.000	8.6	0.000	1.011	0.0 ± 0.0
	3	491			26.6	0.019	3.142	

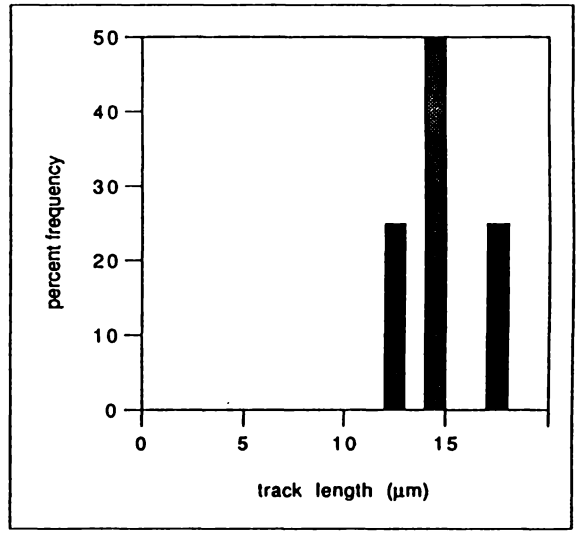
AREA OF BASIC UNIT = 9.89E-07 cm
CHI SQUARED = 3.832406 WITH 19 DEGREES OF FREEDOM
P(chi squared) = 100.0 %
CORRELATION COEFFICIENT = 0.901
VARIANCE OF SQR(Ns) = 0.14
VARIANCE OF SQR(Ni) = 7.21

Ns/Ni = 0.006 ± 0.004
MEAN RATIO = 0.001 ± 0.001

Ages calculated using a zeta of 354.9 ± 4.3 for SRM612 glass
RHO D = 1.545E+06 ; ND = 3056

POOLED AGE = 1.7 ± 1.0 Ma
MEAN AGE = 0.4 ± 0.3 Ma

8902-152



n = 4
Mean = 14.96 µm
Sample std. dev. = 1.57 µm

8902-152 ZIRCON lewis s53/764760 595m

IRRADIATION jmt data:jmt zircon data:lewis zircons:wk028/1
SLIDE NUMBER 1
COUNTED BY: jmt

No.	Ns	Ni	Na	RATIO	U (ppm)	RHOs (E+06)	RHOi (E+06)	F.T AGE (Ma)
1	61	21	6	2.905	0.0	10.280	3.539	163.1 ± 41.4
2	56	20	6	2.800	0.0	9.437	3.370	157.3 ± 41.1
3	52	20	4	2.600	0.0	13.145	5.056	146.2 ± 38.6
4	176	68	12	2.588	0.0	14.830	5.730	145.5 ± 21.0
5	79	27	4	2.926	0.0	19.970	6.825	164.3 ± 36.7
6	257	74	16	3.473	0.0	16.241	4.676	194.5 ± 25.9
7	147	43	8	3.419	0.0	18.579	5.435	191.5 ± 33.4
8	55	15	3	3.667	0.0	18.537	5.056	205.2 ± 59.9
9	140	47	10	2.979	0.0	14.156	4.752	167.2 ± 28.4
10	194	51	9	3.804	0.0	21.795	5.730	212.7 ± 33.7
11	64	25	6	2.560	0.0	10.785	4.213	143.9 ± 34.1
12	194	42	9	4.619	0.0	21.795	4.719	257.4 ± 44.1
13	99	36	12	2.750	0.0	8.342	3.033	154.5 ± 30.2
14	58	12	4	4.833	0.0	14.661	3.033	269.1 ± 85.5
15	93	32	8	2.906	0.0	11.754	4.044	163.2 ± 33.6
	1725	533			0.0	14.908	4.606	

AREA OF BASIC UNIT = 9.89E-07 cm
CHI SQUARED = 13.72774 WITH 14 DEGREES OF FREEDOM
P(chi squared) = 47.0 %
CORRELATION COEFFICIENT = 0.930
VARIANCE OF SQR(Ns) = 8.62
VARIANCE OF SQR(Ni) = 2.36

Ns/Ni = 3.236 ± 0.160
MEAN RATIO = 3.255 ± 0.184

Ages calculated using a zeta of 133.9 ± 1.4 for CN1 glass
RHO D = 8.493E+05 ; ND = 4200

POOLED AGE = 181.4 ± 9.6 Ma
MEAN AGE = 182.5 ± 10.9 Ma

8902-153 APATITE lewis s54/853708 455m

IRRADIATION jmt data:jmt apatite data:lewis apatites:wk017/16
SLIDE NUMBER 1
COUNTED BY: jmt

No.	Ns	Ni	Na	RATIO	U (ppm)	RHOs (E+06)	RHOi (E+06)	F.T AGE (Ma)
1	1	28	8	0.036	34.8	0.126	3.539	8.4 ± 8.6
2	1	18	6	0.056	29.9	0.169	3.033	13.1 ± 13.5
3	0	45	9	0.000	49.8	0.000	5.056	0.0 ± 0.0
4	0	34	12	0.000	28.2	0.000	2.865	0.0 ± 0.0
5	0	24	16	0.000	14.9	0.000	1.517	0.0 ± 0.0
6	1	56	12	0.018	46.4	0.084	4.719	4.2 ± 4.3
7	0	5	6	0.000	8.3	0.000	0.843	0.0 ± 0.0
8	0	2	40	0.000	0.5	0.000	0.051	0.0 ± 0.0
9	1	38	16	0.026	23.6	0.063	2.401	6.2 ± 6.3
10	0	35	20	0.000	17.4	0.000	1.769	0.0 ± 0.0
11	0	33	10	0.000	32.8	0.000	3.337	0.0 ± 0.0
12	0	36	8	0.000	44.8	0.000	4.550	0.0 ± 0.0
13	1	46	24	0.022	19.1	0.042	1.938	5.1 ± 5.2
14	0	16	8	0.000	19.9	0.000	2.022	0.0 ± 0.0
15	0	2	9	0.000	2.2	0.000	0.225	0.0 ± 0.0
16	1	164	30	0.006	54.4	0.034	5.527	1.4 ± 1.4
17	1	16	15	0.062	10.6	0.067	1.079	14.7 ± 15.2
18	0	14	12	0.000	11.6	0.000	1.180	0.0 ± 0.0
19	0	38	16	0.000	23.6	0.000	2.401	0.0 ± 0.0
20	2	57	12	0.035	47.3	0.169	4.803	8.3 ± 6.0
	9	707			24.3	0.031	2.474	

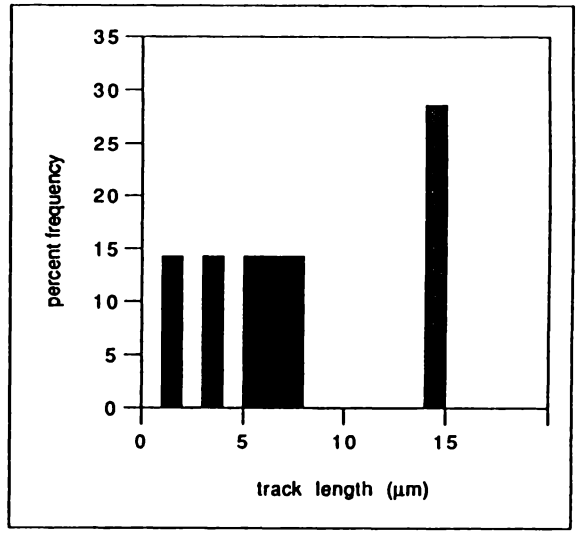
AREA OF BASIC UNIT = 9.89E-07 cm
CHI SQUARED = 13.78749 WITH 19 DEGREES OF FREEDOM
P(chi squared) = 79.6 %
CORRELATION COEFFICIENT = 0.409
VARIANCE OF SQR(Ns) = 0.29
VARIANCE OF SQR(Ni) = 6.29

Ns/Ni = 0.013 ± 0.004
MEAN RATIO = 0.013 ± 0.004

Ages calculated using a zeta of 354.9 ± 4.3 for SRM612 glass
RHO D = 1.331E+06 ; ND = 3291

POOLED AGE = 3.0 ± 1.0 Ma
MEAN AGE = 3.1 ± 1.1 Ma

8902-153



n = 7
Mean = 7.57 µm
Sample std. dev. = 4.70 µm

8902-153 ZIRCON lewis s53/853708 455m

IRRADIATION jmt data:jmt zircon data:lewis zircons:wk037/10
SLIDE NUMBER 1
COUNTED BY: jmt

No.	Ns	NI	Na	RATIO	U (ppm)	RHOs (E+06)	RHOi (E+06)	F.T.AGE (Ma)
1	50	11	4	4.545	0.0	12.639	2.781	316.8 ± 105.6
2	141	79	9	1.785	0.0	15.841	8.875	126.3 ± 17.9
3	107	44	9	2.432	0.0	12.021	4.943	171.4 ± 30.8
4	403	145	42	2.779	0.0	9.702	3.491	195.5 ± 19.2
5	51	19	6	2.684	0.0	8.595	3.202	189.0 ± 50.9
6	142	70	12	2.029	0.0	11.965	5.898	143.3 ± 21.1
7	55	15	3	3.667	0.0	18.537	5.056	256.7 ± 74.9
8	23	8	2	2.875	0.0	11.628	4.044	202.2 ± 83.0
9	39	10	4	3.900	0.0	9.858	2.528	272.7 ± 96.8
10	76	18	10	4.222	0.0	7.685	1.820	294.8 ± 77.4
11	44	24	6	1.833	0.0	7.415	4.044	129.7 ± 33.0
	1131	443			0.0	10.688	4.186	

AREA OF BASIC UNIT = 9.89E-07 cm
CHI SQUARED = 21.5859 WITH 10 DEGREES OF FREEDOM
P(chi squared) = 1.7 %
CORRELATION COEFFICIENT = 0.964
VARIANCE OF SQR(Ns) = 18.09
VARIANCE OF SQR(Ni) = 8.66

Ns/Ni = 2.553 ± 0.143
MEAN RATIO = 2.977 ± 0.292

Ages calculated using a zeta of 133.9 ± 1.4 for CN1 glass
RHO D = 1.067E+06 ; ND = 6342

POOLED AGE = 179.8 ± 10.5 Ma
MEAN AGE = 209.3 ± 20.8 Ma

8902-154 ZIRCON lewis s54/917697 425m

IRRADIATION jmt data:jmt zircon data:lewis zircons:wk029/17
SLIDE NUMBER 1
COUNTED BY: jmt

No.	Ns	Ni	Na	RATIO	U (ppm)	RHOs (E+06)	RHOi (E+06)	F.T.AGE (Ma)
1	68	27	4	2.519	0.0	17.189	6.825	152.9 ± 34.9
2	22	9	1	2.444	0.0	22.245	9.100	148.5 ± 58.8
3	228	56	15	4.071	0.0	15.369	3.775	245.4 ± 36.9
4	157	56	12	2.804	0.0	13.229	4.719	170.0 ± 26.6
5	42	15	4	2.800	0.0	10.617	3.792	169.8 ± 51.2
	517	163			0.0	14.521	4.578	

AREA OF BASIC UNIT = 9.89E-07 cm
CHI SQUARED = 5.087356 WITH 4 DEGREES OF FREEDOM
P(chi squared) = 27.8 %
CORRELATION COEFFICIENT = 0.952
VARIANCE OF SQR(Ns) = 18.58
VARIANCE OF SQR(Ni) = 4.20

Ns/Ni = 3.172 ± 0.285
MEAN RATIO = 2.928 ± 0.295

Ages calculated using a zeta of 133.9 ± 1.4 for CN1 glass
RHO D = 9.177E+05 ; ND = 4538

POOLED AGE = 192.0 ± 17.6 Ma
MEAN AGE = 177.4 ± 18.2 Ma

8902-155 APATITE lewis s54/968703 410m

IRRADIATION jmt data:jmt apatite data:lewis apatites:wk017/15
SLIDE NUMBER 1
COUNTED BY: jmt

No.	Ns	Ni	Na	RATIO	U (ppm)	RHOs (E+06)	RHOi (E+06)	F.T.AGE (Ma)
1	0	4	15	0.000	2.7	0.000	0.270	0.0 ± 0.0
2	0	22	24	0.000	9.2	0.000	0.927	0.0 ± 0.0
3	0	30	15	0.000	20.0	0.000	2.022	0.0 ± 0.0
4	1	37	12	0.027	30.9	0.084	3.118	6.3 ± 6.4
5	0	9	28	0.000	3.2	0.000	0.325	0.0 ± 0.0
6	0	20	12	0.000	16.7	0.000	1.685	0.0 ± 0.0
7	0	3	18	0.000	1.7	0.000	0.169	0.0 ± 0.0
8	1	4	15	0.250	2.7	0.067	0.270	58.4 ± 65.3
9	1	71	18	0.014	39.5	0.056	3.988	3.3 ± 3.3
10	0	7	9	0.000	7.8	0.000	0.786	0.0 ± 0.0
11	0	27	40	0.000	6.8	0.000	0.682	0.0 ± 0.0
12	3	18	32	0.167	5.6	0.095	0.569	39.0 ± 24.3
13	0	9	8	0.000	11.3	0.000	1.138	0.0 ± 0.0
14	0	8	12	0.000	6.7	0.000	0.674	0.0 ± 0.0
15	1	103	40	0.010	25.8	0.025	2.604	2.3 ± 2.3
16	0	18	12	0.000	15.0	0.000	1.517	0.0 ± 0.0
17	0	1	16	0.000	0.6	0.000	0.063	0.0 ± 0.0
18	0	7	14	0.000	5.0	0.000	0.506	0.0 ± 0.0
19	0	4	15	0.000	2.7	0.000	0.270	0.0 ± 0.0
20	1	29	15	0.034	19.4	0.067	1.955	8.1 ± 8.2
21	0	4	15	0.000	2.7	0.000	0.270	0.0 ± 0.0
22	0	2	6	0.000	3.3	0.000	0.337	0.0 ± 0.0
23	0	53	12	0.000	44.3	0.000	4.466	0.0 ± 0.0
24	2	11	18	0.182	6.1	0.112	0.618	42.5 ± 32.7
25	2	98	15	0.020	65.5	0.135	6.606	4.8 ± 3.4
26	0	0	9	0.000	0.0	0.000	0.000	0.0 ± 0.0
27	0	15	9	0.000	16.7	0.000	1.685	0.0 ± 0.0
28	1	16	9	0.062	17.8	0.112	1.798	14.6 ± 15.1
	13	630			13.6	0.028	1.376	

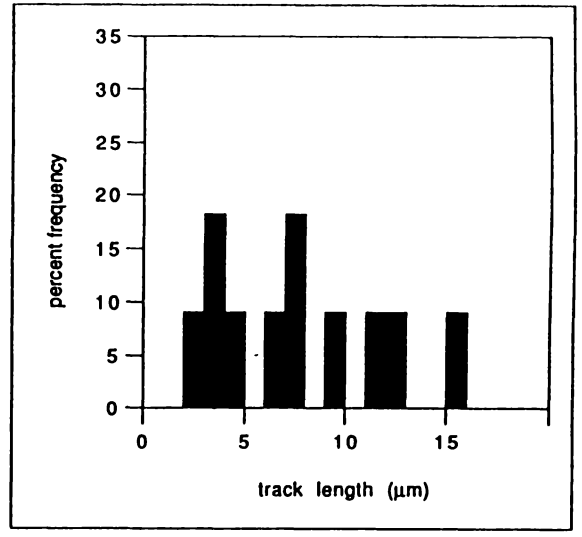
AREA OF BASIC UNIT = 9.89E-07 cm
CHI SQUARED = 43.18296 WITH 27 DEGREES OF FREEDOM
P(chi squared) = 2.5 %
CORRELATION COEFFICIENT = 0.408
VARIANCE OF SQR(Ns) = 0.33
VARIANCE OF SQR(Ni) = 6.44

Ns/Ni = 0.021 ± 0.006
MEAN RATIO = 0.027 ± 0.012

Ages calculated using a zeta of 354.9 ± 4.3 for SRM612 glass
RHO D = 1.322E+06 ; ND = 3270

POOLED AGE = 4.8 ± 1.4 Ma
MEAN AGE = 6.4 ± 2.8 Ma

8902-155



n = 11
Mean = 7.70 µm
Sample std. dev. = 4.14 µm

8902-155 ZIRCON lewis s54/968703 410m

IRRADIATION jmt data:jmt zircon data:lewis zircons:wk029/16
SLIDE NUMBER 1
COUNTED BY: jmt

No.	Ns	NI	Na	RATIO	U (ppm)	RHOs (E+06)	RHOi (E+06)	F.T.AGE (Ma)
1	194	54	14	3.593	0.0	14.011	3.900	215.0 ± 33.3
2	40	13	4	3.077	0.0	10.111	3.286	184.6 ± 59.0
3	59	14	4	4.214	0.0	14.914	3.539	251.5 ± 74.9
4	59	37	6	1.595	0.0	9.943	6.235	96.3 ± 20.3
5	93	29	20	3.207	0.0	4.702	1.466	192.2 ± 41.0
6	32	11	6	2.909	0.0	5.393	1.854	174.6 ± 61.1
	477	158			0.0	8.932	2.958	

AREA OF BASIC UNIT = 9.89E-07 cm
CHI SQUARED = 12.23116 WITH 5 DEGREES OF FREEDOM
P(chi squared) = 3.2 %
CORRELATION COEFFICIENT = 0.880
VARIANCE OF SQR(Ns) = 8.99
VARIANCE OF SQR(Ni) = 2.63

Ns/Ni = 3.019 ± 0.277
MEAN RATIO = 3.099 ± 0.356

Ages calculated using a zeta of 133.9 ± 1.4 for CN1 glass
RHO D = 9.089E+05 ; ND = 4499

POOLED AGE = 181.1 ± 17.0 Ma
MEAN AGE = 185.9 ± 21.6 Ma

8902-156 APATITE lewis s54/047724 380m

IRRADIATION jmt data:jmt apatite data:lewis apatites:wk017/14
SLIDE NUMBER 1
COUNTED BY: jmt

No.	Ns	NI	Na	RATIO	U (ppm)	RHOs (E+06)	RHOI (E+06)	F.T.AGE (Ma)
1	3	72	20	0.042	36.3	0.152	3.640	9.7 ± 5.7
2	0	3	8	0.000	3.8	0.000	0.379	0.0 ± 0.0
3	2	55	12	0.036	46.2	0.169	4.634	8.5 ± 6.1
4	2	27	6	0.074	45.4	0.337	4.550	17.2 ± 12.6
5	0	2	25	0.000	0.8	0.000	0.081	0.0 ± 0.0
6	2	16	18	0.125	9.0	0.112	0.899	29.1 ± 21.8
7	2	7	28	0.286	2.5	0.072	0.253	66.2 ± 53.1
8	0	17	12	0.000	14.3	0.000	1.432	0.0 ± 0.0
9	0	10	15	0.000	6.7	0.000	0.674	0.0 ± 0.0
10	0	7	12	0.000	5.9	0.000	0.590	0.0 ± 0.0
11	0	3	9	0.000	3.4	0.000	0.337	0.0 ± 0.0
12	1	33	30	0.030	11.1	0.034	1.112	7.1 ± 7.2
13	2	69	16	0.029	43.5	0.126	4.360	6.7 ± 4.8
14	2	8	16	0.250	5.0	0.126	0.506	58.0 ± 45.9
15	2	11	24	0.182	4.6	0.084	0.463	42.2 ± 32.5
16	3	96	24	0.031	40.4	0.126	4.044	7.3 ± 4.3
	21	436			16.0	0.077	1.603	

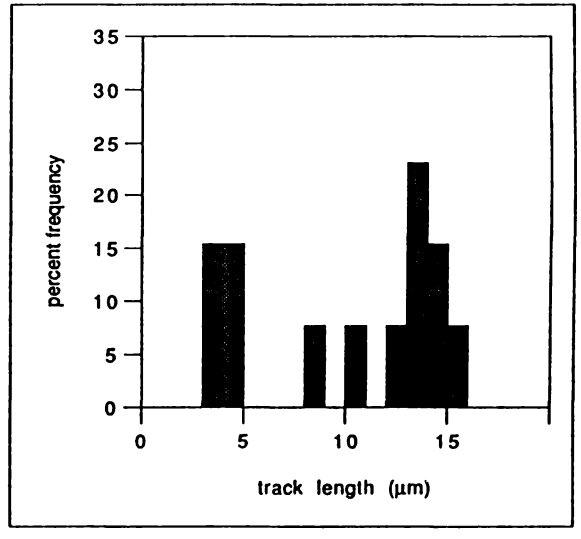
AREA OF BASIC UNIT = 9.89E-07 cm
CHI SQUARED = 20.85149 WITH 15 DEGREES OF FREEDOM
P(chi squared) = 14.2 %
CORRELATION COEFFICIENT = 0.696
VARIANCE OF SQR(Ns) = 0.54
VARIANCE OF SQR(Ni) = 7.14

Ns/Ni = 0.048 ± 0.011
MEAN RATIO = 0.068 ± 0.023

Ages calculated using a zeta of 354.9 ± 4.3 for SRM612 glass
RHO D = 1.313E+06 ; ND = 3248

POOLED AGE = 11.2 ± 2.5 Ma
MEAN AGE = 15.8 ± 5.4 Ma

8902-156



n = 13
Mean = 10.23 µm
Sample std. dev. = 4.42 µm

8902-156 ZIRCON lewis s54/047724 380m

IRRADIATION jmt data:jmt zircon data:lewis zircons:wk029/15
SLIDE NUMBER 1
COUNTED BY: jmt

No.	Ns	Ni	Na	RATIO	U (ppm)	RHOs (E+06)	RHOi (E+06)	F.T AGE (Ma)
1	51	16	6	3.188	0.0	8.595	2.696	189.7 ± 54.5
2	57	45	8	1.267	0.0	7.204	5.688	76.0 ± 15.2
3	93	32	12	2.906	0.0	7.836	2.696	173.1 ± 35.6
4	148	122	10	1.213	0.0	14.965	12.336	72.8 ± 9.0
5	65	27	8	2.407	0.0	8.215	3.413	143.7 ± 33.0
6	102	24	8	4.250	0.0	12.892	3.033	251.6 ± 57.3
7	189	50	12	3.780	0.0	15.925	4.213	224.3 ± 35.9
8	231	69	12	3.348	0.0	19.464	5.814	199.0 ± 27.5
9	123	49	8	2.510	0.0	15.546	6.193	149.8 ± 25.5
10	128	103	12	1.243	0.0	10.785	8.679	74.6 ± 10.0
11	127	70	10	1.814	0.0	12.841	7.078	108.6 ± 16.3
12	124	48	12	2.583	0.0	10.448	4.044	154.1 ± 26.4
	1438	655			0.0	12.322	5.613	

AREA OF BASIC UNIT = 9.89E-07 cm
CHI SQUARED = 88.32374 WITH 11 DEGREES OF FREEDOM
P(chi squared) = < 0.1 %
CORRELATION COEFFICIENT = 0.515
VARIANCE OF SQR(Ns) = 5.79
VARIANCE OF SQR(Ni) = 4.39

Ns/Ni = 2.195 ± 0.103
MEAN RATIO = 2.542 ± 0.292

Ages calculated using a zeta of 133.9 ± 1.4 for CN1 glass
RHO D = 9.019E+05 ; ND = 4460

POOLED AGE = 131.2 ± 6.6 Ma
MEAN AGE = 151.7 ± 17.7 Ma

8902-157 APATITE lewis s54/116716 335m

IRRADIATION jmt data:jmt apatite data:lewis apatites:wk017/13
SLIDE NUMBER 1
COUNTED BY: jmt

No.	Ns	NI	Na	RATIO	U (ppm)	RHOs (E+06)	RHOI (E+06)	F.T.AGE (Ma)
1	21	82	16	0.256	52.0	1.327	5.182	59.0 ± 14.5
2	2	16	9	0.125	18.0	0.225	1.798	28.9 ± 21.7
3	0	18	12	0.000	15.2	0.000	1.517	0.0 ± 0.0
4	0	9	16	0.000	5.7	0.000	0.569	0.0 ± 0.0
5	0	5	9	0.000	5.6	0.000	0.562	0.0 ± 0.0
6	1	39	12	0.026	33.0	0.084	3.286	5.9 ± 6.0
7	0	4	9	0.000	4.5	0.000	0.449	0.0 ± 0.0
8	1	20	16	0.050	12.7	0.063	1.264	11.6 ± 11.9
9	2	30	15	0.067	20.3	0.135	2.022	15.4 ± 11.3
10	19	88	16	0.216	55.8	1.201	5.561	49.8 ± 12.6
11	2	6	16	0.333	3.8	0.126	0.379	76.7 ± 62.7
12	2	16	9	0.125	18.0	0.225	1.798	28.9 ± 21.7
13	4	45	40	0.089	11.4	0.101	1.138	20.6 ± 10.7
14	0	21	14	0.000	15.2	0.000	1.517	0.0 ± 0.0
15	3	16	12	0.188	13.5	0.253	1.348	43.3 ± 27.2
16	8	33	15	0.242	22.3	0.539	2.224	55.9 ± 22.1
17	0	29	18	0.000	16.4	0.000	1.629	0.0 ± 0.0
18	5	11	24	0.455	4.7	0.211	0.463	104.4 ± 56.4
19	36	290	35	0.124	84.1	1.040	8.378	28.7 ± 5.1
	106	778			25.2	0.342	2.513	

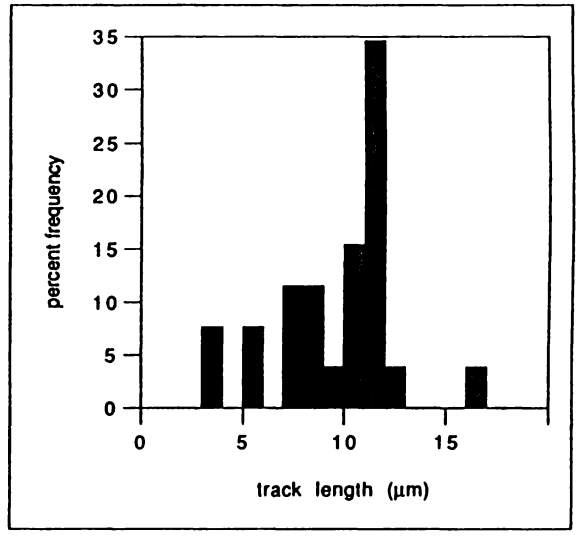
AREA OF BASIC UNIT = 9.89E-07 cm
CHI SQUARED = 37.77263 WITH 18 DEGREES OF FREEDOM
P(chi squared) = 0.4 %
CORRELATION COEFFICIENT = 0.921
VARIANCE OF SQR(Ns) = 3.01
VARIANCE OF SQR(Ni) = 12.01

Ns/Ni = 0.136 ± 0.014
MEAN RATIO = 0.121 ± 0.030

Ages calculated using a zeta of 354.9 ± 4.3 for SRM612 glass
RHO D = 1.305E+06 ; ND = 3226

POOLED AGE = 31.5 ± 3.3 Ma
MEAN AGE = 27.9 ± 7.0 Ma

8902-157



n = 26
Mean = 9.66 µm
Sample std. dev. = 2.79 µm

8902-157 ZIRCON lewis s54/116716 335m

IRRADIATION jmt data:jmt zircon data:lewis zircons:wk037/12
SLIDE NUMBER 1
COUNTED BY: jmt

No.	Ns	Ni	Na	RATIO	U (ppm)	RHOs (E+06)	RHOi (E+06)	F.T.AGE (Ma)
1	51	15	4	3.400	0.0	12.892	3.792	238.4 ± 70.1
2	200	81	15	2.469	0.0	13.482	5.460	174.0 ± 23.1
3	114	43	12	2.651	0.0	9.606	3.623	186.7 ± 33.5
4	252	84	18	3.000	0.0	14.156	4.719	210.8 ± 26.8
5	55	17	4	3.235	0.0	13.903	4.297	227.1 ± 63.1
6	111	39	8	2.846	0.0	14.029	4.929	200.2 ± 37.4
7	58	16	4	3.625	0.0	14.661	4.044	253.9 ± 71.8
8	408	140	27	2.914	0.0	15.279	5.243	204.9 ± 20.3
9	58	37	6	1.568	0.0	9.774	6.235	111.0 ± 23.4
10	155	74	12	2.095	0.0	13.060	6.235	147.9 ± 21.0
11	95	39	8	2.436	0.0	12.007	4.929	171.7 ± 32.8
12	59	20	6	2.950	0.0	9.943	3.370	207.4 ± 53.8
13	88	26	6	3.385	0.0	14.830	4.382	237.4 ± 53.1
14	45	12	4	3.750	0.0	11.375	3.033	262.5 ± 85.4
15	508	250	45	2.032	0.0	11.414	5.617	143.5 ± 11.3
	2257	893			0.0	12.749	5.044	

AREA OF BASIC UNIT = 9.89E-07 cm
CHI SQUARED = 26.60178 WITH 14 DEGREES OF FREEDOM
P(chi squared) = 2.2 %
CORRELATION COEFFICIENT = 0.972
VARIANCE OF SQR(Ns) = 24.04
VARIANCE OF SQR(Ni) = 11.71

Ns/Ni = 2.527 ± 0.100
MEAN RATIO = 2.824 ± 0.161

Ages calculated using a zeta of 133.9 ± 1.4 for CN1 glass
RHO D = 1.067E+06 ; ND = 6342

POOLED AGE = 178.1 ± 7.6 Ma
MEAN AGE = 198.6 ± 11.8 Ma

8902-158 APATITE lewis s54/139643 290m

IRRADIATION jmt data:jmt apatite data:lewis apatites:wk017/12
SLIDE NUMBER 1
COUNTED BY: jmt

No.	Ns	Ni	Na	RATIO	U (ppm)	RHOs (E+06)	RHOi (E+06)	F.T.AGE (Ma)
1	10	32	28	0.312	11.7	0.361	1.156	71.5 ± 25.9
2	6	14	24	0.429	6.0	0.253	0.590	97.8 ± 47.8
3	10	14	16	0.714	8.9	0.632	0.885	162.2 ± 67.3
4	14	39	10	0.359	39.9	1.416	3.943	82.0 ± 25.6
5	6	10	12	0.600	8.5	0.506	0.843	136.5 ± 70.6
6	20	49	12	0.408	41.7	1.685	4.129	93.2 ± 24.8
7	14	34	50	0.412	6.9	0.283	0.688	94.0 ± 29.9
8	15	45	15	0.333	30.7	1.011	3.033	76.2 ± 22.8
9	0	10	15	0.000	6.8	0.000	0.674	0.0 ± 0.0
10	5	14	16	0.357	8.9	0.316	0.885	81.6 ± 42.6
11	1	10	12	0.100	8.5	0.084	0.843	23.0 ± 24.1
12	8	13	15	0.615	8.9	0.539	0.876	140.0 ± 63.0
13	2	8	6	0.250	13.6	0.337	1.348	57.2 ± 45.3
14	2	5	12	0.400	4.3	0.169	0.421	91.3 ± 76.4
15	21	88	24	0.239	37.5	0.885	3.707	54.6 ± 13.3
16	2	9	35	0.222	2.6	0.058	0.260	50.9 ± 39.8
17	5	20	24	0.250	8.5	0.211	0.843	57.2 ± 28.6
18	4	25	24	0.160	10.6	0.169	1.053	36.7 ± 19.8
19	10	25	16	0.400	16.0	0.632	1.580	91.3 ± 34.2
20	0	8	9	0.000	9.1	0.000	0.899	0.0 ± 0.0
	155	472			12.9	0.418	1.273	

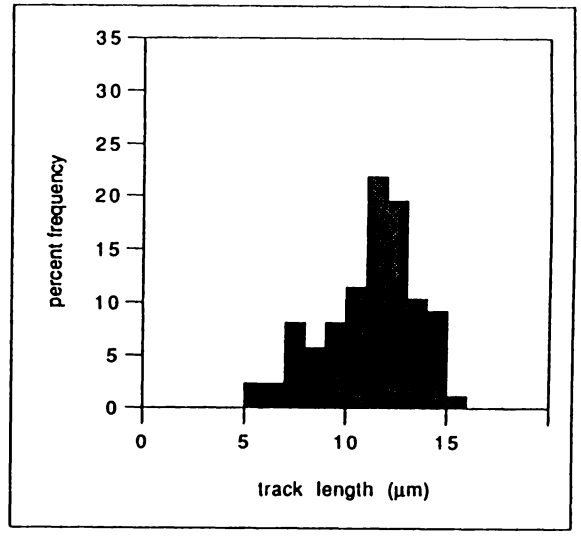
AREA OF BASIC UNIT = 9.89E-07 cm
CHI SQUARED = 20.70377 WITH 19 DEGREES OF FREEDOM
P(chi squared) = 35.3 %
CORRELATION COEFFICIENT = 0.883
VARIANCE OF SQR(Ns) = 1.75
VARIANCE OF SQR(Ni) = 3.29

Ns/Ni = 0.328 ± 0.030
MEAN RATIO = 0.328 ± 0.042

Ages calculated using a zeta of 354.9 ± 4.3 for SRM612 glass
RHO D = 1.296E+06 ; ND = 3204

POOLED AGE = 75.1 ± 7.1 Ma
MEAN AGE = 75.0 ± 9.7 Ma

8902-158



n = 87
Mean = 11.28 µm
Sample std. dev. = 2.23 µm

8902-158 ZIRCON lewis s54/139643 290m

IRRADIATION jmt data:jmt zircon data:lewis zircons:wk029/13
SLIDE NUMBER 1
COUNTED BY: jmt

No.	Ns	Ni	Na	RATIO	U (ppm)	RHOs (E+06)	RHOi (E+06)	F.T.AGE (Ma)
1	244	64	24	3.812	0.0	10.280	2.696	222.3 ± 31.5
2	150	66	12	2.273	0.0	12.639	5.561	133.5 ± 19.9
3	211	176	32	1.199	0.0	6.667	5.561	70.7 ± 7.3
4	219	129	24	1.698	0.0	9.226	5.435	100.0 ± 11.2
5	296	168	28	1.762	0.0	10.689	6.067	103.7 ± 10.2
6	204	82	15	2.488	0.0	13.751	5.527	146.0 ± 19.3
7	171	110	18	1.555	0.0	9.606	6.179	91.6 ± 11.3
8	50	39	6	1.282	0.0	8.426	6.572	75.6 ± 16.2
9	144	37	12	3.892	0.0	12.133	3.118	226.9 ± 42.0
10	285	144	21	1.979	0.0	13.722	6.933	116.4 ± 12.1
11	52	32	6	1.625	0.0	8.763	5.393	95.7 ± 21.6
12	142	67	15	2.119	0.0	9.572	4.516	124.5 ± 18.6
	2168	1114			0.0	10.292	5.288	

AREA OF BASIC UNIT = 9.89E-07 cm
CHI SQUARED = 76.98103 WITH 11 DEGREES OF FREEDOM
P(chi squared) = < 0.1 %
CORRELATION COEFFICIENT = 0.773
VARIANCE OF SQR(Ns) = 10.74
VARIANCE OF SQR(Ni) = 7.22

Ns/Ni = 1.946 ± 0.072
MEAN RATIO = 2.140 ± 0.255

Ages calculated using a zeta of 133.9 ± 1.4 for CN1 glass
RHO D = 8.863E+05 ; ND = 4383

POOLED AGE = 114.5 ± 4.7 Ma
MEAN AGE = 125.8 ± 15.2 Ma

8902-159 APATITE lewis s54/159584 245m

IRRADIATION jmt data:jmt apatite data:lewis apatites:wk017/11
SLIDE NUMBER 1
COUNTED BY: jmt

No.	Ns	Ni	Na	RATIO	U (ppm)	RHOs (E+06)	RHOi (E+06)	F.T.AGE (Ma)
1	6	19	10	0.316	19.6	0.607	1.921	71.7 ± 33.6
2	11	19	4	0.579	48.9	2.781	4.803	130.9 ± 49.7
3	20	62	18	0.323	35.4	1.123	3.483	73.3 ± 18.9
4	4	9	4	0.444	23.2	1.011	2.275	100.7 ± 60.6
5	10	26	24	0.385	11.1	0.421	1.095	87.2 ± 32.5
6	2	3	3	0.667	10.3	0.674	1.011	150.5 ± 137.4
7	4	14	3	0.286	48.0	1.348	4.719	64.9 ± 36.8
8	8	28	12	0.286	24.0	0.674	2.359	64.9 ± 26.1
9	9	26	4	0.346	66.9	2.275	6.572	78.6 ± 30.4
10	2	3	2	0.667	15.4	1.011	1.517	150.5 ± 137.4
11	20	58	12	0.345	49.7	1.685	4.887	78.3 ± 20.4
12	3	20	6	0.150	34.3	0.506	3.370	34.2 ± 21.2
13	17	34	6	0.500	58.3	2.865	5.730	113.2 ± 33.7
14	12	24	4	0.500	61.8	3.033	6.067	113.2 ± 40.1
15	4	10	3	0.400	34.3	1.348	3.370	90.7 ± 53.7
16	7	28	6	0.250	48.0	1.180	4.719	56.8 ± 24.1
17	22	41	9	0.537	46.9	2.472	4.606	121.4 ± 32.2
18	3	10	4	0.300	25.7	0.758	2.528	68.2 ± 44.9
19	25	68	9	0.368	77.8	2.809	7.640	83.4 ± 19.6
20	12	37	6	0.324	63.5	2.022	6.235	73.6 ± 24.5
21	12	28	18	0.429	16.0	0.674	1.573	97.1 ± 33.6
	213	567			34.9	1.290	3.433	

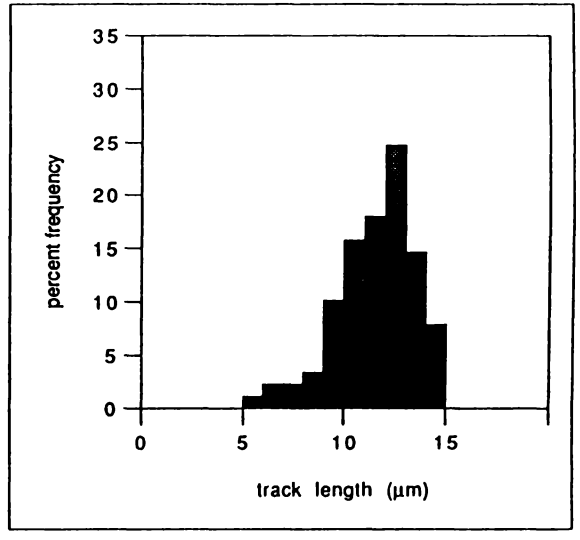
AREA OF BASIC UNIT = 9.89E-07 cm
CHI SQUARED = 10.7734 WITH 20 DEGREES OF FREEDOM
P(chi squared) = 95.2 %
CORRELATION COEFFICIENT = 0.922
VARIANCE OF SQR(Ns) = 1.25
VARIANCE OF SQR(Ni) = 3.22

Ns/Ni = 0.376 ± 0.030
MEAN RATIO = 0.400 ± 0.029

Ages calculated using a zeta of 354.9 ± 4.3 for SRM612 glass
RHO D = 1.287E+06 ; ND = 3183

POOLED AGE = 85.2 ± 7.1 Ma
MEAN AGE = 90.7 ± 6.9 Ma

8902-159



n = 89
Mean = 11.58 µm
Sample std. dev. = 1.87 µm

8902-159 ZIRCON lewis s54/159584 245m

IRRADIATION jmt data:jmt zircon data:lewis zircons:wk029/12
SLIDE NUMBER 1
COUNTED BY: jmt

No.	Ns	Ni	Na	RATIO	U (ppm)	RHOs (E+06)	RHOi (E+06)	F.T.AGE (Ma)
1	124	60	12	2.067	0.0	10.448	5.056	120.4 ± 19.1
2	68	17	6	4.000	0.0	11.459	2.865	231.1 ± 62.8
3	263	105	24	2.505	0.0	11.080	4.424	145.7 ± 17.0
4	57	19	8	3.000	0.0	7.204	2.401	174.1 ± 46.2
5	114	29	16	3.931	0.0	7.204	1.833	227.2 ± 47.4
6	97	26	10	3.731	0.0	9.808	2.629	215.8 ± 47.8
7	106	43	12	2.465	0.0	8.932	3.623	143.4 ± 26.1
8	121	27	12	4.481	0.0	10.195	2.275	258.4 ± 55.2
9	194	77	18	2.519	0.0	10.898	4.325	146.5 ± 19.9
10	68	20	9	3.400	0.0	7.640	2.247	197.0 ± 50.2
11	176	86	20	2.047	0.0	8.898	4.348	119.3 ± 15.8
12	36	10	4	3.600	0.0	9.100	2.528	208.4 ± 74.6
13	224	60	15	3.733	0.0	15.099	4.044	216.0 ± 31.6
14	110	38	16	2.895	0.0	6.951	2.401	168.1 ± 31.8
	1758	617			0.0	9.767	3.428	

AREA OF BASIC UNIT = 9.89E-07 cm
CHI SQUARED = 27.85192 WITH 13 DEGREES OF FREEDOM
P(chi squared) = 0.9 %
CORRELATION COEFFICIENT = 0.914
VARIANCE OF SQR(Ns) = 8.51
VARIANCE OF SQR(Ni) = 4.62

Ns/Ni = 2.849 ± 0.133
MEAN RATIO = 3.170 ± 0.207

Ages calculated using a zeta of 133.9 ± 1.4 for CN1 glass
RHO D = 8.787E+05 ; ND = 4345

POOLED AGE = 165.5 ± 8.3 Ma
MEAN AGE = 183.8 ± 12.5 Ma